ЖУРНАЛ
ЭКСПЕРИМЕНТАЛЬНОЙ И ТЕОРЕТИЧЕСКОЙ
ФИЗИКИ
АКАДЕМИЯ НАУК СССР

SOVIET PHYSICS

JETP

VOLUME 2 NUMBER 4

A Translation

of the

Journal of Experimental and Theoretical Physics

of the

Academy of Sciences of the USSR

JULY, 1956

Published by the

AMERICAN INSTITUTE OF PHYSICS
INCORPORATED

SOVIET PHYSICS
JETP

A translation of the Journal of Experimental and Theoretical Physics of the USSR.

A publication of the
AMERICAN INSTITUTE OF PHYSICS

Governing Board

FREDERICK SEITZ, *Chairman*
ALLEN V. ASTIN
ROBERT F. BACHER
H. A. BETHE
J. W. BUCHTA
S. A. GOUDSMIT
DEANE B. JUDD
HUGH S. KNOWLES
W. H. MARKWOOD, JR.
WILLIAM F. MEGGERS
PHILIP M. MORSE
BRIAN O'BRIEN
HARRY F. OLSON
R. F. PATON
ERIC RODGERS
RALPH A. SAWYER
WILLIAM SHOCKLEY
H. D. SMYTH
J. H. VAN VLECK
MARK W. ZEMANSKY

Administrative Staff

HENRY A. BARTON,
Director
GEORGE B. PEGRAM,
Treasurer
WALLACE WATERFALL,
Executive Secretary
THEODORE VORBURGER,
Advertising Manager
RUTH F. BRYANS,
Publication Manager
EDITH I. NEFTEL,
Circulation Manager
KATHRYN SETZE,
Assistant Treasurer
MELVIN LOOS,
Consultant on Printing

American Institute of Physics Advisory Board on Russian Translations

ELMER HUTCHISSON, *Chairman*
DWIGHT GRAY, MORTON HAMERMESH, VLADIMIR ROJANSKY, VICTOR WEISSKOPF

Editor of SOVIET PHYSICS
ROBERT T. BEYER, DEPARTMENT OF PHYSICS, BROWN UNIVERSITY, Providence, R.I.

SOVIET PHYSICS is a bi-monthly journal published by the American Institute of Physics for the purpose of making available in English reports of current Soviet research in physics as contained in the Journal of Experimental and Theoretical Physics of the Academy of Sciences of USSR. The page size of SOVIET PHYSICS will be 7⅞" x 10½", the same as other Institute journals.

Transliteration of the names of Russian authors follows the system employed by the Library of Congress.

This translating and publishing project was undertaken by the Institute in the conviction that dissemination of the results of researchs everywhere in the world is invaluable to the advancement of science. The National Science Foundation of the United States encouraged the project initially and is supporting it in large part by a grant.

The American Institute of Physics and its translators propose to translate faithfully all the material in the Journal of EXPERIMENTAL & THEORETICAL PHYSICS OF THE USSR appearing after January 1, 1955. The views expressed in the translated material, therefore, are intended to be those expressed by the original authors, and not those of the translators nor of the American Institute of Physics.

One volume is published annually. Volume 1 (1955) contains three issues. Subsequent volumes, beginning with January 1956, will contain six issues.

Subscription Prices:

Per year (6 issues)	
United States and Canada	$30.00
Elsewhere	32.00
1st Volume (3 issues)	
United States and Canada	$15.00
Elsewhere	16.00
Back Numbers	
Single copies	$ 6.00

Subscriptions should be addressed to the American Institute of Physics, 57 East 55 Street, New York 22, New York.

Copyright by American Institute of Physics 1956

SOVIET PHYSICS

JETP

SOVIET PHYSICS JETP VOLUME 2, NUMBER 4 JULY, 1956

On the Macroscopic Theory of Superconductivity

V. L. GINZBURG

P. N. Lebedev Physical Institute, Academy of Sciences, USSR

(Submitted to JETP editor August 12, 1954)
J. Exper. Theoret. Phys. USSR **29**, 748-761 (December, 1955)

The question of the basic equations of the macroscopic theory of superconductivity in steady and alternating fields is discussed in connection with some recent researches. Particular attention is paid to clarification of the character of the conclusions which can be made on the basis of measurements of the surface impedance of the metal.

HE macroscopic theory of superconductivity, the basic problem of which consists in establishing the connection between current density **j** in a superconductor and the electric and magnetic field strengths **E** and **H** plays an exceptionally important rọle in the study of superconductivity. This relation between **j** and **E**, **H** in the superconducting state has a non-trivial character (in contrast, for instance, to Ohm's law $\mathbf{j} = \sigma \mathbf{E}$, which in most cases determines the relation in the nonsuperconducting state); moreover, the establishment of the relation is absolutely necessary for quantitative interpretation of experiments in superconductivity. Again, the microtheory of superconductivity can hardly be constructed and developed if we do not know those macroscopic relations which must be obtained as a result of a detailed consideration of the motion of the electrons in the metal. In view of what has been said, it is easy to understand the considerable attention which has been paid to the macrotheory of superconductivity, to which several special monographs and reviews have been devoted (see, for instance, references 1, 2).

An important step in the construction of a macrotheory of superconductivity was the theory of F. and H. London (1935) in which the basic equation[1,2] is

$$\operatorname{curl} \Lambda \mathbf{j}_s = -(1/c)\mathbf{H}. \tag{1}$$

If we restrict ourselves to the case of a steady field, then Eq. (1), together with Maxwell' equations, is sufficient for determining the density $\mathbf{j}_s$ of the superconducting current and the field **H** in the superconductor. Thus, for a massive superconductor $\mathbf{j}_s = (c/4\pi\delta_0)\mathbf{H}$, $\mathbf{H} = \mathbf{H}_0 e^{-z/\delta_0}$, where $\mathbf{H}_0$ is the field at the boundary of the metal, the z axis is directed along the normal of the boundary surface into the metal and $\delta_0 = (\Lambda c^2/4\pi)^{1/2}$. The parameter Λ may be conveniently expressed in terms of the concentration n_s of the "superconducting electrons";

$$\lambda = m/e^2 n_s, \qquad \delta_0 = \sqrt{\Lambda c^2/4\pi} = \sqrt{mc^2/4\pi e^2 n_s}, \tag{2}$$

where e and m are the charge and the mass of a free electron. The macrotheory based on Eq. (1) turns out to be in qualitative agreement with ex-

---

[1] F. London, *Superfluids, I, Macroscopic Theory of Superconductivity*, New York, 1950.

[2] V. L. Ginzburg, Usp. Fiz. Nauk **42**, 169, 333 (1950).

periments made in weak fields, such that $H \ll H_k$ (H_k is the critical field). In fields $H \sim H_k$, however, such as cocur in the destruction of superconductivity by a field, in the intermediate state, and so on, Eq. (1) and the theory connected with it are completely inapplicable (see reference 2) and require generalization. A macrotheory of superconductivity which can be used in fields of any magnitude was developed only fairly recently[2,3]. Here Eq. (1) is replaced by the relations

$$\frac{1}{2m}\left(-i\hbar\nabla - \frac{e}{c}\mathbf{A}\right)^2\Psi + \alpha\Psi + \beta|\Psi|^2\Psi = 0, \tag{3}$$

$$\mathbf{j}_s = -\frac{ie\hbar}{mc}\left(\Psi^*\nabla\Psi - \Psi\nabla\Psi^*\right) - \frac{e^2}{mc}|\Psi|^2\mathbf{A},$$

where $\mathbf{A}$ is the vector potential, which, if we assume div $\mathbf{A} = 0$, satisfies the equation $\Delta\mathbf{A} = -(4\pi/c)\mathbf{j}_s$. In a weak field we may consider that $|\Psi|^2 = -\alpha/\beta = |\Psi_\infty|^2 = \text{const}$, and consequently $\mathbf{j}_s = -(e^2/mc)|\Psi|^2\mathbf{A}$, from which, after applying the operation curl, we obtain Eq. (1) with $\Lambda = m/e^2|\Psi|^2$, i.e., $|\Psi|^2 = n_s$.

The further development of the theory[3] and comparison of it with experimental data and, in particular, with the specially designed experiments of Zavaritskii has turned out to be very sucessful[4-10]. However, in the papers of Pippard[11,12] is is asserted that even in weak fields (1) is not applicable, and consequently, that it is essential to make some modification of Eq. (3), which leads to (1) in weak fields. The considerations of Pippard, which are based on experimental material, deserve careful attention. In part 1 of the present article we discuss this question and come to the conclusion that Pippard's replacement of the differential equations (1) or (3) by certain integral equations is not justified. In parts 2 and 3 we discuss the question of the behavior of superconductors in fields which are not steady (as was assumed above in part 1), but are time variable at high frequencies, up to the optical part of the spectrum. Particular attention is devoted to clarifying the character of the conclusions which can be made from the results of measurements of the surface impedance of superconductors.

1. CHARACTER OF THE BASIC EQUATIONS OF THE MACROTHEORY OF SUPERCONDUCTIVITY IN A STEADY FIELD

Pippard's remarks are to a large extent based on interesting experimental data and confirm the conclusion that (1) is not valid in strong fields. At the same time it is easy to see that all the new facts (with one possible exception which will be pointed out below) agree at least qualitatively with the theory[3], in which there appear parameters α and β or the directly measurable quantities:

$$\delta_0 = \sqrt{mc^2\beta/4\pi e^2|\alpha|} \tag{4}$$

$$= \sqrt{mc^2/4\pi e^2 n_s}, \quad H_{\kappa M} = \sqrt{4\pi\alpha^2/\beta},$$

$$\varkappa = (mc/|e|\hbar)\sqrt{\beta/2\pi} = (\sqrt{2}|e|/\hbar c)H_{\kappa M}\delta_0^2$$

(δ_0 is the penetration depth of a weak field, H_{kM} is the critical field for the bulk metal). The quantity $|\Psi_\infty|^2 \equiv n_s = -\alpha/\beta$ is not directly measurable, so in the expression for δ_0 we may take e^2/m to be the same as for free electrons without making any assumption of a physical nature (for further details, see references 2, 3 and 18). Thus, the "concentration of superconducting electrons" is by definition given by

$$n_s = mc^2/4\pi e^2\delta_0^2 = 2.83\cdot 10^{11}\,\delta_0^{-2}, \tag{5}$$

where δ_0, as in all that follows, is measured in centimeters. The same of course applies also to

---

[3] V. L. Ginzburg and L. D. Landau, J. Exper. Theoret. Phys. USSR **20**, 1064 (1950).

[4] V. P. Silin, J. Exper. Theoret. Phys. USSR **21**, 1330 (1951).

[5] V. L. Ginzburg, Dokl. Akad. Nauk SSSR **83**, 385 (1952).

[6] V. N. Zavaritskii, Dokl. Akad. Nauk SSSR 78, 665 (1951); **85**, 749 (1952).

[7] V. L. Ginzburg, J. Exper. Theoret. Phys. USSR **23**, 236 (1952).

[8] V. L. Ginzburg, Usp. Fiz. Nauk **48**, 25 (1952).

[9] A. A. Abrikosov, Dokl. Akad. Nauk SSSR **86**, 489 (1952).

[10] A. V. Gurevich, J. Exper. Theoret. Phys. USSR **27**, 195 (1954).

[11] A. B. Pippard, Proc. Roy. Soc. (London) **216**, 547 (1953).

[12] A. B. Pippard, Physica **19**, 765 (1953).

(1) snd (2); the suggestion sometimes made that the mass $m = 9.1 \times 10^{-28}$ should be replaced by some effective mass m_{eff} is based to a large extent on a misunderstanding.

In references 2 and 3 it is assumed that the charge e appearing in (3) and in the expression for κ in (4) is equal to the charge of the free electron $|e| = 4.8 \times 10^{-10}$. In this case

$$\varkappa = 2 \cdot 16 \times 10^{7} H_{\text{KM}} \delta_0^2 \qquad (6)$$

and only two parameters, δ_0 and $H_{k\text{M}}$ enter into the theory. The assumption seems to be a fairly natural one, but may not necessarily be true (this was already noted in reference 8, p. 107). If the charge e in (3) is not equal to that of a free electron* then three parameters (δ_0, $H_{k\text{M}}$ and κ) enter into the theory[3]. Verification of the theory is possible in this case also, since the same quantity κ enters, for instance, both into the expression for the surface energy and the expression determining the dependence of the penetration depth on the applied magnetic field. Thus perhaps we should not take it for granted, as is done by Faber[13] and Bardeen[14], that the theory[3] is uniquely linked with (6), although this does seem the most probable hypothesis.

The experimental data given in references 13 and 14 are not very precise, but nevertheless suggest the possibility that the value of κ is two or three times larger than that given by (6); in other words,

$$\varkappa = (\sqrt{2}\, |e_{\text{eff}}| / \hbar c) H_{\varkappa\text{M}} \delta_0^2 \qquad (7)$$

$$= 2.16 \cdot 10^{7} (e_{\text{eff}} / e) H_{\varkappa\text{M}} \delta_0^2,$$

where $(e_{\text{eff}}/e) \sim 2$ or 3. Since the ratio e_{eff}/e if $e_{\text{eff}} \neq e$ may change from metal to metal there is no reason for supposing[13] that even if $\sqrt{\kappa} \ll 1$ the quantity $\Delta H_{k\text{M}} \delta_0$ should have the same value for all metals close to T_k according to the theory[3] (here $\Delta = \sigma_{ns} / (H_{k\text{M}}^2 / 8\pi)$, where σ_{ns} is the surface energy at the boundary between normal and superconducting phases). In support of the hypothesis that $e_{\text{eff}}/e > 1$ there are some data on the dependence of the penetration depth of magnetic field. However, the whole question of the value of the ratio e_{eff}/e remains completely open from an experimental point of view, and it is quite possible that $e_{\text{eff}}/e = 1$, as is more probable, if not indeed necessary, on theoretical grounds. Verification of the theory by measurement of Δ and the field dependence of δ for one and the same specimen is therefore particularly needed, (if the theory is true then the values of κ obtained from both experiments should coincide)*.

---

* It must be pointed out that the introduction of a nonuniversal charge $e_{\text{eff}} \neq e = 4.8 \times 10^{-10}$ is not free from serious objection (the author owes this remark to L. D. Landau). Thus, if the superconductor is nonuniform, e_{eff} will depend on the coordinates and this will upset the gauge invariance of the theory. However, to take account of nonuniformity of the metal might require just such a generalization of the theory[3], which was developed only for uniform media where this difficulty does not arise.

[13] T. E. Faber, Proc. Roy. Soc. (London) **223**, 174 (1954).

[14] J. Bardeen, Phys. Rev. **94**, 554 (1954).

* It should be noted that the theory[3] has been worked out only for temperatures close to T_k, since it is only in this region that the dependence of δ_0 and $H_{k\text{M}}$ on $(T_k - T)$, and the expression for the free energy in terms of $|\Psi|^2$, are reliably known. For lower temperatures, down to $T = 0$, the generalization of the theory[3] is not uniquely indicated, even if we assume on empirical grounds particular forms of the dependence of δ_0 and $H_{k\text{M}}$ on T. One variant of such a possible generalization of the theory[3] has been considered recently by Bardeen[14] who assumed that $H_{k\text{M}} = H_0(1 - (T/T_k)^2)$, $F_{n0} = -(H_0^2/4\pi)(T/T_k)^2$ and $\delta_0^2 = \delta_{00}^2/(1 - (T/T_k)^4)$. The same forms of temperature dependence of $H_{k\text{M}}$ and δ_0, which are in agreement with experiment to a first approximation, can be obtained by assuming (as in reference 3) that

$$F_{s0} = F_{n0} + \alpha |\Psi|^2 + \tfrac{1}{2}\beta |\Psi|^4,$$

but supposing, as in reference 14, that the dependence of α and β on T has the form:

$$\alpha = -A \frac{1 - (T/T_k)^2}{1 + (T/T_k)^2}, \qquad A = \frac{e^2 H_0^2 \delta_{00}^2}{mc^2},$$

In this case all the formulas of the theory[3] remain in force, if we understand by α and β, the above functions of T. However, such a generalization of the theory, as also that given by Bardeen[14], has only a limited value, since the exact form of the dependence of F_{s0} on $|\Psi|^2$ is unknown, and the expressions given for

Within the framework of the phenomenological theory the parameters δ_0 and H_{kM} are completely independent. From the microscopic point of view, as far as can be said in the present state of the theory[8], only two parameters should enter into the theory: the breadth of the gap in the energy spectrum determining in the first place the field H_{kM} $(T = 0)$, and the concentration $n_s(T = 0) \equiv n_{s0}$, determining the penetration depth at $T = 0$. The quantity n_{s0}, according to the available data (see reference 2 and below) is several times smaller than the concentration of the conduction electrons in the normal state and may depend on the treatment of the metal, presence of impurities, etc. Moreover, if we examine the path by which the quantity n_{s0} enters the microtheory (see reference 8, pp. 40-42), we have some reason for supposing that the value of n_{s0} is the higher the nearer the metal is to an ideal one. Pippard's experiments[11] support this supposition since in the case he investigated, the addition of impurities caused an increase of δ_0 (i.e., a diminution of n_{s0}). The fact that H_{kM} and T_k are only slightly changed cannot be regarded as surprising in view of what has been said, and in any case does not contradict existing theoretical ideas. Thus, the contrary assertion by Pippard does not appear to us to be well founded. The only known experimental result which evidently contradicts the theory[3] (also the London theory, which is a special case of it) is the non-monotonic dependence of penetration depth on the angle between the current and the tetragonal axis for mono-crystalline tin (see references 11 and 15 and the literature quoted there)*. However, the experiments in question[11] were carried out at high frequencies and not for the static conditions which have been implied in the preceding discussion. Moreover, as pointed out by Shoenberg (reference 15, p. 161) and Khaikin[16], there are various reasons for doubting the validity of the experimental data and thus the question of the anisotropy of the penetration depth (in particular, in a static or low frequency field) remains open.

In view of all that had been said, we do not see any reason, for the time being, to believe the conclusion that (1) is already invalid at low fields. Moreover, the equation proposed by Pippard to replace it,

$$\Lambda \mathbf{j}_s = -\frac{3}{4\pi\xi_0}\int \frac{\mathbf{r}\,(\mathbf{r}\mathbf{A})\,e^{-r/\xi}dV}{r^4} \tag{8}$$

seems to be unsuitable for a variety of reasons. Indeed, as is clear from Eq. (8) or similar ones*, the density of superconducting current $\mathbf{j}_s(\mathbf{r})$ is determined by the field in a region of dimensions of order $\sim \xi$ around the point $\mathbf{r}$ and the properties of specimens of dimensions $d \ll \xi$ must differ radically from the properties of the bulk metal. Further, the parameters ξ_0 and ξ in (8) are such that for an ideal metal $\xi_0 = \xi \sim 10^{-4}$, and for addition of impurities the parameter ξ diminishes so that $0 \leq \xi \leq \xi_0$. From this it follows that films of pure metal with the same value of T_k as bulk specimens should behave anomalously if their thickness d is such that $d \lesssim \xi_0 \sim 10^{-4}$. However, it is known from experiments[6,15] that such films behave in agreement with the theory[3] and the penetration depth δ_0 is about the same for them as for the bulk metal. The situation is similar also for superconducting colloids, as Pippard himself points out[11]. The properties of specimens of small dimensions indicate that in weak fields the current density $\mathbf{j}_s(\mathbf{r})$ is determined by a region around the point $\mathbf{r}$ of dimensions $\xi \ll d_{\min} \sim 10^{-6}$ ($d_{\min}$ is the minimum thickness of a film with values of T_k and δ_0 the same as for bulk metal). In the framework of the macrotheory this means that the connection between

---

the functions $H_{kM}(T)$ and $\delta_0(T)$ are also only approximate. Nevertheless, this generalization may be useful, since the exact form of the function $F_{s0}(|\Psi|^2)$, as is clear from Bardeen, is of little importance within certain limits, for instance, from the point of view of calculating the quantity σ_{ns} (though of course in calculating other quantities the form of the function $F_{s0}(|\Psi|^2)$ may be more important). A more detailed discussion of the application of the theory[3] at all temperatures will be given in a forthcoming paper by the author.

* Generalization of Eqs. (1) and (3) to the anisotropic case leads[7] to a monotonic dependence of δ_0 for change of θ from 0 to $\pi/2$ (θ is the angle between the current and the symmetry axis).

[15] D. Shoenberg, *Superconductivity*, Cambridge, 1952.

* Equation (8) is not gauge invariant and consequently must be replaced, for instance, by

$$\operatorname{curl} \Lambda \mathbf{j}_s = -(3/4\pi\xi_0)\int r^{-4}\,\mathbf{r}(\mathbf{r}\mathbf{H})\,e^{-r/\xi}dV$$

(reference 12, p. 772). We shall not go into this question in detail, since it is not particularly relevant to the discussion in the text.

[16] M. S. Khaikin, J. Exper. Theoret. Phys. USSR **28**, 115 (1955); Soviet Physics JETP **1**, 164 (1955).

$\mathbf{j}_s$ and the field is not of an integral character, and for a weak field, where the theory must be linear, we are led in a natural manner to Eq. (1)[1,2]. Equation (1) has, moreover, a clear meaning from the point of view of quantum theory*. Equations of the type (8) are on the contrary obtained by Pippard only by an analogy with the theory of the anomalous skin effect, although there do not appear to be any grounds for developing an analogy between the superconducting current and the normal current in the conditions of either the normal or the anomalous skin effect.

Thus, there are many convincing considerations in favor of the validity of Eq. (1), and the question of the nonvalidity of (1) in weak fields need, in our opinion, only be seriously discussed when this is demanded by new experiments (which should in the first place clear up the question of the character of the anisotropy of penetration depth of static, or sufficiently low frequency fields).

2. BEHAVIOR OF SUPERCONDUCTORS IN A HIGH FREQUENCY FIELD (GENERAL CONSIDERATIONS)

In part 1 we discussed the behavior of superconductors in a constant field. In an alternating field, and in particular, in a high-frequency field, the situation is in general a good deal more complicated, in the first place because of losses and the anomalous character of the skin-effect in metals at low temperatutes. Bearing in mind this complication and the detailed arrangements of the relevant experiments, we shall limit ourselves, in the case of the high frequency fields, to the situation of weak fields ($H \ll H_k$), where the problem can be treated as linear, and moreover, we shall be concerned only with the infleunce of the metal on the field outside it (for instance, in a resonator). In these conditions, and allowing for the smallness of the penetration depth of the field into the metal, the effect of the metal can be described by a single complex quantity which may depend on the frequency ω. Such a quantity is the surface impedance Z (or a function of it):

$$Z(\omega) = R(\omega) + iX(\omega) = \frac{4\pi}{c}\left[\frac{E_x}{H_y}\right]_0, \qquad (9)$$

where the subscript 0 indicates that the components E_x and H_y are to be taken at the surface of the metal (the z-axis is directed into the metal).

If the relation between the current and the field in the metal is such that we can introduce a complex dielectric constant $\epsilon'(\omega)$, then

$$Z(\omega) = \frac{4\pi}{c\sqrt{\varepsilon'(\omega)}}, \qquad (10)$$

$$\varepsilon' = \varepsilon - i\frac{4\pi\sigma}{\omega} = \frac{16\pi^2}{c^2Z^2}$$

$$= \frac{16\pi^2}{c^2}\frac{(R^2 - X^2) - 2iXR}{(X^2 + R^2)^2}.$$

For normal incidence of a plane wave on a plane boundary between a vacuum and the medium, Eq. (10) is exact, but for oblique incidence of the wave on the boundary, and generally for an arbitrary field in the vacuum at the boundary, the impedance will in general depend on the character of this field, i.e., it is not a characteristic of the medium alone. However, for metals, where the field in the metal diminishes very rapidly, the quantity Z, for a plane boundary, does not depend on the character of the field, if only terms up to the order of $1/\epsilon'$ are considered (see reference 17, Sec. 19). Thus, in practice, if the condition

$$16\pi^2/c^2|Z|^2 = |\varepsilon'| \gg 1, \qquad (11)$$

---

* In reference 3 the current density $\mathbf{j}_s(\mathbf{r})$ depends on field over the whole region, since the function $\Psi(\mathbf{r})$ is not constant [as it is in the limiting form (1)]. However, the connection between remote regions established in this way is realized in a way which is characteristic of quantum mechanics, and not by the introduction of integral operators. It should be noted in this connection that in (3) the term $(\hbar^2/2m)\nabla^2\Psi$, if Ψ changes appreciably over a distance δ_0/κ, is of order $\alpha\Psi$, which is large. Thus, this term is also large and cannot be considered simply as the first term in an expansion of the type $a\nabla^2\Psi + b\nabla^2(\nabla^2\Psi) + \ldots$ In our opinion the prominence of the expression $(\hbar^2/2m)\nabla^2\Psi$ is explained by the fact that the Ψ-function introduced in reference 3 is closely connected with the true Ψ-function of the electrons in the metal; in the equation for the latter, however, there enters only the differential operator of the kinetic energy-- $(\hbar^2/2m)\nabla^2$. It should be noted in this connection, that the expression obtained in reference 3 for the surface energy, $\sigma_{ns} = H^2_{kM}\delta_0/\sqrt{2}3\pi\kappa$ is obtained also, as far as order of magnitude is concerned, from the uncertainty principle if we take account of the fact that the thickness of the transition layer between phases is $\sim \delta_0/\kappa$ (from the uncertainty principle it is evident that $\sigma_{ns} \sim \frac{\hbar^2_{ns}}{2m(\delta_0/\kappa)^2}\,\frac{\delta_0}{\kappa} \sim \frac{H^2_{kM}\delta_0}{2\pi\kappa}$).

[17] Ia. L. Alpert, V. L. Ginzburg and E. L. Feinberg, *Propagation of Radio Waves*, Gostekhizdat, 1953.

is fulfilled, as it is with a large margin for metals, the impedance may be considered as characteristic of the metal alone, as was mentioned above*.

This conclusion is valid even if it is not possible to introduce a quantity ϵ' characterizing the metal, but the metal may still be considered as a "good conductor". This is always the case, at least up to frequencies higher than those of visible light (see reference 18, Sec. 2).

It should be noted too, that where the impedance is not universal, it can still be used if the character of the external field is determined. The question of the existence of a universal impedance independent of the character of the external field can be decided experimentally, for instance, by a study of the reflection of plane waves of incidence for various angles.

The impedance can always be written in the form

$$Z(\omega) = \frac{4\pi}{c\sqrt{\varepsilon'_{\text{eff}}(\omega)}}, \tag{12}$$

$$\varepsilon'_{\text{eff}} \equiv \varepsilon_{\text{eff}} - i\frac{4\pi\sigma_{\text{eff}}}{\omega}$$

$$\equiv \varepsilon_{1\,\text{eff}} - i\varepsilon_{2\,\text{eff}} = \frac{16\pi^2}{c^2Z^2},$$

where $\epsilon'_{\text{eff}}(\omega)$ is a new complex quantity playing the role of an effective dielectric constant of the metal. In the special case of normal skin-effect, of course, $\epsilon'_{\text{eff}} = \epsilon'$. Generally, however, ϵ'_{eff} coincides with the complex dielectric constant of a medium that would have exactly the same effect on the external field as the metal if it were put in its place. From this it is clear that from measurement of the impedance alone, bringing in no additional considerations, it is impossible to conclude that the metal cannot be characterized by a parameter ϵ'. Such a conclusion indeed cannot be made without going outside the framework of phenomenological concepts, but only from a determination of the field in the metal itself (the possibility of such measurements is not excluded in principle, but there is no need to consider them as yet). These remarks make evident the unsoundness of attempts[19] to establish, on the basis of impedance measurements, that the relation between field and current in a superconductor is not a differential one. We should, incidentally, qualify what has just been said by pointing out that we have been talking up to now of an isotropic body; if there is anisotropy, i.e., no equivalence between the x and y axes, the question of the possibility of characterizing the field in the metal by some tensor ϵ'_{ik} can be decided by investigating the dependence of $Z(\omega)$ on the angle between the crystal axis and the field (see Pippard[11]). Because of this, experiments on anisotropic specimens at high frequencies (e.g., tin), are particularly important, as has already been mentioned in Sec. 1.

We shall now discuss some general properties of the functions $Z(\omega)$ and $\epsilon'_{\text{eff}}(\omega)$. It can be shown that the quantities $Z(\omega)$ and $\epsilon'_{\text{eff}}(\omega)$, considered as functions of a complex variable ω, have neither poles nor zeros in the lower half-plane (the time dependence is determined by the factor $e^{i\omega t}$) or on the real axis, with the exception, perhaps, only of the point $\omega = 0$. We shall not here discuss the proof of this statement, which follows essentially from the requirement of satisfying the principle of causality, particularly as it has recently been discussed by the author elsewhere[20] (see also reference 17, Sec. 83).

In the static case, for superconductors $[E_{x,y}]_0 = 0$ and consequently $Z(0) = 0$; for nonsuperconductors the quantity $Z(0)$ is likewise finite. Thus the function $Z(\omega)$ has no poles along the whole real axis and below it; hence,

$$\oint_L \frac{Z(\omega') - Z(\infty)}{\omega' - \omega}\,d\omega' = 0, \tag{13}$$

in particular, if the closed contour L is made up of the real axis and the path along a semicircle below the point $\omega' = \omega$ (where ω is some real frequency) and an infinite lower semicircle. The integral around the infinite semicircle vanishes, and consequently (13) can be written in the form

$$i\pi\{Z(\omega) - Z(\infty)\} + \int_{-\infty}^{+\infty} \frac{Z(\omega') - Z(\infty)}{\omega' - \omega}\,d\omega' = 0, \tag{14}$$

---

* Under condition (11) we have, for any angle of incidence of the wave on the surface

$$Z(\omega) = (4\pi/c)[E_x/H_y]_0 = -(4\pi/c)[E_y/H_x]_0.$$

[18] V. L. Ginzburg and G. P. Motulevich, Usp. Fiz. Nauk **55**, 469 (1955).

[19] A. A. Galkin and M. I. Kaganov, J. Exper. Theoret. Phys. USSR **25**, 761 (1953).

[20] V. L. Ginzburg, Akust. Zh. **1**, 31 (1955).

where, as in all that follows, the principal value of the integral should be understood. Further, from the requirements that $[H_{x,y}]_0$ should be real for $[E_{x,y}]_0$ real, it follows that on the real axis $Z(-\omega) = Z^*(\omega)$, i.e., $R(-\omega) = R(\omega)$ and $X(-\omega) = -X(\omega)$. Thus, if we separate (14) into its real and imaginary parts we obtain without difficulty

$$R(\omega) - R(\infty) = -\frac{2}{\pi}\int_0^\infty \frac{\omega'[X(\omega') - X(\infty)]}{\omega'^2 - \omega^2}\,d\omega', \tag{15}$$

$$X(\omega) - X(\infty) = \frac{2\omega}{\pi}\int_0^\infty \frac{[R(\omega') - R(\infty)]}{\omega'^2 - \omega^2}\,d\omega'.$$

For $\omega \to \infty$, the metal has no effect on the propagation of the wave, and consequently $X(\infty) = 0$ and $R(\infty) = 4\pi/c$. However, the transition to the limit of very high frequencies must be considered with some care in view of the limited applicability of the formulas for surface impedance[20]. In this connection we note that the equation $X(\infty) = 0$ follows directly from the second of the equations (15) and the fact that $X(0) = 0$. Moreover, the value of $R(\infty)$ is of little importance, since in the second of the equations (15), $\int_0^\infty \frac{R(\infty)}{\omega'^2 - \omega^2}\,d\omega' = 0$ (the integral to be taken as the principal value), so that $R(\infty)$ does not really enter, while in the first of the equations (15), $R(\infty)$ can be elimiated by taking the difference of the expression for two frequencies. Thus,

$$R(\omega_2) - R(\omega_1) = -\frac{2}{\pi}\int_0^\infty \left\{\frac{1}{\omega'^2 - \omega_2^2} - \frac{1}{\omega'^2 - \omega_1^2}\right\} X(\omega')\,\omega'\,d\omega', \tag{16}$$

$$X(\omega) = \frac{2\omega}{\pi}\int_0^\infty \frac{R(\omega')\,d\omega'}{\omega'^2 - \omega^2}.$$

The second of these relations is particularly useful for quantitative estimates, since the quantity $R(\omega)$ is easier to measure, and moreover is always positive. This is evident from the fact that R is directly connected with the heat developed in the metal

$$Q = (c/4\pi)^2\,|H_0|^2\,R/2, \tag{17}$$

where Q is the mean quantity of heat developed per unit time per unit area of the metal surface (the metal specimen is considered as sufficiently thick to absorb the wave completely) and H_0 is the amplitude of the high-frequency magnetic field at the surface ($[H]_0 = H_0 e^{i\omega t}$).

If we introduce resistive and reactive skin-depths $\delta_r(\omega)$ and $\delta_0(\omega)$ in the usual way, defined by

$$R(\omega) = (2\pi\omega/c^2)\,\delta_r(\omega), \qquad X(\omega) = (4\pi\omega/c^2)\,\delta_0(\omega), \tag{18}$$

then, for instance, the second of the equations (18) may be rewritten in the form

$$\delta_0(\omega) = \frac{1}{\pi}\int_0^\infty \frac{\omega'\delta_r(\omega')\,d\omega'}{\omega'^2 - \omega^2}. \tag{19}$$

To improve the convergence of the integral in the region of high frequency (in this connection see reference 20) it is appropriate to determine not the quantity $\delta_0(\omega)$ itself, but the difference $\delta_0(\omega_2) - \delta_0(\omega_1)$, in terms of $\delta_r(\omega')$, or, in particular, the difference:

$$\delta_0(\omega) - \delta_0(0) = \frac{1}{\pi}\int_0^\infty \left\{\frac{1}{\omega'^2 - \omega^2} - \frac{1}{\omega'^2}\right\}\delta_r(\omega')\,\omega'\,d\omega', \tag{20}$$

where $\delta_0(0) \equiv \delta_0$ is the penetration depth of a weak static magnetic field as used in Sec. 1. Equation (20) was given earlier by Pippard[11], and used successfully by him for estimating the dependence of δ_0 on ω.

It is also useful to obtain formulas analogous to those given for the quantity $\epsilon'_{\mathrm{eff}}(\omega)$. According to (12)

$$R^2 = \frac{8\pi^2}{c^2}\,\frac{\varepsilon_{\mathrm{eff}} + \sqrt{\varepsilon_{\mathrm{eff}}^2 + (4\pi\sigma_{\mathrm{eff}}/\omega)^2}}{\left[\varepsilon_{\mathrm{eff}}^2 + (4\pi\sigma_{\mathrm{eff}}/\omega)^2\right]},$$

$$X^2 = \frac{8\pi^2}{c^2}\,\frac{-\varepsilon_{\mathrm{eff}} + \sqrt{\varepsilon_{\mathrm{eff}}^2 + (4\pi\sigma_{\mathrm{eff}}/\omega)^2}}{\left[\varepsilon_{\mathrm{eff}}^2 + (4\pi\sigma_{\mathrm{eff}}/\omega)\right]} \tag{21}$$

$$\varepsilon_{\mathrm{eff}} = -\frac{16\pi^2}{c^2}\,\frac{X^2 - R^2}{(X^2 + R^2)^2}, \qquad \sigma_{\mathrm{eff}} = \frac{8\pi\omega}{c^2}\,\frac{XR}{(R^2 + X^2)^2},$$

where the root must always be taken as positive. For $\omega \to 0$, the penetration depth of the field into the superconductor is given by $\delta_0(\omega) \to \delta_0(0) \equiv \delta_0$ and is finite; consequently, $X(\omega) = \text{const}\ \omega$. Further, the quantity σ_{eff} for $\omega \to 0$ is certainly finite; (the static conductivity $\sigma(0)$ is finite; σ_{eff} in the theory of the anomalous skin effect is also finite, and finally because the function $\sigma_{\text{eff}}(\omega)$ is even, σ_{eff} would vary as ω^{-2} if it had a pole, and thus would lead to $X \sim \omega^{3/2}$ instead of $X \sim \omega$). From this and from (21) it is clear that $\epsilon_{\text{eff}} = -\omega_s^2/\omega^2$, $R = \text{const} \cdot \omega^2$ and

$$\varepsilon'_{\text{eff}} = -\omega_s^2/\omega^2 \equiv -c^2/\delta_0^2\omega^2 \ \ (\text{for} \ \ \omega \to 0), \tag{22}$$

if we consider only the leading term.

It should be noted that if the differential relation (1) is valid for an alternating field (for $T \to 0$, and before the onset of quantum absorption) we have

$$\varepsilon'_{\text{eff}} = \varepsilon' = \varepsilon = \varepsilon_0(\omega) - \frac{4\pi e^2 n_s}{m\omega^2} \equiv \varepsilon_0(\omega) - \frac{c^2}{\delta_0^2\omega^2}, \tag{23}$$

where $\epsilon_0(\omega)$ is the part of ϵ not connected with the superconducting electrons (for further details, see references 2 and 21). Equation (23) is of course consistent with (22).

The presence of a pole proportional to ω^{-2} distinguishes a superconductor from normal conductors for which $\epsilon' = \epsilon - i4\pi\sigma/\omega$, where $\epsilon(0)$ and $\sigma(0)$ are finite. It is just because of this that the proof given below and the corresponding equations are somewhat different from those ordinarily used for nonsuperconductors (see, for instance, reference 17, Sec. 83, and reference 20).

Bearing in mind what has been said, we see that the integral

$$\oint \frac{\omega' \{\varepsilon'_{\text{eff}}(\omega') - \varepsilon'_{\text{eff}}(\infty)\}\, d\omega'}{\omega' - \omega} = 0$$

taken along the same contour as in (13), but with an additional detour around the semicircle below the point $\omega' = 0$, vanishes. Proceeding just as we did in going from (13) to (15), we obtain

$$\varepsilon_{\text{eff}}(\omega) = 1 - \frac{\omega_s^2}{\omega^2} + \frac{2}{\pi}\int_0^\infty \frac{\omega'\varepsilon'_{2\text{eff}}(\omega')\, d\omega'}{\omega'^2 - \omega^2}$$

$$\equiv 1 - \frac{\omega_s^2}{\omega^2} + 8\int_0^\infty \frac{\sigma_{\text{eff}}(\omega')\, d\omega'}{\omega'^2 - \omega^2}, \tag{24}$$

$$\sigma_{\text{eff}}(\omega) = -\frac{1}{2\pi^2}\int_0^\infty \frac{\omega'^2\{\varepsilon_{\text{eff}}(\omega') - 1\}\, d\omega'}{\omega'^2 - \omega^2} \tag{25}$$

$$= -\frac{\omega^2}{2\pi^2}\int_0^\infty \frac{\varepsilon_{\text{eff}}(\omega') - 1}{\omega'^2 - \omega^2}\, d\omega'$$

$$-\frac{1}{2\pi^2}\int_0^\infty \{\varepsilon_{\text{eff}}(\omega') - 1\}\, d\omega',$$

where we have also taken into account that along the real axis $\epsilon'_{\text{eff}}(-\omega) = \epsilon^*_{\text{eff}}(\omega)$ and that $\epsilon'_{\text{eff}}(\infty) = 1$ (vacuum). Equations (24) and (25) are valid of course for any medium. In the nonsuperconducting state, where $\epsilon_{\text{eff}}(\omega)$ has no singularity at $\omega = 0$, we have from (25)

$$\sigma_{\text{eff}}(0) = -\frac{1}{2\pi^2}\int_0^\infty [\varepsilon_{\text{eff}}(\omega') - 1]\, d\omega' \tag{26}$$

Where it is possible to introduce the quantity $\epsilon'(\omega)$ for all frequencies, (24) and (25) give the relation between $\epsilon(\omega)$ and $\sigma(\omega)$. It has already been pointed out that $R(\omega)$ is always positive; for the same reason $\sigma(\omega)$ is always positive and therefore, as is clear from (10), in the region where we can make use of the concept ϵ', $X(\omega) > 0$. From the meaning of the quantities $X(\omega)$ and $\delta_0 = c^2X/4\pi\omega$ [22], we must suppose that for a plane metallic surface $X(\omega) > 0$ and consequently, $\sigma_{\text{eff}}(\omega) > 0$ [see Eq. (21)].

In the infra-red part of the spectrum, at least for metals such as Ag, Au and Cu, there is a region in which

$$\varepsilon'_{\text{eff}} \approx \varepsilon \approx -4\pi e^2 n_0/m\omega^2 = -\omega_0^2/\omega^2, \tag{27}$$

where n_0 is by definition the concentration of free electrons in the metal (see references 2, 18, where

---

[21] V. L. Ginzburg, J. Exper. Theoret. Phys. USSR **21**, 979 (1951).

[22] E. Maxwell, P. W. Marcus and J. C. Slater, Phys. Rev. **76**, 1332 (1949).

n_0 is denoted by N). Unfortunately, it has not been strictly established for any superconductor whether a region exists in which (27) holds sufficiently accurately, but this is very probable and will be assumed in what follows.

According to the available data (which need improvement), we have, from optical measurements, $n_0 = 6 \times 10^{22}$ for tin[2,18], while the estimate from (17) (based on reference 21) gives $n_0 = 2.7 \times 10^{22}$ for tin, and this estimate is if anything, too low.

Comparing (27) and (24), where it is sufficiently accurate to neglect unity, we obtain the summation rule *,

$$n_0 = n_s + \int_0^\infty n_c(\omega')\,d\omega'; \qquad (28)$$

$$n_c(\omega) = 2m\sigma_{\text{eff}}(\omega)/\pi e^2,$$

since $\omega_0^2 = 4\pi e^2 n_0/m$ and $\omega_s^2 = 4\pi e^2 n_s/m$ (to avoid a frequently occurring misconception, we emphasize again that everywhere above e and m are by definition just the charge and mass of the free electron). Equation (28), like all the other equations obtained, is valid for any temperature T; n_0 is practically independent of temperature, while $n_s = 2.83 \times 10^{11}\delta_0^{-2}$ [see Eq. (5)] and varies in such a way that for $T = T_k$, $n_s = 0$, while for $T = 0$, n_s has its maximum value n_{s0}. For tin, for $T \to 0, \delta_0 \sim 5 \times 10^{-6}$ and $n_{s0} \sim 1.1 \times 10^{22}$ (the use of alternative data leads to an even smaller value of n_{s0}). Thus, according to all the available data, $n_{s0} < n_0$, from which it follows that for $T \to 0$ and for sufficiently low frequencies, where absorption is absent, part of the free electrons becomes superconducting and part goes into some kind of bound state. From this evident limitation and lack of foundation of the so-called "two-fluid model" of superconductors become clear (see, for instance, reference 15, p. 194).

3. BEHAVIOR OF SUPERCONDUCTORS IN HIGH-FREQUENCY FIELDS (CALCULATION OF SURFACE IMPEDANCE)

In the general case, taking account of (24), we may write

$$\varepsilon'_{\text{eff}}(\omega) = \varepsilon_c(\omega) - (\omega_s^2/\omega^2) - 4\pi i\sigma_{\text{eff}}(\omega)/\omega \qquad (29)$$

$$\varepsilon_c(\omega) = 1 + 8\int_0^\infty \frac{\sigma_{\text{eff}}(\omega')}{\omega'^2 - \omega^2}\,d\omega' .$$

For $T \to 0$, and not too high frequencies, $R \to 0$ and consequently, $\sigma_{\text{eff}} \to 0$. In this case (29) coincides with (23), obtained from (1), but with the difference that according to (23), the field in the metal decays exponentially, (since $\epsilon'_{\text{eff}} = \epsilon'$), while nothing can be said about the law of decay from (29). If the considerations pointing to the validity of (1) in a static field are indeed correct (see Sec. 1), then for frequencies such that $\sigma_{\text{eff}} \to 0$ for $T \to 0$, it is justified to apply (1) and (23) (this follows in particular from the fact that $\delta_0(\omega)$ changes very little in comparison with δ_0 right up to frequencies of order 10^{10} (see reference 11). With increasing frequency, absorption must set in, analogous to the inner photo-effect (we shall call this "quantum absorption") and we should expect that the threshold frequency, ω_k, for quantum absorption should be given by

$$\omega_k \sim kT_k/\hbar \sim 10^{11} \text{ to } 10^{12}; \qquad (30)$$

$$\lambda_k = 2\pi c/\omega_k \sim 0.1 \text{ to } 1 \text{ cm}$$

For tin, according to Fawcett[23], $\lambda_k < 0.83$ cm. There are unfortunately no measurements in the region of shorter waves or for other metals in spite of the fact that such experiments are possible, and their importance was emphasized more

---

* Actually in (28) the upper limit should not be infinity but of the order of the maximum frequency for which (27) is still valid. It is supposed, however, as is usually valid, that to the accuracy with which we are working, it is permissable to replace the finite limit by infinity.

[23] E. Fawcett, Proc. Phys. Soc. (London) **66A**, 1071 (1953).

than 10 years ago[24]. For $T > 0$, $\sigma_{\rm eff} > 0$ even for $\omega < \omega_k$, on account of the appearance in the superconductor of "normal" electrons (excitations), so that for $T \to T_k$, $\sigma_{\rm eff} \to \sigma_{{\rm eff}n}$, where $\sigma_{{\rm eff}n}$ is the effective conductivity in the normal state. The "normal" electrons in the superconductor also make their contribution to $\epsilon_c(\omega)$, and it is convenient to write (though this has a rather formal character)

$$\varepsilon_c(\omega) = \varepsilon_0(\omega) + \varepsilon_n(\omega), \tag{31}$$

where ϵ_n is the contribution to ϵ_c from the "normal" electrons*, and ϵ_0 is the contribution of the "bound" electrons. For $T \to 0$ and $\omega < \omega_k$, $\epsilon_n(\omega) \to 0$, while ϵ_0 for $\omega \ll \omega_k$ is constant and may be estimated with the help of (28):

$$\varepsilon_0(\omega) \approx 8 \int_0^\infty \frac{\sigma_{\rm eff}(\omega')\,d\omega'}{\omega'^2 - \omega^2} \tag{32}$$

$$= \frac{4\pi e^2}{m} \int_0^\infty \frac{n_c(\omega')\,d\omega'}{\omega'^2 - \omega^2} \sim \frac{4\pi e^2 (n_0 - n_{s0})}{m\omega_k^2}$$

$$\sim \frac{4\pi e^2 n_0}{m\omega_k^2} \sim \frac{4\pi e^2 n_0}{m\,(kT_k/\hbar)^2} \sim 10^8 \text{ to } 10^{10}.$$

For $\omega \sim \omega_k$ the dependence of ϵ_0 on ω must already be appreciable. The estimate (32) coincides, as is to be expected, with that given in reference 2; the nature of the estimate is such that even the value $\epsilon_0 \sim 10^7$ would not apparently be contradictory. From the experimental data[19,22] for tin it is probably possible to deduce only that for $\lambda \sim 1$ cm, $\epsilon_0 \ll \omega_s^2/\omega^2 \sim 10^9$; a value $\epsilon_0 \sim 10^8$ is quite compatible with (32) and with this estimate. For $T \to T_k$, ϵ_0 and ϵ_n tend to their respective values in the normal state, where $\epsilon_0 \sim 1$.

It is natural to try to calculate the quantities $\epsilon_n(\omega)$ and $\sigma_{\rm eff}(\omega)$ connected with the "normal" electrons in the same way as is done in the theory of the anomalous skin-effect in metals in the normal state[25,26]. We need only consider the case of the extreme anomalous skin-effect, where the mean free path is much greater than the skin depth ($l \gg \delta$). Under these conditions the calculation of Z for superconductors has been carried out both on the basis of the kinetic equations for the normal electrons[22,27], and on the basis[2,21] of the simpler "ineffectiveness concept"[26] which is essentially of a dimensional character. Although they are more complicated, the calculations[22,27] are more consistent with the model assumed (free electrons in a medium with $\epsilon = \epsilon_0 - c^2/\delta_0^2\omega^2$). On the other hand this model itself, in its application to the "normal" electrons in a superconductor, is completely without foundation, particularly if we take account of the possibility of quantum absorption, which for $T > 0$ may take place even for $\omega < \omega_k$ *. In this connection the calculations in reference 21 are to be preferred, as being less tied to a particular model. In general it can be said that reliable calculations of Z or $\epsilon_{\rm eff}$ in superconductors are not yet possible, and it is therefore useful to carry out the calculations by a variety of methods. From comparison of the results it is possible to assess to a certain extent how reliable the calculations are. In the simplest, and therefore most convenient variant of the calculations, using the method of dimensions, it is assumed[21] that

---

* To avoid misunderstanding we must point out that in references 2 and 21 and in a number of other papers, the whole contribution of the "normal" electrons is included in $\sigma_{\rm eff}$, which is a complex quantity (in the present paper $\sigma_{\rm eff}$ is real). It is evident that $-4\pi i\sigma_{\rm eff}/\omega$ in references 2 and 21 is equal to $\epsilon_n - 4\pi i\sigma_{\rm eff}/\omega$ in the notation of the present paper [see Eqs. (29) and (31)].

[24] V. L. Ginzburg, J. Exper. Theoret. Phys. USSR **14**, 134 (1944).

* For quantum absorption in a particular range of frequencies the relevant part of $\sigma_{\rm eff}$ is presumably σ_k, where σ_k is a quantity analogous to the ordinary conductivity. In this case $\sigma_{\rm eff} = \sigma_k + \sigma'_{\rm eff}$ where $\sigma'_{\rm eff}$ is an effective conductivity connected with the normal electrons, which in the region of the anomalous skin-effect is completely different from the "ordinary" (static) conductivity of the "normal" electrons [see Eq. (33)].

[25] G. Reuter and E. H. Sondheimer, Proc. Roy. Soc. (London) **195A**, 336 (1948); E. H. Sondheimer, Proc. Roy. Soc. (London) **224A**, 260 (1954).

[26] A. B. Pippard, Proc. Roy. Soc. (London) **191A**, 385, 399 (1947); **224A**, 273 (1954).

[27] A. A. Abrikosov, Dokl. Akad. Nauk SSSR **86**, 43 (1952).

$$\varepsilon'_{\text{eff}} = \varepsilon_s - i\,\frac{4\pi\sigma}{\omega}\,\frac{2\pi}{\sqrt{3}}\,\frac{\delta'}{l}, \qquad (33)$$

$$\delta' = -\frac{ic}{\omega\sqrt{\varepsilon'_{\text{eff}}}},$$

$$\varepsilon_s = \varepsilon_0 - \frac{c^2}{\delta_0^2\omega^2},$$

where l is the mean free path and σ the static conductivity of the "normal" electrons in the superconductor (this means that for normal skin-effect conditions the normal current density in the superconductor would be $j_n = \sigma E$). The conductivity due to quantum absorption is of course not taken into account in (33). From (33) it follows that the quantity $y = \sqrt{\epsilon'_{\text{eff}}} = 4\pi/cZ$ is determined by the equation

$$y^3 - \varepsilon_s y + 8\pi^2 c\sigma/\sqrt{3}\omega^2 l = 0.$$

Hence, as was shown in reference 8, we have

$$\varepsilon_s \equiv \varepsilon_0 - \frac{c^2}{\delta_0^2\omega^2} = -\frac{16\pi^2}{c^2}\,\frac{(X^2-3R^2)}{(X^2+R^2)^2}, \qquad (34)$$

$$\sigma/l = (16\pi\omega^2/c^4)\sqrt{3}R\,(X^2+R^2)^{-2}.$$

The coefficient in front of δ'/l in (33) is chosen so that in the normal state (for $\epsilon_s \to 0$) we should have

$$Z = Z_n = (\sqrt{3}\pi\omega^2 l/c^4\sigma)^{1/3} \qquad (35)$$

$$\times\,(1+\sqrt{3}i);\ X = \sqrt{3}R,$$

i.e., so that the relation should apply which is obtained in the more rigorous theory (for the normal state) for diffuse reflection of the electrons at the surface.

With the same assumption, the kinetic calculation[27] gives

$$\varepsilon_s = \varepsilon_0 - c^2/\delta_0^2\omega^2 \qquad (36)$$

$$= -(4\pi^2/c^2)\,X^2(X^2+R^2)^{-2}(3-\eta),$$

$$\sigma/l = (16\pi\omega^2/3c^4)\cdot X^3(X^2+R^2)^{-3}(1+\eta),$$

$$R/X = \frac{1}{2\pi}\left[2\sqrt{\eta}\tan^{-1}\sqrt{\eta} - \ln\left(\frac{1+\eta}{4}\right)\right],$$

where for $\eta < 0$ we must replace $\sqrt{\eta}\tan^{-1}\sqrt{\eta}$ by $-\sqrt{|\eta|}\tanh^{-1}\sqrt{|\eta|}$; a graph of the function $\eta(R/X)$ is given by Abrikosov[27]. For $\eta = 3$, it is evident that $\epsilon_s = 0$, and (36) goes over into (35) just as does (34): for $\eta = -1$ and $\epsilon_s < 0$ we have $\sigma = 0$ and $\epsilon_s = -16\pi^2/c^2X^2$; this last result follows directly from (34) for $\sigma = 0$*. To facilitate comparison between (34) and (36) it is convenient to express them in the forms:

$$\varepsilon_s = -16\pi^2 c^{-2}X^{-2}\varphi_1(R/X), \qquad (34a)$$

$$\sigma/l = 16\sqrt{3}\pi\omega^2 c^{-4}X^{-3}f_1(R/X),$$

$$\varepsilon_s = -16\pi^2 c^{-2}X^{-2}\varphi_2(R/X), \qquad (36a)$$

$$\sigma/l = 16\sqrt{3}\pi\omega^2 c^{-4}X^{-3}f_2(R/X),$$

where the form of the functions $\varphi_{1,2}$ and $f_{1,2}$ is evident from comparison with (34) and (36). These functions are plotted in Figs. 1 and 2 (the points $R/X = 0$ and $R/X = 1/\sqrt{3} = 0.58$ correspond to $T = 0$ and $T = T_k$), and it can be seen that the differences between (34) and (36) are not large and indeed probably within the precision which either formula can claim (except possibly in the regions close to $T = T_k$ and $T = 0$ where φ_1, φ_2 and f_1, f_2, respectively, approach zero). From the point of view of the microtheory of superconductivity, the

---

* Equation (33) is valid only if the wave decays rapidly as one goes into the metal, so that for $\sigma = 0$ it is necessary that $R = 0$ and $\epsilon_s < 0$; in the case of (36), for $\sigma = 0$ and $\epsilon_s > 0$, $\eta \to \infty$, $X = 0$ and $R = 4\pi/c\sqrt{\epsilon_s}$, which corresponds to a transparent body. As is clear from (34), for instance, ϵ_s can in principle change sign. At the point where $\epsilon_s = 0$, $X = \sqrt{3}R$ and if $\omega < \omega_k$ the superconductor becomes transparent. In all probability, the frequency ω_0 for which $\epsilon_s = 0$ is greater than ω_k, so that transparency does not occur (in this connection it is important that in the relevant frequency range ϵ_0 may depend appreciably on ω). The introduction of a universal impedance is possible only if $|\epsilon'_{\text{eff}}| \gg 1$, and consequently the region close to the point $\epsilon_s = 0$ requires special consideration if σ_{eff} is close to zero. Generally speaking, the formulas given above are not valid in this region, but their use for deciding the question of the existence of this region is quite permissable.

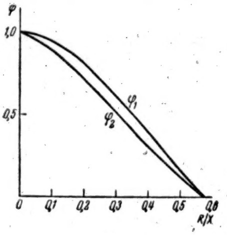

FIG. 1

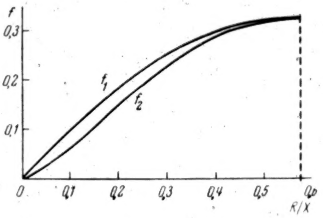

FIG. 2

most interesting feature is the value of $\epsilon_s(\omega)$ at low temperatures; this can be determined from measurements of $X(\omega)$ (R has only secondary importance in the determination of ϵ_s, since in the region concerned $R^2/X^2 \ll 1$ for $\omega < \omega_k$ and, for instance, $\varphi_1 = 1 - 5(R/X)^2$. In this region, we have from (34) $\sigma/l = 16\sqrt{3} \times \pi\omega^2 c^{-4} X^{-4} R \simeq \sqrt{3}\omega^2\epsilon_s^2 R/16\pi^3$, so by measuring R (calorimetrically, for instance), we can find σ/l*, using the static value of δ_0 (which is permissible as long as $|\epsilon_s| \gg \epsilon_0$). The accuracy of such a determination cannot of course exceed that of the formulas (34) and (36) themselves. We shall not discuss here the question of the measurement of Z for superconducting films (see references 8 and 21).

In conclusion, we should like once more to emphasize the importance, from the point of view of studying superconductivity, of optical measurements of n_0 [see (27)] and measurements of $\epsilon'_{\text{eff}}(\omega)$ in the region of centimeter and millimeter waves for various superconductors.

Translated by D. Shoenberg
269

---

* In the region $\epsilon_s = -c^2/\delta_0\omega^2$, it follows from the relation given for σ/l and (35) that $R/R_n \sim \delta_0^2\omega^{4/3}$. According to Galkin and Bezuglyi[28], just such a dependence is found in tin for $\omega < 3 \times 10^{11}$. A deviation from this dependence, within the framework of the approximation used, would indicate an influence of the term ϵ_0 in the expression $\epsilon_s = \epsilon_0 - (c/\delta_0\omega)^2$.

[28] A. A. Galkin and P. A. Bezuglyi, Dokl. Akad. Nauk SSSR **97**, 217 (1954).

SOVIET PHYSICS JETP VOLUME 2, NUMBER 4 JULY, 1956

The Strong Coupling Theory of Meson Fields. II

B. T. GEILIKMAN
Moscow State Teachers' Institute

(Submitted to JETP editor June 17, 1954)
J. Exper. Theoret. Phys. USSR **29**, 430-438 (October, 1955)

In an earlier paper the problem of nucleons interacting with a meson field has been treated by perturbation theory, using as the expansion parameter the reciprocal coupling constant. On that basis in the present paper the interaction of two nucleons, the scattering of mesons from nucleons, and the bound states of mesons are calculated for the case of the infinitely heavy nucleons.

1. IN a previous paper[1] the theory of a meson field interacting with infinitely heavy nucleons has been treated by perturbation theory using the inverse coupling constant as the expansion parameter. We shall here be concerned with the solution of the equations of the zeroth and first approximations.

We first shall obtain the solutions of the zero order approximation, Eq. (14) in I (notation the same as in I):

$$\left\{\frac{g^2}{2}\int\sum_{\alpha}^{3}[|O_\alpha(\mathbf{r})|_{\lambda\lambda}-2O_\alpha(\mathbf{r})] \times |O_\alpha(\mathbf{r}')|_{\lambda\lambda}G(\mathbf{r},\mathbf{r}')\,d\mathbf{r}\,d\mathbf{r}'\right\}\psi_\mu^0=E_\mu^0\psi_\mu^0; \tag{1}$$

which describes a neutral pseudoscalar, a charged scalar or a charged pseudoscalar field interacting with one nucleon.

For the first case (1) has the form

$$[A+(\mathbf{B},\vec{\sigma})]\psi_\mu^0=E_\mu^0\psi_\mu^0;$$

$$A=\frac{I_p}{2}(\vec{\eta})^2;\quad \mathbf{B}=-I_p\vec{\eta};$$

$$I_p=\frac{g^2}{\varkappa^2}\int\frac{\partial^2G(\mathbf{r},\mathbf{r}')}{\partial x\,\partial x'}U(\mathbf{r})\,U(\mathbf{r}')\,d\mathbf{r}\,d\mathbf{r}'\approx\frac{g^2}{\varkappa^2a^3};$$

$$\vec{\eta}=\{\vec{\sigma}\}_{\lambda\lambda}.$$

We shall now introduce a coordinate system $\bar{x}$, $\bar{y}$, $\bar{z}$ such that $\bar{z}$ is parallel to $\vec{\eta}$ (the angle between $\bar{z}$ and $\vec{\eta}$ is zero or π). Then $\eta_{\bar{x}}=\eta_{\bar{y}}=0$ and (1) becomes

$$(A+B_{\bar{z}}\,\sigma_{\bar{z}})\,\psi_\mu^0=E_\mu^0\psi_\mu^0,\quad |B_{\bar{z}}|=B. \tag{2}$$

The Hamiltonian H^0 can be diagonalized also by the known unitary transformation[2]

$$\Lambda=\begin{vmatrix}\cos\frac{\vartheta}{2}e^{-i[(\alpha/2)-(\pi/4)]} & i\sin\frac{\vartheta}{2}e^{-i[(\alpha/2)-(\pi/4)]}\\ i\sin\frac{\vartheta}{2}e^{i[(\alpha/2)-(\pi/4)]} & \cos\frac{\vartheta}{2}e^{i[(\alpha/2)-(\pi/4)]}\end{vmatrix};\quad \vartheta=\arccos\frac{\eta_z}{\eta},\quad \alpha=\operatorname{arctg}\frac{\eta_y}{\eta_x}.$$

The eigenvalues of (2) are: $E_1^0=A+B_{\bar{z}}$; $E_2^0=A-B_{\bar{z}}$. In the first case we obtain from

$$\eta_\alpha=(\psi_{\lambda\lambda}^{0*}(s,\eta_\alpha),\ \sigma_\alpha\psi_{\lambda\lambda}^0(s,\eta_\alpha)) \tag{3}$$

[see Eq. (15) in I] for $\lambda=1$, $\eta_{\bar{z}}^{(1)}=1$; for $\lambda=2$, $\eta_{\bar{z}}^{(2)}=-1$. The Hamiltonians H_1^0 and H_2^0 and their respective eigenvalues are

$$H_1^0=I_p\left(\frac{1}{2}-\sigma_{\bar{z}}\right);\quad \psi_{11}^0=\begin{vmatrix}1\\0\end{vmatrix};\quad \psi_{12}^0=\begin{vmatrix}0\\1\end{vmatrix};$$

$$E_{11}^0\equiv E_1^0=-\frac{I_p}{2};\quad E_{12}^0=\frac{3}{2}I_p.$$

$$H_2^0=I_p\left(\frac{1}{2}+\sigma_{\bar{z}}\right);\quad \psi_{22}^0=\begin{vmatrix}0\\1\end{vmatrix};\quad \psi_{21}^0=\begin{vmatrix}1\\0\end{vmatrix};$$

$$E_{22}^0=-\frac{I_p}{2};\quad E_{21}^0=\frac{3}{2}I_p.$$

---

[1] B. T. Geilikman, J. Exper. Theoret. Phys. USSR **29**, 417 (1955); hereinafter quoted as I.

[2] L. de Broglie, *L'électron magnétique*, Paris, 1934, p. 127.

In the case $H_2^0 = A - I_p(\vec{\eta}, \vec{\sigma})$, clearly all directions in $\vec{\sigma}$ space are equivalent, and therefore the direction of $\vec{\eta}$, and therewith $\bar{z}$, is arbitrary. However, for any given direction of $\bar{z}$ the projections of $\vec{\eta}$ are well defined: for $\lambda = 1$, $\eta_{\bar{z}} = 1$; for $\lambda = 2$, $\eta_{\bar{z}} = -1$. This is similar to the case of the angular momentum vector **L** of a particle moving in a central field, where any frame of reference can be used, and therefore the direction of $|\mathbf{L}|_{nn}$ is also arbitrary. In fact, projecting **L** on the z-axis, we obtain $|\mathbf{L}_z|_{nn} = m\hbar$ and $|\mathbf{L}_x + i\mathbf{L}_y|_{nn}$ $= h \left| e^{i\varphi}\left(\frac{\partial}{\partial\vartheta} + i \operatorname{ctg}\vartheta \frac{\partial}{\partial\varphi}\right)\right|_{nn} = 0$; $|\mathbf{L}_x|_{nn}$ $= |\mathbf{L}_y|_{nn} = 0$, or, the vector $|\mathbf{L}|_{nn}$ is parallel to the z-axis. Despite the arbitrary direction of the z-axis the projections $|\mathbf{L}|_{nn}$ onto it are fully determined and correspond to a certain set of ψ-functions. The direction used for the projection does not enter into our expressions of the energy in any order of approximation in analogy to the case of a particle in a central field.

Similarly, in the case of a symmetric scalar field,

$$H^0 = A + (\mathbf{B}, \vec{\tau}); \quad A = \frac{I_s}{2}(\vec{\eta})^2;$$

$$\mathbf{B} = -I_s\vec{\eta}; \quad \vec{\eta} = \{\vec{\tau}\}_{\lambda\lambda};$$

$$I_s = g^2 \int G(\mathbf{r}, \mathbf{r}')\, U(\mathbf{r})\, U(\mathbf{r}')\, d\mathbf{r}\, d\mathbf{r}'; \quad I_s \approx g^2/a.$$

For the axis $\bar{z}$, parallel to $\vec{\eta}$, we find

$$H^0 = A + B_{\bar{z}}\tau_{\bar{z}}; \quad \eta_{\bar{x}} = \eta_{\bar{y}} = 0.$$

For $\lambda = 1$:

$$\eta_{\bar{z}}^{(1)} = 1; \; H_1^0 = I_s\left(\frac{1}{2} - \tau_{\bar{z}}\right); \quad \psi_{11}^0 = \begin{vmatrix} 1 \\ 0 \end{vmatrix};$$

$$\psi_{12}^0 = \begin{vmatrix} 0 \\ 1 \end{vmatrix}; \; E_{11}^0 = -\frac{I_s}{2}; \quad E_{12}^0 = \frac{3}{2} I_s.$$

For $\lambda = 2$:

$$\eta_{\bar{z}}^{(2)} = -1; \; H_2^0 = I_s\left(\frac{1}{2} + \tau_{\bar{z}}\right); \quad \psi_{22}^0 = \begin{vmatrix} 0 \\ 1 \end{vmatrix};$$

$$\psi_{21}^0 = \begin{vmatrix} 1 \\ 0 \end{vmatrix}; \quad E_{22}^0 = -\frac{I_s}{2}; \; E_{21}^0 = \frac{3}{2} I_s.$$

Actually, the direction of the $\bar{z}$-axis is determined by the experimental conditions, i.e., by a not-charge-invariant perturbation. Under usual circumstances the charge of a nucleon, i.e., τ_z, is well defined. Therefore, here $\vec{\eta}$ is parallel to the z-axis and the $\bar{z}$-axis coincides with the z-axis.

In the case of a nonsymmetric scalar field ($\tau_3 = \gamma_1 + \gamma_2\tau_z$), there exists a preferred direction in τ-space, namely the z-axis, and therefore the direction of the vector $\{\vec{\tau}\}_{\lambda\lambda}$ is not arbitrary, and $E_{11}^0 \neq E_{22}^0$ (the self energy of the proton and the neutron differ).

We shall now investigate the symmetric pseudoscalar field:

$$H^0 = A + \sum_{\alpha,k}^{3,3} B_{\alpha k}\tau_\alpha\sigma_k; \tag{4}$$

$$A = \frac{I_p}{2}\sum_{\alpha,k}^{3.3} \xi_{\alpha k}^2; \quad B_{\alpha k} = -I_p\xi_{\alpha k};$$

$$\xi_{\alpha k} = |\tau_\alpha\sigma_k|_{\lambda\lambda}.$$

We shall choose a system of coordinates in the $\vec{\tau}$ and $\vec{\sigma}$ space such that the matrix $\xi_{\alpha k}$ is diagonal[3,4]: $\xi_{\alpha k} = \xi_k\delta_{\alpha k}$. Then

$$H^0 = A + \sum_{k}^{3} B_{kk}\tau_k\sigma_k.$$

We now apply a unitary transformation to H^0:[3]

$$S = \frac{1}{\sqrt{2}}(\sigma_{\bar{x}} + i\tau_{\bar{y}}).$$

$$S^{-1}H^0S$$
$$= A - B_1\tau_{\bar{z}} - B_2\sigma_{\bar{z}} - B_3\tau_{\bar{z}}\sigma_{\bar{z}} \qquad (B_{kk} = B_k).$$

The eigenvalues are

$$E_1^0 = A - B_1 - B_2 - B_3;$$
$$E_2^0 = A + B_1 + B_2 - B_3;$$
$$E_3^0 = A - B_1 + B_2 + B_3;$$
$$E_4^0 = A + B_1 - B_2 + B_3.$$

According to Eqs. (3) and (15) of I we have, for $\lambda = 1$,

---

[3] G. Wentzel, Helv. Phys. Acta **16**, 551 (1943).

[4] W. Pauli and S. Dancoff, Phys. Rev. **62**, 85 (1942).

$$\xi_1^{(1)} = \xi_2^{(1)} = \xi_3^{(1)} = -1;$$

$$H_1^0 = I_p\left(\frac{3}{2} - \tau_{\bar z} - \sigma_{\bar z} - \tau_{\bar z}\,\sigma_{\bar z}\right);$$

$$\psi_{11}^0 = u_1;\ \psi_{12}^0 = u_2;$$

$$\psi_{13}^0 = u_3;\ \psi_{14}^0 = u_4,$$

with

$$u_1 = \begin{vmatrix}1\\0\\0\\0\end{vmatrix};\ u_2 = \begin{vmatrix}0\\1\\0\\0\end{vmatrix};\ u_3 = \begin{vmatrix}0\\0\\1\\0\end{vmatrix};\ u_4 = \begin{vmatrix}0\\0\\0\\1\end{vmatrix};$$

$$E_{11}^0 = -\frac{3}{2}I_p;\ E_{12}^0 = E_{13}^0 = E_{14}^0 = \frac{5}{2}I_p.$$

For $\lambda = 2$:

$$\xi_1^{(2)} = \xi_2^{(2)} = 1;\ \xi_3^{(2)} = -1;$$

$$H^0 = I_p\left(\frac{3}{2} + \tau_{\bar z} + \sigma_{\bar z} - \tau_{\bar z}\sigma_{\bar z}\right);$$

$$\psi_{22}^0 = u_4;\ \psi_{21}^0 = u_3;\ \psi_{23}^0 = u_2;$$

$$\psi_{24}^0 = u_1;\ E_{22}^0 = -\frac{3}{2}I_p;$$

$$E_{21}^0 = E_{23}^0 = E_{24}^0 = \frac{5}{2}I_p.$$

For $\lambda = 3$:

$$\xi_1^{(3)} = -1;\ \xi_2^{(3)} = \xi_3^{(3)} = 1;$$

$$H_3^0 = I_p\left(\frac{3}{2} - \tau_{\bar z} + \sigma_{\bar z} + \tau_{\bar z}\sigma_{\bar z}\right);$$

$$\psi_{33}^0 = u_2;\ \psi_{31}^0 = u_1;\ \psi_{32}^0 = u_3;$$

$$\psi_{34}^0 = u_4;\ E_{33}^0 = -\frac{3}{2}I_p;$$

$$E_{31}^0 = E_{32}^0 = E_{34}^0 = \frac{5}{2}I_p.$$

For $\lambda = 4$:

$$\xi_1^{(4)} = \xi_3^{(4)} = 1;\ \xi_2^{(4)} = -1;$$

$$H_4^0 = I_p\left(\frac{3}{2} + \tau_{\bar z} - \sigma_{\bar z} + \tau_{\bar z}\sigma_{\bar z}\right);$$

$$\psi_{44}^0 = u_3;\ \psi_{41}^0 = u_4;\ \psi_{42}^0 = u_2;\ \psi_{43}^0 = u_1;$$

$$E_{44}^0 = -\frac{3}{2}I_p;\ E_{41}^0 = E_{42}^0 = E_{43}^0 = \frac{5}{2}I_p.$$

Knowing $\psi_{\lambda\lambda}^0$ it is possible to find the diagonal matrix elements of the spin operators $\{\tau'_\alpha \vec{\sigma}'\}_{\lambda\lambda} = \{S^{-1}\tau_\alpha\vec{\sigma}\,S\}_{\lambda\lambda}$ which enter the expressions for the magnetic moments [Eq. (26) in I]. We then obtain for M_z in the zeroth approximation

$$M_z = -\left(\frac{g^2\alpha}{\hbar c}\frac{e}{\varkappa^2 a} + \frac{e\hbar}{4mc}\right)|\tau_{\bar z}\sigma_{\bar z}|_{\lambda\lambda}$$

$$= \mp\left(\frac{g^2\alpha}{\hbar c}\frac{e}{\varkappa^2 a} + \frac{e\hbar}{4mc}\right).$$

The magnetic moments of the proton and the neutron differ only in sign.

It may be noted that the field φ_α^0 is fully determined by the parameters η_α, η_k, $\xi_{\alpha k}$ which are found when solving Eq. (1), and that the η_α, $\xi_{\alpha k}$ differ for different λ. For example, in the case of a scalar symmetric field $\varphi_{\bar x}^0 = \varphi_{\bar y}^0 = 0$ for $\lambda = 1, 2$; $(\varphi_{\bar z}^0)_{\lambda=1} = \dfrac{g}{c\sqrt{4\pi}} \int G(\mathbf{r}, \mathbf{r}')\,U(\mathbf{r}')\,d\mathbf{r}'$; $(\varphi_{\bar z}^0)_{\lambda=2} = -(\varphi_{\bar z}^0)_{\lambda=1}$. As a result of the fact that φ_α^0 is fully determined by solving the equations of the zeroth order, the character of the fields φ_α is purely oscillatory in all its degrees of freedom (the Hamiltonian $H_{\lambda 2}$ splits into a sum of harmonic oscillator Hamiltonians). This is not so in the theory of molecules (see I). Since the electronic energy $E_m^0(\mathbf{R}_i)$ depends only on the distance between the nucleon positions, $|\mathbf{R}_i - \mathbf{R}_j|$, the minimizing of the energy yields only $3n - 6$ ($3n - 5$ for $n = 2$) relative distances. In these $3n - 6$ degrees of freedom the motion is oscillatory in character; the remainder are translatory (motion of the center of mass) and rotational (rotation of the molecule as a whole) in character.

In all three cases of symmetric coupling, the eigenvalues $E_{\lambda\lambda}^0$ are the same for the different λ as to be expected. This degeneracy disappears only in the higher approximations when real mesons appear. However, for a particular Hamiltonian H_λ^0 the eigenvalues $E_{\lambda\lambda}^0$ are not degenerate:

$E^0_{\lambda\mu} \neq E^0_{\lambda\lambda}$ for $\mu \neq \lambda$. A mathematical degeneracy is absent.

2. We shall now consider two nucleons interacting with a pseudoscalar neutral field. According to Eq. (30) of I the zero order Hamiltonian for this case is

$$H^0 = A + (\mathbf{B}_\mathrm{I}, \vec{\sigma}_\mathrm{I}) + (\mathbf{B}_\mathrm{II}, \vec{\sigma}_\mathrm{II}); \tag{5}$$

$$A = \frac{I_p}{2}[(\vec{\eta}_\mathrm{I})^2 + (\vec{\eta}_\mathrm{II})^2] + \frac{1}{2}\sum_{i,k}^{3,3} K_{ik}\,\eta_{\mathrm{I}i}\eta_{\mathrm{II}k};$$

$$B_{\mathrm{I}k} = -\eta_{\mathrm{I}k} I_p - \sum_l^3 \eta_{\mathrm{II}l} K_{kl};$$

$$B_{\mathrm{II}k} = -\eta_{\mathrm{II}k} I_p - \sum_l^3 \eta_{\mathrm{I}l} K_{lk};$$

$$\vec{\eta}_{\mathrm{I,II}} = \{\vec{\sigma}_{\mathrm{I,II}}\}_{\lambda\lambda};$$

$$K_{ik} = \frac{g^2}{\varkappa^2}\int U_\mathrm{I}(\mathbf{r} - \mathbf{r}_\mathrm{I})\, U_\mathrm{II}(\mathbf{r}' - \mathbf{r}_\mathrm{II})$$

$$\times \frac{\partial^2 G(\mathbf{r}, \mathbf{r}')}{\partial x_i \partial x'_k}\, d\mathbf{r}\, d\mathbf{r}' = \delta_{ik} K_1 + n_i n_k K_2;$$

$$\mathbf{n} = \frac{\mathbf{r}_\mathrm{II} - \mathbf{r}_\mathrm{I}}{r_\mathrm{I,II}} \equiv \frac{\mathbf{r}_\mathrm{I,II}}{r_\mathrm{I,II}};$$

For

$$\mathbf{r}_\mathrm{I,II} \gg a \quad K_1 \approx -\frac{g^2}{\varkappa^2}\frac{1}{r_\mathrm{I,II}}\frac{d}{dr_\mathrm{I,II}} G(\mathbf{r}_\mathrm{I}, \mathbf{r}_\mathrm{II});$$

$$K_2 \approx r_\mathrm{I,II}\frac{dK_1}{dr_\mathrm{I,II}}.$$

Therefore,

$$H^0 = \frac{I_p}{2}[(\vec{\eta}_\mathrm{I})^2 + (\vec{\eta}_\mathrm{II})^2] + K_1(\vec{\eta}_\mathrm{I}, \vec{\eta}_\mathrm{II})$$

$$+ K_2(\mathbf{n}, \vec{\eta}_\mathrm{I})(\mathbf{n}, \vec{\eta}_\mathrm{II}) - I_p[(\vec{\eta}_\mathrm{I}, \vec{\sigma}_\mathrm{I})$$

$$+ (\vec{\eta}_\mathrm{II}, \vec{\sigma}_\mathrm{II})] - K_1[(\vec{\sigma}_\mathrm{I}, \vec{\eta}_\mathrm{II}) + (\vec{\sigma}_\mathrm{II}, \vec{\eta}_\mathrm{I})]$$

$$- K_2[(\vec{\sigma}_\mathrm{I}, \mathbf{n})(\vec{\eta}_\mathrm{II}, \mathbf{n}) + (\vec{\sigma}_\mathrm{II}, \mathbf{n})(\vec{\eta}_\mathrm{I}, \mathbf{n})].$$

We now choose in the $\vec{\sigma}_\mathrm{I}$, $\vec{\sigma}_\mathrm{II}$ space a frame of reference such that the axes $\bar{z}_\mathrm{I}$ and $\bar{z}_\mathrm{II}$ are parallel to $\mathbf{B}_\mathrm{I}$ and $\mathbf{B}_\mathrm{II}$, respectively. Then $\eta_{i\bar{x}} = \eta_{i\bar{y}} = 0$ ($i = \mathrm{I, II}$) or, $\vec{\eta}_\mathrm{I} \parallel \mathbf{B}_\mathrm{I}$ and $\vec{\eta}_\mathrm{II} \parallel \mathbf{B}_\mathrm{II}$. Now, $\mathbf{B}_i = a_i\vec{\eta}_\mathrm{I} + b_i\vec{\eta}_\mathrm{II} + c_i\mathbf{n}$; so $\vec{\eta}_\mathrm{I} \parallel \mathbf{n}$ and $\vec{\eta}_\mathrm{II} \parallel \mathbf{n}$, and finally

$$H^0 = A + B_{\mathrm{I}\bar{z}}\sigma_{\mathrm{I}\bar{z}} + B_{\mathrm{II}\bar{z}}\sigma_{\mathrm{II}\bar{z}};$$

$$B_{\mathrm{I}\bar{z}} = -I_p\eta_{\mathrm{I}\bar{z}} - K_p\eta_{\mathrm{II}\bar{z}};$$

$$B_{\mathrm{II}\bar{z}} = -I_p\eta_{\mathrm{II}\bar{z}} - K_p\eta_{\mathrm{I}\bar{z}}; \quad K_p = K_1 + K_2.$$

The eigenvalues are

$$E^0_1 = A + B_{\mathrm{I}\bar{z}} + B_{\mathrm{II}\bar{z}}; \quad E^0_2 = A - B_{\mathrm{I}\bar{z}} - B_{\mathrm{II}\bar{z}};$$

$$E^0_3 = A - B_{\mathrm{I}\bar{z}} + B_{\mathrm{II}\bar{z}};$$

$$E^0_4 = A + B_{\mathrm{I}\bar{z}} - B_{\mathrm{II}\bar{z}}.$$

For $\lambda = 1$:

$$\eta^{(1)}_{\mathrm{I}\bar{z}} = \eta^{(1)}_{\mathrm{II}\bar{z}} = 1; \quad E^0_{11} = -I_p - K_p.$$

For $\lambda = 2$:

$$\eta^{(2)}_{\mathrm{I}\bar{z}} = \eta^{(2)}_{\mathrm{II}\bar{z}} = -1; \quad E^0_{22} = -I_p - K_p.$$

For $\lambda = 3$:

$$\eta^{(3)}_{\mathrm{I}\bar{z}} = -1; \quad \eta^{(3)}_{\mathrm{II}\bar{z}} = 1; \quad E^0_{33} = -I_p + K_p.$$

For $\lambda = 4$:

$$\eta^{(4)}_{\mathrm{I}\bar{z}} = 1; \quad \eta^{(4)}_{\mathrm{II}\bar{z}} = -1; \quad E^0_{44} = -I_p + K_p.$$

We see that $\vec{\eta}_\mathrm{I}$, $\vec{\eta}_\mathrm{II}$ are parallel to $\mathbf{n}$, which is a preferred direction in this case of two nucleons. Similarly, we obtain for a scalar symmetric field [Eq. (30) in I]

$$H^0 = A + (\mathbf{B}_\mathrm{I}, \vec{\tau}_\mathrm{I}) + (\mathbf{B}_\mathrm{II}, \vec{\tau}_\mathrm{II}); \tag{6}$$

$$A = \frac{I_s}{2}[(\vec{\eta}_\mathrm{I})^2 + (\vec{\eta}_\mathrm{II})^2] + K_s(\vec{\eta}_\mathrm{I}, \vec{\eta}_\mathrm{II});$$

$$\mathbf{B}_\mathrm{I} = -\vec{\eta}_\mathrm{I} I_s - \vec{\eta}_\mathrm{II} K_s;$$

$$\mathbf{B}_\mathrm{II} = -\vec{\eta}_\mathrm{II} I_s - \vec{\eta}_\mathrm{I} K_s;$$

$$K_s = g^2\int U_\mathrm{I}(\mathbf{r})\, U_\mathrm{II}(\mathbf{r}')\, G(\mathbf{r}, \mathbf{r}')\, d\mathbf{r}\, d\mathbf{r}'.$$

For the choice of axes z_{I} and z_{II} parallel to $\mathbf{B}_{\mathrm{I}}$ and $\mathbf{B}_{\mathrm{II}}$, respectively, we find

$$H^0 = A + B_{\mathrm{I}\bar{z}}\tau_{\mathrm{I}\bar{z}} + B_{\mathrm{II}\bar{z}}\tau_{\mathrm{II}\bar{z}}\,.$$

For $\lambda = 1$:

$$\eta^{(1)}_{\mathrm{I}\bar{z}} = \eta^{(1)}_{\mathrm{II}\bar{z}} = 1;\ E^0_{11} = -I_s - K_s;$$

For $\lambda = 2$:

$$\eta^{(2)}_{\mathrm{I}\bar{z}} = \eta^{(2)}_{\mathrm{II}\bar{z}} = -1;\ E^0_{22} = -I_s - K_s;$$

For $\lambda = 3$:

$$\eta^{(3)}_{\mathrm{I}\bar{z}} = -1;\ \eta^{(3)}_{\mathrm{II}\bar{z}} = 1;\ E^0_{33} = -I_s + K_s;$$

For $\lambda = 4$:

$$\eta^{(4)}_{\mathrm{I}\bar{z}} = 1;\ \eta^{(4)}_{\mathrm{II}\bar{z}} = -1;\ E^0_{44} = -I_s + K_s.$$

In all cases we obtain an interaction of the Yukawa type. But the $E^0_{\lambda\lambda}$ for two nucleons are already not the same: $E^0_{11} = E^0_{22}$ and $E^0_{33} = E^0_{44}$, but $E^0_{11} \neq E^0_{33}$ [these cases differ by having parallel or antiparallel (ordinary and isotopic) spins].

3. We shall now investigate the first approximation for the simple case of the symmetric scalar field. Equation (20) of I, describing the motion of a meson interacting with a nucleon, for $\lambda = 1$ has the form

$$(\varkappa^2 - \Delta)\varphi_{\alpha k} - d_s U(\mathbf{r}) \sum_{\beta=1}^{3} \left(|\tau_\beta|_{12}|\tau_\alpha|_{21} + |\tau_\alpha|_{12}|\tau_\beta|_{21}\right)\int U(\mathbf{r}')\varphi_{\beta k}(\mathbf{r}')\,d\mathbf{r}' = \frac{\omega_k^2}{c^2}\varphi_{\alpha k}; \tag{7}$$

$$d_s = 2\pi g^2/I_s.$$

In the frame of reference $\bar{x}$, $\bar{y}$, $\bar{z}$ we have $|\tau_{\bar{x}}|_{12} = |\tau_{\bar{x}}|_{21} = 1$; $|\tau_{\bar{y}}|_{12} = -|\tau_{\bar{y}}|_{21} = -i$; $|\tau_{\bar{z}}|_{12} = |\tau_{\bar{z}}|_{21} = 0$ and we obtain from (7)

$$(\varkappa^2 - \Delta)\varphi_{\bar{x}} - 2d_s U(\mathbf{r})\int \varphi_{\bar{x}}(\mathbf{r}')U(\mathbf{r}')\,d\mathbf{r}' = \frac{\omega^2}{c^2}\varphi_{\bar{x}}; \tag{8}$$

$$(\varkappa^2 - \Delta)\varphi_{\bar{y}} - 2d_s U(\mathbf{r})\int \varphi_{\bar{y}}(\mathbf{r}')U(\mathbf{r}')\,d\mathbf{r}' = \frac{\omega^2}{c^2}\varphi_{\bar{y}};$$

$$(\varkappa^2 - \Delta)\varphi_{\bar{z}} = \frac{\omega^2}{c^2}\varphi_{\bar{z}}.$$

The equations for $\lambda = 2$ are identical.

It should be mentioned that only the full field $\Phi_\alpha = \varphi^0_\alpha + \varphi_\alpha$ obeys charge invariance but not the fields φ^0_α and φ_α separately. Because $\varphi^0_{\bar{x}} = \varphi^0_{\bar{y}} = 0$ and only $\varphi^0_{\bar{z}} \neq 0$, the component $\varphi_{\bar{z}}$ is also singled out.

We see that in the case of $\varphi_{\bar{x}}$ and $\varphi_{\bar{y}}$ the meson is being attracted by the nucleon. In the limiting case $a \to 0$ and for $\epsilon' = \epsilon - \mu c^2 \ll \mu c^2$ we obtain (taking, for example, $U = 3/4\pi a^3$ for $r \leq a$; $U = 0$ for $r > a$, and $I_s \approx 3g^2/2a$)

$$-\frac{\hbar^2}{2\mu}\Delta\varphi_{\bar{x}} - \frac{4\pi\hbar^2}{3\mu}\lim_{a\to 0} aU(\mathbf{r})\varphi_{\bar{x}} = \varepsilon'\varphi_{\bar{x}}.$$

The depth of the potential well $U_0 \approx \hbar^2/\mu a^2$, and so the condition $U_0 \ll \hbar^2/\mu a^2$ for the absence of bound states (see I) is not fulfilled. Therefore, with the above choice of $U(\mathbf{r})$ there are isobars possible even for $a \to 0$; $\epsilon' \approx g^0$.

Under usual experimental conditions the charge of a nucleon, i.e., τ_z, is fully determined, and therefore $\vec{\eta}$ is parallel to the z-axis. Therefore, here the $\bar{z}$-axis coincides with the z-axis, and $\varphi_{\bar{z}} = \varphi_z$. From Eq. (8) one can see that in the first approximation neutral mesons, (φ_z) do not interact with fixed nucleons. (This does not apply to a pseudoscalar field.)

If $\epsilon \geq \mu c^2$ we obtain for φ_x ($a_x = 1$) the following equation [see (23) in I)

$$\varphi_x = e^{i(\mathbf{k},\mathbf{r})}$$

$$+ \frac{d_s}{2\pi}\int \frac{e^{ik|\mathbf{r}-\mathbf{r}'|}}{|\mathbf{r}-\mathbf{r}'|}U(\mathbf{r}')\,d\mathbf{r}' \int U(\mathbf{r}'')\varphi_x(\mathbf{r}'')\,d\mathbf{r}''$$

and a similar expression for φ_y. Here one has to take $d_s = 2\pi g^2/[I_s - (\epsilon/2)]$ [see (25) in I). The solution has the form

$$\varphi_x = e^{i(\mathbf{k},\mathbf{r})} + \frac{d_s}{2\pi}\left(1 - \frac{d_s}{2\pi}\int \frac{e^{ik|\mathbf{r}-\mathbf{r}'|}}{|\mathbf{r}-\mathbf{r}'|} U(\mathbf{r})\, U(\mathbf{r}')\, d\mathbf{r}\, d\mathbf{r}'\right)^{-1}$$

$$\int e^{i(\mathbf{k},\mathbf{r}')} U(\mathbf{r}')\, d\mathbf{r}' \int \frac{e^{ik|\mathbf{r}-\mathbf{r}'|}}{|\mathbf{r}-\mathbf{r}'|} U(\mathbf{r}')\, d\mathbf{r}'.$$

Expanding in a series in powers of ka and κa we obtain for $r \to \infty$

$$\varphi_x \approx e^{i(\mathbf{k},\mathbf{r})}$$

$$- \frac{1 - k^2a^2/5}{(\varepsilon/2g^2) + \varkappa + ik - 3a(\varkappa^2 + k^2)/8} \frac{e^{ikr}}{r} \quad (r_1 = 0).$$

For the scattering cross section for charged mesons, not considering absorption processes, we then obtain $\left(\varphi_- = \frac{1}{\sqrt{2}}(\varphi_x - i\varphi_y);\right.$ $\left.\varphi_+ = \frac{1}{\sqrt{2}}(\varphi_x - i\varphi_y)\right)$:

$$d\sigma = \frac{(1 - k^2a^2/5)^2 d\Omega}{[(\varepsilon/2g^2)^2 + \varkappa - 3a(\varkappa^2 + k^2)/8]^2 + k^2}; \tag{9}$$

$$d\Omega = 2\pi \sin\vartheta\, d\vartheta.$$

We now shall go to the limit $a = 0$. Here, naturally, the self energy $E^0_{\lambda\lambda} = \infty$, but the cross section $d\sigma$ as well as the bound state energy ϵ' of the meson (see above) approach a finite limit.

$$d\sigma = \frac{d\Omega}{[(\varepsilon/2g^2)^2 + \varkappa]^2 + k^2}.$$

For a neutral pseudoscalar field Eq. (20) of I has the form

$$(\varkappa^2 - \Delta)\varphi - 2d_p\left[\frac{\partial U}{\partial x}\int \frac{\partial U'}{\partial x'} \varphi(\mathbf{r}')\, d\mathbf{r} + \frac{\partial U}{\partial y}\int \frac{\partial U'}{\partial y'} \varphi(\mathbf{r}')\, d\mathbf{r}'\right] = \frac{\omega^2}{c^2}\varphi;$$

$$d_p = 2\pi \frac{g^2}{\varkappa^2}\left(I_p - \frac{\varepsilon}{2}\right)^{-1}.$$

The solution for $\epsilon \geq \mu c^2$ is

$$\varphi = e^{i(\mathbf{k},\mathbf{r})} + \left(\frac{2\pi}{d_p} - \int \frac{e^{ik|\mathbf{r}-\mathbf{r}'|}}{|\mathbf{r}-\mathbf{r}'|} \frac{\partial U}{\partial x} \frac{\partial U'}{\partial x'}\, d\mathbf{r}\, d\mathbf{r}'\right)^{-1}$$

$$\times\left[\int \frac{\partial U(\mathbf{r}')}{\partial x'} e^{i(\mathbf{k},\mathbf{r}')}\, d\mathbf{r}' \int \frac{e^{ik|\mathbf{r}-\mathbf{r}'|}}{|\mathbf{r}-\mathbf{r}'|} \frac{\partial U(\mathbf{r}')}{\partial x'}\, d\mathbf{r}'\right.$$

$$\left. + \int \frac{\partial U(\mathbf{r}')}{\partial y'} e^{i(\mathbf{k},\mathbf{r}')}\, d\mathbf{r}' \int \frac{e^{ik|\mathbf{r}-\mathbf{r}'|}}{|\mathbf{r}-\mathbf{r}'|} \frac{\partial U(\mathbf{r}')}{\partial y'}\, d\mathbf{r}'\right];$$

$$\{\vec{\sigma}\}_{\lambda\lambda} \parallel [\mathbf{k}\times\mathbf{k}'].$$

Up to terms $(ka)^2$ and $(\kappa a)^2$ the meson scattering cross section is given by

$$d\sigma = \frac{k^4\cos^2\vartheta\,(1 - k^2a^2/5)^2\, d\Omega}{[(\varepsilon\varkappa^2/2g^2) + I_0(\varkappa^2 + k^2)/3 - \varkappa^3/3]^2 + k^6/9}, \tag{10}$$

$$I_0 = \int U(\mathbf{r})\, U(\mathbf{r}') \frac{d\mathbf{r}\, d\mathbf{r}'}{|\mathbf{r}-\mathbf{r}'|} \approx \frac{3}{2a};$$

$$\text{for } a \to 0 \quad d\sigma \to 0.$$

In the case of two nucleons, their being in a bound state can lead to an additional interaction between them in the order g^0. Actually, the energy ϵ depends, generally speaking, on the distance r_{12} and can even become zero at a certain distance $r_{12} = r_k$. The energy of the system has [in the absence of real mesons ($n_{k\rho} = 0$)] up to terms of order g^0 the form

$$E^0_\lambda + E_{\lambda\lambda} = E^0_\lambda(r_{12}) + \sum_{\varepsilon_i < \mu c^2} \frac{\varepsilon_i(r_{12})}{2} + \sum_{\hbar\omega_k > \mu c^2} \frac{\hbar\omega_k}{2}.$$

This way the term $\sum_{\epsilon_i < \mu c^2} \epsilon_i/2$ in the zero order energy of the meson field, as well as E^0_λ depends on r_{12}.

4. The results here obtained differ significantly from earlier work (see, for example, references 3-8). However, it can be shown that the quoted

---

[5] G. Wentzel, Helv. Phys. Acta **13**, 269 (1940); **14**, 633 (1941).

[6] R. Serber and S. Dancoff, Phys. Rev. **63**, 143 (1943).

[7] W. Pauli and S. Kusaka, Phys. Rev. **63**, 400 (1943).

[8] W. Pauli, *Meson Theory of Nuclear Forces.*

papers contain essential errors. It should be pointed out, first, that the replacement of the operators $\vec{\sigma}$ and $\vec{\tau}$ by classical unit vectors in reference 8 seems to be inadmissible. The transition to the classical case corresponds to a situation with large quantum numbers. However, the spin operators have just two quantum states, and a transition to classical mechanics seems to be meaningless.

In references 3-7 the operators $\vec{\sigma}$ and $\vec{\tau}$ have been retained and the quantum mechanical Hamiltonian has been used. For the zeroth order Hamiltonian the correct potential enervy V_f, diagonalized in the spin variables, has been obtained. However, it has been incorrectly assumed that the level $E^0 = (5/2\,I)$ for the pseudoscalar symmetric field and $E^0 = (3/2\,I)$ for the scalar symmetric or the pseudoscalar neutral field obtains for the real state of the system. As has been shown above, the energy is actually the same for all cases of symmetric coupling ($E^0_{\lambda\lambda} = E^0_{\lambda'\lambda'}$). The relations ($E^0 = (5/2I)$ and $E^0 = (3/2I)$ hold for the eigenvalues of the auxiliary orthonormal functions $\psi^0_{\lambda\mu}$ for $\mu \neq \lambda$ (see I).

A more serious shortcoming in references 3-7 seems to be the assumption that because of the large difference $E^0 = (3/2I)(5/2I)$ between the unperturbed and the perturbed level, one can neglect transitions from the unperturbed to the perturbed level. Therefore, in the higher approximations the spin operator $O_\alpha \Phi_\alpha$ is replaced by its diagonal elements (see, for example, Sec. 5 of reference 4 and III A of reference 6). Now the perturbation $H^{(1)}$ is of first order g, and therefore, its nondiagonal elements yield in the second approximation terms of zero order in g [see (19) in I; these nondiagonal elements actually correspond to transitions to the real level $E^0_{\lambda\lambda'}$, but in a state $\psi^0_{\lambda\mu}$ with $\lambda \neq \mu$]. In this way even the terms of order g^0 have not been correctly obtained in references 3-7, and the energy of the isobars, which has geen given in these references, actually is of the order g^{-2}. Furthermore, only one spin state of the system with $\lambda = \mu$ is considered, i.e., one projection of $<\vec{\sigma}>$, $<\vec{\tau}>$, $<\tau_\alpha \vec{\sigma}>$; as has been seen above, the direction of the vectors is arbitrary. But it was inferred in these papers that, by solving the equation of zero order, one can only obtain the absolute value of the vectors $<\vec{\sigma}>$, $<\vec{\tau}>$, $<\tau_\alpha \vec{\sigma}>$; therefore, angular variables were introduced in isospace to describe the rotational degrees of freedom of the vectors $<\vec{\sigma}>$, $<\vec{\tau}>$, $<\tau_\alpha \vec{\sigma}>$ (a, b, c or $e_{\alpha k}$ for the pseudoscalar and ϑ for the scalar field, see references 4-6). However, as shown above, the vectors $<\vec{\sigma}>$, $<\vec{\tau}>$, $<\tau_\alpha \vec{\sigma}>$ are fully determined solving (1), although for symmetric coupling the direction of these vectors turns out to be arbitrary. By the introduction of the angular variables the number of the degrees of freedom is arbitrarily increased while no conditions are imposed on the old variables, the spin variables of the nucleons and the field oscillators *. Finally, corrections to the energy are not calculated in references 3-7 in the straightforward and unique way of perturbation theory, but by applying a series of unitary transformations which are different for the different cases. Here the calculations are rendered very involved by the fact that the zero order field φ^0_α is an operator and not a classical quantity; therefore, the field of the real mesons and the corresponding momentum turn out not to be canonical variables. The involved character of the calculations explains the occurrence of a number of actual mistakes in these references which have been pointed out by the author[9].

---

* *Note added in proof:* These critical remarks apply to a great extent to recently published papers by J. Pekar, J. Exper. Theoret. Phys. USSR 27,398, 411,579 (1954).

[9] B. Geilikman, Dokl. Akad. Nauk SSSR **90**, 991 (1953).

Translated by M. Danos
222

SOVIET PHYSICS JETP VOLUME 2, NUMBER 4 JULY, 1956

Investigation of the Origin of Levels of Electron Localization in Zinc Sulphide Phosphors

N. V. ZHUKOVA
Moscow State University

(Submitted to JETP editor July 1, 1954)
J. Exper. Theoret. Phys. USSR **29**, 680-692 (November, 1955)

The role of copper and oxygen in the formation of three bands of localization levels of electrons in ZnS-Cu phosphor is clarified by the method of temperature controlled luminescence. The action of iron, nickel and cobalt on the separate maxima of the temperature controlled luminescence curve is examined. It is found that Fe and Ni in small concentrations may sharply increase the intensity of luminescence.

1. INTRODUCTION

PROLONGED emission of phosphors is caused by the freeing of electrons from special localized centers in the crystal structure, where they are trapped when the phosphor is excited. Typical phosphors generally have several kinds of energy levels of localization of electrons, differing in their depth, each of which takes part in a definite way in the process of phosphor luminescence. It is clear from this that the electron localization levels play an exceptionally important role in the kinetics of phosphorescence.

The question of the origin of electron localization levels has not been adequately investigated up to the present time. According to the generally accepted opinion, the places in the crystal structure which are deformed by the inclusion of the activator ions, are also the places of electron localization. However, each phosphor must be separately investigated to determine which set of levels is connected (and to what extent) with one or the other activator. Also, the influence of the other components of the phosphor and of the so-called extinguishers of luminescence, such as iron, nickel and cobalt, on the formation of localized levels is very little understood.

The most widely studied class of phosphors are the zinc sulphides which found wide practical application. It is known that a typical ZnS-Cu phosphor has three bands of electron localization of different depth. The depth of the levels in each band is characterized by a temperature at which most of the electrons stored on the levels of a given band are freed. Hereinafter, the three bands of electron localization of the ZnS-Cu phosphor will be indicated in the order of increasing depth by numbers I, II and III; the depths of these bands are characterized by temperature ranges -140 to -110° C, -60 to -40° C, +20 to +50° C, respectively.

The most thoroughly investigated is the III band of levels. According to references 1 and 2, the origin of this band is connected with the presence of copper. However, in references 3 and 4 this band is explained by the presence of oxygen in the lattice of ZnS. Wee see that there is no agreement on the nature of this most highly investigated band of electron localization. Concerning the origin of bands I and II, there are even less data available. Kreger[3] considers that the band II ($T = -50$ to -25° C) originates by the penetration of copper into the lattice ZnS. According to the opinion of Hoogenstraten[4], it is caused by the presence of complex Cu^+O^{-2}. Hoogenstraten connects the origin of band I with presence of sulphur ion vacancies in the ZnS lattice if oxygen ions enter into the composition of the phosphor; in the absence of oxygen, ions of the type Cl^- are considered the cause of formation of the I band of levels.

Our work is devoted to the further clarification of influence of the components of the ZnS-Cu phosphor on the formation of its levels of localization. To carry out this work we have changed, in different respects, the composition of the investigated samples and have determined their curves of light emission as a function of temperature.

2. DESCRIPTION OF THE EXPERIMENTAL METHOD

In order to establish more accurately the composition of the investigated ZnS-Cu phosphor samples, their preparation was carried out by ourselves. For the preparation of the phosphors,

---

[1] G. F. Garlick, A. F. Wells and M. F. Wilkins, J. Chem. Phys. 17, 399 (1949).

[2] R. Bube, Phys. Rev. 80, 655 (1950).

[3] F. A. Kreger and J. A. Dikhoff, J. Electrochem. Soc. 99, 144 (1952).

[4] W. Hoogenstraten, J. Electrochem. Soc. 100, 356 (1953).

we had at our disposal specially purified zinc suplhide and alkaline halide melts. The copper, and also Fe, Ni and Co, used as activators were in the form of chloride salts marked "chemically pure". Quartz and ceramic vessels only were used in the preparation of the samples. Heat treatment was performed in closed quartz crucibles at a temperature of 1100° C for a period of 15 minutes.

For the investigation, samples ~ 10 μ thick were deposited by precipitation from alcohol on mica plates ~ 7 μ thick.

As the basic method of investigation, we chose the temperature controlled luminescence method which consists of a measurement of the intensity of the excited luminescence at low temperatures of the phosphor as a function of this temperature. A very important requirement of this method is the uniform heating of the phosphor in the process of excitation. Otherwise, the entire picture of resulting levels is distorted.

The area under the curve of the temperature controlled luminescence or the height of its maximum (if the width does not change and on the assumption that in the given range of temperatures there is no temperature extinction) is proportional to the number of localized electrons on the levels of a given depth under given conditions of excitation. The latter conclusion cannot be considered strictly true since electrons which are elevated from the levels of localization into the conduction bands may undergo secondary localization, which may disturb the proportionality between the intensity of illumination corresponding to the maximum of the temperature controlled luminescence curve and the number of electrons localized on the levels of a given depth. However, as we shall see below, a series of experiments shows that under conditions of our experiment, the abovementioned proportionality is preserved with very good approximation. The method of temperature controlled luminescence is therefore very convenient for the study of the origin of the electron localization levels, which in this case is reduced to the determination of the cause of the formation of separate maxima in the curve of the temperature controlled luminescence.

To achieve temperature controlled luminescence, we have constructed special equipment which permits us to obtain quite accurately a linear relationship between the time of heating and the temperature of the excited phosphor. A sketch of the experimental arrangement is shown in Fig. 1. The equipment consists of a massive brass rod with a cavity for the sample. The sample was fastened by a special movable holder. The temperature of the phosphor was measured by a thermocouple. The heating wire was wound over the entire surface of the rod. The rod was placed in a Dewar vessel with windows for excitation of the sample under observation.

For the purpose of cooling the sample prior to excitation, liquid nitrogen was poured into the Dewar. The measurement of the temperature controlled luminescence was begun 15 seconds after the end of the excitation. The temperature of the phosphor was increasing at a steady rate of 0.25 degree/sec. The curve of variation of temperature with time is shown in Fig. 2.

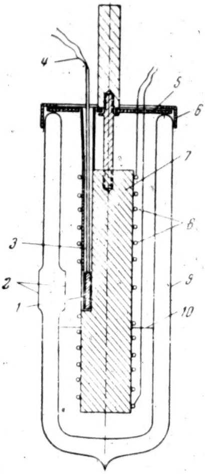

FIG. 1. Experimental equipment for obtaining thermoluminescence. *1.* Sample, in holder; *2.* Windows of the Dewar vessel; *3.* Copper tube for the thermocouple wires; *4.* Thermocouple output; *5.* Textolite cover; *6.* Metal collar; *7.* Brass rod; *8.* Heater; *9.* Dewar vessel; *10.* Level of liquid nitrogen.

The described construction of the equipment permitted us (1) to change samples without changing the fixed position of the phosphor being investigated; (2) to excite the phosphor at any temperature in the range of − 190° C to + 100° C and maintain the temperature constant with an accuracy of ±2° during a 10-15 min interval, and (3) to insure a strictly constant rate of heating during the experiment.

Excitation of the phosphor was made using lamp PRK-4 with a filter which transmits a section of the mercury spectrum from $\lambda_{max} = 436\ m\mu$ to $\lambda_{max} = 366\ m\mu$. Duration of the excitation was 10 minutes. The radiation of the phosphor was measured visually by means of the luminescence photometer GOI.

3. THE ROLE OF ACTIVATORS Cu, Zn AND OXYGEN IN THE FORMATION OF ELECTRON LOCALIZATION LEVELS

As pointed out above, it had not been clearly established until recently, which of the bands of local levels, and to what extent, are formed by copper. We have therefore prepared a series of samples whose copper concentration varied from 3×10^{-6} to 10^{-3} gm/gm and measured their curves of temperature luminescence (Fig. 3).

The curves obtained had three basic maxima, the mean positions of which correspond to the temperatures -120°, -60° and +20° C. It should be noted that the maxima in curves I ($T = -120°$ C) and II ($T = -50°$ C) exhibit a nonsymmetrical form, indicating that these bands of local levels represent a superposition of several narrower

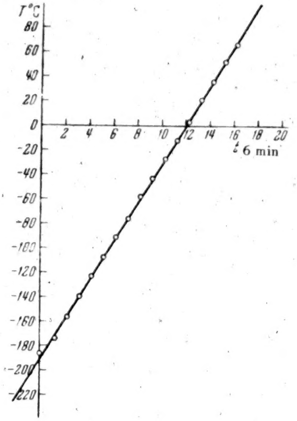

FIG. 2. Variation of the phosphor temperature in time.

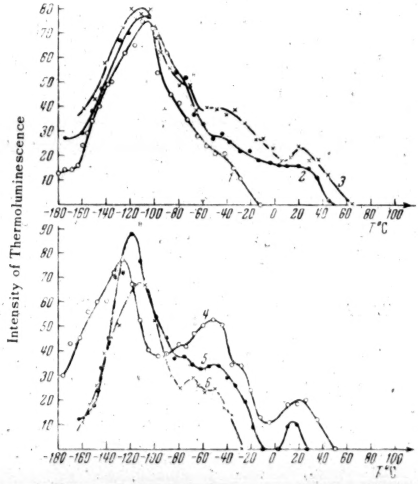

FIG. 3. Thermoluminescence curves of samples of ZnS-Cu phosphor with copper concentration in gm/gm: *1.* 3×10^{-6}; *2.* 3×10^{-5}; *3.* 10^{-4}; *4.* 3×10^{-4}; *5.* 6×10^{-4}; *6.* 10^{-3}.

bands. In further experiments, it was found that concentrations of oxygen as well as iron, nickel and cobalt produce different effects in the various regions of the II maximum. This enabled us to divide the region of maximum II into three sections bounded by the temperatures from -90° to -60°, from -60° to -40° and from -40° to 0° C.

Figure 3 shows that the introduction of copper and the increase of its concentration changes the intensity of maxima II ($T = -60°$ C) and III ($T = +20°$ C) and has almost no influence on the intensity of the maximum I ($T = -120°$ C).

Figure 4 shows the change in the intensity of maxima II and III in relation to the intensity of maximum I as a function of copper concentration.

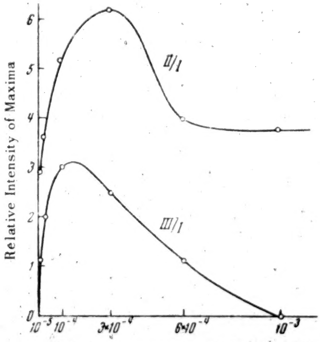

FIG. 4. Concentration of Cu in gm/gm.

The appearance of maximum III with the increase of copper concentration, the fact that this maximum reaches a peak at the concentration of about 1.5×10^{-4} gm/gm and then completely disappears at the concentration of 10^{-3} gm/gm , leads to the conclusion that the presence of copper is necessary for the formation of maximum III. This confirms the similar qualitative conclusions made by previous investigators[1,2]. It is possible that, besides copper, oxygen also has an influence on the formation of maximum III, as recent experiments of Hoogenstraten[4] have shown. However, it is not clear from these experiments whether the presence of oxygen is a necessary condition for the formation of band III or only intensifies this band. Further experiments are necessary to clarify this point.

The change in the maximum III with the increased concentration of copper is qualitatively and quantitatively analogous to the corresponding change in intensity of the green emission band ($\lambda_{max} = 530$ mμ) and the complementary absorption of the copper centers[2,5]. As shown in reference 5, the introduction of copper into zinc sulphide leads to the complementary absorption in the region 350-450 mμ which increases with the increased concentration of copper. This is accompanied by a simultaneous increase in intensity of the green emission band. At copper concentration of $\sim 10^{-4}$ gm/gm, the growth of the complementary absorption stops and its abrupt decrease begins. Simultaneously, the green band decreases in intensity and at concentrations of $\sim 10^{-3}$ completely disappears.

The above analogy indicates that the III band of electron localization levels is directly connected with the copper luminescent centers and that its disappearance at concentrations $\sim 10^{-3}$gm/gm as well as the disappearance of the green emission band and of the complementary absorption of copper, is explained by the transition of a portion of the copper into a nonluminescent state. It follows from this that if copper ceases to be the source of luminescent centers, it does no longer provide any centers of electron localization.

It is seen from Figs. 3 and 4 that not only maximum III but also maximum II increases with the increase of copper concentration. Beginning with the concentration of 3×10^{-4} gm/gm, the intensity of II maximum as well as that of the III maximum decreases but only up to a certain definite value. Further increase in the copper concentration has practically no effect on the intensity of the II maximum. Considerable change in intensity of the II maximum with change in copper concentration indicates that the II maximum is connected with the penetration of copper into the ZnS lattice. The general increase in intensity of the II maximum takes place mainly at the expense of the intensity growth in the temperature regions of -60° to -40° and from -40° to 0° C. It follows, therefore, that these very sections of the II maximum are connected with the presence of copper in the ZnS lattice. The intensity in the -90° to -60° region of temperature changes only slightly with the increase of copper concentration.

The difference in the shapes of the two curves

---

[5] M. N. Alentsev and A. A. Cherepnev, J. Exper. Theoret. Phys. USSR 26, 473 (1954).

of Fig. 4 indicates that besides copper, some other components of the nonactivated ZnS influence the formation of the II maximum. In order to study the nature of this maximum more fully, we have prepared three samples of the ZnS phosphor without addition of the copper activator but with different degrees of admission of air during the heat treatment. The curves of the temperature controlled luminescence for these samples are shown in Fig. 5. Increase of air admission corresponds to an increase in the labeling number on the curves of Fig. 5.

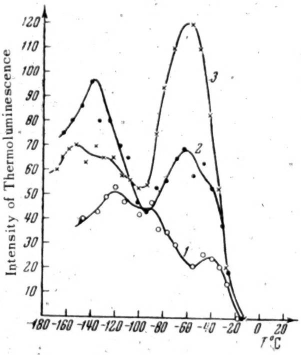

FIG. 5.

In all cases, the curves exhibited only maxima I and II. The absence of maximum III confirms the conclusion reached above concerning the connection of this maximum with the presence of copper in the ZnS lattice. These samples had only traces of copper. At room temperature, these samples exhibited a blue phosphorescence of very low persistence. It is characteristic that the high temperature portion (from -40° C to 0° C) of the II maximum is completely absent in the curves under consideration. This indicates that the origin of the latter is also connected with the presence of copper in the ZnS lattice.

As seen from Fig. 5, the intensity of the maximum II changes considerably depending on the conditions of heat treatment. High rate of air admission during the heat treatment (curve *3*) increases the intensity of maximum II almost fivefold compared with the intensity corresponding to the heat treatment at the low rate of air admission (curve *1*). Increased intensity of the II maximum is at the expense of growth of intensity in the temperature regions from -90° to -60° and from -60° to -40° C due to the increase of the amount of oxygen in the ZnS lattice. The conclusion concerning the possibility of the influence of oxygen on the formation of levels of electron localization is in agreement with references 3 and 4.

It was shown above that the origin of the central portion of the II maximum (from -60 to -40° C) is connected with the presence of copper. Its existence in the curve *1*, Fig. 5, is apparently due to traces of copper in the ZnS lattice. Its considerable growth in intensity with the increase of oxygen in the ZnS lattice indicates that the origin of this portion of the II maximum is apparently due to the combination of oxygen and copper. Considerable growth in intensity of the low temperature portion of the II maximum (from -90° to -60° C) with the increase of the oxygen content and the fact that an increase of copper concentration has almost no effect on the intensity (see Fig. 3), lead to the conclusion that the origin of this portion of the II maximum is due to the presence of oxygen in the ZnS lattice.

We now turn to the discussion of the origin of the I maximum. From Figs. 3 and 5, it can be seen that neither oxygen nor copper cause the formation of the I maximum. The conclusion that the nature of maximum I is entirely different from that of maxima II and III is very clearly confirmed from the study of influence of the melting processes on the formation of the levels of electron localization[6]. On the other hand, it is clear that the excess zinc which is the second activator in all activated zinc sulphide phosphors, can produce levels of electron localization. The presence of excess zinc in ZnS phosphors and its role as an activator was established by experiments of Bundel and Rusanova[7] and others. Inasmuch as neither the II nor III maximum is connected with the presence of zinc, it is natural to suppose, by the process of exclusion, that the only remaining maximum(I) is connected with the excess zinc.

Confirmation of this assumption follows from the comparison of the spectra of instantaneous illumination of ZnS-Cu phosphor samples with the curves of the temperature controlled luminescence. Fig. 6 contains curves for two samples; the first was prepared without alloying; the second with the introduction of 25% NaCl. Figure 7 shows the luminescence spectra of these samples. These figures show that almost complete destruction of

---

[6] N. V. Zhukova, Dokl. Akad. Nauk SSSR **85**, 981 (1952)

[7] A. A. Bundel and A. I. Rusanova, Izv. Akad. Nauk SSSR, Ser. Fiz. **13**, 173 (1949).

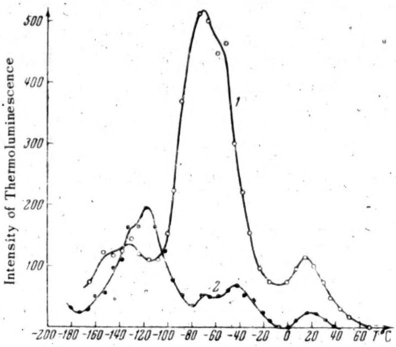

FIG. 6. Thermoluminescence curves of phosphor samples ZnS-Cu 3×10^{-4} gm/gm. Curve *1*--without the melt; Curve *2*--with 25% NaCl.

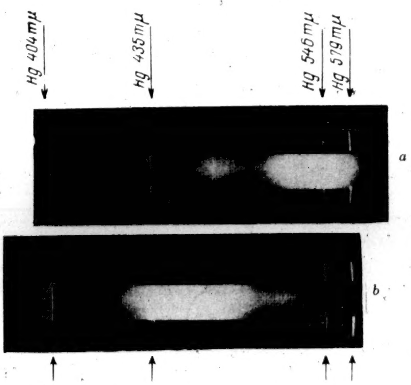

FIG. 7. Luminescent spectra of samples ZnS-Cu 3×10^{-4} gm/gm. *a.* Without melt; *b.* With 25% NaCl.

maxima II and III carries with it the destruction of the green band with $\lambda_{max} = 530\ m\mu$. This is understood since the green band is associated with copper, and the maxima II and III, as shown above, are connected with the presence of copper in the ZnS lattice.

As a result of the sharp decrease in intensity of the green band, there appeared a bright light blue band with $\lambda_{max} = 460\ m\mu$. The work of Alentsev and Cherepneva[5] has definitely established that this luminescent band belongs only to the excess of zinc. The accompanying preservation and even increase in the area of the first maximum (Curve 2, Fig. 6) indicates that the first band of levels of electron localization as well as the blue luminescent band with $\lambda_{max} = 460$ *mμ*, in all probability, belongs to the same centers, i.e., excess zinc.

4. THE INFLUENCE OF IRON, NICKEL AND COBALT ON THE THERMOLUMINESCENCE OF ZnS-Cu PHOSPHOR

In the course of preparation of ZnS-Cu phosphor samples, we have encountered the strong influence of iron, nickel and cobalt on the thermoluminescence of the samples being investigated, which presented a considerable difficulty. Although the quenching action of these elements on the luminescence of zinc sulphide phosphors has long been known, their quenching of thermoluminescence has been very little investigated. Neither has the question been cleared up whether the quenching action of iron, nickel and cobalt is explained by the decrease (up to complete destruction) of the possibility of electron localization or by the increase in the number of radiationless transitions associated with the freeing of levels.

In this connection, it was of interest to investigate how the quenching of the different maxima of thermoluminescence take place. For this purpose, we have prepared three series of ZnS-Cu phosphor samples with different concentrations of Fe, Ni and Co. The curves of thermoluminescence of these samples are shown in Figs. 8, 9 and 10. They show a considerable reduction in the maxima of the curves of thermoluminescence with the increase in the concentration of iron, nickel and cobalt. It is seen from Fig. 10 that, in addition to the usual quenching action, cobalt at concentrations of 10^{-6} gm/gm forms new local levels which are deeper than all previously existing

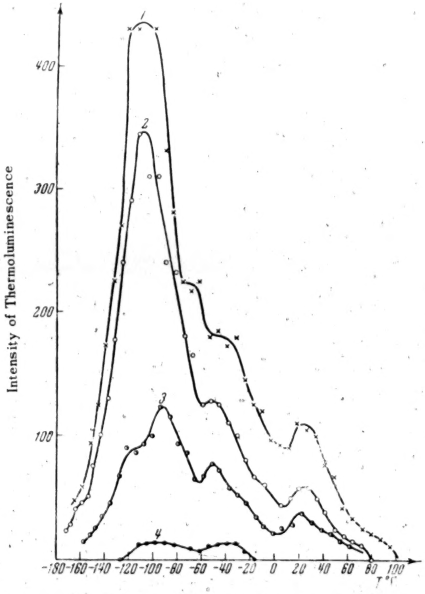

FIG. 8. Thermoluminescence curves of samples of ZnS-Cu phosphor with different concentration of iron in gm/gm. *1.* without Fe; *2.* 10^{-5}; *3.* 6×10^{-5}; *4.* 10^{-4}.

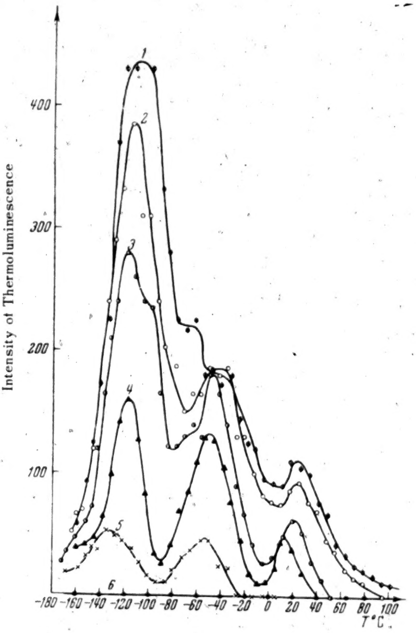

FIG. 9. Thermoluminescence curves of samples ZnS-Cu with different concentrations of nickel in gm/gm. *1.* without nickel; *2.* 10^{-7}; *3.* 10^{-6}; *4.* 3×10^{-6}; *5.* 6×10^{-6}; *6.* 10^{-5}.

levels. As the concentration of cobalt is increased to 10^{-5} gm/gm, I, II and III maxima are completely extinguished and there remains only a newly formed maximum at $T = 80°$ C. The ability of cobalt to form a new band of localization levels was noted in references 4 and 8.

Into all samples prepared for the investigation of the action of iron, nickel and cobalt, 10% molten NaCl was introduced at a copper concentration of 6×10^{-5} gm/gm. This caused a sharp increase of the I maximum and therefore maximum II is not as pronounced. Nevertheless, the nonsymmetrical form of the latter is clearly visible as before. Increased concentration of iron, nickel and cobalt influenced unequally the regions of the II maximum contained in the temperature regions from -90° to -60° on one side and from -60° to -40° and from -40° to 0° C on the other.

In Fig. 11 there is shown the change in intensity of the separate maxima in the curves of thermoluminescence as a function of concentration of the quenching agents. The changes in the maximum II are shown by the curves corresponding to the low temperature (-90° to -60° C) and the high temperature (-60° to 0° C) regions of the maximum II.

The following table contains data showing the factors of intensity decrease of each maximum in the thermoluminescence of the phosphor ZnS, Cu 6×10^{-5} gm/gm, 10% NaCl by the introduction of one of the investigated quenching agents in

---

[8] E. S. Krylova, Dokl. Akad. Nauk SSSR **64**, 495 (1949).

TABLE

Number and temperature of maximum in °C / Quenching agent	I	II		III
	−120	Low temperature portion	High temperature portion	+ 20
Fe	1.16	1.12	1.20	1.37
Ni	8.6	11.2	4.5	Complete
Co	43	15	2.6	1.7

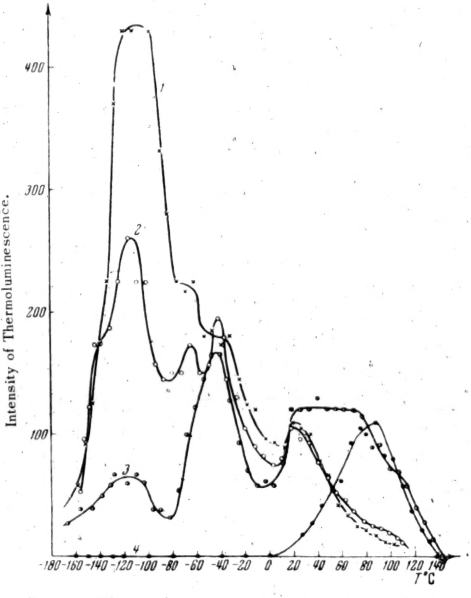

FIG. 10. Thermoluminescence curves of samples ZnS-Cu phosphor with different concentrations of cobalt in gm/gm. *1.* Without Co; *2.* 10^{-7}; *3.* 10^{-6}; *4.* 10^{-5}.

the quantity of 6×10^{-6} gm/gm. (In the case of cobalt, the intensity of the III maximum was taken as equal to the intensity at $T = +20°$ C.)

The comparison of the quenching of the same maximum by different elements shows that for the I maximum, as well as for the low temperature portion of the II maximum, the strongest quenching agent is cobalt, the weakest is iron. For the high temperature portion of the II maximum and basic maximum III, the strongest quenching agent is nickel, the weakest is iron. If we compare the quenching of different maxima by one and the same

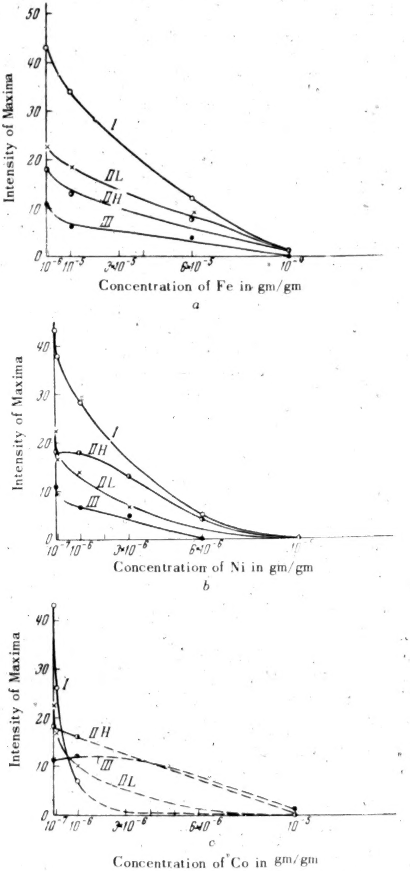

FIG. 11. Variation of intensity of the separate maxima in the thermoluminescence curves with the change of concentration of the quenching agents. O - I maximum; × - II maximum (low temperature portion); ● - III maximum.

quenching agent, it appears that iron (in concentrations of up to 10^{-5} gm/gm) lowers the intensity of III and of the high temperature portion of II maxima to a greater degree than it lowers the intensity of the I maximum and of the low temperature portion of the II maximum. In the cases of cobalt and nickel, I and the low temperature portion of II maximum are quenched to a greater extent than III and the high temperature portion of II maximum.

We have discovered an intersesting phenomenon

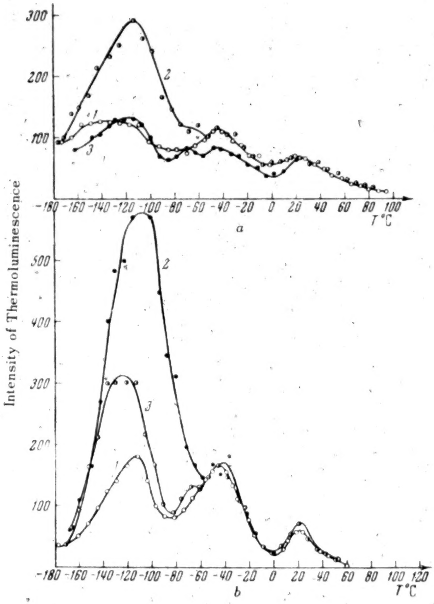

FIG. 12. Thermoluminescence curves of samples ZnS-Cu phosphor with 10% NaCl, with iron and nickel. *a.* Cu 10^{-5} gm/gm, *1* - without Fe and Ni, *2* - 10^{-6} Fe, *3* - 10^{-7} Ni. *b.* Cu 3×10^{-4} gm/gm, *1* - without Fe and Ni, *2* - 10^{-6} Fe, *3* - 10^{-7} Ni.

in 4 samples of ZnS-Cu phosphor when small quantities (10^{-7}, 10^{-6} gm/gm) of quenching elements were introduced (Fig. 12). Introduction of 10^{-6} gm/gm of Fe into a sample of phosphor ZnS, Cu 3×10^{-4} gm/gm caused a sharp increase (approximately threefold) in intensity of maximum I ($T = -120°$ C) and had no effect on the intensity of maxima II and III. By the introduction into a sample of the same composition of 10^{-7} gm/gm Ni instead of Fe, the intensity of maximum I increased 1.7 times. The effect was repeated, but was less pronounced, when the same quantities of Fe and Ni were introduced into two other samples of ZnS-Cu phosphors of concentration 10^{-5} gm/gm.

The spectra of these samples have not displayed the bands characteristic of Fe and Ni luminescence. This led us to believe that Fe and Ni are capable of influencing, i.e., increasing, the possibility of localizing electrons. It is therefore considered possible that the quenching of the zinc sulphide phosphors by these elements after illumination is to be explained by the destruction of the phosphor's ability to localize electrons at the levels. The latter conclusion agrees with the data in the work of references 9 and 10, where it is shown that zinc sulphide phosphors containing nickel do not exhibit the existence of localized electrons when in a state of excitation. Note

---

[9] G. Garlick and A. Gibson, Proc. Phys. Soc. (London) **60**, 574 (1948).

[10] C. Bull and D. Mason, J. Opt. Soc. Amer. **10**, 718 (1951).

that as shown in Fig. 12, in the case of thermoluminescence of the ZnS phosphor, the transition of electrons from shallow to deep levels is insignificant. Indeed, the sharp increase in the I maximum, and the fact that II and III maxima remain unchanged, contradict the assumption that a large number of secondary localizations of electrons takes place in the process of thermoluminescence.

A sharp increase in the number of electrons in small local levels of the phosphor should have caused the growth of maxima II and III, which is actually not observed as Fig. 12 shows.

The expressed statement concerning the unimportance of secondary localization in the thermoluminescence of zinc phosphors is also confirmed by the following data. We have conducted an experiment to investigate the distribution of electrons in local levels of ZnS-Cu phosphor excited at different temperatures. For this purpose, samples were first excited at the temperature of liquid nitrogen and, in subsequent experiments, at higher temperatures (up to + 20° C), after which we have plotted the curves of thermoluminescence. The number of electrons stored on the levels of any one band at a definite temperature was determined by planimetric measurement of the area of the corresponding maximum, determined by the curve of electroluminescence. It was found that the number of electrons stored at deep levels is 20-25% higher at high excitation temperatures compared with the number at low excitation temperatures. This is explained by the impossibility of binding electrons to low levels at high excitation temperatures and their secondary localization at deep levels. It is clear from this that if in the process of excitation, when the number of electrons in the low local levels is continuously being restored, only a small fraction of them (20-25%) undergoes secondary localization to deeper levels, then in the process of thermoluminescence, when the number of electrons in low local levels is not replenished by excitation, the number of secondary localizations will be considerably less than 25%. We are referring to reference 11, in which it is shown by use of ZnS-Cu, Pb phosphor as an example, that there exists a great number of optically freed secondary electron localizations, while secondary localizations are practically absent in the process of thermoluminescence.

It can be stated, on the basis of what has been presented and as mentioned in the introduction, that, with certain approximation, the heights of the maxima of the thermoluminescent curves for our phosphors, under conditions of our experiments, are proportional to the number of electron filled levels.

5. CONCLUSION

I. The study of the origin of each maximum of the thermoluminescence curve for ZnS-Cu phosphor permits the following deductions:

(1) Maximum I ($T = -120°$ C) is apparently conditioned by the presence of excess zinc in the ZnS lattice.

(2) The maximum II ($T = -60°$ C) consists of three parts bound by temperatures −90° to −60°, −60° to −40° and −40° to 0° C. The origin of these parts is connected with the presence in the lattice of oxygen, combination of oxygen and copper, and copper, respectively.

(3) Maximum III ($T = +20°$ C) is formed by the luminescent centers of copper.

The existence of the Cu and Zn activators is therefore the main cause of giving rise to levels of electron localization. In addition, oxygen plays an important role in their formation.

II. The study of the quenching action of iron, nickel and cobalt on the thermoluminescence of ZnS-Cu phosphor shows that cobalt exhibits a stronger quenching action on low temperature maxima than on the high temperature maxima. It was established that as a consequence of this regular behavior, cobalt in concentrations of 10^{-6} gm/gm forms a new high temperature maximum ($T = +80°$ C). The differences in the quenching of different maxima by nickel are less pronounced. Iron, unlike cobalt, quenches high temperature maxima more effectively than the low temperature maxima. It was established that as a consequence of this regular behavior, nickel, expecially in small concentrations of 10^{-7}–10^{-6} gm/gm, produces a sharp increase in the intensity of the low temperature maximum ($T = -120°$ C) while the intensities of the II and III maxima remain unchanged. The latter effect indicates that there were few secondary electron localizations under the conditions of our experiments.

This investigation was carried out under the supervision of Prof. V.L. Levshin to whom the author expresses deep gratitude for his continuous interest in this work.

---

[11] G. F. Garlick and D. E. Mason, J. Electrochem. Soc. **96**, 90 (1949).

Translated by J. L. Herson
254

SOVIET PHYSICS JETP VOLUME 2, NUMBER 4 JULY, 1956

The (d, p) Reaction on Heavy Nuclei

K. A. Ter-Martirosian
Leningrad Physico-Technical Institute, Academy of Sciences, USSR

(Submitted to JETP editor July 28, 1954)
J. Exper. Theoret. Phys. USSR **29**, 713-729 (December, 1955)

The differential cross section for the (d, p) reaction on a heavy nucleus is calculated for the case where the effect of the Coulomb field is fundamental in determining the angular distribution. The differential cross section over the region of large angles increases with increasing angle, while the behavior of the cross section is weakly dependent on the angular momentum l_n of the state into which the neutron is captured. The total cross section is determined and the factor multiplying the exponential is estimated.

At the present time, the (d, p) reaction has been studied in detail mainly on light nuclei, where the effect of the Coulomb field of the nucleus is not very important. In this case, the protons which are formed emerge mainly in the forward direction and their angular distribution depends strongly on the angular momentum l_n of the state into which the neutron is captured. These experimental data are in good agreement with a formula proposed by Butler[1]; however, it is still not clear why this agreement occurs, since the approximations used by Butler actually correspond to the Born approximation[2], whose applicability to the calculation of the (d, p) reaction has no basis whatever.

We shall consider a different case of the (d, p) reaction—on heavy nuclei, for low energy E_d of the incident deuterons ($E_d < Ze^2/R_0$), where the effect of the Coulomb field of the nucleus is the main factor in determining the angular distribution. In this case the protons from the (d, p) reaction emerge mainly backward, and their angular distribution depends weakly on l_n. In our case, the whole calculation can be made consistently on the basis of the methods of perturbation theory, which is known to be applicable for large Z and small E_d, because of the smallness of the matrix elements containing the Coulomb wave functions in the repulsive field.

The total cross section for the (d, p) reaction on heavy nuclei (i.e., the Oppenheimer-Phillips process) was calculated by perturbation methods in a whole series of older papers[3-6,7], whose authors limited their considerations to just the spherically symmetric part of the functions $\psi_{\mathbf{k}_d}(\mathbf{r})$ and $\psi_{\mathbf{k}_p}^{(-)}(\mathbf{r})$, describing the motion (in the field of the nucleus) of the incident deuterons and emerging protons, with momenta $\hbar\mathbf{k}_d$ and $\hbar\mathbf{k}_p$ at infinity. To calculate the angular distribution, it is necessary to consider all terms in the expansion of these functions in spherical waves. This is the basic difference between our calculations and those of Lifshitz[7].

1. THE AMPLITUDE FOR THE (d, p) REACTION

The exact value f_{ex} of the amplitude for the reaction $d + A \to B + p$ is given by the formula

$$f_{\text{ex}} = -\frac{1}{4\pi}\frac{2M}{\hbar^2}\int \Psi_B^*(R, \mathbf{r}_n)\,\psi_{\mathbf{k}_p}^{(-)*}(\mathbf{r}_p)\,[V_{np} \tag{1}$$

$$+ V'_p]\,\Psi_{\mathbf{k}_d}^{(\text{ex})}(R, \mathbf{r}_n, \mathbf{r}_p)\,dR\,d\mathbf{r}_n\,d\mathbf{r}_p$$

(the derivation of this formula by the usual methods is given in an Appendix at the end of the paper). Here $V_{np} = V_{np}(|\mathbf{r}_n - \mathbf{r}_p|)$ is the interaction energy of a neutron and a proton whose coordinates are $\mathbf{r}_n$ and $\mathbf{r}_p$, $V'_p = V_p(\mathbf{r}_p, R) - Ze^2/r_p$ is the energy of interaction of the proton with the nucleons of nucleus A minus the Coulomb energy, R represents the collection of coordinates of the nucleons of nucleus A, at whose center of mass the origin is located, Ψ_B is the wave function of the final nucleus B, $\psi_{\mathbf{k}_p}^{(-)}(\mathbf{r}_p)$ is the Coulomb wave function describing the motion of the proton; as $r_p \to \infty$, it reduces to a sum of an incident plane wave (corresponding to the momentum $\hbar\mathbf{k}_d$) and an outgoing spherical wave*. $\Psi_{\mathbf{k}_d}^{(ex)}$ denotes the exact wave function of the system; to go over from the exact formula (1) to the formula given by the first approximation of perturbation theory, we replace it by the "incident" wave, i.e., by

---

[1] S. T. Butler, Proc. Roy. Soc. (London) **208A**, 559 (1951).

[2] E. Gerjuoy, Phys. Rev. **91**, 645 (1953).

[3] J. R. Oppenheimer and M. Phillips, Phys. Rev. **48**, 500 (1935).

[4] H. A. Bethe, Phys. Rev. **53**, 39 (1938).

[5] P. L. Kapur, Proc. Roy. Soc. (London) **163A**, 553 (1937).

[6] G. M. Volkoff, Phys. Rev. **57**, 866 (1940).

[7] E. M. Lifshitz, J. Exper. Theoret. Phys. USSR **8**, 930 (1938).

$$\Psi_A(R)\,\varphi_{\mathbf{k}_d}(\mathbf{r}, \vec{\rho});$$

$$\mathbf{r} = {}^1/_2(\mathbf{r}_n + \mathbf{r}_p), \quad \vec{\rho} = \mathbf{r}_n - \mathbf{r}_p.$$

Here Ψ_A is the eigenfunction of the nucleus A, while $\varphi_{\mathbf{k}_d}$ describes the motion of the deuteron in the pure Coulomb field Ze^2/r_p:

$$\left\{\left[-\frac{\hbar^2}{4M}\nabla_r^2 + \frac{Ze^2}{|\mathbf{r} - {}^1/_2\vec{\rho}\,|}\right] + \left[-\frac{\hbar^2}{M}\nabla_\rho^2 + V_{np}(\rho)\right] - (E_d - \varepsilon_d)\right\}\varphi_{\mathbf{k}_d}(\mathbf{r}, \vec{\rho}) = 0,$$

with momentum $\hbar\mathbf{k}_d$ at infinity ($E_d = \hbar^2 k_d^2/4M$, $\epsilon_d = 2.23$ mev is the binding energy of the deuteron). Replacing $\Psi_{\mathbf{k}_d}^{(ex)}$ by $\Psi_A\,\varphi_{\mathbf{k}_d}$ and neglecting in (1) the potential V_p', which differs from zero only for $r_p \leq R_0$ --in the interior of the nucleus A, where $\psi_{\mathbf{k}_p}^{(-)}$ and $\varphi_{\mathbf{k}_d}$ are exponentially small (if Z is large and E_d small), we obtain $f_{ex} \to f_1$, where

$$f_1 = -\frac{1}{4\pi}\frac{2M}{\hbar^2}\int \Phi_n^*(\mathbf{r} + {}^1/_2\vec{\rho})\,\psi_{\mathbf{k}_p}^{(-)*} \times (\mathbf{r} - {}^1/_2\vec{\rho})\,V_{np}(\rho)\,\varphi_{\mathbf{k}_d}(\mathbf{r}, \vec{\rho})\,d\mathbf{r}\,d\vec{\rho}. \tag{2}$$

The function

$$\Phi_n(\mathbf{r}_n) = \int \Psi_A^*(\mathbf{R})\,\Psi_B(R, \mathbf{r}_n)\,dR \tag{3}$$

is the wave function of the neutron in the final state. This same value of f_1 can be obtained by the standard methods of perturbation theory as the matrix element for the transition between the nonorthogonal states $\Psi_A\varphi_{\mathbf{k}_d}$ and $\Psi_B\,\psi_{\mathbf{k}_p}^{(-)}$.

In the region of values of r_p and r_n greater than R_0, which is the important region in the integrals (1) and (2), $\Psi_{\mathbf{k}_d}^{(ex)}$ is a sum of an "incident" wave $\Psi_A\varphi_{\mathbf{k}_d}$ and various scattered waves (caused solely by nuclear interaction*), whose amplitude decreases exponentially with increasing Z and decreasing E_d. Therefore, the difference $f_{ex} - f_1$ is smaller [i.e., Eq. (2) is more exact] and the perturbation series converges the more rapidly, the larger Z becomes and the smaller E_d.

We express (2) in a form suitable for computation. The regions which are important in the integral (2) are $r > R_0$, and small values $\rho < r_0$, where r_0 is the range of the potential V_{np}; i.e., the important region is $\frac{1}{2}\rho \ll r$ (r_0 is always much smaller than R_0). In this region the variables r and ρ in the equation for $\varphi_{\mathbf{k}_d}$ are separable, and its solution to terms of order $(\rho/2r)^2 < (r_0/2R_0)^2$ has the simple form: $\varphi_{\mathbf{k}_d} \approx \varphi_d(\rho)\,\psi_{\mathbf{k}_d}(\mathbf{r})$, where φ_d is the internal wave function of the deuteron:

$$\varphi_d = \sqrt{\frac{\xi_d\varkappa_d}{2\pi}}\,\frac{1}{\rho}\,e^{-\varkappa_d\rho} \quad \text{for } \rho > r_0,$$

($\kappa_d = (M\epsilon_d)^{1/2}/\hbar$, $\xi_d \simeq 3/2$ is a correction factor for normalization) and $\psi_{\mathbf{k}_d}$ is the solution of the equation

$$\left(-\frac{\hbar^2}{2M}\nabla^2 + \frac{Ze^2}{r} - E_d\right)\psi_{\mathbf{k}_d} = 0,$$

---

* We always normalize the wave functions of the continuous spectrum to unit amplitude at infinity.

* The scattering of the deuteron in the Coulomb field is already taken into account in the "incident" wave $\Psi_A\,\varphi_{\mathbf{k}_d}$; for this reason the word "incident" is given in quotation marks.

which, for $r \to \infty$, goes over into a sum of plane and spherical outgoing waves. In other words, in the region of small $\rho/2r$, which is important in the integral (2), the polarization of the deuteron by the Coulomb field is unimportant*. Substituting this value of $\varphi_{\mathbf{k}_d}$ in (2), and setting $\psi^{(-)}_{\mathbf{k}_p}(\mathbf{r} - \tfrac{1}{2}\vec{\rho}) \approx \psi^{(-)}_{\mathbf{k}_p}(\mathbf{r})$, $\Phi_n(\mathbf{r} + \tfrac{1}{2}\vec{\rho}) \approx \Phi_n(\mathbf{r})$, which are correct up to terms in the squares of the quantities $k_p r_0/2$ and $\kappa_n r_0/2$ ($\kappa_n = (2M|E_n|)^{1/2}/\hbar$, $|E_n|$ is the neutron binding energy in nucleus B), which are small compared to unity**, we obtain

$$f_1 = 2\sqrt{\frac{\xi_d \varkappa_d}{2\pi}} \int \Phi_n^*(\mathbf{r})\, \psi^{(-)*}_{\mathbf{k}_p}(\mathbf{r})\, \psi_{\mathbf{k}_d}(\mathbf{r})\, d\mathbf{r}, \tag{4}$$

since

$$-\frac{1}{4\pi}\frac{2M}{\hbar^2}\int V_{np}(\rho)\, \varphi_d(\rho)\, d\vec{\rho} \approx \sqrt{\frac{\xi_d \varkappa_d}{2\pi}}.$$

A formula completely analogous to (4) was obtained by Landau and Lifshitz[8], in considering the (d, np) reaction (breakup of the deuteron in the field of the nucleus). In this reaction the final state of the neutron is a state of free motion, so that Ψ_B can be represented approximately[8] in the form $\Psi_A \sqrt{\dfrac{d\mathbf{k}_n}{(2\pi)^3}}\, e^{i\mathbf{k}_n \mathbf{r}_n}$, i.e., according to (3) $\Phi_n(\mathbf{r}_n)$ is a plane wave $\sim e^{i\mathbf{k}_n \mathbf{r}_n}$ (if we do not take into account the change of the neutron wave function under the action of the nuclear force field, which is actually not small).

2. THE NEUTRON WAVE FUNCTION $\Phi_n(\mathbf{r})$

In the region $r > R_0$, which is important in (4), the function $\Phi_n(r)$ of Eq. (3) satisfies the equation:

$$-(\hbar^2/2M)\,\nabla^2\Phi_n = E_n\Phi_n,$$

where $E_n = W_B - W_A$ is the binding energy of the neutron in nucleus B (W_B and W_A are the energies of nuclei B and A), and in accordance with the transformation properties of Ψ_A and Ψ_B under rotation and inversion of the coordinate axes, has the form:

$$\Phi_n(\mathbf{r}, \xi_n) \tag{5}$$

$$= \sum_{j_n = |J_A - J_B|}^{J_A + J_B} C^{J_B M_B}_{J_A M_A j_n \mu_n} \sum_{\sigma_n = \pm 1/2} C^{j_n \mu_n}_{s_n \sigma_n l_n m_n} \chi_{s_n}$$

$$\times\ \sigma_n(\xi_n)\, \Phi_{j_n l_n m_n}(\mathbf{r}),$$

$$\Phi_{j_n l_n m_n}(\mathbf{r}) = \eta_{j_n l_n} \frac{v_{l_n}(\varkappa_n r)}{r}\, e^{-\varkappa_n r}\, Y_{l_n m_n}(\vartheta\varphi),$$

$$v_{l_n} = \sum_{\nu=0}^{l_n} \frac{(l_n + \nu)!}{\nu!\,(l_n - \nu)!}\frac{1}{(2\varkappa_n r)^\nu}.$$

[From now on we write $\Phi_n(\mathbf{r})$ as $\Phi_n(\mathbf{r}, \xi_n)$, i.e., we include the neutron spin variable.] Here $J_A M_A$, $J_B M_B$ are the angular momenta of nuclei A and B, $j_n \mu_n$, $l_n m_n$ and $s_n = \tfrac{1}{2}$, σ_n are the quantum numbers of the total, orbital and spin angular momenta of the neutron (for given j_n, l_n is $j_n + \tfrac{1}{2}$ or $j_n - \tfrac{1}{2}$, depending on the parity of Ψ_A and Ψ_B), $C^{j\mu}_{j_1\mu_1 j_2\mu_2}$

---

* In papers 3-6 the amplitude (2) was written in the form

$$f_1 = -\frac{1}{4\pi}\frac{2M}{\hbar^2}\int \Psi_B^*(R, \mathbf{r}_n)$$

$$\psi^{(-)*}_{\mathbf{k}_p}(\mathbf{r}_p)\, V_n(\mathbf{r}_n, R)\, \Psi_A(R)\, \varphi_{\mathbf{k}_d}(\mathbf{r}, \vec{\rho})\, d\mathbf{r}_n\, d\mathbf{r}_p,$$

so that the important regions in the integral are $r_n \leq R_0$, $r_p > R_0$, i.e., $\rho/2 \approx r$. In this region we have to take into account the deformation of φ_d under the influence of the Coulomb field, and $\varphi_{\mathbf{k}_d}$ has a very complicated structure; the authors of the papers cited limited themselves to the setting up of the spherically symmetric part of $\varphi_{\mathbf{k}_d}$.

** The linear terms in the expansions of $\psi^{(-)}_{\mathbf{k}_p}(\mathbf{r} - \tfrac{1}{2}\vec{\rho})$ and $\Phi_n(\mathbf{r} = \tfrac{1}{2}\vec{\rho})$ in powers of ρ vanish when we integrate over the direction of $\vec{\rho}$ in (2). The quadratic terms are small: $(k_p r_0/2)^2 \sim E_p(\text{mev})/40$, $(\kappa_n r_0/2)^2 \sim E_n(\text{mev})/40$.

[8] L. D. Landau and E. M. Lifshitz, J. Exper. Theoret. Phys. USSR **18**, 750 (1948).

are the Clebsch-Gordon coefficients, $\chi_{s_n \sigma_n}$ is the spin function of the neutron, $\kappa_n = (2M|E_n|)^{1/2}/\hbar$ for $E_n < 0$ and $\kappa_n = -ik_n = -i(2ME_n)^{1/2}/\hbar$ for $E_n > 0$. $\eta_{j_n l_n}$ in (5) is a constant depending on the structure of the nucleus. It can be estimated most simply as follows. We first consider those levels of nucleus B for which the neutron energy E_n is positive. If the function (5) is properly normalized (in accordance with the normalization of Ψ_B so that the integral of $|\Psi_B|^2$ over the interior of the nucleus is unity) the total radial flux of neutrons is

$$\frac{\hbar k_n}{M}\frac{1}{2J_B+1}\sum_{M_A M_B}\int |r\Phi_n(\mathbf{r})|^2_{r\to\infty}\, d\Omega$$

$$= \frac{\hbar k_n}{M}\sum_{j_n}|\eta_{j_n l_n}|^2$$

and is equal to the neutron width $\Gamma_n/\hbar = \sum_{j_n}\Gamma_{j_n l_n}/\hbar$. Thus,

$$|\eta_{j_n l_n}|^2 = (M/\hbar^2 k_n)\,\Gamma_{j_n l_n}.$$

We know[9] that

$$\Gamma_{j_n l_n}$$

$$= 2k_n R_0 |v_{l_n}(-ik_n R_0)\, e^{ik_n R_0}|^{-2}\,[-f'_{j_n l_n}(W_B)]^{-1},$$

where the function in the square brackets depends on the nuclear structure (W_B is the energy of nucleus B). In order to estimate it, we consider the special case $j_n = \frac{1}{2}$, $l_n = 0$, when[9,10] $\Gamma_{\frac{1}{2}0} = (1/2\pi)(E_n/E_0)^{1/2}\, D_{\frac{1}{2}0}(W_B)$, where D is the level spacing and $E_0 \approx 0.7$ mev. Comparing this value with the general expression given above, and setting $\hbar/\sqrt{2ME_0} = \xi_{\frac{1}{2}0}/\kappa_d$ [where $\xi_{\frac{1}{2}0} = (\epsilon_d/2E_0)^{1/2} \approx 1.25$] for convenience in writing, we have:

$$[-f'_{\frac{1}{2},0}(W_B)]^{-1} = \frac{\xi_{\frac{1}{2},0}}{4\pi\kappa_d} D_{\frac{1}{2},0}(W_B).$$

We keep this same estimate for $l_n \neq 0$, setting

$$[-f'_{j_n l_n}(W_B)]^{-1} = \frac{\xi_{j_n l_n}}{2\pi\kappa_d} D_{j_n l_n}(W_B),$$

where $\xi_{j_n l_n}$ is a constant of the order of unity. Then

$$\Gamma_{j_n l_n} \tag{6a}$$

$$= \frac{k_n \xi_{j_n l_n}}{2\pi\kappa_d\, |v_{l_n}(-ik_n R_0)\exp\{ik_n R_0\}|^2} D_{j_n l_n}(W_B),$$

$$|\eta_{j_n l_n}|^2 = \frac{\kappa_d \Gamma_{j_n l_n}}{\sqrt{2\epsilon_d E_n}} = \frac{\xi_{j_n l_n}\kappa_d}{2\pi}$$

$$\times |v_{l_n}(-ik_n R_0)\exp\{ik_n R_0\}|^{-2}\frac{D_{j_n l_n}(W_B)}{\epsilon_d}.$$

Thus, the condition that the integral of $|\Psi_B|^2$ over the interior of the nucleus be equal to unity determines $|\eta_{j_n l_n}|^2$ as an analytic function of the neutron energy E_n. The form of this function does not change when we go from levels of nucleus B with $E_n > 0$ to levels with $E_n < 0$; when this is done we must write κ_n in place of $-ik_n$ on the right-hand side of (6a)*:

$$|\eta_{j_n l_n}|^2 = \frac{\xi_{j_n l_n}\kappa_d}{2\pi} \tag{6b}$$

$$\times\ |v_{l_n}(\kappa_n R_0)\exp\{-\kappa_n R_0\}|^{-2}\cdot\frac{D_{j_n l_n}(W_B)}{\epsilon_d}.$$

Formulas (5)-(6) completely determine $\Phi_n(\mathbf{r})$ over the region which is important in the integral (4).

---

[9] H. Feshbach, D. R. Peaslee and V. F. Weisskopf, Phys. Rev. **71**, 145 (1947).

[10] A. I. Akhiezer and I. Ia. Pomeranchuk, *Some Problems of Nuclear Theory*, GITTL, 1950.

* This same value (6b) can be gotten directly from the condition that the integral of $|\Psi_B|^2$ over the interior of the nucleus be equal to unity. We emphasize once more that the constants κ_d and ϵ_d of the theory of the deuteron are introduced here only for convenience in writing the formulas.

3. THE DIFFERENTIAL CROSS SECTION

Since the spin of the neutron was included in (5) to make our formulas precise, we shall give the expression (4) for the amplitude including the spins of all the particles:

$$f_1 = \sqrt{\frac{2\xi_d\varkappa_d}{\pi}}\int \left(\Phi_n^*(\mathbf{r}, \xi_n)\,\psi_{\mathbf{k}_p}^{(-)*}(\mathbf{r})\cdot\chi^*_{s_p\sigma_p}(\xi_p),\right.$$

$$\left.\psi_{\mathbf{k}_d}(\mathbf{r})\,\chi_{s_d\sigma_d}(\xi_n\xi_p)\right)d\mathbf{r},$$

where $\chi_{s_p\sigma_p}$ and $\chi_{s_d\sigma_d}$ are the spin functions of the proton and deuteron ($s_p = 1/2$, $s_d = 1$). Substituting Φ_n from (5), we express the differential cross section for the (d, p) reaction

$$d\sigma = \frac{1}{(2s_d+1)(2J_A+1)}\sum_{M_A\sigma_d,\, M_B\sigma_p}|f_1|^2\frac{v_p}{v_d}\,d\Omega_p,$$

$$\left(\frac{v_p}{v_d} = \frac{2k_p}{k_d}\right)$$

in the form

$$d\sigma = \frac{2J_B+1}{2(2J_A+1)}\sum\nolimits_{j_n} d\sigma_{j_n l_n}, \tag{7}$$

$$d\sigma_{j_n l_n} = \frac{1}{2l_n+1}\sum_{m_n=-l_n}^{l_n}|f^{(1)}_{l_n m_n}(\vartheta_p)|^2\frac{2k_p}{k_d}\,d\Omega_p;$$

$$f^{(1)}_{l_n m_n}(\vartheta_p) = \sqrt{\frac{2\xi_d\varkappa_d}{\pi}}\,\eta_{j_n l_n} \tag{8}$$

$$\times\int v_{l_n}(\varkappa_n r)\,e^{-\varkappa_n r}\,Y^*_{l_n m_n}(\vartheta\varphi)\,\psi_{\mathbf{k}_p}^{(-)*}(\mathbf{r})\,\psi_{\mathbf{k}_d}(\mathbf{r})\frac{d\mathbf{r}}{r}.$$

Here we have made use of the facts that

$$\sum_{\sigma_p\sigma_d}\Big|\sum_{\sigma_n}A_{\sigma_n}(\chi^*_{s_n\sigma_n}\chi^*_{s_p\sigma_p},\ \chi_{s_d\sigma_d})\Big|^2 = \frac{3}{2}\sum_{\sigma_n}|A_{\sigma_n}|^2,$$

$$\sum_{(M_B-M_A=\mu_n)}{}' C^{J_BM_B}_{J_AM_A,\, j_n\mu_n}C^{J_BM_B}_{J_AM_A,\, j'_n\mu_n} = \frac{2J_B+1}{2j_n+1}\,\delta_{j_n j'_n};$$

$$\sum_{(\mu_n-\sigma_n=m_n)}{}' C^{j_n\mu_n}_{s_n\sigma_n,\, l_n m_n}C^{j_n\mu_n}_{s_n\sigma_n,\, l'_n m_n} = \frac{2j_n+1}{2l_n+1}\,\delta_{l_n l'_n}.$$

The A_{σ_n} are arbitrary quantities: $\sum'_{(\mu_n-\sigma_n=m_n)}$ denotes summation over all values of μ_n and σ_n for which $\mu_n - \sigma_n = m_n$, where m_n is fixed. We note that formulas (7)-(8) correspond to the formulas of Butler.

We omit from the integral (8) the region of integration $r \leq R_0$, which is unimportant in the case we are considering, and set:

$$f^{(1)}_{l_n m_n} = \sqrt{\frac{2\xi_d\varkappa_d}{\pi}} \tag{8a}$$

$$\times\int_{(r>R_0)}\Phi^*_{j_n l_n m_n}(\mathbf{r})\,\psi_{\mathbf{k}_p}^{(-)*}(\mathbf{r})\,\psi_{\mathbf{k}_d}(\mathbf{r})\,d\mathbf{r}.$$

For large Z, (8a) practically coincides with (8); on the other hand, if we formally set $Z = 0$ in (8a), so that $\psi^{(-)*}_{\mathbf{k}_p}\psi_{\mathbf{k}_d} = \exp\{i(\mathbf{k}_d - \mathbf{k}_p)\cdot\mathbf{r}\}$, then (8a) and (5) give Butler's[1] result:

$$f^{(1)}_{l_n m_n} = \sqrt{\frac{\xi_d\varkappa_d}{2\pi}}\,\eta_{j_n l_n}\frac{4\pi i^{l_n}R_0^2\,Y^*_{l_n m_n}(\vartheta_q\varphi_q)}{\varkappa_d^2 + (^1/_2\mathbf{k}_p - \mathbf{k}_d)^2}$$

$$\times\left[G_{l_n}(qr)\frac{d}{dr}\left(\frac{v_{l_n}(\varkappa_n r)}{r}e^{-\varkappa_n r}\right)\right.$$

$$\left.-\frac{dG_{l_n}(qr)}{dr}\frac{v_{l_n}(\varkappa_n r)}{r}e^{-\varkappa_n r}\right]_{r=R_0},$$

where $q = |\mathbf{k}_d - \mathbf{k}_p|$, $G_{l_n}(x) = \sqrt{\pi/2x}\,J_{l_n+1/2}(x)$, $J_{l_n+1/2}$ is a Bessel function.

Thus (8a) is an interpolation formula, correct for large Z and reducing to Bulter's formula in the limit $Z \to 0$. In the following we shall limit ourselves to the case of large Z and shall use (8) rather than (8a), with the value of Φ_n given by (5) even for $r \leq R_0$, since it is more convenient to calculate the integral over the whole space. Thus the results which we shall obtain do not reduce to Butler's for $Z \to 0$.

4. ANGULAR DISTRIBUTION

In the quasiclassical case which we are considering, when Z is large and E_d small, and $\alpha_d = Ze^2/\hbar v_d > 1$, $\alpha_p = Ze^2/\hbar v_p > 1$ ($v_p = \sqrt{2E_p/M}$, $v_d = \sqrt{E_d/M}$), the angular distribution and the variation of the cross section with energy depend weakly on l_n. In fact, in this case the factor

$$e^{-\varkappa_n r}\psi_{\mathbf{k}_p}^{(-)*}(\mathbf{r})\,\psi_{\mathbf{k}_d}(\mathbf{r})$$

$$= \exp\{-\varkappa_n r + \ln[\psi_{\mathbf{k}_p}^{(-)*}\psi_{\mathbf{k}_d}]\}$$

in the integral (8) varies exponentially as a function of **r**.

The value of the integral of such a rapidly varying function is determined by its value in the neighborhood of the saddle point $\mathbf{r}_1(r_1, \vartheta_1, \varphi_1)$, at which $F(\mathbf{r}) = -\kappa_n r + \ln[\psi_{\mathbf{k}_p}^{(-)*}\psi_{\mathbf{k}_d}]$ is an extremum. Therefore, the slowly varying spherical functions in (8) can be evaluated at $\vartheta = \vartheta_1$ and $\varphi = \varphi_1$ and removed from the integral; if* $\kappa_n r_1 > l_n(l_n + 1)/2$ then the function $v_{l_n} = 1 + l_n(l_n + 1)/2\kappa_n r + \ldots$ in the remaining integral can be replaced by its asymptotic value $v_{l_n} \approx 1$. This gives

$$f_{l_n m_n}^{(1)} \tag{9}$$

$$= \sqrt{2\xi_d\varkappa_d/\pi}\,\eta_{j_n l_n}\sqrt{4\pi}\,Y_{l_n m_n}(\vartheta_1, \varphi_1)\,I_0(\vartheta_p),$$

$$I_0(\vartheta_p) = \frac{1}{\sqrt{4\pi}}\int e^{-\varkappa_n r}\psi_{\mathbf{k}_p}^{(-)*}(\mathbf{r})\,\psi_{\mathbf{k}_d}(\mathbf{r})\,\frac{d\mathbf{r}}{r}.$$

Substituting $f_{l_n m_n}^{(1)}$ in (7) and using the fact that

$$\frac{4\pi}{2l_n + 1}\sum_{m_n = -l_n}^{l_n} |Y_{l_n m_n}(\vartheta_1, \varphi_1)|^2 = 1,$$ we get

$$d\sigma_{j_n l_n} = a_{j_n l_n}\varkappa_d^2\,|I_0(\vartheta_p)|^2\,\frac{2k_p}{k_d}\,d\Omega_p. \tag{10}$$

Here $a_{j_n l_n}$ denotes a dimensionless constant, independent of ϑ_p and E_d and equal, according to (6a, b), to:

$$a_{j_n l_n} = \frac{2\xi_d}{\pi}\frac{|\eta_{j_n l_n}|^2}{\varkappa_d} \tag{11}$$

$$= \begin{cases} \dfrac{\sqrt{2}\,\xi_d}{\pi}\dfrac{\Gamma_{j_n l_n}}{\sqrt{\varepsilon_d E_n}}, & E_n > 0 \\[2ex] \dfrac{\xi_d\xi_{j_n l_n}}{\pi^2}\dfrac{D_{j_n l_n}(W_B)\exp\{2\varkappa_n R_0\}}{\varepsilon_d\,|v_{l_n}(\varkappa_n R_0)|^2}, & E_n < 0. \end{cases}$$

Thus only the absolute value of the cross section depends on l_n, and not its variation with angle and energy.

After substituting in (9) the exact values of the Coulomb functions:

$$\psi_{\mathbf{k}_d} = \sqrt{2\pi\alpha_d}\exp\{-\pi\alpha_d + i\mathbf{k}_d\cdot\mathbf{r}\}\,F(-i\alpha_d,$$

$$1,\ i(k_d r - \mathbf{k}_d\cdot\mathbf{r})),$$

$$\psi_{\mathbf{k}_p}^{(-)*} = \sqrt{2\pi\alpha_p}\exp\{-\pi\alpha_p - i\mathbf{k}_p\cdot\mathbf{r}\}\,F(-i\alpha_p,$$

$$1,\ i(k_p r + \mathbf{k}_p\cdot\mathbf{r}))$$

the integral can be computed exactly (similar integrals were evaluated by Sommerfeld[11,12]). The details are given in the Appendix, where it is shown that

$$I_0(\vartheta_p) = \frac{4\pi^{3/2}\sqrt{\alpha_d\alpha_p}}{(\boldsymbol{k}_d - \boldsymbol{k}_p)^2 + \varkappa_n^2}\exp\{-\pi(\alpha_d + \alpha_p)\}$$

$$\times\left[\frac{(\varkappa_n - ik_d)^2 + k_p^2}{\varkappa_n^2 + (\boldsymbol{k}_d - \boldsymbol{k}_p)^2}\right]^{i\alpha_d}$$

$$\times\left[\frac{(\varkappa_n - ik_p)^2 + k_d^2}{\varkappa_n^2 + (\boldsymbol{k}_d - \boldsymbol{k}_p)^2}\right]^{i\alpha_p}\frac{F(-i\alpha_d, -i\alpha_p, 1, -\zeta)}{1 + \zeta}.$$

The argument ζ of the hypergeometric function depends on the angle ϑ_p between $\mathbf{k}_d$ and $\mathbf{k}_p$:

---

* This condition is almost always fulfilled if l_n is not very large and $|E_n|$ is not very small. For an estimate, we can use the value $r_1 = Ze^2/[E_d + (\sqrt{2|E_n|} - \sqrt{\varepsilon_d})^2]$, which was gotten[7] in calculating an integral of the type of (9) by the saddle-point method. Then

$$\varkappa_n r_1 = 0{,}15Z\frac{\sqrt{2\varepsilon_d|E_n|}}{E_d + (\sqrt{2|E_n|} - \sqrt{\varepsilon_d})^2}$$

$$\left(0{,}15 = \frac{e^2}{\hbar}\sqrt{\frac{M}{\varepsilon_d}}\right).$$

which, for heavy nuclei, gives a value of about ten for $\kappa_n r_1$.

[11] A. Sommerfeld, *Atombau und Spectrallinien IIB.*, Braunschweig, 1939.

[12] A. Sommerfeld, Ann. d. Physik 11, 257 (1931).

$$\zeta = \zeta_0 \sin^2(\vartheta_p/2); \quad \zeta_0 = \frac{4k_d k_p}{(k_d - k_p)^2 + \varkappa_n^2}$$

$$= \frac{4\sqrt{2E_d(E_d + Q)}}{(\sqrt{2E_d} - \sqrt{E_d + Q})^2 + E_n},$$

where $Q = E_p - E_d = -E_n - \epsilon_d$ is the Q of the reaction. For $E_n < 0$, κ_n is real, so that the quantities in square brackets in $I_0(\vartheta_p)$ are complex:

$$(\varkappa_n - ik_d)^2 + k_p^2 = -(k_d^2 - \varkappa_n^2 - k_p^2)$$

$$- 2ik_d\varkappa_n = c_1 e^{-i(\pi - \varphi_d)},$$

$$(\varkappa_n - ik_p)^2 + k_d^2 = (k_d^2 + \varkappa_n^2 - k_p^2)$$

$$-2ik_p\varkappa_n = c_2 e^{-i\varphi_p},$$

where c_1 and c_2 are the moduli of the complex quantities, and the phases are determined (for $E_n < 0$) by the equations:

$$\operatorname{tg}\varphi_d = \frac{2\varkappa_n k_d}{k_d^2 - k_p^2 - \varkappa_n^2} = \frac{2\sqrt{2|E_n|E_d}}{E_d + \varepsilon_d - 2|E_n|}, \tag{12a}$$

$$0 \leqslant \varphi_d \leqslant \pi,$$

$$\operatorname{tg}\varphi_p = \frac{2\varkappa_n k_p}{k_d^2 - k_p^2 + \varkappa_n^2} = \frac{2\sqrt{|E_n|(E_d + Q)}}{E_d + \varepsilon_d},$$

$$0 \leqslant \varphi_p \leqslant \frac{\pi}{2}.$$

According to (12a), the angles φ_d and φ_p go to zero for $|E_n| \to 0$, and obviously remain equal to zero for any $E_n > 0$, when $\kappa_n = -ik_n$ is a pure imaginary number:

$$E_n > 0, \quad \varphi_d = \varphi_p = 0. \tag{12b}$$

We can therefore write, for $E_n > 0$ and $E_n < 0$:

$$|I_0(\vartheta_p)| = \frac{4\pi\sqrt{\pi\alpha_d\alpha_p}}{(k_d - k_p)^2 + \varkappa_n^2} \exp\{-(\alpha_d\varphi_d - \alpha_p\varphi_p)\}$$

$$\times \left| \frac{e^{-\pi\alpha_p} F(i\alpha_d, i\alpha_p, 1, -\zeta)}{1 + \zeta} \right|$$

or, according to (10):

$$d\sigma_{j_n l_n} = a_{j_n l_n} \frac{8\pi^2\varkappa_d^2\alpha_d}{[(k_d - k_p)^2 + \varkappa_n^2]^2} \tag{13}$$

$$\times \exp\{-2(\alpha_d\varphi_d - \alpha_p\varphi_p)\} N(\zeta)\, d\Omega_p,$$

where the function

$$N(\zeta) = 2\pi\alpha_d \left| \frac{e^{-\pi\alpha_p} F(i\alpha_d, i\alpha_p, 1, -\zeta)}{1 + \zeta} \right|^2 \tag{14}$$

determines the dependence of the cross section on ϑ_p. In the case we are considering, when $\alpha_d > 1$, or $\alpha_p > 1$, the hypergeometric function has the following asymptotic value:

$$|F(i\alpha_d, i\alpha_p, 1, -\zeta)|^2 \tag{15}$$

$$\approx \frac{1 + \zeta}{2\pi\alpha_d\zeta} \frac{\exp\{2\pi\alpha_p + 2(\alpha_d\psi_d - \alpha_p\psi_p)\}}{\sqrt{(4\rho/\zeta) - (1 - \rho)^2}},$$

the derivation of which is given in the Appendix. The angles ψ_d and ψ_p are defined by the equations

$$\cos\psi_d = \frac{(1 - \rho)\zeta + 2}{2\sqrt{1 + \zeta}}, \quad 0 \leqslant \psi_d \leqslant \pi, \tag{16}$$

$$\cos\psi_p = \frac{(1 - \rho)\zeta - 2\rho}{2\rho\sqrt{1 + \zeta}}, \quad 0 \leqslant \psi_p \leqslant \pi, \tag{16a}$$

where $\rho = \alpha_p/\alpha_d = k_d/2k_p = (E_d/2E_p)^{1/2}$. The equality (15) is valid for not too small ζ--roughly speaking, until $\zeta \sim 1/\alpha_d$; more precisely, for $\zeta > \zeta'$, where

$$\frac{\zeta'^2}{1 + \zeta'} \sqrt{(4\alpha_d\alpha_p/\zeta') - (\alpha_d - \alpha_p)^2} = \min\left\{\frac{\alpha_p}{\alpha_d}, \frac{\alpha_d}{\alpha_p}\right\}$$

(cf. the Appendix). If $\zeta \to 0$, then $|F(i\alpha_d, i\alpha_p, 1, -\zeta)/(1 + \zeta)| \to 1$. Therefore:

$$N(\zeta) = \begin{cases} [\zeta(1+\zeta)\sqrt{(4\rho/\zeta)-(1-\rho)^2}]^{-1}\exp\{2(\alpha_d\psi_d-\alpha_p\psi_p)\}, & \text{if} \quad \zeta > \zeta', \\ 2\pi\alpha_d \exp\{-2\pi\alpha_p\}, & \text{if} \quad \zeta \to 0, \end{cases} \tag{17}$$

or

$$N(\zeta) = \exp\{\alpha_d L_\rho(\zeta)\} / M_\rho(\zeta), \tag{18}$$

where

$$L_\rho(\zeta) = 2(\psi_d - \rho\psi_p), \quad L_\rho(0) = -2\pi\rho,$$

$$M_\rho(\zeta) = \zeta(1+\zeta)\sqrt{(4\rho/\zeta)-(1-\rho)^2},$$

$$M_\rho(0) = 1/2\pi\alpha_d.$$

Graphs of the functions $L_\rho(\zeta)$ and $M_\rho(\zeta)$ are shown in Fig. 1. As we see from the figure, $L_\rho(\zeta)$ increases with increasing ζ [reaching zero for $\zeta = 4\rho/(1-\rho)^2$, while $\zeta_0 < 4\rho/(1-\rho)^2$ throughout]. This increase causes an exponential increase in $N(\zeta)$, i.e., in the cross section, with increasing ϑ_p.

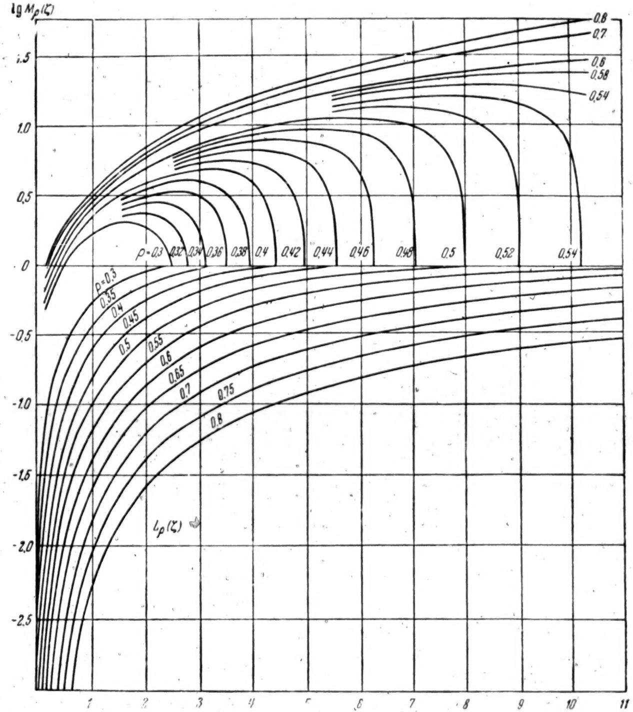

FIG. 1

The function $N(\zeta)$ is a maximum for $\vartheta_p = \pi$, $\zeta = \zeta_0$; for small $\pi - \vartheta_p$, its dependence on $\pi - \vartheta_p$ is approximately a Gaussian. This can be seen by expanding $L_\rho(\zeta)$ in series in powers of $\zeta_0 - \zeta = \zeta_0 \cos^2(\vartheta_p/2) \approx \zeta_0(\pi - \vartheta_p)^2/4$:

$$L_\rho(\zeta) = L_\rho(\zeta_0) - \frac{\varkappa_d}{k_p(1+\zeta_0)}(\zeta_0 - \zeta) + \cdots$$

(since $\left(\frac{dL_\rho}{d\zeta}\right)_{\zeta_0} = \frac{\sqrt{(4\rho/\zeta_0) - (1-\rho)^2}}{1+\zeta_0}$,

$\left.\sqrt{\frac{4\rho}{\zeta_0} - (1-\rho)^2} = \frac{\varkappa_d}{k_p}\right]$) and neglecting the change of the factor $M_\rho(\zeta)$ outside of the exponential in (18). We then get:

$$N(\zeta) \simeq A \exp\{-(\pi - \vartheta_p)^2 \delta^{-2}\},$$

$$\pi - \vartheta_p \ll 1,$$

where

$$\delta^2 = \frac{(k_d - k_p)^2 + \varkappa_n^2}{\alpha_d \varkappa_d k_d}$$

$$= \frac{(\sqrt{2E_d} + \sqrt{E_d + Q})^2 + Q + \varepsilon_d}{\beta \varepsilon_d},$$

$$\beta = \frac{Ze^2}{h}\sqrt{\frac{M}{\varepsilon_d}} = 0.15\,Z.$$

The width δ of the angular distribution is smaller, the larger Z and the smaller E_d, and the higher the nuclear level into which the neutron is captured (i.e., the smaller Q). This conclusion also follows from consideration of the angular distribution curves of Fig. 2 for various cases (the curves are drawn on a logarithmic scale).

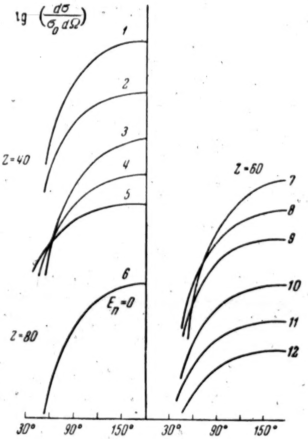

FIG. 2. $1 - E_n = -2$, $2 - E_n = -4$, $E = 2$ mev; $3 - E_n = 1$, $4 - E_n = 0$, $5 - E_n = -2$, $E = 4$ mev; $6 - E_n = 0$, $E = 6$ mev; $7 - E_n = 0$, $8 - E_n = -2$, $9 - E_n = -4$, $E = 4$ mev; $10 - E_n = 0$, $11 - E_n = -2$, $12 - E_n = -4$, $E = 6$ mev

5. TOTAL CROSS SECTION

In order to calculate the total cross section, we integrate (13) over ϑ_p; noting that $d\Omega_p = (4\pi/\zeta_0)\, d\zeta$, we get the integral:

$$\int N(\zeta)\, d\Omega_p = \frac{4\pi}{\zeta_0}\int_0^{\zeta_0} N(\zeta)\, d\zeta$$

$$= \frac{4\pi}{\zeta_0}\int_0^{\zeta_0} \frac{\exp\{\alpha_d L_\rho(\zeta)\}\, d\zeta}{\zeta(1+\zeta)\sqrt{\frac{4\rho}{\zeta} - (1-\rho)^2}},$$

in which, because of the decrease of $L_\rho(\zeta)$ with increasing $\zeta_0 - \zeta$, the values of ζ near to ζ_0 are important. Therefore, as before, we expand $L_\rho(\zeta)$ in powers of $x = \zeta_0 - \zeta$ and extend the x integration to infinity. This gives

$$\int N(\zeta)\, d\Omega_p$$

$$= \frac{\pi}{4\alpha_d}\left[\frac{(k_d - k_p)^2 + \varkappa_n^2}{k_d \varkappa_d}\right]^2 \exp\{\alpha_d L_\rho(\zeta_0)\}$$

(the factor in front of the exponential was taken outside the integral and evaluated at $\zeta = \zeta_0$).

According to (13) we then have:

$$\sigma_{j_n l_n} = 2\pi^3 a_{j_n l_n} k_d^{-2} \exp\{-\beta\Phi(E_d, E_n)\}, \quad (19)$$

$$\begin{aligned}\beta\Phi(E_d, E_n) &= 2(\alpha_d\varphi_d - \alpha_p\varphi_p) - \alpha_d L_\rho(\zeta_0) \\ &= 2[\alpha_d(\varphi_d - \psi_d^{(0)}) - \alpha_p(\varphi_p - \psi_p^{(0)})]\end{aligned}$$

(where $\alpha_d = \beta\sqrt{\epsilon_d / E_d}$, $\alpha_p = \beta\sqrt{\epsilon_d / 2E_p}$). $\psi_d^{(0)}$ and $\psi_p^{(0)}$ are the angles (16) for $\zeta = \zeta_0$. Writing

$$\Phi(E_d, E_n) = \eta_d \sqrt{4\varepsilon_d / E_d} - \eta_p \sqrt{2\varepsilon_d / E_p}, \quad (20a)$$

and using (12a, b)-(16), we express $\eta_d = \varphi_d - \psi_d^{(0)}$ and $\eta_p = \varphi_p - \psi_p^{(0)}$ directly in terms of E_d and E_n:

$$E_n > 0 \begin{cases} \operatorname{tg}\eta_d = \sqrt{2E_d\varepsilon_d} / [E_n - (E_d + Q)], & -\pi \leqslant \eta_d \leqslant 0, \\ \operatorname{tg}\eta_p = 2\sqrt{2(E_d + Q)\varepsilon_d} / [E_n - (E_d + Q) - 2\varepsilon_d], & -\pi \leqslant \eta_p \leqslant 0, \end{cases} \quad (20b)$$

$$E_n < 0 \begin{cases} \operatorname{tg}\dfrac{\eta_d}{2} = (\sqrt{2|E_n|} - \sqrt{\varepsilon_d})\, E_d^{-1/2}, & -\pi \leqslant \eta_d \leqslant \pi \\ \operatorname{tg}\dfrac{\eta_p}{2} = (\sqrt{|E_n|} - \sqrt{2\varepsilon_d})\,(E_d + Q)^{-1/2} & -\pi \leqslant \eta_p \leqslant \pi. \end{cases}$$

These formulas can also be written in the following form ($E_n \gtrless 0$):

$$\Phi(E_d, E_n) = 2\mathrm{Re}\left\{\sqrt{\frac{4\varepsilon_d}{E_d}} \operatorname{arc\,tg} \frac{\sqrt{-2E_n} - \sqrt{\varepsilon_d}}{\sqrt{E_d}} - \sqrt{\frac{2\varepsilon_d}{E_p}} \operatorname{arc\,tg} \frac{\sqrt{-E_n} - \sqrt{2\varepsilon_d}}{\sqrt{E_p}}\right\}$$

$$= 2\,\mathrm{Im}\left\{\sqrt{\frac{4\varepsilon_d}{E_d}} \operatorname{arc\,cosh} \frac{E_d^{1/2}}{[E_d + (\sqrt{\varepsilon_d} - \sqrt{-2E_n})^2]^{1/2}} - \sqrt{\frac{2\varepsilon_d}{E_p}} \operatorname{arc\,cosh} \frac{E_p^{1/2}}{[E_d + (\sqrt{\varepsilon_d} - \sqrt{-2E_n})^2]^{1/2}}\right\}.$$

In this form, $\Phi(E_d, E_n)$ coincides with the expression obtained by Lifshitz[7]. It is not difficult to see that the initial formula of his calculation[7] can be gotten from (8) and (9), if instead of $\psi_{\mathbf{k}_p}^{(-)}$ and $\psi_{\mathbf{k}_d}$, we substitute the spherically symmetric parts of those functions in the quasiclassical approximation, and apply the saddle-point method to evaluate the integral

$$\int_0^\infty \exp\left\{-\beta\sqrt{2\varepsilon_d}\left[\int_{E_d}^{x} \sqrt{2(y - E_d)}\,\frac{dy}{y^2} - \int_{E_p}^{x} \sqrt{y - E_p}\,\frac{dy}{y^2} - \frac{\sqrt{-E_n}}{x}\right]\right\} dx,$$

to which (9) then reduces. (x and y are reciprocal to r: $x = Ze^2/r$.)

Figure 3 shows curves of the dependence of $\Phi(E_d, E_n)$ on $(|E_n| / 2\epsilon_d)^{1/2}$ for the values of $(E_d/\epsilon_d)^{1/2}$ marked on the individual curves. The curves were constructed for the region $E_n < 0$, and their behavior agrees with the analysis of the behavior of the functions $\Phi(E_d, E_n)$ which was given by Lifshitz.

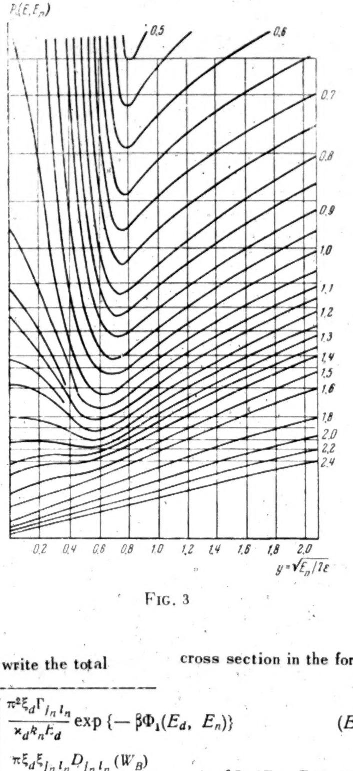

FIG. 3

Substituting (11) in (19), we write the total cross section in the form:

$$\sigma_{j_n l_n} = \begin{cases} \dfrac{\pi^2 \xi_d \Gamma_{j_n l_n}}{\varkappa_d k_n E_d} \exp\{-\beta\Phi_1(E_d, E_n)\} & (E_n > 0) \\ \dfrac{\pi \xi_d \xi_{j_n l_n} D_{j_n l_n}(W_B)}{2\varkappa_d^2 E_d \, | v_{l_n}(\varkappa_n R_0)|^2} \exp\{-\beta\Phi_1(E_d, E_n)\} & (E_n < 0); \end{cases}$$

where $\beta\Phi_1 = \beta\Phi - 2\varkappa_n R_0$, i.e., $\Phi_1 = \Phi - \sqrt{8\epsilon_d |E_n| / B}$, $B = Ze^2/R_0$ is the height of the Coulomb barrier.

Finally, we calculate the overall cross section

$$\sigma_{\text{tot}} = \sum \frac{2J_B + 1}{2(2J_A + 1)} \Sigma_{j_n} \sigma_{j_n l_n} \qquad (22)$$

(summed over all levels of nucleus B with $E_n < 0$) for capture of the neutron into any level with $E_n < 0$ of a heavy nucleus, whose levels are distributed in the region $E_0 \simeq 0$. [Capture in a level with $E_n > 0$ would actually lead to the (d, np) reaction.] Then in the summation in (22) we need only include levels with $l_n = 0$, i.e, $J_B = J_A \pm 1/2$, since $e^{-\beta\Phi_1}$ drops rapidly* with increasing $|E_n|$ so that only levels with small

---

[*] We should keep in mind the case when $(E_d/\epsilon_d)^{1/2} \geq 1.8$, where, according to Fig. 3, Φ increases approximately linearly with increasing $|E_n|^{1/2}$.

$|E_n|$ are important in the summation, while for small $|E_n|$, the quantity $|v_{l_n}(\kappa_n R_0)|^{-2}$ is proportional to $E_n^{l_n}$. Going over from a summation over levels to an integration [the sum over levels is equal to $\int d|E_n|/D(W_B)$], and using the fact that on the average $\overline{2J_B+1} = 2J_A + 1$ (if $J_B = J_A \pm 1/2$), we get from (21):

$$\sigma_{\text{tot}} = \frac{1}{2}\,\frac{\pi\xi_d\xi_{1/2,0}}{2\varkappa_d^2}\int\limits_0^{|E_n^0|}\exp\{-\beta\Phi_1(E_d,\,E_n)\}\,\frac{d|E_n|}{E_d}, \tag{23a}$$

$|E_n^0|$ is the binding energy of the neutron in the ground state of nucleus B. The integral can be calculated approximately, by expanding $\Phi_1(E_d, E_n)$ in powers of $|E_n|^{1/2}$:

$$\beta\Phi_1(E_d,\,E_n) = \beta\Phi(E_d,\,0) + \sqrt{\frac{8}{E_0}}\,\frac{B - E_d - \varepsilon_d}{E_d + \varepsilon_d}\sqrt{|E_n|},\quad E_0 = \frac{\hbar^2}{MR_0^2}$$

[according to (20a, b), $(\partial\Phi/\partial|E_n|^{1/2})_{E_n=0} = \sqrt{3\epsilon_d}/(E_d+\epsilon_d)$] and extending the integration over $|E_n|^{1/2}$ to infinity. We obtain

$$\sigma_{\text{tot}} = \frac{\pi\xi_d\xi_{1/2,0}}{16\varkappa_d^2}\,\frac{E_0}{E_d}\left(\frac{E_d + \varepsilon_d}{B - E_d - \varepsilon_d}\right)^2\exp\{-\beta\Phi(E_d,\,0)\}, \tag{23b}$$

where, according to formulas given earlier,

$$\Phi(E_d,\,0) = 2\left(\sqrt{\frac{2\varepsilon_d}{E_p}}\operatorname{arc\,tg}\sqrt{\frac{2\varepsilon_1}{E_p}} - \sqrt{\frac{4\varepsilon_d}{E_d}}\operatorname{arc\,tg}\sqrt{\frac{\varepsilon_d}{E_d}}\right).$$

6. THE REGION OF VALIDITY OF THE CALCULATION

We must emphasize that the region of applicability of formulas (18)-(23) is very limited. The fundamental reason for this is related to our having neglected all terms Δf proportional to the value of $\psi^{(-)*}_{\mathbf{k}_p}\psi_{\mathbf{k}_d}$ in the region inside the nucleus[*] compared to the amplitude f_1 given by formulas (4)-(8). According to (13), f_1 is proporportional to the exponential

$$\exp\left\{\frac{\beta}{2}\Phi(E_d,\,E_n) - \frac{1}{2}\ln\frac{N(\zeta_0)}{N(\zeta)}\right\},$$

while we have dropped terms corresponding to the value of $\psi^{(-)*}_{\mathbf{k}_p}\psi_{\mathbf{k}_d}$ for $r = R_0$, which in the quasiclassical approximation (if we consider only S-waves) is determined by the exponential

$$\exp\{-{}^1/_2\,\beta\Phi_z(E_d,\,E_n)\},$$

$$\Phi_z = 2\sqrt{\frac{4\varepsilon_d}{B}}\left\{\gamma\left(\frac{E_d}{B}\right) + \frac{1}{\sqrt{2}}\gamma\left(\frac{E_p}{B}\right)\right\},$$

$$\gamma(\varkappa) = \sqrt{\varkappa}\arccos\sqrt{\varkappa} - \sqrt{1-\varkappa}.$$

If we assume (as is verified by calculation) that the factors in front of the exponentials in Δf and f_1 are of the same order, then we find that neglecting Δf compared to f_1 is permissible if

$$\beta(\Phi_z - \Phi) - \ln\frac{N(\zeta_0)}{N(\zeta)} > 2. \tag{24}$$

---

[*] In particular, we substituted into (8) the incorrect value (5) for Φ_n in the region $r < R_0$. If the correct value is substituted, the region inside the nucleus automatically gives a small contribution to the integral (8), because of the rapid oscillation or the damping of Φ_n in this region.

This condition severely limits the values of Z, E_d and ϑ_p. It is well satisfied only for heavy nuclei ($Z > 50$), for $E_d < B$, and under conditions where the angle ϑ_p is not small. Thus, even for heavy nuclei, formulas (17)-(18) give the proton angular distribution correctly only in the region of large values of ϑ_p. This significantly decreases the reliability of the data given in Sec. 5 on total cross sections; for more accurate calculations, we would have to start not from (8), but from (8b), where the region inside the nucleus is taken into account completely.

The author expresses his thanks to Academician L. D. Landau for discussion and many valuable comments. The present calculation was carried out in 1951, in connection with experimental work of Academician P. I. Lukirskii and Prof. Iu. A. Nemilov.

APPENDIX

I. DERIVATION OF FORMULA (1) FOR f_{ex}

We multiply both sides of the Schrodinger equation:

$$\left\{-\frac{\hbar^2}{2M}\nabla^2_{r_p}+\left[-\frac{\hbar^2}{2M}\nabla^2_{r_n}+V_n(\mathbf{r}_n, R)+\mathscr{H}_A(R)\right]\right.$$

$$+V_p(\mathbf{r}_p, R)$$

$$\left.+V_{np}(|\mathbf{r}_n-\mathbf{r}_p|)\right\}\Psi^{(\text{ex})}_{\mathbf{k}_d}=(E_p+W_B)\Psi^{\text{ex}}_{\mathbf{k}_d}$$

[$\hat{\mathscr{H}}_A(R)$ is the Hamiltonian of nucleus A, $E_p+W_B = E_d-\epsilon_d+W_A$] by $\Psi^*_B(R, \mathbf{r}_n)$ and integrate over R and $\mathbf{r}_n$. This gives:

$$\left[-\frac{\hbar^2}{2M}\nabla^2_{r_p}-E_p\right]F(\mathbf{r}_p) \qquad \text{(a)}$$

$$=-\int\Psi^*_B[V_p+V_{np}]\Psi^{(\text{ex})}_{\mathbf{k}_d}\,dR\,d\mathbf{r}_n,$$

where the function

$$F(\mathbf{r}_p)=\int\Psi^*_B(R, \mathbf{r}_n)\Psi^{(\text{ex})}_{\mathbf{k}_d}(R, \mathbf{r}_n, \mathbf{r}_p)dR\,d\mathbf{r}_n$$

for $r_p\to\infty$ has the form $F(\mathbf{r}_p)\sim r_p^{-1}f_{\text{ex}}\exp\{i(k_pr_p-\alpha_p\ln 2k_pr_p)\}$ [the outgoing wave is distorted by the Coulomb field, since the potential on the right side of (a) drops like $1/r_p$ as $r_p\to\infty$]. We consider an equation of somewhat more general form than (a), which we get if we add to both sides of (a) the term $V^0_p(r_p)F(\mathbf{r}_p)=\int\Psi^*_BV^0_p(r_p)\Psi^{(\text{ex})}_{\mathbf{k}_d}\times dR\,d\mathbf{r}_n$, where $V^0_p(r_p)$ is an arbitrary function which goes over into Ze^2/r_p for $r_p\to\infty$:

$$\left[\nabla^2_{r_p}-\frac{2M}{\hbar^2}V^0_p+k^2_p\right]F(\mathbf{r}_p) \qquad \text{(b)}$$

$$=\frac{2M}{\hbar^2}\int\Psi^*_B[V_{np}+V'_p]\Psi^{(\text{ex})}_{\mathbf{k}_d}\,dR\,d\mathbf{r}_n;$$

Here $V'_p=V_p-V^0_p$; as $r_p\to\infty$, V'_p drops faster than $1/r_p$.

To solve Eq. (b), we note that the function

$$G(\mathbf{r}_p, \mathbf{r}'_p)=k_p\sum_{l_pm_p}\mathscr{H}_{l_p}(r_p)Y_{l_pm_p}(\vartheta_p, \varphi_p)$$

$$\times L_{l_p}(r'_p)Y^*_{l_pm_p}(\vartheta'_p, \varphi'_p), \quad r_p>r'_p$$

(with a similar definition for $r_p<r'_p$, with the coordinates r_p and r'_p interchanged on the right side), satisfies the equation

$$\left[\nabla^2_{r_p}-2M\hbar^{-2}V^0_p+k^2_p\right]G(\mathbf{r}_p, \mathbf{r}'_p)=\delta(\mathbf{r}_p-\mathbf{r}'_p)$$

and, for $r_p\to\infty$, has the form

$$G(\mathbf{r}_p, \mathbf{r}'_p)\approx\frac{1}{r_p}\exp\{i(k_pr_p-\alpha_p\ln 2k_pr_p)\} \qquad \text{(c)}$$

$$\times\sum_{l_pm_p}\exp\left\{-i\frac{l_p\pi}{2}+i\eta_{l_p}\right\}L_{l_p}(r'_p)$$

$$\times Y^*_{l_pm_p}(\vartheta'_p, \varphi'_p)Y_{l_pm_p}(\vartheta_p, \varphi_p)$$

$$=(1/4\pi r_p)\exp\{ik_pr_p-\alpha_p\ln 2k_pr_p)\}\psi^{(-)*}_{\mathbf{k}_p}(\mathbf{r}'_p).$$

Here $L_{l_p}(r_p)Y_{l_pm_p}(\vartheta_p\varphi_p)$ is the solution, which remains finite for $r_p\to 0$, of the equation

$$[\nabla^2_{r_p}-2M\hbar^{-2}V^0_p+k^2_p]L_{l_p}(r_p)Y_{l_pm_p}(\vartheta_p, \varphi_p) \qquad \text{(d)}$$

$$=0,$$

so that

$$L_{l_p}(r_p) \approx (k_p r_p)^{-1} \sin\left(k_p r_p - \frac{l_p \pi}{2} + \eta_{l_p} - \alpha_p \ln 2k_p r_p\right), \quad \text{if} \quad r_p \to \infty;$$

$\mathcal{H}_{l_p}(r_p) Y_{l_p m_p}(\vartheta_p, \varphi_p)$ is the other solution (singular for $r_p \to 0$) of the same equation, so

$$\mathcal{H}_{l_p}(r_p) \approx (k_p r_p)^{-1} \exp\left\{i\left(k_p r_p - \frac{l_p \pi}{2} + \eta_{l_p} - \alpha_p \ln 2k_p r_p\right)\right\}, \quad \text{if} \quad r_p \to \infty.$$

Finally,

$$\psi_{\mathbf{k}_p}^{(-)}(\mathbf{r}_p) = 4\pi \sum_{l_p, m_p} \exp\left\{\frac{i l_p \pi}{2} - i\eta_{l_p}\right\} L_{l_p}(r'_p) Y_{l_p m_p}(\vartheta'_p, \varphi'_p) Y_{l_p m_p}(\vartheta_p, \varphi_p)$$

is the solution of the same equation (d), which for $r_p \to \infty$ becomes a sum of a plane wave (with wave vector $\mathbf{k}_p = k_p \mathbf{r}_p / r_p$) and an outgoing spherical wave distorted by the Coulomb field.

It is clear that the required solution of Eq. (b) has the form:

$$F(\mathbf{r}_p) = -\int G(\mathbf{r}_p, \mathbf{r}'_p) \{2M\hbar^{-2} \int \Psi_B^*(R, \mathbf{r}_n) [V_{np}(|\mathbf{r}_n - \mathbf{r}'_p|)$$

$$+ V'_p(\mathbf{r}'_p, R)] \Psi_{\mathbf{k}_d}^{(ex)}(R, \mathbf{r}_n, \mathbf{r}'_p) \, dR \, d\mathbf{r}_n\} \, d\mathbf{r}'_p.$$

For $r_p \to \infty$, $F(r_p)$ according to (c) has the form of an outgoing wave, while (c) gives the value of the amplitude f_{ex} which appears on the right of Eq. (1) in the body of the paper. For the special choice $V_p^0 = Ze^2/r_p$, V'_p has the value $V_p - Ze^2/r_p$ given in the text.

II. CALCULATION OF THE INTEGRAL $I_0(\vartheta_p)$.

(Cf. REFS. 11, 12)

We substitute into the integral (9) given in the text the expressions for the Coulomb functions, where we use for the hypergeometric function $F(\alpha, \gamma, z) = e^{z} F(\gamma - \alpha, \gamma, -z)$ the representation[12]:

$$F(\gamma - \alpha, \gamma, -z) = \frac{\Gamma(\gamma)}{\Gamma(\gamma - \alpha)} z^{(1-\gamma)/2} e^{z} \int_0^\infty u^{(\gamma - 1 - 2\alpha)/2} J_{\gamma - 1}(2\sqrt{zu}) e^{-u} \, du. \tag{e}$$

This gives:

$$I_0(\vartheta_p) = \frac{\sqrt{\pi \alpha_p \alpha_d} \exp\{-\pi(\alpha_p + \alpha_d)\}}{\Gamma(1 + i\alpha_p) \Gamma(1 + i\alpha_d)} \int_0^\infty v^{i\alpha_d} e^{-v} \, dv \int_0^\infty u^{i\alpha_p} e^{-u} \, du \, X(u, v), \tag{f}$$

$$X(u, v) = \int \exp\{-[\varkappa_n + i(k_d + k_p)] r\} J_0(2\sqrt{ik_d \eta v}) J_0(2\sqrt{ik_p \xi' u}) \frac{d\mathbf{r}}{r}.$$

Here, $\eta = r - \mathbf{r} \cdot \mathbf{k}_d / k_d$, $\xi = r + \mathbf{r} \cdot \mathbf{k}_d / k_d$ (or $\eta' = r - \mathbf{r} \cdot \mathbf{k}_p / k_p$, $\xi' = r + \mathbf{r} \cdot \mathbf{k}_p / k_p$) are parabolic coordinates,

$$\xi' = \xi \cos^2(\vartheta_p / 2) + \eta \sin^2(\vartheta_p / 2)$$

$$+ 2\sqrt{\xi\eta} \cos(\vartheta_p / 2) \sin(\vartheta_p / 2) \cos \varphi,$$

where $\cos\vartheta_p = \mathbf{k}_p \cdot \mathbf{k}_d / k_p k_d$, φ is the angle between the planes of the vectors $\mathbf{k}_d$, $\mathbf{k}_p$ and $\mathbf{k}_d$, $\mathbf{r}$. The calculation of $X(u, v)$ is conveniently done in the parabolic coordinates ξ, η, φ, in which $r = \frac{1}{2}(\xi + \eta)$, $d\mathbf{r} = \pi r d\xi d\eta d\varphi / 2\pi - 2(ik_p u \xi')^{1/2} = (\sigma^2 + \rho^2 - 2\sigma\rho\cos(\pi - \varphi))^{1/2}$, where $\sigma = 2(ik_p \xi u)^{1/2}\cos(\vartheta_p/2)$, $\rho = 2(ik_p u\eta)^{1/2} \times \sin(\vartheta_p/2)$. According to the addition theorem:

$$J_0(2\sqrt{ik_p u\xi'}) = \sum_{n=-\infty}^{\infty} J_n(\sigma) J_n(\rho) e^{in(\pi-\varphi)},$$

so that the integration over φ in $X(u, v)$ gives simply

$$\int_0^{2\pi} J_0(2\sqrt{ik_p u\xi'})\, d\varphi / 2\pi = J_0(\sigma) J_0(\rho),$$

from which $X(u, v) = \pi \mathfrak{J}_1 \mathfrak{J}_2$,

where

$$\mathfrak{J}_1 = \int_0^{\infty} e^{-a\xi} J_0(\sigma)\, d\xi = (1/a)\exp\left\{- i\frac{k_p u}{a}\cos^2\frac{\vartheta_p}{2}\right\};$$

$$\mathfrak{J}_2 = \int_0^{\infty} e^{-a\eta} J_0(\rho) J_0(2\sqrt{ik_d v\eta})\, d\eta = \frac{1}{2}\exp\left\{- i\frac{k_p u}{a}\sin^2\frac{\vartheta_p}{2} - i\frac{k_d v}{a}\right\} \times J_0\left(\frac{2\sqrt{k_p k_d uv}}{a}\sin\frac{\vartheta_p}{2}\right),$$

and $a = \frac{1}{2}[\kappa_n - i(k_p + k_d)]$. In this integration we have used the general formula:

$$\int_0^{\infty} e^{-au} J_m(\alpha u^{1/2}) J_m(\beta u^{1/2})\, du = \frac{i^m}{a} e^{(\alpha^2+\beta^2)/4a} J_m\left(\frac{\alpha\beta}{2ia}\right).$$

Thus

$$X(u, v) = \frac{\pi}{a^2}\exp\{-i(k_p u + k_d v)/a\} \times J_0\left(\frac{2}{a}\sqrt{k_p k_d uv}\sin\frac{\vartheta_p}{2}\right).$$

Substituting this value in (f), keeping in mind Eq. (e), and noting that

$$F(\alpha\beta\gamma z) = \frac{1}{\Gamma(\alpha)}\int_0^{\infty} e^{-u} u^{\alpha-1} F(\beta, \gamma, uz)\, du,$$

we get:

$$I_0(\vartheta_p) = \frac{\pi^{3/2}\sqrt{\alpha_p\alpha_d}}{a^2}\left(\frac{a}{a + ik_d}\right)^{i\alpha_d+1} \times \left(\frac{a}{a + ik_p}\right)^{i\alpha_p+1} e^{-\pi(\alpha_p+\alpha_d)} \times F(i\alpha_d + 1, i\alpha_p + 1, 1, -\zeta),$$

where $\zeta = \dfrac{k_d k_p}{(a + ik_d)(a + ik_p)}\sin^2\dfrac{\vartheta_p}{2} = \zeta_0 \sin^2\dfrac{\vartheta_p}{2}$.

Substituting the value

$$F(i\alpha_d + 1, i\alpha_p + 1, 1, -\zeta) = (1 + \zeta)^{-i\alpha_p - i\alpha_d - 1} F(-i\alpha_d, -i\alpha_p, 1, -\zeta),$$

we then have:

$$I_0(\vartheta_p) = \frac{\pi^{3/2}\sqrt{\alpha_p\alpha_d}\exp\{-\pi(\alpha_d + \alpha_p)\}}{(a + ik_p)(a + ik_d)} \times \left(\frac{a}{(a + ik_d)(1 + \zeta)}\right)^{i\alpha_d} \times \left(\frac{a}{(a + ik_p)(1 + \zeta)}\right)^{i\alpha_p} \frac{F(-i\alpha_d, -i\alpha_p 1, -\zeta)}{1 + \zeta}.$$

After some elementary transformations, one gets from this to the value given in the text.

III. THE ASYMPTOTIC FORM OF $|F(i\alpha_d, i\alpha_p, 1, -\zeta)|^2$ FOR $\alpha_d > 1$

For $\alpha_d > 1$, the contour integral

$$F(i\alpha_d, i\alpha_p, 1, -\zeta)$$

$$= \frac{1}{2\pi i}\int\limits_C \left(\frac{u}{u-1}\right)^{i\alpha_p}(1+\zeta u)^{-i\alpha_d}\frac{du}{u}$$

$$= \int\limits_C \exp\{\alpha_d\varphi(u)\}\frac{du}{2\pi i u}$$

(where the contour C encircles the points + 1 and − 1 on the real axis) can be evaluated by the saddle-point method; the result, according to Sommerfeld[11], is

$$|F(i\alpha_d, i\alpha_p, 1, -\zeta)|^2 \qquad \text{(g)}$$

$$= |\exp\{\alpha_d\varphi(u_0)\}(2\pi\alpha_d|\varphi_0''|u_0)^{-1/2}|^2,$$

where

$$\varphi(u) = i\ln u^\rho(u-1)^{-\rho}(1+\zeta u)^{-1}, \quad \rho = \alpha_p/\alpha_d;$$

$$u_0 = \frac{1-\rho}{2} + \frac{i}{2}\sqrt{\frac{4\rho}{\zeta} - (1-\rho)^2} \qquad \text{is the}$$

solution of the equation $\varphi'(u_0) = 0$,

$$|\varphi_0''| = |\varphi''(u_0)| = \left| -\zeta\frac{2u_0 - (1-\rho)}{(u_0^2 - u_0)\left(\frac{1}{\zeta} + u_0\right)} \right|$$

$$= \frac{\zeta^2\sqrt{(4\rho/\zeta) - (1-\rho)^2}}{\rho(1+\zeta)}$$

[in the last equation we use the fact that $|(u^2 - u_0)(u_0 + \zeta^{-1})| = |-\rho(u_0 + \zeta^{-1})^2| = \rho(1+\zeta)\zeta^{-2}$]. It is assumed throughout that $\rho < 1$, but since $F(i\alpha_d, i\alpha_p, 1, -\zeta)$ is symmetric in α_d and α_p, the final formula is also valid for $\rho > 1$. Substituting the values of $|\varphi_0''|$ and u_0 in (g), and using $|u_0|^2 = \rho/\zeta$ and

$$\alpha_d[\varphi(u_0) + \varphi^*(u_0)] = 2\pi\alpha_p + 2(\alpha_d\psi_d - \alpha_p\psi_p),$$

where ψ_d and ψ_p are the angles defined in (16), we obtain for $|F(i\alpha_d, i\alpha_p, 1, -\zeta)|^2$ the value (15) given in the text. The saddle-point method is applicable if

$$\alpha_d|\varphi_0''| = \zeta^2[(\alpha_d\alpha_p/\zeta)$$

$$- (\alpha_p - \alpha_d)^2]^{1/2}/\rho(1+\zeta) > 1.$$

This condition limits the values of ζ to those satisfying the inequality $\zeta > \zeta'$ given in the text.

Translated by M. Hamermesh
266

SOVIET PHYSICS JETP VOLUME 2, NUMBER 4 JULY, 1956

Theory of Magnetic Susceptibility in Metals at Low Temperatures

I. M. LIFSHITZ AND A. M. KOSEVICH
Physico-Technical Institute, Academy of Sciences, Ukrainian SSR

(Submitted to JETP editor July 17, 1954)
J. Exper. Theoret. Phys. USSR **29**, 730 (December, 1955)

The magnetic properties of electrons in a metal are investigated for the case of an arbitrary dispersion law. The energy levels are found for a quasi-particle under an arbitrary dispersion law in a magnetic field, and the magnetic moment of a gas of such quasi-particles is computed, spin paramagnetism being taken into account. It is shown that the periods and amplitudes of the oscillations are determined by the form of the Fermi boundary surface. Knowledge of these quantities permits one to reconstruct the form of the Fermi surface and the values of the velocities upon it.

INTRODUCTION

THE question of the electron-energy spectrum is of central importance in the construction of a quantum theory of metals. There is every reason to suppose that the electron spectrum for metals is of the Fermi type. This implies that at low temperatures the electrons in the metal, interacting with one another and with the lattice, may be replaced for thermodynamic purposes by an ideal Fermi gas of charged particles following some dispersion law $\mathcal{E} = \mathcal{E}(p_x, p_y, p_z)$. The majority of the thermodynamic and kinetic properties of a degenerate Fermi gas, however, are highly insensitive to the dispersion law, as a consequence of which their investigation does not permit one to draw any conclusions concerning the form of the law.

Substantially different in this respect is the behavior of certain magnetic properties of metals – in particular, oscillations of the magnetic susceptibility – which, it appears, depend strongly upon the electron energy spectrum and may serve to distinguish it uniquely.

The periodic dependence of the magnetic susceptibility upon the field at low temperatures (the De Hass – Van Alphen effect) has by now been observed for a large number of metals (Bi, Sb, Hg, Zn, Cd, Be, C, Mg, Ga, In, Sn, Tl, Al)[1] and may be regarded as a property common to all metals. At the same time, the quantitative theory of this phenomenon had until recently been worked out only for the case of an electron gas following a quadratic dispersion law[2, 2a].

The quadratic dispersion law is correct for an electron in a metal only in the lower part of the appropriate energy zone, and may be used to investigate the magnetic properties of metals having a small number of conduction electrons (such as Bi). In general, however, there is no justification for the use of a quadratic dispersion law, as a consequence of which it is essential to determine to just what extent the peculiarities of the effect are to be attributed to the electronic dispersion law. Certain qualitative considerations associated with this circumstance have been presented earlier by Onsager[3]. A qualitative theory has been offered in a paper by the present authors[4].

The present article contains a detailed presentation of the results published earlier in the brief communication[4], with, in addition, a treatment of the spin paramagnetism (a treatment of spin paramagnetism for the case of a quadratic dispersion law has been given elsewhere [2a]).

1. ENERGY LEVELS OF A QUASI-PARTICLE IN A MAGNETIC FIELD

We investigate the motion of a charged quasi-particle under a general dispersion law

---

[1] B. Verkin, B. Lazarev, N. Rudenko, J. Exper. Theoret. Phys. USSR **20**, 93, 995 (1950); **21**, 658(1951); Dokl. Akad. Nauk SSSR **80**, 45 (1951); the collection *"In Memory of Sergei Ivanovich Vavilov"*, Acad. Sci. USSR Press, 1952. B. Verkin, Dokl. Akad. Nauk SSSR **81**, 529 (1951); B. Verkin, I. Mikhailov, J. Exper. Theoret. Phys. USSR **24**, 324 (1953); **25**, 471 (1953).

[2] L. Landau, Z. f. Phys. **64**, 629 (1930); Supplement to the article: D. Shoenberg, Proc. Roy. Soc. **170A**, 341 (1939).

[2a] A. Akhiezer, Dokl. Akad. Nauk SSSR **23**, 872 (1939); Iu. Rumer, J. Exper. Theoret. Phys. USSR **18**, 1081 (1948); G. Zil'berman, J. Exper. Theoret. Phys. USSR **21**, 1209 (1951); E. Sondheimer, A. Wilson, Proc. Roy. Soc. (London) **210A**, 173 (1951).

[3] L. Onsager, Phil. Mag. **43**, 1006 (1952)

[4] I. Lifshitz and A. Kosevich, Dokl. Akad. Nauk SSSR **96**, 963 (1954).

$$\mathscr{E} = \mathscr{E}(p_x, p_y, p_z) \qquad (1.1)$$

in a homogeneous magnetic field.

If the magnetic field **H** is directed along the z - axis, the Hamiltonian for such a particle in the magnetic field is obtained formally by replacing in (1.1) the momentum component p_i by the linear momentum operator $\check{P}_i$, the latter being interrelated by the commutation rules:

$$[\check{P}_y, \check{P}_x] = \frac{e}{c}H, \; [\check{P}_y, \check{P}_z,] = [\check{P}_x, \check{P}_z] = 0 \qquad (1.2)$$

This relation between $\check{P}_x$ and $\check{P}_y$ corresponds to the adjustable relation between the generalized coordinate and the generalized momentum: $[\check{P}_y, \check{Q}_y] = 1$.

The role of the generalized coordinate operator is played here by the operator $(c/eH)\check{P}_x$: Therefore the quasi-classical quantization condition

$$\frac{1}{2\pi}\oint P_y dQ_y = (n+\gamma)\hbar$$

may be written in the form:

$$(c/2\pi eH)\oint P_y dP_x = (n+\gamma)\hbar \quad (0<\gamma<1) \qquad (1.3)$$

(for the case of a quadratic dispersion law $\gamma = \frac{1}{2}$; in the general case, however, γ may differ from $\frac{1}{2}$).

The integral $\oint P_y dP_x$ defines the area bounded by the plane closed curve

$$\mathscr{E}(P_x, P_y, P_z) = E = \text{const}, \qquad P_z = p_z = \text{const}, \qquad (1.4)$$

which allows (1.3) to be written in the more symmetrical form:

$$S(E, p_z) \equiv \iint dP_x dP_y = (n+\gamma)\, 2\pi\hbar \frac{eH}{c}, \qquad (1.5)$$

the double integral being taken over the region bounded by the curve (1.4). Here $S(E, p_z)$ is the area intercepted on the surface of constant energy

$$\mathscr{E}(P_x, P_y, P_z) = E \qquad (1.6)$$

by a plane perpendicular to the direction of the magnetic field.

The condition (1.5) specifies, in the quasi-classical approximation, the implicit dependence of the energy of a quasi-particle in a magnetic field upon the quantum number n:

$$E = E_n(p_z; H). \qquad (1.7)$$

In accordance with (1.5), the distance between the energy levels will be

$$\Delta E_n = E_{n+1} - E_n = 2\pi\hbar eH/(c\partial S/\partial E).$$

If the quasi-particle possesses spin ½ and has a magnetic moment $\frac{1}{2}\mu_0 = \frac{1}{2}(e\hbar/m_0 c)$, then in the expression for the energy of such a particle the two possible orientations of the spin relative to the direction of the magnetic field **H** must be taken into account:

$$E = E_n(p_z; H) \pm {}^1/_2\,\mu_0 H. \qquad (1.8)$$

Thus, the energy levels in a magnetic field of a quasi-particle having an arbitrary dispersion law and a spin ½, which we shall henceforth refer to as an electron, are given by the expression (1.8); m_0, which appears in the definition of μ_0, represents the mass of the electron.

It should be remarked that the components p_i in (1.1) for electrons in a metal are components of a quasi-momentum. This fact, however, does not affect the results obtained, provided that the surface (1.6) does not intersect itself, and that each of the curves (1.4) is located within one of the cells of the reciprocal lattice. In addition, the radius of curvature of the electron trajectory must clearly be assumed to be large compared to the lattice constant.

2. CALCULATION OF THE MAGNETIC MOMENT

The magnetic moment **M** of the electron gas is found by taking the derivative of the thermodynamic potential Ω with respect to the field : $\mathbf{M} = -\partial\Omega/\partial\mathbf{H}$. To determine the thermodynamic potential Ω we make use of the usual formula of statistical mechanics:

$$\Omega = -\Theta \sum_s \ln\left\{1 + \exp\frac{\zeta - E(s)}{\Theta}\right\}, \qquad (2.1)$$

where $E(s)$ is the energy of the electron in the state s, ζ is the chemical potential, $\Theta = kT$, and the summation is performed over all of the possible states s of the individual electron. The energy

$E(s)$ for an electron in a state with given p_z, n, and direction of spin is given by the expression (1.8).

Since, in computing the number of states, the commutation relations (1.2) rather than the dispersion law for the electrons are the essential factor, the number of states is calculated by the same method as that used by Landau for free electrons[2]; in particular, it is possible to state that the number of states of momentum p_z in the interval $(p_z, p_z + \Delta p_z)$ for a given n and a given spin orientation is equal to

$$V\frac{eH}{4\pi^2\hbar^2 c}\Delta p_z.$$

Therefore, (2.1) may be rewritten in the form:

$$\Omega = -V\frac{eH}{4\pi^2\hbar^2 c}\sum_{\text{spin}}\sum_{n=0}^{\infty}\Theta\int_{-\infty}^{\infty}dp_z \tag{2.2}$$

$$\times\ln\left\{1+\exp\frac{\zeta - E_n(p_z;H)\mp {}^1/_2\mu_0 H}{\Theta}\right\}.$$

Representing the expression following the summation sign in (2.2) by $\varphi(n)$, we use for the summation over n the Poisson formula[5]:

$$\Omega = -V\frac{eH}{4\pi^2\hbar^2 c}\sum_{\text{spin}}\left\{\frac{1}{2}\varphi(0)+\int_0^{\infty}dn\,\varphi(n)\right.$$

$$\left.+2\sum_{k=1}^{\infty}\int_0^{\infty}dn\,\varphi(n)\cos 2\pi kn\right\}.$$

Inasmuch as $\gamma \to \frac{1}{2}$ for $E_n \to E_0$, it may readily be shown that the thermodynamic potential can be written in the following form:

$$\Omega = -V\frac{eH}{4\pi^2\hbar^2 c}\sum_{\text{spin}}\left\{\int_{-{}^1/_2}^{\infty}dn\,\varphi(n)\right. \tag{2.3}$$

$$\left.+2\,\mathrm{Re}\sum_{k=1}^{\infty}\int_{-{}^1/_2}^{\infty}dn\,\varphi(n)\,e^{2\pi kin}\right\}.$$

The first term inside the curly brackets corresponds to the continuous energy spectrum. It can easily be shown that this term will contribute only to the spin paramagnetism of the electron gas. Introducing the symbol $\epsilon = \zeta \pm \frac{1}{2}\mu_0 H$, we obtain

$$J_1 = \int_{-{}^1/_2}^{\infty}dn\,\varphi(n)$$

$$= \Theta\int_{-{}^1/_2}^{\infty}dn\int_{-\infty}^{\infty}dp_z\ln\{1+e^{(\epsilon-E_n)/\Theta}\}$$

$$= \Theta\int_0^{\infty}dE\ln\left\{1+e^{(\epsilon-E_n)/\Theta}\right\}\int_{S>0}dp_z\left(\frac{\partial n}{\partial E}\right),$$

where $S = S(E, p_z)$.

The relation between E and n is given by the expression (1.5), and hence

$$\frac{\partial n}{\partial E} = \frac{c}{2\pi e\hbar H}\frac{\partial S}{\partial E}; \tag{2.4}$$

$$J_1 = \frac{\Theta c}{2\pi e\hbar H}\int_0^{\infty}dE \tag{2.5}$$

$$\times\ln\{1+e^{(\epsilon-E)/\Theta}\}\int_{S>0}dp_z\left(\frac{\partial S}{\partial E}\right).$$

Taking into consideration the nature of the limits of integration for the inner integral in (2.5), we write

$$J_1 = \frac{\Theta c}{2\pi e\hbar H}\int_0^{\infty}dE \tag{2.6}$$

$$\times\ln\{1+e^{(\epsilon-E)/\Theta}\}\frac{d}{dE}\int_{S>0}dp_z S(E, p_z)$$

$$= \frac{c}{2\pi e\hbar H}\int_0^{\infty}\frac{dE}{e^{(E-\epsilon)/\Theta}+1}\int_{S>0}S(E, p_z)\,dp_z.$$

We now note that the inner integral in (2.6) gives the volume bounded by the surface of constant energy E in momentum space. Representing this volume by $U(E)$, and introducing the expression

$$W(\epsilon) = \int_0^{\infty}\frac{U(E)\,dE}{e^{(E-\epsilon)/\Theta}+1},$$

we obtain

$$J_1 = \frac{c}{2\pi e\hbar H}W(\epsilon). \tag{2.7}$$

Making use of the fact that $\mu_0 H \ll \zeta$, we can expand $W(\epsilon)$ in powers of $\mu_0 H$, stopping with the second-order terms. If we insert this expansion into (2.3) and sum over the two possible spin orientations, it is seen that the corresponding part of the thermodynamic potential Ω is equal to

---

[5] Courant and Hilbert, "*Methods of Mathematical Physics*", v. I.

$$\Omega_1 = -\frac{V}{8\pi^3\hbar^3}\left[2W(\zeta) + \left(\frac{\mu_0 H}{2}\right)^2 \frac{d^2 W(\zeta)}{d\zeta^2}\right]. \qquad (2.8)$$

J_1, therefore, actually contributes only to the spin paramagnetism of the electron gas:

$$M_{1z} = \mu_0 V \frac{1}{16\pi^3\hbar^3} \frac{d^2 W(\zeta)}{d\zeta^2} \mu_0 H. \qquad (2.9)$$

The expression (2.9) has a simple physical interpretation. Under the condition $\Theta \ll \zeta$, which we shall consider always to be fulfilled, one can set

$$W(\zeta) \approx \int_0^\zeta U(E)\, dE,$$

which implies

$$\frac{d^2 W(\zeta)}{d\zeta^2} \approx \frac{dU(\zeta)}{d\zeta}.$$

The product

$$\frac{V}{8\pi^3\hbar^3} \frac{dU(\zeta)}{d\zeta} = \rho(\zeta) \qquad (2.10)$$

gives the number of states per unit energy interval at the Fermi boundary energy; (2.9) may therefore be written in the form

$$M_{1z} = {}^1/_2\, \mu_0 \rho(\zeta) \mu_0 H. \qquad (2.11)$$

The diamagnetism of the electron gas and the De Haas - Van Alphen effect are described by the second term in the curly brackets in (2.3). Using (1.5) and (2.4), we can transform the integrals entering into this term:

$$J(k) = \int_{-1/2}^{\infty} dn\, \varphi(n)\, e^{2\pi k i n}$$

$$= \Theta \int_{-1/2}^{\infty} dn \int_{-\infty}^{\infty} dp_z \ln\left\{1 + \exp\frac{\varepsilon - E_n}{\Theta}\right\} e^{2\pi k i n}$$

$$= \frac{\Theta c}{2\pi e\hbar} \int_0^\infty dE \ln\left\{1 + \exp\frac{\varepsilon - E}{\Theta}\right\}$$

$$\times \int_{S>0} dp_z \left(\frac{\partial S}{\partial E}\right) \exp\left\{\frac{kc}{e\hbar H} S(E, p_z) - 2\pi k i\gamma\right\}.$$

Integration by parts leads to the expression

$$J(k) = \frac{c}{2\pi e\hbar H} \int_0^\infty dE\, f\left(\frac{E - \varepsilon}{\Theta}\right)$$

$$\times \int_0^E dE' \int_{S>0} dp_z \frac{\partial S(E', p_z)}{\partial E'} \qquad (2.12)$$

$$\times \exp\left\{i \frac{kc}{e\hbar H} S(E', p_z) - 2\pi k i\gamma\right\};$$

$f(x)$ represents the Fermi distribution function: $f(x) = (1 + e^x)^{-1}$.

In computing the inner double integral in (2.12) we make use of the fact that under the assumption of very large numbers $(c/2\pi e\hbar H)S = n + \gamma$. This permits the use of the method of stationary points for the asymptotic evaluation of the integral. It is found that the major contribution to $J(k)$ comes, first, from integration in the vicinity of the peaks in the extremum point of $S(E', p_z)$, for $E' = E$ - i.e., the point at which $\partial S(E, p_z)/\partial p_z = 0$ – and second, from integration in the vicinity of the region of integration: $E' = E$, $S(E, p_z) = 0$. As regards the integration about the stationary point, this yields the oscillating part of $J(k)$ (cf. Appendix), corresponding to the oscillating part of the magnetic moment. Integration about the peak $E' = E$, $S(E, p_z) = 0$, yields the nonperiodic part of $J(k)$, which determines the diamagnetism of the electron gas. The neighborhood of $S(E, p_z) = 0$, however, corresponds to small values of the quantum number n [cf. Eq. (1.5)], for which the energy levels calculated in the quasi-classical approximation (Section 1) are, generally speaking, incorrect. Therefore the nonperiodic part of $J(k)$, an expression for which is given in the Appendix, can give the correct figure for the diamagnetism of the electron gas only in the special case for which the quasi-classical energy levels coincide with the true levels for all n (for instance, in the case of a quadratic dispersion law).

The first term in the asymptotic expansion of the inner double integral about the stationary point leads to the following expression for $J(k)$:

$$J(k) = \frac{1}{\sqrt{2\pi}} \left(\frac{e\hbar H}{c}\right)^{1/2} \frac{1}{k^{3/2}} \qquad (2.13)$$

$$\times \exp\left\{-2\pi k i\gamma \mp i\frac{\pi}{4} - i\frac{\pi}{2}\right\}$$

$$\times \int_0^\infty dE f\left(\frac{E - \varepsilon}{\Theta}\right) \left|\frac{\partial^2 S(E, p_z)}{\partial p_z^2}\right|_m^{-1/2}$$

$$\times \exp\left\{i \frac{kc}{e\hbar H} S_m(E)\right\}.$$

We have represented by $S_m(E)$ the extremal value of $S\,(E,\ p_z)$ for constant E. If $S_m(E)$ represents a maximum for the intercepted area, then the phase $i\pi/4$ takes the minus sign in (2.13), while if $S_m(E)$ is a minimum area, the phase $i\pi/4$ takes the plus sign. The derivative $(\partial^2 S/\partial p_z^2)_m$ is taken at the extremal point.

To compute the integral in equation (2.13) we make use of the fact that, under the assumption that $dS_m(E)/dE \neq 0$, and for the evident inequality $\Theta \ll \epsilon$, the major contribution to the integral comes from the integration about the point at which the function $f\,[(E-\epsilon)/\Theta]$ varies most rapidly; i.e., about $E=\epsilon$. Therefore, expanding $S_m(E)$ in powers of $E-\epsilon$ and integrating, we obtain

$$\int_0^\infty dE\, f\left(\frac{E-\varepsilon}{\Theta}\right)\left|\frac{\partial^2 S}{\partial p_z^2}\right|_m^{-1/2}\exp\left\{i\,\frac{kc}{e\hbar H}\,S_m(E)\right\}$$

$$\approx \frac{e\hbar H}{kc}\,\Psi(k\lambda)\,\frac{\exp\left\{-i\,\frac{\pi}{2}+i\,\frac{kc}{e\hbar H}S_m(\varepsilon)\right\}}{\left|\frac{\partial^2 S}{\partial p_z^2}\right|_m^{1/2} dS_m(\varepsilon)/d\varepsilon}, \qquad (2.14)$$

where $\Psi(z) = z\ \ \sinh z$, and $\lambda = (\pi c\Theta/e\hbar H)\times(dS_m(\epsilon)/d\epsilon)$.

Inserting the expression (2.14) into (2.13), we obtain:

$$J(k) = -\frac{1}{\sqrt{2\pi}}\left(\frac{e\hbar H}{c}\right)^{5/2},$$

$$\times\ \frac{1}{k^{5/2}}\,\frac{\Psi(k\lambda)\exp\left\{i\,\frac{kc}{e\hbar H}S_m(\varepsilon)\mp i\,\frac{\pi}{4}-2\pi k i\gamma\right\}}{\left|\partial^2 S(\varepsilon,\ p_z)/\partial p_z^2\right|_m^{1/2} dS_m(\varepsilon)/d\varepsilon}. \qquad (2.15)$$

We compute the second term in the curly brackets of (2.3) by summing over k:

$$2\mathrm{Re}\sum_{k=1}^{\infty} J(k)$$

$$= -\frac{2}{\sqrt{2\pi}}\left(\frac{e\hbar H}{c}\right)^{5/2}\left|\frac{\partial^2 S(\varepsilon,\ p_z)}{\partial p_z^2}\right|_m^{-1/2}\left(\frac{dS_m(\varepsilon)}{d\varepsilon}\right)^{-1} \qquad (2.16)$$

$$\times\sum_{k=1}^{\infty}\frac{1}{k^{5/2}}\Psi(k\lambda)\cos\left[\frac{kc}{e\hbar H}S_m(\varepsilon)\mp\frac{\pi}{4}-2\pi k\gamma\right].$$

In summing over the two spin orientations it is possible, in all of the expressions in (2.16) except the argument of the cosine, simply to replace ϵ by ζ. In the argument of the cosine, however, it is necessary to expand $S_m(\epsilon)$ in powers of $\mu_0 H$, stopping with the first power of $\mu_0 H$:

$$S_m(\varepsilon) = S_m(\zeta) \pm \frac{1}{2}\,\mu_0 H\,\frac{dS_m(\zeta)}{d\zeta}.$$

Taking this into account in the summation, we obtain as the final expression for the oscillating part of the thermodynamic potential Ω, corresponding to the second term in the curly brackets of (2.3):

$$\Omega_2 = \frac{V}{\pi^2\sqrt{2\pi}\,\hbar^3}\left(\frac{e\hbar H}{c}\right)^{5/2}\left|\frac{\partial^2 S}{\partial p_z^2}\right|_m^{-1/2}\left(\frac{dS_m}{d\zeta}\right)^{-1} \qquad (2.17)$$

$$\times\sum_{k=1}^{\infty}\frac{\Psi(k\lambda)}{k^{5/2}}\cos\left[\frac{kc}{e\hbar H}S_m(\zeta)\mp\frac{\pi}{4}-2\pi k\gamma\right]$$

$$\times\ \cos\left[\frac{k}{2m_0}\,\frac{dS_m(\zeta)}{d\zeta}\right].$$

In order to determine that part of the magnetic moment which is contributed by (2.17) we must differentiate Ω_2 with respect to the magnetic field intensity. In this differentiation the factors preceding the cosine, which vary slowly with H, need not be differentiated at all; it is necessary only to differentiate the cosine, whose argument depends upon H. We have, therefore, for the component of the moment in the direction of the magnetic field*:

$$M_{\mathrm{osc}} = -\frac{V}{\pi^2\sqrt{2\pi}\,\hbar^3}\left(\frac{e\hbar}{c}\right)^{3/2}\frac{S_m(\zeta)\sqrt{H}}{\left|\partial^2 S/\partial p_z^2\right|_m^{1/2} dS_m/d\zeta}$$

$$\times\sum_{k=1}^{\infty}\frac{1}{k^{3/2}}\Psi(k\lambda) \qquad (2.18)$$

$$\times\sin\left[\frac{kc}{e\hbar H}S_m(\zeta)\mp\frac{\pi}{4}-2\pi k\gamma\right]$$

$$\times\cos\left[\frac{k}{2m_0}\,\frac{dS_m(\zeta)}{d\zeta}\right].$$

Combining (2.8) and (2.17) as well as (2.11) and (2.18), and taking into consideration the diamagnetism of the electron gas, we write the final expressions for the thermodynamic potential Ω and the magnetic moment:

$$\Omega = -\frac{V}{4\pi^3\hbar^3}\,W(\varepsilon) - V\,\frac{1}{2}(\chi_1+\chi_2)H^2 \qquad (2.19)$$

---

* Throughout what follows, the values given are those of the component M_z of the momentum in the direction of **H**. The corresponding oscillating component M_x of the momentum in the perpendicular direction is obtained by multiplying (2.18) by $(1/S_m)(\partial S_m/\partial\vartheta)$ (ϑ being the angle in the x-z plane).

$$+\frac{V}{\pi^2\sqrt{2\pi}\,\hbar^3}\left(\frac{e\hbar H}{c}\right)^{3/2}\left|\frac{\partial^2 S}{\partial p_z^2}\right|_m^{-1/2}\left(\frac{dS_m}{d\zeta}\right)^{-1}$$

$$\times\sum_{k=1}^{\infty}\frac{\Psi(k\lambda)}{k^{3/2}}\cos\left[\frac{kc}{e\hbar H}S_m(\zeta)\right.$$

$$\left.\mp\frac{\pi}{4}-2\pi k\gamma\right]\cos\left[\frac{k}{2m_0}\frac{dS_m(\zeta)}{d\zeta}\right];$$

$$M = V(\chi_1+\chi_2)H \tag{2.20}$$

$$-\frac{4V}{\hbar^3(2\pi)^{3/2}}\left(\frac{e\hbar}{c}\right)^{3/2}\frac{S_m(\zeta)\sqrt{H}}{\left|\partial^2 S(\zeta,p_z)/\partial p_z^2\right|_m^{1/2}dS_m(\zeta)/d\zeta}$$

$$\times\sum_{k=1}^{\infty}\frac{\Psi(k\lambda)}{k^{3/2}}\sin\left[\frac{kc}{e\hbar H}S_m(\zeta)\right.$$

$$\left.\mp\frac{\pi}{4}-2\pi k\gamma\right]\cos\left[\frac{k}{2m_0}\frac{dS_m(\zeta)}{d\zeta}\right].$$

Here χ_1 represents the spin paramagnetic susceptibility of the electron gas, determined from (2.11), and χ_2 is the constant part of the diamagnetic susceptibility (cf. Appendix).

We may remark that the nonperiodic part of the magnetic moment [the first two terms in (2.20)] is of little interest, inasmuch as it is obscured in metals by other effects (for example, by the atomic magnetism). The oscillating part of the magnetic moment, to the analysis of which we now turn, is of primary interest.

3. ANALYSIS OF RESULTS

From the formula for the magnetic moment (2.20) it can be seen that the amplitude and period of the oscillations in the magnetic moment are fully determined by the extremal value of the area on the Fermi boundary surface intercepted by the plane $P_{\times}H$=const., and by the derivatives of the area intercepted on the Fermi surface at the extremal point.

For a quadratic dispersion law

$$\mathscr{E}=\frac{1}{2m}(p_x^2+p_y^2+p_z^2) \tag{3.1}$$

we have

$$S(E,p_z)=2\pi m(E-(p_z^2/2m));$$

$$S_m(E)=2\pi mE,\quad dS_m(E)/dE=2\pi m,$$

$$|\partial^2 S/\partial p_z^2|=2\pi;\ \gamma={}^1/_2.$$

In this case the expression (2.20) goes over into the usual formula for the magnetic moment of a gas of free electrons[2].

For a temperature of absolute zero or for very strong magnetic fields, in which case $\lambda \ll 1$, the function $\Psi(k\lambda)$ may be replaced in (2.20) by unity; then the oscillating part of the magnetic moment is given by the formula:

$$M_{\text{osc}}=-\frac{4V}{\hbar^3(2\pi)^{3/2}}\left(\frac{e\hbar}{c}\right)^{3/2} \tag{3.2}$$

$$\times\frac{S_m(\zeta)\sqrt{H}}{\left|\partial^2 S(\zeta,p_z)/\partial p_z^2\right|_m^{1/2}dS_m(\zeta)/d\zeta}$$

$$\times\sum_{k=1}^{\infty}\frac{1}{k^{3/2}}\sin\left[\frac{kc}{e\hbar H}S_m(\zeta)\mp\frac{\pi}{4}\right.$$

$$\left.-2\pi k\gamma\right]\cos\left[\frac{k}{2m_0}\frac{dS_m(\zeta)}{d\zeta}\right].$$

For small fields, $\lambda \gg 1$ and $\Psi(k\lambda)\approx 2k\lambda e^{-k\lambda}$; and therefore only one term (for $k = 1$) of the summation in expression (2.20) need be taken, which yields

$$M_{\text{osc}}=-A(H,\zeta)\sin\left[\frac{c}{e\hbar H}S_m(\zeta)\mp\frac{\pi}{4}-2\pi\gamma\right], \tag{3.3}$$

where

$$A(H,\zeta)=\frac{4V}{\hbar^3(2\pi)^{3/2}}\left(\frac{e\hbar}{c}\right)^{1/2}$$

$$\times\frac{\Theta S_m(\zeta)e^{-\lambda}}{\left|\partial^2 S(\zeta,p_z)/\partial p_z^2\right|_m^{1/2}\sqrt{H}}\cos\left[\frac{1}{2m_0}\frac{dS_m(\zeta)}{d\zeta}\right].$$

Since we used the thermodynamic potential Ω in calculating the magnetic moment, ζ and H must in consequence be regarded as independent variables. In actual applications of Eqs. (2.20), (3.2), and (3.3), however, one must take into consideration the dependence of ζ upon H, determined by the constancy of the number of particles N:

$$N=-\partial\Omega(\zeta,H)/\partial\zeta=\text{const.}$$

This dependence is, however, sufficiently weak that it may be neglected. It is easy to convince oneself of this by evaluating the part of ζ which depends upon the magnetic field. The expression for $\Omega(\zeta, H)$ is given by formula (2.19); in differentiating this with respect to ζ we retain, as before, only the first few terms in the expansion in powers of H. Then

$$N = \frac{V}{4\pi^2\hbar^3}\frac{dW(\zeta)}{d\zeta} - \frac{V}{2\pi^2\hbar^3}\left(\frac{e\hbar H}{c}\right)^{3/2}\frac{\sqrt{2\pi}}{\left|\partial^2 S(\zeta, p_z)\,\partial^2 p_z\right|_m^{1/2}} \times \sum_{h=1}^{\infty}\frac{1}{k^{3/2}}\Psi(k\lambda)\sin\left[\frac{kc}{ehH}S_m(\zeta) \mp \frac{\pi}{4} - 2\pi k\gamma\right]\cos\left[\frac{k}{2m_0}\frac{dS_m(\zeta)}{d\zeta}\right]. \tag{3.4}$$

Under the assumptions we have made ($\Theta \ll \zeta$), $dW(\zeta)/d\zeta = U(\zeta)$; this is the volume in momentum space enclosed by the Fermi boundary surface. If we introduce this notation into formula (3.4), and for simplicity designate the summation in the second term of this formula by $G(\zeta,H)$, we obtain

$$U(\zeta_0) = U(\zeta) - \left(\frac{e\hbar H}{c}\right)^{3/2}\frac{2\sqrt{2\pi}\,G(\zeta, H)}{\left|\partial^2 S(\zeta, p_z)/\partial p_z^2\right|_m^{1/2}}, \tag{3.5}$$

where ζ_0 is the chemical potential at $H = 0$.

Assuming a small increment to ζ dependent upon the magnetic field H, we may set

$$\zeta = \zeta_0(1 + \xi(H)), \quad \xi \ll 1.$$

Expanding the quantities in (3.5) which depend upon ξ in powers of ξ and stopping after the first few terms, we have

$$U(\zeta_0) = U(\zeta_0) + \xi\zeta_0\frac{dU(\zeta_0)}{d\zeta_0} - \left(\frac{e\hbar H}{c}\right)^{3/2}\frac{2\sqrt{2\pi}\,G(\zeta_0, H)}{\left|\partial^2 S(\zeta_0, p_z)/\partial p_z^2\right|_m^{1/2}}$$

whence it follows that

$$\xi(H) = \frac{2\sqrt{2\pi}}{\zeta_0 dU(\zeta_0)/d\zeta_0}\left(\frac{e\hbar H}{c}\right)^{3/2}\frac{G(\zeta_0, H)}{\left|\partial^2 S(\zeta_0, p_z)/\partial p_z^2\right|_m^{1/2}}. \tag{3.6}$$

Inasmuch as the summation $G(\zeta, H)$ appearing in (3.6) is of the order of unity, while $|\partial^2 S/\partial p_z^2|_m^{1/2}$ is a nondimensional quantity representing the anisotropy of the Fermi boundary surface (for the case of a spherical surface it is equal to $\sqrt{2\pi}$), the quantity $\xi(H)$ is determined by the ratio $(e\hbar H/c)^{3/2}/\zeta_0(dU(\zeta_0)/d\zeta_0)$. If the cases in which the anisotropy of the Fermi surface is anomalously large are neglected, then it is possible to assume that $U(\zeta_0) \sim [S(\zeta_0)]^{3/2}$ where $S(\zeta_0)$ is the mean area intercepted on the Fermi surface by the planes p_z = const. This permits setting, in order of magnitude

$$\zeta_0\frac{dU}{d\zeta_0} \sim U(\zeta_0) \sim [S(\zeta_0)]^{3/2} \sim \left[\zeta_0\frac{dS}{d\zeta_0}\right]^{3/2},$$

and we can write

$$\xi(H) \sim \left(\frac{e\hbar H}{c}\right)^{3/2}\Big/\zeta_0\frac{dU(\zeta_0)}{d\zeta_0} \sim \left(\frac{e\hbar H}{\zeta_0 c}\Big/\frac{dS(\zeta_0)}{d\zeta_0}\right)^{3/2}. \tag{3.7}$$

We note here that, as follows from (1.5), the mean distance between neighboring energy levels near the boundary energy is equal to

$$\Delta E = \frac{2\pi e\hbar H}{c}\Big/\frac{dS(\zeta_0)}{d\zeta_0}.$$

The distance between the levels is assumed to be considerably less than the boundary energy ζ_0; from (3.7), therefore, we obtain the following evaluation of $\xi(H)$:

$$\xi(H) \sim (\Delta E/\zeta_0)^{3/2} \ll 1. \tag{3.8}$$

Thus, the quantity $\xi(H)$, determined by the expression (3.6), is actually small in magnitude. For the case of the quadratic dispersion law (3.1)

$$\xi(H) = \left(\frac{e\hbar H}{mc\zeta_0}\right)^{3/2}\frac{G(\zeta_0, H)}{2\pi\sqrt{2}} \sim \left(\frac{e\hbar H}{mc\zeta_0}\right)^{3/2} = \left(\frac{\mu H}{\zeta_0}\right)^{3/2} \ll 1.$$

As regards the argument of the sine in (2.20), (3.2), or (3.3), its dependence upon the magnetic field is incorporated in the expression

$$\frac{c}{e\hbar H}S_m(\zeta) = \frac{c}{e\hbar H}\left[S_m(\zeta_0) + \xi\zeta_0\frac{dS_m(\zeta_0)}{d\zeta_0}\right] = \frac{c}{e\hbar H}S_m(\zeta_0) + \frac{2\sqrt{2\pi}}{dU(\zeta_0)/d\zeta_0}\left(\frac{e\hbar H}{c}\right)^{1/2}\frac{G(\zeta_0, H)\,\dfrac{dS_m(\zeta_0)}{d\zeta_0}}{\left|\partial^2 S(\zeta_0, p_z)/\partial^2 p_z\right|_m^{1/2}} \tag{3.9}$$

The second term in (3.9) is equal in order of magnitude to $(\Delta E/\zeta_0)^{1/2} \ll 1$; the periodic dependence of the magnetic moment upon the magnetic field is therefore fully determined by the first term in (3.9):

$$\frac{c}{e\hbar H} S_m(\zeta) \approx \frac{c}{e\hbar H} S_m(\zeta_0) \,. \qquad (3.10)$$

It follows from (3.8) and (3.9) that ζ may be replaced by ζ_0 in Eqs. (2.19) and (2.20), as well as in (3.2) and (3.3), and the period of the oscillations may be represented in the form

$$\Delta\left(\frac{1}{H}\right) = \frac{2\pi e\hbar}{cS_m(\zeta_0)} \,. \qquad (3.11)$$

In the event that there are several unfilled zones, in which the classical motion of the electron is independent – i.e., when the Fermi surface is reduced to a few closed surfaces – each group of electrons has its own $S_m(E)$ and makes its own oscillatory contribution to the magnetic moment. If in this case the boundary energy ζ is found to be distributed about the lower part of the unfilled zone, we may content ourselves with the representation

$$\mathcal{E}(P_x, P_y, P_z) = \varepsilon_0 + \left(\frac{P_x^2}{2m_1} + \frac{P_y^2}{2m_2} + \frac{P_z^2}{2m_3}\right)$$

The maximum area intercepted on the ellipsoid $\mathcal{E}(P_x, P_y, P_z) = E$ by the plane $\mathbf{P} \times \mathbf{H} =$ const. will be

$$S_m = 2\pi m(E - \varepsilon_0),$$

$$m = (m_1 m_2 m_3)^{1/2} / (m_1\alpha_1^2 + m_2\alpha_2^2 + m_3\alpha_3^2)^{1/2}$$

where the α_i are the direction cosines of the magnetic field vector H in the system of the crystallographic axes. This yields for the corresponding factor $\partial S_m/\partial E = 2\pi m$ and period

$$\Delta\left(\frac{1}{H}\right) = \frac{\mu}{\zeta - \varepsilon_0} \qquad \left(\mu = \frac{e\hbar}{mc}\right).$$

In the case of a nearly-filled zone the energy at the upper boundary has the form

$$\mathcal{E}(P_x, P_y, P_z) = \varepsilon_0' - \left(\frac{P_x^2}{2m_1} + \frac{P_y^2}{2m_2} + \frac{P_z^2}{2m_3}\right),$$

which yields

$$\partial S_m/\partial E = -2\pi m \text{ and } \Delta\left(\frac{1}{H}\right) = \frac{\mu^*}{\varepsilon_0' - \zeta}$$

$$\mu^* = e\hbar/m^*c,$$

$$m^* = (m_1^* m_2^* m_3^*)^{1/2} / (m_1^*\alpha_1^2 + m_2^*\alpha_2^2; m_3^*\alpha_3^2)^{1/2}.$$

In the presence of strong mass anisotropy even a slightly mosaic structure leads to obscuration or complete obliteration of the oscillations in the event that the number of electrons in the corresponding zone is large. This obscuration of the phase of the oscillatory term may be represented in the form

$$\Delta\varphi = \frac{\zeta - \varepsilon_0}{\mu H}\frac{\Delta m}{m} \sim \frac{\zeta - \varepsilon_0}{\mu H}\Delta\vartheta,$$

where $\Delta\vartheta$ is the angle of mosaicity. For $\Delta\vartheta \gg 1$ the oscillations disappear. Therefore, only those groups of electrons or holes in which the number of particles is extremely small will participate in the effect. Oscillations having smaller periods can appear only for sufficiently high fields. Since, however, the curvature of the surface corresponding to an anomalously small number of electrons is as a rule extremely high (anomalously small electronic "masses"), even in this case there is no foundation for assuming a quadratic dispersion law.

Thus, the occurrence of the experimentally observable De Haas-Van Alphen in a large group of metals provides grounds for assuming that the presence of zones having an anomalously small number of electrons is a general property of metals. It is possible that the appearance of these zones is connected with interactions between the electrons and the lattice. The discovery of an isotopic effect might serve to confirm such a supposition.

Finally we turn our attention to the fact that careful experimental measurement of the period of the oscillations in the magnetic moment $\Delta(1/H)$, as well as of the amplitude of the oscillations and the temperature dependence, would permit the reconstruction of the form of the Fermi boundary surface, and would also permit the determination of the velocity of the electrons upon this surface – i.e., the problem may be solved in an inverse sense, so to speak, to that in which we have solved it. The feasibility of this procedure is a consequence of the fact that the period of the oscillations determines the extreme value $S_m(\zeta)$ of the area intercepted on the Fermi boundary surface by the planes perpendicular to the direction of the magnetic field, while the amplitude of the oscillations and the temperature dependence determine $dS_m(\zeta)/d\zeta$ and $|\partial^2 S(\zeta, p_z)/\partial p_z^2|_m$. As has been demonstrated in a paper by Lifshitz and Pogorelov[6], a knowledge of these quantities, under quite general assumptions, is adequate for the solution of the inverse problem.

If it is assumed that the Fermi boundary surface has a center of symmetry and that the extremal intercept is the central one, then the length of the radius vector **r**, extending from the center to the surface in the direction **e** (**e** being the unit vector), is determined by the formula[6]

$$\pi r^2(\mathbf{e}) = X_{\mathbf{e}}(0) - \int_0^1 [X_{\mathbf{e}}(u) - X_{\mathbf{e}}(0)]\frac{du}{u^2} \quad (3.12)$$

We have introduced here the representation

$$X_{\mathbf{e}}(u) = \frac{1}{2\pi}\int [S_m(\zeta)]_{\mathbf{n}}\delta(\mathbf{ne} - u)\, d\Omega_{\mathbf{n}}$$

where $[S_m(\zeta)]_{\mathbf{n}}$ is the area intercepted on the boundary surface $\mathcal{E}(P_x, P_y, P_z) = \zeta$ by a plane through the center normal to a given unit vector **n**, $\partial(z)$ is the delta-function, and $d\Omega_{\bar{n}}$ is the element of solid angle in the direction **n**.

Having determined the form of the surface $r(\mathbf{e})$, and knowing the quantity $dS_m(\zeta)/d\zeta$, one may readily determine the velocity of the electrons on the boundary surface.

For the magnetic fields under which the measurements of the De Haas-Van Alphen effect have been conducted ($H \sim 10^4$ gauss) the periods observed experimentally for the oscillations are determined, as we have pointed out, by those zones having an anomalously small number of electrons; for this reason the method described above can be used to reconstruct the Fermi boundary surface for these zones alone. Measurements in considerably stronger fields are needed before it will be possible to draw any conclusions regarding the form of the boundary surface for the normal energy zones.

APPENDIX

We shall evaluate the integral

$$I = \iint dE'dp_z \frac{\partial S(E', p_z)}{\partial E'} \times \exp\left\{i\frac{kc}{e\hbar H}S(E', p_z) - 2\pi k\gamma i\right\}$$

in which the region of integration is bounded by the straight line $E' = E$ and the curve $S(E', p_z) = 0$. We shall not specify the extremely weak dependence of γ on E' and p_z.

Assuming that $\partial S(E', p_z)/\partial E' \neq 0$, we may conclude that the primary contribution to I is provided by integration in the neighborhood of the point on the boundary of the region of integration $E' = E$ for which $\partial S(E, p_z)/\partial p_z = 0$, in the vicinity of the point $E' = p_z = 0$, for which $\partial S(0, p_z)/\partial p_z = 0$, and about the peaks of the region of integration[7].

1) In integrating about the stationary point on the straight line $E' = E$ we expand $S(E', p_z)$ in a power series in $(E' - E)$ and $(p_z - p_m)$ (p_m corresponding to the stationary point), stopping after the first nonvanishing terms:

$$I_1 = \frac{\partial S(E, p_m)}{\partial E}\exp\left\{i\frac{kc}{e\hbar H}S(E, p_m) - 2\pi ki\gamma\right\} \times \int_{E-0}^{E} dE \int_{p_m-0}^{p_m+0} dp_z \exp\left\{i\frac{kc}{e\hbar H}\left[(E' - E)\frac{\partial S}{\partial E} + \frac{1}{2}(p_z - p_m)^2\frac{\partial^2 S}{\partial p_z^2}\right\}\right.$$

After further computation we obtain

$$I_1 \sim \left(\frac{e\hbar H}{kc}\right)^{3/2}\frac{\sqrt{2\pi}}{|\partial^2 S/\partial p_z^2|_m^{1/2}}\exp\left\{i\frac{kc}{e\hbar H}S(E, p_m) - 2\pi ki\gamma - i\frac{\pi}{2} \mp i\frac{\pi}{4}\right\}$$

The sign of the last term in the exponent agrees with the sign of $\partial^2 S(E, p_m)/\partial p_m^2$.

In computing the integral we have made use of the following asymptotic formula:

$$\int_{x_0} f(x)\exp\{\pm iW(x - x_0)\}\, dx \sim f_n\frac{\Gamma(n+1)}{W^{n+1}}\exp\left\{\pm i\frac{n+1}{2}\pi\right\}, \quad (W \gg 1),$$

assuming that in the neighborhood of $x = x_0$ the function $f(x)$ has the form $f(x) \approx f_n(x - x_0)^n$.

The expression obtained for I_1 determines the oscillatory part of $J(k)$; if it is inserted into equation (2.12), setting $S_m(E) = S(E, p_m)$, the latter will yield (2.13).

2) Designating by $\pm p_0$ the values of p_z corresponding to the peaks in the region of integration, we investigate the integral in the

---

[6] I. Lifshitz, and A. Pogorelov, Dokl. Akad. Nauk SSSR **96**, 1143 (1954).

[7] J. Corput. Proc. Acad. Sci. (Amsterdam) **51**, 650 (1948).

vicinity of one of the peaks

$$I_2 \approx \frac{\partial S(E, p_0)}{\partial E} e^{-2\pi k i \gamma} \int\limits_{p_0-0}^{p_0} dp_z \int^{E} dE'$$

$$\times \exp\left\{i \frac{kc}{e\hbar H}\left[(p_z - p_0)\frac{\partial S}{\partial p_0} + (E' - E)\frac{\partial S}{\partial E}\right]\right\}$$

The lower limit of the integral over E' lies on the curve $S(E', p_z) = 0$. Near the peak it is possible to make the substitution

$$E' = E + (p_0 - p_z)\left(\frac{\partial S}{\partial p_0} \Big/ \frac{\partial S}{\partial E}\right)$$

With substitution of variables we have

$$I_2 \sim \left(\frac{e\hbar H}{kc}\right)^2 \frac{e^{-2\pi k i \gamma}}{\partial S(E, p_0)/dp_0} \int\limits_0 dx e^{-ix} \int\limits_0^{-x} dy e^{-iy}$$

Computing the integral using the above formula we obtain:

$$I_2 \sim \left(\frac{e\hbar H}{kc}\right)^2 \frac{\sin 2\pi k\gamma - \cos 2\pi k\gamma}{\partial S(E, p_0)/\partial p_0}(1 + ia)$$

where a is some real quantity; its value is not important, since we shall be interested only in the real part of I.

Inserting I_2 into (2.12) we obtain the corresponding contribution to the real part of $J(k)$:

$$\mathrm{Re}\{J(k)\}$$

$$\sim \frac{e\hbar H}{c} \frac{\sin 2\pi k\gamma - \cos 2\pi k\gamma}{2\pi k^2} \int\limits_0^\infty \frac{f\left(\frac{E-\varepsilon}{\Theta}\right) dE}{\partial S(E, p_0)/\partial p_0}.$$

Noting that the region of integration has two symmetrical peaks, we write the expression for that part of the thermodynamic potential Ω and the magnetic moment M which is determined by the quantity I_2 in the form:

$$\Omega = -V \frac{1}{\hbar^3}\left(\frac{e\hbar H}{c}\right)^2 \frac{1}{\pi^3} \sum_{k=1}^{\infty} \frac{\sin 2\pi k\gamma - \cos 2\pi k\gamma}{k^2}$$

$$\times \int\limits_0^\infty \frac{f\left(\frac{E-\zeta}{\Theta}\right) dE}{\partial S(E, p_0)/\partial p_0} \qquad \text{(P.1)}$$

$$M = V \frac{2}{\pi^3} \frac{e^2}{\hbar c^2} H \sum_{k=1}^{\infty} \frac{\sin 2\pi k\gamma - \cos 2\pi k\gamma}{k^2} \qquad \text{(P.2)}$$

$$\times \int\limits_0^\infty \frac{f\left(\frac{E-\zeta}{\Theta}\right) dE}{\partial S(E, p_0)/\partial p_0}$$

These expressions describe the constant part of the diamagnetism of the electron gas. In the case of the quadratic dispersion law (3.1) $\partial S(E, p_z)/\partial p_0 = -2\pi\sqrt{2mE}$ and (P.2) goes over into the familiar Landau formula.

In the general case, however, our formulas for the constant part of the diamagnetic susceptibility may turn out to be incorrect, since it is impossible to use the quasi-classical energy levels in the vicinity of $S(E, p) = 0$. The diamagnetic susceptibility of the electron gas is determined by the electrons near the Fermi boundary surface[8], while the expressions (P.1) and (P.2) are determined by all of the electrons together.

3). One can readily convince oneself that integration about the point $E' = p_z = 0$ yields a a contribution to the real part of I which is small in comparison with the real parts of I_1 and I_2; we shall not, therefore, investigate it.

---

[8] R. Peierls, Physik. **80**, 763 (1933); A. Wilson, *Quantum Theory of Metals*.

Translated by S. D. Elliot
267

SOVIET PHYSICS JETP VOLUME 2, NUMBER 4 JULY, 1956

The de Haas-van Alphen Effect in Thin Metal Layers

A. M. KOSEVICH AND I. M. LIFSHITZ
Physico-Technical Institute of the Academy of Sciences of the Ukrainian SSR

(Submitted to JETP editor July 19, 1954)
J. Exper. Theoret. Phys. USSR **29**, 743-747 (December, 1955)

The magnetic properties of electrons in thin metal layers are discussed for an arbitrary law of dispersion. The energy levels of quasi-particles with an arbitrary law of dispersion in a magnetic field in the presence of a transverse potential field are determined. The oscillating part of the magnetic moment of a gas of such quasi-particles is calculated and general formulas are used for investigating the de Haas-van Alphen effect in thin metal layers. It is shown that the periods and amplitudes of the oscillations are determined by the form of the limiting Fermi surface and depend appreciably on the ratio of the thickness of the layer to the "radius of the classical orbits" of the quasi-particles.

1. IN previous papers by the authors[1] a method of quasi-classical quantization of the motion of charged particles with an arbitrary law of dispersion $\mathcal{E}(p_x, p_y, p_z)$ in a uniform magnetic field was proposed. This method can be extended to the quantization in a magnetic field in the presence of an additional field $U(y)$.

For a magnetic field **H** along the z axis, the components of the kinetic momentum operator **P** may be conveniently chosen as

$$\check{P} = \check{p}_x + \frac{e}{c}Hy = -i\hbar\frac{\partial}{\partial x} + \frac{e}{c}Hy,$$

$$\check{P}_y = -i\hbar\frac{\partial}{\partial y},\ \check{P}_z = \check{p}_z = -i\hbar\frac{\partial}{\partial z}$$

i.e., taking $y = (\check{P}_x - \check{p}_x)c/eH$.

Thus, the Hamiltonian of the particles has the form

$$\mathscr{E}^*(P_x, P_y, P_z) = \mathscr{E}(P_x, P_y, P_z) + U[(P_x - p_x)c/eH]$$

Classical motion of the particles is described by the equations

$$\mathscr{E}^*(P_x, P_y, P_z) = \text{const}, \quad P_z = p_z = \text{const}, \quad p_x = \text{const},$$

and quasi-classical quantization is given by[1]

$$\iint dP_x dP_y \equiv S(E, p_z, p_x; H) = (n+\gamma)\frac{2\pi e\hbar H}{c}, \quad 0 < \gamma < 1 \tag{1}$$

where the integral is to be taken over the region bounded by the plane curve

$$\mathscr{E}(P_x, P_y, P_z) + U[(P_x - p_x)c/eH] = E = \text{const} \tag{2}$$

$$P_z = p_z = \text{const}, \quad p_x = \text{const}.$$

Equation (1) implicitly determines the dependence of the energy level E on the quantum number n and the components p_z and p_x:

$$E = E_n(p_z, p_x; H). \tag{3}$$

Having in mind the application of the formulas obtained to the study of the electron gas in a metal layer of finite thickness, we take $U(y)$ as having the form of infinitely high potential walls at the metal surface:

$$U(y) = 0, \quad |y| < a; \quad U(y) = \infty, \quad |y| \geqslant a \tag{4}$$

where a is the half-thickness of the layer. For this case the region (2) is given by the conditions

$$\mathscr{E}(P_x, P_y, P_z) = E, \quad |P_x - p_x| < \frac{|e|H}{c}a, \quad P_z = p_z = \text{const}, \quad p_x = \text{const}. \tag{5}$$

---

[1] I. M. Lifshitz and A. M. Kosevich, Dokl. Akad. Nauk SSSR **96**, 963 (1954); A. M. Kosevich and I. M. Lifshitz, J. Exper. Theoret. Phys. USSR **29**, 730 (1955).

Let $R_2(p_z, E)$ be the right-hand extreme value of the P_x coordinate of the plane closed curve

$$\mathscr{E}(P_x, P_y, P_z) = E, \quad P_z = p_z = \text{const}, \tag{6}$$

and $R_1(p_z, E)$ the left-hand extreme value of the P_x coordinate of the curve (Fig. 1). If

$$R_2(p_z, E) < p_x + \frac{|e|H}{c}a, \tag{7}$$

$$R_1(p_z, E) > p_x - \frac{|e|H}{c}a,$$

then the closed curve (6) lies completely between the straight lines $P_x = p_x \pm eHa/c$ (Fig. 1), and the quasi-particle can be considered as "free" and its energy levels are determined by the formulas given earlier^1.

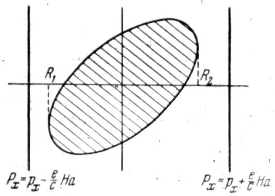

FIG. 1.

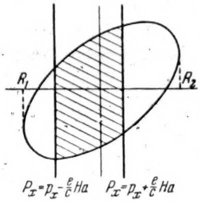

FIG. 2

If the condition (7) is not satisfied, then the area of the region (5) entering into (1) is the area bounded by the curve (6) and the straight lines (or only one of them) $P_x = p_x \pm eHa/c$ (Fig. 2). Since this area depends on a, the energy levels in this case will also depend on a:

$$E = E_n(p_z, p_x; H, a). \tag{8}$$

2. Knowing the values of the energy levels (3) or (8) of a single particle, we can determine the oscillating part of the magnetic moment of a Fermi gas consisting of such particles. The magnetic moment of the gas contained in a volume having linear dimensions L in the x and z directions is given by

$$M = -2\frac{L^2}{(2\pi\hbar)^2}\sum_n \int dp_x \times \int dp_z \frac{\partial E_n(p_z, p_x; H)}{\partial H} f\left(\frac{E-\zeta}{\Theta}\right) \tag{9}$$

where $f(\epsilon)$ is the Fermi distribution function $f(\epsilon) = (e^\epsilon + 1)^{-1}$, ζ is the chemical potential and $\Theta = kT$.

To separate out the oscillating part of the magnetic moment, we use the Poisson formula, replacing the summation with respect to n by an integration. The relevant part of the formula has the form

$$M_{\text{osc}} = -\frac{L^2}{\pi^2\hbar^2}\sum_{k=1}^{\infty} \text{Re}\left\{\int_0^\infty \varphi(E_n)\exp(2\pi kin)\,dn\right\}; \tag{10}$$

where $\varphi(E_n)$ denotes the expression under the summation sign in (9).

Taking account of (1) and the equation $\partial E/\partial H = (S - H\frac{\partial S}{\partial H})/H\frac{\partial S}{\partial E}$ which follows from it, we can go over in the integrals of (10) to an integration with respect to E

$$I_k = \int_0^\infty \varphi(E_n) e^{2\pi kin}\,dn = \frac{c}{2\pi e\hbar H^2} e^{-2\pi ki\gamma}\int_0^\infty dE f\left(\frac{E-\zeta}{\Theta}\right) \times \left\{\iint_{S>0} dp_x dp_z\left(S - H\frac{\partial S}{\partial H}\right)\exp\left[ikcS/e\hbar H\right]\right\}, \tag{11}$$

where $S = S(E, P_z, P_x; H)$. Since the argument of the exponential in (11) is, according to our assumptions, a very large number, we can apply the method of steepest descent to calculate the integral in curly brackets. If we assume the stationary point $(\partial S/\partial p_x = \partial S/\partial p_z = 0)$ to be isolated, we obtain

$$I_k \approx \frac{1}{kH} \exp\left\{-2\pi k i\gamma \pm i\frac{\pi}{4} \pm i\frac{\pi}{4}\right\}$$

$$\times \int_0^\infty dE \frac{S_m - H(\partial S/\partial H)_m}{\left|\left(\frac{\partial^2 S}{\partial p_z^2}\right)\left(\frac{\partial^2 S}{\partial p_x^2}\right) - \left(\frac{\partial^2 S}{\partial p_x \partial p_z}\right)^2\right|_m^{1/2}}$$

$$\times f\left(\frac{E-\zeta}{\Theta}\right) \exp\left[ikcS_m(E, H)/e\hbar H\right].$$

where $S_m(E, H)$ is the extreme value of $S(E, p_z, p_x; H)$ for constant E. The sign of the phase $i\pi/4$ is the same as the sign of the derivative $(\partial^2 S/\partial p_z^2)_m$ or $(\partial^2 S/\partial p_x^2)_m$ taken at the extreme point.

Because of the extreme steepness of the function $f[(E-\zeta)/\Theta]$ in the neighborhood of $E \approx \zeta$, the main contribution to I_k for $\Theta \ll \zeta$ comes from the integration close to the limiting energy. This integration finally gives

$$I_k \approx -\frac{1}{k^2}\frac{e\hbar}{c} \frac{S_m(\zeta, H) - H(\partial S/\partial H)_{m,\zeta}}{\left|\left(\frac{\partial^2 S}{\partial p_x^2}\right)\left(\frac{\partial^2 S}{\partial p_z^2}\right) - \left(\frac{\partial^2 S}{\partial p_x \partial p_z}\right)^2\right|_{m,\zeta}^{1/2} \frac{\partial S_m(\zeta, H)}{\partial \zeta}} \Psi(k\lambda)$$

$$\times \exp\left[i\frac{kcS_m(\zeta, H)}{e\hbar H} + i\frac{\pi}{2} \pm i\frac{\pi}{4} \pm i\frac{\pi}{4} - 2\pi k i\gamma\right], \tag{12}$$

where

$$\Psi(z) = \frac{z}{\sinh z}, \quad \lambda = \frac{\pi c\Theta}{e\hbar H}\frac{\partial S_m(\zeta, H)}{\partial \zeta}.$$

As can be seen from (12) the period of oscillation is given by

$$\Delta\left(\frac{1}{H}\right) = \frac{2\pi e\hbar}{c} / \left|S_m(\zeta, H) - H(\partial S_m(\zeta, H)/\partial H)\right|, \tag{13}$$

which shows that the period $\Delta(1/H)$ of oscillation depends on the value of the magnetic field H.

3. We shall now apply the general formulas obtained for a gas of quasi-particles in an arbitrary potential field to the case of an electron gas in a metal layer of finite thickness whose walls we shall replace by the infinitely high potential walls (4). The calculation of the integral I_k in this case is somewhat changed. This is connected with the fact that for

$$R_2(p_z^0, \zeta) < p_x + \frac{|e|H}{c}a,$$

$$R_1(p_z^0, \zeta) > p_x - \frac{|e|H}{c}a,$$

the energy levels are independent of p_x, where p_z^0 corresponds to the maximum value $S_m^0(\zeta)$ of the area of cross section $S^0(\zeta, p_z)$ of the surface $\mathcal{E}(P_x, P_y, P_z) = \zeta$ by planes $\mathbf{PH} = \text{const}$. Thus the expression for I_k assumes different forms for different ratios of the thickness $2a$ of the layer, to the "diameter" cD/eH of the orbit of the quasi-particle:

1) If
$$D(p_z^0, \zeta) \equiv R_2(p_z^0, \zeta) - R_1(p_z^0, \zeta) < 2\frac{eH}{c}a,$$

$$I_k \approx -\left[\frac{eH}{c}2a - D(p_z^0, \zeta)\right]$$

$$\times \frac{(e\hbar/c)^{1/2} S_m^0(\zeta)\Psi(k\lambda^0)}{k^{3/2}\sqrt{2\pi H}\left|\partial^2 S^0(\zeta, p_z)/\partial p_z^2\right|_m^{1/2}}$$

$$\times \frac{\exp\left\{ikcS_m^0(\zeta)/e\hbar H - 2\pi k i\gamma + i\left(\frac{\pi}{2} \pm \frac{\pi}{4}\right)\right\}}{\partial S_m^0(\zeta)/\partial\zeta}, \tag{14}$$

where

$$\lambda^0 = \frac{\pi c\Theta}{e\hbar H}\frac{dS_m^0(\zeta)}{d\zeta}.$$

2) If $D(p_z^0, \zeta) > 2(eH/c)a$ the expression for I_k is the same as (12), where $S(E, p_z, p_x; H)$ is to be understood as the area bounded by the curve (5) and the straight lines $P_x = p_x \pm eHa/c$.

The corresponding periods of oscillation of magnetic moment in these two cases are given by different formulas, namely,

a) for $D < 2eHa/c$, the period of oscillation is given by

$$\Delta\left(\frac{1}{H}\right) = \frac{2\pi e\hbar}{c} \Big/ S_m^0(\zeta),$$

where $S_m^0(\zeta)$ is the extreme area bounded by the curve (6) for $E = \zeta$;

b) for $D > 2eHa/c$ the period is given by (13), where $S_m(\zeta, H)$ is to be understood as the extreme value of the "cut-off" area (Fig. 2). Since $S_m(\zeta, H)$ depends on a, the period $\Delta(1/H)$ in this case depends both on the magnetic field and the thickness of the layer.

It should be noted that for the electron gas in a metal layer, the dependence of the period $\Delta(1/H)$ on H occurs only for thicknesses smaller than the mean "radius" of the electron orbit. However, the dependence of the amplitude of the oscillations on the layer thickness begins to appear at larger thicknesses [see Eq. (14)].

For an electron gas with a quadratic law of dispersion $\mathcal{E} = p^2/2m$, the curve (6) is a circle and $D(p_z^0, \zeta) = 2\sqrt{2m\zeta}$ $(p_z^0 = 0)$. As has been pointed out, the formula for the magnetic moment of such a gas in a metal layer depends on the size of the ratio

$$\sqrt{\delta} = 2a \Big/ \frac{c}{eH} D = eHa / c\sqrt{2m\zeta}.$$

For $\delta > 1$ the oscillating part of the magnetic moment is given by (10) and (14), where

$$S_m^0(E) = 2\pi m E,$$

$$dS_m^0/dE = 2\pi m, \quad |\partial^2 S/\partial p_z^2| = 2\pi,$$

and for $\delta < 1$, by (10) and (12) in which we must use the relations

$$S_m(\zeta, H) = 4m\zeta\left(\sqrt{\delta(1-\delta)} + \sin^{-1}\sqrt{\delta}\right);$$

$$\partial S_m(\zeta, H)/\partial\zeta = 4m \sin^{-1}\sqrt{\delta},$$

$$H(\partial S/\partial H)_{m,\zeta} = 8m\zeta\sqrt{\delta(1-\delta)},$$

$$|\partial^2 S/\partial p_z^2|_{m,\zeta} = 4\sin^{-1}\sqrt{\delta},$$

$$|\partial^2 S/\partial p_x^2|_{m,\zeta} = 4\sqrt{\delta/(1-\delta)}, \quad \partial^2 S/\partial p_x\,\partial p_z = 0.$$

The expressions obtained for the oscillating part of the magnetic moment of a free electron gas from the general formulas (10), (12) and (14) go over into the expressions obtained earlier by the authors from direct calculations[2]. We give here only the formulas for the periods of oscillation

$$\Delta(1/H) = e\hbar/mc\zeta, \qquad \delta > 1;$$
$$\Delta(1/H) = \pi e\hbar/2mc\zeta\left|\sqrt{\delta(1-\delta)} - \sin^{-1}\sqrt{\delta}\right|, \quad \delta < 1. \qquad (15)$$

Equation (15) gives the explicit dependence of the period of oscillation on H and the layer thickness a for $\delta < 1$.

It should be noted that, in determining the magnitude of the extreme area of cross section of the Fermi surface from experimental data, it should be possible to establish that the dependence of the period $\Delta(1/H)$ on H appears at thicknesses $a \sim 10^{-4}$ to 10^{-5} cm (in fields $H \sim 10^3$ to 10^4 oe).

In order to apply the above results to the investigation of the magnetic properties of metallic films, it is essential that the metallic film, or the packet of metallic films, should be nearly a single crystal or else the scatter of the orientations of the single crystals will lead to smearing out or complete extinction of the oscillations of the magnetic moment.

---

[2] I. M. Lifshitz and A. M. Kosevich, Dokl. Akad. Nauk SSSR **91**, 795 (1953).

Translated by D. Shoenberg
268

SOVIET PHYSICS JETP VOLUME 2, NUMBER 4 JULY, 1956

Thermal and Galvanometric Effects in Strong Fields at Low Temperatures

G. E. ZIL'BERMAN

(Submitted to JETP editor July 17, 1954)
J. Exper. Theoret. Phys USSR **29**, 762-769 (December, 1955)

The thermoelectromotive force, resistance and Hall effect are considered on the basis of a two band model for a metal in a magnetic field at low temperatures.

THE kinetic energy of electrons in a magnetic field, in a plane perpendicular to the direction of H, is quantized[1]. This holds both for free electrons and for electrons in a metal[2-4], independently of their dispersion law[5]. Because of the quantization of the energy, all the physical quantities that depend on the distribution of the electrons in the quantized levels, will oscillate upon a change in H. The oscillation of the magnetic susceptibility has been studied in greatest detail [5-9]; however, a study of the behavior of other physical quantities (resistance, Hall effect, thermal emf, etc.) upon variation of H is of interest for the electron theory of metals. It was pointed out by Akhiezer[6], on the basis of the research work of Titeica[10], that the resistance of metals (in accord with published experiments[11,12]) must oscillate upon variation of the magnetic field. Blokhintsev and Nordheim[13] investigated the increase of resistance in a magnetic field. Davydov and Pomeranchuk[14], making use of the particular case of a two band model for bismuth, showed that, along with the oscillations, there was observed an unlimited increase in the resistance of bismuth in a magnetic field. Their expressions applied only to bismuth, and in view of their complicated character, were unsuitable for comparison with experiment. Kohler[15] obtained a simple expression for the resistance in a magnetic field, but he did not take into account the quantization of the energy of the electrons.

In the present research, we have considered the behavior of the resistance, Hall effect and thermal emf (in the isotropic case) for a two band model of a metal in a strong magnetic field at low temperatures.

In place of the inequality $\omega\tau \ll 1$ ($\omega = eH/mc$, τ is the free path time for the electron in the metal), which allows us to write down the kinetic equation in the usual way, we shall assume the inverse inequality to be valid: $\omega\tau \gg 1$. In this case the quantization is preserved, in spite of collisions with the lattice.

1. EIGENFUNCTIONS AND THE ENERGY OF THE ELECTRONS

For free electrons in a magnetic field $H = H_z$ (described by the vector potential $A_x = -H_y$, $A_y = A_z = 0$) and an electric field $F = F_y$, we have the equation

$$\mathscr{H}\psi = -\frac{\hbar^2}{2m}\Delta\psi \tag{1}$$

$$+ i\mu Hy\frac{\partial\psi}{\partial x} + \frac{e^2H^2y^2}{2mc^2}\psi + eFy\psi = E\psi,$$

where $\mu = e\hbar/mc$, e = absolute value of the electronic charge. The solution of this equation has the form

$$\psi_{k_1 n k_3} \tag{2}$$

$$= \frac{\exp\{i(k_1x + k_3z)\}}{2\sqrt{L_1L_3\alpha_0}}\varphi_n\left(\frac{y}{\alpha_0} - \frac{\hbar ck_1}{\alpha_0 eH} + \frac{Fmc^2}{\alpha_0 eH^2}\right),$$

---

[1] L. D. Landau, Z. Phys. **64**, 629 (1930)

[2] R. Peierls, Z. Phys. **80**, 763 (1933)

[3] G. E. Zil'berman, J. Exper. Theoret. Phys. USSR **23**, 49 (1952)

[4] G. E. Zil'berman, J. Exper. Theoret. Phys. USSR **25**, 313 (1953)

[5] I. M. Lifshitz and A. M. Kosevich, Dokl. Akad. Nauk SSSR **96**, 953 (1954); I. M. Lifshitz and A. V. Pogorelov, Dokl. Akad. Nauk SSSR **96**, 1143 (1954)

[6] A. I. Akhiezer, Dokl. Akad. Nauk SSSR **23**, 872 (1939)

[7] L. D. Landau, Appendix to the paper of D. Shöenberg Proc. Roy. Soc. (London) **170**A341 (1939)

[8] G. E. Zil'berman, J. Exper. Theoret. Phys. USSR **21**, 1209 (1951)

[9] B. I. Verkin, B. G. Lazarev and N. S. Rudenko, J. Exper. Theoret. Phys. USSR **20**, 93 (1950); **25**, 471 (1953); **20**, 995 (1950); Dokl. Akad. Nauk SSSR **69**, 773 (1949); **73**, 59 (1950); **81**, 529 (1951); *Memorial Volume for S. I. Vavilov*, Academy of Sciences Press, 1952, p. 344.

[10] S. Titeica, Ann. Physik **22**, 129 (1953)

[11] W. J. de Hass, L. W. Schubnikov, Leiden Comm. 207 and 210 (1930); B. G. Lazarev, N. M. Makhimovich and E. A. Parphenova, J. Exper. Theoret. Phys. USSR **9**, 1169 (1939).

[12] E. S. Borovik, *Doctoral Dissertation*, Kharkov University, 1954.

[13] D. I. Blokhintsev and L. Nordheim, Z. Phys. **84**, 168 (1933).

[14] B. I. Davydov and I. Ia. Pomeranchuk, J. Exper. Theoret. Phys. USSR **9**, 1295 (1939)

[15] M. Kohler, Ann. Physik **6**, 18 (1949)

where $\alpha_0 = (\hbar c/eH)^{1/2}$; φ_n = Chebyshev-Hermite functions;

$$E_{k_1 n k_3} = E_{n k_3} + \hbar c k_1 E / H, \tag{3}$$

$$E_{n k_3} = \mu H (n + {}^1/_2) + \hbar^2 k_3^2 / 2m\,.$$

We note that $\hbar c k_1 F/H = eFy_0$, where y_0 is the equilibrium position. To the state (2) there corresponds the current

$$i_x = -ecF/H, \; i_y = 0. \tag{4}$$

We now pass over to electrons in a lattice, wherein we shall make use of the approximation of strongly coupled electrons, employing the rather simplified method of Peierls[2]. If $\varphi_0(\mathbf{r})$ is the eigenfucntion of the electron in an atom located at the point $\mathbf{n} = 0$, then (see reference 4) we have for the electron in the atom at the point $\mathbf{n}$ (if the magnetic field directed along the axis oz is described by the potential $A_y = Hx$):

$$\varphi_{\mathbf{n}}(\mathbf{r}) = \exp\{-i\alpha_0^{-2} n_1 y\}\, \varphi_0(\mathbf{r} - \mathbf{n}). \tag{5}$$

For an electron in the periodic field of the lattice, we have

$$\frac{1}{2m}\left(\hat{\mathbf{p}} + \frac{e}{c}A\right)^2 \psi + (V_p + eFy)\,\psi = E\psi. \tag{6}$$

We seek the solution of this equation in the form

$$\psi = \sum_{\mathbf{n}} a_{\mathbf{n}} \varphi_{\mathbf{n}}(\mathbf{r}), \tag{7}$$

where the function $\varphi_{\mathbf{n}}(\mathbf{r})$, which is defined by Eq. (5), satisfies the equation

$$\frac{1}{2m}\left(\hat{\mathbf{p}} + \frac{e}{c}\mathbf{A}\right)^2 \varphi_{\mathbf{n}} \tag{8}$$

$$+ [V(\mathbf{r} - \mathbf{n}) + eFy]\,\varphi_{\mathbf{n}} = E_{\mathbf{n}} \varphi_n,$$

$V(\mathbf{r} - \mathbf{n})$ is the field in an isolated atom at the point $\mathbf{n}$. For the coefficients $a_{\mathbf{n}}$ we get (assuming the neighboring $\varphi_{\mathbf{n}}$ to be slightly overlapping)

$$\varepsilon a_{\mathbf{m}} = \sum_{\mathbf{n}} a_{\mathbf{n}} \varepsilon_{\mathbf{mn}}; \qquad \varepsilon = E - E_a \tag{9}$$

(E_a are the eigenvalues in the isolated atom),

$$\varepsilon_{\mathbf{mn}} \tag{10}$$

$$= \exp\{i\alpha_0^{-2}(m_1 - n_1) n_2\}\, [A(\mathbf{m} - \mathbf{n}) + eFn_2 \delta_{\mathbf{mn}}].$$

The exchange integral $A(\mathbf{q})$ is equal to

$$A(\mathbf{q}) = \int \varphi_0^*(\mathbf{r} - \mathbf{q})\, \varphi_0(\mathbf{r})\, [V_p(\mathbf{r}) - V(\mathbf{r})]\, d\tau \tag{11}$$

It is not difficult to obtain the operator $\hat{\varepsilon}$ from the matrix elements (10). It has the form

$$\hat{\varepsilon} = \sum_{\mathbf{q}} A(\mathbf{q})\, e^{-i\mathbf{q}\hat{\mathbf{R}}} + eFy, \tag{12}$$

where $\hat{\mathbf{R}} = [\hat{\mathbf{p}} + (e/c)\mathbf{A}]/\hbar$ (e is the absolute value of the electronic charge), while $A_x = -H_y$, $A_y = A_z = 0$, and $\mathbf{q}$ is the lattice vector.

Writing the operator $\hat{\varepsilon}$ in the form (12), we have neglected the noncommutability of the components of the operator $\hat{\mathbf{R}}$ (a = lattice constant):

$$a\hat{R}_x a\hat{R}_y - a\hat{R}_y a\hat{R}_x = -ia^2/\alpha_0^2, \tag{13}$$

inasmuch as $a^2/\alpha_0^2 \ll 1$, which takes place even in very strong magnetic fields (in order that this ratio be unity, the field must be of the order of 10^8- 10^9 oersteds).

Since the exchange integral $A(\mathbf{q})$ increases very rapidly with q, we can write Eq. (12) for the cubic lattice in the form:

$$\hat{\varepsilon} = A_{00} \tag{14}$$

$$+ 2A_1(\cos a\hat{R}_1 + \cos a\hat{R}_2 + \cos a\hat{R}_3) + eFy.$$

We consider the field F small, so that the following inequality is satisfied: $eFN\alpha_0 \ll \mu H$, where $N = \sqrt{2n+1}$, $N\alpha_0$ is the amplitude of oscillation of the electron. Below the upper band we can expand in a cosine series, neglecting two terms. Then the operator (14) is identical with the operator (1), if we introduce the effective mass

$$m_{\text{eff}} = m_1 = -\hbar^2 / 2A_1 a^2$$

These operators have identical eigenfunctions[*] [Eq. (2)] and, if we select the value of the energy at $k_1 = 0$ as zero, identical eigenvalues (3).

---

[*] In the approximation of strong coupling of the electrons, for $ka \ll 1$, the function $U_k(\mathbf{r})$ in the expression $\psi = \exp\{i\mathbf{k}\cdot\mathbf{r}\} \sum \exp\{i\mathbf{k}\cdot(\mathbf{n} - \mathbf{r})\}\, \varphi_0(\mathbf{r} - \mathbf{n}) = \exp\{i\mathbf{k}\cdot\mathbf{r}\}\, U_k(r)$ depends very weakly on $\mathbf{k}$, since $|\mathbf{r} - \mathbf{n}| \lessapprox a$, and therefore the rapidly oscillating factor of $U_{\mathbf{k}}(\mathbf{r})$ can be considered constant in the calculation of arbitrary matrix elements from functions in the region $ka \ll 1$. In the presence of a magnetic field, Eq. (2) appears in place of $e^{i\mathbf{kr}}$.

Above the lower band we can again expand Eq. (14) in a series, neglecting the quadratic terms. By means of a transformation of the eigenfunctions [multiplication of them by $\exp\{\pm(i\pi/a)(x+y+z)\}$] we can reduce the problem to Eq. (1) here also. However, the effective mass, $-m_2$, is now given by

$$m_{\text{eff}} = -m_2 = \hbar^2/2A_2a^2, \quad m_{\text{eff}} < 0.$$

The eigenfunctions will have the form

$$\psi_{k_1nk_3} \tag{15}$$

$$= \sqrt{2}\,\begin{matrix}\sin\\ \cos\end{matrix}\,\frac{\pi}{a}(x+y+z)\,\frac{\exp\{i(k_1x+k_3z)\}}{2\sqrt{L_1L_3\alpha_0}} \times \varphi_n\left(\frac{y}{\alpha_0} - \frac{\hbar ck_1}{\alpha_0 eH} - \frac{Fm_2c^2}{\alpha_0 eH^2}\right).$$

Here the square of the first factor (which is rapidly oscillating and identical for all $\psi_{k_1nk_3}$) can be replaced by ½ in the calculation of the matrix elements.

The energy of the electron can be written as

$$E_{k_1nk_3} \tag{16}$$

$$= A_0 - \mu_2 H\left(n + \frac{1}{2}\right) - \frac{\hbar^2k_3^2}{2m^2} + \frac{\hbar ck_1F}{H}$$

Here A_0 is the overlap of the lower and upper bands.

The same current corresponds to the state (15) and to the state (2). The same result obtains in classical physics: the velocity of the electron has the mean value cF/H in the field $F = F_y$, $H = H_z$ and depends neither on its mass nor on its charge. The current density for all electrons in the first (upper) band will be $j_{x_1} = -(ecF/H)N_1$; N_1 = number of electrons in this zone per cm^3. The current density in the second (lower) zone will be equal to $j_{x_2} = (ecF/H)N_2$ if we take it into account that the current which corresponds to a filled band is zero. Here N_2 is the number of free states in the lower band (number of holes). The resulting current density along the ox axis will be

$$j_x = -(ecF/H)(N_1 - N_2). \tag{17}$$

The overlapping of the bands A_0 and the Fermi level E_0 (for $H = 0$, $T = 0$) are connected with the numbers N_1 and N_2 by the relations

$$N_1 = (8\pi/3h^3)(2m_1E_{00})^{3/2};$$

$$N_2 = (8\pi/3h^3)[2m_2(A_0 - E_{00})]^{3/2}.$$

2. THE CURRENT IN THE DIRECTION OF THE ELECTRIC FIELD

The current in the direction of the electric field F_y is brought about by transport of electrons because of collisions with the lattice^{10}. At the very low temperatures of interest to us we can consider only scattering by distortions of the lattice.

The current I_y through the plane $y = 0$ is equal to the number of transfers across this plane per second, multiplied by the charge on the electron:

$$I_y = \frac{2\pi e}{\hbar}\left(\frac{L_1L_3}{\pi^2}\right)^2 \tag{18}$$

$$\times \int\limits_{k_1>0}\int\limits_{\varkappa_1<0}\sum_{n,m}\int\limits_{k_3\varkappa_3} |V_{k_1nk_3;\,\varkappa_1m\varkappa_3}|^2\,\delta(E_{k_1nk_3} - E_{\varkappa_1m\varkappa_3})$$

$$\times [f_{k_1}(E_{nk_3})(1 - f_{\varkappa_1}(E_{m\varkappa_3})) - f_{\varkappa_1}(E_{m\varkappa_3})$$

$$\times (1 - f_{k_1}(E_{nk_3}))]\,dk_1\,d\varkappa_1\,dk_3\,d\varkappa_3.$$

Here $V_{k_1nk_3\varkappa_1m\varkappa_3}$ is the matrix element of the perturbation V, produced by the transfer:

$$V_{k_1nk_3;\,\varkappa_1m\varkappa_3} \tag{19}$$

$$= \frac{1}{4L_1L_3\alpha_0}\int \exp\{-i(k_1-\varkappa_1)x - i(k_3-\varkappa_3)z\}$$

$$\times \varphi_n\left(\frac{y}{\alpha_0} - \frac{\hbar ck_1}{\alpha_0 eH} + \frac{Fmc^2}{\alpha_0 eH^2}\right)$$

$$\times \varphi_m\left(\frac{y}{\alpha_0} - \frac{\hbar c\varkappa_1}{\alpha_0 eH} + \frac{Fmc^2}{\alpha_0 eH^2}\right) V\,d\tau.$$

The argument of the distribution function f will be E_{nk_3} [Eq. (3)], not $E_{k_1nk_3}$, inasmuch as $\hbar ck_1F/H$ plays the rôle of a potential energy in the electric field. The index k_1 of the function f is introduced for the case in which there is a weak temperature gradient in the metal.

In a way similar to that used in reference 10, we can show that the function f is identical, up to terms of order F^2, with the usual Fermi function, provided that the temperature gradient is proportional to the field F (thermo-emf). The proof is based on the fact that in Eq. (20) below [as also in Eq. (18)],

$$\left(\frac{\partial f}{\partial t}\right)_{\text{coll}}=\frac{2L_1L_3}{\pi\hbar}\sum_m\int_{-\infty}^{+\infty}d\varkappa_1\int_{-\infty}^{+\infty}d\varkappa_3\,|V_{k_1nk_3;\,\varkappa_1m\varkappa_3}|^2\,\delta(E_{k_1nk_3}-E_{\varkappa_1m\varkappa_3})$$
$$\times[f_{k_1}(E_{nk_3})(1-f_{\varkappa_1}(E_{m\varkappa_3}))-f_{\varkappa_1}(E_{mk_3})(1-f_{k_1}(E_{nk_3}))],\qquad(20)$$

the integration over $\varkappa_1$ is effectively between the limits

$$-\alpha_0(M+N)\leqslant\alpha_0^2(\varkappa_1-k_1)\leqslant\alpha_0(M+N),\qquad(21)$$
$$N=\sqrt{2n+1},\quad M=\sqrt{2m+1},$$

since the matrix element (19) differs from zero only in this interval. The integral (20) depends on the field F only in the combination $eF\alpha_0^2(k_1-\varkappa_1)$, but in the expansion in powers of F and integration, such terms drop out, in view of the condition (21). This will be true even in the case in which there is a temperature gradient in the metal, a gradient proportional to the field. We can then write

$$f_{\varkappa_1}=f_{k_1}+(\varkappa_1-k_1)\frac{\hbar c}{eH}\left[\frac{\partial T}{\partial y}\frac{\partial f_{k_1}}{\partial T}+\frac{\partial E_0}{\partial y}\frac{\partial f_{k_1}}{\partial E}\right],\qquad(22)$$

where E_0 is the Fermi level.

In the calculation of Eq. (18) we make use of the smallness of the difference $E_{nk_3}-E_{m\varkappa_3}$ and of the expansion (22):

$$I_y=\frac{2\pi ed_0^2}{\hbar}\left(\frac{L_1L_2}{\pi^2}\right)^2\Bigg\{\left(-eF-\frac{\partial E_0}{\partial y}\right)\int\limits_{k_1>0}\int\limits_{\varkappa_1<0}\sum_{m,\,n}\int\limits_{k_3\varkappa_3}|V_{k_1nk_3;\,\varkappa_1m\varkappa_3}|^2$$
$$\times\,\delta(E_{k_1nk_3}-E_{\varkappa_1m\varkappa_3})(k_1-\varkappa_1)\frac{\partial f_{k_1}}{\partial E_{nk_3}}\,dk_1\,d\varkappa_1\,dk_3\,d\varkappa_3$$
$$-\frac{1}{T}\frac{\partial T}{\partial y}\int\limits_{k_1>0}\int\limits_{\varkappa_1<0}\sum_{m,\,n}\int\limits_{k_3\varkappa_3}|V_{k_1nk_3;\,\varkappa_1m\varkappa_3}|^2\,\delta(E_{k_1nk_3}-E_{\varkappa_1m\varkappa_3})(k_1-\varkappa_1)\qquad(23)$$
$$\times\,(E_{nk_3}-E_0)\frac{\partial f_{k_1}}{\partial E_{nk_3}}\,dk_1\,d\varkappa_1\,dk_3\,d\varkappa_3\Bigg\}.$$

To calculate the matrix element (19) which determines the probability of elastic scattering on distortions of the periodic potential of the lattice, randomly located in the crystal, we assume that the difference V between the real and ideal periodic potential can be expressed in the form

$$V=V_0\sum_{\mathbf{p}}\delta(\mathbf{r}-\mathbf{p}),\qquad(24)$$

where the summation is carried out over all the nodes where distortion takes place. We assume such a form of V completely if the scattering of electrons located near the boundary of the band is considered.

Making use of the independence of the location of neighboring distortions, we can calculate the matrix element of the perturbation and carry out the integration over k_1, $\varkappa_1$, $\varkappa_3$, after which Eq. (23) takes the form

$$I_y=V_0^2n_{\text{d}}\,\frac{L_1L_3me}{\alpha_0^2\,6\,\pi^3\hbar^3}\Bigg\{\left(-eF-\frac{\partial E_0}{\partial y}\right)\sum_{m,\,n}\int\limits_{k_3}\frac{M^2+N^2}{\sqrt{k_3^2+2\alpha_0^{-2}(n-m)}}\frac{\partial f}{\partial E_{nk_3}}\,dk_3$$
$$-\frac{1}{T}\frac{\partial T}{\partial y}\sum_{m,\,n}\int\limits_{k_3}\frac{M^2+N^2}{\sqrt{k_3^2+2\alpha_0^{-2}(n-m)}}\frac{\partial f}{\partial E_{nk_3}}(E_{nk_3}-E_0)\,dk_3\Bigg\}.\qquad(25)$$

Here n_d is the concentration of the distortions. Summation over m is obtained with the aid of Poisson's formula and yields

$$\sum_m \frac{M^2+N^2}{\sqrt{k_3^2+2\alpha_0^{-2}(n-m)}} \tag{26}$$

$$= \frac{2\sqrt{2}\hbar}{\sqrt{m_0}(\mu H)^2}\left[\frac{2}{3}E_{nk_3}^{3/2}+\mu H\left(n+\frac{1}{2}\right)E_{nk_3}^{1/2}\right]$$

$$+\frac{2\hbar\sqrt{2\pi}}{\sqrt{m_0}(\mu H)^{3/2}}\sum_{q=1}^{\infty}\frac{(-1)^q}{\sqrt{2\pi q}}\cos\left(\frac{2\pi q E_{nk_3}}{\mu H}-\frac{\pi}{4}\right)$$

$$\times\left(E_{nk_3}+\mu H\left(n+\frac{1}{2}\right)\right)$$

We substitute this in Eq. (25), sum over n and integrate over k_3, thus obtaining the final expression for I_y. This expression is very cumbersome, but it becomes appreciably simpler if the following inequalities are satisfied:

$$\exp\{2\pi^2 kT/\mu H\}\gg 1,$$
$$kT \lesssim \mu H,\quad \mu H/E_0\ll 1, \tag{27}$$
$$kT/E_0\ll 1.$$

These conditions are usually satisfied in the theory of diamagnetism at low temperatures.

For the current density in the direction OY we get, for electrons in the lower levels of the upper band:

$$j_{y_1}=\frac{m_1^4 C}{H^2}\left\{\left(eF+\frac{\partial E_0}{\partial y}\right)\left[\frac{8}{3}E_0^2+0{,}6\mu_1 HE_0-\frac{40\pi^2\sqrt{2}}{3}\frac{kTE_0^{3/2}}{\sqrt{\mu_1 H}}e^{-\gamma_1}\cos\left(\varepsilon_1-\frac{\pi}{4}\right)+\ldots\right]\right.$$
$$\left.+k^2T\frac{\partial T}{\partial y}\left[\frac{16\pi^2}{9}E_0+\frac{\pi^2}{5}\mu_1 H-\frac{40\pi}{3\sqrt{2}}\frac{\sqrt{\mu_1 H}}{kT}E_0^{3/2}e^{-\gamma_1}(1-\gamma_1)\sin\left(\varepsilon_1-\frac{\pi}{4}\right)+\ldots\right]\right\}; \tag{28}$$

$$C=V_0^2 n_{\mathrm{d}}\frac{2c^2}{3\pi^3 e\hbar^7};\quad \gamma_1=\frac{2\pi^2 kT}{\mu_1 H};\quad \varepsilon_1=\frac{2\pi E_0}{\mu_1 H}; \tag{29}$$

and for the electrons in the upper part of the lower band:

$$j_{y_2}=\frac{m_2^4 C}{H^2}\left\{\left(eF+\frac{\partial E_0}{\partial y}\right)\left[\frac{8}{3}(A_0-E_0)^2+0{,}6\mu_2 H(A_0-E_0)\right.\right.$$
$$\left.-\frac{40\pi^2\sqrt{2}}{3}\frac{kT(A_0-E_0)^{3/2}}{\sqrt{\mu_2 H}}e^{-\gamma_2}\cos\left(\varepsilon_2-\frac{\pi}{4}\right)+\ldots\right]-$$
$$-k^2T\frac{\partial T}{\partial y}\left[\frac{16\pi^2}{9}(A_0-E_0)+\frac{\pi^2}{5}\mu_2 H-\right.$$
$$\left.\left.-\frac{40\pi}{3\sqrt{2}}\frac{\sqrt{\mu_2 H}}{kT}(A_0-E_0)^{3/2}e^{-\gamma_2}(1-\gamma_2)\sin\left(\varepsilon_2-\frac{\pi}{4}\right)+\ldots\right]\right\}; \tag{30}$$

$$\gamma_2=2\pi^2 kT/\mu_2 H,\qquad \varepsilon_2=2\pi(A_0-E_0)/\mu_2 H. \tag{31}$$

3. THERMOELECTRIC FIELD

The theory of the thermal emf in a magnetic field, based on the kinetic equation[15], shows that, upon unbounded increase in H, the longitudinal electric field (in the direction of the temperature gradient) becomes significantly greater than the transverse (their ratio is of the order of $\omega\tau$). We make the assumption that this conclusion is qualitatively correct in the case of interest to us: $\omega\tau\gg 1$, although the kinetic equation, strictly speaking, is valid only for $\omega\tau<1$. An independent argument in favor of our assumption is the fact that a thermoelectric field exists in the longitudinal direction, even in the absence of a magnetic field, while, under such conditions, there is no such field in the transverse direction. Moreover, the change of thermal emf is always small in a magnetic field (experiments have not yet been carried out at low temperatures).

If our assumption is correct, we can obtain the thermoelectric field F by making use of Eqs. (28) and (30), and the equation

$$j_{y_1} + j_{y_2} = 0.$$

In this case the H^{-2} in front of Eqs. (28) and (30) drops out, as a result of which the terms which increase rapidly with field are absent in the thermal emf case, in contradistinction to the cases of resistance and the Hall coefficient. If the above mentioned assumption is not correct, then such terms can appear in the thermal emf. We get

$$eF = -\frac{\partial E_0}{\partial y} - \frac{2}{3}\frac{\partial T}{\partial y}\frac{\pi^2 k^2 T^2}{m_1^4 E_0^2 + m_2^4 (A_0 - E_0)^2}\Big\{ m_1^4 E_0 - m_2^4 (A_0 - E_0)$$
$$\frac{9}{80}(\mu_1 H m_1^4 - \mu_2 H m_2^4) + \frac{15}{2\pi\sqrt{2}}\frac{m_1^4 \sqrt{\mu_1 H} E_0^{3/2}}{kT} e^{-\gamma_1}(1-\gamma_1)\sin\left(\varepsilon_1 - \frac{\pi}{4}\right) \tag{32}$$
$$+ \frac{15}{2\pi\sqrt{2}}\frac{m_2^4 \sqrt{\mu_2 H}(A_0 - E_0)^{3/2}}{kT} e^{-\gamma_2}(1-\gamma_2)\sin\left(\varepsilon_2 - \frac{\pi}{4}\right) + \ldots \Big\}.$$

In the single band model we have

$$eF = -\frac{\partial E_0}{\partial y} - \frac{2}{3}\frac{\partial T}{\partial y}\frac{1}{E_0}\left[1 - \frac{9}{80}\frac{\mu H}{E_0} + \frac{15}{2\pi\sqrt{2}}\frac{\sqrt{\mu H E_0}}{kT} e^{-\gamma}(1-\gamma)\sin\left(\varepsilon - \frac{\pi}{4}\right) + \ldots\right];$$
$$\frac{\partial E_0}{\partial y} = \frac{\partial E_0}{\partial T}\frac{\partial T}{\partial y} = k\frac{\partial T}{\partial y}\left[-\frac{\pi^2}{6}\frac{kT}{E_0} + \pi^{3/2}(1-\gamma)\sqrt{\frac{\mu H}{2\pi E_0}} e^{-\gamma}\sin\left(\varepsilon - \frac{\pi}{4}\right) + \ldots\right].$$

Thus the thermal emf must oscillate upon change of H, like the other physical quantities. The oscillating term has the factor $\sqrt{\mu H E_0}/kT$, of the same order of magnitude as the corresponding term $(\sqrt{\mu H E_0}/kT)\,(kT/\mu H)^2$ in the expression for the magnetic susceptibility.

4. RESISTANCE IN A TRANSVERSE MAGNETIC FIELD AND THE HALL EFFECT

The relative positions of the components of the current and field in the specimen are shown in Fig. 1. In the absence of a temperature gradient, the entire current is directed along the ξ axis.

The resistance in the magnetic field is $\rho_H = F_\xi / j = (j_y / j^2) F$, where $j_y = j_{y_1} + j_{y_2}$. Making use of Eqs. (28), (30) we obtain

$$\rho_H = \frac{CH^2 (f_1 + f_2)}{ec^2 H^2 (N_1 - N_2)^2 + cC^2 (f_1 + f_2)^2}, \tag{33}$$

where

$$f_1 = \frac{8}{3}E_0^2 m_1^4 \Big(1 + \frac{9}{40}\frac{\mu_1 H}{E_0}$$
$$- 5\pi^2\sqrt{2}\frac{kT}{\sqrt{\mu_1 H E_0}} e^{-\gamma_1}\cos\left(\varepsilon_1 - \frac{\pi}{4}\right) + \ldots\Big) \tag{34}$$

and f_2 is obtained from f_1 by replacing m_1 by m_2, and E_0 by $A_0 - E_0$. Equation (33) is valid only for $\omega\tau \gg 1$ (in strong fields). For $N_1 = N_2$, ρ_H increases proportionally to H^2, while for $N_1 \neq N_2$, saturation is observed.

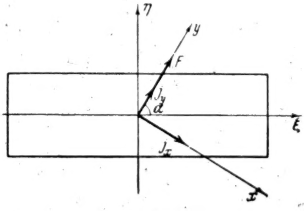

FIG. 1

The ratio F_η / F_ξ, introduced by Borovik[1,2] as a characteristic of the Hall effect at low temperatures, is equal to

$$\frac{F_\eta}{F_\xi} = \frac{j_x}{j_y} = \frac{-H(N_1 - N_2)}{C(f_1 + f_2)}. \tag{35}$$

Equations (33) and (34) are in conformity with the classification of metals[1,2] according to the type of dependence of the resistance and the Hall field on the direction of the magnetic field. If $N_1 \neq N_2$, the resistance increases up to saturation and the Hall field is proportional to H. If $N_1 = N_2$, the resistance increases in proportion to H^2, and the Hall field is very small. It follows from Eq. (35) that in this case $F_\eta = 0$; this is dependent on our approximation (in the expression for the current j_x, there must appear terms of much higher order relative to $(\omega\tau)^{-1}$, which leads to a decrease of F_η in strong fields; this has also been observed[12]).

The oscillations of the resistance and the Hall field must differ in phase by π; this has been observed in the experiments of Borovik[12]. The mobility of the electrons enters only into the current j_y; therefore, if the resistance decreases under external pressure (as a consequence of the increase in the exchange integral A and, consequently, the decrease of the effective mass m), then the Hall field must increase. This has also been observed by Alekseevskii and Brandt[16].

The expression (28) for the current density (for $dT/dy = 0$) can be written in the form

$$j_y = \sigma F(\omega\tau)^{-2}, \tag{36}$$

which follows from the theory of Kohler[15] for $\omega\tau \gg 1$. In such a case, if we assume $\sigma = e^2 n\tau/m$, we can estimate the mean free time of the electrons. If we keep in Eq. (28) only the principal term $(8/3)E_0^2$, we get

$$1/\tau = V_0^2 n_d 2m \sqrt{2mE_0}/3\pi\hbar^4. \tag{37}$$

while for the mean free path we get

$$1/l = (1/\tau)\sqrt{m/2E_0} = 2V_0^2 n_d\, m^2/3\pi\hbar^4, \tag{38}$$

and $1/l$, as always, in scattering on impurities or distortions, is proportional to the concentration of the impurities and does not depend on the concentration of electrons.

If we also keep all the other terms in Eq. (28), then the free time of the electrons on the Fermi surface oscillates upon change of the magnetic field:

$$\frac{1}{\tau} = \frac{2V_0^2 n_d m}{3\pi\hbar^4}\sqrt{2mE_0}\left(1 + \frac{9}{40}\frac{\mu H}{E_0}\right. \tag{39}$$
$$\left. - 5\pi^2\sqrt{2}\frac{kT}{\sqrt{\mu\hbar E_0}}e^{-\gamma}\cos\left(\varepsilon - \frac{\pi}{4}\right) + \ldots\right)$$

Here we assume E_0 to be a constant quantity, since the corrections will be of a higher order of smallness than the terms considered.

The author takes this occasion to express his thanks to Professor I. M. Lifshitz for his discussions of the work.

---

[16] N. E. Alekseevskii and N. G. Brandt, Proceedings of the Conference on Low temperature Magnetism, Kharkov, 1954.

Translated by R. T. Beyer
270

SOVIET PHYSICS JETP VOLUME 2, NUMBER 4 JULY, 1956

Magnetic Properties of Trivalent Ions of Europium and Samarium

A. S. BOROVIK-ROMANOV AND N. M. KREINES
Moscow State Institute
of Standards and Measuring Instruments

(Submitted to JETP editor August 10, 1954)
J. Exper. Theoret. Phys. USSR **29**, 790-797 (December, 1955)

The magnetic susceptibilities of Eu_2O_3, Sm_2O_3 (in two crystalline modifications) and $Sm_2(C_2O_4)_3 \cdot 10H_2O$ have been measured from 12 to 300° K. A strong dependence of the magnetic properties of the samarium ion on the crystalline structure of the compound in which it occurs was found. With a decrease in the effect of the crystalline field, the experimental curves of the temperature dependence of the magnetic susceptibility approximate the theoretical curve of Van Vleck for free ions. An apparatus for measuring magnetic susceptibility over a wide temperature interval is described.

---

1. INTRODUCTION

THE investigation of the magnetic properties of the rare earth elements has played a significant role in the study of the structure of atomic electron shells. The magnetic susceptibility of the majority of the compounds of the rare earth elements satisfies the Curie law. The compounds of europium and samarium are an exception. The splitting of the deepest multiplet levels is very small for the ions of these elements. The difference in energy between the first excited level and the ground state $E_1 - E_0$ is comparable with the energy of thermal motion even at room temperatures. The magnitude of $(E_1 - E_0)/k \sim 1400°$ K for samarium. As Van Vleck has shown[1], this must lead to intrinsic anomalies in the temperature dependence of the magnetic susceptibility. For an explanation of the magnetic properties of europium and samarium, two circumstances must be considered.

1. The smallness of the difference $E_1 - E_0$ indicates a significant effect of the quadratic term in the energy of interaction of the magnetic moment of the atom with the magnetic field. Instead of the simple Curie law for the magnetic susceptibility, there results in this case the more complicated expression

$$\chi_J = \frac{Ng^2\mu_0^2 J(J+1)}{3kT} + N\alpha_J, \qquad (1)$$

in which there enters the temperature independent term $N\alpha_J$. The latter arises when account is taken of nondiagonal matrix elements of the square of the magnetic moment. In the region of low temperatures the first term predominates, and the susceptibility varies in inverse proportion to the temperature. As the temperature is increased, the susceptibility approaches a constant limit. The magnetic susceptibility of the trivalent ion of samarium must satisfy this law for low temperatures.

2. Moreover, because of the smallness of the multiplet splitting, a considerable portion of the ions are in excited states even at room temperatures. Formula (1) will be correct for such a group of ions, occurring in the equation with a given value of J. Van Vleck has derived the following general formula for the total susceptibility:

$$\chi = \sum_J \chi_J (2J+1)\exp\{-E_J/kT\} \Big/ \sum_J (2J+1)\exp\{-E_J/kT\}. \qquad (2)$$

The magnetic susceptibility of Eu^{+++} must satisfy this dependence. $E_1 - E_0$ for samarium is sufficiently large up to ~ 150° K this summation may be limited to only its first term. The testing of Van Vleck's theory at the lowest possible temperatures is of very great interest. Sufficiently complete experimental results were not obtained in the works completed earlier by Wiersma and

---

[1] J.H.Van Vleck, *The Theory of Electric and Magnetic Susceptibilities*, Oxford, 1932.

Schultz[2] and by Trapnell and Selwood[3]. The present work is devoted to an experimental investigation of the magnetic properties of the trivalent ions of europium and samarium at low temperatures.

2. APPARATUS AND SAMPLES

The Faraday method, based on the measurement of the force exerted on a small sample placed in an inhomogeneous field, was used in the measurement of the magnetic susceptibility.

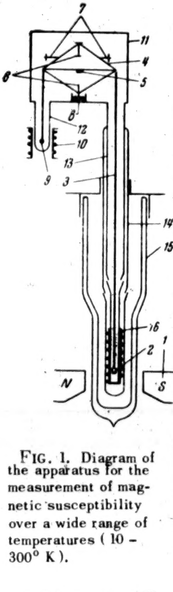

FIG. 1. Diagram of the apparatus for the measurement of magnetic susceptibility over a wide range of temperatures (10 – 300° K).

A general view of the apparatus is schematically represented in Fig. 1. The magnetic field, in which the sample *2* under investigation was placed, was produced by the electomagnet *1*. Powdered samples were placed in a quartz tube of diameter 3 mm and height 5 mm. The tube was suspended by a long quartz thread *3* from one end of the beam of a balance which served for the measurement of the force exerted on the sample. The balance beam *4* had an arm 3 cm in length; it was reinforced by a tension member *5* made of bronze strip of thickness 30 μ and width 0.6 mm. Screws *6* and *7* served for the adjustment of the center of gravity and the attainment of equilibrium in the absence of the field. The balance was provided with an oil damper *8*. The position of the balance was observed by the deflection of a light beam on a scale located 2 m away. The force acting on the sample was balanced by the force of interaction of the magnetic field of the compensating coil *10*, fed with alternating current, on a piece of permalloy suspended from the other arm of the beam. The tube containing the sample and the counterweight of permalloy were suspended from the beam arms by quartz threads (diameter 50 μ). The balance and the suspended sample were enclosed in a hermetically sealed system consisting of the cover *11* and the glass tubes *12* and *13*. The lower part of the tube *13* was removable (as a section) and had at the end a copper tube *16*. Calibration of the entire apparatus was done by means of standard weights, certified by the All-Union Institute of Metrology.

In order to allow the measurement of the magnetic susceptibility over a wide range of temperatures, the tube *13*, in which the sample was located, was surrounded with a vacuum jacket *14*. This entire system was immersed in the Dewar *15*, filled with either liquid nitrogen or hydrogen. A heating coil was wound on the copper tube *16*. By sending current through the heater with a vacuum of $\sim 10^{-3}$ mm Hg in the jacket, we can easily cover the two continuous temperature ranges from 20 to 90° K and from 77 to 300° K.

The temperature was measured by means of a copper-constantan thermocouple soldered to the copper tube. It was ascertained that the temperature of the sample was always sufficiently close to the temperature of the copper tube surrounding it.

The described apparatus allowed the measurement of the magnetic susceptibility over a wide temperature interval.

The sensitivity of the balance was $\sim$0.003 mg per 1 mm deflection of the light beam. Three field intensities, from 2 to 6 kilo-oersteds, depending on the susceptibility of the sample, were used in the susceptibility measurements. With a maximum field intensity and with a sample of weight $\sim$10 mg, the sensitivity of the arrangement was $\sim 10^{-8}$ cgsu per 1 mm deflection of the light beam. We estimate the accuracy of the determination of the absolute value of the susceptibility as 3-4%. The accuracy of the relative measurements was $\sim$1.5%.

All the samples we investigated had the form of microcrystalline powders. Measurements were made on portions of $\sim$10 mg, and were made on at least two portions of each compound. The majority of the compounds were kindly prepared for us by I. N. Zaozerskii and were of special purity. The quantity of impurities in the sample of Eu_2O_3 did not exceed 0.1% and was less than 0.01% in the samples of Sm_2O_3 (I) and $Sm_2(C_2O_4)_3 \cdot 10H_2O$. On being stored for a long time, the oxides of samarium and europium absorb carbon dioxide and water. Hence, they were all kept at a temperature of 800° C for two hours before the measurements. In the case of samarium, measurements were also made with unheated oxides. In this latter case a correction was made for the weight of the absorbed carbon dioxide and water.

---

[2] E. C. Wiersma and B. H. Schultz, Physica **13**, 171 (1933).

[3] B. M. W. Trapnell and P. W. Selwood, Nature **169**, 840 (1952).

3. MAGNETIC SUSCEPTIBILITY OF Eu_2O_3

One sample of Eu_2O_3 was investigated. A diamagnetic correction, which we took as -0.35×10^{-6} cgsu, corresponding to the results of the measurement[2] of the susceptibility of La_2O_3, was made to the measured specific susceptibility.

The temperature dependence which we obtained for the gram-atomic magnetic susceptibility of the Eu^{+++} ion is shown in Fig. 2. The dashed curve was given in reference 3 on the basis of values of the susceptibility at only 4 temperatures. (The experimental values are indicated by small crosses.) The results of Trapnell and Selwood agree sufficiently well with our results, although they drew their curve erroneously because of an insufficiency of experimental points.

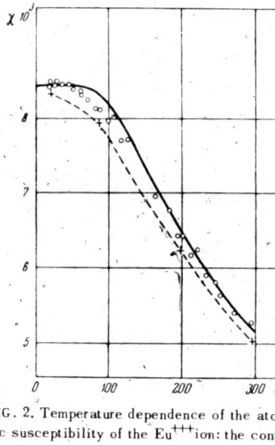

FIG. 2. Temperature dependence of the atomic magnetic susceptibility of the Eu^{+++} ion: the continuous curve is according to the theory of Van Vleck[1], the points + are the results of Trapnell and Selwood[3], and the points O are the results of the present work.

As is clear from Fig. 2 our results agree quite well with the theoretical conclusions of Van Vleck[1,4]. At low temperatures, for which all the europium ions are in the ground state with $J = 0$, only the constant term remains in Eq. (2): $\chi_0 = N\alpha_0$. The susceptibility actually remains constant up to $\sim 40°$ K. From the magnitude of this susceptibility, χ_0 $(Eu^{+++}) = 8.42 \times 10^{-3}$ cgsu, the difference in energy between the ground and first excited levels can be calculated. The value which we obtained, $E_1 - E_0 = 250$ cm^{-1}, lies essentially lower than the value of 400 cm^{-1} obtained from spectroscopic data[5]. However, it agrees well with the value calculated by Van Vleck for a shielding constant of $\sigma = 34$. It should also be noted that the value of the overall width of the multiplet ~ 5200 cm^{-1} calculated from our value of $E_1 - E_0$ coincides with the value 5000 cm^{-1} obtained from spectroscopic results.

The number of ions in the ground state decreases with an increase in temperature, and the susceptibility which depends on these ions falls according to the law $\chi = N\alpha_0 / (1 + 3\exp\{-(E_1 - E_0)/kT\})$. The overall susceptibility falls somewhat more slowly, since the ions which are in excited states also contribute to the susceptibility. Our results agree quite well with Van Vleck's formula (2) if we take $E_1 - E_0 = 250$ cm^{-1}. A small discrepancy is observed only in the region 60–100° K, where the values of the susceptibility lie somewhat below the theoretical curve.

4. MAGNETIC PROPERTIES OF THE TRIVALENT ION OF SAMARIUM

The magnetic properties of Sm^{+++} were studied in two compounds: Sm_2O_3 and $Sm_2(C_2O_4)_3 \cdot 10H_2O$. Two samples of Sm_2O_3 were investigated: one sample (I) a product of the Kahlbaum firm, the purity of which, according to the results of a spectroscopic analysis*, was not less than 99.0%, and the other sample (II) prepared by I. N. Zaozerskii. The latter sample was of very high purity ($\sim$ 99.99%). Investigations were carried out with both samples, both before heating them and after heating them.

Preliminary experiments on the magnetic susceptibility of both samples of Sm_2O_3 gave a basis for supposing that we had to do with two crys-

---

[4] A. Frank, Phys. Rev. 39, 119 (1932).

* The authors extend their thanks to S. A. Borovik, who carried out the spectral analysis of this compound.

[5] M. A. El'jashevich, *Spectra of the Rare Earths*, 1953.

talline modifications. X-ray photographs* confirmed that for sample I the crystalline structure of the heated compound differed essentially from the structure of the unheated compound, while for sample II both structures were nearly the same. It is known from the literature (see, for example, reference 6) that at room temperatures Sm_2O_3 has a body-centered cubic lattice (of the type of Mn_2O_3) with 16 molecules in the elementary cell. A new crystalline modification is formed at a temperature of 720° C. This modification has been little studied; it has a pseudotrigonal structure. Evidently in the freshly heated sample I we were concerned with the supercooled high temperature pseudotrigonal modification of Sm_2O_3. The remaining forms had the cubic structure. It should be emphasized that in the very pure compound (sample II) supercooling does not occur, and we are at all times, both before and after the heating, concerned only with the equilibrium low temperature modification. We assume that the presence of impurities in sample I facilitated the formation of the high temperature modification.

The results of the investigation of the temperature dependence of the magnetic susceptibility of both samples are given in Fig. 3. Within the limits of error of the measurements, all the points lie on two separate curves. Curve 2 corresponds to the results obtained for the heated sample I, that is, for the pseudotrigonal structure of Sm_2O_3. The results obtained at Leyden[2] in 1936 are also put with this curve. The results obtained for both unheated samples describe curve *1*. The results obtained for the heated sample II also coincide with them. Thus this curve corresponds to the cubic modification of Sm_2O_3.

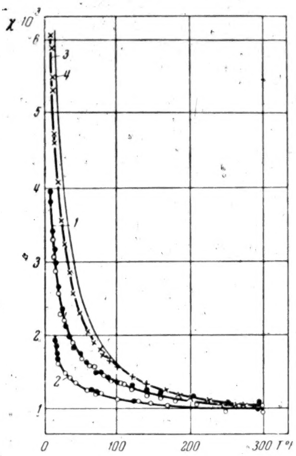

FIG. 3. Temperature dependence of the atomic magnetic susceptibility of the Sm^{+++} ion. Curve *1* is for the cubic modification of Sm_2O_3: O for sample I, ● for sample II; curve *2* is for the pseudotrigonal modification of Sm_2O_3: O for sample I, ● for the Leyden results[2]; curve *3* is for $Sm_2(C_2O_4)_3 \cdot 10H_2O$; curve *4* is the theoretical curve[1].

Both curves agree qualitatively with the theoretical curve of Van Vleck, although the quantitative discrepancies, especially at low temperatures, are very significant. It would be natural to suggest that these discrepancies depend on the effect of the crystalline field (see below). Hence it would be desirable to carry out an investigation of the magnetic properties of Sm^{+++} in another compound, where the effect of the crystalline field would be smaller. Samarium oxalate ($Sm_2(C_2O_4)_3 \cdot 10H_2O$), a salt favorably distinguished by its great number of molecules of water of crystallization and the constancy of their number, was chosen. The H_2O molecules surround the Sm ion in the crystal of the salt and significantly lower the inhomogeneous crystalline field acting on the ion. The results obtained for the sample of $Sm_2(C_2O_4)_3 \cdot 10H_2O$ are also given in Fig. 3 (curve *3*). They much more nearly coincide with the theoretical curve, deviating from it by only 20% for 20° K.

With the aid of the value of $\chi(Sm^{+++}) = 1.07 \times 10^{-3}$ cgsu (at 293° K), obtained for $Sm_2(C_2O_4)_3 \cdot 10H_2O$ by formula (2), the difference in energy between the two lowest levels of the Sm^{+++} multiplet was calculated. The value $E_1 - E_0 = 1020\,cm^{-1}$ (equivalent to 1470° K) obtained agrees sufficiently well with the value 1100 cm^{-1} obtained from spectroscopic results[5]. It lies between the two values (1070 cm^{-1} and 932 cm^{-1}) theoretically calculated by Van Vleck[1] for the two shielding constants $\sigma = 33$ and $\sigma = 34$.

---

* The x-ray photographs of the samples were taken by V. P. Tarasova and D. I. Graevskaia, with the kind assistance of V. I. Iveronova. The authors express to them their deepest thanks.

[6] V. I. Iveronova, V. P. Tarasova and M. M. Umanskii, Vestn. Moscow Univ. 8, 37 (1951).

The significant deviations of our results for the magnetic susceptibility of the two modifications of Sm_2O_3 from the theoretical curve for free Sm^{+++} ions must be explained by the effect of the crystalline field. The question of the effect of the crystalline field on the magnetic properties of the ions of the rare earth elements has been considered in a number of theoretical investigations[7-9]. In particular, the effect of the crystalline field on the magnetic properties of Sm^{+++} in the salt $Sm_2(SO_4)_3 \cdot 7H_2O$ was investigated by Miss Frank[10]. However, her considerations were limited to the temperature region 70-300° K, where the effect of the crystalline field may be considered insignificant.

The crystalline field splits the sixfold degenerate ground level of the samarium ion ($^6H_{5/2}$) into three twofold sublevels, each of which may be characterized by the effective magnetic quantum number $\pm M_{i\ \mathrm{eff}}$. In this case the value of the susceptibility will be determined not by formula (1), but by the more complicated formula

---

$$\chi = \frac{Ng^2\mu_0^2}{kT} \frac{M_{1\ \mathrm{eff}}^2 + M_{2\ \mathrm{eff}}^2 \exp\{-\Delta W_1/kT\} + M_{3\ \mathrm{eff}}^2 \exp\{-\Delta W_2/kT\}}{1 + \exp\{-\Delta W_1/kT\} + \exp\{-\Delta W_2/kT\}} + N\alpha, \qquad (3)$$

---

where ΔW_1 and ΔW_2 are the energy differences between the two corresponding upper and lower sublevels. The values of the effective magnetic quantum numbers of each of the sublevels are obtained as a linear combination of the magnetic quantum numbers of the free ion[5] M:

$$M_{i\ \mathrm{eff}} = \sum_M |\alpha_M^i|^2 M, \qquad (4)$$

where the α_M^i are the coefficients in the expansion of the wave functions corresponding to the ith sublevel, for the wave functions of the ion in a field of cylindrical symmetry. The general solution of the problem of the calculation of the particular form of formula (3) requires a knowledge of the symmetry of the crystalline field and the form of its potential. However, in many cases it may be assumed that the $M_{i\ \mathrm{eff}}$ are approximately equal to the corresponding values of the magnetic quantum number of the free ion[11,12,5]. For Sm^{+++} one should put into the formula the respective values $M = \pm 1/2$, $\pm 3/2$, $\pm 5/2$. We have taken $M_1 = \pm 1/2$, $M_2 = \pm 3/2$, $M_3 = \pm 5/2$.

By comparing the resulting formula with the experimental results, we determined the values of the parameters ΔW_1 and ΔW_2 which occur in the formula. For the cubic modification of Sm_2O_3 we obtained: $\Delta W_1 = 0$ and $\Delta W_2 = 52$ cm^{-1} (equivalent to 73° K). For the pseudotrigonal modification of Sm_2O_3 we found $\Delta W_1 = 20$ cm^{-1} (29° K) and $\Delta W_2 = 150$ cm^{-1} (218° K).

Our experimental results are shown in the graph of Fig. 4, where the coordinates are $1/\chi$ and T. Curve *4* of this graph corresponds to Van Vleck's formula (1), curves *1* and *3* were calculated according to formula (3), using the values of the constants introduced above. Although a rather rough assumption on the replacement of M_{eff} by M was made in the construction of these curves, a consideration of them gives a basis for some general conclusions. First, when the corresponding set of constants is used in Eq. (3), it will describe with a sufficient degree of accuracy the results obtained for the magnetic susceptibility of the samarium ion in various compounds. Second, for all the compounds of samarium which were investigated, the value of the effective magnetic quantum number corresponding to the lower sublevel must be less than the M_{eff} corresponding to the upper sublevel, since only in this case do we obtain curves situated above the curves for the free ions. Giesekus[12], in his calculations on the splitting of the levels in $Sm_2(BrO_3)_3 \cdot 9H_2O$ ar-

---

[7] H. Bethe, Ann. Physik 3, 133 (1929).

[8] H. Kramers, Proc. Amst. Acad. 35, 1272 (1932).

[9] W. G. Penney and R. Schlapp, Phys. Rev. 41, 194 (1932).

[11] K. Hellwege, Ann. Physik 4, 95 (1948).

[12] H. Giesekus, Ann. Physik 8, 350 (1951).

[10] A. Frank, Phys. Rev. 48, 765 (1935).

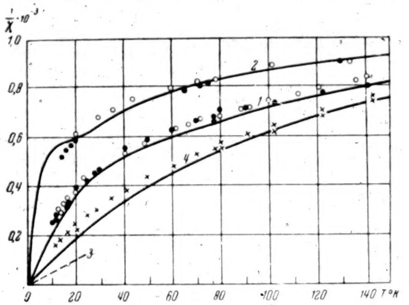

FIG. 4. Temperature dependence of the reciprocal of the atomic magnetic susceptibility of the Sm^{+++} ion. Curve *1* is for the cubic modification of Sm_2O_3: O for sample I, ● for sample II, the continuous curve is by formula (3) ($\Delta W_1 = 0$, $\Delta W_2 = 52$ cm^{-1}); curve *2* is for the pseudotrigonal modification of Sm_2O_3: O for sample *1*, ● for the Leyden results[2], the continuous curve is by formula (3) ($\Delta W_1 = 20$ cm^{-1}, $\Delta W_2 = 150$ cm^{-1}); curve *3* is the straight line example explained in the text; curve *4* is the theoretical curve for free ions.[1]

rived at the opposite result.

Third, for sufficiently low temperatures the magnetic susceptibility must follow the Curie law $\chi = C/T$, in which $C = (Ng^2\mu_0^2/k)\times(\Sigma M_{\mathrm{eff}}^2/i)$, where the summation is taken over all the M_{eff} of the lower sublevel and i is the degree of degeneracy of this sublevel. For the cubic modification of Sm_2O_3 the magnitude $(1/i)\Sigma M_{\mathrm{eff}}^2$ must be of the order 10/8, that is, approximately 2.3 times as small as the value $J(J+1)/3 = 35/12$ obtained for the sixfold degenerate level $^6H_{5/2}$. The value of C for an ion in the crystalline field will always be less than the value of C for a free ion if the M_{eff} of the lower sublevel is less than the M_{eff} of the upper sublevel. As an example, the straight line 3 – $1/\chi = T/C_1$, where C_1 is calculated on the assumption that the lower sublevel has $M_{\mathrm{eff}} = \pm 5/2$, is drawn in Fig. 4.

It should be remarked that, although from 300° K to ~ 70° K the results obtained for $Sm_2(C_2O_4)_3 \cdot 10H_2O$ very nearly coincide with Van Vleck's curve, the experimental points deviate from this curve at low temperatures and approach curve *1*.

CONCLUSIONS

In summing up the work reported, we may draw the following general conclusions:

1. The temperature dependence of the magnetic susceptibility of Eu_2O_3 agrees sufficiently well with the theoretical dependence of Van Vleck. The small deviation in the region 40 – 80° K may be explained by the splitting up of the first excited level, since this must lead to the decrease in susceptibility beginning at lower temperatures.
2. The magnetic properties of the Sm^{+++} ion (especially at low temperatures) depend very strongly on the crystalline lattice in which it is found.
3. When a small amount of impurities is present, samarium oxide which has been heated to 800° C keeps the crystalline structure of the high temperature phase when it is cooled to room temperature. The magnetic properties of the equilibrium and supercooled phases of Sm_2O_3 are essentially different at low temperatures. The deviation of the temperature dependence of the magnetic susceptibility of both crystalline forms of Sm_2O_3 from Van Vleck's theory for free ions may be qualitatively explained by the splitting of the ground state of Sm^{+++} in the field of the lattice.

4. The temperature variation of the magnetic susceptibility of samarium oxalate, for which the effect of the crystalline field should be small, is very close to the theoretical curve for free ions.

5. Energy differences between the first excited state and the ground state were calculated from the magnetic data. The values obtained (250 cm^{-1} for Eu^{+++} and 1020 cm^{-1} for Sm^{+++}) agree quite well with spectroscopic results.

In conclusion, the authors wish to express their deep gratitude to Professor P. G. Strelkov for his constant interest in the work and to Professor I. N. Zaozerskii, who kindly prepared the samples and gave us a number of valuable suggestions.

Translated by M. G. Gibbons
273

SOVIET PHYSICS JETP VOLUME 2, NUMBER 4 JULY, 1956

Methods of Investigating the Width of Raman Lines and Their Application

P. A. BAZHULIN, S. G. RAUTIAN, A. I. SOKOLOVSKAIA AND M. SUSHCHINSKII
P. N. Lebedev Institute of Physics, Academy of Sciences, USSR

(Submitted to JETP editor July 15, 1954)
J. Exper. Theoret. Phys. USSR 29, 822-829 (December, 1955)

The effect of various factors on the observed width of Raman lines was considered, and methods of excluding the effect of these factors on the results of measurements are described. Results are given of measurements of the width of a number of Raman lines using a prism spectrograph with large dispersion. A comparison is made of the data obtained with data found by other methods.

1. STUDIES of the width and the form of Raman lines are of great interest from the viewpoint of obtaining data on intramolecular and intermolecular interactions. The knowledge of the width of these lines is also very important for the correct selection and substantiation of the methods of measuring intensities. However, the width and the form of lines remain (up to the present time) the least investigated parameters in Raman spectra, owing to the fact that their investigation is associated with great experimental difficulties. These difficulties were, apparently, successfully overcome for the first time in the work of Sterin[1], although attempts to carry out such measurements were made many times previously[2,3]. In the work of Sterin two Raman lines were studied with the aid of a Fabry-Perot etalon: the line $\Delta\nu = 992$ cm^{-1} of benzene and $\Delta\nu = 802$ cm^{-1} of cyclohexane. Irrespective of the fact that these belong to the strongest (and narrowest) Raman lines, the interferometric method of measuring proved very difficult. Hence, this method would not be very suitable for the study of weaker lines. Also, additional difficulties arise when it is necessary to study the wider lines, owing to the fact that the dispersion region of the Fabry-Perot interferometer is inadequate. For this reason, we developed indirect methods for the evaluation of the widths of the Raman lines. Such indirect methods are the "photometric" method, based on the study of the dependence of the intensity of lines on the width of slit of the spectrograph[4,5], and the method of the "effective width" of lines, based on a comparison of the integral intensities with the intensities at the maximum of the lines[6,7,8]. These indirect methods are essentially based on the data obtained in the work of

---

[1] Kh. E. Sterin, Dissertation, Inst. of Physics, Acad. Sci. USSR, 1949; Izv. Akad. Nauk SSSR, Ser. Fiz. 14, 411 (1950).

[2] P. P. Shorygin, Zh. Fiz. Khim. 15, 1072 (1941).

[3] A. C. Manzies, Proc. Roy. Soc. (London) 172, 89 (1939).

[4] M. M. Sushchinskii, Izv. Akad. Nauk SSSR, Ser. Fiz. 11, 348 (1947).

[5] M. M. Sushchinskii, Trudy Fiz. Inst. Akad. Nauk 5, 185 (1950);

[6] M. M. Sushchinskii, Izv. Akad. Nauk SSSR, Ser. Fiz. 14, 387 (1950).

[7] M. M. Sushchinskii, J. Exper. Theoret. Phys. USSR 22, 765 (1952).

[8] M. M. Sushchinskii, Izv. Akad. Nauk SSSR, Ser. Fiz. 17, 608 (1953).

Sterin[1].

The development of indirect methods does not minimize, of course, the importance of studying the forms and the widths of lines by direct methods, the more so because the indirect methods are not suitable for the study of the line contours. In addition, for the development and substantiation of the above-mentioned indirect methods of evaluating the width of lines, the data of Sterin are not sufficient, since they relate only to a class of the sharpest Raman lines. Therefore, the problem arose of obtaining by direct methods new data on the width and shape of lines of various types. The present work deals with the development of a procedure for measuring the width and the contour of Raman lines with the aid of a spectrograph of medium dispersion. We have also compiled the data of measurements for a number of different types of Raman lines.

2. In the study of spectral lines it is necessary to take into account a number of factors exerting an influence on their observable width and shape. Such distorting factors can be diffraction on the aperture diaphragm of the spectrograph, defects in the optical system, the final value of the width of slit and the resolving capacity of the photolayer. In the case of Raman lines, it is also necessary to take into account the width of the exciting line. The broadening produced by each of the factors enumerated above can be characterized as an "apparatus function," which corresponds to the action of a given factor under the condition of a neglibibly small effect of all the other factors. In order to illustrate the role of each of the distorting factors, we have compiled in Table I an approximate evaluation of the width of the apparatus function corresponding to each of these effects for several types of spectrographs. For the characteristic of diffraction broadening the values of the normal width of slit are given by

$$S_0 = \frac{\lambda f}{d} D,$$

where f is the focal distance, d the effective diameter of the objective of the collimator, D the linear dispersion of the instrument. We have not taken into account the effect of defects in the optical system of the spectrograph, since these are to some degree individual characteristics. For the apparatus function of the photolayer, in agreement with the data of the photoplates used, we assumed a width of the order of 0.015 mm. The value of the width of the exciting line was taken as that of a lamp with cooled electrodes[9] from the measurements with a Fabry-Perot etalon.

TABLE I

Spectrograph	Actual Relative Opening	Magnification	Linear Dispersion*, cm^{-1} mm	S_0, cm^{-1}	Apparatus function of the Photolayer, cm^{-1}	Real Width of Exciting Line, cm^{-1}	Observed Width of Exciting line***, cm^{-1}
ISP-51	1:6	0.9	140	0.36	2.1	0.2	2.5
V-III	1:11	0.7	56	0.21	0.8	0.2	1.0
Diffraction Lattice** . .	1:12	1.0	28	0.14	0.4	0.2	0.7

* All data given are calculated for the line 4358 Å.

** This apparatus will be described in more detail separately.

*** When a narrow slit is used for the photographing of the spectra.

Some idea of the total action of all the distorting factors considered above is given by the observed width of the exciting line. The values of this quantity for the three spectrographs we have considered are given in the last column of Table I.

---

[9] M. L. Sosinskii, Izv. Akad. Nauk SSSR, Ser. Fiz. 17, 621 (1953).

3. It should be kept in mind that the distorting action of each of the factors considered above depends not only on the width and on the shape of the corresponding apparatus functions, but also on the shape of the lines under investigation. Therefore, a separate account of the effect of each of the distorting factors in the study of the width and the shape of Raman lines is associated with considerable difficulties. However, an individual account of these factors is not at all requried: in order to exclude completely the effect of all the distorting factors, and to find the real contour from the observed contour of a Raman line, it is sufficient to have the data on the observed contour of the exciting line. This problem was considered in detail in a previous paper[10]. According to the data of this study, for the real contour of the Raman line φ_k we have:

$$\varphi_{\text{K}}(\lambda) = \frac{1}{2\pi}\int_{-\infty}^{+\infty} \frac{K(u)}{K_{\text{B}}(u)} e^{-i\lambda k}\, du, \tag{1}$$

where

$$K(u) = \frac{1}{\sqrt{2\pi}}\int_{-\infty}^{+\infty} k(x)\, e^{iux}\, dx;$$

$$K_{\text{B}}(u) = \frac{1}{\sqrt{2\pi}}\int_{-\infty}^{+\infty} k_{\text{B}}(x)\, e^{iux}\, dx,$$

and $k(x)$ and $k_{\text{B}}(x)$ are the observed contours of the Raman and the exciting line, respectively. It is significant that for the determination of the real contour of the Raman lines it is not required to know the apparatus function of the spectral instrument used and the real contour of the exciting line, the experimental determination of which is associated with great difficulties; however, the observed contours of the Raman line $k(x)$ and the exciting line $k_{\text{B}}(x)$, entering into the expressions for $K(u)$ and $K_{\text{B}}(u)$, can be determined comparatively simply.

Calculations by Eq. (1) can be carried out very easily, when the observed contour of the exciting line is disperse Examples of finding the real contours of the Raman lines of various shape for this case are given in reference 10. If, however, the observed contour of the exciting line $k_{\text{B}}(x)$ is not disperse, then we may consider the dispersed curve $k_{\text{D}}(x)$ as having the same width as the first approximation, and the difference

$$\Delta k_{\text{B}} = k_{\text{B}} - k_{\text{D}} \tag{2}$$

as the correction. Moreover,

$$K_{\text{B}}(u) = \frac{1}{\sqrt{2\pi}}\int_{-\infty}^{+\infty} [k_{\text{D}}(x) + \Delta k_{\text{B}}(x)]\, e^{iux}\, dx = K_{\text{D}}(u) + \Delta K_{\text{B}}(u), \tag{3}$$

where

$$\Delta K_{\text{B}}(u) = \frac{1}{\sqrt{2\pi}}\int_{-\infty}^{+\infty} \Delta k_{\text{B}}\, e^{iux}\, dx.$$

Substituting (3) into (1), and assuming approximately that

$$\frac{1}{K_{\text{B}}} \approx \frac{1}{K_{\text{D}}}\left[1 - \frac{\Delta K_{\text{B}}}{K_{\text{D}}}\right],$$

we find:

$$\varphi_{\text{K}}(\lambda) = \frac{1}{2\pi}\int_{-\infty}^{+\infty} \frac{K(u)}{K_{\text{D}}(u)}\, e^{-i\lambda u}\, du - \frac{1}{2\pi}\int_{-\infty}^{+\infty} \frac{K(u)}{K_{\text{D}}(u)}\,\frac{\Delta K_{\text{B}}(u)}{K_{\text{D}}(u)}\, e^{-i\lambda u}\, du. \tag{4}$$

The second term of this expression represents the correction to the contour of the Raman line which should be introduced so as to take into account the deviation of the observed contour of the existing line from the dispersed curve.

Our experiment shows that approximating the observed contour of the exciting line with the dispersed curve gives in practice satisfactory results in the majority of cases. Of the factors which may lead to deviations from the dispersion, the most significant, apparently, is the fairly wide slit width with which, for a number of reasons, it is necessary to photograph Raman spectra. When the same width of slit is used for photographing the exciting line, the latter will be distorted in such a manner that in its observed contour the drop in intensity at the edges will occur faster than in the dispersed curve of the same width. In this case, instead of calculating the correction by Eq. (4), a faster and more effective solution of the problem of obtaining the real contour of the Raman line from the observed contour may be attained by an initial exclusion of the effect of the width of slit.

---

[10] M. M. Sushchinskii, J. Exper. Theoret. Phys. USSR **25**, 87 (1953).

Methods for the exclusion of the width of slit are developed in the work of Rayleigh[11], Runge[12], Paschen[13] and others. For our purpose, it is sufficient to use the simplest Rayleigh version which consists in the following: Under conditions of almost incoherent illumination of the spectrograph slit, the observed contour of the spectral line can be expressed in the form

$$f(x)=\frac{1}{2s}\int_{x-s}^{x+s}\psi(\lambda)\,d\lambda, \tag{5}$$

where $2s$ is the width of the slit, and $\psi(\lambda)$ is the contour of the line at an infinitely narrow slit depending on all the other distorting factors. Approximating the function $\psi(\lambda)$ along the length of the slit by the parabola

$$\psi(\lambda)=a\lambda^2+b\lambda+c, \tag{6}$$

we obtain:

$$f(x)=\psi(x)+as^2/3. \tag{7}$$

Assuming that the change in a is small when we substitute $\psi(x)$ by $f(x)$, we find a from the observed distribution; then

$$\psi(x)=f(x)-as^2/3. \tag{8}$$

Rayleigh proposed the use of a graphic method, instead of the analytical, for the determination of the correction $as^2/3$, which can be reduced to the following: from the points $x-s$ and $x+s$ on the abscissa perpendiculars are extended until they cross the curve $f(x)$; the points of intersection are joined by a chord, and one third of the cut-off ab (Fig. 1) is added (or subtracted) to the ordinates $f(x)$. Carrying out the same operation for a number of points x, it is possible to construct the complete contour of the line corresponding to an infinitely narrow slit (this operation does not take more than 10-15 minutes).

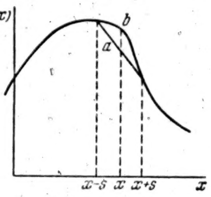

FIG. 1. A graphical method for excluding the effect of the width of slit.

Thus, we can exclude the distortions produced by the extremity of the width of slit in the combination line. In order to take into account the remaining factors, the exciting line is photographed with a slit of not more than 0.2 - 0.3 s_0. Then, the limitations superimposed by the partial incoherence of the illumination are removed, and the distorting effect of the slit is negligibly small, since its width is 10-15 times smaller than the width of the remaining apparatus function. Account of the remaining apparatus distortions (together with the exciting line) is taken by the methods described above.

Thus, the procedure which we are proposing for the investigation of the contours and the width of the Raman lines can be reduced to the following:

a) The photographing of the Raman spectra with the aim of obtaining the highest possible intensity may be carried out with a sufficiently wide slit. The width of slit, however, should not exceed one half of the width of the line studied; under this condition the distortions introduced by the slit are still negligible;

b) When at the width of slit, with which the photographing of the Raman spectra is carried out, the observed contour of the exciting line is found to be dispersed, then to obtain the real contour of the Raman lines from their observed contour can be reduced to the analytical operations described in reference 10. In the simplest case, when the observed contour of the Raman line is also dispersed, then it is only necessary to subtract the observed width of the exciting line from the observed width of the Raman line ; moreover, the real contour of the Raman line remains dispersed;

---

[11] Rayleigh, Phil. Mag. 42, 441 (1871).

[12] C. Runge, Z. Math. 42, 205 (1897).

[13] F. Paschen, Wied. Ann. 60, 712 (1897).

c) When the contour of the exciting line differs noticeably at the width of slit used in the photographing of Raman spectra from the dispersed (whereupon the drop in intensity at the edges of the line occurs faster than for a dispersed line of the same width), then the photographing of the exciting line should be carried out at a narrow slit (several times smaller than the normal width of slit). Thus the distorting effect of the slit is removed and the contour of the line should approach that of the dispersed. The distorting effect of the slit on the contour of the Raman line is excluded by the graphic method described above. From the "restored" contour of the Raman line its real contour can be obtained as in step b) (by using the contour of the exciting line photographed with a narrow slit);

d) It may be found that the contour of the exciting line photographed with a narrow slit differs noticeably from the dispersed. In this case the required corrections may be found by Eq. (4).

For the practical application of the methods described in this section it is, of course, necessary to take into account the actual accuracy of measurements. An analysis of the material available at our disposal shows that the corrections for the deviations of the contour lines from the dispersed form are not very significant. With a limited accuracy of measurement, attempts to make the data more precise by introducing such corrections may prove illusory. Thus, in many cases, the introduction of corrections is not justified, and the actual refinement of the data can be carried out by a simple subtraction of the observed widths of the Raman and the exciting lines.

4. Using the methods described, the width of the Raman lines in the spectra of a number of hydrocarbons was measured. The photographing was carried out with a triprism spectrograph V III* (the parameters of the instrument are given in Table I.) The width of slit used in the photographing of the Raman spectra was 0.03 mm, which corresponded to 1 cm^{-1} in the spectrum (the given spectrograph has a magnification of 0.7; the dispersion of the instrument in the region of the line 4358 Å represents 56 cm^{-1} per 1 mm). The photographing of the exciting line (the source --a lamp with cooled electrodes) was carried out also with a slit of 0.03 mm in one series of the experiments, and with a slit of 0.002 mm in the second series. For the exact installation and measurement of the width of slit the diffraction method described in reference 15 was used.

The spectra were photographed on "Zenit 700" plates. The exposure on the average was 7 hours. The photometering was carried out on the microphotometer MF-2 with a 30-fold magnification, at a slit width of the photometer 0.15-0.20 mm.

The observed width of the exciting line in the photographing with a slit width of 0.002 mm was equal to

$$\delta_{\text{B}} = 0.019 \pm 0.003 \text{ mm}$$

or 0.1 ± 0.15 cm^{-1} in the spectrum. The measurements carried out with lines of the iron spectrum, obtained at the same slit width, showed that the width of the apparatus function is maintained over the length of the spectral region in which the Raman lines were located.

When photographing with a width of slit of 0.03 mm, the observed width of the exciting line was equal to 0.028 ±0.003 mm (or 1.6 cm^{-1} in the spectrum). The study of the contours of the exciting line showed that they approximate the dispersed. However, the drop in the intensity when moving away from the maximum of the line occurs somewhat more rapidly than for the dispersed curve. These deviations are more noticeable when the exciting line is photographed at a width of slit of 0.03 mm. Hence, in the refinement of the data of the Raman lines we excluded the effect of the width of slit by the method described in Sec. 3. It was found in practice that the exclusion of the width of slit introduces into the final results a small, but systematic correction amounting to 0.2-0.3 cm^{-1} for narrow lines, and 0.3-0.5 cm^{-1} for wide lines.

The deviations from dispersion of the exciting line, obtained with a narrow slit, give a correction which, when evaluated by formula (4), is found to be within the limits of experimental errors. Therefore, this correction was not taken into account.

The results which we have obtained for a number of Raman lines are given in Table II. The investigation of the line contours showed that, within the limits of experimental errors, they can all be described by the dispersion curve.

---

* The measurements of the width of Raman lines with the aid of the spectrograph were carried out also by Chulanovskii and co-authors[14]. However, the procedure they used is suitable only for fairly narrow lines.

[14] V. M. Chulanovskii and A. Mironova, Izv. Akad. Nauk SSSR, Ser. Fiz. 12, 560 (1948); V. M. Chulanovskii, M. P. Burgova and A. N. Mironova, Izv. Akad. Nauk SSSR, Ser. Fiz. 14, 406 (1950).

TABLE II

Substance	$\Delta\nu$, cm^{-1}	I_∞	δ cm^{-1}	I_0 ISP-51*	δ_{eff} cm^{-1}	δ_{cal} cm^{-1}	I_0 V-III
Toluene	521	210	3.2	100	2.1	2.3	80
	1031	230	2.0	130	1.8	1.8	120
	1211	260	3.4	120	2.2	2.7	100
	1605	310	6.5	85	3.6	7.5	50
Cyclohexane	802	500	2.0	250	2.0	2.0	250
	1029	480	10	105	4.6	11	65
	1267	440	11	90	4.9	12	—
	1445	470	12	85	5.5	14	50
Cyclopentane	889	550	9	150	3.7	8	90
	1031	270	20	44	6.2	16	18
	1449	300	17	42	7.2	19	21
Cyclopentane	900	350	5.2	140	2.5	3.7	—
	1108	460	6.6	130	3.5	7.0	—
	1614	380	3.2	150	2.5	3.7	—
Methylcyclohexane . . .	770	300	3.2	115	2.6	4.0	—

* The data on the intensities at the maximum of the lines (ISP-51), used in the Table, were obtained by taking into account a great many repeated measurements of these values, carried out by Kh. E. Sterin and V. T. Aleksanian at the Commission on Spectroscopy in the Dept. of Physico-Math. Sciences, Academy of Sciences, USSR.

5. The selection of the objects for investigation was determined in this study mainly by the desire to obtain data for lines of diversified width belonging to different classes of hydrocarbons and types of vibrations, so as to obtain material which could be used for a more strict substantiation of the method of the effective width of lines, proposed previously[6-8]. In the method mentioned, the evaluation of the width of lines δ_{eff} was carried out by a comparison of the integral intensities I_∞ with the intensities I_0 at the maximum of the lines

$$\delta_{eff} = I_\infty / I_0. \qquad (9)$$

When using this method, the required normalization should be based on the data of direct measurements of the width of several lines. Up to the present time such measurements are only those of Sterin relating to two completely symmetrical lines: benzene ($\Delta\nu = 992$) and cyclohexane ($\Delta\nu = 802$), with a width of 1.8 and 1.9 cm^{-1}, respectively. In subsequent investigations it was found that such a normalization cannot be used for lines differing greatly in width, since the ratio of the intensities at the maximum I_0 for lines of different width, generally speaking (see reference 5), does not correspond to the ratio of these values at an infinitely narrow exciting line. But, according to the meaning of Eq. (9), the values of I_0 for the photographic conditions enter into it. Under these conditions the distortions associated with the end width of the exciting line (and apparatus distortions) are completely excluded. When we use values for I_0 not obtained under such "ideal" conditions, the values of δ_{eff} determined by Eq. (9) will have a definite provisory meaning, since they are singularly connected with the real width of lines δ. However, δ_{eff} and δ, generally speaking, no longer coincide.

In order to correlate the values obtained by the method of the effective width of lines (using for I_0 the data of investigation[16]) with the results of the direct measurements of δ, we compared the

---

[15] E. Prenss, Spectr. Acta **4**, 412 (1950).

two values for a number of lines. It was found that the relationship between $\delta_{\rm eff}$ and δ (at $\delta_{\rm eff} > 2$; the region $\delta_{\rm eff} < 2$ was not investigated in detail) can be expressed by the formula

$$\delta = \alpha(\delta_{\rm eff} - \beta), \tag{10}$$

where $\alpha = 3.4$; $\beta = 1.4$.

This relationship is shown in Fig. 2, where $\delta_{\rm eff}$ is plotted along the abscissa and the values of δ from the data of our measurements along the ordinate (see Table II). In the calculations of $\delta_{\rm eff}$ we have used for I_0 the data of reference 16, and for I_∞ the values measured by the photoelectric method, described previously[17]. As is evident, the deviations between the direct and indirect methods of measuring the width of lines with such a recalculation of the values $\delta_{\rm eff}$ do not exceed the limits of experimental errors. In the last column of Table II are given the relative intensities of the lines obtained by using a narrow exciting line. One can see that for the wide lines, when using a narrow exciting line, the value of I_0 is actually smaller than the corresponding intensities obtained when using a wide exciting line.

The possibility of obtaining the actual widths of lines (using the graduated graph) from the values of $\delta_{\rm eff}$, found by Eq. (9), also provides the possibility of transferring from the values of I_0, obtained in reference 16 with an instrument of medium dispersion (type ISP-51) and with a fairly wide exciting line (~ 2 cm^{-1}), to such values of I_0 which correspond to "ideal" conditions of photographing. In fact, if we know I_∞ (which can be determined, at least in principle, without great difficulties) and if we know $\delta_{\rm eff}$, then it is possible to find [by Eq. (10)] the actual line widths δ. Then, obviously, the values I_∞/δ will give the intensities I_0 reduced to ideal conditions of photographing.

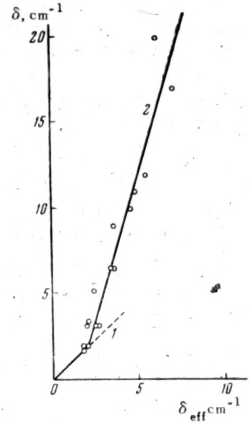

FIG. 2. The dependence of the effective width on the actual width of line. $1 - \delta = \delta_{\rm eff}$ (ideal conditions of photography); $(\delta_{\rm eff} - \beta)$.

It should be noted that all the measurements of I_0 in investigation[16] are expressed in the absolute scale, at the basis of which are placed the data of a number of typical lines for several standard hydrocarbons. To such hydrocarbons belong benzene, cyclohexane, methylcyclohexane, toluene and cyclopentane. Therefore, the finite scale should be based on careful measurements of the intensities of the typical lines of such hydrocarbons. Such measurements were carried out with great care by Kh. E. Sterin and V. T. Aleksanian, to whom we express our thanks for providing these data.

In conclusion we wish to express our gratitude to Academician G. S. Landsberg for constant attention to this work and for valuable suggestions.

Translated by E. Rabkin
277

---

[16] P. A. Bazhulin et al, Izv. Akad. Nauk SSSR, Otd. Khim. Nauk 1, 14 (1941); 3, 198 (1943); 1, 7 (1946); 6, 480 (1949); 5, 501 (1950). P. A. Bazhulin and Kh. E. Sterin, Izv. Akad. Nauk SSSR, Ser. Fiz. 11, 456 (1947).

[17] M. M. Sushchinskii, J. Exper. Theoret. Phys. USSR 20, 304 (1950).

SOVIET PHYSICS JETP   VOLUME 2, NUMBER 4   JULY, 1956

Propagation of a Short Pulse in a Semiconductor Bounded by Two Hole-Electron Transistors

E. I. ADIROVICH AND V. G. KOLOTILOVA
P. N. Lebedev Physical Institute, Academy of Sciences, USSR

(Submitted to JETP editor July 19, 1954)
J. Exper. Theoret. Phys. USSR **29**, 770-777 (December, 1955)

Herein is presented a calculation of the propagation of a short pulse in a semiconductor bounded by two hole-electron transistors, one of which ($x = 0$) is positive and the other ($x = w$) has a negative bias such that a semiconducting triode system exists. The form of the impulse is approximated by a δ-function. With the aid of Laplace transforms we obtained the current in p-representation at any semiconductor section. Transforming to the original representation at $x = w$ permits one to obtain the expression for the collector current $i(w, t)$ and clarifies the influence of diffusion and recombination of the nonequilibrium current carriers in a semiconductor on the form of the impulse at the collector.

1. GENERAL SOLUTION OF THE PROBLEM

LET us consider a semiconductor doped with a conducting impurity, bounded at $x = 0$ (emitter) and $x = w$ (collector) by hole-electron transistors. No electric field exists within a semiconductor and the changes in the concentration of the current carriers (deficit type of conduction) can be specified only through two mechanisms: 1. diffusion and 2. disturbance of the thermodynamic equilibrium between thermal creation and electron-hole pair recombinations. The conservation equation and the expression for the current have the following form:

$$\frac{\partial n_{\text{h}}}{\partial t} + \frac{1}{q}\operatorname{div}\mathbf{j} = g - \frac{n_{\text{h}}}{\tau}, \quad \frac{1}{q}j = -D\frac{\partial n_{\text{h}}}{\partial x}, \tag{1}$$

from which it follows that the concentration of deficit carriers (holes) is specified by the equation

$$\frac{\partial n_{\text{h}}}{\partial t} + \frac{n_{\text{h}} - n_0}{\tau} - D\frac{\partial^2 n_{\text{h}}}{\partial x^2} = 0. \tag{2}$$

Here n_0 is the equilibrium concentration of holes; for equilibrium the source function g, representing thermal creation of electron-hole pairs in a unit volume, equals the numbers of recombinations, i.e., n_0/τ.

Separating the stationary solution $n_{\text{st}}(x)$, which satisfies the equation

$$\frac{n_{\text{st}} - n_0}{\tau} - D\frac{d^2 n_{\text{st}}}{dx^2} = 0 \tag{3}$$

with given stationary boundary conditions (constant potentials for the hole-electron transistors), one obtains for

$$n = n_{\text{h}} - n_{\text{st}} \tag{4}$$

the equation

$$\frac{\partial n}{\partial t} + \frac{n}{\tau} - D\frac{\partial^2 n}{\partial x^2} = 0, \tag{5}$$

with the boundary conditions[*]

$$n(w, t) \equiv 0, \qquad \frac{\partial n}{\partial x}(0, t) = -\frac{N}{D}\delta(t) \tag{6}$$

and the initial conditions

$$n(x, 0) \equiv 0 \text{ with } 0 < x \leqslant w. \tag{7}$$

With the help of the assumption[1]

$$n(x, t) = y(x, t)e^{-t/\tau} \tag{8}$$

Eq. (5) is transformed to a pure diffusion equation

$$\frac{\partial v}{\partial t} - D\frac{\partial^2 y}{\partial x^2} = 0 \tag{9}$$

with the previous boundary and initial conditions.

Performing the Laplace transformation[2] on the function $y(x, t)$

---

[*] N equals the concentration of current carriers in the base produced by the introduced delta impulse

$$-qD\int_0^\infty \frac{\partial n}{\partial x}(0, t)\,dt = qN\int_0^\infty \delta(t)\,dt = qN.$$

[1] E. I. Andirovich, Dokl. Akad. Nauk SSSR **86**, 1085 (1952).

[2] M. A. Lavrent'ev and B. V. Shabat, *Methods of Function Theory of Complex Variable*, GITTL, 1951.

$$y(x, t) \doteq F(x, p) = \int_0^\infty y(x, t)\, e^{-pt}\, dt, \tag{10}$$

we find that $F(x, p)$ satisfies the equation

$$\frac{d^2F}{dx^2} - \frac{p}{D} F = 0 \tag{11}$$

with the conditions

$$F(w, p) \equiv 0, \qquad \frac{dF}{dx}(0, p) = -\frac{N}{D}. \tag{12}$$

The solution to Eqs. (11) and (12) is

$$F(x, p) = \frac{N \operatorname{sh} k(w - x)}{Dk \operatorname{ch} kw}, \tag{13}$$

where

$$k = \sqrt{p/D}. \tag{14}$$

The dispersion in the concentration of non-equilibrium carriers, specified by a δ-current pulse on the emitter, can be represented by the general formula

$$n_h(x, t) \tag{15}$$

$$= n_{st}(x) + \frac{e^{-t/\tau}}{2\pi i} \frac{N}{D} \int_{a-j\infty}^{a+j\infty} \frac{\operatorname{sh} k(w - x)}{k \operatorname{ch} kw} e^{pt}\, dp.$$

Here

$$n_{st}(x) \tag{16}$$

$$= n_0 \left(1 + \frac{(i_1/n_0) \operatorname{sh} \varkappa (w - x) - qD\varkappa \operatorname{ch} \varkappa x}{qD\varkappa \operatorname{ch} \varkappa w}\right)$$

is the stationary distribution satisfying the given bias on the hole-electron transistors.

The corresponding stationary component of the hole current is

$$i_{st}(x) = \frac{i_1 \operatorname{ch} \varkappa (w - x) + qDn_0\varkappa \operatorname{sh} \varkappa x}{\operatorname{ch} \varkappa w}. \tag{17}$$

At the emitter, $i_{st}(0) = i_1$, and at the collector,

$$i_{st}(w) = \frac{i_1 + qDn_0\varkappa \operatorname{sh} \varkappa w}{\operatorname{ch} \varkappa w}, \tag{18}$$

where $\kappa = (D\tau)^{-1/2}$.

2. COLLECTOR CURRENT

The variable component of the hole current (deficit type of conduction) specified by a δ-impulse on the emitter equals

$$\begin{aligned} i(x, t) &= -qD \frac{\partial n(x, t)}{\partial x} \\ &= -qDe^{-t/\tau} \frac{\partial y(x, t)}{\partial x}. \end{aligned} \tag{19}$$

Transforming to the p-representation we obtain from Eqs. (13) and (19) that

$$-qD \frac{\partial y(x, t)}{\partial x} \doteq \Phi(x, p) \tag{20}$$

$$\equiv -qD \frac{dF}{dx} = \frac{qN \operatorname{ch} k(w - x)}{\operatorname{ch} kw}.$$

Returning to the original representation for Eq. (20) and inserting it into (19), one obtains the expression for the current* at any section x. At the collector, i.e., at $x = w$,

$$e^{t/\tau} i(w, t) \doteq \Phi(w, p) = \frac{qN}{\operatorname{ch} kw}. \tag{21}$$

Expressing $\Phi(w, p)$ by an exponential series[3], we have

$$\Phi(w, p) = 2 \sum_{n=1}^{\infty} (-1)^{n+1} e^{-(2n-1)kw} \tag{22}$$

---

* $i(x, t)$ is the excess over the stationary current $i_{st}(x, t)$ and corresponds to the given boundary conditions.

[3] I. M. Ryzhik and T. C. Gradshtein, *Tables of Integrals, Sums, Series and Products*, GITTL, 1951.

and transforming each term of (22) to the original representation[4] we obtain the series

$$I(\xi) = \frac{i(w,t)}{i_0} \tag{23}$$

$$= \frac{e^{-\lambda^2\xi}}{\xi^{3/2}} \sum_{n=1}^{\infty} (-1)^{n+1}(2n-1)\, e^{-(2n-1)^2/\xi},$$

which represents the collector current in general form. Here

$$\xi = t/\Theta, \quad \lambda^2 = \Theta/\tau, \tag{24}$$

$$i_0 = 2qN/\sqrt{\pi}\Theta, \quad \Theta = w^2/4D.$$

We approximate the collector current, in series (23), by the S-sum,

$$I(\xi) \cong I_s(\xi) \tag{25}$$

$$= \xi^{-3/2} e^{-\lambda^2\xi} \sum_{n=1}^{s} (-1)^{n+1}(2n-1)\, e^{-(2n-1)^2/\xi},$$

and evaluate the region of validity and degree of accuracy of this approximation. It is evident that

$$I(\xi) - I_s(\xi) = P_s(\xi) \tag{26}$$

$$= \xi^{-3/2} e^{-\lambda^2\xi} \sum_{n=s+1}^{\infty} (-1)^{n+1}(2n-1)\, e^{-(2n-1)^2/\xi}.$$

With

$$\xi < 8(s+1)/\ln\frac{2s+3}{2s+1} \tag{27}$$

the remaining term, $P_s(\xi)$, is an alternating series whose terms decrease monotonically with increasing n. Consequently,

$$|P_s|(\xi)| < \xi^{-3/2} e^{-\lambda^2\xi}(2s+1)\, e^{-(2s+1)^2/\xi} \tag{28}$$

and, for $I(\xi)$ one can write upper and lower limits,

$$I_s(\xi) < I(\xi) < I_{s+1}(\xi), \quad \text{if } s \text{ is even,} \tag{29}$$

$$I_s(\xi) > I(\xi) > I_{s+1}(\xi), \quad \text{if } s \text{ is odd.}$$

To determine the accuracy of the approximation we consider

$$\frac{|I_{s+1}(\xi) - I_s(\xi)|}{I_s(\xi)} \tag{30}$$

$$= \frac{(2s+1)\, e^{-(2s+1)^2/\xi}}{\sum_{n=1}^{s} (-1)^{n+1}(2n-1)\, e^{-(2n-1)^2/\xi}} \leqslant \varepsilon,$$

from which we can determine the time interval ξ' during which the collector current can be represented by $I_s(\xi)$ with an accuracy ϵ. Here we must require that

$$\xi' < 8(s+1)/\ln\frac{2s+3}{2s+1}; \tag{31}$$

otherwise the duration of the determined interval is not ξ' but the right-hand side of the previous inequality.

We shall show that specification of the collector current for any value of the lifetime τ by a three term formula, $I_3(\xi)$, is sufficient; in the given cases it was possible to restrict onself to approximations with two and, in some cases, with one term of the series (23).

3. CASE OF LARGE LIFETIMES FOR THE NON-EQUILIBRIUM CURRENT CARRIERS

Let us consider the case $\lambda^2 \to 0$, or correspondingly, $4D\tau/w^2 \to \infty$. In Fig. 1 we have shown the curves I_1^∞, I_2^∞ and I_3^∞ which are one, two, and three term approximations [see Eq. (23)] to the collector current I^∞.

The superscript ∞ indicates that these solutions represent currents obtained in the absence of recombination ($\tau = \infty$). The maxima of all three

---

[4] V. A. Ditkin and P. I. Kuznetsov, *Handbook of Operational Calculus*, GITTL, 1951.

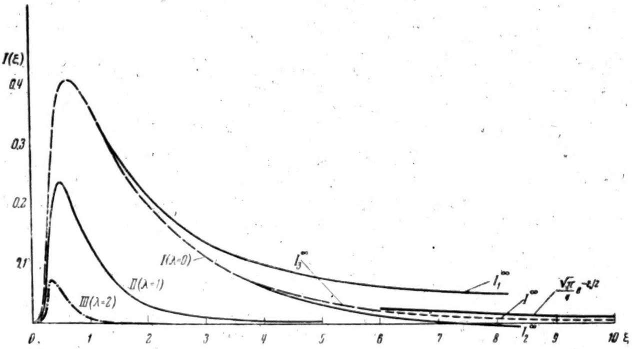

FIG. 1

approximations are identical and occur at the value $\xi = 0.67$. The value of I_1^∞ falls to half maximum at $\xi_1 = 2.1$; I_2^∞ and I_3^∞ at the value $\xi_{2,3} = 2$. From Fig. 1 and Eq. (30) it is seen that the first term of the series (23) approximates the collector current with an accuracy of $\epsilon = 0.01$ down to $\xi = 1.4$; the first two terms down to $\xi = 3.7$; the first three terms down to $\xi = 6.1$. For I_1^∞, condition (27) is satisfied up to $\xi = 3.1$, i.e., no additional restriction is imposed. At $\xi = 6$ the value of the current is 26 times smaller than the maximum. Consequently, the three term formula $I_3^\infty(\xi)$ gives a sufficiently accurate expression for the collector current over the total range. The two term formula $I_2^\infty(\xi)$ is a satisfactory representation of $i(w, t)$ for values of the time less than the time of maximum. In those cases, when the problem is confined to the half-maximum of the curve $i(w, t)$, i.e., to times for which the current, after passing through its maximum value, has decreased by no more than a factor of two, then the value of the collector current agrees with $I_1^\infty(\xi)$ to within 5%.

For greater times, the actual curve should be approximated by a larger number of terms of the series (23) since, with $\xi \gg 1$, i.e., for $t \gg w^2/4D$, the series (23) converges slowly. According to Tauber's theorem[5] the form of the asymptotic solution as $\xi \to \infty$ can be obtained from the series expansion of $\Phi(w, p)$ in powers of kw,

$$\Phi(w, p)|_{p\to 0} = qN/\left(1 + \frac{k^2w^2}{2}\right). \tag{32}$$

Transforming this equation to the original representation, we find

$$I^\infty(\xi)|_{\xi\to\infty} = \frac{\sqrt{\pi}}{4}e^{-\xi/2}. \tag{33}$$

Equation (33) is shown in Fig. 1 beginning at $\xi = 6$. For all larger ξ, the asymptotic expression (33) approximates $I^\infty(\xi)$ from above, since in the transition to the asymptotic representation (32), positive terms were truncated in the denominator. Consequently, for later times, when $I_3^\infty(\xi)$ does not give a good approximation to the actual current, $I^\infty(\xi)$ is bounded between the axis and the exponential (33). In Fig. 1, $I^\infty(\xi)$ is shown in this region as a dashed curve.

We shall write the final formula in different variables. With relative accuracy to $\epsilon = 0.01$, we have

$$i(w, t) = \frac{qNw}{\sqrt{\pi D t^3}}\left(e^{-w^2/4Dt}\right.$$
$$\left. - 3e^{-9w^2/4Dt} + 5e^{-25w^2/4Dt}\right) \tag{34}$$

with $t \leq 1.52\, w^2/D$. Up to $t = 0.93\, w^2/D$ one can, with the same degree of accuracy, use the first two terms, and, to $t = 0.35\,w^2/D$, the first term. Indeed, this last gross approximation permits one to obtain the major part of the current impulse on the collector, up to the point where the curve has fallen to approximately half its maximum value.

---

[5] I. M. Ryzhik and I. C. Gradshtein, loc. cit.

4. CASE OF MODERATE AND SMALL LIFETIMES

In those cases in which it is not permissible to disregard the recombination of carriers, one obtains for the collector current,

$$I(\xi) = e^{-\lambda^2\xi} I^\infty(\xi), \tag{35}$$

where $I^\infty(\xi)$ is the value of the collector current with $\tau = \infty$ and is given by the series expression on the right in (23). Inasmuch as the evaluation of the values of ξ' is independent of λ, the results are correct for any value of τ. But, because of the exponential factor in (35), i.e., $e^{-\lambda^2\xi}$, $I(\xi)$ falls faster for the same value of ξ. The three term approximation $I_3^\infty(\xi)$, which was accurate to $\epsilon = 0.01$, was good for ξ's up to the point where the current is 1/26 its peak value; here, however, for $\lambda = 1\,(\tau = w^2/4D)$, the current in the same interval, $\xi \leq 6.1$, falls to 1/1000 its peak value. The same situation holds for the other approximations; the smaller the recombination time, the more complete the expression for the collector current. Thus it follows that the approximate expressions for the collector current derived above, i.e., $I_3(\xi)$, $I_2(\xi)$, $I_1(\xi)$, hold to the same accuracy for any value of τ.

To find the magnitude and location of the peak current for the general case $\lambda \neq 0$ one can use the condition resulting from (35) that

$$\left.\frac{d\ln I^\infty(\xi)}{d\xi}\right|_{\xi=\xi_{\max}} = \lambda^2. \tag{36}$$

From (36) it is seen that the recombination process hastens the occurrence of the maximum current at the collector, since we have, with $\lambda \neq 0$

$$(dI^\infty/d\xi)|_{\xi_{\max}} > 0.$$

In the vicinity of the maximum

$$I^\infty(\xi) \cong I_1^\infty(\xi) = \xi^{-3/2}e^{-1/\xi}. \tag{37}$$

Consequently,

$$\xi_{\max} = \frac{3}{4\lambda^2}\left[\sqrt{1+\frac{16}{9}\lambda^2} - 1\right]. \tag{38}$$

Likewise,

$$I_{\max} = \xi_{\max}^{-3/2}\exp\{-\lambda^2\xi_{\max}\}\exp\{-1/\xi_{\max}\}. \tag{39}$$

The asymptotic expression for $I(\xi)$ for large times is, for $\tau \neq 0$,

$$I(\xi)|_{\xi\to\infty} \cong \frac{\sqrt{\pi}}{4}e^{-(1/4+\lambda^2)\xi}. \tag{40}$$

Curve *II* in Fig. 1 represents the time history of the collector current for $\lambda = 1$, i.e., for $\tau = w^2/4D$. As was mentioned above, in this case the current does not fall from its peak value in the interval $t \leq \frac{1.52\,w^2}{D}$ by a factor of 26 as for $\lambda = 0$ (curve *I*), but by a factor of 1000. At $t = 0.93\,w^2/D$ the current has decreased to 1/14 its peak value. Consequently, for moderate values of the lifetimes ($\lambda \simeq 1$), the two term formula I_2 fully serves as a sufficient approximation to the collector current.

For small $\tau\,(\lambda > 1)$, the current, over its entire range, for all practical purposes is given by

$$I(\xi) \approx I_1(\xi) = \xi^{-3/2}e^{-\lambda^2\xi}e^{-1/\xi}. \tag{41}$$

Thus, for example, with $\lambda = 2$ the collector current at $\xi = 1.4$, where the approximation given by (41) is accurate to 1%, is 1/25 its peak value (curve *III* in Fig. 1).

Curves *I*, *II* and *III* in Fig. 1 demonstrate the dependence of the form of the impulse at the collector on the lifetime of the nonequilibrium current carriers in a semiconductor.

5. THE INFLUENCE OF BOUNDARY CONDITIONS ON THE ELECTRON PROCESSES IN THE VOLUME OF A SEMICONDUCTOR

To clarify the influence of boundaries we shall compare the results obtained above with the results for the propagation of a δ-impulse in a semi-infinite semiconductor $(0 \leq x \leq w)$. The mathematical formulation of the problem differs from the preceding only in the fact that the condition $n = 0$ occurs not at $x = w$ but at $x = \infty$. For this case, the concentration and current of nonequilibrium carriers have the following representation

$$e^{t/\tau} n^*(x,t) \doteqdot F^*(x,p) = \frac{N}{Dk}\, e^{-kx}, \tag{42}$$

$$e^{t/\tau} i^*(x,t) \doteqdot \Phi^*(x,p) = qNe^{-kx}.$$

Comparing these with the corresponding representations for a semiconducting layer of thickness w [Eqs. (13) and (20)] we see that the two agree when $k \gg (w-x)^{-1}$, i.e., when

$$p \gg D(w-x)^{-2}. \tag{43}$$

Thus as $p \to \infty$, $t \to 0$, which indicates that for all $x < w$ the diffusion process proceeds from the start the same in a semi-infinite semiconductor as in a bounded semiconductor. Departures occur when $t \simeq t_0$, corresponding to $p = D(w-x)^{-2}$, i.e., that much earlier the smaller the separation $(w-x)$. The inequality (43) indicates that at the collector ($x = w$), the process differs from that in a semi-infinte semiconductor right from the beginning (i.e., at $t = 0$, corresponding to the establishment of a δ-impulse on the emitter). In particular, [consider Eq. (21)],

$$\Phi(w,p)|_{p\to\infty} = 2qNe^{-kw} = 2\Phi^*(w,p), \tag{44}$$

i.e., at the beginning of the process, the collector current is twice the current which would be obtained at the distance w from the emitter in a semi-infinite medium. The reason for this is the absence of a partial counter current of deficit carriers which is specified by the assigned potential on the collector. Associated with the maintenance of a small constant concentration of deficit carriers, $n(w,t) \simeq 0$, is a faster diffusion rate which involves a more rapid decrease of current, so that as $t \to \infty$, the collector current becomes much smaller than the current at $x = w$ in a semi-infinite conductor. In Fig. 2, the currents $i(w,t)$ and $i^*(w,t)$ for $\tau = \infty$ are represented, corresponding respectively to the bounded and semi-infinite case. The given potential which specifies $n(w,t) \simeq 0$ not only doubles the maximum and sharpens it but, in addition, introduces a sharper decrease for later times. Instead of the current falling off like $t^{-3/2}$ (for $t \gg w^2/4D$)

$$i^*(w,t) \equiv \frac{wN}{2\sqrt{\pi D t^3}}\, e^{-w^2/4Dt} \approx \frac{\text{const}}{t^{3/2}}, \tag{45}$$

as in a semi-infinite semiconductor, the current behaves exponentially

$$i = 2qNDw^{-2}e^{-2Dt/w^2}. \tag{46}$$

Figure 2 illustrates these effects.

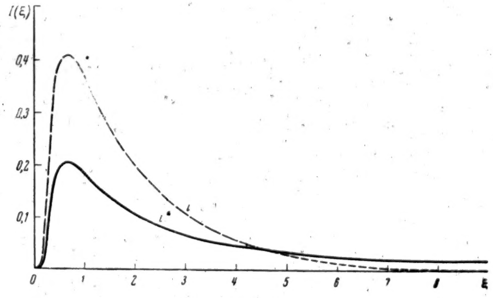

FIG. 2

We note that the recombination of nonequilibrium current carriers also produce a change in the time dependence through the exponential factor $e^{-t/\tau}$ for late times (i. e., $e^{-t/\tau}$ predominates over $t^{-3/2}$). Likewise, the main portion of the impulse is decreased (i.e., the value of i_{max}).

Within the volume of the semiconductor the same effects as at the collector are realized (i.e., greater currents at first and a greater decrease near the tail of the passing impulse) but they are smaller in magnitude the greater the distance from the collector and begin to be noticed only at large intervals of time after the onset of the diffusion process.

Correct to a constant factor, Eq. (23) represents the transient characteristics[6] of a semiconducting triode

$$g(\xi)=\frac{dh(\xi)}{d\xi}=\frac{2}{\sqrt{\pi}}\,J(\xi)\,. \tag{47}$$

We note further that the influence of finite lifetime on the electronic processes in a semiconducting layer is represented by a multiplicative factor $e^{-t/\tau}$ only for a δ-impulse. For other kinds of signal shapes, assumption (8) implies that τ appears in the second boundary condition of (6), and consequently the diffusion and recombination process cannot be separated.

Translated by A. Skumanich
271

---

[6] V. P. Siforov, *Radio Principles*, p. 58, 1954.

SOVIET PHYSICS JETP VOLUME 2, NUMBER 4 JULY, 1956

Fission of Heavy Nuclei by High Energy Neutrons*

V. I. GOL'DANSKII, V. S. PEN'KINA AND E. Z. TARUMOV
Academy of Sciences, USSR

(Submitted to JETP editor July 11, 1955)
J. Exper. Theoret. Phys. USSR **29**, 778-789 (December, 1955)

Results of experiments on the fission of various heavy nuclei in the region $Z = 74$-92 by neutrons of nominal energy of 120 and 380 mev are presented. An evaluation of threshold for fission connected with previous neutron emission is based on a comparison of the binding and critical fission energies. The average number of neutrons emitted during the fission of a heavy nucleus is evaluated.

1. INTRODUCTION

IN the course of the experimental work of the past few years various peculiar characteristics of the fission of heavy nuclei by high energy nucleons have been discovered and investigated. These differed in many respects from the previous work on fission by slow neutrons.

The first stage of the interaction of a high energy nucleon with a complex nucleus is an internal cascade, including one or several nucleon collisions within the nucleus. Struck nucleons may either fly out of the nucleus without further collisions or may stick within the nucleus, expending their kinetic energy in further collisions. At the end of the internal cascade, the nucleus remains hot, i.e., in an excited state, and the cooling of such a nucleus may take the form of multiple emission of particles. In the case of heavy nuclei, the fission process may offer strong competition to the multiple emission of particles. One can imagine two extreme cases of fission of a highly excited nucleus: the fission takes place with the loss of an excitation energy that is far larger than the critical fission energy, the fissioning nucleus having been very highly heated (high temperature fission); or the fission is preceded by multiple emission of particles (especially neutrons), after which the remaining excitation energy of the nucleus barely exceeds the critical fission energy ("emissive fission").

Such a division into high temperature and emissive fission is of course arbitrary, since all intermediate cases can occur. However, this division is useful for understanding characteristics of nuclear fission caused by high energy nucleon bombardment.

During slow neutron induced fission, a characteristic double-humped fission fragment spectrum (in both mass and energy) is observed. With increase in bombardment energy, the valley between the humps gradually smoothes out, and at high energies, for example in the fission of of uranium by 380 mev α - particles[1], or in the fission of bismuth by 190 mev deuterons[2], a strong single-humped fragment mass spectrum is observed. Chemical analysis of the fission fragments leads to the conclusion that the maximum of the mass spectrum is some 3-6 mass units lighter than half the sum of the nuclear and incident particle masses.

Such reduction of the fission fragment mass is connected with the emission of a large number of nucleons (chiefly neutrons) during fission of a heavy nucleus induced by a high energy particle. This emission may precede "emissive" fission, or may follow high temperature fission from an excited state; in this case neutrons are emitted by the fission fragments. The shape of the fission fragment mass spectrum for slow or fast nucleon induced fission has not been explained. Energetically, fission into fragments of equal mass is generally most efficient, i.e., a single-humped fission fragment mass spectrum. The occurrence of a two humped mass spectrum in low energy induced fission has been connected by several authors[3] with the fact that such a spectrum allows the formation of many fission fragments of magic neutron number ($N = 50$ and 82). From this viewpoint a two-humped mass spectrum is indicative of fission of a heavy nucleus from a state of weak excitation. The radical change in character of the spectrum of the mass fragments with increase of the bombardment energy may then be considered as an argument in support of high temperature fission from a highly excited state. However, this conclusion is opposed by the appearance among high energy induced fission fragments of large numbers of heavy nuclei of β^+ or K active isotopes (especially for $A \gtrsim 125$ – in uranium fission). Appearance of such neutron-deficient fragments allows the conclusion that most of the neutron emission takes place before fission, that is, the process is "emissive" fission.

---

*The experimental part of this work was completed in 1950-1951.

[1] P. O'Connor and G. Seaborg, Phys. Rev. **74**, 1189 (1948).

[2] R. Goeckermann and I. Perlman, Phys. Rev. **76**, 628 (1949).

[3] D. Brunton, Phys. Rev. **76**, 1798 (1949); L. Meitner, Nature **165**, 561 (1950).

Experiments determining kinetic energy of the fragments in the fission of uranium and thorium by 90 mev neutrons[4], as well as in the fission of uranium by stopping π - mesons[5] show that the total energy of the two fragments is not higher than is characteristic for slow neutron fission.

This fact also supports, although it does not prove, interpretation of the process as emissive fission, since neutron emission by highly excited fission fragments must be over in $\tau \sim 10^{-15} - 10^{-16}$ second, and the remaining observable energy will be determined solely by the coulomb repulsion.

Further evidence toward the emissive fission viewpoint is offered by the bombardment energy dependence of the fission cross sections for nuclei of $Z = 74$-83. As we know, the fission cross section of such nuclei as U^{238} and Th^{232} increases rapidly for excitation energies several mev higher than threshold. It reaches some tenths of a barn, and is fairly insensitive to further increase of energy. The partial level widths of these nuclei for fission and for neutron emission are of the same order of magnitude. Below are shown upper limits to the fission cross section of nuclei from W to Bi by 14 mev neutrons[6], and the critical fission energy for the corresponding compound nuclei calculated from data[7]:

	Bi^{209}	Pb^{204}	Pb^{206}	Pb^{207}	Pb^{208}	Hg^{200}	Au^{197}	Ir^{193}	W^{184}
E_{crit} (mev)	9.5	9.3	10.6	11.1	11.4	12.1	13.0	15.0	19.5
$\sigma_f \times 10^{29}$ (cm^2)	1.4	130	8.2	8.6	3.7	0.67	1.2	1.5	1.2

In all the above cases, the excitation energy of the compound nucleus is greater than the fission threshold; for W^{184} it is greater by only 0.3 mev, while for Bi^{209} it is almost 9 mev greater. Nevertheless, the upper limits for the fission cross section of the above nuclei (with the exception of Pb^{204}) are about 10^{-29}cm^2, which points to the smallness of the fission widths compared to the neutron widths of these nuclei.

It follows from the statistical model that increase of excitation energy in a region considerably higher than the critical fission energy is accompanied by roughly equal increases of the neutron and fission widths (equal to within an exponential coefficient). It is therefore hard to imagine that the fission cross sections of the above nuclei could increase appreciably with higher energy in the case of high temperature fission. However, the fission cross section of bismuth with 84 mev neutrons[8] is at least 1300 times larger than at 14 mev. On the other hand, the ratio of fission cross section of Pb^{204} and Pb^{208} decreases with increasing bombardment energy, from 35 (neutrons, 14 mev) to 3.5 (deuterons[2], 100 mev). It is thus natural to assume that the fission cross section at high excitations is determined, not by the fission width of the initial nucleus, but by that of a nucleus which has already amitted several neutrons.

Due to the above arguments, we based the analysis of our experimental data (completed in 1950-1951) on the emissive nature of fission. Seeking to determine the average number of neutrons emitted during a fission process, we proceeded from the assumption[9] that the neutron emission takes place until the critical fission energy becomes lower than the neutron binding energy. The calculation of the average number of neutrons on this assumption proved to be in satisfactory agreement with independent experimental determinations.

All the above facts served as a more or less indirect confirmation of the predominance of emissive fission over high temperature fission. A recent paper by Dauthett and Templeton[10] described an attempt to prove experimentally the emission of neutrons before fission.

---

[4] J. Jungerman and S. Wright, Phys. Rev. **76**, 1112 (1949).

[5] S. Al-Salam, Phys. Rev. **84**, 254 (1954); N. A. Perfilov and H. S. Ivanova, J. Exper. Theoret. Phys. USSR **29**, 551 (1955); Soviet Phys. JETP.

[8] E. Kelly and C. Wiegand, Phys. Rev. **73**, 1135 (1948).

[6] A. Phillips, L. Rosen and R. Taschek, Phys. Rev. **75**, 919 (1949).

[7] D. Hill and J. Wheeler, Progress of the Physical Sciences **52**, 83, 239 (1954).

[9] V. I. Gol'danskii, Report of Inst. Chem. Phys., Acad. Sci. USSR, 1950.

[10] E. Dauthett and D. Templeton, Phys. Rev. **94**, 128 (1954).

These workers compared the range of particular fission fragments (for example Sr^{89}, Ag^{111}, Ba^{140}) in the fission of U^{238} by 18 mev deuterons and by 335 mev protons. It turned out that for fission by high energy protons the fragment energies were several mev lower. Such energy reduction is connected with mass reduction of the fragment pair by previous neutron emission. In these cases, the number of neutrons emitted before the U^{238} fission was 6-8 (Ba^{140} fragment) to 21-22 (Sr^{89} fragment). The quantitative results of reference 10 are evidently not sufficiently precise, but the qualitative demonstration of the emission nature of fission seems to be valid.

2. DESCRIPTION OF THE EXPERIMENTS

In our experiments, performed in 1950-1951 with the synchrocyclotron at the Institute of Nuclear Problems of the Academy of Sciences, USSR, we investigated the fission of U^{235} and U^{238} by neutrons of 120 and 380 mev, excitation functions for neutron fission of bismuth in the energy interval 120-380 mev, and the fission of Th, Pb, Tl, Au, Pt, and W by 380 mev neutrons.

The neutrons used in the 1950 experiments were obtained by stripping 280 mev deuterons in a 16 mm (14.2 g/cm^2) copper target. The energy spectrum of such neutrons is a bell shaped curve with a maximum and average energy of $\sim$ 120 mev and a half width $\sim$ 40 mev.

The neutrons used in the 1951 experiments were obtained by charge exchange of protons in a 25 mm (4.6 g/cm^2) beryllium target. The target was placed at various distances from the center of the magnet – 153, 195, and 220 cm, which corresponded to proton energies of 260, 400, and 490 mev. The charge exchange neutron energy spectrum is considerably more smeared out than that for stripping reaction neutrons. The energy spectrum of charge exchange neutrons at a proton energy of 490 mev is shown in reference 11. We are calling these (from the position of the spectrum maximum) 380 mev neutrons. Actually the average effective energy for such neutrons depends on the threshold and excitation function shape of the detector used. In the case of the bismuth fission the effective energy was close to 340 mev. The maxima of the charge exchange neutron spectra for proton energies of 260 and 400 mev, obtained by interpolation of various charge exchange spectra, were close to 210 and 315 mev respectively.

The fission process was observed by counting pulses due to fission fragments in ionization chambers. Figure 1 shows the ionization chamber used. Electrodes were aluminum rings to which 20μ aluminum foil was glued. A layer of the fissioning material of area 8.5 or 12 cm^2 was deposited on both sides of the working electrodes. Collecting electrodes were less than 10 mm from the working electrodes, which is less than the range of fragments at atmospheric pressure. The chambers were filled with chemically pure argon at a pressure of about 800 mm Hg.

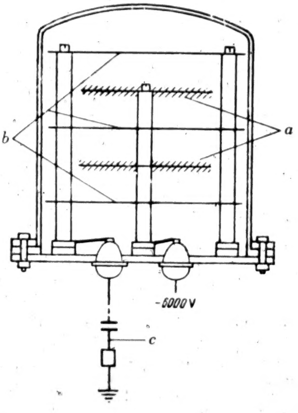

FIG. 1. Drawing of the ionization fission fragment chamber. *a* – the fissioning material; *b* – collecting electrodes; *c* – to amplifier grid.

Electronics consisted of a preamplifier, wide band amplifier, discriminator, scaler, and mechanical register.

The preamplifier was located in the synchrocyclotron room next to the ionization chamber. Signal was conducted out by a 40 meter armored coaxial cable to the amplifier.

Two types of linear amplifier were used in this work (LU-1 and LU-2). The upper frequency limit of LU-1 was 1.3 mc with an amplification factor 20,000 to 25,000.

The upper frequency limit of LU-2 was 8 mc, with an amplification factor of 8,000 to 10,000. Figure 2 shows the dependence of chamber count-

---

[11] V. P. Dzhelepov and Iu. M. Kazarinov, Dokl. Akad. Nauk SSSR **99**, 939 (1954).

ing rate on the discriminator clamp voltage for the fission of U, Bi, and W. The noise level was some 50-60 times less than the smallest fission fragment pulse. α-particle signals were up to 0.1 the size of the fission fragment pulse. The basic difficulty of measurement was connected with the necessity of cutting off possible registration of the frequently collected charged particles which originated in the chamber gas or walls and electrodes due to high energy neutron collisions. The difficulty depends to a large extent on the pulsed nature of the accelerator; it increases as the fission cross section of the investigated nucleus decreases, since in this case low neutron beam currents are convenient for removal of the background, but necessitate measurements of long duration. The necessity of removing the background demands the use of wide band amplifiers. Special experiments carried out in chambers without the fissioning layers showed that the background under typical working conditions was small (order of several percent) even compared to the fission effect of wolfram.

As can be seen from Fig. 2, in all cases investigated, there was observed a sufficiently wide plateau, where the counting rate varied weakly with the discriminator clamping level. Thus for uranium the plateau stretched from 5 to 12 volts, with a slope of 3% per volt. This slope was evidently connected with fringe effects, the effect of fissioning material layer thickness, and the emission of fragments at various angles. Measurements were carried out at the center of each plateau.

Thin layers of U^{235} and U^{238} were deposited on the aluminum cathode by electrolysis of a solution of uranium nitrate in absolute alcohol (~ 1 g/liter), using a platinum anode. With a current density of 0.5 ma/cm^2, a firm yellow-green deposit of thickness ~ 0.5 mg/cm^2 was formed in 10 minutes. The thickness of uranium on the working electrodes was 0.15 - 0.5 mg/cm^2. In view of the impossibility of baking the aluminum foils (with consequent change of the uranium to higher oxides), we assumed that the composition of the fissioning layer was between UO_2 (11.9% oxygen by weight) and U_2O_3 (9.2% oxygen by weight), i.e., we assumed that the layer was 89.5% uranium by weight. The U^{235} content of the isotope mixture used was 92.6%, so that 82.8% of the fissioning layer was U^{235}. The U^{235} ionization chambers were shielded by boron carbide and cadmium to eliminate the background due to fission by thermal neutrons. A thorium layer of ~ 1 mg/cm^2 was deposited on the aluminum foil in the form of a suspension of finely ground ThO_2 in acetone with 1% (by weight) organic binder. Layers of bismuth, lead and thallium (1 - 1.5 mg/cm^2) were produced by vacuum evaporation onto the aluminum foil, while the gold and platinum layers (~ 0.8 mg/cm^2) were produced by cathode sputtering.

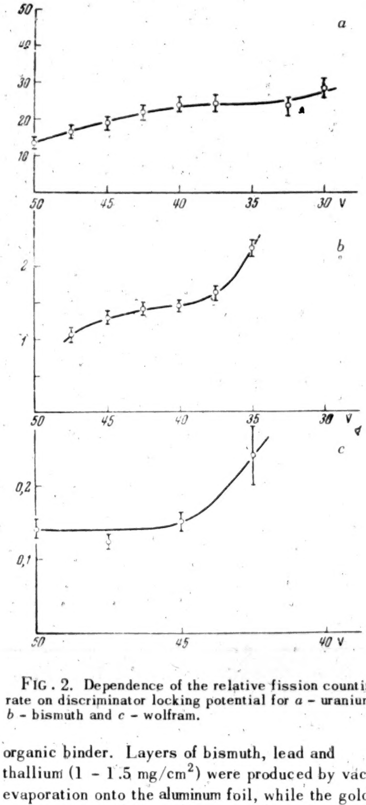

FIG. 2. Dependence of the relative fission counting rate on discriminator locking potential for *a* - uranium, *b* - bismuth and *c* - wolfram.

Wolfram was electrolytically deposited onto a copper cathode, (with platinum anode) in a bath consisting of 125 gm H_2WO_4 and 330 gm Na_2CO_3 per liter of solution. With a current density of 50 ma/cm^2, a silvery metallic deposit was formed in 30 minutes, with thickness ~ 0.8 mg/cm^2. From the data of reference 12 the composition by weight of wolfram in such a deposit is ~ 65%.

---

[12] V. I. Lainer and N. G. Kudriavtsev, *Fundamentals of Electroplating*, ch. 2, ONTI, USSR, 1938.

To determine the cross section, the incident neutron current was measured with the aid of carbon activated in the $C^{12}(n,2n)C^{11}$ reaction. The absolute detection efficiency of the activity of the product of this reaction – the C^{11} isotope (the count of the carbon detectors) was measured in special experiments. The cross section of $C^{12}(n,2n)C^{11}$ at $E_n = 90$ mev is 0.022 barns[13] and at 380 mev it is 0.021 barns[14]. The latter quantity was obtained in reference 14 by the comparison of *np* scattering data with the activation of carbon detectors, using our data for the count of these detectors. Therefore, possible errors in the absolute value of the activation cross section and in the count of the carbon detectors tend to cancel for $E_n = 380$ mev.

In a series of the special experiments, during which good constancy of the high energy neutron current was maintained, the fission cross section of bismuth was obtained by comparison with the carbon detectors. For subsequent determinations of fission cross sections of other nuclei, a bismuth fission chamber was used to monitor the neutron beam. In such a comparison, fluctuations of the neutron intensity could not affect the measured quantities.

The accuracy of the absolute values of the fission cross sections given below is connected with the determination of the bombarding neutron current with the carbon detectors and with statistical errors, and is taken as 20-30% for $E_n = 120$ mev and 15-25% for $E_n = 380$ mev. It must be noted that in the determination of the bombarding neutron current with carbon detectors, the magnitude of the current is lowered for the registration of U and Th fission and is raised for the lighter nuclei, the amount of rise increasing with the fission threshold. Therefore the fission cross sections indicated below are undoubtedly too high for U and Th, and too low for the other nuclei. Furthermore, the average effective neutron energy causing the fission is higher the greater the fission threshold and the faster the growth of the fission cross section with energy. The indicated errors are common to all work with high energy neutrons where it is impossible to define a narrow region in the neutron energy spectrum. Approximate evaluation of low energy neutron admixture in the outgoing spectrum shows that the increase of fission cross section of U and Th is not greater than 5-10%. Corrected values of the bismuth fission cross section, taking account of the spectrum shape and the excitation function, are shown in Fig. 3. Such a correction was not performed for the lighter nuclei because of insufficient data on the dependence of their fission cross section on energy.

Data on high energy neutron fission cross sections of nuclei from U to W from our work (no superscript) as well as from other authors[8,15,16] are given in Table 1.

TABLE I. Fission cross sections of heavy nuclei for high energy neutrons (in barns).

E_n (mev)	U^{235}	U^{238}	Th	Bi	Pb	Tl	Au	Pt	Re	W
84	—	1.4[8]	1[8]	0.019[8]	0.0055[8]	0.0032[8]	0.0021[8]	0.00095[8]	—	—
120	1.5	1.14	1[15]	0.036	0.020[16]	0.010[16]	0.010[16]	—	0.0017[15]	0.0011[15]
380	1.24	1.03	0.9	0.074	0.033	0.019	0.020	0.012	—	0.0038

Figure 3 shows the excitation function for the fission of bismuth, for a nominal neutron energy (curve 1) and corrected for the spectrum shape (curve 2). Values up to 84 mev and for 270 mev are taken from the literature;[8,17] the remaining points are from our work. The satisfactory agreement of all points confirms the determination of the absolute fission cross section.

---

[13] E. McMillan and H. York, Phys. Rev. **73**, 262(1948).

[14] K. O. Oganesian, Report Inst. Nuclear Problems, Acad. Sci. USSR, 1953.

[15] V. P. Dzhelepov, B. M. Golovin, Iu. M. Kazarinov, Report Inst. Nuclear Problems, Acad. Sci. USSR, 1950.

[16] A. A. Reut, G. I. Celivanov and V. V. Iur'ev, Report Ins. Nuclear Problems, Acad. Sci. USSR, 1950.

[17] W. Knox, Phys. Rev. **81**, 687 (1951).

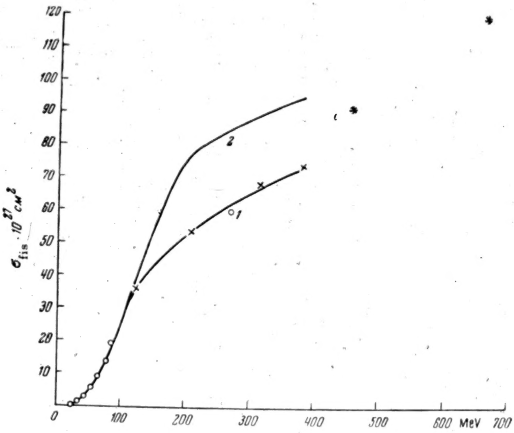

FIG. 3. Dependence of fission cross section of bismuth on neutron energy. 1 – without corrections for the energy spectrum of the incident neutrons; 2 – with such correction. The stars indicate data on the fission of bismuth by protons[23].

3. EVALUATION OF THRESHOLD FOR EMISSIVE FISSION

During the excitation of a heavy nucleus to high energies, the most likely processes are apparently emission of neutrons and fission. It is clear from the facts given in the introduction that the fission widths for stable nuclei from Bi to W are much narrower than the corresponding neutron widths. Evidently according to the emission of neutrons, the ratio of the fission width to the total width, which determined the probability for fission, must increase with increase of the parameter Z^2/A. Since there are no qualitative data relating the fission probability and the neutron emission for a highly excited nucleus, we have, in treating our experimental data, made the assumption[9] that emissive fission does not take place earlier than the moment at which the binding energy of the next neutron (increasing with the neutron emission) becomes larger than the critical fission energy of the remaining nucleus (which decreases according to the number of emitted neutrons).

The neutron binding energy is calculated from the Weizsacker-Fermi formula:

$$E_{bn} = -5{,}32 - 8{,}68\,A^{-1/3} + (Z^2/A)(77{,}4\,A^{-1} + 0{,}195\,A^{-1/3}) \pm 33{,}5\,A^{-3/4}. \quad (1)$$

The last term is added for even-even and odd-even nuclei (i.e., for even $N = A - Z$), and is subtracted for even-odd and odd-odd nuclei (i.e., with odd N). To determine the binding energy for nuclei with odd A, the last term should be used with $A - 1$ instead of A. For heavier, even N nuclei, whose neutron binding energy is higher, and for which, in general, the indicated conditions for emissive fission are satisfied,

$$E_{bn} \approx -6{,}16 + (Z^2/A)(77{,}4\,A^{-1} + 0{,}195\,A^{-1/3}). \quad (2)$$

In the determination of the neutron binding energy for nuclei with $A > 208$, in agreement with reference 18, a correction term should be put in which reduces the binding energy by

---

[18] O. Stern, Revs. Mod. Phys. **21**, 316 (1949).

$$\Delta E = 1.97 \exp\{-(A-208)/208\}\ \text{MeV}. \qquad (3)$$

In determining the neutron binding energy from Eqs. (2) and (3) we are naturally not taking account of the fluctuations in nuclear density connected with the filling of shells.

To calculate the critical fission energy, use was made in reference 9 of the results of the first paper of Bohr and Wheeler[19]; in our earlier paper[20] we worked from the results of Frankel and Metropolis[21]. However evaluation of the fission threshold from reference 21 produces values that are too high – for example the calculated threshold of U^{238} is higher by 1.7 mev than that experimentally observed, and for Th^{232} by 2.8 mev. Thus, our use[20] of the results of reference 21 for the evaluation of the critical fission energy gave high values for the number of neutrons emitted before the neutron binding energy is comparable to the fission barrier*.

Below we have made use of the results of a recent paper by Hill and Wheeler[7] to determine the critical fission energy. This gives

$$E_{fis} = 13A^{2/3}\xi_{max} \qquad (4)$$

in good agreement with the experimental value. The quantity

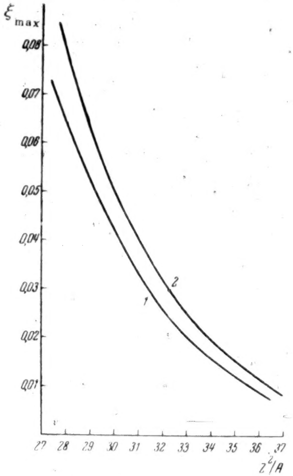

FIG. 4

FIG. 4. Dependence of the quantity ξ_{max} in the critical energy expression on the parameter Z^2/A; *1* – according to Hill and Wheeler[7] ($E_{fis} = 13A^{2/3}\xi_{max}$); *2* – according to Frankel and Metropolis[21] ($E_{fis} = 14A^{2/3}\xi'_{max}$).

---

[19] N. Bohr and J. Wheeler, Phys. Rev. **52**, 426 (1939).

[20] V. I. Gol'danskii, E. Z. Tarumov and V. S. Pen'kina, Dokl. Akad. Nauk SSSR **101**, 1027 (1955).

[21] S. Frankel and N. Metropolis, Phys. Rev. **72**, 914 (1947).

* It must be noted that a rough extrapolation was used in the series of values from reference 20 presented in Table I, and no account was taken of the difference in binding energy for nuclei with odd *N* and *Z*, so that these results are only of qualitative value.

$$\xi_{max} = f(x) = 0.728\,(1-x)^3 - 0.661\,(1-x)^4 + 3.330\,(1-x)^5,$$

where $x = (Z^2/A)\,/\,(Z^2/A)_{initial}$, and $(Z^2/A)_{initial} = 46.78$. The dependence of ξ_{max} on Z^2/A is shown by curve 1, Fig. 4. For comparison, curve 2 shows the corresponding dependence according to Frankel and Metropolis [21], who give

$$E_{fis} = 14A^{2/3}\xi'_{max} \qquad (5)$$

Using (2), (3), and (4), we determined the mass number A_c at which the neutron binding energy becomes greater than the critical fission energy for various nuclei. The dependence of A_c on Z is shown in Fig. 5. The main results of the calculations are presented in Table 2.

The first column of this table gives the mass number of the most stable isotopes or the average mass number of the natural isotopic mixture. The second column shows calculated values (according to reference 7) of the critical fission energy for the initial nucleus, while column four shows this for a nucleus of mass number A_c, as given in column three. The fifth column gives the fission parameter Z^2/A_c. The next three columns give the minimum number of neutrons (not counting the incident neutron) which must be emitted by the nucleus before emissive fission, with the emission of only neutrons, or with the addition of one or two protons. The last three columns show the values of the energy spent in the case of emissive fission with the emission of neutrons only, – the binding energy E_b of $N_c = A - A_c$ neutrons, their average kinetic energy (E_{kin}), and the average total energy of such a fission ($E_{tot} = E_b + E_{kin} + E_c$). The average neutron kinetic energy was calculated from the relation $\overline{E}_{kin} = 2T$, where the nuclear temperature T is connected to the excitation energy U by the relation $T = \alpha\sqrt{U}$. For this calculation we

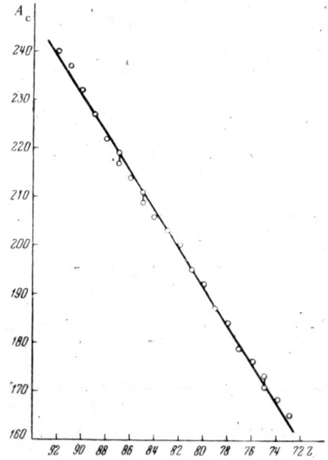

FIG. 5

FIG. 5. Dependence of the mass number A_c (at which the critical fission energy, calculated according to Hill and Wheeler[7], becomes less than the neutron binding energy) on atomic number Z.

TABLE II. Evaluation of emissive fission thresholds.

Nucleus	E'_{fis} (mev)	A_c	E_{fis} (mev)	Z^2/A_c	Number of emitted neutrons			Binding energy of N_c neutrons E_b(mev)	Kinetic energy of N_c neutrons E_{kin} (mev)	Total fission energy E_{tot}. (mev)
					Only n N_c	1 p	2 p			
$_{92}U^{235}$	4.4	(240)	(5.7)	(35.27)	0	0	1	—	—	4.4
$_{92}U^{238}$	5.2	(240)	(5.7)	(35.27)	0	0	4	—	—	5.2
$_{91}Pa^{231}$	4.6	(237)	(6.2)	(34.94)	0	0	2	—	—	4.6
$_{90}Th^{232}$	6.2	232	6.2	34.91	0	4	8	—	—	6.2
$_{89}Ac^{227}$	6.3	227	6.3	34.89	0	4	6 (8)	—	—	6.3
$_{88}Ra^{226}$	7.1	222	6.1	34.88	4	6 (8)	10	25	8	39
$_{87}Fr^{223}$	7.4	219	6.5 (6)	34.56	4 (6)	8	10 (12)	25 (38)	8 (12)	39 (56)
		(217)		(34.88)						
$_{86}Rn^{222}$	8.8	214	6.4	34.56	8	10 (12)	14	50	22	78
$_{85}At^{210}$	6.6	211	7 (6.3)	34.24	0 (1)	3	5	(6.4)	(1.1)	6.6
		(209)		(34.57)						(13.8)
$_{84}Po^{209}$	7.7	206	6.8	34.25	3	5	7	19	7	33
$_{83}Bi^{209}$	9.3	203	7.3	33.94	6	8	12	39	15	61
$_{82}Pb^{206}$	10.1	200	7.7	33.62	6	10	12	41	15	64
$_{81}Tl^{204}$	11.6	195	7.6	33.65	9	11	15	63	28	99
$_{80}Hg^{201}$	12.6	192	8.1	33.33	9	13	15	63	29	100
$_{79}Au^{197}$	12.4	187	7.9	33.37	10	12	16	74	35	117
$_{78}Pt^{195}$	13.6	184	8.3	33.07	11	15	17	82	42	132
$_{77}Ir^{192}$	15.5	179	8.3	33.12	13	15	17 (19)	98	53	159
$_{76}Os^{190}$	16.6	176	8.7	32.82	14	16 (18)	20	106	59	174
$_{75}Re^{186}$	16.9	173	~~9.1 (8.3)~~	32.51	13 (15)	17	19	100 (118)	54 (67)	163
		(171)		(32.89)						(193)
$_{74}W^{184}$	18.9	168	8.8	32.60	16	18	—	128	73	210
$_{73}Ta^{181}$	19.7	165	9.5	32.30	16	—	—	128	74	212

took the numerical value of α directly from the model of a Fermi gas which gives $\alpha = 2.92\, A^{-1/3}$ (for a Fermi surface of 21 mev). The calculation of the critical fission energy according to Hill and Wheeler[7], and the improvement of the calculation of A_c and the neutron binding energy taking account of whether the nucleus is even or odd, gives a significantly reduced value of N_c and the energy of emissive fission compared to reference 20, so that the results shown in Table 2 are close to our previous evaluations given in reference 9.

It follows from the above assumptions on the conditions for emissive fission that we may consider the fission section of each nucleus as the cross section of emission before fission of $N > N_c = A - A_c$ neutrons. Then the fission cross section of the given nucelus is

$$\sigma_{N_c} = \sigma_0 \int_{N_c}^{\infty} w(n)\, dn,$$

where σ_0 is the fission cross-section of a nucleus which can divide without the emission of neutrons, and $w(n)$ is the normalized probability of emission before fission of n neutrons. Comparing the fission cross sections of various nuclei, it is possible to determine the function $w(n)$, i.e., distribution of the fission-accompanying neutron stars by the number of prongs, as well as to determine the average number of neutrons (for $n > N_c$) emitted by the given nucleus before fission. It is necessary in such an evaluation to take account of the possibility that the excited nucleus will emit charged particles in addition to neutrons before fission. From their investigation of uranium fission in thick emulsions by 150 and 380 mev neutrons, the authors of reference 22 conclude that, in practice , the emission of one charged particle should be taken into account in each case of fission. We shall therefore work on the assumption that in each fission event one proton is emitted either during the internal cascade or in the subsequent evaporation process. Then we may, using the data of Table I, and taking the fission cross section of U^{238} for σ_0, determine the dependence of σ/σ_0 on N_c shown in Fig. 6. From this dependence and the

---

[22] G. E. Belovitskii, T. A. Romanova, L. V. Sukhov and I. M. Frank, J. Exper. Theoret. Phys. USSR **29**, 537 (1955); Soviet Phys. JETP **2**, 493 (1956)

assumption that one proton is emitted before fission, we obtain the following values for the number of neutrons emitted before fission of U^{238} for various bombarding energies: $E_n = 84$ mev, $\bar{N} = 6.0$; $E_n = 120$ mev, $\bar{N} = 6.7$; $E_n = 380$ mev, $\bar{N} = 7.1$ (here the incident neutron is already taken into account). For lighter nuclei, the average number of neutrons emitted before fission turns out to be higher – for example in bismuth (from Fig. 5), normalizing to $\sigma = \sigma_0$, we obtain $E_n = 84-380$ mev, $\bar{N} = 11-11.5$ (counting the incident neutron).

The results obtained are in satisfactory agreement with purely radiochemical investigation of the fission products of uranium[1] and bismuth[2] in high energy reactions; the average number of neutrons emitted during a fission event was there found to be 6-12 for uranium and 12 for bismuth. In comparing our values of $\bar{N}$ with those found by other methods, it should be borne in mind that the smeared out energy spectrum of the bombarding neutrons which raises the fission cross sections of U and Th, and lowers the fission cross sections of the lighter nuclei, has the effect of somewhat lowering the value of $\bar{N}$. The excitation energy necessary for emissive fission shown in Table II for nuclei heavier than Ta, and calculated by us for lighter nuclei in reference 9, is also in satisfactory agreement with the results of emulsion studies of emissive fission by Shamov[23].

Such agreement with experiment seems to justify the simple qualitative interpretation we have made of the fission of heavy nuclei by high energy particles, based on equating the neutron binding energy with the critical fission energy of the nucleus after the emission of neutrons.

The comparisons between experiment and calculation can not aspire to be quantitatively exact, if only because the data represent averages over the isotopic composition of the elements and over the energy spectrum of the bombarding neutrons. However, even the qualitative observations allow some conclusions to be drawn about the general nature of fission of various nuclei by high energy particles, and allow the proposal of some experiments to check on the assumptions that were made above. For example, it follows from Fig. 6 that the ratio $\sigma/\sigma_0 = f(N_c)$ falls off very rapidly for nuclei lighter than thorium. If we take into account the lowering of the fission cross sections of lighter nuclei by the smearing of the neutron energy spectrum, then the tails of the curves on Fig. 6 for $z = 74-78$ are raised strongly. The dependence of σ/σ_0 on N_c is then divided into three regions – slow decrease (from U to Th, and for nuclei lighter than Au), and a region of fast decrease from Th to Au. The existence of three such regions is apparently connected with the fact that for nuclei from U to Th and lighter than Au in the present energy interval, fission may occur with the emission of less than $N_c = A - A_c$ neutrons. This conclusion is in agreement with the theoretical results of Geilikman[24], who examined the thermodynamics of excited and fissioning nuclei. He concluded that high temperature fission from a highly excited state may compete with emissive fission for the heaviest nuclei where $\sigma_{fis} \approx \sigma_{geom}$, and for the relatively light nuclei, which must emit a very large number of neutrons for emissive function.

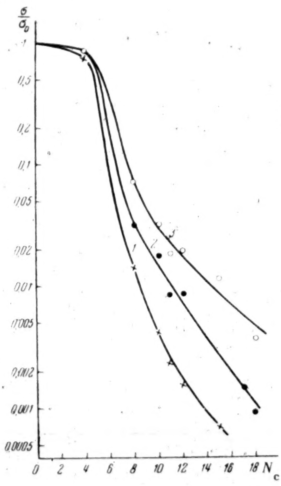

FIG. 6. Dependence of the fission cross section of nuclei on the minimum number of neutrons which must be emitted before fission (assuming that one proton is also emitted). *1* – $E_n = 84$ mev; *2* — $E_n = 120$ mev; *3* – $E_n = 380$ mev.

Similar conclusions can be drawn from recent

---

[23] V. P. Shamov, Dissertation, Radium Inst. Acad. Sci. (RIAN), 1955.

[24] B. T. Geilikman, Report of the Acad. Sciences USSR, 1950.

Soviet work on the fission of heavy nuclei by high energy particles using emulsions[25] as well as radiochemical methods[26,27].

To check on the assumptions we have made it would be desirable to perform experiments with monoenergetic neutrons. It would be interesting to to measure the fission cross section for separated isotopes – particularly those with neutron deficit, in which case fission does not require multiple emission of neutrons. The fission cross sections of some similar isotopes (for example $At^{207-209}$) must be of the order of $10^{-25}cm^2$. The combination of data on emissive fission of various isotopes at high energies may be used to determine the neutron widths and fission widths of strongly excited heavy isotopes with neutron deficits, which are not at all formed in experiments at low energies.

---

[25] N. A. Perfilov, N. S. Ivanovna. O. V. Lozhkin, V. I. Ostroumov and V. P. Shamov, paper at the July 1955 meeting of the Academy of Sciences, USSR.

[26] A. P. Vinogradov, I. P. Alimarin, V. I. Baranov, T. V. Baranova, A. K. Lavrukhina and F. I. Pavlotskaia, paper at the July 1955 meeting of the Academy of Sciences, USSR.

[27] B. V. Kurchatov, V. N. Mekhedov, M. Ia. Kuznetsova and L. N. Kurchatova, paper at the July 1955 meeting of the Academy of Sciences, USSR.

Translated by G. L. Gerstein
272

SOVIET PHYSICS JETP VOLUME 2, NUMBER 4 JULY, 1956

Investigation of the Structure of the Surface of Films of Copper Oxide on Different Faces of a Monocrystal of Copper, and the Determination of the Contact Potential Difference between These Surfaces

N. B. GORNY
Leningrad Electrotechnical Institute of Communications

(Submitted to JETP editor July 3, 1954)
J. Exper. Theoret. Phys. USSR **29**, 808-816 (December, 1955)

The structure of the surfaces of films of copper oxide formed on various faces of a monocrystal of copper is investigated using the method of diffraction of slow electrons. It is found that on faces (100) and (111) of a monocrystal of copper there is formed a monocrystalline film of Cu_2O with a (111) plane parallel to the base. On face (110) a monocrystalline film of Cu_2O is also formed but with a less perfect crystalline structure and with a (110) surface plane. Investigation of the contact potential difference by the method of displacement of the volt-ampere characteristic curves demonstrated that films of Cu_2O on faces (100) and (111) of a monocrystal of copper have the same work function (0.2V), and consequently, have the same crystalline orientation. The film of Cu_2O on the (110) face of copper possesses a larger work function (0.3v), and also has stronger adsorptivity of residual gases than films of Cu_2O on faces (100) and (111), which indicates a difference in the properties (orientations) of the film of Cu_2O on face Cu (110) and of films of Cu_2O on faces Cu (100) and (111).

IN order to clarify the results obtained during the investigation of secondary electron emission from the surfaces of various faces of a monocrystal of copper which were covered with films of copper oxide[1], it was necessary to determine the crystalline structure of these films and also the work function of the surface of these films. With this aim in mind, we carried out investigations of the surface structure of monocrystalline specimens by the method of diffraction of slow electrons and the contact potential difference between the surfaces of the investigated specimens.

Numerous investigations have demonstrated that after pure copper, polycrystalline or monocrystalline, is exposed to the atmosphere for a certain length of time, its surface undergoes oxidation. A film of copper oxide several tens of Å in thickness[2,3] forms at atmospheric pressure and at room temperature. According to references 4 and 5, the thickness of a film of copper oxide on the surfaces of monocrystals of copper having various crystallographic directions varies. However, the data in these two references do not coincide. Various conditions of film formation (temperature, pressure of the gaseous medium, etc.) can lead to varying results with regard both to thickness of film as well as the structure of the film itself. Apparently, the very mechanism of formation of the films differs at low and high temperatures[2]. The conditions under which Gwathmey and Benton[5] carried out their oxidation processes most closely resembled ours. They found that the thickness of a layer of copper oxide decreases on the planes of a monocrystal of copper according to the following order: (100), (111), (110). The results of the work in reference 6 also agree with these results. During the investigations recently carried out by Rhodin[7] it was demonstrated that the thickness of the oxide film which formed on the (100) face of a monocrystal of copper increases rapidly at first, and then remains almost unchanged (up to 40 hours). At room temperature, the thickness of the oxide film on the (100) face attains 15Å.

---

[1] N. B. Gorny, J. Exper. Theoret. Phys. USSR **26**, 79, 327 (1954).

A number of researchers have been occupied with the study of the structure of copper oxide films formed on the various faces of a monocrystal of copper, with the aid of the method of diffraction of fast electrons or of X-rays. However, the results of these investigations show no conformity. Pinsker and Tatarinova[8] are of the belief that, aside from a certain quantity of copper oxide in the form of a polycrystalline powder, the basic mass of Cu_2O is precisely oriented with respect to the metallic copper. Pinsker[9] indicates that, according to the degree of increase in the concentration of the oxide phase of the monocrystalline film of copper, a precise mutual orientation takes place between the Cu_2O and the copper, during the course of which three basic types of orientation are observed: on the (100) faces of the copper the copper oxide distributes itself with faces (111), (110) and (100). In references 10, 11 the authors come to the conclusion that an oxide film of monocrystalline structure forms on the (110) and (111) faces of monocrystal of copper, while a homogeneous face of Cu_2O film distributes itself parallel to the face of the copper. The (100) face of the copper is covered by (111) planes of copper oxide.

THE INVESTIGATED SPECIMENS AND THE VACUUM TUBE DEVICE

After the orientation of the copper monocrystal was determined by optical means, and the basic crystallographic directions on the monocrystal were noted[12], three discs having a diameter of approximately 10 mm and a thickness of 0.6-0.8 mm were cut from the copper; the surfaces of these discs coincided with various crystalline faces, namely: (001), (011), and (111).

After fabrication of the discs and a preparatory mechanical and electrical polishing process, they were etched with a special mixture (see reference 12) in order to make sure that the superficial layer, which was deformed during the mechanical processing, was completely removed by the electrolytic polishing process, and in order to check the crystalline orientation of the planes of the discs, according to the method described in reference 12. Then the discs were polished mechanically with a thin paste of GOI and, finally, they were polished electrolytically to a mirrorlike finish. In addition to this, a disc having exactly the same dimensions was prepared from a fragment of polycrystalline copper and polished in the same manner.

Immediately following their fabrication, the specimens were mounted in place in the tube. The tube was subjected to a lengthy process of evacuation, while the space representing the electron trap of the tube (normally filled with liquid air) was heated to room temperature for a period of time sufficient to rid it of water vapor. Subsequent de-gassing of the tube was carried out over a period of 4 days at a tube temperature of up to 450°C; the metal parts were subjected to a supplementary heating process by means of electron bombardment and by high frequency currents till they glowed deep red. After attainment of a high vacuum (less than 10^{-6} mm mercury) the tube was sealed off and the getters were vaporized in special compartments of the tube.

---

[2] N. Cabrera and N. F. Mott, Reports of P[illegible]g. in Phys. **12**, 174 (1949).

[3] U. R. Evans, *Metallic Corrosion Passivity and Protection*, E. Arnold, 1949.

[4] J. Bernard and J. Talbot, Comptes rend. **225**, 411 (1947).

[5] A. T. Gwathmey and A. F. Benton, J. Phys. Chem. **46**, 969 (1942).

[6] P. A. Thissen and H. Schütze, A. anorg. allgem. Chemie **233**, 35 (1937).

[7] T. N. Rhodin, J. Amer. Chem. Soc. **72**, 5102 (1950).

[8] Z. G. Pinsker, *Diffraction of Electrons*, Acad. Sci. Publishing House, 1949.

[9] A. G. Pinsker, Izv. Akad. Nau, SSSR, Ser. Fiz. **13**, 473 (1949).

[10] K. H. Moore, Ann. Physick **33**, 133 (1938).

[11] E. Menzel, A. anorg. Chemie, **256**, 49 (1948) (Annals of the All-Union Mineralogical Society).

[12] N. B. Gorny, Zap. Vses. Mineral Ob-va **80**, 245 (1951).

It was expedient to carry out the investigation of the structure of the surfaces and the contact potential differences in the very same tube and under the very same conditions prevailing during the investigation of secondary emission. We employed a relatively simple tube construction, which made it possible to carry out the investigation of both the secondary emission and the diffraction of the electrons as well as the contact potential difference.

In the vaccum tube which we utilized (Fig. 1) a narrow electron beam emitted from the tantalum electron gun impinged perpendicularly on a platform consisting of a tungsten disc situated at the center of the sphere represented by the vacuum tube; the platform could be turned by means of electromagnets and set to the desired position. The specimens undergoing investigation were fastened to the platform – these were monocrystals of copper with planes corresponding to faces (001), $(0\bar{1}1)$ and (111), and polycrystalline copper. By preliminary experiments using the method of cathode luminescence, the position of the electron spot issuing from the gun was determined relative to the light spot. The diameter of the electron spot was of the order of 1 - 1.5 mm.

INVESTIGATION OF THE SURFACE STRUCTURE OF FILMS OF Cu_2O

In investigating the surface structure of the specimens, we employed the method of diffraction of slow electrons, measuring the dependence of the current at a constant angle on the energy of a primary cluster of electrons.

A tantalum Faraday shield measuring 8 × 5 mm (Fig. 1) was used as an electron receiver during the investigation of diffraction. The current in the cylinder was measured by a vacuum tube electrometer having a sensitivity of 10^{-15} A/mm at an input resistance of 10^{10} ohms.

In order to avoid leakage losses to the glass support of the Faraday cylinder, a protective cylinder is employed which is held at the same potential as the Faraday cylinder. With the same aim in mind, the surface of the support is deliberately enlarged, and on the outside the point of issuance and the entire glass base are covered with ceresin to increase the degree of isolation. A retarding potential is applied to the outer cylinder, which prevents the possibility of entry into the receiver of any electrons which have lost energy greater than one electron volt. The actual value for the accelerating potential, which depended on the contact potentials and on the voltage drop across the cathode filament, was determined experimentally. The retarding potential at which the current in the receiver becomes equal to zero, is apparently equal to the actual value of the accelerating potential. From this, it is possible to find a correction factor, which it is necessary to apply to the reading of the voltmeter measuring the accelerating potential.

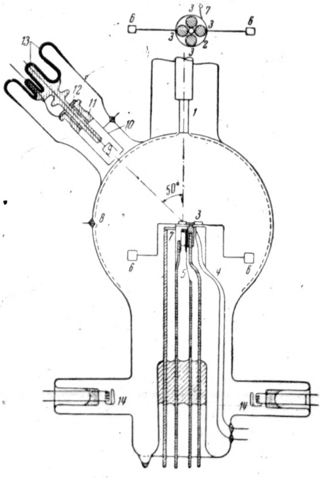

FIG. 1. Vacuum tube device. *1* – electron gun; *2* - platform; *3* - objects under investigation; *4* - thermocouple; *5* - heater filament; *6* - small iron rods imbedded in glass; *7* - locking spring; *8* - collector; *9* - Faraday cylinder; *10* - cylinder with diaphragm; *11* - quartz tube; *12* – protective cylinder; *13* - ceresin; *14* — getter.

In order to prevent distortion of the trajectory of the electrons in the tube during the measurements, the earth's magnetic field was compensated for by two Helmholtz coils having a diameter of 1 m.

The experimental data we obtained are presented in Fig. 2. The abscissa shows the energy of the incident electrons in volts; the ordinate gives the number of electrons distributed without velocity loss (or more precisely, which have lost no more than 1 v) in the Faraday cylinder. The ordinate is in arbitrary units. The measurements were carried out at room temperature and at specimen temperatures of 350 ° and 450°C. Heating was accomplished by a heater filament located inside the platform

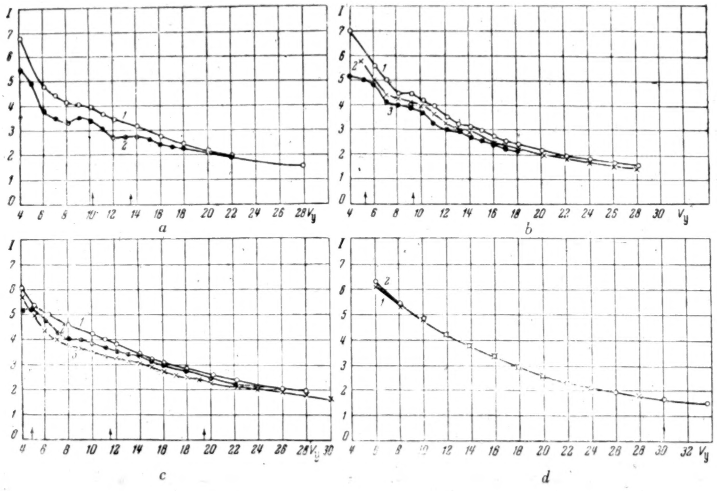

FIG. 2. Diffraction curves obtained: *a* – from the (100) plane of a monocrystal of copper (plane (111) of copper oxide); *b* – from the (111) plane of a monocrystal of copper (plane (111) of copper oxide); *c* – from the (110) plane of a monocrystal of copper (plane (110) of copper oxide); curve *2* is obtained at 450°C, curve *1* at 350°C; *d* – are curves obtained from the surface of polycrystalline copper (polycrystalline surface of copper oxide). All curves *1* are obtained at room temperature: in graphs *a*, *b*, and *d*, curves *2* are obtained at 350° and curve *3* at 450°C.

Investigations demonstrated that the magnetic field of the tungsten spiral used for heating affected the measurements, and for this reason before each reading, after the temperature of the specimens had been brought to its predetermined value and had been maintained for the predetermined length of time, the heating current was turned off.

The presence of maxima in the diffraction curves of the monocrystalline copper specimens indicates a monocrystalline structure of the surface. It is necessary to point out that the diffraction maxima obtained are weakly expressed and rather broad. This is most probably a result of the nonsymmetrical positioning of the receiver and the electron gun, as has been indicated in the investigations of Lashkarev[13], who observed an abrupt drop in the intensity of expression of the maxima upon changing from a symmetrical to a nonsymmetrical receiver with respect to the electron gun. In the case of the polycrystalline specimen (Fig. 2d) the scattering curve proved to be smooth and without maxima, both at room temperature and at elevated temperatures.

---

[13] V. E. Lasharev, *Diffraction of Electrons*, GTTI, 1933.

We attempted to compute the diffraction maxima, hypothesizing that the scattering originated in the copper lattice; however, negative results were obtained. It was then that we attributed these maxima to scattering from the monocrystalline film of copper oxide formed on the surface of the monocrystal of copper.

Copper oxide, in crystallizing, forms a volume-centered crystalline lattice with a periodicity of 4.26 Å. The values for the energy of the electrons, at which the maxima appear on the diffraction curves, conform with the following hypotheses as to the disposition of the crystalline lattice of the copper oxide on the copper lattice. On face Cu (111) there is formed a monocrystalline film of oxide with a (111) face parallel to the base, but rotated 30° about the vertical axis with respect to the copper lattice (Fig. 3a). On face Cu (001) there is formed a monocrystalline film of copper oxide with a (111) face parallel to the base, whereas the edge of the (111) face of the Cu_2O is rotated 15° about the vertical axis with respect to the edge of Cu face (001) (Fig. 3b). A (011) face of copper oxide, rotated about the vertical axis by an angle of 35° is located on Cu face (011) (Fig. 3c). The dispositions of the lattices of copper oxide on copper described above agree with the data obtained in references 6, 9, 10. This sort of accretion of copper oxide on copper is apparently connected with the magnitudes of the constants of the copper (3.6 Å) and Cu_2O (4.26 Å) lattices. The most favorable conjectures of the lattices of copper oxide and copper are obtained with the dispositions indicated above.

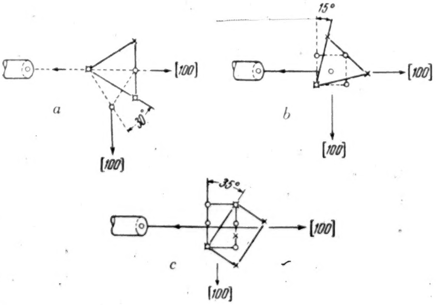

FIG. 3. Schematic of the mutual dispositions of the lattices of copper oxide and copper. The broken line represents the lattice of copper, and the solid line the lattice of Cu_2O. The primary cluster of electrons falls on the monocrystals from above. The arrows show the direction of the dispersed electrons to the Faraday cylinder. The zones of the copper lattice are shown in each drawing.

The arrows on the diffraction graphs (Fig. 2) show the potentials corresponding to the wavelengths, computed on the basis of interferential conditions, for the maxima for normal electron fall (for our specimens). The correspondence of the potentials at which the experimental maxima were obtained with the computed maxima is satisfactory.

Here it may be noted that while in the investigation of copper oxide on monocrystals of copper having (001) and (111) planes maxima were obtained even at room temperature of the specimens, and the positions of these maxima remained unchanged even at a temperature of 350°C (Figs. 2a and 2b), in the curves for copper oxide on the (1 1 0) plane of a monocrystal of copper there are no expressed maxima either at room temperature or at 350°C, and only at 450°C did a weakly expressed maximum appear. These data indicate a less perfect monocrystalline structure of the copper oxide film on the (1 1 0) face of copper than on the (1 1 1) and (1 00) faces of copper, apparently as a result of lesser thickness. According to the data by Pinsker, thinner layers of copper oxide have a less perfect, dispersive structure formed of tiny monocrystals[8].

We also investigated the effect of temperature on the intensity of reflection of the electrons for all specimens. Figure 4 shows the experimental results we obtained. The abscissa represents the time in minutes from the instant the heating current was switched off, at $t = 450°C$ (reduction of temperature); the ordinate is the intensity of scattering of electrons (in relative units) with energy conditions unchanged. The intensity of scattering of the electrons for the two investigated surfaces – the (1 1 1) plane of copper oxide on the (1 00) face of the copper (Fig. 4a and also Fig. 2a) and the (1 1 1) plane of copper oxide on the (1 1 1) face of the copper (Fig. 2b) – decreases as the temperature goes up. These data coincide with the results obtained by Kalashnikov and Zamsha on a monocrystal of silver[14]. However, for the (11 0) plane of copper oxide on the (1 1 0) face of copper, the intensity of dispersion of the electrons at first drops, and then only upon continued reaction in temperature, increases (Fig. 4b). These data for a film of copper oxide on the (110) face of copper, and the circumstance noted above that for such a film weakly expressed maxima are observed only at a temperature of 450°C, and at lower temperatures (350°C and room temperature) they are not expressed in the diffraction curves, can be explained by the more powerful adsorption of residual gases on the oxide film formed on the (1 1 0) face of the copper as a result of its imperfect structure. This has been confirmed by a recently published research paper[15].

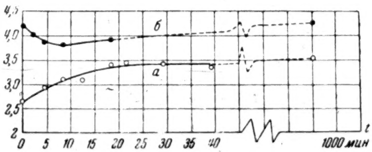

FIG. 4. Effect of change in temperature on the intensity of reflection: *a* - from the (1 1 1) plane of copper oxide; *b* - from the (11 0) plane of copper oxide.

INVESTIGATION OF THE CONTACT POTENTIAL DIFFERENCE

In order to check the correctness of our conclusions that a monocrystalline film of copper oxide having the same orientation with respect to the (1 1 1) plane and parallel to the base accumulates on the (001) and (1 1 1) faces of monocrystals of copper, we carried out measurements of the contact potential difference by the method of displacement of the volt-ampere characteristic curve[16,17].

A series of investigations[18-20] have shown that the work function differs for various faces of a monocrystal of one and the same metal. If the contact potential difference between the two monocrystalline planes of the very same substance is equal to zero, i.e., if these planes possess the same work function, then with a high degree of probability one may conclude that these planes represent the same crystalline faces.

---

[14] S. G. Kalashnikov and O. I. Zamsha, J. Exper. Theoret. Phys. USSR **9**, 1408 (1939).

[15] T. N. Rhodin, J. Amer. Chem. Soc. **72**, 5691 (1950).

[16] B. M. Tsaryev, *The contact potential difference*, GITTL, Moscow, 1949.

[17] P. A. Anderson, Phys. Rev. **47**, 958 (1935).

[18] S. T. Martin, Phys. Rev. **56**, 947 (1939).

[19] M. H. Nichols, Phys. Rev. **57**, 297 (1940).

[20] P. A. Anderson, Phys. Rev. **59**, 1034 (1941).

The contact potential difference between the investigated specimens was measured in the very same vacuum tube device which was used in investigating the diffraction of the electrons. An extremely important requirement for these measurements was the specification that the primary current be maintained constant (within limits of 0.5%).

This was accomplished by connecting a constant resistance into the heating circuit, and regulation of the heating current was accomplished (extremely smoothly) by means of two potentiometrically connected, plug-in type resistance boxes. The magnitude of the primary current could be judged from the readings of the microammeter. During these experiments, compensation for the earth's magnetic field was performed by two Helmholtz coils.

Figure 5 shows the experimentally determined curves for the investigated specimens. The values of the current across the individual specimens are graphed along the ordinate in relative units, while the difference between the unvarying accelerating potential and the varying retarding potential $V_y - V_z$ is graphed along the abscissa. The potentials were measured with an accuracy of ± 0.02 v. The displacement of the volt-ampere curves in the steep portion determines the contact potential difference between the corresponding specimens.

At room temperature (Fig. 5a) the contact potential difference between all the specimens is almost equal to zero, and consequently, the work function, too, is almost the same for all the investigated planes at room temperature. Upon increasing the temperature to 350°the work functions of the monocrystalline planes changed – they increased (Fig. 5b) with respect to the polycrystalline surface and with respect to the work function for these planes at room temperature, and in this instance to the greatest degree for plane (110). At a still higher temperature (450°C) (Fig. 5c) the work function of plane (110) grew even greater, exceeding the work function of the polycrystalline surface by $\Delta\varphi = 0.5$ v. As for the work functions of both planes of the films of copper oxide formed on the (001) and (111) faces of copper, at room temperature they were the same; upon raising the temperature to 350°C they changed equally with respect to the work function of the polycrystalline surface (by $\Delta\varphi = 0.2$v); and upon raising the temperature to 450°C their work functions remained unchanged and almost equal for both of the planes. Upon raising the temperature to 500°C, the disposition of the volt-ampere curves for all the investigated specimens remained the same as at 450°C.

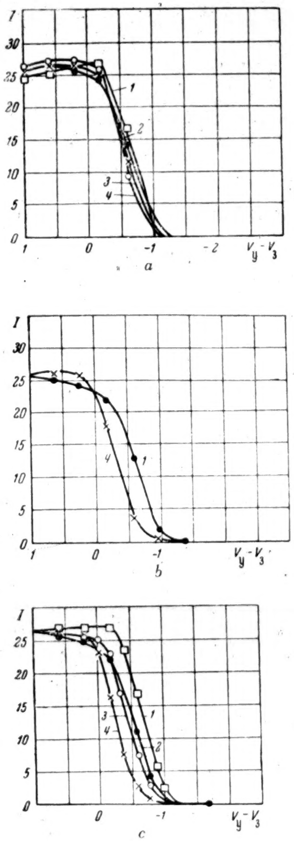

FIG. 5. Volt-ampere characteristic curves, obtained: *a* – at room temperature of the specimens; *b* - at a temperature of the specimens equal to 350°C; *c* - at a temperature of the specimens equal to 450°C. Curves *1* for films of Cu_2O on polycrystalline copper; *2* – for films of Cu_2O on the (111) face of copper; *3* – for films of Cu_2O on the (100) face of copper and *4* – for films of Cu_2O on the (110) face of copper.

EVALUATION OF THE RESULTS

On the basis of our experimental data, we can draw the following conclusions. The value of the contact potential differences among all the specimens, which is almost equal to zero at room temperature, indicates that at that temperature all the specimens are covered with adsorbed molecules of residual gas. Upon increasing the temperature to 350°C the oxide film on the polycrystalline copper and the oxide films on the (100) and (111) faces of the copper monocrystal clear themselves of adsorbed molecules of gas. The surface of the oxide film on the (110) copper face was cleared of molecules of residual gas only at 450°C, which is indicated by the change in its work function during increase in temperature right up to 450°C (Fig. 5), and also by the appearance of diffraction maxima only at this temperature (Fig. 2c). The course of change in intensity of scattering with decrease in temperature (Fig. 2c) also indicates more powerful adsorption of the molecules of the residual gases on the oxide film*, formed on the (110) face of the copper as a result of the less perfect crystalline structure of this film as compared to the films formed on copper faces (100) and (111). The less perfect crystalline structure, as we have already mentioned, apparently is connected with the lesser thickness of the film on the (110) face of the copper.

The equal values for the work function of the two copper oxide films, formed on faces (100) and (111) of the monocrystal of copper, confirm our conclusion (based on our investigations of the diffraction of electrons) as to the formation of similarly oriented films of copper oxide (with a (111) plane parallel to the base) on these Cu faces. The work function of films of Cu_2O on the (110) face of Cu differs from the work function for films of Cu_2O on the (100) and (111) faces of copper, which indicates a different crystalline orientation of this film, in conformity with the results obtained in the investigations of their structure by the method of electron diffraction.

In connection with the results obtained, we would like to make the following two remarks: 1) These results are in conformity with general considerations, which consist of the fact that a crystalline face in which the superficial atoms are more densely packed (as is the case with volume-centered cubic lattice (110)[21] should have a greater work function than a face with less dense concentration of the surface atoms (111). 2) At the same time that the work function for the (111) plane of the copper oxide remains unchanged (with change in temperature from 350°C to 450°C), the diffraction curve for the same plane (Fig. 3b) changes with change in temperature over the same range. This apparently confirms the conclusions of Farnsworth[22] with regard to the fact that only the upper atomic layer affects the diffraction, while the work function depends on a deeper layer.

The vacuum tube device described in this article (Fig. 1) was also utilized in the investigation of secondary emission from the examined surfaces of the monocrystalline specimens of copper[1]. The data obtained in the present work made it possible to explain the following peculiarities of the secondary emission for the investigated monocrystalline surfaces (for a more detailed account see reference 1).

For the monocrystalline specimens of copper with superficial planes (100) and (111), the same values for the coefficient of secondary emission δ and the same course of the curves $\delta = f(V_p)$ were obtained. Here V_p is the energy of the primary electrons. This agreement is attributed to the fact that the same monocrystalline films of copper oxide with (111) surface planes form on the monocrystalline (100) and (111) surface planes of copper.

The relative variation in δ with change in temperature from 20° to 500°C for the (111) plane of copper oxide are less than the relative variations in δ with change in temperature within the same limits for the (110) plane of copper oxide. This result points to the presence of greater contamination by molecules of residual gas at room temperature on the (110) plane of the copper oxide than on the (111) plane. The data obtained in this work with regard to the fact that a monocrystalline film of copper oxide on the (110) face of copper possesses a less perfect crystalline structure, and consequently, also greater capability of adsorption than a monocrystalline film of copper oxide with a (1 1 1) surface plane, conforms with the result given above.

---

* This conclusion is verified by Rhodin[15], who discusses investigations of the heat of adsorption of nitrogen on polycrystalline copper and on the faces of a monocrystal of copper covered with a film of copper oxide; the investigations employed the method of measuring the adsorption with the aid of vacuum-type microbalance scales for several values of temperature. The investigations demonstrated that the heat of adsorption differs for various surfaces and increases according to the following order: pollycrystalline surface ~ 2500 cal/mol; (111) face ~ 3300 cal/mol; (100) face ~ 3500 cal/mol; and (110) face ~ 4000 cal/mol.

[21] K. Khering and M. Nikol's, *Thermoelectronic Emission*, IIL, 1950.

[22] H. E. Farnsworth, Phys. Rev. **81**, 652 (1951).

The coefficient of secondary emission δ for the monocrystalline specimen with a (1 1 0) surface plane at a temperature of 500°C has a somewhat lesser value than for the two other monocrystalline specimens of copper oxide with a (1 1 1) surface plane at the same temperature. This may result from the fact that the work function of the (11 0) plane of copper oxide is greater than the work function of the (1 1 1) plane of copper oxide.

It may be noted that the juxtaposition of the results of the investigation of the structure of the surface of monocrystalline films of copper oxide and the contact potential difference between them, with the results of the investigation of secondary emission for these films, proved to be extremely useful in the explanation of these results.

Translated by A. Certner
275

SOVIET PHYSICS JETP VOLUME 2, NUMBER 4 JULY, 1956

Experiments on the Investigation of the Breakdown of NaCl Crystals

N. M. MELANKHOLIN AND V. R. REGEL'
Institute of Crystallography, Academy of Sciences, USSR

(Submitted to JETP editor June 14, 1954)
J. Exper. Theoret. Phys. USSR 29, 817-821 (December, 1955)

The development of cracks during the stretching of specimens of NaCl monocrystals was studied by the method of cinematography in polarized light. It was shown that the cracks spread intermittently. The development of the cracks is prevented by the shearing bands which they have to cross. It is assumed that the propagation of the cracks is prevented by the regions of the shearing bands in which compression stresses are present. Regions of shearing bands having stretching stresses apparently do not prevent their development.

A CONSIDERABLE number of investigations have been devoted to the study of the processes of shear origination and the breakdown of NaCl monocrystals. Of these investigations, the studies of Stepanov and his co-workers[1-7] are of great importance. In these studies the process of the artificial origination of shear and that of the appearance of cracks was investigated. However, the main conclusions regarding the relationships of the appearance and of the growth of cracks in crystals were arrived at by Stepanov on the basis of indirect experiments[8-10], and the data of direct observations are cited by him only in one investigation[4], and these are limited to a small number of experiments. On the basis of his investigations, Stepanov arrives at definite conclusions regarding the relationship between the appearance of cracks and shear-origination, stating that the formation of shear facilitates the origination of cracks. The effect of plastic deformation on the development of an already initiated origin of a crack hardly received any attention in these investigations. In the present investigation we are continuing the studies of Stepanov on the phenomena of the breakdown of NaCl monocrystals by direct observations of the origination and growth of cracks. Observations of shear-origination were also carried out simultaneously. The results of the latter observations will be published in another paper.

The growth of cracks was observed on specimens subjected to a gradually increasing stretching tension. The direct observation of the stretched specimens under a microscope in polarized light using crossed polaroids was later replaced by microcinematography under the same conditions. The specimens studied were of rectangular cross section having an area of 15-30 mm^2 and a length of 40-50 mm, and were spalled along the cleavage planes from natural crystals of rock salt of the Artemov region.

All the specimens studied were subjected to an initial anneal, which was carried out in accordance with the following schedule: first the specimens were heated gradually for two hours in a muffle furnace up to a temperature of 600° C. They were maintained at this temperature for 2-2½ hours, then gradually cooled for 4-5 hours, down to a temperature of 200° C. After this the furnace was disconnected. As a result of such an anneal, the primary shear bands (present in the nonannealed specimens and clearly visible with crossed polaroids) disappeared or became hardly noticeable. The annealed specimens were washed with water so as to remove the surface defects as much as possible.

Copper foil terminals were glued with BF-2 glue to the ends of the specimens. These terminals were used to secure the specimens to the ends of a self-centered suspension device. As shown by our experiment, such a simple device of attaching the terminals was found to be very reliable and

---

[1] A. V. Stepanov, J. Exper. Theoret. Phys. USSR 17, 606 (1947).

[2] A. V. Stepanov, J. Exper. Theoret. Phys. USSR 18, 741 (1948).

[3] A. V. Stepanov and E. A. Mil'kamanovich, J. Exper. Theoret. Phys. USSR 18, 773 (1948).

[4] A. V. Stepanov, J. Exper. Theoret. Phys. USSR 18, 776 (1948).

[5] A. V. Stepanov and E. A. Mil'kamanovich, J. Exper. Theoret. Phys. USSR 21, 401 (1951).

[6] A. V. Stepanov and E. A. Mil'kamanovich, J. Exper. Theoret. Phys. USSR 21, 409 (1951).

[7] A. V. Stepanov, Izv. Akad. Nauk SSSR, Ser. Fiz. 17, 342 (1953).

[8] A. V. Stepanov, J. Exper. Theoret. Phys. USSR 7, 1168 (1937).

[9] A. V. Stepanov, J. Exper. Theoret. Phys. USSR 7, 663 (1937)

[10] A. V. Stepanov, Izv. Akad. Nauk SSSR, Otd. Matem. estest. nauk 6, 797 (1937).

can be recommended for use not only with NaCl crystals, but also with crystals of other substances.

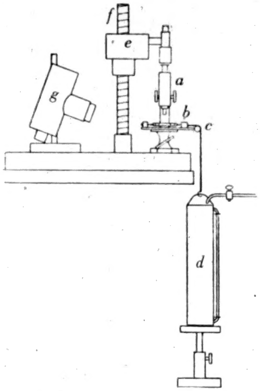

FIG. 1. Diagram of the apparatus for the microcinematography of the process of shear origination and breakdown in monocrystals.

A special apparatus was set up for the microfilming of the growth of cracks (Fig. 1). A heavy brass frame *b*, having two adapters (stationary and movable), was fastened to the table of the microscope. The terminals, glued to the specimens under investigation, were attached to this frame, and the movable adapter was connected to a copper truss spanned over the clock *c*. A high cylindrical vessel *d*, filled with water slowly flowing out through a syphon, was suspended from a hook which was attached to the end of the truss. A communicating vertical tube was attached to the vessel, making it possible to take readings of the quantity of water poured into the vessel by the scale marked on it. A 16 mm cine-camera *e*, which was attached to the vertical column *f*, was installed under the microscope. A projection lamp *g* of 300 W with a condenser was used as the light source.

Owing to the comparative slowness of the processes under study, the photographig was slow. For the automatic control of the photographing, a so-called *Zeitraffer** was developed--it is an instrument which makes it possible to regulate and maintain a constant frequency during photographing. The *Zeitraffer* made it possible, when necessary, to change over quickly from one frequency of photographing to another, and it also ensured the automatic switching on of the projector a definite time before the photographing of each frame, and switching off after the picture was taken, when the time interval between frames was fairly long.

In the majority of experiments the photography was carried out within the time intervals of 8 seconds. The rate of loading was of the order of 5 gm/mm^2 per minute, varying (within small limits) from experiment to experiment, and even during the experiment. In several of the experiments, the further loading was stopped after attaining a definite tension and continuous photographing was carried out at constant tension. In these cases the time intervals between the frames was increased to 15 minutes and longer. Noting down from time to time the value of the load and the corresponding number of the frame during the experiment, it was possible later, when analyzing the film obtained, to establish which of the processes originate or develop for the particular loads.

In order to facilitate the origination of cracks, scratches perpendicular to the length of the ribs of the specimen were made (prior to the experiment) on two adjacent faces of each specimen with the aid of a Martens sclerometer. Later the scratches were made not with a sclerometer, which produces a plastic line with smooth straight edges, but with a thin sharp needle producing a frangible line with broken edges. Such a line gave rise to more microdefects from which the breakdown of the specimen could originate.

The specimen was fastened into adapters in a position such that one of its side faces was perpendicular to the optical axis of the microscope. The crossed polaroids (one of which was fastened on the table and the other on the object of the microscope) were installed in a manner such that the vibrations which pass through them were parallel, and perpendicular to the axis of the specimen. With such a position of the polaroids, the axis of the optical indicatrix, produced by the stretching, was parallel to the direction of the vibrations in one of the polaroids and, therefore, the stretched specimen remained opaque in the crossed polaroids. On the dark background of the specimen, the end of each crack is always clearly visible owing to the presence around it of overstrain, which produces local translucencies in the form of two or four light beams issuing from the end of the crack (Fig. 2*a*).

In addition to the cracks, there are also clearly visible on the dark background of the specimen the

---

* The apparatus was developed and constructed at our request by V. G. Govorkov to whom the authors express their gratitude.

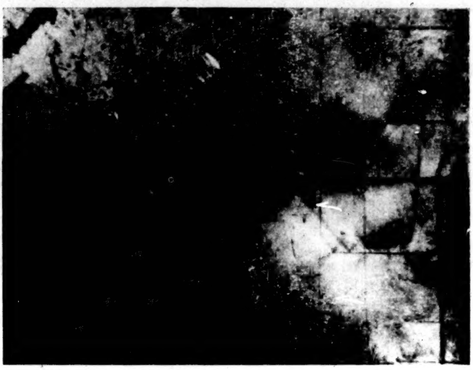

a

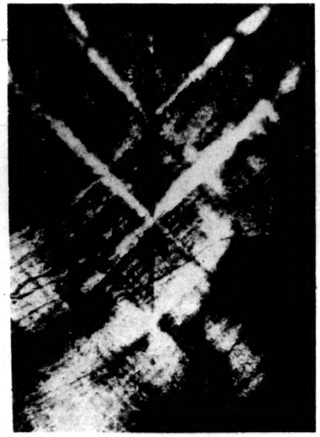

b

FIG. 2. Microphotographs of cracks in NaCl crystals (crossed polaroids): *a* – cracks originated during the stretching of the specimen; *b* – a crack spreading along the cleavage plane during the spalling of the specimen. Magnification × 22.

light shearing bands produced along the planes (110), in which the stresses are no longer orientated along the axis of the specimen, but approximately along the shears. The most intense shear bands emanate from the trace of the scratch. It should be noted that the observations of the shear bands in two directions, perpendicular to two adjacent faces of the specimen, show that frequent, intensely developed shear bands can be observed at sufficient tension only in one of these directions, while in the other one can see only relatively rare single traces of slipping.

Observation of the growth of cracks and the microcinematography of this process were hindered by the condition that the growth of cracks, as a rule, does not start from the scratch. Therefore, even in the cases when the scratch was made with a needle instead of the sclerometer, it was not possible to predict where the origins of the cracks will appear, and which of these will prove to be the most dangerous and will lead to the breakdown of the specimen. Only in the last experiments we found a method of initiating origins of cracks artificially by pressing lightly with a sharp razor blade on the rib of the specimen. When this is done, a small crack is produced at the rib itself, which, at sufficient load, begins to grow, extending into the interior of the specimen and finally leading to its breakdown. However, this method was only slightly used in our experiments, since by the time we discovered it, all the main experiments on the study of the development of cracks, designated for this investigation, had already been carried out.

The breakdown of the specimens occurred mainly at tensions of ~ 200 gm/mm^2 (varying within the limits 175 to 285 gm/mm^2). The growth of the crack, leading to the breakdown of the specimen, always begins at the rib, apparently from some microdefect which was not removed by the washing of the specimen. The cracks begin to grow noticeably at tensions of 140 to 185 gm/mm^2. In some of the experiments, the specimens studied were maintained for 24 hours and longer under a constant load. Moreover, no further growth was observed in the cracks which were sufficiently well developed.

As was stated, under our experimental conditions the breakdown almost never occurred along the scratches made on the surface of the specimen. Of the 24 specimens studied at a gradually increasing load, only three broke down along the scratches, and two of these did not break down along the scratches from which the most intensely developed shears issued. Only one of the specimens broke down along the scratch with intense shears, similar to the case described by Stepanov[4]; moreover, this breakdown occurred at the instant when the apparatus received a strong knock. All our experiments showed that the crack, having originated at the rib of the specimen, does not spread uniformly in all the directions, but at first always proceeds as a narrow band along that face of the specimen which is located in the zone of intense shears. The growth of the crack, moreover, proceeds intermittently and is visible to the eye when the specimen is observed under the microscope. Wherever there is a halt in the growth of the crack a pair of crossed shears is produced along both planes of sliding at the end of the crack. These shears form a row of small squares by crossing each other. The common diagonal of the squares is the crack (Fig. 2 *a*); in some cases the squares are almost of the same dimensions, in others they gradually decrease.

A similar picture is observed also in the cases when the crack results from causes other than of stretching the specimen. In Fig. 2 *b*, for example, one of the specimens is shown which has a crack produced along the cleavage plane during a longitudinal spalling of the specimen (by knocking along the scalpel); the crack in this case did not reach the end of the specimen.

Such an intermittent development of the crack may be observed when we analyze the surface of rupture of the specimen, which has a definite relief showing the history of the process of propagation of the crack during breakdown. The subsequent positions of the edge of the crack are visible on the surface of rupture in the form of a number of concentric contours. These contours are crossed by a system of lines indicating the directions of the propagation of cracks in all the sections of the surface.

The picture observed on the surface of rupture makes it possible to subdivide it into two parts. In Fig. 3, the first section of the surface of rupture is shown on a slightly enlarged scale (this occupies a relatively small portion of the surface of rupture). The growth of the crack in this stage of the breakdown proceeded mainly along the edge of the specimen in a direction shown by the arrow *A* in Fig. 3. The development of the crack in a direction perpendicular to the arrow proceeded much slower.

In Fig. 3 *b*, a general picture of the surface of rupture is given, from which it is evident that, after overcoming a certain "barrier", the crack begins to propagate only in the direction perpendicular to the initial direction (shown by arrow *B*);

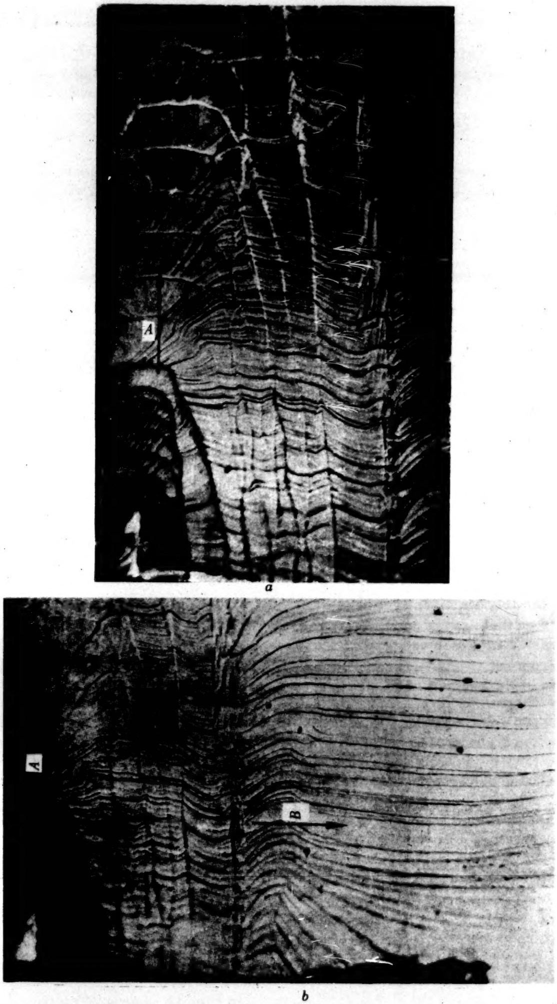

FIG. 3. Microphotograph of the surface of rupture of the NaCl crystal. The relief of the surface shows that the crack, having started from the angle of the specimen, had spread mainly along one side of the specimen (*A*), and only after having traversed the whole of the specimen, it began to grow in a perpendicular direction (*B*). *a* – magnification × 30; *b* – magnification × 20.

in this second section of the surface of rupture we no longer observe transverse contours, indicating the existence of halts in the development of the crack.

Frequently, during the loading, a row of cracks is produced simultaneously on the specimens. These cracks can be observed through a microscope, as well as by the naked eye in reflected light. In the latter case the cracks are clearly visible as light bands proceeding, as a rule, either along one of the faces, or along the two opposite faces of the specimen (Fig. 4). The plane of the cracks is perpendicular to the ribs of the specimen. Generally, as soon as one of such cracks approaches the opposite edge of the specimen, its total breakdown occurs in a very brief interval of time. During this time the crack no longer develops in a direction perpendicular to its initial direction of propagation.

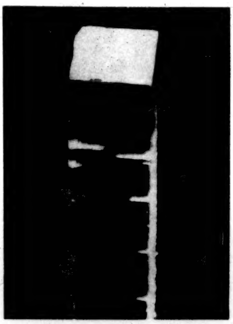

FIG. 4. A view of the cracks in reflected light. It can be observed that the cracks develop in the form of bands only along the two opposite faces.

It is of interest to note that in the microphotographs of the cracks during the initial stage of their development it is clearly evident that the width of the crack increases noticeably from its end towards the beginning (Fig. 5). Therefore, the crack does not have an elliptical cross section, as was assumed by some investigators (such an assumption was introduced, for example, by Griffiths for the simplification of the mathematical calculations), but it has a wedge-like form (as was assumed by Frenkel'[11]).

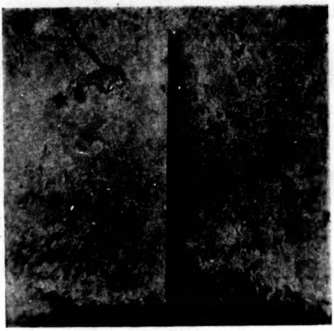

FIG. 5. Microphotograph of a crack developing from the angle of the specimen. The wedge-like appearance of the crack can be observed. Magnification × 30.

Thus, from the observations described above, it follows that during the initial stage of growth, the crack spreads easily in a direction parallel to the planes of strongly developed shear, but it crosses them with difficulty. In some of the specimens one can see clearly that the further growth of the crack is hindered by the intense shear against which the end of the crack thrusts (Fig. 6). Also, in agreement with this is the fact noted above, that the cracks do not originate from the scratches accompanied by intensely developed shears, and originate rarely from the scratches with weak shears, irrespective of the fact that the scratch is undoubtedly accompanied by microdefects, which facilitate the origination of cracks. The growth of a crack may begin from the scratch only in the case when the microdefects necessary for the origin of the crack, with the exception of the microdefects produced by the deposition of the scratch, are removed from the surface of the specimen by careful washing. Since the scratch itself cannot prevent the development of a crack, it is possible to assume that its growth is prevented by the intensely developed shears, always proceeding from the scratch.

One may suppose that the growth of cracks is prevented, on the one hand, by a dislocation in the homogeneity of the crystalline lattice and, on the other hand, by the presence of compression stresses in the vicinity of the sliding surfaces. The regions of the shear bands having stretching stresses apparently should not prevent the de-

---

[11] Ia. I. Frenkel', Zh. Tekhn. Fiz. 22, 1857 (1952).

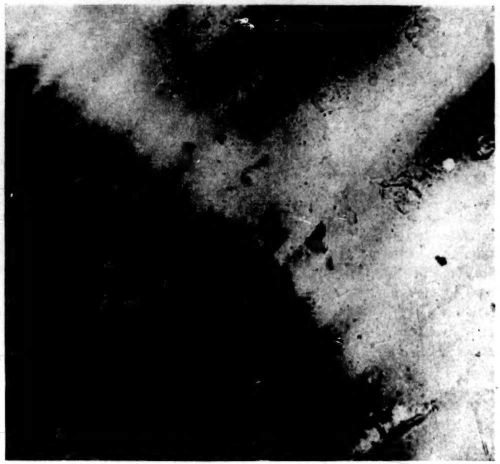

FIG. 6. Microphotograph of a crack stopped at the line of shear (crossed polaroids).

velopment of cracks.

From the above one can assume that the plastic deformation of the NaCl crystal leads to its localized strengthening, which prevents the development of cracks. If this assumption is true, then one may consider that the process of shear origination does not prepare the breakdown of the NaCl crystal and does not facilitate it, as it was supposed earlier, but, on the contrary, hinders it. Plastic deformation, apparently, only accompanies the breakdown of the crystal, having been produced by the same causes, that is, by the action of tensions and by the presence of microdefects. Of course, the processes of shear origination always precede the breakdown of the crystal, but this is dependent only on the fact that these proceed at lower tensions than the breakdown; otherwise, they could not take place at all.

In the light of the above, one can explain the fact of the strengthening of the NaCl crystals, which have undergone plastic deformation when stretched in water, expressly as the result of the hindrance of the growth of cracks by the shears. This excludes the second of the two explanations of this fact proposed by Klassen-Nekhliudova[12], which is based completely on the ideas of Stepanov.

The investigation carried out shows that direct observation of the origination and growth of cracks in crystals can provide additional new material, substantiating or disproving the conclusions drawn indirectly from the experiments on the determination of the strength of crystals. Further work in this direction and, in particular, the obtaining of quantitative data on the kinetics of the growth of cracks in crystals, are highly desirable. The conclusions of Stepanov regarding the effect of plastic deformation on the appearance of origins of breakdown (but not on the growth of cracks) should also be substantiated by direct experiments.

In conclusion, the authors express their gratitude to Professor Klassen-Nekhliudova for valuable suggestions and discussion of this work.

Translated by E. Rabkin
276

---

[12] M. V. Klassen-Nekhliudova, J. Exper. Theoret. Phys. USSR 6, 584 (1936).

SOVIET PHYSICS JETP VOLUME 2, NUMBER 4 JULY, 1956

Method of Determination of Parameters of Ferromagnetic Resonance from Experimental Data

A. I. PIL'SHCHIKOV
Moscow State University

(Submitted to JETP editor June 23, 1954)
J. Exper. Theoret. Phys. USSR **29**, 798-807 (December, 1955)

A calculation of the conditions for the extrema of the magnetic permeabilities in the region of ferromagnetic resonance is carried out. On the basis of the results obtained, formulas are derived for the determination of the gyromagnetic ratio and the relaxation time from experimental data. In the proposed method the calculation of the parameters of ferromagnetic resonance is carried out for fields of magnitudes corresponding to extrema of the magnetic permeabilities. Consequently, the necessity of calculating the maximum value of the magnetic permeability μ_k (or ρ'), which is the source of a large error (greater than 25%) in the determination of the relaxation time, disappears. It is shown that the method of calculation of g and T for fields of the extrema is applicable in cases where it is impossible to calculate the maximum values of the permeability μ_k (or ρ').

1. INTRODUCTION

THE phenomenon of ferromagnetic resonance was discovered and first studied in 1911-1913 by Arkad'ev[1,2]. While investigating the behavior of iron and nickel in high frequency electromagnetic fields (of wavelengths from 1.7 to 73 cm) he discovered, in the wavelength region from 2-6 cm, a band of dispersion of the magnetic permeability and maximum absorption of electromagnetic energy. He explained the results which he obtained as consequences of the resonance of elementary magnetic dipoles.

In these works Arkad'ev first introduced the complex magnetic permeability of the material

$$\mu' = \mu - i\rho'$$

and showed that as the frequency of the external magnetic field is changed under given conditions, there must exist a band of dispersion of μ and a maximum in ρ'.

Dorfman[3] was the first to explain the phenomenon of ferromagnetic resonance on the basis of quantum mechanics, while Landau and Lifshitz[4] carried out a theoretical calculation of the magnetic permeability of a single crystal for alternating fields without hysteresis. Starting from contemporary ideas of magnetic structure and processes of ferromagnetic magnetization, they obtained formulas determining the dependence of the real and imaginary parts of the complex magnetic permeability of the material on the frequency of the external field. It was shown in this work that for definite frequencies of the external field there must exist a resonance absorption of electromagnetic energy and a dispersion of the magnetic permeability. Frenkel'[5], in a quantum calculation of the resonance absorption in paramagnetics, also considered the question of the quantum treatment of ferromagnetic resonance.

Further theoretical works[6-8] developed the basic ideas of Arkad'ev, Landau and Lifshitz. In these works studies were made of the effect of the finite dimensions of the sample (demagnetizing field), the magnetic crystallographic anisotropy of a ferromagnetic, and eddy currents on the phenomenon of ferromagnetic resonance. In the works of Kittel[6] and Bloembergen[8], a calculation of the high-frequency magnetic permeability is carried out for the case of a homogeneously magnetized single crystal under the action of a weak alternating magnetic field. In this calculation no account is taken of hysteresis nor of possible inhomogeneous conditions for the various parts of the ferromagnetic.

---

[1] V. K. Arkad'ev, Zh. Russ. Fiz. Obschestva **44**, 165 (1912).

[2] V. K. Arkad'ev, Zh. Russ. Fiz.-Hhim. Obschestva, ch. fiz. **45**, 302 (1913).

[3] J. Dorfman, Z. Physik **17**, 98 (1923).

[4] L. D. Landau and E. M. Lifshitz, Physik. Z. Sowjetunion **8**, 153 (1935).

[5] Ia. I. Frenkel', J. Exper. Theoret. Phys. USSR **15**, 8 (1945).

[6] C. Kittel, Phys. Rev. **70**, 281 (1946); **73**, 155 (1948).

[7] J. H. Van Vleck, Phys. Rev. **78**, 266 (1950); Physica **17**, 234 (1951).

[8] N. Bloembergen, Phys. Rev. **78**, 572 (1950).

However, the formulas obtained by these authors for the magnetic permeability seem at present to be quite correct and give satisfactory agreement with experimental results. According to reference 8, the dependence of the real and imaginary parts of the complex magnetic permeability of the substance on the constant magnetic field and on the frequency of the alternating magnetic field, with account being taken of the relaxation time, may be written (for a polycrystal) in the form:

$$\mu = \frac{\omega_1^2(\omega_0^2-\omega^2)}{(\omega_0^2-\omega^2)^2+(4\omega^2/T^2)}+1, \tag{1}$$

$$\rho' = \frac{\omega_1^2(2\omega/T)}{(\omega_0^2-\omega^2)^2+(4\omega^2/T^2)}, \tag{2}$$

where

$$\omega_0^2 = \gamma^2[H+(N_y-N_z)I_s] \times [H+(N_x-N_z)I_s]+T^{-2}, \tag{3}$$

$$\omega_1^2 = 4\pi\gamma^2 I_s[H+(N_y-N_z)I_s]. \tag{4}$$

N_x, N_y, N_z are the demagnetizing factors along the corresponding axes, I_s is the saturation magnetization of the sample, T is the transverse relaxation time, ω is the angular frequency of the alternating magnetic field, H is the external constant magnetic field, $\gamma = eg/2mc$ is the gyromagnetic ratio for the electron, g is the Landé splitting factor. It is supposed here that the constant magnetic field is directed along the Z axis and the high-frequency magnetic field along the X axis. The effective magnetic permeabilities as given by the coefficient of absorption μ_k and the index of refraction μ_n, are connected with the magnetic permeabilities of the substance by the relations[9]:

$$\mu_k = \sqrt{\mu^2+\rho'^2}+\rho', \tag{5}$$

$$\mu_n = \sqrt{\mu^2+\rho'^2}-\rho'. \tag{6}$$

Ferromagnetic resonance under conditions of a simultaneous constant magnetic field and a high-frequency magnetic field perpendicular to it, both acting on the ferromagnetic, has been studied in many experimental works[10-16]. In these experiments the frequency of the alternating magnetic field was fixed and the constant magnetic field was changed. The results of the experiments with polycrystalline samples and single crystals, with metals and polyconductor (ferrite) ferromagnetics, basically confirmed the theoretical calculations and made it possible to establish the fact that the splitting factor g determined from experiments on ferromagnetic resonance is, in the overwhelming majority of cases, greater than two. The value of the magnetomechanical factor determined from gyromagnetic experiments, g', is always less than 2. Kittel[17], and subsequently Van Vleck[7], gave an explanation of this discrepancy depending on the spin-orbit interaction. However, their formula $g-2=2-g'$ is not confirmed by the experimental results: it turns out that in the majority of cases $g-2>2-g'$.

One of the most essential questions of the theory of ferromagnetic resonance is the question of the width of the absorption curve. The theoretical calculations give a result smaller than that obtained from the experimental data. In connection with this it should be noted that the above indicated discrepancies between the experimental and theoretical results should not be considered as due solely to the imperfections of the theory. It is also necessary to give attention both to the more exact development of the actual methods used in the measurements and to the development and substantiation of methods of determining the parameters of ferromagnetic resonance (g, T) from the experimental data.

In the determination of the splitting factor g it is customary under the condition of maximum absorption of electromagnetic energy to neglect the term containing the relaxation time[3]. This neglect could be considered legitimate if there were obtained from the experimental data at least an estimate of the relaxation time. However, the methods of determining the relaxation time are very often either insufficiently substantiated or involve large errors. The relaxation time is often determined by making use of the approximate relation $\mu_{k\,\max} = 2\rho'_{\max}$, from which it follows that:

---

[9] V. K. Arkad'ev, *Electromagnetic Processes in Metals*, vol. II, Energoizdat, Moscow, 1936.

[10] E. K. Zavoiskii, J. Exper. Theoret. Phys. USSR 17, 883 (1947).

[11] W. A. Jager and R. M. Bozorth, Phys. Rev. 72, 80 (1947).

[12] A. F. Kip and R. D. Arnold, Phys. Rev. 75, 1556 (1949).

[13] V. N. Lazukin, Izv. Akad. Nauk SSSR, Ser. Fiz. 16, 510 (1952).

[14] I. A. Shekhtman, Izv. Akad. Nauk SSSR, Ser. Fiz. 16, 498 (1952).

[15] W. A. Yager, Phys. Rev. 75, 316 (1949).

[16] W. A. Yager and F. R. Merritt, Phys. Rev. 75, 318 (1949).

[17] C. Kittel, Phys. Rev. 76, 743 (1949).

$$1/T = \omega_1^2/\omega\mu_{k\,\max}.$$

A calculation of $\mu_{k\,\max}$ is essential for this method of determining the relaxation time. Such a calculation involves a large error, and under certain experimental conditions it is impossible to carry it out. Thus, for example, in the case where the measurement is carried out with the help of a cavity resonator, it is necessary to calculate its quality factor Q_0, which is determined only from the losses in the ferromagnetic walls[8]. A calculation of the quality factor can be carried out for resonators of simple form, but cannot be carried out for resonators of complicated form, since the structure of the high-frequency field in the cavity of the resonator is very inexactly known. Consequently, this method of determining the relaxation time cannot be applied with resonators of complicated form. In those cases where the calculation may be carried out, it gives too large a value Q_0, since, on account of irregularities and scratches commensurate with the depth of penetration of the field into the metal, the operating surface of the wall is greater than that obtained by calculation. Bloembergen[8] estimates that the error in the calculation of Q_0 does not exceed 10%, but he does not substantiate his estimate.

A comparison of the experimental and theoretical calues of the quality factor[18] shows that the indicated discrepancy is significantly larger than 10%, increases with increasing frequency and depends very strongly on the treatment of the wall surfaces. This latter fact makes the estimation of the error in such a calculation difficult. Even with an error of 10% in Q_0, the error in the calculation of $\mu_{k\,\max}$ reaches 25%. However, it is significantly larger, since Q_0 is calculated with an error of more than 10%, especially in the wavelength region $\lambda < 3$ cm.

In order to calculate $\mu_{k\,\max}$ one must know μ_k for some value of the external magnetic field. It is customary to take $\mu_k' = 1$ for magnetic fields in which suppression of ferromagnetic resonance occurs. Such a choice of μ_k imposes definite requirements on the manner of conduction of the experiment, since a suppression of the resonance must necessarily be obtained, that is, one must necessarily use a constant magnetic field significantly exceeding the resonance field. This requirement complicates the experiment and very often is not fulfilled even with the use of comparatively strong fields (curves for nickel and supermalloy[8] for a frequency of 9030 *mc* and for supermalloy[11,15,16] for a frequency of 24,000 *mc*). Bloembergen[8], in a calculation of the relaxation time for frequencies of the order of 24,000 *mc* (nickel and supermalloy), uses the value of μ_k for $H = 0$. The choice of this value ($\mu_k' = 0.8-0.9$ was taken in reference 8) was determined by the condition of the best coincidence of the experimental and theoretical curves in the region of minimum absorption. This manner of computing the relaxation time, based on the selection of a value of μ_k, is not completely convincing.

In connection with the fact that at the present time theoretical and experimental works are directed toward the detailed study of the phenomena of ferromagnetic resonance and the obtaining of qualitative results, there arises the necessity of developing such methods of measurement and of treatment of experimental data as will guarantee increased accuracy in the determination of the parameters of ferromagnetic resonance. Hence the aim of the present work is the analysis of the dependence of the magnetic permeabilities in the region of ferromagnetic resonance on the constant magnetic field and the determination of the conditions under which maxima and minima in the magnetic permeabilities of the substance (μ, ρ') and in the effective magnetic permeabilities (μ_n, μ_k) will occur. On the basis of the obtained conditions on the extrema, methods are found for determining the splitting factor and the relaxation time from the experimental data (absorption curve and dispersion curve). Theoretical curves giving the dependence of μ, ρ', μ_n and μ_k on the constant magnetic field H are given in the Figure.

The region of maximum absorption (maximum ρ' or μ_k) and the region of dispersion (minimum and maximum μ or maxima in μ_n) are investigated in the overwhelming majority of the experimental works. The structure of the expression and the course of the curves for μ and ρ' and for μ_n and μ_k

---

[18] F. Horner et. al., J. Inst. Elec. Engrs. (London) 93, 21 (1946).

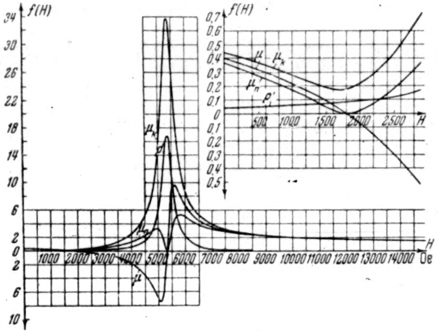

Theoretical dependence of the magnetic susceptibilities during ferromagnetic resonance. $\omega = 15.3 \times 10^{10} mc$, $4\pi I_0 = 6000$ gauss, $N_x = N_z = 0$, $g = 2.24$, $1/T = 5 \times 10^9$ sec^{-1}.

in the Figure are close to the formulas and the course of the curves for dispersion and absorption in optics. Consequently, we may surmise that the difference in the fields corresponding to the maximum and minimum $\mu(H)$ and the difference in the fields corresponding to the maxima in $\mu_n(H)$ are determined by the relaxation time.

In the investigation of ferromagnetic resonance the experimental data are obtained in the form of the dependences on the magnetic field of magnitudes proportional to the square root of μ_k or ρ' (for example, the attenuation of a cavity resonator with a ferromagnetic wall) and the square root of μ_n or μ (the resonance frequency of such a resonator). The positions of the extrema of these quantities will coincide with the extrema of the corresponding magnetic permeability. Hence, in order to determine the parameters of ferromagnetic resonance (γ, g, T) it is necessary to find the conditions for extrema in $\mu(H)$, $\rho'(H)$, $\mu_n(H)$ and $\mu_k(H)$.

Before beginning the determination of the conditions for the extrema, we note the following special feature of the calculations which are to be carried out: all the conditions for the extrema are obtained as approximations, an evaulation of the accuracy of which is carried out, proceeding from the magnitudes of the quantities characteristic of samples made from metallic ferromagnetics in the form of plates for the wavelength region above 1 cm. For the evaluation, we take the following values of the quantities: field corresponding to maximum absorption $H_0 = 10^3$ oersteds; $N_x = N_z = 0$ (small in comparison with N_y); $4\pi I_s = 10^4$ gauss; $\omega^2 = 10^{20}$ sec^{-2}; $\gamma^2 = 3 \times 10^4$ oersteds^{-2} sec^{-2}; $T^{-2} = 10^{20}$ sec^{-2}; $\omega_1^2 = 10^{22}$ sec^{-2}.

2. CONDITION FOR MAXIMUM $\rho'(H)$

The condition for an extremum in $\rho'(H)$ can be reduced to a second degree equation relating to the quantity $\alpha = \omega_0^2 - \omega^2$. Making use of an evaluation of the quantities entering into this equation, we obtain the following approximate magnitudes of the roots:

$$\alpha_1 = \frac{2\omega^2}{T^2\omega_1^2}, \quad \alpha_2 = 2\omega_1^2. \tag{7}$$

The first root gives the condition for maximum ρ',

$$\omega_0^2 = \omega^2\left(1 + \frac{2}{T^2\omega_1^2}\right),$$

or, with an exactitude of the order of 2%, $\omega_0 = \omega$. This equation determines the field $H_{0\rho'}$ corresponding to the maximum value of $\rho'(H)$.

The second root determines a field of order $8\pi I_s$, and for it this estimate of magnitude is incorrect.

3. CONDITIONS FOR EXTREMA IN $\mu(H)$

The condition for an extremum in $\mu(H)$ can be written in the form:

$$\alpha^3-\beta\alpha^2+\alpha+\beta=0,$$

where

$$\omega_0^2-\omega^2=(2\omega/T)\alpha,\quad \beta=\omega_1^2T/2\omega.$$

Using the ordinary method of solving cubic equations[19] we obtain approximate expressions for the roots, neglecting terms of order $1/\beta^2 \ll 1$,

$$\alpha_1=-1+\beta^{-1},\quad \alpha_2=1+\beta^{-1},\quad \alpha_3=\beta.$$

Then the conditions for the extrema of $\mu(H)$ can be written in the form

$$\omega_{01\mu}^2-\omega^2=-\frac{2\omega}{T}\left(1-\frac{2\omega}{T\omega_{11\mu}^2}\right); \tag{8}$$

$$\omega_{02\mu}^2-\omega^2=\frac{2\omega}{T}\left(1+\frac{2\omega}{T\omega_{12\mu}^2}\right), \tag{9}$$

where

$$\omega_{01\mu}^2=\omega_0^2(H_{1\mu}),\qquad \omega_{02\mu}^2=\omega_0^2(H_{2\mu}),$$

$$\omega_{11\mu}^2=\omega_1^2(H_{1\mu}),\qquad \omega_{12\mu}^2=\omega_1^2(H_{2\mu}),$$

$H_{1\mu}$ and $H_{2\mu}$ are the values of the constant magnetic field which correspond to the minimum and maximum values of $\mu(H)$. The root α_3 gives a condition analogous to (7).

4. CONDITIONS FOR MAXIMUM $\mu_k(H)$

The determination of the conditions for maximum $\mu_k(H)$ leads to the necessity of solving an algebraic equation of higher than the fourth degree. Consequently, in the solution of this equation it is necessary to use approximate methods, taking into account the character of the behavior of the functions $\mu(H)$ and $\rho'(H)$. In the region of maximum $\rho'(H)$ the values of $\mu(H)$ are near unity and are small in comparison with the values of $\rho'(H)$ in this region. Hence we may suppose that the conditions for maxima in $\mu_k(H)$ and $\rho'(H)$ are near each other. Starting from this, the condition for maximum $\mu_k(H)$ can be written in the form: $\omega_0^2=\omega^2(1+\alpha)$, assuming that $\alpha \ll 1$. The equation $d\mu_k/dH=0$ leads to a linear equation in α, and, on evaluating the quantities entering into it, we obtain:

$$\alpha=4/3\omega^2T^2.$$

Consequently, the condition for maximum $\mu_k(H)$ will be:

$$\omega_{0k}^2=\omega^2\left(1+\frac{4}{3\omega_{1k}^2T^2}\right),\quad \omega_{1k}^2=\omega_1(H_{k0}) \tag{10}$$

This equation determines the constant magnetic field H_{0k} for which maximum $\mu_k(H)$ occurs, that is, maximum absorption of the energy of the high-frequency field in the case where the penetration depth is less than the thickness of the sample. In accordance with the accepted evaluation of the quantities involved, we may write, with an accuracy of 1-2%, $\omega_{0k}=\omega$. If we use the values of the quantities which were assumed for this evaluation, then $H_{0\rho'}-H_{0k}\approx 1$ oersted, that is, the difference in the fields corresponding to the maximum values of μ_k and ρ' lie within the limits of the error in the measurement of the field.

5. CONDITION FOR MAXIMA IN $\mu_n(H)$

An analysis of the equation $d\mu_n/dH=0$ shows that it becomes considerably simpler and can be solved exactly if we assume

$$\frac{d\omega_1^2}{dH}=0;\quad \mu=\frac{\omega_1^2(\omega_0^2-\omega^2)}{(\omega_0^2-\omega^2)^2+(4\omega^2/T^2)}. \tag{11}$$

We can substantiate the first simplifying condition to a certain extent by the fact that the basic course of the dependence of the magnetic permeability on the constant magnetic field is determined mainly by the field entering into ω_0^2. The second condition receives some confirmation from the fact that the calculation is carried out for a region of field near the region of maximum absolute values of μ, which are determined by the first component in (1). The considerations introduced make it possible to suppose that the conditions for extrema in $\mu_n(H)$ found on the basis of the simplifying assumptions will be near the conditions for the extrema which are obtained if we take account of the exact expression for μ and the dependence of ω_1^2 on the field. Solving the equation $d\mu_n/dH = 0$ while taking account of (11), we obtain the following conditions for the extrema:

---

[19] L. Ia. Okunev, *Higher Algebra*, Gostekhizdat, 1949.

$$\omega_{01}^2 - \omega^2 = -2\sqrt{3}\,\omega/T, \tag{12}$$

$$\omega_{02}^2 - \omega^2 = 2\sqrt{3}\,\omega/T.$$

If we now take account of the dependence of ω_1^2 on H and the exact expression for μ in the form (1), then the solution of the equation $d\mu_n/dH = 0$ in the region of fields $H > H_{0k}$ can be sought in the form:

$$\omega_0^2 - \omega^2 = (2\sqrt{3}\,\omega/T)(1 + \alpha),$$

assuming $\alpha \ll 1$. The equation $d\mu_n/dH = 0$ can be reduced to a linear equation in α (neglecting terms of order α^2 and higher in comparison with unity), and we then obtain

$$\alpha = \frac{8\sqrt{3}}{3}\,\frac{\omega}{T\omega_1^2}. \tag{13}$$

For the assumed estimate of magnitudes, $\alpha = 0.05$. The problem of the extrema in the region of fields $H < H_{0k}$ is solved analogously. As a result of these calculations, we obtain the conditions for the first and second maxima of $\mu_n(H)$ in the form:

$$\omega_{01n}^2 - \omega^2 = -\frac{2\sqrt{3}\,\omega}{T}\left(1 - \frac{8\sqrt{3}}{3}\,\frac{\omega}{T\omega_{11n}^2}\right), \tag{14}$$

$$\omega_{02n}^2 - \omega^2 = \frac{2\sqrt{3}\,\omega}{T}\left(1 + \frac{8\sqrt{3}}{3}\,\frac{\omega}{T\omega_{12n}^2}\right) \tag{15}$$

where

$$\omega_{01n}^2 = \omega_0^2(H_{1n}), \qquad \omega_{02n}^2 = \omega_0^2(H_{2n}),$$

$$\omega_{11n}^2 = \omega_1^2(H_{1n}), \qquad \omega_{12n}^2 = \omega_1^2(H_{2n}),$$

H_{1n} and H_{2n} are the magnitudes of the constant magnetic field corresponding to the first and second maxima of $\mu_n(H)$. From the evaluation of α there follows the possibility of using Eqs. (12) and (13) as approximate conditions for the extrema in $\mu_n(H)$. The error in using these approximate conditions may be estimated from Eqs. (14) and (15).

6. METHOD OF DETERMINING THE GYROMAGNETIC RATIO AND THE RELAXATION TIME FROM EXPERIMENTAL DATA

In the investigation of ferromagnetic resonance in metallic ferromagnetics, one most frequently meets with cases in which the penetration depth is less than the thickness of the sample, and the absorption is determined by μ_k and the phase relationships by μ_n. Hence, let us consider a means of determining the parameters of ferromagnetic resonance in this case, assuming that H_{0k}, H_{1n} and H_{2n} are known from experimental results. Using Eqs. (14) and (15), we obtain

$$\omega_{02n}^2 - \omega_{01n}^2 = \frac{4\sqrt{3}\,\omega}{T}\left(1 - \frac{4\sqrt{3}\,\omega}{T}\,\frac{\omega_{12n}^2 - \omega_{11n}^2}{\omega_{12n}^2\omega_{11n}^2}\right).$$

Taking into account the evaluation of the magnitudes entering into the second member in the parantheses, and assuming $H_{2n} - H_{1n} = 5 \times 10^2$ oersteds, we obtain $\omega_{12n}^2 - \omega_{11n}^2 \approx 10^{21}$. Consequently, allowing an error of less than 0.3%, we can discard the second member in the parentheses. Then the expression for the determination of the relaxation time will be [using Eq. (3)]:

$$\frac{1}{T} = \frac{\gamma^2(H_{2n} - H_{1n})[H_{1n} + H_{2n} + (N_x + N_y - 2N_z)I_s]}{4\sqrt{3}\,\omega}. \tag{16}$$

In the determination of the relaxation time it is not always possible to use the formula obtained. Thus in the wavelength region $\lambda > 5$ cm the first maximum μ_n lies at comparatively weak fields, in which the sample is not magnetized to saturation. Hence the position of the first maximum μ_n does not correspond to the conditions considered in Sec. 5, and the magnitude of the field corresponding to this maximum cannot be used for a calculation of the relaxation time.

The experimental results in the indicated region allow the use of the field determining the maximum μ_k and the second maximum μ_n. Using Eqs. (10) and (15) and assuming $H_{2n} - H_{0k} \approx 10^2$ oersteds, we obtain the following expression for the determination of the relaxation time:

$$\frac{1}{T}=\frac{\omega_{02n}^2-\omega_{0k}^2}{2\sqrt{3}\,\omega}\left(1-\frac{22\sqrt{3}}{9}\frac{\omega}{T\omega_{12n}^2}\right). \qquad (17)$$

The second member in the parentheses ~ 0.03; consequently, discarding it, we obtain an expression for the relaxation frequency ($1/T$) increased by approximately 3%:

$$\frac{1}{T} \qquad (18)$$

$$=\frac{\gamma^2(H_{2n}-H_{0k})\,[H_{0k}+H_{2n}+(N_x+N_y-2N_z)\,I_s]}{2\sqrt{3}\,\omega}.$$

In the study of ferromagnetic resonance in the region of comparatively short waves, a fairly strong field is necessary in order to obtain the second maximum of μ_n. If the second maximum of μ_n is not obtained experimentally, then we may use the fields corresponding to the first maximum of μ_n and to the maximum μ_k. As a result of an analogous calculation we obtain:

$$\frac{1}{T}=\frac{\omega_{0k}^2-\omega_{01n}^2}{2\sqrt{3}\,\omega}\left(1+\frac{22\sqrt{3}}{9}\frac{\omega}{T\omega_{11n}^2}\right), \qquad (19)$$

or, approximately (the magnitude of $1/T$ will be decreased by 3%),

$$\frac{1}{T} \qquad (20)$$

$$=\frac{\gamma^2(H_{0k}-H_{1n})\,[H_{1n}+H_{0k}+(N_x+N_y-2N_z)\,I_s]}{2\sqrt{3}\,\omega}.$$

The formulas obtained for the calculation of the relaxation time are not of equally good accuracy. As follows from the very derivation of the formulas, the determination of the relaxation time by the two maxima in μ_n is considerably more exact. Consequently, if the conditions of the experiment allow the use of the two maxima, it is necessary to use Eq. (16). The results of the calculation of the relaxation time using Eqs. (18) and (20) can be made more exact if we introduce corrections in accordance with Eqs. (17) and (19) and calculate the first approximation for $1/T$. In the terms determining the correction, the value of $1/T$ should be taken from estimates according to Eqs. (18) and (20).

Any of the formulas (16), (18) and (20) can be written in the form

$$1/T=\gamma^2 p, \qquad (21)$$

where p is determined, depending on the extrema with respect to which the calculation of the relaxation time has been carried out, by comparison of Eq. (21) with Eqs. (16), (18) and (20).

The condition for maximum μ_k may be written in the form

$$\omega^2=\gamma^2 q+T^{-2}, \qquad (22)$$

$$q=[H_{0k}+(N_x-N_z)\,I_s] \qquad (23)$$

$$[H_{0k}+(N_y-N_z)\,I_s].$$

From Eqs. (21) and (22) we obtain a formula for the determination of the gyromagnetic ratio:

$$\gamma^2=-\frac{q}{2p^2}+\frac{1}{p}\sqrt{\frac{q^2}{4p^2}+\omega^2}. \qquad (24)$$

Formula (24) makes possible the determination of the gyromagnetic ratio from the values of the field corresponding to maxima of μ_k and μ_n, taking account of the $1/T^2$ term in expression (3) for ω_0^2. Naturally, the use of formula (24) for the calculation of the gyromagnetic ratio makes sense only in case the relaxation frequency $1/T$ is commensurate with the frequency of the electromagnetic field, ω. If $1/T\omega \ll 1$, then it is simpler to use the formula $\gamma=\omega/\sqrt{q}$.

If there exist conditions in the experiment such that the depth of penetration of the field into the ferromagnetic is considerably greater than the thickness of the sample, then the absorption is determined by ρ' and the phase relations by μ. In this case, using the conditions for extrema in ρ' and μ, and carrying out an analogous calculation, we obtain the following relationship:

$$\frac{1}{T}=\frac{\omega_{02\mu}^2-\omega_{01\mu}^2}{4\omega}\left(1+\frac{\omega}{T}\frac{\omega_{12\mu}^2-\omega_{11\mu}^2}{\omega_{12\mu}^2\,\omega_{11\mu}^2}\right).$$

If we assume that $H_{2\mu}-H_{1\mu}=3\times10^2$ oersteds, then the second member in the parentheses is of the order of 10^{-3}; consequently, allowing an error of the order of 0.1%, we may write:

$$\frac{1}{T} = \frac{\gamma^2 (H_{2\mu} - H_{1\mu}) [H_{1\mu} + H_{2\mu} + (N_x + N_y - 2N_z) I_s]}{4\omega}. \tag{25}$$

On using the maxima of μ and ρ',

$$\frac{1}{T} = \frac{\omega^2_{02\,\mu} - \omega^2_{0\rho'}}{2\omega}\left(1 - \frac{\omega}{T\omega^2_{12\,\mu}}\right),$$

or, approximately (with an error of ~ 1%),

$$\frac{1}{T} = \frac{\gamma^2 (H_{2\mu} - H_{0\rho'}) [H_{0\rho'} + H_{2\mu} + (N_x + N_y - 2N_z) I_s]}{2\omega}. \tag{26}$$

For the case of the minimum of μ and the maximum of ρ',

$$\frac{1}{T} = \frac{\omega^2_{0\rho'} - \omega^2_{01\,\mu}}{2\omega}\left(1 + \frac{\omega}{T\omega^2_{11\,\mu}}\right),$$

or, with an error of ~ 1%,

$$\frac{1}{T} = \frac{\gamma^2 (H_{0\rho'} - H_{1\mu}) [H_{1\mu} + H_{0\rho'} + (N_x + N_y - 2N_z) I_s]}{2\omega}. \tag{27}$$

The remarks concerning the accuracy of Eqs. (16), (18) and (20) and concerning the introduction of the corrections for the calculation of the first approximation for the determination of the relaxation frequency also are completely applicable to formulas (25), (26) and (27).

CONCLUSIONS

The proposed method of treating the experimental data for the determination of the parameters of ferromagnetic resonance uses, besides the usual initial data (ω, N_x, N_y, N_z, I_s), the values of the constant magnetic field which correspond to the extrema in μ_k and μ_n (or ρ' and μ). The essential advantages of this method, in comparison with the method based on the calculation of the maximum value of μ_k (or ρ') are:

1. The necessity of calculating the resonator's quality factor Q_0, which depends on the losses in the ferromagnetic walls of the resonator, disappears. This considerably broadens the possibilities in the study of ferromagnetic resonance, since resonators of complicated form, for which such a calculation is impossible, can be used. We can dispense with the rather complicated technology of soldering the sample to the wall of the resonator (see, for example, reference 8) and instead can place the sample in a suitable place in the cavity of the resonator.

In the case of resonators of simple form, the error in the calculation of Q_0 has as basic source the error in the determination of the relaxation time, which exceeds 25%. The basic error in the determination of the relaxation time by the fields of the extrema is connected with the error in the determination of the difference of the fields corresponding to the extrema, which error depends to a considerable extent on the sharpness of the extrema. The difference of these fields ordinarily consists of a few hundred oersteds and can be determined with an accuracy of not less that 5%. This guarantees a more exact result for the relaxation time.

2. In the use of the proposed method of treating the experimental data in order to determine g and T, the suppression of the resonance is not required. Consequently, in carrying out the experiment we can use a considerably smaller region of constant magnetic fields. It is sufficient that the experimental data be obtained in a region which includes the extrema of μ_n (or μ), and it is even sufficient to obtain one of these extrema and the maximum of μ_k (or ρ').

3. In case the suppression of the resonance is obtained, the use of the values of g and T obtained by the proposed method makes possible the determination of the absolute value of the magnetic permeabilities μ_n, μ_k, μ, ρ' and the estimation of the quality factor Q_0 from experimental data.

It should be noted that it is necessary, in using the method of the fields of the extrema, to obtain the absorption and dispersion curves experimentally. This complicates the experiment somewhat, but with present day technique the measurements do not present great difficulties.

The author wishes to express his gratitude to Professor S. D. Gvozdover, under whose direction the present work was carried out.

Translated by M. G. Gibbons
274

SOVIET PHYSICS JETP VOLUME 2, NUMBER 4 JULY, 1956

On the Lowering of the Luminescence Yield of Phosphors in Intense Excitation

V. V. ANTONOV-ROMANOVSKI AND L. A. VINOKUROV
P. N. Lebedev Physical Institute, Academy of Sciences, USSR

(Submitted to JETP editor July 15, 1954; after revision June 11, 1955)
J. Exper. Theoret. Phys. USSR **29**, 830-833 (1955)

It is shown that the lowering of the luminescent output of ZnS-Cu and ZnS-Cu, Co phosphors with intense excitation is conditioned to a considerable degree by the illuminating action of the exciting light and by the fact that the recombination of optical electrons or "holes" results in radiationless transitions. The same causes result in the fact that the total illumination, as determined from the curve of increasing illumination, turns out to be considerably smaller than the total illumination as determined from the curve of the extinction process.

1. INTRODUCTION

IT is known that minute quantities of impurities frequently act as extinguishers of luminescence of crystal phosphors. The ZnS-Cu phosphor with traces of the iron group elements is a classic example. In spite of the great number of published works in this field[1-11] no definite results have yet been obtained in the understanding of the mechanism of extinction by impurities in typical phosphors – i.e., in luminescent substances which exhibit the phenomenon of recombination. This is apparently due to the fact that the authors of the referenced works have not taken into consideration certain, only recently investigated phenomena in the field of luminescence [for example: the luminescent action of the exciting light and the possible difference in the effectiveness of irradiation for recombination of thermal and optical, (i.e., liberated by light) electrons][12-16].

In this work, using phosphors ZnS-Cu and ZnS-Cu, Co, we show that with high degree of excitation, these phenomena can substantially influence the magnitude of the luminescent output and determine the relation between the output and the intensity of the exciting light. By taking these phenomena into account it is possible to explain why, with excitation of high intensity, the total light output as determined from the curve of increasing luminescence turns out to be considerably smaller than the total light output determined from the curve of extinction.

2. INVESTIGATION OF THE DEPENDENCE OF LIGHT OUTPUT ON THE INTENSITY OF THE EXCITING LIGHT

In the investigation of the equilibrium luminescent output q of ZnS-Cu phosphor for different intensities E of the exciting light we have established together with Alentsev[17] that q is constant only for moderate values of E ("plateau" region); for this case $q \sim 1$. Outside the "plateau" the value of q falls both in the direction of increasing and decreasing E. The fall of q at high values of E was explained by the increase of that portion of the excitation energy which is absorbed by the localized electrons and the ionized luminescent centers (the luminescent action

---

[1] L. Levy and D. W. West, Trans. Farad. Soc. **35**, 128 (1939).

[2] N. R. Nail, D. Pearlman and F. Urbach, *Luminescent Materials, Symposium*, 1948, p. 190; J. Opt. Soc. Am. **39**, 690 (1949)

[3] S. Roberts, Science **112**, 427 (1950).

[4] C. G. Hill and H. A. Klasens, J. Electrochem. Soc. **96**, 275 (1949)

[5] J. Saddy and N. Arpiarian, Comp. rend. **230**, 1948 (1950).

[6] N. Arpiarian, Compt. rend. **233**, 387 (1951); J. phys. radium **14**, 552 (1953).

[7] N. Arpiarian and D. Curie, Compt. rend. **234**, 75 (1952).

[8] R. H. Bube, S. Larach and R. E. Schräder, Phys. Rev. **92**, 1135 (1953).

[9] H. Goberecht and W. Kunz, Z. Physik **136**, 21 (1953).

[10] F. I. Vergunas and Iu. M. Saichenko, J. Exper. Theoret. Phys. USSR **24**, 470 (1953).

[11] W. Hoogenstraaten and H. A. Klasens, J. Electrochem. Soc. **100**, 366 (1953).

[12] V. V. Antonov-Romanovskii, Izv. Akad. Nauk SSSR Ser. Fiz. **13**, 91 (1949); **15**, 637 (1951).

[13] R. Ellickson, J. Opt. Soc. Am. **36**, 264 (1946).

[14] Z. L. Morgenshtern, Dokl. Akad. Nauk SSSR **54**, 791 (1946).

[15] C. Bull and D. E. Mason, J. Opt. Soc. Am. **41**, 718 (1951).

[16] L. A. Vinokurov, Dokl. Akad. Nauk SSSR **85**, 529 (1952).

[17] M. H. Alentsev, V. V. Antonov-Romanovskii and L. A. Vinokurov, Dokl. Akad. Nauk SSSR **96**, 1133 (1954).

of the exciting light), the concentration of which increases with the increase of E. This in turn leads to an increase in the number of electrons and "holes" the recombination of which does not produce any radiation^3. The reduction of q for low values of E was explained by the accompanying increase of the role of external quenching which is a linear reaction (proportional to the concentration of the ionized centers n) while the luminescent processes are reactions of the second order (proportional to n^2).

We have conducted similar investigations of the dependence of q on E for ZnS-Cu,Co phosphors. We have measured not the quantity q itself but the intensity of equilibrium luminescence which is a quantity proportional to q.

$$I_\infty = aq. \tag{1}$$

Since the introduction of Co does not result in any change of the absorption in the region of excitation, a = constant.

The results turned out to be similar to those obtained with pure phosphors of ZnS-Cu, i.e., there is a plateau with a drop in q to the right and to the left of it. It can therefore be considered that the cause of the drop in q outside the plateau for the ZnS-Cu,Co phosphor is the same as for the ZnS-Cu phosphor. Besides the similarity, there is also a difference in that, even in the plateau region, $q \ll 1$. The reason for this general reduction in the values of the ordinates in the q vs. E curve will be discussed by us in a later paper.

In the previously mentioned work, the dependence of q on E for the ZnS-Cu phosphor was investigated at various temperatures in order to prove the correctness of the assumptions made concerning the general lowering of the value of q. As expected, it turned out that the heating results in the displacement of the plateau into the region of higher values of E. It can be shown that the same data also give certain quantitative support to these assumptions.

Indeed, the lowering of q with increase of E begins at the moment ($E = E'$), when the probability of the optical liberation of the electron (or "hole") $w_E = \alpha E$ (α = constant) becomes comparable with that of thermal liberation $w_T = w_0 \exp\{-\epsilon/kT\}$ (w_0 = const., ϵ = binding energy of the electron, k = Boltzman's constant) i.e., when

$$\alpha E' \sim w_0 e^{-\epsilon/kT} \tag{2}$$

It follows from (2) that

$$\lg \frac{E_2'}{E_1'} \approx \frac{\epsilon}{k}\left(\frac{1}{T_1} - \frac{1}{T_2}\right), \tag{3}$$

where indexes 1 and 2 refer to two different temperatures. If we make use of the data for $T_1 = 20°\mathrm{C}$ and $T_2 = 100°\mathrm{C}$ taken from the work of Alentsev et al[17], we obtain

$$\epsilon \sim 0.3 \text{ ev}. \tag{4}$$

This result agrees with values ϵ(ϵ = 0.3 – 0.5 ev), for the phosphor ZnS-Cu obtained by other methods[18].

The results obtained in this manner can serve as a new confirmation of the theory that the lowering of q outside the "plateau" region is connected with the luminescent action of the exciting light. However, with the action of the exciting light, there is associated not only the lowering of q in the plateau region but also, as will be shown later, a decrease in total illumination, as determined from the curve of increasing luminescence, compared with that determined from the extinction curve.

3. DEPENDENCE OF THE RATIO OF TOTAL LIGHT OUTPUTS DETERMINED FROM THE CURVES OF RISE AND EXTINCTION OF LUMINESCENCE ON THE INTENSITY OF THE EXCITING LIGHT

The total light output determined from the curve of rising luminescence is given as

$$L_p = \int_0^\infty (I_\infty - I_\vartheta)\, d\vartheta, \tag{5}$$

where ϑ = time elapsed from the beginning of excitation and I_ϑ = intensity of light at the time ϑ.

The total light output, evaluated from the curve of extinction of luminescence, is equal to

$$L_3 = \int_0^\infty I_t\, dt, \tag{6}$$

where t = time elapsed from the cessation of excitation. It is generally assumed that

$$L_p / L_3 = 1. \tag{7}$$

However, such equality requires that the following conditions be fulfilled:

---

[18] V. V. Antonov-Romanovskii, Dokl. Akad. Nauk SSSR **20**, 361 (1938); Izv. Akad. Nauk SSSR Ser. Fiz. **10**, 477 (1946).

1) that the light output associated with recombination of electrons and "holes"

$$q = \text{constant} \tag{8}$$

during the time of increasing luminescence, as well as during the time of extinction of luminescence even if quenching exists.

2) that the ionization per unit time remains constant during the excitation time.

Tolstoi[19] has shown that with external quenching which follows the first order kinetic law

$$L_p / L_3 > 1. \tag{9}$$

The inequality of L_p and L_3 in this case is associated with the nonfulfillment of condition (8).

By measuring L_p and L_3 for phosphors ZnS-Cu, and ZnS-Cu,Co, we have obtained the following results: Under weak excitation, when the effect of the extinction is present, inequality (9) is confirmed (Table I). Under strong excitation (Table II) the opposite is true.

TABLE I. Values of L_p/L_3 at weak excitation and $T = 80°C$ for phosphors ZnS-Cu and ZnS-Cu,Co (thin layer).

E (Rel. Intensity of exciting light)	Cu (3×10^{-4}), Co (0)	Cu (3×10^{-4}), Co (10^{-6})
11	—	1.43
2.4	1.64	2.50
1.0	2.17	3.00

TABLE II. Values of L_p/L_3 at intensive excitation and $T = 20°C$ for phosphors ZnS-Cu and ZnS-Cu,Co (thin layer).

E	Cu (3×10^{-4}), Co (0)	Cu (3×10^{-4}), Co (10^{-7})	Cu (3×10^{-4}), Co (10^{-6})
800	—	—	0.41
200	0.38	0.33	—
3.5	—	—	0.73
1.0	0.73	0.60	—

$$L_p / L_3 < 1. \tag{10}$$

This result can be explained as follows: Inasmuch as L is relatively high at high values of E, and the action of the exciting light plays an important role in the kinetics of phosphorescence (a portion of the excitation energy is captured by the localized electrons or "holes"), the results are that:

1. During the excitation of the phosphor, as L is increasing, its optical characteristics may change, which may result in the violation of condition (2).

2. Optical electrons and "holes" which appear during excitation enter into recombination which, in the case of phosphors ZnS-Cu and ZnS-Cu,Co, does not result in radiating transitions. This results in the violation of condition (8), since there are no such losses during the extinction in view of the absence of electrons and "holes".

RESULTS

The results obtained indicate that:

1. The causes of the decrease in the light output outside the "plateau" region for the ZnS-Cu,Co phosphor are the same as for the ZnS-Cu phosphor. At low intensities of the exciting light, this decrease is caused by the rising role of the external quenching, at high intensities – by the luminescent action of the exciting light and by the fact that only recombination of thermal electrons produces radiation.

2. As a result of the phenomena described the ratio of light outputs $L_p/L_3 < 1$ for high intensity of excitation.

3. In all works on investigation of the nature of the extinction process of ZnS-Cu phosphor by the elements of the iron group*, in which the phenomena associated with the luminescent action of the exciting light have not been considered, the interpretation of the results may be more or less incorrect.

---

[19] N. A. Tolstoi, Dokl. Akad. Nauk SSSR **95**, 249 (1954).

* Preliminary experiments have shown that the action of Ni and Fe are very similar to the action of Co, but there is also a considerable difference. For example, while infra-red radiation of wavelengths $\lambda = 0.8$ and $\lambda = 1.3\,\mu$ quenches the luminescence of ZnS-Cu,Co, in the case of ZnS-Cu, Ni only radiation $\lambda = 1.3\,\mu$ produces quenching, and radiation $\lambda = 0.8\,\mu$ produces a noticeable intensification.

Translated by J. L. Hersen
278

SOVIET PHYSICS JETP VOLUME 2, NUMBER 4 JULY, 1956

Some Problems in Recombination Luminescence Associated With Various Forms of Excitation in KCl-Tl Phosphors

I. P. SHCHUKIN
P. N. Lebedev Physical Institute, Academy of Sciences, USSR

(Submitted to JETP editor July 15, 1954)
J. Exper. Theoret. Phys. USSR **29**, 834-846 (December, 1955)

The efficiency of activator-produced radiative electron recombination has been measured in KCl-Tl phosphors using excitation by ultraviolet light, x-rays and γ-rays. An estimate is made of the quenching probability at the luminescence center – the Tl^+ ion. The existence of a transfer of excitation energy from the host material to the activator is confirmed. The predominating process is found to be the transfer of phosphorescence excitation energy associated with Tl^+ ionization. A decrease in the activator absorption is found upon stimulation of the phosphor; this is connected with the Tl^+ ionization.

INTRODUCTION

LUMINESCENCE in KCl-Tl phosphors has been extensively investigated. Bünger and Flechsig[1] have shown that luminescence in the phosphor KCl-Tl includes two processes: a short-time fluorescence having a duration of the order of 5×10^{-5} sec and a prolonged phosphorescence. The fluorescence spectrum and the phosphorescence spectrum are identical and consist of two wide bands with maxima at ~ 300 and 460 mμ[1]. According to Bünger[2] the quantum yield in fluorescence reaches 80% while that of phosphorescence is ~5% (for ultraviolet excitation). Hilsch and Pohl[3,4] found that the absorption of pure KCl has a maximum at ~ 163 mμ and a longwave edge extending to ~200 mμ. Koch[5] and other authors[6,7] have shown that the introduction of Tl into the lattice leads to the appearance of new absorption bands with the strongest having maxima at ~ 195 and 250 mμ*. The absorption of radiation in the longwave band gives rise only to fluorescence, while in the shortwave band both fluorescence and phosphorescence are excited[9].

Theoretical and experimental work by Johnson and Williams[10,11] indicates that the absorption bands with maxima at 195 and 250 mμ and the emission bands with maxima at 300 and 460 mμ are caused by electronic transitions in the Tl^+ ion which replaces the cation K^+ and whose levels are affected by the interaction with the lattice; the processes connected with fluorescence occur entirely within the luminescence center and their duration is determined by the lifetime of the electron in the excited level.

The fact that the fluorescence and phosphorescence spectra coincide is a reasonable basis for assuming that the final radiative transitions in phosphorescence occur at the same centers and even between the same levels as those in fluorescence, and that the only essential difference between these processes is one of kinetics. The kinetics of phosphorescence in KCl-Tl phosphors has been studied in detail by Antonov-Romanovskii[12]. On the basis of an analysis (using ultraviolet light) of the decay curves obtained at various excitation levels he reached the conclusion that phosphorescence in KCl-Tl stems from a recombination mechanism.

At the present time the kinetics of recombination luminescence is visualized as follows. With absorption of radiation at a luminescence center, an electron makes a transition to an excited level of the center; it can return to the ground state either emitting radiation (fluorescence) or not emitting radiation (in which case the excitation energy is converted into heat); it can also, by virtue of the energy evolved in the displacement of the nuclei to a new equilibrium position and thermal lattice vibrations, be transferred from the excited level to the conduction band, thus effecting ionization of the luminescence center. Ionization may be accompanied by energy absorption in the host material. Electrons excited to the conduction band are captured by various lattice defects. After being freed from the trap levels and a number of subsequent captures these electrons recombine with the ionized luminescence centers. An electron recombining with an ionized luminescence center initially falls into an excited level whence it falls to the ground state with the emission of a luminescence quantum (or by a radiationless mechanism).

---

*At higher Tl concentrations KCl-Tl spectra become more complicated[8].

[1] W. Bünger and W. Flechsig, Z. Physik 67, 42(1931).

[2] W. Bünger, Z. Physik 66, 31 (1930).

[3] R. Hilsch and R. W. Pohl, Z. Physik 59, 812 (1930).

[4] R. Hilsch, Z. Physik 44, 421 (1927).

[5] R. Koch, Z. Physik 57, 638 (1929).

[6] H. Lorenz, Z. Physik 46, 558 (1928).

[7] M. Forro, Z. Physik 56, 534 (1929).

[8] K. V. Shalimova, Dokl. Akad. Nauk SSSR 70, 225 (1950).

[9] W. Von-Meyeren, Z. Physik 61, 321 (1930).

[10] F. E. Williams, J. Phys. Chem. 57, 780 (1953); J. Chem. Phys. 19, 457 (1951).

[11] P. D. Johnson and F. E. Williams, J. Chem. Phys. 20, 124 (1952).

[12] V. V. Antonov-Romanovskii. Dissertation Tr. Inst. Fiz. Akad. Nauk SSSR, II 2-3, 157 (1942).

This description of the kinetics of phosphorescence explains both the coincidence of the fluorescence and phosphorescence spectra and the impossibility of exciting phosphorescence with radiation at ~ 250 mμ subsequent to the absorption of a quantum of energy at this wavelength; the energy evolved in the transition of the nuclei to a new equilibrium position is found to be inadequate for the transfer of an electron from an excited level to the conduction band[13]. In the following, only recombination luminescence in KCl-Tl will be discussed.

The study of various trapping sites for free electrons is of great importance in the kinetics of phosphorescence. Trap sites in the phosphor KCl-Tl have been investigated by Johnson and Williams[13] using ultraviolet radiation, and by Parfianovich[14] and Lushchik[36] who used excitation by ultraviolet light and x-rays. The latter have shown that the trap sites in KCl-Tl having the deepest electron levels are the anion vacancies. As is well known, the capture of electrons[15] and polarons[16] at these vacancies leads to the formation of so-called F-centers which give rise to additional absorption having a maximum at 560 mμ in KCl. Parfianovich reports that phosphorescence due to the emptying of electrons from shallow and medium trap levels decays in the course of several hours at room temperature; thus, KCl-Tl phosphors which have been stored for a sufficient time following excitation should contain electrons only in the lowest levels – those of the halide vacancies (F- levels).

2. FORMULATION OF THE PROBLEM

This work was undertaken with two objectives in mind; 1) an investigation of one of the aspects of the complicated recombination luminescence process, namely, the determination of the efficiency of radiative electron recombination produced by the activator Tl^+, i.e., the ratio of the number of quanta emitted in the luminescence of Tl^+ to the total number of recombining electrons**, and 2) an elucidation of the question of excitation energy migration in KCl-Tl phosphors.

It was found to be extremely important that identical studies be made when using the different excitation methods – ultraviolet radiation, x-rays and γ-rays. The measurement of the efficiency of radiative recombination for excitation by ultraviolet radiation, in which virtually only the activator is ionized makes possible an estimate of the quenching probability in the luminescence center. The measurement of recombination efficiency for excitation by x-rays or γ - rays, which ionize both the activator and the material, permits a clarification of the question of excitation energy migration in the phosphor.

In order to measure the radiative electron recombination efficiency it is necessary to determine the number of quanta emitted in the Tl^+ luminescence and the number of recombining electrons by independent means. The number of quanta radiated in a given volume can be determined easily, since KCl-Tl phosphors can be prepared in the form of large transparent single-crystals. To determine the number of recombining electrons advantage was taken of the fact that a phosphor which has been stored for a sufficiently long time after excitation contains electrons only at the halide vacancies; the concentration of these F - centers can easily be determined from absorption measurements. Thus, the problem resolves itself into the measurement of the ratio of the number of emitted quanta to the number of destroyed F-centers in phosphors which

---

[13] P. D. Johnson and F. E. Williams, J. Chem. Phys. **21**, 125 (1953).

[14] I. A. Parfianovich, J. Exper. Theoret. Phys. USSR **24**, 117 (1953).

[15] F. Seitz, Rev. Mod. Phys. **18**, 384 (1946).

[16] S. I. Pekar, *Studies in the Electron Theory of Crystals*, State Tech. Press, 1951.

[36] Ch. B. Lushchik, Abstract of Dissertation, Leningrad State University (1954).

**In general, recombination can occur at "holes" both in the host material and the activator.

have been stored under suitable conditions.

F-electrons can be liberated from the trapping site by two means: heating of the phosphor or exposure to yellow light which is absorbed by the F-centers. The second technique was employed since the intense heating required for thermal destruction of F-centers causes a considerable quenching of the luminescence (cf. reference 14). The liberated F-electrons undergo secondary capture at shallower trap levels from which they again can be freed by either thermal or optical processes. In the present work photostimulation of the light sum was carried out with infrared radiation in order to achieve a more rapid liberation of the electrons from shallow levels*.

In the course of this work a new effect was discovered, namely, a decrease in the activator absorption upon stimulation. A supplementary investigation was undertaken to examine this effect and to make use of it in a number of quantitative measurements. From a comparison of the activator absorption in colored and non-colored crystals (if the concentrations of the activator and the F-centers are known) one can determine the concentration of "holes" in the activator and the host material; from this, conclusions can be drawn regarding the predominant process in the transfer of excitation energy from the host material to the activator under γ-stimulation.

3. METHOD OF MEASUREMENTS

This work was carried out on single crystals of KCl-Tl grown from the melt by a technique due to Kyropoulos[17]. Although 0.1 mole percent Tl was introduced into the phosphor, polarographic analysis of the grown crystal revealed an activator concentration of $\sim 5\times10^{-3}$ mole percent. Thin layers, 1-4 mm in thickness, were cut off for the large, single-crystal measurements.

The ultraviolet source was an aluminum arc and associated condensing system, and the excitation was carried out without filters. The exposure time varied from 5 min to 15 hours. The x-ray source was a copper-anode tube operated with an accelerating voltage of 37 kv and a current of 10 ma. Exposures varied from 5 to 20 hours.+ A preparation of Co^{60} (energy of the quanta 1.33 and 1.17 mev) of 150 mc served as the source of γ-rays. Exposure time was varied from 2.5 to 72 days.

All absorption measurements were performed with the SF-4 spectroscope. The apparatus for the stimulation of the light sum and the measurement of the number of quanta consisted of two incandescent lamps (one with a yellow filter, the other with infrared) and a visual photometer, calibrated in apostilbs. By inserting a criss-cross yellow filter in the photometer in front of the eyepiece we were able to carry out phosphorescence decay measurements during continuous exposure to the yellow F-light (in doing this the transmission of the filter was taken into account in measuring the luminescence).

Mollwo and Ross[18] have given a formula for determining the concentration of F-centers (per cm^3)

$$N_F = 1.31\,\frac{n_0}{(n_0^2+2)^2}\,k_{\max}\,\Delta H, \tag{1}$$

where n_0 is the index of refraction at the maximum of the F-band, $k_{\max}$ is the absorption coefficient in cm^{-1} at the maximum and ΔH is the half-width of the F-band in electron-volts. This formula, which is valid only for a uniform distribution of F-centers, can be generalized to the case of an arbitrary distribution of the concentration over the thickness of the layer. In this case, the number of F-centers located in a parallelepiped having a 1 cm^2 base and a height equal to the thickness of the layer can be written (per cm^2)

$$N_F = 1.31\cdot10^{17}\,\frac{n_0}{(n_0^2+2)^2}\left(\int_0^d k_{\max}\,dx\right)\Delta H$$

$$= 1.31\cdot10^{17}\,\frac{n_0}{(n_0^2+2)^2}\,(-\ln D)_{\max}\,\Delta H,$$

where D is the transparency of the layer and the subscript "max" refers to the maximum value of the quantity ($-\ln D$) within the limits of the F-band.

Substituting the value $n_0 = 1.5$ in the last formula we obtain:

$$N_F = 1.1\cdot10^{16}\,(-\ln D)_{\max}\,\Delta H, \tag{2}$$

where N_F is given per cm^2.

Formula (2) was used in the calculations with ultraviolet and x-ray excitation (large gradient in the concentration of F - centers) and also in the case of excitation by γ-rays (uniform concentration). This was done since, experimentally, the number of quanta radiated by the same parallelepiped is determined directly. In the case of γ-excitation, if desired, the quantity N_F/cm^3 can be obtained easily by dividing by d.

---

* Yellow light transfers the electron only to an excited level of the F-center[15] from which it is usually transferred to the conduction band via a thermal mechanism. Under the present conditions infrared radiation can also promote this transfer.

+ Certain measurements were performed using x-ray excitation from a tube operated at 180 kv.

[17] S. Kyropoulos, Z. Physik **63**, 849 (1930).

[18] E. Mollwo and W. Ross, Gött. Nach. 1, 107 (1938).

To measure the number of radiated luminescence quanta it is necessary to determine the total luminescence energy radiated in the ultraviolet band and the visible band. In visual photometry this can be done through the use of the known relative energy distribution over the spectrum. In KCl-Tl phosphors the measurement of the number of quanta is made possible by virtue of the well-known fact that both bands maintain a constant relation between themselves during decay.

For light rays emanating from a crystal with an index of refraction n_0 into air, the solid angle is modified by a factor of n^2 (for perpendicular incidence and a small solid angle) because of refraction at the interface. This causes a reduction of the energy intensity by a factor n^2 in the output flux of the crystal[19]. Therefore, the experimentally observed intensity must be multiplied by a factor n^2, and also by a factor 4π when account is taken of the isotropy of the radiation within the crystal. The conversion from the visual experimental measurement of the light intensity in apostilbs to the energy intensity in erg/cm^2-ster-sec is carried out with a calculation of the relative distribution of the luminescence energy in the spectrum $I(\lambda)$, the sensitivity curve of the eye and the well-known relationships between luminance and energy units.

The formula for determining the number of quanta radiated in all directions by a parallelepiped with a 1 cm^2 base and a height equal to the thickness of the layer is of the form:

$$n_{\mathrm{qu}} = 4\pi C\left(\frac{n_1^2\int\limits_{\lambda_1} I(\lambda)\,d\lambda}{h\bar{\nu}_1\int\limits_0^\infty v(\lambda)\,I(\lambda)\,d\lambda}+\frac{n_2^2\int\limits_{\lambda_2} I(\lambda)\,d\lambda}{h\bar{\nu}_2\int\limits_0^\infty v(\lambda)\,I(\lambda)\,d\lambda}\right)\Delta S_n, \qquad (3)$$

where the integrals in the numerator indicate the total energy in relative units radiated in each of the two luminescence bands and the integral in the denominator is the luminescence energy with a visibility-curve correction for dark vision; ΔS_n denotes the light sum in apostilb-seconds being radiated in the direction normal to the surface of the crystal; n_1 and n_2 are the refractive indices for KCl at the two band-maxima; $h_{\bar{\nu}_1}$ and $h_{\bar{\nu}_2}$ are the mean radiated quanta for both bands in ergs and C is the proportionality factor for conversion from luminescence units into energy units at the maximum sensitivity of the eye ($C = 0.5$ erg/asb-sec-cm^2-sterad).

The energy distribution in the KCl phosphorescence spectrum was determined by photographic methods and the following formula was used:

$$n_{\mathrm{qu}} = 1.84\cdot 10^{11}\,\Delta S_n. \qquad (4)$$

The measurements of the efficiency of radiative electron recombination were carried out in the following manner. Following excitation by ultraviolet radiation, x-rays or γ-rays , the phosphor was stored in darkness for 15-18 hours in order to reduce the emission to a point where it would be invisible even with good darkness adaptation of the eye. As has been pointed out above, such a phosphor contains electrons only in the F - levels. Then the SF-4 spectrometer was used to measure the absorption of the crystal in the F - band and the number of F - centers N_F/cm^2 was determined from Eq. (2). The crystal was then placed directly in front of the objective of the photometer with its grain perpendicular to the rays of the eye and the emission of the light sum was stimulated by simultaneous exposure to yellow light and infrared radiation. The light sum in apostilb-seconds was determined from a measurement of the area under the decay curve and then the number of quanta emitted in the luminescence due to the recombination of the excited F-electrons $n_{\mathrm{qu}}/\mathrm{cm}^2$ was calculated by use of Eq. (4). Finally the radiative electron recombination efficiency $\rho = n_{\mathrm{qu}}/N_F$

---

[19] M. H. Alentsev, J. Exper. Theoret. Phys. USSR **21**, 133 (1951).

was determined**. All measurements were performed at room temperature.

4. RESULTS FOR EXCITATION BY ULTRAVIOLET RADIATION

The results of measurements of the efficiency of radiative electron recombination for excitation by ultraviolet radiation are shown in Fig. 1. The dependence of the quantity ρ^{phot} on the number of F- centers N_F/cm^2 is shown. The value of ρ^{phot} varies between the limits 0.35 and 0.47, but this scatter is explained by the experimental errors: errors in the absorption measurements for small numbers of F-centers and errors in the measurement of the stimulated light sum. Within the limits of these errors ($\approx$ 20%) the quantity ρ^{phot} can be taken as constant and it may be assumed that $\rho^{phot}_{ave} \approx 0.4$.

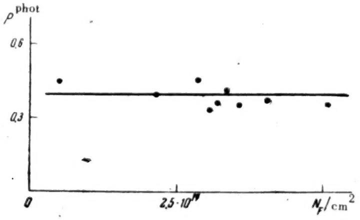

FIG. 1. Efficiency of radiative electron recombination as a function of the number of F-centers (photoexcitation).

In recombination with positive "holes", electrons can undergo both radiative and non-radiative transitions. Physically speaking, the quantity ρ is the ratio of the number of radiative transitions to the total number of transitions and therefore permits a determination of the fraction of non-radiative transitions $(1 - \rho)$ i.e., an estimate of the quenching probability. In recombination with "holes" in the host material, as a rule, all electrons carry out non-radiative transitions*, but after recombination with ionized luminescence centers (within the center), only a certain fraction do so, depending on the properties of the center, the temperature, and the energy of the recombining electrons.

Two processes lead to the appearance of "holes" in the host material. First, the passive absorption of energy by the host lattice which leads to its ionization. Second, direct ionization of the activator alone in which it is possible for electrons to be transferred from a filled band to free levels of the activator by thermal or optical mechanisms, thus producing "holes" in the host material. This second mechanism was first proposed by Antonov-Romanovskii[1 2] and used, for example, by Vinokurov[21] in explaining the exponential decay curve in the temperature quenching of ZnS-Cu phosphors and also by Antonov-Romanovskii, Alentsev and Vinokurov[22] in the interpretation of the non-linear dependence of the luminescence intensity of ZnS-Cu phosphors on the intensity of the exciting radiation at low intensities.

The quenching connected with non-radiative transitions in the recombination of electrons with "holes" in the host material (regardless of its origin) can be described as "external" since it occurs outside of the luminescence center. Quenching within the center, on the other hand, may be described as "internal". We shall show that in KCl-Tl phosphors excited by ultraviolet radiation one is dealing essentially with "internal quenching".

As has already been noted, the data of references 3-5 indicate that absorption in the host material has a maximum at ~ 163 mμ, and a longwave edge extending to ~ 200 mμ and is insignificant as compared with activator absorption in the region in which the two overlap (~ 195 mμ). In the region of the spectrum which corresponds to absorption by the host material, radiation from the aluminum arc is absorbed by a 10 cm thickness of air and consequently does not reach the phosphor; in the region in which the spectra overlap, the activator absorption considerably exceeds the weak absorption edge of the host lattice. This means that absorption in the host material is insignificant and that radiation from the arc ionizes the activator almost exclusively.

It will be shown below, on the basis of absorption measurements, that in a crystal which has been stored after exposure to the arc, the number of "holes" in the host material is negligible

---

**Kats[20] has performed similar absolute measurements by different methods on certain non-activated alkali-halide crystals, colored by ultraviolet irradiation at room temperature.

*This holds true if there is no energy transfer to the activator.

[20] M. L. Kats, J. Exper. Theoret. Phys. USSR **18**, 164 (1948).

[21] L. A. Vinokurov, Dokl. Akad. Nauk, SSSR **85**, 529 (1952).

[22] V. V. Antonov-Romanovskii, M. L. Alentsev and L. A. Vinokurov, Dokl. Akad. Nauk SSSR **96**, 1133 (1954).

compared to the number in the activator. The fact that ρ^{phot} is approximately independent of N_F provides a basis for assuming that there is no electron transfer (in the destruction of the F-centers) by thermal or optical mechanisms from the lower bands to free levels of the activator.

Hence, it may be assumed that in photoexcitation of KCl-Tl phosphors, it is principally "internal quenching" which occurs. We now estimate the probability for this quenching.

The quantity ρ can be written in the following form:

$$\rho = \frac{n_{\text{qu}}}{N_F} = \frac{\alpha n_{\text{a}}^0}{n_{\text{a}}^0 + n_s^0} = \frac{\alpha}{1 + n_s^0 / n_{\text{a}}^0}, \qquad (5)^*$$

where n_{a}^0 and n_s^0 are, respectively, the number of "holes" in the activator and the host material prior to the destruction of the F-centers, and α is the probability for radiative transitions in the luminescence center. In photoexcitation, as we have indicated above, $n_s^0 \ll n_{\text{a}}^0$. Thus, using Eq. (5) we obtain $\rho^{\text{phot}} \approx \alpha$ and the quenching probability in the luminescence center is approximately 0.4.

In certain phosphors, it has been shown[23,24] that electrons ejected from trap levels by thermal or optical mechanisms have different probabilities for radiative transitions within the luminescence center. We have performed special experiments to measure the quantity ρ in the case where electrons were ejected from shallow trap levels and excited F-center levels in KCl-Tl phosphors by purely thermal means; the results are the same as those obtained with infrared stimulation.

5. RESULTS FOR EXCITATION BY X-RAYS AND γ-RAYS

In Fig. 2 are shown the results of the measurements of ρ using γ-excitation. The value of ρ^{γ} varies from 0.13 to 0.21, but within the limits of the errors (especially at small concentrations of the F-centers) it can be considered as constant and it may be assumed that $\rho^{\gamma}_{\text{ave}} \approx 0.16$. Comparison of the results obtained with photoexcitation and γ-excitation yield the ratio $\rho^{\text{phot}}_{\text{ave}} / \rho^{\gamma}_{\text{ave}} \approx 2.5$.

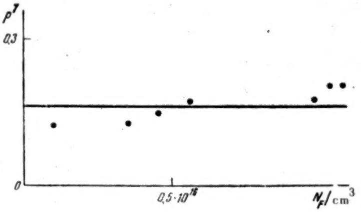

FIG. 2. Efficiency of radiative electron recombination as a function of the number of F-centers (γ-excitation).

The results obtained with x-ray excitation are shown in Fig. 3. Within the limits of the errors of the measurements ρ^r can again be taken as constant**, and it may be assumed that $\rho^r_{\text{ave}} \approx 0.1$. Comparison with $\rho^{\text{phot}}_{\text{ave}}$ yields $\rho^{\text{phot}}_{\text{ave}} / \rho^r_{\text{ave}} \approx 4$.

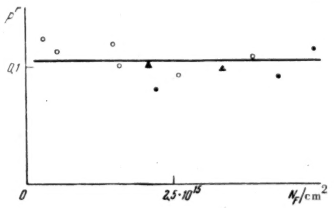

FIG. 3. Efficiency of radiative electron recombination as a function of the number of F-centers (excitation by x-rays of varying degrees of "hardness"). ○– ΔV =37 kv; ●-ΔV=180 kv; ▲-ΔV=37 kv (thermal emptying of electrons from shallow trap levels).

The low values of $\rho^{\gamma}_{\text{ave}}$ and ρ^r_{ave} as compared with $\rho^{\text{phot}}_{\text{ave}}$ can be explained by the fact that in excitation by x-rays and γ-rays it cannot be assumed that $n_s^0 \ll n_{\text{a}}^0$, i.e., recombinations with "holes" in the host material (non-radiative transitions) cannot be neglected . On the other hand, using the actual concentration of the activator (5×10^{-3} mole percent) one might expect results differing considerably from those given above. Since secondary electrons play such an important role in the ionization of the material when excitation by x-rays or γ-rays is used, the formula for electron ionization losses (Bethe formula[26]) can be used to estimate the ratio of the number of "holes" in the host material to the number of "holes" in the activator:

---

*Equation (5) is valid only in those cases in which there is no transfer of "holes" between the host material and the activator during the time in which electrons are liberated from the F-levels.

[23] Z. L. Morgenshtern, Dokl. Akad. Nauk SSSR **54**, 721 (1946).

[24] R. Ellickson, J. Opt. Soc. Amer. **36**, 264 (1946).

**Relative measurements of the dependence of the light sum on the concentration of F-centers in some x-rayed alkali-halide phosphors have been performed by Parfianovich[25] and also reveal a proportionality between these quantities.

[25] I. A. Parfianovich, Izv. Akad. Nauk SSSR, Ser. Fiz. **15**, 669 (1951).

$$\left(-\frac{dE}{dx}\right)_{\text{ion}} = \frac{2\pi e^4 N Z}{mv^2}\, C, \tag{6}$$

where e, m, and v are the charge, mass, and velocity of the ionizing electron, N is the concentration of atoms; Z is the number of electrons in an atom of the material through which the electron moves,and C is a quantity which depends on v and also somewhat on the mean ionization potential of the atoms in the medium.

Thus we have:

$$\frac{n_s^0}{n_a^0} \sim \frac{N_{\mathrm{K}^+}Z_{\mathrm{K}^+} + N_{\mathrm{Cl}^-}Z_{\mathrm{Cl}^-}}{N_{\mathrm{Tl}^+}Z_{\mathrm{Tl}^+}} \approx 10^4.$$

Substituting this value in (5) and using the value found for α , we obtain $\rho^{\gamma}_{\text{theo}} \sim \rho^{r}_{\text{theo}} \sim 4 \times 10^{-5}$ while the experimental values are $\rho^{\gamma}_{\text{exp}} \approx 0.16$ and $\rho^{r}_{\text{exp}} \approx 0.1$.

Thus

$$\rho^{\gamma}_{\text{exp}} \gg \rho_{\text{theo}} \quad \text{and} \quad \rho^{r}_{\text{exp}} \gg \rho_{\text{theo}}.$$

6. SENSITIZATION OF Tl^+ LUMINESCENCE IN KCl-Tl PHOSPHORS WITH EXCITATION BY X-RAYS OR γ- RAYS

The fact that the experimental value of ρ is considerably larger than the theoretical value in the case of excitation by x-rays or γ-rays is an indication of the transfer of excitation energy from the host material to the activator; this follows since it is only the activator which radiates, and energy transferred to it causes an increase in the value of ρ. In the following, only the transfer of energy which occurs in the excitation of phosphorescence will be considered, since fluorescence was not studied. These transfer processes, regardless of the particular mechanism, involve the following. Energy is absorbed in the host material and by some means a free electron is created which is then captured at a trap level (for example, an F-level); radiation from the activator occurs in the subsequent recombination of such an electron.

Two cases of the transfer of energy can be visualized.

Case 1. As is apparent from Eq. (5), ρ^{γ} and ρ^{r} become larger with a decrease in the ratio n_s^0 / n_a^0, i.e., with an increase in the fraction of ionized luminescence centers. Under Case 1 there are two different possible mechanisms for the transfer of energy to the activator which lead to a lower value of n_s^0 / n_a^0.

a) The first mechanism is connected with the diffusion of "holes" (originating in the host material) to the activator upon ionization. In the energy band description this means that electrons can make transitions from the lower levels in the Tl^+ ions to the filled band, recombining with "holes". In KCl-Tl phosphors, apparently this transfer of "holes" can occur only during the excitation time.

This conclusion is reached on the basis of the high stability of the F-centers (the concentration of F-centers does not change even after several days). Stability of this kind is possible only under conditions in which there are no direct transitions of F-electrons into the filled bands and this situation obtains only when the "holes" in the host material are rigidly connected to lattice defects and are not free to diffuse. Diffusion of "holes" to the activator during excitation reduces the ratio n_s^0/n_a^0.

b) The second possibility for the transfer of energy from the host lattice to the activator is the transfer by exchange resonance mechanisms. Here again only those processes are considered which lead to a reduction in the value of n_s^0/n_a^0.

Vavilov[27] has developed a theory for the migration of excitation energy in exchange resonance interactions between molecules in solutions of fluorescence materials. In crystals, Frankel has introduced the notion of a particular excited state – the exciton; migration of the exciton in crystals can be considered as the transfer of excitation energy by a resonance mechanism from one atom to its neighbor and so on. Dexter[28] has recently considered theoretically the problem of the transfer of excitation energy in crystal phosphors and has shown, in particular, that when excitons are created there is a high probability for the transfer of their energy to the activator.

---

[26] E. Fermi, *Nuclear Physics*.

[27] S. I. Vavilov, *Microstructure of Light (Studies and Notes)*, Acad. Sci. Press, Moscow, 1950.

[28] D. L. Dexter, J. Chem. Phys. **21**, 836 (1953).

In the excitation of phosphors by x-rays or γ-rays, it is apparent that ionization should be accompanied to some degree by the creation of excitons. An exciton created in the host material during excitation migrates through the lattice and can transfer its energy to the activator ion. The electron in Tl^+ makes a transition to an excited level; then in a time of 10^{-12}– 10^{-13} sec, displacement of the lattice nuclei to a new equilibrium position occurs (lattice relaxation). By virtue of the energy evolved in this displacement and to some degree the energy of the thermal lattice vibrations, the electron is transferred into the conduction band – thus effecting ionization of the luminescence.

This process tends to increase the value of n_a^0 and hence to reduce n_s^0/n_a^0. Another process may also be a factor. Energy is liberated in the recombination of the electron with a "hole" in the host material both during excitation and during the decay of phosphorescence (again, the creation of an exciton is possible); this energy is transferred to the Tl^+ ion by a resonance mechanism resulting in its ionization and repeated electron capture. This process also tends to increase n_a^0 and thus to reduce n_s^0/n_a^0.

Thus both mechanisms considered under Case 1 ("hole" and resonance) lead to a lower value of the ratio n_s^0/n_a^0. In this case the value of ρ is to be determined from Eq. (5).

Case 2. There is another means by which excitation energy can be transferred to the activator; this does not involve a reduction of n_s^0/n_a^0 but none the less results in an increase of ρ^γ and ρ^r. In this case the following process takes place. Energy is liberated in the recombination of an electron with a "hole" in the host material; this energy is transferred to the activator ion by a resonance mechanism. By virtue of this energy, an electron in the Tl^+ ion makes a transition to an excited level, whence it returns to the ground state by a radiative or non-radiative process. This situation is different from that considered under Case 1 in that only excitation of Tl^+ occurs and not ionization.

An essential feature of this process is the fact that the ratio of "holes" n_s^0/n_a^0 remains equal to the theoretical value ($\sim 10^4$) and Eq. (5) is no longer valid. In this case the values of ρ^γ and ρ^r should be determined by the following formula:

$$\rho = \frac{\alpha n_a^0 + \alpha'\beta n_s^0}{n_a^0 + n_s^0} = \frac{\alpha + \alpha'\beta n_s^0/n_a^0}{1 + n_s^0/n_a^0}, \qquad (7)$$

where β is the probability for the transfer of energy from the host material to the activator and α' is the probability of radiation in the Tl^+ ion which is excited by the transferred energy. Generally speaking, the quantity α which denotes the probability for radiation in Tl^+ after recombination of a free electron is not equal to α'. It is apparent from this formula that an increase in ρ^γ or ρ^r depends on the term $\alpha'\beta n_s^0/n_a^0$ which appears in the denominator and which is a function of the probability of energy transfer.

In order to determine which of the two energy-transfer processes is the predominant one, we used the experimental data to make an estimate of the ratio n_s^0/n_a^0. This estimate can be carried out by exploiting an effect which was found in the KCl-Tl phosphor; namely, the decrease in the absorption of the activator Tl^+ which occurs in excitation of the phosphor.

7. VARIATION OF THE ABSORPTION OF THE ACTIVATOR Tl^+ IN EXCITATION AND DETERMINATION OF THE CONCENTRATION OF "HOLES"

A decrease in the activator absorption was observed in the case of excitation by ultraviolet radiation and γ-radiation, (no experiment was performed with x-ray excitation).

It may be remarked that this is the first case in which a decrease in the absorption of the activator Tl^+ has been observed. Urbach and others[29] have observed a similar effect in the activator Eu^{+++} in SrS-Eu, Sm and Anikina[30] in the activators Ce^{+++} and Eu^{+++} in the phosphors SrS-Eu, Sm and SrSCaS-Ce, Sm. In the work of Arsanjewa[31], on the other hand, an increase in the absorption of x-rayed alkali-halide-Tl phosphors was reported; in this same paper and in a paper by Schulman et al[32] a decrease in the absorption of the activator Pb^+ in the phosphor NaCl-Pb was observed. Schulman has interpreted this diminution on the basis of the conversion of the activator ions to quasi-neutral atoms (or double valence ions to single valence ions) in the capture of electrons separated from the host material. In a paper which appeared recently, Andrianov and Kats[33] explain in the same way the decrease of the absorption of the activator in the phosphor KCl-Sn following x-ray excitation.

---

[29] F. Urbach, H. Hemmendinger and D. Pearlman, *Preparation and Characteristics of Solid Luminescent Materials, Symposium*, London, 1948, p.279.

[30] L. I. Anikina, Abstract of Dissertation, Inst. Fiz. Akad. Nauk SSSR, 1953.

[31] A. Arsanjewa, Z. Physik 57, 163 (1929).

[32] J. H. Schulman, R. J. Ginther and C. C. Klick, J. Opt. Soc. Amer. **40**, 854 (1950).

The possibility of the formation of quasi-neutral silver atoms and single valence copper in excited alkali -halide phosphors such as NaCl-Ag and NaCl-Cu has been shown in references 34 and 35. By analogy, the decrease in the absorption of the activator Tl^+ in KCl-Tl phosphors can be explained not only by the ionization of Tl^+ but also by the capture of an electron near the Tl^+, causing its conversion to Tl^0; this explanation becomes more convincing when one considers the fact that Lushchik[36] has verified experimentally the existence of trap levels associated with the activator in the phosphor KCl-Tl. In view of what has been said above concerning deep levels, however, it may be assumed that the trapping levels associated with Tl are not as deep as the F-levels and that after 15-18 hours of decay the phosphor contains electrons only in the F-levels. Making this assumption, we now calculate the number of "holes" n_a^0 and n_s^0 in 1 cm^2 of the surface of a phosphor which has been stored after excitation.

The relative reduction of the Tl^+ absorption in a colored crystal which has been allowed to decay as compared with a non-colored crystal yields the fraction of ionized luminescence centers δ. In general, the number of F-electrons is equal to the sum of the number of "holes" in the host material and the number of "holes" in the activator; the results of a polarographic analysis give the concentration of Tl^+ in the phosphor as $N_{Tl^+} = 7 \times 10^{17}/cm^3$. The average measurements in a layer with a thickness of 0.09 cm are as follows:

$$\delta \sim 0{,}006 \text{ and } N_F \approx 3.3 \cdot 10^{14}/cm^2,$$

from which we obtain

$$N_{Tl+}/cm^2 = (N_{Tl+}/cm^3)\,d = 7 \cdot 10^{17} \cdot 0.09 = 0{,}63 \cdot 10^{17}/cm^2,$$
$$n_a^0 = \delta N_{Tl+} \sim 0{,}006 \cdot 0{,}63 \cdot 10^{17} \sim 3{,}8 \cdot 10^{14}/cm^2$$

and

$$n_s^0 = N_F - n_a^0 \sim 0.$$

Thus in photoexcitation it may be assumed that $n_s^0 \ll n_a^0$.

If one assumes that in photoexcitation $N_F \approx n_a^0$, it is possible to get an approximate solution to the converse problem,i.e., having measured experimentally N_F and δ, one can determine the activator concentration N_{Tl^+}.

The decrease in the activator absorption was also observed with γ-excitation.

The results of measurements of the absorption in the Tl^+ band (maximum at 245 mμ) for phosphors which were colored by γ-rays, and for others which were not (all phosphors were stored in darkness), are presented in Fig. 4a. The concentrations of F-centers are shown in the Table and the corresponding F-bands are shown in Fig. 4a and Fig. 4b.

It should be pointed out that the proportionality between δ and N_F serves as evidence of the fact that the reduction in the activator absorption in stored phosphors depends only on the Tl^+ ionization and the electrons in the F-levels, i.e., the deepest levels.

The concentration of holes n_s^0 and n_a^0 can be calculated by this same method. In all three cases this ratio is found to be:

$$n_s^0/n_a^0 \sim 0{,}4. \tag{8}$$

On the other hand, the value of n_s^0/n_a^0 as determined from the value of ρ^γ using Eq. (5), which is valid only for the first energy-transfer case, we have:

$$n_s^0/n_a^0 \approx 1{,}5. \tag{9}$$

The approximate agreement of these values (order of magnitude) indicates * that case 1 is the important one, since calculations made using case 2 result in a discrepancy between measured and calculated values of n_s^0/n_a^0 which is of order 10^4.

---

[33] A. S. Andrianov and M. L. Kats, Dokl. Akad. Nauk SSSR **96**, 253 (1954).

[34] J. H. Schulman, R. J. Ginther, C. C. Klick, R. S. Alger and R. A. Levy, J. App. Phys. **22**, 1479 (1951).

[35] M. L. Kats, J. Exper. Theoret. Phys. USSR **23**, 720 (1952); Dokl. Akad. Nauk. SSSR **85**, 757 (1952).

* A discrepancy of a factor of 3 can easily be explained by the experimental errors (particularly in the delicate absorption measurements).

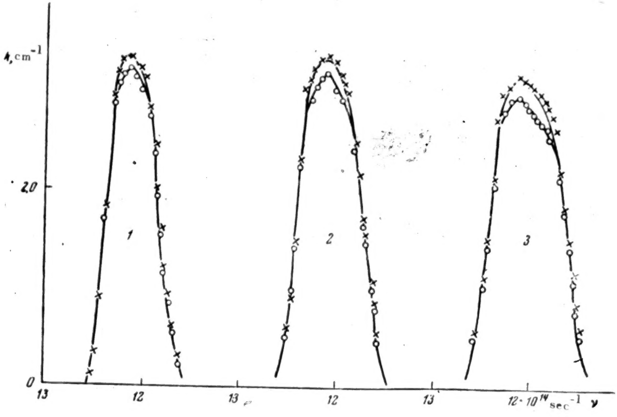

FIG. 4a. Reduction of absorption in the Tl$^+$ activator band for a phosphor colored by γ-irradiation as compared with a non-colored phosphor for the following exposure times: *1* -- 15 days; *2* - 35 days; *3* - 72 days.

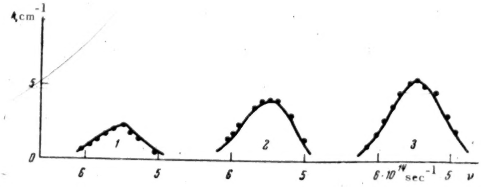

FIG. 4b. *F*-bands for the same exposures given in Fig. 4a.

TABLE

$N_{\mathrm{Tl}^+} \approx 7 \cdot 10^{17}/\mathrm{cm}^3$

Exposure time in days	δ	$N_F/\mathrm{cm}^3 \cdot 10^{-16}$	$N_F/\delta \cdot 10^{-17}$
15	0.0095	0.9	9.48
35	0.016	1.64	10.2
72	0.022	2.15	9.77

In conclusion the author wishes to express his gratitude to V. V. Antonov-Romanovskii for guidance in this work, to Z. L. Morgenshtern for the determination of the concentration of Tl⁺ in the phosphor and for a careful reading of the entire manuscript, to M. N. Alentsev and M. D. Galanin for critical comment, to A. A. Bundel for providing the x-ray apparatus and to E. E. Bukke for help in performing the experiment.

Translated by H. Lashinsky
279

SOVIET PHYSICS JETP VOLUME 2, NUMBER 4 JULY, 1956

Photochemical Conversion of Color Centers in Heated Crystals of Potassium Chloride

A. A. SHATALOV
Kiev State University

(Submitted to JETP editor July 19, 1954)
J. Exper. Theoret. Phys. USSR 29, 847-856 (December, 1955)

The results of investigating the photochemical conversion of F-centers in KCl crystals at temperatures of 270-300° C, leading to the complete disappearance of absorption F-bands and their replacement by analogous symmetrical bell-shaped band (X-bands) displaced by 0.5 ev towards the long wavelength region, are described.

At lower temperatures (250-150° C), exposure to light similarly results in the complete disappearance of F-bands and their replacement by wider and lower symmetrical absorption bands somewhat displaced toward the long wavelength region.

The temperature dependence of absorption X-bands is characterized by increasing height, narrowing, and displacement of the bands towards shorter wavelengths, upon cooling. Preliminary measurements of the kinetics of the photochemical conversion process of F-centers are reported for different temperatures. A hypothesis connecting the observed thermophotochemical F-center conversions with the formation process of colloidal alkali metal is proposed. The possible mechanism of converting F-centers into F_2-centers is deduced.

1. STATEMENT OF THE PROBLEM AND THE METHOD OF MEASUREMENT

THE rapid growth of the various applications of electron flow in dielectric crystals and semiconductors has necessitated an experimental and theoretical investigation of localized electron concentrations near different lattice imperfections. The knowledge of the properties and the structure of such states is imperative, in particular, for the understanding of early stages of thermal and photochemical processes involved in coloring transparent solids.

For certain applications, it is also particularly important to understand the conversion of initial "atomic" color centers into colloidal aggregates containing millions of neutral metal atoms.

Recently it has been repeatedly admitted in the literature that silver halide is not useful in the detailed study of the photochemical process, despite its practical importance in such processes. Even at room temperatures, the significantly high mobility of the cations causes considerable difficulty in investigating the correspondingly rapid coagulation of silver following exposure to visible light. Moreover, the investigation of photochemical conversions by means of absorption spectra is further limited in the visible region by self-absorption by the lattice. Much more suitable for such investigations are monocrystals of alkali-halides This is due to their higher melting points, the correspondingly higher temperatures of other transitions depending on ionic mobility, their insensitiveness to visible light under normal conditions, and the transparency of pure compounds in a wide spectral range.

Taking into account these advantages and the observation first made by Kravtse[1] in 1928, and fully accepted today[2], viz., the analogy between photochemical processes in silver halides and alkali halides, it is natural to use alkali-halides in the role of "models" for silver halides in the solution of many problems.

For these "models", as distinct from silver halide*, the name F-center was adopted for the initial atomic centers of high-temperature colloidal coagulates.

---

* Kirillov[3] has shown that for silver halide the absorption centers are intermediate between atomic and colloidal. However, the initial primitive absorption centers were not observed experimentally. The possibility of identifying with F-centers absorption bands observed by Meikliar[4] near the actual absorption edge of AgBr and AgCl crystals, irradiated by ultraviolet or heated, is open to discussion[5].

[1] S. I. Vavilov, Uspekhi. Fiz. Nauk 27, 106 (1945).

[2] P. V. Meinkliar, Uspekhi Nauch. Fotogr. 1, 149 (1951).

[3] E. A. Kirillov, Izv. Akad. Nauk SSSR, Ser. Fiz. 12, 533 (1948); Uspekhi. Nauch. Fotogr. 1, 183 (1951).

[4] P. V. Meikliar, Izv. Akad. Nauk SSSR, Ser. Fiz. 26, 129 (1952).

[5] O. F. Tomasevich, Thesis, Kiev State University, (1952).

Despite the apparent multi-stepped process of colloid formation, up to now it has been possible to obtain the final products of this process in alkali halide crystals only in the form of multi-atomic particles of alkali metal**.

Certain foreign investigators have even reached the conclusion*** that at temperatures allowing ionic mobility only "coarse" photochemical conversions take place, intimately associated with the permissability of ionic transitions. Finer photochemical reactions, determined by photo-transitions of electrons and also their local fixation (except *F*-centers), can only be accomplished at low temperatures.

It is not possible to agree with this conclusion because in the first stages of the photochemical coagulation process even the simplest conversions are essential, beginning with the action of individual photons, through their statistical distribution in the crystal lattice, to their absorption by the *F*-centers. However, until very recently, it has not been possible to determine what the nature of this initial light effect is and what local electronic conditions follow immediately after the photochemical annihilation or combination of *F*-centers, i.e., it was not possible to determine the intermediate production of atomic and colloidal centers, which, without any doubt, exist here similarly as in silver halide.

Wishing to advance the explanation of this question, we attempted to study changes in absorptivity of KCl crystals containing *F*-centers under the influence of light at elevated temperatures. Some of the results of our measurements have been described in a preliminary publication[7] In the present publication we describe in greater detail the applicable method and further investigations.

The absorption spectra of alkali halide crystals additionally colored were studied on specimens "frozen to room temperature after coloring at elevated temperatures. The temperature dependence of absorption was studied by heating and cooling these specimens to the desired temperature. This method is not without fault, however, since in cooling, no matter how quickly done, as well as in heating, it is possible that processes changing the distribution an properties of the color centers take place in the crystals. Such processes may be: the crystals becoming transparent, possible conversion of the centers, coagulation of colloids, etc. This shortcoming cannot be circumvented in the measurement of absorption by crystals colored in alkali-metal vapors.

The overwhelming majority of foreign investigations have been, and are presently being carried out, on crystals colored by exactly this process. Yet, an alkali halide crystal can be easily colored additively by diffusing the color from a sodium electrode into a warmed crystal[8]. In this method, the electrons enter the crystal voluntarily (electron diffusion) or under the coercion of an applied field. Taking advantage of this application, we developed a method[9] for obtaining colors of uniform intensity by forming them in a homogeneous electrical field with the aid of planar parallel electrodes. The method of coloring with a sodium electrode eliminates the need of a vacuum and if an applied electric field is used it is possible to make the crystal transparent repeatedly, and to color it.

The utilization of this method permitted us to measure the absorption spectra of the crystals, located directly in the oven, at various temperatures and degrees of coloration. The samples under investigation were potassium chloride monocrystals grown by the method of Kiropulius with every precaution being taken to attain maximum purity. A ray diagram of the actual experimental arrangement is schematically pictured in Fig. 1.

The samples were cleaved from a monocrystal to a size approximately 2.5 × 1.5 × 0.5 cm, carefully polished on two sides and placed between two sodium electrodes with the aid of a support *A*. This assembly was placed in a horizontal cylindrical oven, *B* supplied with transparent windows, *C*. The light from a rectangular 30 watt tungsten source, *D*, powered by a storage battery, passed through a condenser lens which focused the light on to the surface of the crystal plate *E*. The transmitted light passed

---

** The explanation of low, longwave absorption bands obtained by Petroff[6] and other investigators in terms of absorption by aggregates of atomic centers resulting from light acting on the *F*-centers at low temperatures appears highly debatable.

***See the foreward written by R. W. Pohl and H. C. Pick to the investigation by Petroff[6].

[6] St. Petroff, Z. Physik 127, 443 (1950).

[7] A. A. Shatalov, Dokl. Akad. Nauk SSSR 92, 3 (1953).

[8] S. A. Artsybyshev, Trudy Phys. Inst. Akad. Nauk SSSR 1, 3 (1938).

[9] A. A. Shatalov, Trudy Phys. Facult. Kiev State University 6, 43 (1952).

through another lens which focused the light on an aperture, F, placed in front of a UM-2 glass monochromator. The intensity of the light passing through the monochromator was measured with a galvanometer and a photosensitive element (selenium, FES, FES-U), which was sensitive to the various spectral regions.

Since we were only interested in measuring the change of shape and position of the peaks and not the absolute value of the absorption coefficient μ, we did not have to measure the thickness d, of the the absorbing layer, and we selected the magnitude of $\ln \frac{I_0}{I} = \mu d$ as a measure of the absorption.

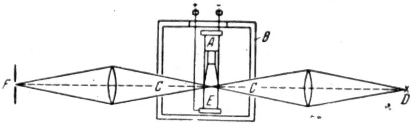

FIG. 1.

The intensity of the incident beam, I_0, was measured by passing the light through the crystal, made transparent by reversing the applied field. In this way, we could avoid all the errors arising from surface reflections, surface irregularities, etc., since the same conditions were used for measuring I and I_0.

The simplest effect of the intensity of the light on the crystal could be realized in the following way. The beam of light used for the measurement constituted a light probe formed by the focal spot on the crystal surface. Its intensity depended, therefore, on the conditions of focusing (area of spot) and on the variable intensity of the light source. Later, the effect of the light was also realized on large uniformly lighted areas.

2. EXPERIMENTAL RESULTS

As has been reported previously[7], the light absorbed in the range of an F-band does not lead to its destruction up to temperatures of ~ 300° C. However, upon slight further cooling, a distinct light sensitivity of the F-centers develops resulting in a conversion, during a few seconds following the beginning of the exposure, from a blue-violet atomic coloring of the crystal into a less intense (due to absorption near the boundary of the visible spectrum) blue having a greenish tinge.

As soon as the light source was turned on, a small "window" formed on the uniformly colored background due to the F-centers. This window had sharply outlines boundaries corresponding exactly to the shape of the light probe. Within the area of this window, the above-described color changes took place, corresponding to the formation of new color centers. The further path of the light beam passed only through the region of the new color, making possible the measurement of the absorption spectra of this region. The degree of complete "saturation" attained could be measured by observing the galvanometer indicator after rotating the monochromator to the position corresponding to the wavelength of the F-peak. Experiments with copper sulfate and yellow glass filters, serving to connect the long and short wavelength ends of the spectrum, permitted the determination of the photoactivity of the light absorbed in the region of the F-band.

By means of measurements at temperatures of 300-270° C, it was determined that the effect of exposure to light resulted in a replacement of the F-peaks in the long wavelength region by bell-shaped absorption bands centered approximately near 740 $m\mu$. In all other regards, the new absorption band, which we have called the X-band, does not differ significantly from the original F-band.

In Fig. 2, curve a represents the F-band observed at 270° C by a method wherein light pulses are used that are long enough to allow measurement (with a damped galvanometer) but not long enough to allow significant changes in the color centers. Curve *b* shows the change in the absorption of the crystal brought about by continuous exposure of the crystal until it had been "saturated." At the indicated temperatures the *X*-band is thermally unstable, disappearing in a short time interval, depending on the temperature, if the light source is removed. In this case, the crystal returns to its original color and the *F*-band is restored to its former intensity. The *X*-band can be frozen in only by rapidly quenching the crystal to room temperature. In this case, it is perfectly stable both in the dark and under visible light. The photochemical destruction and thermal reconstruction of the *F*-centers can be repeated many times.

Exposure to light at temperatures of 250, 200, and 150° C can also destroy the *F*-band completely. However, essential differences are observed. The optical destruction of the *F*-centers takes place at different rates, passing through a maximum (see below), and decreasing with decreasing temperature.

Moreover, upon termination of the exposure, the newly formed centers disappear more slowly as the temperature decreases until they reach thermal stability, which point is a function of the original *F*-center concentration. The observed thermophotochemical conversions are irreversible, and only by raising the crystal temperature to 270-300° C or higher can the original *F*-band be restored in a purely thermal way. Furthermore, the coloring of the crystal resulting from exposures at lower temperatures is different from the coloring caused by *X*-centers. This difference is characterized by the absorption curves (curves *c* and *d* in Fig. 2) obtained at 250 and 200° C. These curves are symmetrical but show a more rapid decline and displacement toward longer wavelengths as compared to the *X*-bands. The change is proportional to the drop in temperature.

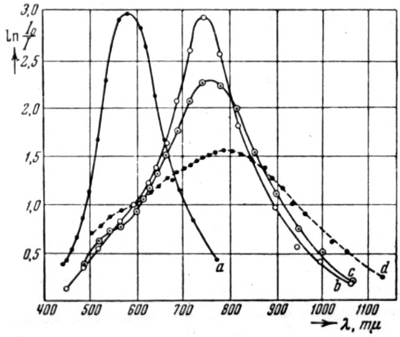

FIG. 2. *a*-*F*-centers, 270° C; *b*-*X*-centers, 270° C; *c*-colloids, 250° C; *d*-colloids, 200° C.

The effect of light below 150° C, when the observable ionic mobility is virtually absent, does not produce complete disappearance of the *F*-band and leads to a considerably slower production of photodisintegrated *F*-centers having absorption curves with many maxima. The investigation of these curves, begun recently by Petroff[6], and their relation to our higher temperature observations will require further study.

By means of additional measurements we have elucidated the nature of the temperature dependence of the new absorption band. It can be seen from the observations reported previously[7] that for any chosen light intensity, provided it is sufficiently great, there exists a limiting temperature above which it is not possible to observe a complete conversion of *F*-centers into *X*-centers. Below this temperature, the observation of thermal changes in the pure X-band is possible only during continuous exposures or else by cooling in darkness until the temperature reaches the range of thermal stability of X-centers. Otherwise, the electrons have an opportunity to return to the F-levels and the changes in the X-bands are not produced solely by temperature change. On the right side of Fig. 3* are shown X-bands measured on the same exposed crystal at 280, 200 and 20° C. Intermediate temperatures yield curves intermediate between those shown. The increasing height and narrowing width of the peak, observed with decreasing temperature, obeys well the constancy of the product of the maximum absorption coefficient times the halfwidth. As is well known, the relation $\mu\delta = \text{const}$ for F-bands has been experimentally proven by many authors, and is quantitatively deduced in Pekar's[10] theory. This product (also constant for the X-bands shown) numerically is almost identically equal to its value for the original F-band measured after additional coloring at 500° C. The temperature dependence of this curve is shown on the left side of Fig. 3 for comparison purposes. As can be seen, the displacement of the two bands is quite different. Instead of the usual pronounced shift in the F-band, the X-band shifts but slightly in the direction of shorter wavelengths upon decreasing the temperature.

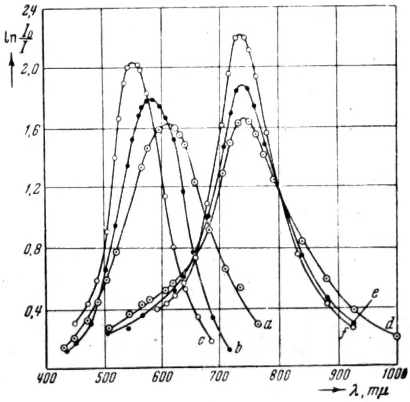

FIG. 3. a–F-centers, 500° C; b–F-centers, 280° C; c–F-centers, 20° C; d–X-centers, 280° C; e–X-centers, 200° C; f–X-centers, 20° C.

The kinetics of the photochemical conversion of F-centers into aggregations absorbing in the inner region of the spectrum can be best evaluated from the decrease in absorption in the F-band or by its increase in newly arising bands. After setting the monochromator on the maximum of an absorption band, the deflections of the galvanometer connected to the photoelement on which the light falls after passing through the crystal and the monochromator are measured. Recording these deflections at fixed time intervals, and assuming the magnitude of $\ln = \frac{I_{0\,\max}}{I_{\max}}$ as a measure of the concentration*, one can obtain an approximate time dependence of the latter for disappearing and newly formed centers under different conditions.

---

* The measurements reported in Fig. 3 were carried out by L. M. Titomir.

[10] S. I. Pekar, *Investigation of the Electronic Theory of Crystals*, GITTL, 1951.

The curves in Fig. 4 are examples of isotherms of time dependent F-center concentrations, obtained by us in this way. The functions at 280-270° C, corresponding to the conversion of F-centers into X-centers, have an exponential character as can be shown by the usual graphical analysis. As the temperature is lowered the curves become hyperbolic and then straighten out to become linear. This lack of congruency in the curves indicates a change in the nature of the F-center destruction mechanism with change in temperature. In addition, the curves show that the rate of conversion also depends on the temperature. It would have been easy to select an observational parameter to follow this dependence if the curves all had the same shape. For example, in the case of an exponential fall-off in the concentration, a useful parameter of process rate (radioactive disintegration) is the so-called disintegration constant (magnitude equal to the reciprocal half-life) which is a coefficient in the exponent and determinable from the slope of the line: logarithm of the concentration vs. time. In this case, as an approximate common characteristic of the observed function, the time τ of half-disintegration of F-centers, can be chosen, i.e,, the time, essentially different for different temperatures, during which the concentration of F-centers is decreased by one-half. The magnitude of the reciprocal of this time can then be used as an indication of the rate of the process.

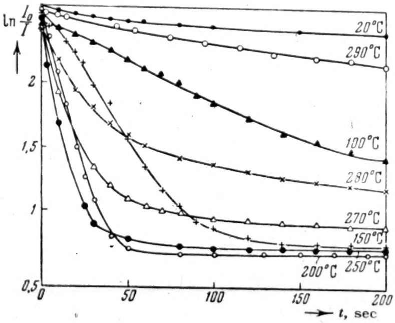

FIG. 4.

If we plot $1/\tau$ as the ordinate and the temperature as the abscissa, we obtain the curve shown in Fig. 5. It shows that the rate of photochemical conversion of F-centers, very small at low temperatures (apparently bounded by an insignificant ionic mobility), grows rapidly with increasing temperature reaching a maximum near 240° C. This part of the curve is reminiscent of temperature dependences (e.g., conductivity or diffusion) governed by the temperature increase in ionic mobility. This fact, as well as the temperatures at which the increased rates begin, convincingly testify that the thermophotochemical conversions of interest to us are connected with ionic rearrangements. After attaining a maximum, the rate curve falls rapidly. This appears to be a consequence of a sharp growth of a reverse thermal decomposition of new formation, beginning at certain temperatures.

We have measured the temperature dependence of reconstitution of f-bands after discontinued exposure, and also the appearance of X-bands and their thermal disintegration. These dependencies, along with quantitative analyses of the kinetics of photochemical conversions of *F*-centers into *X*-centers will be published in the near future.

---

* Since, at not overly large concentrations (in the absence of interactions between centers) the halfwidth of the absorption band is independent of the concentration, the latter can be assumed to be proportional to the absorption coefficient at the maximum, for independent centers and constant temperature.

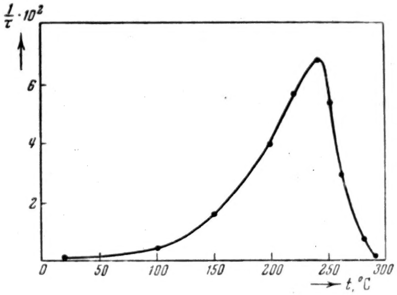

FIG. 5.

3. CONCLUSIONS

The experimental results at our disposal do not permit a complete elucidation of the mechanism of the conversion of *F*-centers into new color centers, nor the determination of the exact nature of the latter, However, the sequence of established facts already gives us reason for connecting the observed conversions with the colloidal coagulation of *F*-centers. This is especially evident for formations characterized by lower and broader curves shifted toward longer wavelengths (see Fig. 2), which can be attributed to absorption by ever increasing colloidal aggregates according to the calculation of Savostianova[11].

As a matter of fact, the color centers observed by us produce absorption bands shifted towards longer wavelengths as compared to the *F*-band and can be obtained as a result of affecting the color of the crystal by heat and light, i.e., the same factors that figure in the processes of colloidal coagulation, specifically at those temperatures at which this coagulation takes place in alkali-halide crystals.

As is well known, the rate of purely thermal colloidal coagulation is practically equal to zero for sufficiently high and sufficiently low temperatures. Consequently, in the process of cooling, it must pass through a maximum. This is apparently the result of the temperature dependence of the following processes: As the temperature lowers, the speed with which the atomic centers conglomerate increases with an initial formation of multiple centers and later of colloidal aggregates. It is believed that the outset of this process must be characterized by a certain saturation concentration of atomic centers in the crystal, which decreases upon cooling, similarly to the process taking place, for example in the precipitation of the solid phase from a saturated liquid solution. Moreover, the rate of the reverse process, i.e., the dissociation of the colloid into atomic centers, is also decreased with lowering temperature. At certain specific temperatures, however, an equilibrium between these two processes exists. If, in a crystal being cooled, after such an equilibrium condition has been reached, the intensity of the first process were to predominate again, the rate of colloidal coagulation could grow without limit. However, this growth is limited by the appearance of a third factor, viz., a rapid decline and, finally, a complete stoppage of the ionic mobility. The influence of this factor sharply decreases the rate of colloid formation, forcing it again to drop from the maximum.

Upon cooling, the state of the crystal immediately preceding the dynamical equilibrium of the processes of coagulation and dissociation, according to our observations, appears at temperatures at which the photochemical formation of X-bands is possible.

---

[11] M. V. Savostianova, Izv. Phys. Mat. Inst. Akad. Nauk SSSR **3**, 169 (1930); Z. Physik **64**, 262 (1930).

From the results of the present investigation, it is possible to reach the conclusion that two processes, analogous to those described above, occur in potassium chloride also. As an additional condition to the process of purely thermal coagulation, there appears here the role of exposure to light. The latter leads to an optical destruction of F-centers at temperatures too high for thermal coagulation. The thermal decomposition of the new formations combined with the reconstitution of F-centers makes up the second process. In this way, exposure to light is capable of initiating photochemical coalescence of atomic centers somewhat earlier than would be the case thermally, and at the same time displaces the initiation of the coagulation process toward higher temperatures, preceding those at which saturation concentrations occur. This latter condition predetermines the thermal instability of X-centers.

The presence of a maximum in the temperature dependence of the ratio in the observed optical process, has been shown by us in Fig. 5. Being bounded on the top by a rapidly growing thermal instability, and at the bottom by a fall-off in ionic mobility, the thermophotochemical process of conversion of F-centers can take place only in a narrow temperature interval. This further shows its similarity to the process of colloid formation.

As far as the nature of X-centers is concerned, we can make a fairly reliable choice between a representation of X-centers as more or less sizable colloidal aggregates containing large numbers of alkali metal* and an assumption that they are simple nuclei, possibly associated with the initiation of colloidal coagulation, being either new mono-atomic centers or small groups of atoms resulting from the coalescence of F-centers. The sequence of arguments[7] convincingly testifies in favor of the second postulate.

A more concretely plausible possibility appears to be a model identifying X-centers with F_2-centers. Such a model agrees well with the observational facts and theoretical considerations of Deigen[13] (the position of an absorption curve's maximum, its intensity, halfwidth, binding energy, etc.). On its basis, the mechanism of photochemical reaction observed by us can be explained more simply as a phototransition of an electron from an absorbing F-center, with simultaneous formation of an F'-center and a halogen vacancy, followed by rapid recombination of the two into a double center according to the scheme: $2F \rightarrow F_2$. As is well known[14], F'-centers are extremely unstable at observational temperatures and would succeed in disintegrating up to the moment at which they are somewhat stabilized by combination with halogen vacancies, if the latter did not occur with sufficient rapidity, caused (aside from significant coulomb fields of opposite charge), by their sufficient mobility.

From this, the role of the presence of intense ionic mobility becomes clear, i.e., the sufficiency of high temperature to make possible X-center formation. The same can be said about the reverse process of rapid destruction of X-bands after terminating the exposure. This can be explained simply by thermal dissociation of double centers made unstable by the presence of ionic mobility. The latter is confirmed by the stability of X-centers following a rapid quenching to room temperature.

The proposed unstable formation, obtained by stabilizing an F'-center by combination with a halogen vacancy, appears to be a realization under rigid conditions of an earlier, experimentally unobserved local state of the electron in the crystal lattice. A more certain determination of its properties can be made only following continued investigation.

---

* This apparently unlikely possibility must be mentioned, since Scott and Smith[12] who obtained a narrow long-wavelength absorption band in a KCl crystal by purely thermal means at very high initial concentrations, attributed this to a colloidal metal distribution and called it colloidal.

[12] A. B. Scott and W. A. Smith, Phys. Rev. **83**, 982 (1951).

[13] M. F. Deigen, J. Exper. Theoret. Phys. USSR **21**, 992 (1951); **24**, 631 (1953).

[14] H. Pick, Ann. d. Physik **31**, 363 (1938).

Translated by L. V. Azaroff
280

SOVIET PHYSICS JETP VOLUME 2, NUMBER 4 JULY, 1956

Anisotropy of the Absorption of Gypsum Crystals in the Infrared Region

G. S. ZAITSEV AND B. C. NEPORENT

(Submitted to JETP editor August 12, 1954)
J. Exper. Theoret. Phys. USSR **29**, 857-863 (December, 1955)

A microscopic adapter and a polarizer were built for the infrared spectrometer, and the anisotropy of absorption and reflection of the gypsum crystals in the region 2-11μ investigated. For a series of spectrum bands corresponding to the vibrations of the molecules of water and $SO_4^{=}$ groups, pleochroism and splitting into variously polarized components were observed. The origins of some bands were determined and conclusions were drawn about the character of coupling of vibrations in the lattice.

1. THE infrared spectra of gypsum crystals have been investigated several times since the end of the last century. The old investigations were reviewed by Shefer and Matossi[1]. Recently Ellis[2] and Louisfert[3] investigated the absorption spectra of gypsum crystals in the wavelength region 0.9-2μ. Miller and Wilkins[4] investigated, together with other inorganic substances, the emulsion of crystalline gypsum powder in an organic oil. Matsumura[5] studied the spectra of a single crystal of gypsum in the region around 3μ.

Also, the Raman spectra of gypsum crystals have been thoroughly investigated. A most thorough investigation of these spectra was made by Krishnan[6]. Investigations in polarized light were carried out by Cabannes and Aynard[7]. They also analyzed the results for vibrations in the 3000 cm^{-1} region.

Gross and Valkov[8] investigated the Raman scattering of gypsum in the region up to 200 cm^{-1}, and they ascribed the detected vibration frequencies to the hydrogen bond.

Stekhanov[9], studying the Raman spectra of gypsum in the region of 3000 cm^{-1}, detected in the neighborhood of the fundamental lines 3486 and 3408 cm^{-1} a number of associated lines at the distance up to 200 cm^{-1}. These lines are ascribed to the intermolecular vibrations.

The purpose of our work was to investigate systematically the anisotropy of the infrared absorption of gypsum crystals in the region of fundamental frequencies.

2. A spectrometer with an auto-collimator provided with a NaCl 70° prism was used in the investigation. The focal distance of the mirrors was 600 mm, the prism height was 70 mm, and the height of the slits up to 30 mm. The radiation detector consisted of a thermo-couple with an electro-optical amplifier.[10] The polarizer was composed of three laminae of selenium, each about 3μ thick. The maximum obtainable polarization exceeds 90%. The polarization planes of the monochromator and the polarizer were parallel to each other. The rotation of the polarization plane with respect to the specimen was realized by the rotation of the latter.

The absorption spectra were obtained by using thin (10-60 μ) sheets of the crystal with a well-defined orientation. The measurements were made by using a microscopic adapter with the spectrometer. The adapter consists of two identical mirror objectives with an aperture of 0.45. The first objective projects a nine-time reduced image of Nernst's rod on the object. The object with the reduced image of Nernst's rod is then magnified nine times and projected by the second objective through the polarizer on the entrance slit of the spectrometer (Nernst's rod appears in its natural size).

---

[1] K. Shefer and F. Matossi, *Infrared spectra*, ONTI, 1935.

[2] J. W. Ellis, Phys. Rev. **38**, 693 (1931).

[3] J. Louisfert, J. Phys. Radium **8**, 22 (1947).

[4] F. A. Miller and H. Wilkins, Anal. Chem. **24**, 1253 (1952).

[5] On Matsumura, Mem. Faculty Sci., Kyusyu Univ, **1B**, 1-3 (1951); Chem. Abst. 4365 i (1952).

[6] R. S. Krishnan, Proc. Ind. Acad. Sci. **A22**, 274 (1945).

[7] J. Cabannes and R. Aynard, J. Phys. Radium **3**, 137 (1942).

[8] E. F. Gross and V. I. Valkov, Dokl. Akad. Nauk SSSR **68**, 473 (1949).

[9] Stekhanov, Dokl. Akad. Nauk SSSR **92**, 281 (1953).

[10] B. P. Kozyrev, Uspehki Fiz. Nauk **44**, 173 (1951).

The use of the micro-adapter was necessary because of the difficulties in preparation of thin sheets of gypsum crystals with various orientations having sufficiently large dimensions. For our measurements specimens of dimensions of 0.2 × 1.5 mm were sufficient.

It is easy to show that, for a given sensitivity threshold of the radiation receiver (which determines the resolving power of the spectrometer), the minimum area of the specimen depends on the aperture of the micro-adapter. The aperture found in micro-objectives for infrared spectrometers is not greater than 0.8, even in objectives of lower image quality. Attempts to use specimens with smaller areas than that determined by the aperture of the micro-adapter and thus not filling completely the monochroator, resulted actually in a sharp reduction of the resolving power of the spectrometer.[11] It should be noticed that, because of its relatively large aperture, the use of the micro-adapter introduces some uncertainty in the results of the experiments. This fact, and also the difficulties in preparation of thin sheets of gypsum crystals having an orientation perpendicular to the principal cleavage plane (010), obliged us to perform a series of measurements by the method of reflection. The source of radiations - Nernst's rod - was projected on the polished surface of the specimen by means of a spherical mirror. By means of a second spherical mirror the image of the source and the surface of the specimen is projected through the polarizer on the entrance slit of the spectrometer. The aperture of the beam is not greater than 0.1; the angle of incidence is 4 °. Under these conditions there is practically no influence of the oblique incidence on the results of the measurements. The polished surfaces had been obtained on a well-developed single gypsum crystal.

3. The gypsum crystal $CaSO_4 \cdot 2H_2O$ belongs to the monoclinic system. The crystal has a laminated structure and the principal cleavage planes separate the layers of water molecules between which the double layers of Ca^{++} ions and of complex ions SO_4^{--} are enclosed..

The structure of an elementary cell of gypsum (Fig. 1) was established by Wooster.[12]

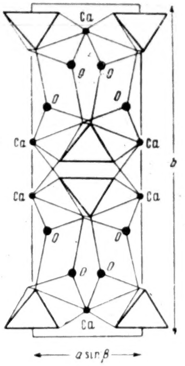

FIG. 1. The unit cell of gypsum according to Wooster. The tetrahedrons represent the SO_4^{--} groups. The positions of the hydrogen atoms of the water molecules are not shown.

Figure 2 (curve *I*) shows the absorption spectrum of a fine gypsum powder $CaSO_4 \cdot 2H_2O$ as compared with the spectrum of $CaSO_4 \cdot 0.5H_2O$ powder (curve *II*) and with the spectrum of anhydrous $CaSO_4$ (curve *III*). It is known that the intense lines in the region 1100-1200 cm^{-1} are related to the vibration of the SO_4^{--} ions. The 1615 cm^{-1} line is obviously caused by deformational vibrations (ν_2) of the crystallization water molecules (in liquid water $\nu_2 = 1640$ cm^{-1}). A weaker line, 1675 cm^{-1}, could be observed in the spectra obtained by several investigators, beginning with Koblentz, but no suggestion was made to explain its origin. The 2220 cm^{-1} line belongs to the crystallization water (Raman frequency); the 2130 cm^{-1} line is due to the SO_4^{--} group (second harmonic of the 1100-1200 cm^{-1} line). In the spectrum band 3300-3600 cm^{-1} very strong absorption is observed. Certainly, here must appear the symmetrical ν_3, and the anti-symmetrical ν_2, vibrations of water molecules (in liquid water ν_1=3450 cm^{-1}; ν_3=3580 cm^{-1}). In the same region also should be situated the harmonics of the 1675, 1615, and 1100-1200 cm^{-1} lines. It is also possible that the 3300-3600 cm^{-1} band is broadened by the presence of hydrogen bonds in the crystal.

---

[11] D. L. Wood, Rev. Sci. Instr. **21**, 764 (1950).

[12] W. A. Wooster, Z. Kristall. **94**, 375 (1936).

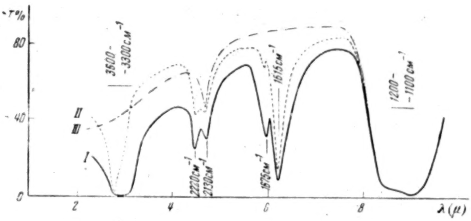

FIG. 2. The absorption spectra of gypsum powders $CaSO_4 \cdot 2H_2O$ (curve *I*), $CaSO_4 \cdot 0.5\,H_2O$ (curve *II*) and $CaSO_4$ obtained by heating to 600° C (curve *III*). *T* is the transmission coefficient of the specimens.

The absorption spectra of a lamina of gypsum 50μ thick, cut parallel to its principal cleavage plane, are represented in Fig. 3. The direction of the light beam coincides in this case with the *b* axis of the crystal. The electric vector was oriented either parallel to the direction of the fibrous cleavage of the crystal (curve II) or perpendicular to it (curve *I*). Curve *III* was obtained for a crystal cut parallel to the *b* axis and to the direction of the fibrous cleavage. The electric vector is in this case perpendicular to the *b* axis. The data obtained indicate a strong anisotropy of absorption of gypsum crystals. It was impossible to obtain a full picture of the directions of maximum absorption for all lines; the attempts to resolve the 3300-3600 cm^{-1} band by using larger dispersion (LiF prism) and smaller thickness of the specimen (up to 2μ) were unsuccessful. It was impossible also to resolve the band around 1100-1200 cm^{-1}. Therefore, an investigation was made of reflection spectra in polarized light. This enabled us to detect many important details. The results of these investigations are represented in Fig. 4. This figure shows also the directions of the incident radiation and of the vibrations of the electric vector.

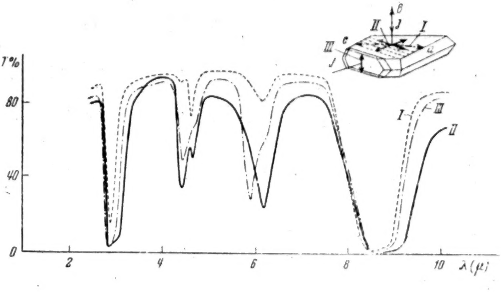

FIG. 3. The absorption spectra of gypsum crystal sheets in polarized light. The orientation of the cuts and the direction of the light polarization are shown in the figure. *T* is the transmission coefficient of the specimens.

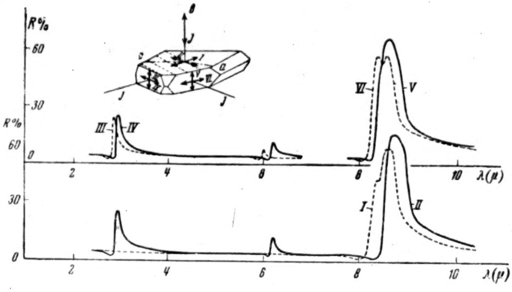

FIG. 4. The reflection spectra of gypsum crystals. The orientation of the polished surfaces and the direction of the polarization are shown in the figure. *R* is the reflection coefficient of the specimen.

The spectrum band 1100-1200cm^{-1} shows a clear anisotropy in the reflection. On curves *I* and *VI* (Fig. 4) two components of this band are resolved. They are situated at about 1180 and 1150 cm^{-1}. A third component appears on graphs *II* and *V*, but it was not possible to resolve it, even when a slit was used with a spectral width of 3 cm $^{-1}$and the crystal cooled to the temperature of the liquid air. The maximum of this component is, according to our estimation, situated at about 1120 cm^{-1}. It should be pointed out that dependence of the maximum on the orientation of the polarization plane is observed also in the second harmonic of the considered vibrations around 2130 cm^{-1} (Fig. 3), but the influence of the neighboring 2220 cm^{-1} line, associated with the crystallization water, makes the study difficult in this case.

The reflection spectra in the region 1615-1675 cm^{-1} shown in Fig. 4 were obtained by taking into account the absorption due to the atmospheric humidity. Here also the dichroism clearly appears. The position of the observed lines, whose maxima are shifted by 5 cm^{-1} in the direction of low frequencies with respect to the lines obtained by absorption, does not depend on the directions of observation and polarization. This is also true for the maxima of reflection in the region of valence vibrations of the water molecules which are situated around 3400 and 3510 cm^{-1}. The second of these maxima is a little deformed because of the superposition of absorption lines of the atmospheric moisture. It is not clear, however, why the broad band of absorption in the region 3000-3600 cm^{-1} appears in the reflection spectrum only in the form of two narrow maxima and, moreover, why the line of absorption observed on curve *I* (Fig. 3) around 3485 cm^{-1} does not appear in the reflection spectrum with corresponding orientation of the electric vector of the incidence radiation. These questions merit further study.

The results discussed above were obtained with an arbitrarily chosen orientation of the electric vector of the incidence radiation. In order to determine the direction of the maximum absorption, the polar diagrams of reflection were measured by rotating the investigated specimen around an axis perpendicular to the reflecting plane without changing the polarization plane. Analogous diagrams were also obtained by absorption. In this case, the spectrometer separated the narrow interval of wavelengths near the maximum of the investigated absorption band. The investigations were made on those specimens which had been used for the measurement of spectra. The obtained curves have a characteristic form of the figure eight. The direction of the greatest absorption coincides clearly with the long of the axis eight.

4. The directions of the absorption maxima were determined for the frequencies 1120, 1150,1180 cm^{-1} associated with the vibrations of atoms of the SO$_4^{--}$ ion, and also for frequencies 1615, 1675, 3400 and 3510 cm^{-1} associated with the vibrations of the molecules of crystallization water. The polar diagrams for the frequencies 1120 and 1180 cm^{-1}, and particularly for the frequency 1150 cm^{-1}, are a little deformed, probably as a consequence of superposition of lines. Nevertheless, the asymmetry of the curves is very great, and the direction of the maximum absorption is defined without ambiguity.

The Table and Fig. 4 show the orientations of the dipoles for fundamental frequencies of vibrations, expressed by means of the angle of elevation ρ and the azimuth φ measured with respect to the axes b and a of the elementary cell of the crystal. The experimental values agree with the values computed on the basis of Wooster's model, according to which eight molecules of water present in the elementary cell of gypsum can be reduced, as a result of the crystal symmetry, to four identical orientations in space. If the dipoles responsible for the infrared absorption of water molecules in the crystal are orientated, as in free molecules, along the diagonal of the triangle H-O-H (ν_1 and ν_2) and along the normal to its plane (ν_3), then for each frequency the four dipoles would be grouped two by two in the directions shown on Fig. 5 and denoted by ν_3 and ν_1, ν_2.

The Directions of the Maximum Absorptions

Vibration Frequency in cm^{-1}	Values calculated on the basis of Wooster's model		Experimental Results	
	ρ_0	φ_0	ρ	φ
3510	40 140	33	0	—
3400	53 127	9	90	3
1675	—	—	0	—
1615	53 127	9	90	3
1180	90	100	90	103
1150	0	—	0	—
1120	90	10	90	25

The directions of the maximum absorption of the lines 1615 and 1675 cm^{-1} coincide with the bisectrices of the angles between the vectors ν_1 and ν_2 Fig. (5).

Both these frequencies should be ascribed to the deformational vibrations of water molecules ν_2; the corresponding line, according to the theory of Davydov,[13] is separated into two mutually perpendicular components. The ratio of intensities of these components is in qualitative agreement with the predictions of the theory. This interpretation agrees with the results obtained by comparison of the spectra of gypsum $CaSo_4 \cdot 2H_2O$ with the spectra of $CaSO_4 \cdot 0.5H_2O$ (Fig. 2). In this last case the line 1675 cm^{-1} is not visible. The observed split of the line 1615-1675 cm^{-1} indicates that deformational vibrations of individual water molecules in the gypsum crystal are not independent of each other and that the absorption and radiation in this special region is linked with the propagation of the excitation wave through the crystal.

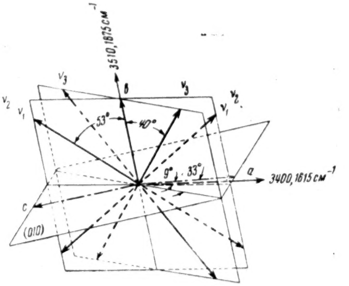

FIG. 5. The directions of the dipoles, corresponding to different vibrations of the water molecules, according to the model of the crystal, Fig. 1. The heavy arrows show the observed direction of the maximum absorption.

One would expect an analogous split of lines related to the valence vibrations of water molecules. In the corresponding region of the spectrum we found, however, the vibrations of two frequencies only: 3510 cm^{-1} oriented (as 1675 cm^{-1}) along the b axis and 3400 cm^{-1} oriented (as 1615 cm^{-1}) in the direction normal to the first one. The first of the frequencies should be related with the asymmetrical (ν_3) and the second with the symmetrical (ν_1), valence vibrations of the water molecules. We did not succeed, however, in detecting second components of these lines. One would conclude therefore from these results that the valence vibrations of individual water molecules in gypsum crystal are independent of each other, and that the excitation by light absorption has a localized character. It still remains unexplained, however, why there is observed for each frequency a single, sharply defined direction of maximum absorption, coinciding with the bisectrix of the smaller angle between the corresponding dipoles (Fig. 5). Inasmuch as the angle between these dipoles is near 90°, with the direction of the incidence light normal to the planes ν_1 and ν_3, the corresponding lines should exhibit only slight anisotropy. It has to be kept in mind that the data considered were obtained only by the reflection method and we see no reason to consider them as complete. It should be noted that Cabannes and Aynard[7], studying the Raman spectrum of gypsum in polarized light, observed also in the same region only two components instead of the expected four. On the other hand, Matsumura[5], whose paper we know only from a digest, discovered in the region of 3μ four components in the absorption spectrum of gypsum crystals. It is thus seen that the spectrum of valence vibrations of crystallization water in gypsum deserves further study.

---

[13] A. S. Davydov, *Theory of Light Absorption in Molecular Crystals*, Trudy. Inst. Phys., Acad. Sci. USSR 1, 1951.

Let us consider the spectrum of the group SO_4^{--}. As known, the vibrations 1100-1200 cm^{-1} have a triple degeneracy. The field of the crystal splits them into three components, which in the slightly perturbed tetrahedron SO_4^{--} should be mutually perpendicular[14]. The orientations of the corresponding dipoles are the same for all SO_4^{--} groups; therefore, it cannot be expected that each of the components would be split.

The orientation of the component 1120 cm^{-1} is not normal to the orientations of two other components (see Table). This deviation exceeds the limits of experimental error and is obviously caused by the asymmetry of the field of the crystal acting on the tetrahedron SO_4^{--}

---

[14] G. Herzberg, *Vibrational and Rotational Spectra of Polyatomic Molecules.*

Translated by E. L. Bergstein
281

Letters to the Editor

Solution of the Equations of Pseudo-scalar Meson Theory with Pseudo-scalar Coupling

I. IA. POMERANCHUK
Academy of Sciences, USSR

(Submitted to JETP editor September 24, 1955)
J. Exper. Theoret. Phys. USSR 29, 869-871
(December, 1955)

THE problem of renormalization of the meson charge g was analyzed in references 1 and 2. It was observed thereby that the expressions determined by Abrikosov and Khalatnikov[3] for the vertex portion Γ, for the nucleon Green's function G, and for the meson Green's function D, are correct only for $g_1^2 \ll 1$ (g_1 is the meson charge prior to re-normalization), as suggested in reference 3, but also for all values of g_1^2.

The proof of this statement contains one point which was not fully analyzed. This concerns the effect of meson-meson scattering at the vertex portion. Even though the simplest diagram *a*, which includes the effect of interest to us (proportional to $[\ln\lambda_p^2\lambda_k^{-2}]^{-1})^*$, is small and cannot play an effective role, nevertheless diagram *b*, which contains one more meson scattering act, turns out to be of the same order as *a*. This raises the problem of summing a large number of various diagrams produced by meson-meson scattering. Although the aggregate of the diagrams can hardly change the conclusion reached in references 1 and 2 that the renormalized meson charge g vanishes, nevertheless reference 2 calls attention to the importance of examining the meson-meson scattering.

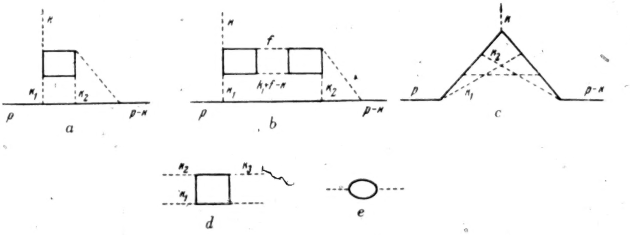

References 1 and 2 employed the double-limit technique developed by Abrikosov and Khalatnikov[3] of cutting-off the divergent terms of the equations that determine G, Γ, and D. The relationship used there for the limiting cut-off momenta for the integration with respect to the nucleon momenta λ_p and the meson momenta λ_k was:

$$\lambda_p: \ln \lambda_p^2\lambda_k^{-2} \gg 1.$$

If this equality is strengthened substantially:

$$\ln \lambda_p^2 m^{-2} \gg \ln \lambda_h^2 m^{-2},\ \lambda_p \to \infty,\ \lambda_h \to \infty, \tag{1}$$

it becomes possible to obtain exact solutions for the equations for G, D and Γ, fully accounting for the meson-meson scattering in such an approximation of a point interaction, considered as a limit of the "spread" interaction[4] with finite λ_p and λ_k. We shall now prove that if equation (1) is used in the pseudo-scalar meson theory with pseudo-scalar coupling, G, D and Γ assume the following values:

$$G = \hat{p}^{-1},\ p^2 \gg m^2. \tag{2}$$

$$\begin{gathered} D = k^{-2}[1 + \pi^{-1} g_1^2 \ln \lambda_p^2 k^{-2}]^{-1},\ \lambda_h^2 \gg k^2 \gg m^2, \\ D = k^{-2},\ k^2 \gg \lambda_h^2; \end{gathered} \tag{3}$$

$$\Gamma(p, p-k; k) = \Gamma_5,\ \lambda_p^2 \gg p^2 \gg m^2, \tag{4}$$

$$\lambda_p^2 \gg (p-k)^2 \gg m^2,\ \lambda_k^2 \gg k^2 \gg m^2,$$

$$\Gamma(p, p-k; k) = 0,\ p^2 > \lambda_p^2 \quad \text{or} \quad k^2 > k_k^2.$$

The only diagram used in equations (2)- (4) is diagram e, contained in the expression for D. We shall now verify that an arbitrary unaccounted diagram is of no significance. Let us examine first an arbitrary n-fold overlapping diagram, contained in $\Gamma(p, p-k; k)$. Let $p^2 \sim (p-k)^2 \sim k^2$. Taking into account that to such a diagram c there corresponds only one logarithmic integration $[p^2 \ll k_1{}^2, k_2{}^2 \ldots k_n{}^2 \ll \lambda_k{}^2]$, we find the value of the operator b, which contains $(n+1)$ D-functions, $(2n+3)$ Γ-functions, and $2(n+1)$ G-functions:

$$b \sim g_1^{2(n+1)} \int\limits_{p^2}^{\lambda_k^2} \frac{dk_1^2}{k_1^2} \left[1 + \frac{1}{\pi} g_1^2 \ln \lambda_p^2 k^{-2}\right]^{-n-1} \tag{5}$$

$$\leqslant \frac{\ln \lambda_k^2 p^{-2}}{[\ln \lambda_p^2 \lambda_k^{-2}]^{n+1}} \ll 1$$

$$[\ln \lambda_p^2 \lambda_k^{-2} = \ln \lambda_p^2 m^{-2} - \ln \lambda_k^2 m_2^{-2} \approx \ln \lambda_p^2 m^{-2}].$$

Here we did not assume $g_1{}^2$ to be small compared with unity. If $n = 0$, we have an aggregate of non-overlapping diagrams equal in the order of magnitude to $\ln(\lambda_k^2 p^{-2}) / \ln(\lambda_p^2 \lambda_k^{-2}) \ll 1$. We see that all the overlapping and nonoverlapping diagrams make a negligible contribution to Γ if (1) is used.

Let us now turn to the meson-meson scattering. The elementary small square (see diagram d) equals $g_1{}^4 \ln \lambda^2{}_p \lambda_k{}^{-2}$, where k^2 is the largest from among $k_1{}^2$, $k_2{}^2$, $k_3{}^2$, $(k_1 + k_2 - k_3)^2$. Accordingly, and also taking into account that only one logarithmic integration corresponds to diagram a [assuming that $p^2 \sim (p-k)^2 \sim k^2$] we obtain in the region $p^2 \ll k_1{}^2 \approx k_2{}^2 \ll \lambda_k{}^2$ the following estimate of the operator a:

$$a \sim g_1^6 \int\limits_{p^2}^{\lambda_k^2} \left[1 + \frac{1}{\pi} g_1^2 \ln \lambda_p^2 k_1^{-2}\right]^{-3} [\ln \lambda_p^2 k_1^{-2}] \frac{dk_1^2}{k_1^2}\cdot$$

$$\leqslant \frac{\ln \lambda_k^2 m^{-2}}{[\ln (\lambda_p^2 m^{-2})]^{-2}} \ll 1.$$

The transition from a to b, involves one more logarithmic integration with respect to f^3, resulting in the factor:

$$g_1^4 \int\limits_{q^2}^{\lambda_k^2} \frac{df^2}{f^2} \left[1 + \frac{1}{\pi} g_1^2 \lambda_p^2 f^{-2}\right]^{-2} \ln \lambda_p^2 f^{-2}$$

$$\approx \frac{\ln \lambda_k^2 m^{-2}}{\ln \lambda_p^2 m^{-2}} \ll 1.$$

We see that condition (1) insures a rapid convergence of the series of consecutive meson-meson scattering acts, making it unnecessary to examine in detail all the meson-meson scattering diagrams.

The above estimates prove the correctness of equations (1)-(3) for any value of $g_1{}^2$. Unlike the case in references 1 and 2, meson-meson scattering is known here to play a negligible role. A consequence of (1)-(2) is the vanishing of the renormalized meson charge.

$$g^2 = g_1^2 [1 + \pi^{-1} g_1^2 \ln \lambda_p^2 m^{-2}]^{-1}$$

$$\to \pi [\ln \lambda_p^2 m^{-2}]^{-2} \to 0.$$

Let us remark that the use of condition (1) simplifies most radically the problem of finding G, D and Γ. The examination given here shows that meson-meson son scattering (without involving the term $\lambda\varphi^4$) does not change the conclusion reached in references 1 and 2, that the renormalized meson charge g vanishes.

Recently Ter-Martirosian, Diatlov, and Sudakov, using a very clever technique, determined the value of aggregate of substantial meson-meson scattering diagrams, and established that in the case when the meson momenta are small compared with certain values of λ, the entire aggregate of the diagrams differs from the simplest diagram d by only a numerical factor. No conditions whatever were imposed here on λ_p and λ_k. The result obtained by Ter-Martirosian, Diatlov, and Sudakov show that the proof that $g = 0$ is independent of the relationship between λ_p and λ_k.

---

[*] We shall use here the symbols of references 1 and 2, except that λ will be used for Λ

[1] I. Ia. Pomeranchuk, Dokl. Akad. Nauk SSSR 104, 51 (1955)

[2] I. Ia. Pomeranchuk, Dokl. Akad. Nauk. SSSR 105, 3 (1955)

[3] A. A. Abrikosov and I. M. Khalatnikov, Dokl. Akad. Nauk. SSSR 103, 993 (1955)

[4] L. D. Landau, A. A. Abrikosov and I. M. Khalatnikov Dokl. Akad. Nauk SSSR, 95, 497 (1954)

Translated by J. G. Adashko
286

Orientation of Planes in Double V° Decay Events

V. M. KHARITONOV
Physical Institute, Academy of Sciences, Armenian SSR

(Submitted to JETP editor August 31, 1955)
J. Exper, Theoret.. Phys. USSR 29, 868-869 (December, 1955)

IN a letter under the same title, Bellam[1] et al considered ten so-called double $V°$ events obtained with a Wilson cloud chamber, two $V°$ decays appearing on the same photograph. The authors assume that both $V°$ particles originated from the same disintegration, and they consider the angles between the plane of their lines of flight and the planes of their decay products. Denoting η_a as the lesser and η_b as the greater of the two angles for a double $V°$ event, the authors plot all ten events as points on an $\eta_b - \eta_a$ plane. Under these circumstances, it turns out that the majority of the points lie in the lower right corner of the graph, i.e., η_a is comparatively small ($< 40°$) as a rule, and η_b is large ($> 40°$ in most cases). On the basis, despite the poor statistics, the authors assume that there is a possibility of some correlation between the directions of the decay planes of the secondary particles and the plane of the $V°$ particles. From this the authors conclude that at least one $V°$ particle has a spin greater than $1/2^2$.

Actually, on the basis of the available statistics and the positions of the points on the graph of reference 1, no conclusions can be made concerning a correlation. From elementary considerations it is apparent that if one does not distinguish the angles for some physical reason, the lesser angles will always be concentrated about a small value, and the larger angles about a large value. For η_a in the interval η_a to $\eta_a + d\eta_a$, and η_b in the interval $\eta_b + d\eta_b$, and for the conditions $\eta_a \leq \eta_b$ and isotropic decay, the probability is

$$\frac{6}{5} \cdot \frac{64}{\pi^4}\left(\frac{\pi}{2} - \eta_a\right)\eta_b\, d\eta_a\, d\eta_b.$$

The figure shows the integral curve of the probabilities W for a number of events lying in the lower right corner of the $\eta_b - \eta_a$ plane, to the right of a line cutting off the axes η_b and η_a with segments γ and $\pi/2 - \gamma$, depending on the magnitude of γ, and plotted with experimental points from reference 1. The arrows show the errors as defined by $\sqrt{N}$. The majority of the experimental points lie satisfactorily close to the calculated curve.

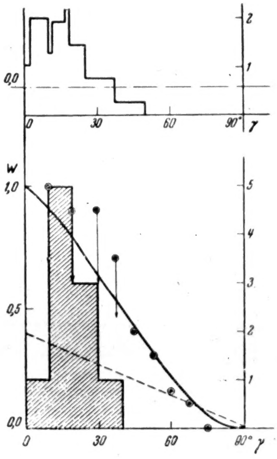

Nevertheless, one can draw certain conclusions concerning the orientations of decay planes if one considers the distribution for angle η_a only. The differential curve of the distribution will appear as a straight line (dotted line in the figure.) Experimental data from reference 1 are shown in the figure in the form of a crosshatched histogram. One may note a grouping of experimental points in the neighborhood of the angle ~ 20°. These values are analogous to those obtained earlier in reference 3 where particles of a definite type $\Lambda_0 \Lambda^-$

were selected (see the upper histogram and the dashed line in the diagram; experimental data are plotted using exact calculations of angle). Analogous grouping is not obtained for angle η_b.

I wish to thank G. S. Saakian for reviewing this communication.

---

[1] J. Bellam, A. L. Hodson, W. Martin, R. Ronald Rau, Geo. T. Reynolds, and S. B. Treiman, Phys. Rev. **97**, 245 (1955).

[2] S. B. Treiman, Geo. T. Reynolds, and A. L. Hodson, Phys. Rev. **97**, 244 (1955).

[3] W. B. Fowler, R. P. Shutt, A. M. Thorndike, and W. L. Whittemore, Phys. Rev. **93**, 861 (1954).

Translated by B. G. Saunders
285

Electroacoustic Waves in a Gas Discharge Plasma with Consideration of Volume Recombination

M. V. Koniukov and Ia. P. Terletskii
Moscow State University

(Submitted to JETP editor, June 12, 1955)
J. Exper. Theoret. Phys. USSR **29**, 874-876 (December, 1955)

IN a previous paper[1] electroacoustic waves were studied, taking into account the production of ionized particles but not considering volume recombination. This occurs along with recombination at walls[2] and plays an important role in some cases (e. g. in molecular gases). The present work deals with the effect of volume recombination on the behavior of electroacoustic waves.

Three possible cases are considered 1. all particles ultimately diffuse to the walls where recombination takes place; 2. recombination takes place only in volume, and 3. both volume recombination and recombination of the walls take place at the same time.

The behavior of the electrons and ions is described by the system of hydrodynamic equations derived earlier[1]. On the assumption that the neutral atoms do not move and that the electrons and ions are separately thermalized, the system of equations becomes (in the notation used earlier)

$$\frac{\partial\sigma^-}{\partial t} + \frac{\partial}{\partial x_\alpha}(\sigma^- v_\alpha^-) = Z^-\sigma^- - R^-\sigma^+\sigma^-, \qquad (1)$$

$$\frac{\partial\sigma^+}{\partial t} + \frac{\partial}{\partial x_\alpha}(\sigma^+ v_\alpha^+) = Z^+\sigma^+ - R^+\sigma^-\sigma^+,$$

$$\frac{\partial}{\partial t}(\sigma^- v_\alpha^-) + \frac{\partial}{\partial x_\rho}(\sigma^- v_\alpha^- v_\rho^-)$$

$$= -\frac{\theta^-}{m^-}\frac{\partial\sigma^-}{\partial x_\alpha} + \frac{e\sigma^-}{m^-}E_\alpha - \alpha_-\sigma^- v_\alpha^-,$$

$$\frac{\partial}{\partial t}(\sigma^+ v_\alpha^+) + \frac{\partial}{\partial x_\rho}(\sigma^+ v_\alpha^+ v_\rho^+)$$

$$= -\frac{\theta^+}{m^+}\frac{\partial\sigma^+}{\partial x_\alpha} - \frac{e\sigma^+}{m^+}E_\alpha - \alpha_+\sigma^+ v_\alpha^+,$$

$$\partial E_\alpha/\partial x_\alpha = 4\pi e(\sigma^-/m^- - \sigma^+/m^+),$$

where $R^-\sigma^+\sigma^-$ and $R^+\sigma^-\sigma^+$ are the mass recombination rates of electrons and ions respectively.

Assuming cylindrical symmetry and neglecting, as before, terms quadratic in the particle velocities, we obtain a set of equations for the relative deviations n^- and n^+ from stationary solutions* $\sigma_0^-(r)$ and $\sigma_0^+(r)$, i.e., setting

$$\sigma^- = \sigma_0^-(1 + n^-), \quad \sigma^+ = \sigma_0^+(1 + n^+), \qquad (2)$$

On replacing $\sigma_0^-(r)$ and $\sigma_0^+(r)$ by their average values over r, the equations become

$$(3)$$

$$\frac{\partial^2 n^-}{\partial t^2} - \frac{\theta^-}{m^-}\frac{\partial^2 n^-}{\partial z^2} + (\alpha_- - Z^- + R^-\overline{\sigma_0^+})\frac{\partial n^-}{\partial t} + \omega_e^2 n^-$$

$$= (\omega_e^2 - \alpha_- R^-\overline{\sigma_0^+})n^+ - R^-\overline{\sigma_0^+}\frac{\partial n^+}{\partial t},$$

$$\frac{\partial^2 n^+}{\partial t^2} - \frac{\theta^+}{m^+}\frac{\partial^2 n^+}{\partial z} + (\alpha_+ - Z^+ + R^+\overline{\sigma_0^-})\frac{\partial n^+}{\partial t} + \omega_i^2 n^+$$

$$= (\omega_i^2 - \alpha_+ R^+\overline{\sigma_0^-})n^- - R^+\overline{\sigma_0^-}\frac{\partial n^-}{\partial t},$$

where ω_e and ω_i are the characteristic frequencies of the electronic and ionic oscillations.

Equations (3) have progressive wave solutions

$$n^- = n_0^- \exp(i\omega t - ikz), \qquad n^+ = n_0^+ \exp(i\omega t - ikz).$$

The dispersion relation between ω and k is determined by the equation:

$$\{k^2 - (m^-/\theta^-)[\omega^2 - i(\alpha_- - Z^- + R^-\overline{\sigma_0^+})\omega - \omega_e^2]\} \tag{4}$$

$$\times\{k^2 - (m^+/\theta^+)[\omega^2 - i(\alpha_+ - Z^+ + R^+\overline{\sigma_0^-})\omega - \omega_i^2]\}$$

$$= (m^-/\theta^-)(m^+/\theta^+)[(\omega_e^2 - \alpha_- R^-\overline{\sigma_0^+})$$

$$+ i\omega R^-\overline{\sigma_0^+}][(\omega_i^2 - \alpha_+ R^+\overline{\sigma_0^-}) + i\omega R^+\overline{\sigma_0^-}]$$

We now consider the three cases mentioned earlier.

1. Volume recombination absent; all electrons and ions produced diffuse to the walls and recombine there. Putting R^- and R^+ equal to zero in Eq. (4), we get

$$\{k^2 - (m^-/\theta^-)[\omega^2 - i(\alpha_- - Z^-)\omega - \omega_e^2]\}$$

$$\times\{k^2 - (m^+/\theta^+)[\omega^2 - i(\alpha_+ - Z^+)\omega - \omega_i^2]\}$$

$$= (m^-/\theta^-)(m^+/\theta^+)\omega_e^2\omega_i^2,$$

in agreement with the earlier result[1].

2. No recombination at walls, the rate of production of particles being in equilibrium with the volume recombination in the stationary state. In this case $Z^- - R^-\sigma_0^+ = Z^+ - R^+\sigma_0^- = 0$, and the dispersion relation becomes

$$[k^2 - (m^-/0^-)(\omega^2 - i\alpha_-\omega - \omega_e^2)]$$

$$\times\quad [k^2 - (m^+/\theta^+)(\omega^2 - i\alpha_+\omega - \omega_i^2)]$$

$$= (m^-/\theta^-)(m^+/\theta^+)[(\omega_e^2 - \alpha R^-\sigma_0^+)$$

$$- i\omega R^-\overline{\sigma_0^+}][(\omega_i^2 - \alpha_+ R^+\overline{\sigma_0^-}) - i\omega R^+\overline{\sigma_0^-}].$$

The zeroth order solutions of this equation are

$$k^2 = (m^-/\theta^-)(\omega^2 - i\alpha_-\omega - \omega_e^2),$$

$$k^2 = (m^+/\theta^+)(\omega^2 - i\alpha_+\omega - \omega_i^2).$$

It is seen that, in contrast to the results of reference 1, there is no variation in the damping coefficient, so that sustained or increasing ionic oscillations are not possible.

3. Both volume and wall recombination present. The zeroth order solutions are

$$k^2 = \frac{m^-}{\theta^-}[\omega^2 - i(\alpha_- - Z^- + R^-\overline{\sigma_0^+})\omega - \omega_e^2],$$

$$k^2 = \frac{m^+}{\theta^+}[\omega^2 - i(\alpha_+ - Z^+ + R^+\overline{\sigma_0^-})\omega - \omega_i^2].$$

Thus the consideration of simultaneous volume recombination and recombination by diffusion to the walls leads to waves with a decreasing damping coefficient. Here, however, in contrast to the previous work, the variation of the damping coefficient depends not just on the rate of ionization but on the difference between that rate and the volume recombination rate.

In summary, it is seen that it is the relative importance of bulk and surface recombination in the stationary state of a gaseous discharge plasma which determines the variation of the damping coefficient of the plasma oscillations with the rate of production of ions. The most rapid decrease in the damping coefficient with increasing ionization occurs when there is negligible diffusion to the walls. The decrease is slower when volume recombination is appreciable and vanishes when it is dominant. Since volume recombination becomes important in discharges in molecular gases it may be expected that no sustained or increasing plasma waves will be possible in them. It should be noted also that in tubes of large section an analogous effect will occur even for a not very large volume recombination rate because of the relative increase of ion loss in volume.

In conclusion we consider it our pleasant duty to thank A. A. Zaitsev for his advice on many questions pertaining to the present paper and also G. V. Spivak for discussions on the physical meaning of the results.

---

* The stationary solutions for this case have been investigated previously[3], starting from the diffusion equation. It is easily shown that the solution in our case has the same form.

[1] M. V. Koniukov and Ia. P. Terletskii, J. Exper. Theoret. Phys. USSR **27**, 542 (1954)

[2] H. Krefft. Phys. Z. **32**, 948 (931); H. Krefft, H. Reger and R. Rompe, Z. techn. Phys. **14**, 242 (1931)

[3] R. Seeliger and A. Kruschke, Phys. Z. **34**, 883 (1933)

Translated by B. Goodman
288

Polarization of the Nuclei of Ferromagnetic Atoms

G. R. KHUTSISHVILI
Institute of Physics
Academy of Sciences, Georgian SSR

(Submitted to JETP editor, July 29, 1955)
J. Exper. Theoret. Phys. USSR 29, 894
(December, 1955)

DURING the past years several indirect methods have been proposed for obtaining oriented nuclei (see references 1,2). Still another method of obtaining polarized nuclei is proposed in the present note.

It is possible to polarize nuclei of ferromagnetic atoms in the following manner. Ferromagnetics which contain nuclei possessing spins are cooled to very low temperatures (for this purpose it is necessary to bring the ferromagnetic into thermal contact with a cooled paramagnetic salt). An external magnetic field exceeding the saturation field is then superimposed on the ferromagnetic. Complete polarization of the shell spins is then obtained.

In turn this brings about a significant polarization of the nuclei (owing to the great magnitude of the field, forming a shell on the nuclei, and also due to the very low temperature) The relaxation of the nuclear spins will be rapid since it is tied in with the interaction of nuclei with the conduction electrons.

The advantage of the ferromagnetic method consists in the fact that by this means a target is obtained free of foreign atoms. The drawback of this method is that it is applicable only for polarization of nuclei of ferromagnetic atoms.

Shchegolev, Alekseevski and Zavaritskii have observed anisotropy in the γ-rays emitted from the nuclei of Co^{60}, when polarized by the ferromagnetic method. At a temperature of the order of 0.05 - 0.08°K intensity, the γ-intensity radiation along the external field is about 10-15% less than in the perpendicular direction.

In conclusion, I wish to express thanks to N. E. Zavaritskii and to I. F. Shchegolev, who reported the results of their measurements.

---

[1] R. J. Blin-Stoyle, M. A. Grace and H. Halban, Progress in Nuclear Physics 3, 63 Pergamon Press, London (1953).

[2] G. R. Khutsishvili, Uspekhi. Fiz. Nauk 53, 381 (1954)

Translated by D. Tarris
300

The Rotation of the Plane of Polarization in Electrolytic Solutions by a Magnetic Field

A. F. KAPUSTINSKII
Institute for General and Inorganic Chemistry,
Academy of Sciences, USSR

(Submitted to JETP editor, April 14, 1955)
J. Exper. Theoret. Phys. USSR 29, 883
(December 1955)

OKAZAKI[1], in a careful study of the Faraday effect, found that in aqueous solutions of strong electrolytes, the effect could be considered as made up of additively of two parts, the so-called molar rotations of the different ions.

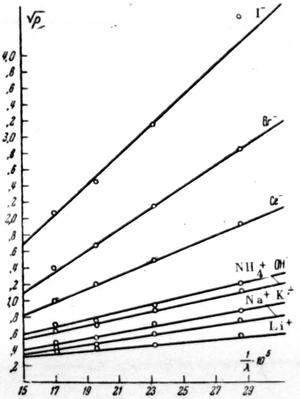

Attention is called here to the increase of the molar rotation ρ with frequency ν of the light which is well represented by the simple relations

Cations: $\nu = A'\rho^{1/2}$,

Anions: $\nu = A''\rho^{1/2} + B$,

A′ and A′′ are constants for a given ion which decrease from ion to ion along with their crystal ionic radii.

Figure 1 shows the agreement of the measured values with the above relations. The values of $\sqrt{\rho}$ were calculated from the data of Okazaki[1] and are also given in the table below.

λ	Li^+	Na^+	K^+	NH_4^+	Cl^-	Br^-	I^-	OH^-
5900	0.378	0.412	0.490	0.632	1.000	1.396	2.057	0.655
5100	0.412	0.458	0.574	0.714	1.204	1.670	2.464	0.728
4300	0.458	0.600	0.707	0.877	1.487	2.145	3.162	0.949
3500	0.583	0.775	0.877	1.127	1.949	2.850	4.470	1.225

---

[1] A. Okazaki, Proc. Phys. - Math. Soc. (Japan) 24, 40 (1942); see also J. Parkington, *A Treatise on Physical Chemistry* (London, 1953) Vol. IV p. 604.

Translated by B. Goodman

Distribution Function of a Non-ideal Bose Gas at the Temperature of Absolute Zero

D. N. ZUBAREV
Mathematical Institute, Academy of Sciences, USSR

(Submitted to JETP editor June 24, 1955)
J. Exper. Theoret. Phys. USSR **29**, 881-882
(December, 1955)

THE distribution function for the momentum molecules of an ideal Bose gas at the temperature of absolute zero has a δ-like character. All the molecules of the gas lie in the lowest energy level with zero momentum. For a non-ideal gas this no longer holds even at absolute zero, owing to the interaction of the molecule with the non zero momentum.

In the work of Bogoliubov and the author[1], the wave function of the lower state of a weakly non-ideal Bose-gas was calculated. In the first approximation it has the form

$$\varphi_0 = \exp\left\{\tfrac{1}{2}\sum_k (1-\lambda_k^{-2})\,\rho_k\rho_{-k}\right\}, \qquad (1)$$

where

$$\rho_k = \frac{1}{\sqrt{N}}\sum_{j=1}^{N}\exp\{-i(kr_j)\}, \qquad (2)$$

$$\lambda_k^4 = \frac{\hbar^2k^2}{V}\left(\frac{N\nu(k)}{4m}+\frac{\hbar^2k^2}{4m}\right)^{-1}, \qquad (3)$$

$\nu(k) = \int\Phi(r)e^{i(kr)}dr$ = Fourier coefficient of energy of interaction $\Phi(r)$, N = number of particles, V = volume of the system, m = mass of the particle.

The function φ_0 corresponds to the zerovibrations of the collective variables ρ_k. By means of this wave function it is possible to find the distribution function for the momentum of molecules of a non-ideal Bose gas. It is possible to show this in the following way. The momentum distribution function permits us to calculate the mean value of operators of the additive type; this depends on the momenta of the particles. If one makes up an arbitrary function of additive type out of the particle momenta:

$$\sum_{j=1}^{N} f(\mathbf{p}_j), \qquad (4)$$

then the determination of its average value leads to the calculation of the integrals over the coordinates of all N particles:

$$N\bar{f} = \frac{\sum\int \varphi_0 f(\mathbf{p}_j)\,\varphi_0\,d\mathbf{r}_1\ldots d\mathbf{r}_N}{\int \varphi_0^2\,d\mathbf{r}_1\ldots d\mathbf{r}_N} \tag{5}$$

$$= N\int w(\mathbf{p})\,f(\mathbf{p})\,d\mathbf{p}\,,$$

where $w(p)$ is the unknown distribution function.

This problem from a mathematical point of view, is similar to the calculation of a contour integral, because we are able to apply the method of computation of integrals of such a type, given in reference 2. If the symmetry of function φ_0 is taken into account, it is sufficient to calculate only one integral, for example $j = 1$. It is convenient to represent the variables ρ_k in the form of a sum of variables ρ'_k (which are constructed exactly as before, but which do not include r_1) and $N^{-1/2}e^{i(kr_1)}$, and then to expand the function in series of these terms. For calculating the integral along $r_2,\ldots,r_N$, it is convenient to consider the ρ'_k as auxiliary variables and take into account their connection with $r_2,\ldots,r_N$, as this was done in reference 2. Finally, the desired integral is represented in a form of a single integral over p. Comparing the coefficients for the arbitrary function $f_{(p)}$, we obtain the distribution function $W(p)$.

Not stopping for details of calculation, which will be given in a later paper, we set forth only the final results of the computations. The distribution function of molecules of a Bose gas of momentum $p = \hbar k$ at the temperature of absolute zero has the form

$$w(\mathbf{p}) = C\delta(\mathbf{p}) + \frac{v}{4(2\pi\hbar)^3}(1-\lambda_p^{-2})\,\lambda_p^2\,, \tag{6}$$

$$C = 1 - \frac{v}{4(2\pi\hbar)^3}\int'(1-\lambda_p^{-2})^2\,\lambda_p^2\,d\mathbf{p}, \tag{7}$$

where $v = V/N$. The distribution function (6) was obtained on the assumption of weak interaction between particles. It agrees with the distribution function of a slightly non-ideal Bose gas, as determined by Bogoliubov[3]. Here we obtained it by another method, that is, we did not utilize a δ-like momentum distribution by way of a zero approximation.

The quantity $\lambda^2{}_k$ is connected with the correlation function $g(r)$

$$g(\mathbf{r}) = 1 + \frac{1}{V}\sum_k(\lambda_k^2 - 1)\,e^{i(kr)}, \tag{8}$$

which is not difficult to determine, if one takes into account that the correlation function for the lower state is proportional to the variation derivative of the energy of the lower state for the interaction function[1]. It is possible to determine $\lambda^2{}_k$ from experimental data on the scattering of slow neutrons in He II[4]; however, in this case it is impossible to compute the small interaction.

---

[1] N. N. Bogoliubov and D. N. Zubarev, JETP **28**, 129 (1955); Soviet Phys. **1**, 83 (1955)

[2] D. N. Zubarev, Dokl. Akad. Nauk. SSSR **45**, 757 (1954)

[3] N. N. Bogoliubov, Izv. Akad. Nauk SSSR, Ser. Fiz. **11**, 77 (1947)

[4] R. P. Feynman, Phys. Rev. **94**, 262 (1954)

Translated by A. A. Silvidi
292

Towards a Statistical Theory of Fission Width

V. G. Nosov
Academy of Sciences, USSR

(Submitted to JETP editor March 30, 1955)
J. Exper. Theoret. Phys. USSR **29**, 880-881
(December, 1955)

AN estimate of fission width has been obtained in a series of works[1,2]. This letter presents the possibility of examining the connection between different rates of fission width, and also of defining it more accurately and extending the field of its applicability.

In the work of Bohr and Wheeler[1], the rate was obtained by application of the methods of classical statistics:

$$\Gamma_f \cong \frac{D}{2\pi}\,N^*(E - E_f), \tag{1}$$

where D is the separation of levels; N^* is the number of levels which are bound. By $N^*(E)$ is understood the number of levels with energy of excitation not exceeding E. In the immediate neighborhood of the fission energy E_f we have $N^*(E-E_f) \cong 1$ and, therefore,

$$\Gamma_f \sim D/2\pi. \tag{2}$$

As is known[3], the classical statistics are applicable for the condition $T >> \hbar\omega$, where T is the temperature and ω is the vibration frequency of the nuclear configuration, associated with fission. In the region $T << \hbar\omega$ it is impossible to use the estimates (1) and (2). In this region, in order to make an estimate of the fission width, valid in all temperature intervals, we represent it in the form $\Gamma f \simeq (\hbar\omega/2\pi)w$ where w is the probability density on the dividing degree of freedom of the energy, exceeding the fission threshold E_f. We estimate this probability, having applied a microcanonical distribution[3] to the nucleus. This distribution takes into account not only the law of conservation of energy, but also the law of conservation of momentum—all states, compatible with the conservation laws, being equally probable. Finally, we obtain

$$\Gamma_f \cong \frac{\hbar\omega}{2\pi}\,\frac{N^*(E-E_f)}{N^*(E)} \tag{3}$$

As it was shown by Landau[4], the density of levels with fixed moment varies, in principle, according to the law $e^{S(E)}$ where S is the entropy. Since $dS/dE = 1/T$, we have $N^*(E) \cong T/D^*$ where D^* is the separation of the levels, which are bound. In view of the fact that, near the threshold, $N^*(E-E_f) \cong 1$, we obtain

$$\Gamma_f \sim (\hbar\omega/T)(D^*/2\pi). \tag{4}$$

In the classical region, $T >> \hbar\omega$, the estimates (3) and (4) pass to that obtained by Bohr and Wheeler (1) and (2), since in this case, as it is not difficult to see, $D^* \cong (T/\hbar\omega)D$. On the other hand, in the opposite limiting case $T << \hbar\omega$ we have $D^* = D$ and therefore,

$$\Gamma_f \sim (\hbar\omega/T)(D/2\pi). \tag{5}$$

The actual values of the quantities $\hbar\omega$ and T for heavy nuclei are not known with any accuracy. We assume for computation that both these values are of the order of 1 mev; however, they can vary several fold. From this point of view the estimate (2) must be considered as the lower estimate of the fission width.

If the full energy of the composite nucleus E significantly surpasses the fission energy, then, as it is not difficult to see from (3)

$$\Gamma_f \sim \frac{\hbar\omega}{2\pi}\exp\left\{-\frac{E_f}{T}\right\}.$$

This rate was also obtained by Kramers[2]; evidently, it is not applicable in the immediate vicinity of the fission threshold.

---

[1] N. Bohr and J. Wheeler, Phys. Rev. 56, 426 (1939)

[2] H. Kramers, Physica 7, 284 (1940)

[3] L. Landau and E. Lifshitz, *Statistical Physics*, State Technical Publication, 1951

[4] L. Landau, J. Exper. Theoret. Phys. USSR **7**, 819 (1937)

Translated by A. A. Silvidi
291

Radiation of Molecules in the Presence of a Strong High-Frequency Field

V. M. FAIN
Gorki State University

(Submitted to JETP editor July 11, 1955)
J. Exper. Theoret. Phys. USSR **29**, 878-880
(December, 1955)

THE absorption of high-frequency radiation in a molecular gas was examined in references 1,2. It will be shown in the present paper that, besides the absorption (and saturation of levels) at a frequency $\omega \approx \omega_{12} = (E_1 - E_2)/h \equiv \omega_0$ (E_1 and E_2 are energy levels of the molecules), there appears a radiation at a frequency Ω_0 [see Eq. (6)], which depends on the matrix element of the dipole moment, corresponding to the transition $E_1 \rightarrow E_2$, and on the field potential of the frequency ω.

We assume that the following conditions are satisfied[1-3]: a) $T \ll 1/\omega \ll \overline{\tau}$, where T is the duration of the molecular collision, and τ is the mean time between collisions; b) $|\omega - \omega_0| \lesssim 1/\tau$ and $|\omega - \omega_{mn}| \gg 1/\tau$, where $m, n = 1,2$; c) molecular collisions re-establish the Boltzman energy distribution; d) $\omega_0 \gg \Omega_0$.

For any ensemble of quantum mechanical systems the density matrix satisfies the following equation:

$$i\hbar\,(\partial\rho/\partial t) = H\rho - H\rho. \qquad (1)$$

In our case the Hamiltonian H of the molecule in the external field $F(t) = F\sin\omega t$ equals

$$H = H_0 - \vec{\mu}F(t) = H_0 + V\sin\omega t, \qquad (2)$$

where H_0 is the Hamiltonian of the free molecule, and $\vec{\mu}$ is the operator of the dipole moment. Selecting the representation in which H_0 is diagonal, we get

$$ih\frac{\partial\rho_{mn}}{\partial t} = \sin\omega t\sum_l (V_{nl}\rho_{lm} - \rho_{nl}V_{lm}). \qquad (3)$$

where $n, m = 1,2$ [according to condition (b)].

According to condition (c), at the moment of collision $t = t_0$:

$$\rho_{12} = \rho_{21} = 0, \quad D \equiv \rho_{22} - \rho_{11} = D_0, \qquad (4)$$

where $D_0 = \rho^0_{22} - \rho^0_{11}$ is the difference in the populations of levels E_2 and E_1 for a free molecule.

In satisfying the conditions (a) and (d) the solution of equation (3), which satisfies the initial condition (4), assumes the form^2:

$$D = D_0(h\Omega_0)^{-2}\{|V_{12}|^2\cos\Omega_0(t - t_0) + (h\delta)^2\}, \qquad (5)$$

where

$$\Omega_0^2 = h^{-2}|V_{12}|^2 + \delta^2, \quad \delta = \omega_0 - \omega. \qquad (6)$$

The mean dipole moment of a molecule equals

$$\langle\mu\rangle = \mathrm{Sp}\,(\rho\vec{\mu}) = \rho_{11}\vec{\mu}_{11} + \rho_{22}\vec{\mu}_{22} + \rho_{12}\vec{\mu}_{21} + \rho_{21}\vec{\mu}_{12}. \qquad (7)$$

On the basis of the correspondence principle we are now in the position to find the radiation from and absorption by the molecular gas. The last two terms in (7) show the contribution to the absorption of electromagnetic radiation of the frequency ω[1,2] We are going to examine, therefore, the first two terms of (7):

$$\langle\vec{\mu}_1\rangle = \rho_{11}\vec{\mu}_{11} + \rho_{22}\vec{\mu}_{22} = {}^1/_2\,[\vec{\mu}_{11} \qquad (8)$$

$$+ \vec{\mu}_{22} + (\vec{\mu}_{22} - \vec{\mu}_{11})\,D_0\Omega_0^{-2}\delta^2]$$

$$+ \frac{1}{2}\,\frac{(\vec{\mu}_{22} - \vec{\mu}_{11})\,D_0\,|V_{12}|^2}{h^2\Omega_0^2}\cos\Omega_0(t - t_0).$$

Here we have used Eq. (5) and the fact that $\rho_{11} + \rho_{22} = 1$. The contribution to radiation is given by the variable part of $<\vec{\mu}_1>$

$$\langle\vec{\mu}\rangle = \vec{\mu}_0\cos\Omega_0(t - t_0), \qquad (9)$$

$$\vec{\mu}_0 = {}^1/_2\,(\vec{\mu}_{22} - \vec{\mu}_{11})\,D_0\,(h\Omega_0)^{-2}\,|V_{12}|^2.$$

Taking into account that the times between the collisions τ are distributed according to the law

$$w(\tau)\,d\tau = (1/\bar{\tau})\,e^{-\tau/\bar{\tau}}\,d\tau,$$

it is possible to find the spectral intensity of the radiation

$$I(\Omega) \backsim [(\Omega_0 - \Omega)^2 + \bar{\tau}^{-2}]^{-1}. \qquad (10)$$

The total radiation intensity equals

$$I_{\mathrm{total}} = (\Omega_0^4/3c^3)\,\mu_0^2. \qquad (11)$$

It is easy to understand the origin of the radiation at the frequency Ω_0 of Eq. (6) on the basis of simple quantum electrodynamic considerations. The system consisting of molecules and an electromagnetic field is actually described by the Hamiltonian $\mathcal{H} = H_0 + H^0_\gamma + {}^1\!/\!_2 V$, where H^0_γ is the Hamiltonian of the free field, and $V/2$ is the energy of interaction [the coefficient 1/2 is necessary to maintain consistency with Eq. (2)]. We shall try to find the solution of the equation

$$\mathcal{H}\psi = \mathcal{E}\psi \qquad (12)$$

in the form of superposition of the solutions of the equation

$$(H_0 + H^0_\gamma)\,\psi^{(0)} = \mathcal{E}^{(0)}\,\psi^{(0)}. \qquad (13)$$

We write

$$\psi = c_1\psi_1^{(0)} + c_2\psi_2^{(0)}, \qquad (14)$$

$$\psi_1^{(0)} = \psi_{1m}^{(0)}\,\Phi_{N_0}(N); \quad \psi_2^{(0)} = \psi_{2m}\,\Phi_{N_0+1}(N);$$

$$\mathcal{E}_1^{(0)} = E_1 + N_0 h\omega; \quad \mathcal{E}_2^{(0)} = E_2 + (N_0 + 1)\,h\omega;$$

$$\mathcal{E}_1^{(0)} \approx \mathcal{E}_2^{(0)},$$

where $\psi^{(0)}_{1m}$, $\psi^{(0)}_{2m}$ are wave functions of the free molecule $\Phi_{N_0}(N)$, $\Phi_{N_{0+1}}(N)$ are wave functions of the free field, and N is the number of photons. Substituting (14) in (12), multiplying first by $\psi^{(0)*}_1$, then by $\psi^{(0)*}_2$, and integrating, we get two equations. The condition of their consistency gives:

$$\mathcal{E}_{1,2} = {}^1\!/_2\,(\mathcal{E}^{(0)}_1 + \mathcal{E}^{(0)}_1) \pm {}^1\!/_2 \sqrt{(\mathcal{E}^{(0)}_1 - \mathcal{E}^{(0)}_2)^2 + |V_{12}|^2}$$

Transitions of the system molecule + field with radiation of quanta of energy $\mathcal{E}_1 - \mathcal{E}_2 = h\Omega_0$ are thus possible. It is also not difficult to demonstrate that the matrix element of the dipole moment corresponding to the transition at the frequency Ω_0 is proportional to $\vec{\mu}_{22} - \vec{\mu}_{11}$.

Let us note that the measurements of the frequency Ω_0 offer the possibility of the experimental determination of the matrix element $|V_{12}|$, which is proportional to the product of the dipole moment and the magnitude of the field intensity F. Such measurements offer a method for the precise determination of the field intensity of frequency ω, if the matrix element $|\vec{\mu}_{12}|$ is known. If conversly, the field intensity of frequency ω is known with sufficient precision, it is possible to determine $\vec{\mu}_{12}$ precisely.

Let us evaluate the order of magnitude of possible frequencies $\Omega_0 \sim |\vec{\mu}_{12}|F/h$. Let $|\vec{\mu}_{12}| \sim 10^{10}\,\mathrm{sec}^{-1}$ and $F = 1$ cgs unit = 300 v/cm; then $\Omega_0 \sim 10^9\,\mathrm{sec}^{-1}$. If, however, $F = 10$ cgs units, then $\Omega_0 = 10^{10}\,\mathrm{sec}^{-1}$. By changing the field intensity at the frequency ω, we can change the frequency Ω, which presents some convenience in the experimental handling of the problem.

In conclusion, let us note that radiation at the frequency Ω_0 will be observed only for molecules whose dipole moments $\bar{\mu}_{11}$ and $\vec{\mu}_{22}$ differ from zero.

---

[1] R. Karplus and J. Schwinger, Phys. Rev. 73, 1020 (1948)

[2] H. Snyder and P. Richards, Phys. Rev. 73, 1178 (1948).

[3] J. Van Vleck and V. Weisskopf Rev. Mod. Phys. 17, 227 (1945).

Translated by S. Feitelberg

Anomalous Skin Effect with Arbitrary Collision Integral

M. Ia. Azbel' and E. A. Kaner
Physico-Technical Institute, Academy of Sciences, Ukrainian SSR

(Submitted to JETP editor July 14, 1955)
J. Exper. Theoret. Phys. USSR **29**, 876-878
(December, 1955)

In previous publications[1,2] an expression was obtained for the surface impedance of metal in the case of anomalous skin effect*. It was then assumed that the integral of collisions can be written with the help of the relaxation time τ in the form:

$$(\partial f/\partial t)_{st} = (f - f_0)/\tau, \tag{1}$$

where f is the electron distribution function, $f_0(\epsilon)$ is the Fermi equilibrium distribution function.

Introduction of the relaxation time can be rigorously established only at high temperatures ($T \gg \Theta$, Θ the Debye temperature). At lower temperatures, the collision integral, in general, cannot be written in form (1), and one must consider an arbitrary collision integral. In the present contribution it is proved that the formula for impedance, obtained in reference 1, is valid for an arbitrary collision integral. Let us note that the left-hand member of (1) is not assumed to be small in comparison with ωf (ω – frequency of external field).

The complete system of equations has the form:

$$\frac{d^2E_\alpha(z)}{dz^2} = \frac{4\pi i\omega}{c^2}\frac{2e^2}{(2\pi\hbar)^3}\int n_\alpha\,[\psi(z;\,\mathbf{n}) - \psi(z;\,-\mathbf{n})]\,dS_p{}^*; \tag{2}$$

$$n_z\frac{\partial\psi(z;\,\mathbf{n})}{\partial z} + \check{L}^{-1}\psi(z;\,\mathbf{n}) = E_\beta(z)\,n_\beta \equiv E_x n_x + E_y n_y; \tag{3}$$

$$\psi(z;\,\mathbf{n})|_{z=+\infty} = 0,$$

$$\psi(0;\,n_x,\,n_y,\,n_z) = q\psi(0;\,n_x,\,n_y,\,-n_z);\quad n_z > 0$$

$$\mathbf{n} = \mathbf{v}/v;\quad \mathbf{v} = \nabla_{\mathbf{p}}\varepsilon(\mathbf{p}). \tag{4}$$

Here $-e(\delta f_0/\delta\epsilon)\,\psi\exp(i\omega t)$ is an addition to the equilibrium distribution function of distribution $f_0(\epsilon)$; $E_\alpha(z)\exp(i\omega t)$ - are the components of the electric field inside the metal; $\check{L}^{-1} = v^{-1}[(\delta/\delta t)_{st} + i\omega\check{I}]$ is operator of the free path length ($\check{I}$ – unit operator)$^{+}$; ϵ, $\mathbf{p}$, $\mathbf{v}$ are the energy, quasi-momentum and velocity of electrons. The parameter q in (4) characterizes reflection of electrons from the surface of metal ($q = 0$ corresponds to diffuse and $q = 1$ to specular reflection). Integration with respect to $dS_\mathbf{p}$ in (2) and below is carried out for all momenta on the Fermi surface $\epsilon(\mathbf{p}) = \epsilon_0$, $n_z \geq 0$.

Axis OZ coincides with the direction of internal normal to the surface of metal.

Writing equation (3) separately for $\psi(z;\mathbf{n})$ and $\psi(z;-\mathbf{n})$ and eliminating $\psi(z;\mathbf{n}) + (z;-\mathbf{n})$, we will obtain an equation for the function $\psi_-(z;\mathbf{n}) = \psi(z;\mathbf{n}) - \psi(z;-\mathbf{n})^{++}$, which determines this current density

$$\frac{\partial^2\psi_-(z;\mathbf{n})}{\partial z^2} - \frac{1}{n_z^2}\check{L}^{-2}\psi_-(z;\mathbf{n}) = \frac{2}{n_z^2}E_\beta(z)\,\check{L}^{-1}n_\beta. \tag{5}$$

In this equation the fact that the main contribution to the current density in the anomalous skin effect comes from electrons with small n_z has been taken into account (see references 1,2). Therefore we may consider that the operator $\check{L}$ acts on functions whose values are taken on the curve $n_z = 0$ on the the Fermi surface.

Continuing functions $E_\alpha(z)$ and $\psi_-(z;\mathbf{n})$, as even functions, into the region of negative z, and going over to Fourier transforms, we find:

$$\mathscr{E}_\beta(t)\left\{t^2\delta_{\alpha\beta} + \frac{4\pi i\omega}{c^2}\frac{2e^2}{(2\pi\hbar)^3}\right. \tag{6}$$

$$\left.\times\int 2n_\alpha[\check{I} + t^2n_z^2\check{L}^2]^{-1}\check{L}n_\beta\,dS_\mathbf{p}\right\}$$

$$= -2E_x'(0) + \frac{4\pi i\omega}{c^2}\frac{2e^2}{(2\pi\hbar)^3}$$

$$\times\int 2n_z^2n_x[\check{I} + t^2n_z^2\check{L}^2]^{-1}\check{I}^2\psi'(0;\mathbf{n})\,dS_\mathbf{p},$$

where $\mathscr{E}_\alpha(t) = \int\limits_{\infty}^{\infty} E_\alpha(z)\exp(-itz)\,dz$ is the Fourier transform of the component of the electric field ($\alpha = x, y$).

Analogously to what was done in references 1,2 it can be shown that the asymptotic expression for the surface impedance, in the limiting case of the anomalous skin effect, is obtained by replacing the integrals in (6) by their asymptotic expressions for large t. In the process the operator $\check{L}$ drops out. In fact, for large t, since operators L and $[\check{I} + t^2n_z{}^2\check{L}^2]^{-1}$ commute,

$$\int n_\alpha[\check{I} + t^2n_z^2\check{L}^2]^{-1}\check{L}n_\beta\,dS_\mathbf{p}$$

$$\approx \frac{1}{t}\int\limits_0^{2\pi}\frac{n_\alpha(\varphi)\,d\varphi}{K(\varphi,\pi/2)}\left\{\int\limits_0^\infty dx\,[\check{I} + x^2\check{L}^2]^{-1}\check{L}\right\}n_\beta(\varphi);$$

$$\left\{\int\limits_0^\infty dx\,[\check{I} + x^2\check{L}^2]^{-1}\check{L}\right\}n_\beta(\varphi)$$

$$= \{\operatorname{arc\,tg} x\check{L}\}_{x\to\infty}n_\beta(\varphi) = \frac{\pi}{2}n_\beta(\varphi).$$

Here $K(\varphi,\vartheta)$ – Gauss curvature of the Fermi surface; α, ϑ – angles of a spherical coordinate system in the velocity space: $\mathbf{n} = (\sin\vartheta\cos\varphi;\ \sin\vartheta\sin\varphi;\ \cos\vartheta)$;

$$n_x(\varphi) = \cos\varphi;\quad n_y(\varphi) = \sin\varphi;$$

$$dS_\mathbf{p} = \sin\vartheta\,d\vartheta\,d\varphi\,/\,K(\varphi,\vartheta).$$

In a similar way one can calculate the asymptotic value of the second integral in Eq. (6).

As a result we arrive at the following integral equation for $\mathscr{E}_\alpha(t)$:

$$\mathscr{E}_\alpha(t) = \frac{-2E_\alpha'(0) + (1-q)\,i\dfrac{6\omega}{c^2}B_\alpha\displaystyle\int\limits_0^\infty\frac{\ln t - \ln\tau}{t^2-\tau^2}\mathscr{E}_\alpha(\tau)\,d\tau}{t^2 + i(3\pi^2\omega/c^2)(B_\alpha/t)}, \tag{7}$$

where B_α is the principal value of the tensor

$$B_{\alpha\beta} = \frac{8e^2}{3(2\pi\hbar)^3}\int_0^{2\pi}\frac{n_\alpha(\varphi)\,n_\beta(\varphi)\,d\varphi}{K(\varphi,\pi/2)}, \tag{8}$$

and the axes X and Y are chosen along its principal axes.

The integral equation (7) is independent of the form of the collision integral and, in particular, coincides with the equation that was obtained when we introduced the relaxation time τ. Therefore we may use immediately the results of the previous work[1] and write down the surface impedance Z_α in the limiting cases of diffuse ($q = 0$) and specular ($q = 1$) reflections of electrons from the surface of the metal:

$$Z_\alpha = R_\alpha + iX_\alpha = -\frac{4\pi i\omega}{c^2}\frac{E_\alpha(0)}{E'_\alpha(0)} \tag{9}$$

$$= \begin{cases} \left(\sqrt{3}\,\dfrac{\pi\omega^2}{c^4B_\alpha}\right)^{1/3}(1+i\sqrt{3}); & q=0. \\ \dfrac{8}{9}\left(\sqrt{3}\,\dfrac{\pi\omega^2}{c^4B_\alpha}\right)^{1/3}(1+i\sqrt{3}); & q=1. \end{cases}$$

$$X_\alpha / R_\alpha = \sqrt{3}. \tag{10}$$

Examination of the integral equation (7) shows that formulas (9) and (10) for the surface impedance are valid with accuracy to within a small numerical factor of the order of unity, for arbitrary linear relation between $\psi(0; n_x, n_y, n_z)$ and $\Psi(0; n_x, n_y, -n_z)$ on the boundary metal - vacuum.

Thus, in the region of the anomalous skin-effect dependence of the surface impedance upon frequency ($Z_\alpha \sim \omega^{2/3}$), its independence of temperature, and relation (10) are all valid not only for arbitrary law of dispersion of electrons $\epsilon = \epsilon(p)$, but also for arbitrary collision integral and any relation $\psi(0; n_x, n_y, n_z[= Q\psi(0; n_x, n_y, -n_z)$ at the boundary metal-vacuum.

In conclusion the authors wish to avail themselves of this opportunity to thank I. M. Lifshitz for the discussion of their results.

---

[*] Anomalous skin effect occurs at high frequencies and low temperatures, when the mean free path of electrons is large compared with the depth of penetration of the field into metal.

[**] Here use is made of the spherical symmetry of Fermi surface.

[+] All operators operate on functions in momentum space.

[++] In so doing we consider that the collision operator has a center of symmetry.

[1] M. I. Kaganov and M. Ia. Azbel', Dokl. Akad. Nauk SSSR **102**, 49 (1955).

[2] G. E. Reuter and E. H. Sonderheimer, Proc. Roy. Soc. (London) **195**, 336 (1949).

Translated by B. Podolsky
289

The Internal Compton Effect

A. M. IAKOBSON
Moscow State Teachers' Institute

(Submitted to JETP editor March 18, 1955)
J. Exper. Theoret. Phys USSR **29**, 703-705
(November, 1955)

THIS letter deals with some conclusions which can be drawn from the theoretical analysis of the internal Compton effect.

In the internal Compton effect, a nucleus jumps from an excited to the ground state, with the result that the atom is ionized and a gamma ray radiated. The emission of an electron and a gamma ray when the nucleus de-excites itself is due to the interaction of the electron with the nucleus and the electromagnetic field: i.e., it is a third order effect. This is presumably why the effect has not been observed till recently. It was in 1953 that Brown and Stump[1] saw a continuous spectrum accompanying internal conversion.

The internal Compton effect was analyzed in reference 1 by use of nonrelativistic perturbation theory, i.e., with the restriction that the energy difference between the excited and ground states was much less than the electron rest energy. In the perturbation theory approach, the internal Compton effect is of third order and considered to take place in the following steps: a virtual gamma ray emitted by the nucleus is scattered from the atomic electrons and as a result a real gamma ray is radiated and an electron ionized.

The initial state (1) of the system consists of an excited nucleus, an electron in its ground state and no quanta. In the final state (2) the nucleus is in its ground state, the electron is in an excited (ionized) state and a gamma ray has been emitted. The perturbation was taken to be the nonrelativistic interaction between a charged particle and the electromagnetic field. Nonrelativistic hydrogen-like wave functions were used for the electrons. The electromagnetic field was quantized with spherical waves. Since the matrix elements of the gamma ray annihilations and creation operators are nonzero only for one quantum transition, the transition of the system from its initial to its final state can take place only through two intermediate states. For example, the nucleus emits a quantum $\hbar c'k'$ and drops to a lower state, which corresponds to the first intermediate state of the system; then the electron absorbs the emitted quantum, and so takes the system into its second intermediate state. After this the electron jumps into its final state, emitting a quantum $\hbar ck$. Thus the matrix element for the transition 1-2 takes the form

$$V_{12}=\sum\frac{V_{1\mathrm{I}}V_{\mathrm{I}\,\mathrm{II}}V_{\mathrm{II}\,2}}{(E_1-E_{\mathrm{I}})(E_1-E_{\mathrm{II}})},$$

where the indices I and II label the intermediate states of the system. The sum is over the nine possible pairs of intermediate states.

The calculations of reference 1 show that the probability of the internal Compton effect is very small, differing from zero only because of the nuclear multipole field. The effect is described by a differential coefficient, which is defined as the ratio of the probability that the process considered takes place to the probability of gamma ray emission when the nucleus makes the same transition. General expressions for these ratios are obtained, relating the various possible types of internal Compton effect to the different possible (electric and magnetic multipole) transitions and the parity of the emitted gamma ray. As is to be expected, these coefficients can be calculated without knowing nuclear ψ-functions and are theoretically obtained independently of any model for nuclear structure.

The final computations of the differential coefficient for the internal Compton effect with the K electrons were made using the Born approximation for the final electron state; only the long wavelength part of the continuous gamma ray spectrum was considered.

It was shown that in the nonrelativistic case, only the internal Compton effect associated with the emission of a dipole gamma ray is of practical importance. The following analytic expressions for the differential coefficient of the internal Compton effect with K electrons were obtained:

$$d\beta_K^{\mathrm{I}}=\frac{8}{3\pi}\left(\frac{l}{l+1}\right)\alpha^2\,[Z\alpha]^3\left[\frac{2mc^2}{\Delta E}\right]^{l+1/2}\frac{dE_K}{E_K},$$

$$d\beta_K^{\mathrm{M}}=\frac{8}{3\pi}\alpha^2\,[Z\alpha]^3\left[\frac{2mc^2}{\Delta E}\right]^{l+1/2}\frac{dE_K}{E_K},$$

where $d\beta_K^{\partial}$ and $d\beta_K^{\mathrm{M}}$ are the differential coefficients of the Compton effect connected with electric and magnetic multipole nuclear transitions, respectively; ΔE is the difference in energy between the excited and ground states of the nucleus; E_K is the energy of the emitted gamma ray; mc^2 is the rest energy of the electron; $\alpha=e^2/\hbar c$ the fine structure constant; Z the nuclear charge and l the angular momentum quantum number which characterizes the multipolarity of the nuclear transition.

We can use this interesting result to compare the differential coefficient of the internal Compton effect with the coefficient of internal conversion. The ratios of the differential coefficient of the internal Compton effect to the corresponding coefficient α_K for internal conversion, connected with the same type of nuclear transition, are all equal and do not depend on the multipole order or on the nuclear charge:

$$\frac{d\beta_K^{\partial}}{\alpha_K^{\partial}}=\frac{d\beta_K^{M}}{\alpha_K^{M}}=\frac{4\alpha}{3\pi}\left[\frac{\Delta E}{mc^2}\right]\frac{dE_K}{E}$$

This suggests that there is a simple connection between the internal Compton effect and the internal conversion process. Indeed, this connection follows from the semi-classical theory of Wang Chang and Falkoff[3], which describes the continuous gamma spectrum associated with beta decay, if we assume that the probability of the internal Compton effect is equal to the product of the probability of internal conversion and the probability that the conversion electron emits a gamma ray as it is knocked out of the atom. The full agreement between the quantum mechanical calculation and the semi-classical theory shows that for small gamma ray energies the internal Compton effect can be considered as two successive, independent processes: internal conversion and subsequent emission of a gamma ray by the emitted electron. This picture of the internal Compton effect also explains why the experimental results of Brown and Stump agree so well with the predictions of a semi-classical theory.

After the present work was finished, a paper[4] appeared on the internal Compton effect associated with a magnetic multipole transition. In this paper the differential coefficient for the particular nuclear transition considered was calculated using Born approximation but without the restriction to nonrelativistic energies. In the overlap region between this paper and the present work, the two results are identical.

---

[1] A. M. Iakobson, Dissertation, Moscow State Teachers' Institute, 1954

[2] H. B. Brown and R. Stump, Phys. Rev. **90**, 1061 (1953)

[3] Wang Chang and Falkoff, Phys. Rev. **76**, 365 (1949)

[4] Larry Spruch and G. Goertzel, Phys. Rev. **94**, 1671 (1954)

Translated by R. Krotkov
261

Radiative Capture of Thermal Neutrons without Formation of a Compound Nucleus

L. K. PEKER

(Submitted to JETP editor July 25, 1955)
J. Exper. Theoret. Phys. USSR **29**, 865-866
(December, 1955)

A LARGE amount of experimental data has recently been accumulated in which it is shown that nuclear reactions may take place at low energies of incident particles (1-10 mev) without the formation of a compound nucleus. For example, in reactions of the (d, p), (d, n) and (p, γ) types, the captured particle has little effect on the structure of the nucleus. The state of the resultant nucleus is most frequently affected by the captured particle, which may be located at successive excited levels.[1-8]. This explains the fact that in the reactions (d, p) and (d, n) the probability of exciting successive single-particle levels is considerably greater than for levels of other types.[1-3] In the present note we wish to draw attention to the fact that such a reaction as the radiative capture of thermal neutrons may also apparently take place without the formation of a compound nucleus.

Let us consider the reaction $\mathrm{Pb}^{206}(n, \gamma)\,\mathrm{Pb}^{207}$. The lower excited levels of Pb^{207} are well known from various sources [α-decay of Po^{211}, K-capture in Bi^{207}, β^--decay of Tl^{207} and (d, p) and (d, t) nuclear reactions].[9-11] The scheme of these levels and their quantum characteristics are shown in the figure. The ground state of Pb^{207}, in accordance with the experimental value of the spin, must be written as $p_{1/2}$. The 870 kev level is excited in α-decay of Po^{211} and in β^--decay of Tl^{207}. Since Tl^{207} has an $s_{1/2}$ ground level (all odd isotopes of $_{81}\mathrm{Tl}$ have spin ½) the 870 kev level must have spin ½ or 3/2. If the spin were 5/2, β-decay to this level would be strongly forbidden ($\Delta I = 2$) and could not be observed. However, this β-transition cannot be an allowed type since the observed intensity of the 870 kev γ-line is small. It is most probably a transition of the first order of forbiddenness. In this case the parity of the 870 kev level is opposed to the parity of the ground state of $_{81}\mathrm{Tl}^{207}$ and consequently, agrees with the parity of the ground state of $_{82}\mathrm{Pb}^{207}$.

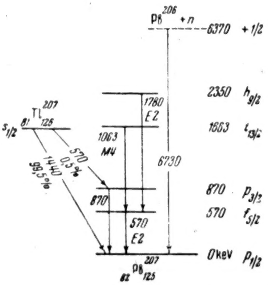

Scheme of the levels of $_{82}\mathrm{Pb}^{207}_{125}$. The dashed line represents the state of Pb^{207} resulting from capture of a thermal neutron; the solid lines are established levels of Pb^{207}. $E\,1$ transitions to the $p_{3/2}$ level which are allowed by the selection rules $(+\tfrac{1}{2} \to p_{3/2})$ are not observed.

The absence of a γ-transition from the isomeric level $i_{13/2}$ to the 870 kev level also indicates that the spin of the 970 kev level must be less than 5/2. The shell model[12,13], in agreement with the data mentioned, describes this as a $p_{3/2}$ level. It must be a hole-level since it is completely filled in the ground state of $_{82}\mathrm{Pb}^{207}$.

Pb^{207} is obtained from the capture of thermal neutrons by Pb^{206}. Since the ground state of the even-even nucleus Pb^{206} is " + 0 " and the thermal neutron has no orbital momentum, Pb^{207} is formed in a + ½ state. Under these conditions, γ-transitions to the $p_{1/2}$ ground state and the 870 kev $p_{3/2}$ state must be of the electric dipole type (the spin changes by one and the parity changes), and since the energies involved in these transitions, 6.73 mev and 5.86 mev, differ little from each other, they should have almost the same intensity.

In actuality only a γ-transition to the ground state is observed in the capture of a thermal neutron by Pb^{207}.[14,15]. The absence of a γ-transition to the $p_{3/2}$ level can be explained by the fact that the radiative capture of thermal neutrons takes place without the formation of a compound nucleus, as a result of which the excitation of $p_{3/2}$ hole-levels is improbable.

---

[1] J. R. Holt and T. N. Marsham, Phys. Rev. **89**, 665 (1953).

[2] J. R. Holt and T. N. Marsham, Proc. Phys. Soc. (London) **66A**, 565 (1953).

[3] C. H. Paris, F. P. G. Valckx and P. M. Endt, Physica **20**, 573 (1954).

[4] C. H. Paris and P. M. Endt, Physica **20**, 585 (1954).

[5] H. H. Woodbury, A. V. Tollestrup and R. B. Day, Phys, Rev. **93**, 1311 (1954).

[6] S. A. Heiberg, D. B. James and T. K. Alexander, Canad. J. Phys. **33**, 34 (1955).

[7] J. B. Warren, K. A. Laurie, D. B. James and K. L. Erdman, Canad. J. Phys. **32**, 563 (1954).

[8] L. A. Sliv and L. K. Peker, J. Exper. Theoret. Phys. USSR **25**, 381 (1953).

[9] W. K. Jentschke, A. C. Juveland and G. H. Kinsey, Phys. Rev. **96**, 231 (1954).

[10] J. Surugue, J. Phys. Radium **7**, 145 (1946).

[11] M. H. Pryce, Proc. Phys. Soc. (London) **65A**, 773 (1952).

[12] M. G. Mayer, Phys. Rev. **78**, 16 (1950).

[13] L. K. Peker, L. A. Sliv and A. V. Zolotavin, Dokl. Akad. Nauk SSSR **88**, 781 (1953).

Translated by I. Emin
283

Possibility of Formation of Penetrating Radiation (μ-Mesons) in the Collision of High Energy Protons with Nuclei

A. N. Novikov, B. M. Pontecorvo
and G. I. Selivanov
Institute for Nuclear Problems, Academy of Sciences, USSR

(Received by JETP editor July 15, 1955)
J. Exper. Theoret. Phys. USSR 29, 889-892
(December, 1955)

It is well known that the interaction of slow μ-mesons with nuclei is extremely small[1]. The process of capturing slow μ^--mesons is assumed to be written in the form[2]

$$\mu^- + p \to \nu + n. \tag{1}$$

Information about the interaction of fast μ-mesons is less certain. In the work in references 3 and 4 it was discovered that for energies exceeding 100 mev, μ-mesons underwent an anomalously greater scattering. The cross section for the anomalous scattering was considerably greater than $10^{-28}\,cm^2$/nucleon, and is in marked disagreement with the existing theory of scattering of these particles in the Coulomb field of a nucleus with a finite radius. Some authors have assumed that the presence of an anomalous scattering indicates the possibility of a non-coulombic interaction for fast μ-mesons and nuclei.**

The starting point of the present work was the assumption that the anomalously large scattering cross section for μ-mesons was due to a specific nuclear interaction. Such a strong interaction cannot be caused by an extremely small probability process of emission by nucleons of μ and ν particles, i.e., processes which are responsible for reaction (1). Generally speaking, the mechanism of scattering of fast μ-mesons by nucleons cannot appear in processes of absorption of slow μ^--mesons, since the probability of capturing slow μ^--mesons by nuclei is extremely small ($\sim 10^6\,sec^{-1}$ for $Z \sim 10$). It is not difficult to see that a strong interaction may be caused by only virtual processes of emission by nuclei of two particles (μ, χ) where the mass of the particle χ may not be less than the μ-meson mass.

It is natural to come to the conclusion that the scattering of μ-mesons depends on the interaction between the nucleon field and the field of a pair of μ-mesons corresponding to the virtual process:

$$(N) \to (N) + (\mu, \mu) \quad (N\text{—Nucleon}). \tag{2}$$

The possibility of a sufficiently strong pair interaction has already been implied many times[6].

In particular, Wentzel[7], proposed a structural theory of π-mesons based on a pair interaction of μ-mesons (μ^+,μ^- or $\mu^\pm,\mu^\circ$)

In the present work it was assumed that the virtual process (2) took place. Moreover, it was assumed that the coupling constant has a value sufficient to explain the "anomalous scattering" and it was considered that, in addition to charged mesons, there also exist hypothetical neutral μ°-mesons. Under these assumptions, the cross section for μ°-meson formation by collisions of protons with nuclei, when the relative energy considerably exceeds the threshold for formation of a pair of μ-mesons, must be 1-10 % of the cross section for formation of π-mesons. An experiment is described below in which an attempt was made to detect μ°- mesons.

The fundamental property of the hypothetical μ°-meson followed from the "anomalous scattering" of μ-mesons as was done above. It is natural to suppose that the cross section $\sigma(\mu^\circ\rightarrow\mu^\pm)$ for the process of exchange scattering of μ-mesons by nucleons

$$\mu^0 + N \rightarrow \mu^\pm + N, \qquad (3)$$

is, as an order of magnitude, the same as the cross section for the usual scattering of charged mesons by nucleons ($\gtrsim 10^{-28}$ cm^2/nucleon if the original assumptions are correct). In connection with this we carried out an experiment to detect μ°-mesons as the products of conversion according to reaction (3).

It is characteristic that the value of the cross section $\sigma(\mu^\circ\rightarrow\mu^\pm)$ ($\approx 10^{-28}$cm^2/nucleon) turns out, on the one hand, to be sufficiently small, so that it gives rise to the large penetrability of μ°-mesons (the mean free path equals several meters of iron) and on the other hand it is sufficiently large so that the μ°-mesons can be detected as a product of this conversion. The large penetrability of this hypothetical radiation permits setting up an experiment for detecting it through the shield of the accelerator, where the background of neutrons is very small. One can expect that at a distance of 40m from the irradiated target of the synchrocyclotron the flux of μ°-mesons $\Phi(\mu^\circ)$ is approximately 1 cm^{-2} sec^{-1} if, of course, it is understood that the assumptions are correct. The estimate of the flux of $\mu^\pm$-mesons, emerging from a thick converter, set at a distance of 40m from the target of the synchrocyclotron, gives $\Phi(\mu^\pm) \sim 0.5$ cm^{-2}min^{-1}.

"The detector of μ°-mesons was a telescope, consisting of a triple bank of proportional counters, connected in coincidence (resolving time 9.3 μ-sec). The effective area of each of the banks is 256 cm^2. An additional bank of proportional counters of effective area 576 cm^2 was placed in front of the converter (a copper block 16 cm thick or a steel block 20 cm thick. It worked in an anti-coincidence system and served to decrease the background of charged particles. The distance between the outside group of counters connected in coincidence was 80cm.

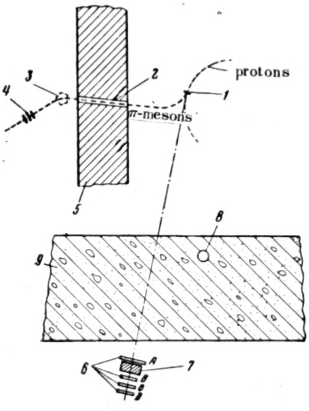

Experimental Arrangement. 1-target; 2-collimator; 3-deflecting magnet; 4-telescope of scintillator detectors, used as a monitor; 5-iron shield; 6-telescope of proportional counters, serving as a "detector of penetrating radiation"; 7-converter; 8-counter, filled with BF$_3$; 9-concrete shield.

The fundamental part of the measurement was made at a time when the synchrocyclotron was used for other experimental work, in which it generated a beam of π-mesons. The carbon target of the synchrocyclotron (2.5 mm thick) was bombarded with protons of energy 670 mev. Charged π-mesons (see Figure) deflected by the fringing field of the accelerator, proceeded through the collimator, were focused by the auxiliary magnet and then were detected by the telescope of scintillating counters. The readings of this telescope in our experiment gave us the possibility of controlling the intensity of the circulating beam of protons. "The detector of μ°-mesons" was situated behind a set of three concrete walls, which in the figure is represented schematically in the form of a single block 8m thick. The distance from the target, exposed to protons, to the detector was 38m. The telescope was aligned tangentially to the equilibrium orbit of the circulating proton beam.

The experimental data are given below

	With accelerator off	With accelerator switched on to full intensity
Triple coincidence counts in 10 min	1.11 ± 0.2[illegible]	1.36 ± 0.31
counts of the first group of counters in 1 min	1582 ± 4	1821 ± 6

As is readily seen, the increase in the counts due to the accelerator is very small. Apparently, it is produced by the diffuse secondary particles originating from the background of neutrons in the shield. The background of chance coincidences is negligibly small. It is determined by the method of out-of-alignment coincidences. The efficiency of the charged particle telescope was determined in a separate experiment. In the limiting case, when it is assumed that the increase in triple coincidences is due entirely to the emission of μ°-mesons from the target, we may on the basis of the given data obtain an upper limit for the flux of $\mu^{\pm}$-mesons originating in the converter. In this way we find that $\Phi(\mu^{\pm}) \ll 3 \times 10^{-3} \text{cm}^{-2} \text{min}^{-1}$. This value is two orders of magnitude smaller than that which was expected in the original assumption. In another experiment where the protons bombarded a beryllium target, we found an analogous result. The conversion of the μ°-mesons in this case took place in a steel block 20cm thick, and with a monitor using a counter filled with BF_3.

To estimate the maximum fraction of μ° -mesons from the recorded effect (see above) we conducted a supplementary experiment. "The detector of μ°-mesons" was turned relative to its initial direction by an angle of 60°. In this way the detection of charged products of the conversion of μ°-particles never took place because the anomalous scattering, according to the experimental data, took place chiefly at small angles. It was found that, within the limits of error of the experimental data obtained with the rotated detector, the results agreed with the data given above. This allowed one to come to the conclusion, that the principle part of the counts detected in this experiment consisted of the background. Nevertheless in the estimate of the upper limit of the cross section for formation of a pair $\mu^{\pm}$,μ° mesons we assumed that the effect was completely due to μ°-mesons.

The upper limit for the value $\sigma_{NN}^{\mu\mu^\circ}$ (the cross section for the emission of a pair from the collision of two nucleons at a relative energy of 680 mev) was estimated by the use of the assumptions-a) the angular distribution of μ-mesons originating in nucleon-nucleon collisions is isotropic in the center of mass system, b)the mean energy of μ°-mesons in the laboratory system ≈130mev, c) the cross section for exchange scattering $\sigma(\mu^\circ \to \mu^{\pm}) \sim 10^{-28} \text{cm}^2/$ nucleon. It was found that $\sigma_{NN}^{\mu\mu^\circ} \ll 7 \times 10^{-31} \text{cm}^2/$ nucleon, i. e, four orders of magnitude smaller than the value of the cross section for the formation of π-mesons.

The result obtained allows one to reach the following conclusions: 1) "The anomalous scattering"** of μ-mesons cannot be explained by an interaction between the nucleon field and the pair field (μ,μ°). 2) The "structural" theory of π-mesons proposed by Wentzel apparently does not conform to reality. 3) The contribution to the pair interaction (μ,μ°) to the nuclear force is insignificant ($\lesssim 10^{-3}$ of the contribution of the π-mesons).

At the time of completion of the present work there was published the work in reference 8 in which an attempt was made to detect pair formation of charged μ-mesons by photons of energy 345 mev on nuclei of Al and Be. The authors came to the conclusion that the relative strength of the interaction (μ^+,μ^-) was similar to our conclusions on the interaction $(\mu^{\pm},\mu^\circ)$.

This report is based on the results of the work completed in 1954 and previously reported in reports of the Institute for Nuclear Problems, Acad. Sci. USSR.

** It has recently been the custom to consider that anomalous scattering was explained rather as a deficiency of the existing theory of coulomb interaction than as a specific nuclear interaction of μ--mesons.

[1] M. Conversi, E. Pancini and O. Piccioni. Phys. Rev. 71,209 (1947).

[2] B. Pontecorvo, Phys. Rev. 72, 246 (1947).

[3] M. L. T. Kannangara and G. S. Shrikantia, Phil. Mag. 44, 1091 (1953).

[4] B. Leontic and A. W. Wolfendale, Phil. Mag 44, 1101 (1953)

[5] See, for example, I. B. McDiarmid, Phil. Mag. 46, 177(1955).

[6] See, for example, R. E. Marshak, *Meson Physics*, 1952.

[7] G. Wentzel, Phys. Rev. 79, 710(1950).

[8] B. T. Feld, A. Julian, A. C. Odian, L. S. Osborne, and A. Wattenberg, Phys. Rev. 96, 1386(1954).

Translated by M. Hamermesh
297

Formation of Neutral π-mesons in ($n-p$) Collisions at Effective Neutron Energies of 590 mev

V. P. Dzhelepov, K. O. Oganesian and
V. B. Fliagin
Institute for Nuclear Problems, Academy of Sciences,
Academy of Sciences, USSR

(Submitted to JETP editor August 2, 1955)
J. Exper. Theoret. Phys. USSR 29, 886-889
(December, 1955)

THE kinematic calculation of the processes of formation of π^0-mesons in collisions of neutrons with free protons:

$$n + p \rightarrow \pi^0 + d, \tag{1}$$

$$n + p \rightarrow \pi^0 + n + p, \tag{2}$$

which are accompanied by the decay of these mesons into two γ-quanta shows that the probability of emission of the γ-quanta at 90° (in the laboratory system) from the beam of neutrons, depends very slightly on the angular distribution of π^0-mesons in the center of mass system of the colliding nucleons as well as on the velocity of the center of mass. This fact makes it possible in principle to determine the sum of the total cross sections for forming π^0-mesons in reactions (1) and (2) by measuring the number of γ-quanta coming out of the target at an angle of 90°.

The arrangement of the apparatus, used in the experiment, is shown in Fig. 1. Neutrons of high energy were generated by bombarding the internal beryllium target of the synchrocyclotron with protons of energy 680 mev. The intensity of the beam of neutrons of energy above 400 mev in the region of the apparatus was $\sim$ 1-2 $\times 10^4$ neutrons/cm^{2}sec. The energy distribution of neutrons in the beam was investigated in a special experiment by Fliagin[1] and is shown in Fig. 2.

Gamma-quanta from the decay of π^0-mesons, generated in the target, were detected in the telescope of two scintillators and one Cerenkov counter labeled in the Figure by the numbers 1, 2 and 3, respectively. The conversion of the

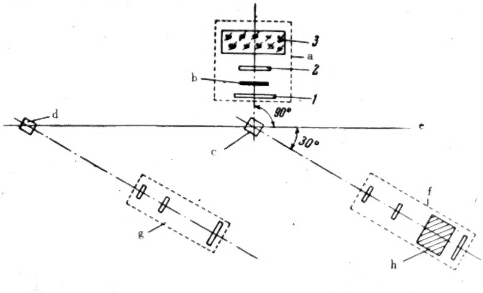

FIG. 1. Scematic Arrangement of the Apparatus
a - telescope-detector of γ-quanta, b - converter, c - target, d - scatterer, e - neutron beam, f - telescope-detector of protons, g - telescope-monitor, h - Tungsten filter

γ-quanta was carried out in a lead plate (converter) of 3 mm thickness, located behind the first counter. This counter serves to prevent the possibility of the detector registering fast charged particles flying from the target, and is connected in anti-coincidence with the counters 2 and 3. The Cerenkov radiation of the conversion electrons in a 3-meter counter, which is a block of plexiglas, was recorded simultaneously on a pair of photo multipliers. All of the relative measurements were carried out with the aid of this detector.

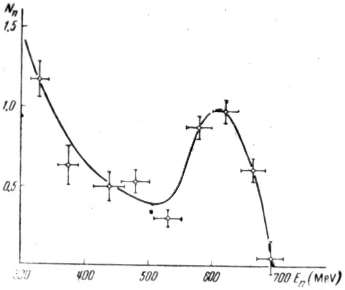

FIG. 2. Energy distribution of Neutrons

The effect of the generation of π^0-mesons in collisions of neutrons with free protons was determined as a difference between the effects of targets of polyethylene and graphite, consisting of an equal number of carbon atoms. By means of this study, carried out with these targets, we have the ratio of the cross sections for emission at angles of 90° (in the laboratory system) of γ-quanta from the decay of π^0-mesons from hydrogen and carbon. This ratio was shown to be equal to

$$\left(\frac{d\sigma_\gamma}{d\Omega}\right)^{\mathrm{H}}_{90^\circ} \Big/ \left(\frac{d\sigma_\gamma}{d\Omega}\right)^{\mathrm{C}}_{90} = 0.215 \pm 0.014. \qquad (3)$$

The absoulute value of the yield of emitted γ-quanta was determined in experiments in which (simultaneously with the measurement of the flux of γ-quanta) we determined the recoil proton flux produced by elastic $(n - p)$ scattering whose cross section for neutrons of mean energy 590 mev had been determined in our laboratory[2]. For this purpose, the telescope which detected γ-quanta, the Cerenkov counter, was replaced by a scintillator. In this manner we eliminated the need of determining the effect of the Cerenkov counter in an auxiliary experiment. The converter in this experiment has a thickness of 1 mm. The telescope which registered the proton recoils was located at an angle of 30° relative to the direction of the neutron beam (see Fig. 1) and acted on the target in common with the γ-detector. In order to use the data of experiments on $(n - p)$ scattering in our work, a tungsten filter was placed in front of the last counter of the telescope-detector of protons. This filter guaranteed an energy threshold for the particle counter the same as the threshold of the detector used in reference 2.

The absolute cross section for the emission of γ-quanta at 90° (in the laboratory system) from the neutron beam for a hydrogen target under the conditions of our experiment is expressed by the following formula:

$$\left(\frac{d\sigma_\gamma}{d\Omega}\right)^{\mathrm{H}}_{90^\circ} = \left(\frac{N_\gamma}{N_p}\right)^{\mathrm{H}} \frac{\Delta\Omega_p \cdot K_p}{\Delta\Omega_\gamma K_\gamma} \left(\frac{d\sigma_{np}}{d\Omega}\right)_{30^\circ}, \qquad (4)$$

where the symbols γ and p stand for the detector of γ-quanta and protons respectively; N = the counting rate of the detector; $\Delta\Omega$ the solid angle intercepted by the detector; k the efficiency of the detector; $(d\sigma_{np}/d\Omega)_{30}$ the elastic $(n$-$p)$ scattering for an angle of 30°, equal, according to reference 2 to $(3.1 \pm 0.2) \times 10^{-27}$ cm^2/steradian.

For determining the values of N_γ^H and N_p^H, we measured simultaneously in both detectors the effect of the carbon target, while the effect of the hydrogen was determined with the help of the known value of Eq. (3). A similar analysis was performed for the proton detector (for 30°).

The coefficient K_p takes into account the absorption of recoil protons by the filter. This coefficient was determined directly from the experiment With this in view, we placed a system of two telescopes in the proton beam emerging from the synchrocyclotron; these registered elastic $(p$-$p)$ events. One of these telescopes was used as described here as the proton detector. The coefficient K_p was determined as the ratio of the counting rates with and without the filter* and was given experimentally as equal to 0.5.

The efficiency for detecting γ-quanta K_γ is equal to the product of the conversion probability p with the coefficient η, which takes into account the loss of electrons owing to scattering in the converter. The probability p is easily calculated on the basis of the known experimental and theoretical work on the total cross section for absorption of γ-rays in lead. The coefficient η was determined by calculating by the method given by Moliere[3]. For a converter of 1 mm thickness and average energy of γ-quanta ~ 100 mev, η is found to be equal to $\sim 1\%$**.

The basic difficulties which arise in trying to determine K_γ, are the following: 1) The energy of π^0-mesons in the center of mass system of the colliding nucleons can take on different values, (2) the unknown form of the angular distribution of π^0-mesons in this system (both factors determine the spectrum of detected γ-quanta). However, as is demonstrated by calculation, the weighted average of K_γ over the spectrum of γ-quanta is slightly dependent on these factors and changes in the range from 0.089 to 0.098 for a mean energy of incident neutrons of 600 mev and a converter thickness of 1 mm.

The effective solid angle of the detector of γ-quanta was found by conducting a separate experiment in which we studied the dependence of the counting rate of the γ-detector on the diameter of the converter.

On the basis of our determination of the values of N, k and $\Delta\Omega$ and also the known cross section $(d\sigma_{np}/d\Omega)_{30^\circ}$ from Eq. (4) for an angle of 90°, we obtain the absolute cross section for the emission of γ-quanta from the decay of π^0-mesons by collisions of neutrons with hydrogen. This cross section equals

$$(d\sigma_\gamma/d\Omega)^{\mathrm{H}}_{90^\circ} = (0.72 \pm 0.18)\cdot 10^{-27}\ \text{cm}^2/steradian. \qquad (5)$$

On account of the non-monoenergetic neutron flux (see Fig. 2) the cross section found by us is averaged over the energy spectrum of the neutrons. For determining the effective energy to which we refer this cross section, we made use of data on relative yields of γ-quanta in the reaction $p + n \rightarrow \pi^0 + (n + p)$ in the proton energy range 490-650 mev obtained in the work of reference 4, data on the formation of π^0 mesons for nucleon energies 340 mev[5] and 400 mev[6] and also for the neutron spectrum shown in Fig. 2. The effective neutron energy in our experiment turned out to be equal to 590 ± 20 mev.

The absolute value of the cross section $(d\sigma_\gamma/d\Omega)^H_{90^\circ}$ as indicated above, enables us to get the total cross section for generating π^0-mesons in $(n$-$p)$ collisions. On the assumption that the angular distribution of π^0-mesons is isotropic in the center of mass system of the colliding nucleons, we derive the value***

$$\sigma^{\pi^0}_{np} = (5.9 \pm 1.5)\cdot 10^{-27}\ \text{cm}^2. \qquad (6)$$

In the case of an angular distribution $\sim \cos^2\theta$ for π^0-mesons having a momentum (in the center of mass system) equal to half the maximum, the cross section turns out to be 5% greater and is

$$\sigma^{\pi^0}_{np} = (6.3 \pm 1.7)\cdot 10^{-27}\ \text{cm}^2. \qquad (7)$$

Comparing the cross section (6) with the cross section measured in reference 5 for protons of energy 340 mev, it is evident that the increase of the cross section for generating π^0-mesons in $(n$-$p)$ collisions in the energy range 340-600 mev is proportional to $k^{3.3 \pm 0.5}$, where k is the maximum meson momentum in the center of mass of the colliding nucleons.

If we use the result of reference 7, in which was determined the cross section for formation of π^0-mesons by protons of 670 mev on neutrons bound in deuterium, and convert this to the energy 590 mev with the aid of the relation $\sigma^{\pi^0}_{pn} \sim k^{3.2}$ given in reference 7, then σ_{pn} is found to equal $(5.3 \pm 1.2) \times 10^{-27}$ cm^2. For the same energy the cross section $\sigma^{\pi^0}_{np}$ obtained by us was somewhat larger, as was to be expected. However, the precision of the results of the two experiments is insufficient to attempt to establish, on the basis of the observed difference in the cross sections for forming π^0-mesons from nucleons that are free or bound in deuterium, a quantitative estimate of the effect of bound nucleons on the process of forming mesons.

For a neutron energy of 590 mev, the cross section for forming π^0-mesons in $(n$-$p)$ collisions appears to be approximately 17% of the total cross section for the $(n$-$p)$ interaction, which at this energy equals $(36 \pm 2) \times 10^{-27}$ cm^2 according to reference 8.

In conjunction with our results and those available in the literature on the cross section for generating π^0-mesons in nucleon-nucleon collisions for $E_{\text{nucl.}} \approx 600$ mev it appears that they satisfy the relation

$$\sigma^{\pi^0}_{np} = {}^1\!/_2\sigma^{\pi^+}_{pp} + \sigma^{\pi^-}_{np} - \sigma^{\pi^0}_{pp} \qquad (8)$$

and, so, do not contradict the requirements of the charge invariance of the nuclear force. If we assume that this hypothesis is correct, then we can take advantage of the resultant equation $\sigma(pp \rightarrow \pi^+, d) = 2\sigma(np \rightarrow \pi^0, d)$. It is then possible to obtain the cross section for formation of π^0-mesons from the reaction (1). Thus, according to the experiment in reference 9, for $E_p = 586$ mev, $\sigma(pp \rightarrow \pi^+ + d)$ equals $(2.95 \pm 0.15) \times 10^{-27}$ cm^2; then for the same energy $\sigma(np \rightarrow \pi^0 + d)$ has to be equal to 1.5×10^{-27} cm^2 Under these conditions it follows that, for an energy of 590 mev, the cross section for generating π^0-mesons in reaction (2) is approximately three times greater than that in reaction (1).

[*] We make use of this opportunity to express our thanks to B. S. Neganov for help rendered to us in conducting this experiment.

[**] The geometry of our γ-detector allows detection of all electrons of energy > 10 mev emitted in a cone of opening angle 40°.

[***] On the assumption of an isotropic angular distribution of π^0-mesons Eq. (3) tells us that the cross section for formation of π^0-mesons from carbon is $\sigma_c^{\pi^0} = 27.4 \pm 6.7 \times 10^{-27}$ cm^2.

---

[1] V. B. Fliagin, Reports Inst. Nuclear Problems Acad. Sci. USSR 1954

[2] Iu. M. Kazarinov, Reports Inst. Nuclear Problems, Acad. Sci. USSR 1954

[3] G. Moliere, Naturforsch. 3a, 78 (1948).

[4] B. D. Balishov, V. A. Zhukov, B. M. Pontecorvo and G. I. Selivanov. Reports, Inst. Nuclear Problems, Acad. Sci., USSR, 1954

[5] R. W. Hales and B. J. Moyer, Phys. Rev. 89, 1047 (1953).

[6] R. A. Shluter, Phys. Rev. 96, 734 (1954)

[7] A. A. Tiapkin, M. S. Kozodaev and Ia. D. Prokoshkin Dokl. Akad. Nauk. SSSR 100, 689 (1955).

[8] V. P. Dzhelepov, Iu. M. Kazarinov, B. M. Golovin, V. B. Fliagin and V. I. Satarov, Izv. Akad. Nauk SSSR Ser. Fiz. 19, 5 (1955).

[9] M. G. Meshcheriakov and B. D. Neganov, Dokl. Akad Nauk. SSSR 100, 677 (1955)

Translated by B. Hamermesh
296

Microwave Spectrum of the C_2H_5Cl Molecule

A. I. Barchukov, T. M. Minaeva and
A. M. Prokhorov
The P. N. Lebedev Physical Institute,
Academy of Sciences, USSR

(Submitted to JETP editor July 19, 1955)
J. Exper. Theoret. Phys. USSR 29, 892 (December, 1955)

We have carried out a preliminary study of the rotational spectrum of the C_2H_5Cl molecule. A short communication on the spectrum of this molecule was published by Wagner and Dailey[1], who studied the transitions $1_{11}-2_{12}$, $1_{10}-2_{11}$, $2_{22}-3_{32}$ and $2_{20}-3_{21}$ in the $C_2H_5Cl^{35}$ molecule, and the $1_{11}-2_{21}$ and $1_{10}-2_{11}$ transitions in the $C_2H_5Cl^{37}$ molecule. From these transitions they obtained the values of the rotational constants B and C, as well as the magnitudes of the quadrupole bonds along the principal axes of inertia.

We have studied additional transitions whose frequencies have the following values, neglecting the effects of quadrupole interactions:

Molecule	Transition	Observed Frequency (mc/sec)
$C_2H_5Cl^{35}$	$0_{00}-1_{01}$	10 246,20 ± 0,05
$C_2H_5Cl^{35}$	$1_{01}-2_{02}$	20 903,80 ± 0,04
$C_2H_5Cl^{37}$	$0_{00}-1_{01}$	10 456,00 ± 0,05

The frequency of the transition line $0_{00}-1_{01}$ coincides with the frequency calculated from the the values for B and C given in reference 1*.

The frequency of the transition $1_{01}-2_{02}$ depends on the rotational constant A; calculation gave the value $A = 30{,}940 \pm 200$ mc/sec. The low accuracy in the determination of A is due to the fact that A enters into the value of the transition frequency $1_{01}-2_{02}$ as a small correction of the form $(B-C)^2/A$, and the magnitudes of B and C are very similar. Note that, in general, the accuracy of determining A is always small if it is determined from transitions involving a change in the dipole moment μ_a. We propose to observe transitions involving the measurement of μ_b. Although these transitions give less intense lines, they provide a more accurate determination of A.

Using the transition $0_{00}-1_{01}$, we have determined the dipole moment μ_a of the $C_2H_5Cl^{35}$ molecule from the Stark splitting of the line which has the hyperfine structure $F = 3/2 - 5/2$, at applied fields of 195 v/cm and 292 v/cm. The calculation of μ_a was carried out using the "weak field" formula. The value found for μ_a was 1.79 ± 0.05 D.

---

[*] The rotational constants for $C_2H_5Cl^{37}$ given in reference 1 are incorrect, and were therefore calculated directly from the line frequencies given therein.

[1] R. S. Wagner and B. P. Dailey, J. Chem. Phys. 22, 1459 (1954).

Translated by D. C. West
298

Concerning the Cross Section of Overcharging of Slow Ions in their own Gas

IA. M. KAGAN AND V. I. Perel'
Karelo-Finnish State University

(Submitted to JETP editor, March 30, 1955)
J. Exper. Theoret. Phys. USSR **29**, 884-886
(December, 1955)

THE value of the effective cross section of overcharging for collisions between ions and atoms of the same gas can be determined from experiments on ion beams as well as from the measurements of the drift velocity of ions in an electric field in a gas. Recent methods, however, require a knowledge of the character of the interaction between ions and atoms. As is well known, with the collision of an ion and atom there occurs a resonance effect along with the possibility of charge exchange. As shown in theoretical calculations[1-4] the effective cross section of overcharging in this case is so large that exchange of momentum is not essential for the majority of collisions. Therefore, a convenient model for describing the interaction of an ion with an atom of the same gas appears to be the proposed Sena model for pure overcharging. This is confirmed also by the measurements of Ziegler[6]. On the basis of this model, wherein it is proposed that the cross section of overcharging does not depend on the relative velocity, Sena obtains, in an elementary way, a formula for the drift velocity of ions in a large field. An exact expression for this case, obtained by means of a solution of the kinetic equation[7] has the form

$$\overline{u} = (2eE/\pi mqN)^{1/2}, \tag{1}$$

where $\overline{u}$ is the drift velocity, e and m the charge and mass of the ions, q the cross section of overcharging, E the field intensity, and N is the atomic concentration. Expression (1) differs from the formula of Sena in the value of the multiplier. In the case of small fields it is possible to make use of the well-known formula[8]

$$\overline{u} = \frac{3\pi^{1/2}eE}{8(mkT)^{1/2}N}\left[\int_0^\infty Qe^{-\lambda^2}\lambda^5 d\lambda\right]^{-1}, \tag{2}$$

where T is the gas temperature and k is the Boltzmann constant,

$$Q = 2\pi\int_0^\pi (1-\cos\theta)\,\sigma(\theta)\sin\theta\, d\theta, \tag{3}$$

$\sigma(\theta)\sin\theta\, d\theta d\phi$ is the effective differential cross section for scattering, θ is the angle of scattering in the center of mass system. In the case under consideration $\sigma(\theta)$ has the form of a sharp maximum near $\theta = 0$ and near $\theta = \pi^2$. The first corresponds to elastic scattering and the second to overcharging. For angles perceptibly different from 0 and π, $\sigma(\theta)$ is small. Therefore, it is possible to write the approximation

$$\sigma(\theta) = \frac{1}{2\pi}[q\delta(1+\cos\theta) + q_1\delta(1-\cos\theta)], \tag{4}$$

where q is the cross sectoin for pure overcharging and q_1 the cross section for scattering; $\delta(x)$ is a delta function. With the hypothesis that q is not dependent on velocity, we obtain from (2) and (3)

$$\overline{u} = 3\pi^{1/2}eE/16\,(mkT)^{1/2}qN. \tag{5}$$

Equation (5) differs in its multiplicative factor from the approximate formula obtained in reference (7) by 10%.

By making use of Eq. (1) it is possible to calculate the cross section of overcharging from the experimental data of Hornbeck and Varney[9,10] for the motion of the ions of an inert gas in a strong field. In the case of a weak field it is possible to make use of Eq. (5) and calculate the cross section of overcharging from the experimental data of Biondi and Chanin[11] for the motion of ions. The values calculated by such a method are shown in the third and fourth columns of the Table. In the first and second columns, there are given for comparison the total cross section q_n and the cross section of overcharging q obtained by Ziegler from experiments with ion beams at ion of ~ 1 ev. The magnitude of the cross section in the Table is given in 10^{-15} cm^2. The cross section obtained from the value of the drift velocity in large fields corresponds to an energy of ion drift of the order of 1-2 ev. They are not in bad agreement with the data of Ziegler (with the exception of helium). The cross sections obtained from the data for the drift velocity in small fields also corresponds to the thermal energy of the ions, but does not exceed the cross sections near large energies. Thus the data in the Table show that the model for pure overcharge with velocity independence of cross section yields fairly good results in a sufficiently wide interval of ion energies. In the work of reference 7 it is shown that this model give good results for the drift velocity, according to the data of references 9 and 10, for all values of the ratio E/p (where p is the reduced pressure) reached in the experiment if they use the cross sections calculated from their data for large fields and the true thermal motion of the atoms.

In the work of Hornbeck and Wannier[12,13] it is attempted to explain the results of measurements of the drift velocity of ions in inert gases by means of a model which assumes isotropic scattering of the ions and atoms. They use this model to calculate the cross section from the drift velocity near large fields and arrive at a value which is in poor agreement with the results of Ziegler (Ziegler attempted to improve the agreement by subtracting (without presenting a reason) the gas kinetic cross section from the actual cross section). Furthermore, this model is not entirely in agreement with the relation obtained by Ziegler between the total cross section and the cross section of overcharging. Recently Wannier[14] rejected this model, and recognized that the model of pure overcharging is actually better. However, the cross section of overcharging calculated by him from the drift velocity in large fields [with the help of Eq. (1)] is not correct, apparently due to an error in conversion. The cross sections of overcharging calculated by the formula of Demkov[3] for He, Ne, A, Kr, Xe are equal respectively to 2.6, 3.0, 4.1, 4.6, and $5.3 \times 10^{-15} \text{cm}^2$. As is evident from the Table, agreement is best of all for He and Ne, and worse for A, Kr, and Xe. This also explains certain divergences between the theoretical and experimental curves for the cross section of the drift velocity of ions in these gases given in reference 7. This divergence is, in our opinion, entirely attributable to the inaccuracy of Demkov's calculation. We note that the determination of the cross section of overcharging made by Sena[15] leads to still worse agreement with the experimental values of the cross section.

Gas	q_n[9]	q[9]	q[9, 10]	q[11]
He	—	4.1	2.6	3.6
Ne	5	4.4	3.15	4.2
A	9	5.5	6.5	7.5
Kr	—	9	7.6	9.2
Xe	13	10.3	9.3	11.3

The calculated mobilities of Massey and Mohr[1], and of Holstein[4] appear to be more accurate, but up to now calculations have only been made for small fields. They agreed well with results of experimental work[11].

---

[1] H. S. W. Massey and C. B. O. Mohr, Proc. Roy. Soc. (London) **A144**, 188 (1934)

[2] H. S. W. Massey and E. H. Burhop, *Electronic and Ionic Impact Phenomena*, Oxford Univ. Press, London (1952).

[3] Iu. N. Demkov Uch. Zap., (Science Memorandum), Leningrad State Univ., No. 146, Series Physical Science 8, 74 (1952)

[4] T. Holstein, J. Phys. Chem. **56**, 832 (1952)

[5] L. A. Sena, J. Exper. Theoret. Phys. USSR **16**, 734 (1946)

[6] B. Ziegler, Z. Phys. **136**, 108 (1953)

[7] Ia. M. Kagan and V. I. Perel', Dokl. Akad Nauk SSSR **98**, 575 (1954)

[8] S. Chapman and T. G. Cowling, *The Mathematical Theory of Nonuniform Gases*, Cambridge University Press (1939)

[9] J. A. Hornbeck, Phys. Rev. **84**, 615 (1951)

[10] R. N. Varney, Phys. Rev. **88**, 362 (1952)

[11] M. A Biondi and L. M. Chanin, Phys. Rev. **94**, 910 (1954)

[12] J. A. Hornbeck and G. H. Wannier, Phys. Rev. **82**, 458 (1951)

[13] J. A. Hornbeck, J. Phys. Chem. **56**, 829 (1952)

[14] G. H. Wannier, Phys. Rev. **96**, 831 (1954)

[15] L. A. Sena, *The Collision of Electrons and Ions with Gas Atoms*, State Publishing House of Technical and Theoretical Literature (1948)

Translated by L. B. Leder
295

The Effect of Pressure on the Superconductivity of Cadmium

N. E. ALEKSEEVSKII AND IU. P. GAIDUKOV
Institute of Physical Problems,
Academy of Sciences, USSR

(Submitted to JETP editor September 7, 1955)
J. Exper. Theoret. Phys. USSR **29**, 898-899
(December, 1955)

THE effect of pressure on the displacement of the critical temperature of a superconductor has been studied by many authors[1-7]. However, they studied only superconductors whose transition temperatures are above 1°K. It seemed interesting to study the effect of pressure on the properties of superconductors with low transition temperatures. Such a superconductor is cadmium, which goes into the superconducting state at 0.54 °K. We measured the critical magnetic field vs. the temperature of samples of polycrystalline cadmium without pressure as well as with pressure.

To obtain temperatures in the interval between 0.06 - 0.6°K we used the method of adiabatic demagnetization of a paramagnetic salt. The pressure was obtained by freezing water in a bomb of fixed volume[8]. Heat contact between the bomb and the salt was realized by means of a thermal conductor *K* (Fig. 1), a copper rod, 2 mm in diameter and 50 mm long, one end of which is pressed into the salt, and the other is cadmium soldered to the plug of the bomb. To assure a reliable contact between the salt and the thermal conductor, thin copper sheets were hard soldered to the end of the thermal conductor and pressed into the salt[9]. The bomb for retaining the pressure was made of beryllium bronze. It had an outer diameter of 10 mm, an inner diameter of 5 mm and a length of 80 mm. To seal the bomb plug a washer of annealed copper was used. The sample was prepared from 99.95% pure cadmium and was in the form of a rod 3 mm in diameter and 20 mm long. To be sure that the sample *O* makes reliable thermal contact with the salt, we soldered it to a small piece of copper wire, 0.5 mm in diameter, which in turn was soldered to the inside of the bomb roof. The solder was pure cadmium. A drawing of the apparatus is shown in Fig. 1. We obtained thermal contact between the salt and the liquid helium by admitting a small quantity of gaseous helium into space *A* through tube *B*. This helium after demagnetization is adsorbed by the salt *F* and in this way the thermal contact between the salt and the liquid helium is broken. The demagnetization was done at a field of 15,000 oersteds and an initial temperature of 1.6 °K. The salt used was iron ammonium alum. After the demagnetization the temperature obtained was of the order of 0.05-0.06

The subsequent warm-up to a temperature of 0.6°K took 4-5 hours. The salt temperature was measured as in former experiments[9] by the displacement of coil *D*, which is connected to the ballistic galvanometer. To determine the critical field of cadmium, the magnetic moment of the sample was measured by means of another coil *E*, which can also be connected to the ballistic galvanometer. The magnetic field was produced by a solenoid wound around the helium dewar. The determination of the pressure in the bomb, *C*, was derived from the displacement of the superconductivity transition of indium[6].

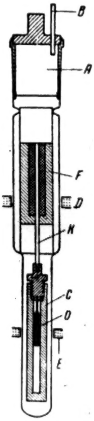

FIG. 1.

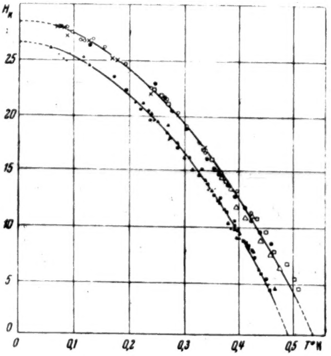

FIG. 2 Measurements 1954 - Without pressure: ◘-Nov. 26; ϴ-Nov. 11; Δ- Nov. 10; O-Nov.2; X-Nov.4. Under pressure: ▲-Nov. 3; ■-Oct. 22; ●-Oct. 28.

The results of the measurements obtained at $p = 0$ and $p = 1550$ atm are shown on Fig. 2. In these experiments the temperature of the sample was assumed to be the same as the temperature of the salt, the truth of which was ascertained in separate experiments. The curves we obtained for the critical fields fit the following formulas well:

$$(H_k/28.5) + (T/0.54)^2 - 1 \text{ for } p = 0$$

$$(H_k/26.5) + (T/0.495)^2 = 1 \text{ for } p = 1550 \pm 50 \text{ atm.}$$

H_k is shown as a function of T^2 on Fig. 3, indicating the accuracy of the derived equations. H_0 and T_k have the following values for cadmium:

at $p = 0$, $H_0 = 28.5$ oersteds, $T_k = 0.540°K$;

at $p = 1550$ atm, $H_0 = 26.5$ oersteds, $T_k = 0.495$.

Thus:

$$\partial T_k/\partial p = 3 \times 10^{-11} °K \text{ dyne}^{-1} \text{ cm}^2$$

$$\partial H_0/\partial p = 1.27 \times 10^{-9} \text{oersteds dyne}^{-1} \text{cm}^2,$$

i.e., they have the same order of magnitude as for other superconductors [6,10]. Thus we note the change of T_k by a pressure ~1500 atm is 8.3%, i.e., slightly larger than the corresponding value for other superconductors.

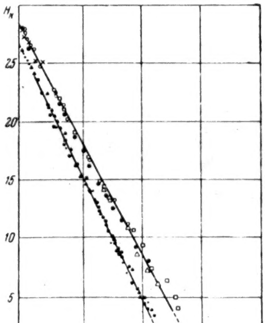

FIG. 3. Same meaning of symbols as in Fig. 2.

---

[1] G. J. Sizoo and H. Kammerlingh-Onnes, Leid. Comm., No. 180c, 1926.

[2] G. J. Sizoo, W. J. de Haas, and H. Kammerlingh-Onnes, Leid. Comm., No. 180c, 1926.

[3] N. R. Alekseevskii, J. Exper. Theoret. Phys. USSR **10**, 746 (1940).

[4] B. G. Lazarev and L. S. Kan, J. Exper. Theoret. Phys. USSR **14**, 463 (1944).

[5] N. E. Alekseevskii and N. B. Brandt, J. Exper. Theoret. Phys. USSR **22**, 200 (1952)

[6] L. S. Kan, B. G. Lazarev, and A. I. Sudovtsev, J. Exper. Theoret. Phys. USSR **18**, 825 (1948).

[7] N. E. Alekseevskii, J. Exper. Theoret. Phys. USSR **19**, 358 (1949)

[8] B. G. Lazarev and L. S. Kan. J. Exper. Theoret. Phys. USSR **14**, 439 (1944).

[9] N. E. Alekseevskii and Iu. P. Gaidukov, J. Exper. Theoret. Phys. USSR **25**, 383 (1953).

[10] D. Shoenberg, Superconductivity, (Cambridge Univ. Press, Cambridge, England, 1952), p. 77.

Translated by S. D. Sydoriak
304

The Quantum Theory of the Magnetostriction of Cubic Monocrystals of Ferromagnetics at Low Temperatures

A. A. GUSEV
Moscow State University

(Submitted to JETP editor November 10, 1954)
J. Exper. Theoret. Phys USSR **29**, 895-897
(December, 1955)

IN an earlier paper[1] we presented a general method for the quantum treatment of the magnetostriction of ferromagnetic single crystals at low temperatures. The results were applied to crystals of hexagonal symmetry.

All the basic physical assumptions of the theory outlined in reference 1 are also valid for the cubic lattice. The special peculiarity of the latter is its much higher symmetry, which in particular, does not permit us to extend the theory of magnetic anisotropy, developed for hexagonal crystals, to cubic crystals.[2] In the case of magnetostriction, this difficulty arises to a significant degree, since the deformation of the lattice by the magnetic forces eliminates the symmetry and there is introduced into the Hamiltonian the operators of magnetoelastic interaction which are quadratic in the spin operators and linear in the components of the deformation tensor. This difficulty affects the consideration of the magneto-elastic anisotropy which appears in the phenomenon of magnetostriction.

The equivalent Hamiltonian of the system in this case has the form

$$\mathscr{H} = G_0 - {}^1/_2 \sum G_{\alpha\beta}(f_1, f_2)\, S_{f_1}^{\alpha} S_{f_2}^{\beta} \tag{1}$$

$$- {}^1/_2 \sum A_{ij}^{\alpha\beta} u_{ij} S_{f_1}^{\alpha} S_{f_2}^{\beta} - \mu H \sum \gamma_\alpha S_f^\alpha,$$

where the summations are carried out over all upper and lower indices appearing in them. The difference from the hexagonal case consists of the fact that the form of the tensors $G_{\alpha\beta}$ and $A_{ij}^{\alpha\beta}$ will be different, corresponding to cubic symmetry of the lattice. In the same way as in reference 1, we write the Hamiltonian in diagonal form:

$$\mathscr{H} = E_0 + \Delta E_0 + \sum_k E_k \hat{\xi}_k^+ \hat{\xi}_k. \tag{2}$$

(All the symbols in Eqs. (1) and (2) have the same meaning as in reference 1). In the case under consideration, the quantity ΔE_0 is small at low temperatures and strong fields in comparison with the remaining terms in Eq. (2), and can be neglected for our purposes. Under these conditions we have for E_0 and E_k, approximately,

$$E_0 = -(N/2)\,[\bar{G}_a + \xi(\gamma_\alpha, \gamma_\beta, u_{ij}) + 2\mu H], \tag{3}$$

$$E_k = 2\mu H + \xi(\gamma_\alpha, \gamma_\beta, u_{ij}) + \beta k^2. \tag{4}$$

Here $\bar{G}_a$ are the mean values of the diagonal terms of the tensor of electron interaction (the exchange integral), $\beta = G_a f^2$, k = wave number, and

$$\xi(\gamma_\alpha, \gamma_\beta, u_{ij}) = \left(u_{11}\overline{A_{11}^{11}} + u_{27}\overline{A_{22}^{11}} + u_{33}\overline{A_{33}^{11}}\right)\gamma_1^2 \tag{5}$$

$$+ \left(u_{11}\overline{A_{11}^{22}} + u_{22}\overline{A_{22}^{22}} + u_{33}\overline{A_{33}^{22}}\right)\gamma_2^2$$

$$+ \left(u_{11}\overline{A_{11}^{33}} + u_{22}\overline{A_{22}^{33}} + u_{33}\overline{A_{33}^{33}}\right)\gamma_3^2$$

$$+ u_{12}\overline{A_{12}^{12}}\gamma_1\gamma_2 + u_{23}\overline{A_{23}^{23}}\gamma_2\gamma_3 + u_{13}\overline{A_{13}^{13}}\gamma_1\gamma_3,$$

where $\overline{A_{ij}^{\alpha\beta}}$ are the mean values of the components of the tensor of magneto-elastic interaction.

Having Eq. (2), it is not difficult to calculate the partition function, and hence the free energy, the magnetoelastic part of which in the same approximation has the form

$$\Psi_{\text{M.y}} = -\frac{N\xi(\gamma_\alpha, \gamma_\beta, u_{ij})}{2V}\varphi(\vartheta, H), \tag{6}$$

where

$$\varphi(\vartheta, H) = 1 - \frac{V}{4N}\left(\frac{\vartheta}{\beta\pi}\right)^{3/2} e^{-2\mu H/\vartheta}, \quad \vartheta = kT. \tag{7}$$

For cubic symmetry of the lattice, the components of the tensor $A_{ij}^{\alpha\beta}$ have the following properties:

$$\overline{A_{11}^{11}} = \overline{A_{22}^{22}} = \overline{A_{33}^{33}} = A_1, \ \overline{A_{12}^{12}} = \overline{A_{23}^{23}} = \overline{A_{13}^{13}} = A_2;$$

$$\overline{A_{ij}^{\alpha\beta}} = 0 \text{ for } (ij) \neq (\alpha\beta).$$

Computing $\xi(\gamma_\alpha, \gamma_\beta, u_{ij})$ and substituting in Eq. (6) we get for $\Psi_{\text{M.y}}$ an expression from consideration of which it is evident that, because of its dependence on $\mu_\alpha u_{ij}$ coincides with the classical expression for the magneto-elastic energy of a cubic crystal. Hence the quantities

$$\left(\overline{A_{ij}^{\alpha\beta}}\, N/2V\right)\varphi(\vartheta, H) \tag{8}$$

play the role of magneto-elastic coefficients; however, in contrast to the classical expressions, they are functions of the temperature and the magnetic field.

In order to obtain expressions for the constants of magnetostriction, we introduce the elastic energy and find the equilibrium values of the components of the deformation tensor $u_{ij} = u_{ij}^0$ from the condition of a minimum. If we substitute these in the formula for the relative extension, we get

$$\lambda_{[100]} = \lambda_{[100]}^0\,\varphi(\vartheta, H), \ \lambda_{[100]}^0 = c_1 A_1 N/V,$$
$$\lambda_{[111]} = \lambda_{[111]}^0\,\varphi(\vartheta, H), \ \lambda_{[111]}^0 = c_2 A_2 N/V. \tag{9}$$

The coefficients c_1 and c_2 depend on the elastic constants of the cubic lattice. As also in the case of the hexagonal crystals, the quantum calculation permits the a priori explanation of both positive and negative value of $\lambda_{[100]}$ and $\lambda_{[111]}$, which the classical theory could not do. Thus we have obtained in clear form the dependence of the constants of magnetostriction of cubic single crystals on temperature and, which is very important, on the external magnetic field.

The quantum theory of magnetostriction of ferromagnetics with a cubic lattice is extremely weakly developed. There is on this problem only the work of Vonsovskii[3], where a theory is given for the high temperature region. In this same work an expression is given (without derivation) for the temperature factor $\varphi(\vartheta, H)$ at low temperatures (for $H = 0$). In the corresponding case one can introduce the expression for $\varphi(\vartheta, 0)$ from the quasi-classical theory of Akulov. There dependence is of the form $\vartheta^{3/2}$ in these expressions; however, our dependence (7), while containing $\vartheta^{3/2}$, possesses a more complicated character (for details, see reference 4).

In the comparison of the expressions for the constants of Anisotropy[3] and the constants of magnetostriction of a hexagonal crystal[1] and a cubic crystal Eq. (9), a definite analogy is noted in their temperature behavior at low temperatures. This circumstance points up the deep connection between the phenomenon of anisotropy and that of magnetostriction, and is determined by the character of the energy spectrum of ferromagnetics at low temperatures. The great variation observed in the temperature dependence of the constants of magnetostriction and anisotropy for medium and high temperatures is connected with the fact that the "gas" of quasi-particles (elementary excitations) ceases to be ideal upon increase in temperature, and other quasi-particles (especially phonons), their interaction with ferromagnons begins to play an important role, and the individuality of the lattice appears strongly. These circumstances disrupt the apparent universality at low temperatures and lead to a series of complicated effects.

The theory developed by us, as noted in reference 1, applies primarily to liquid hydrogen temperatures. The development of a systematic quantum mechanical theory of magnetoelastic phenomena for intermediate temperatures and in the region of the Curie point is an important problem of the quantum theory of magnetism that is still unsolved.

---

[1] A. A. Gusev, J. Exper. Theoret. Phys. USSR **29**, 181 (1955); Soviet Phys. JETP

[2] S. V. Tiablikov, J. Exper. Theoret. Phys. USSR **20**, 661 (1950).

[3] S. V. Vonsovskii, J. Exper. Theoret. Phys. USSR **10**, 761 (1940).

[4] A. A. Gusev, Dissertation, Moscow State University 1954.

Translated by R. T. Beyer
302

The Study of Relativistic Particles by the Use of Nuclear Emulsions in a Pulsed Magnetic Field

V. M. LIKHACHEV, A. V. KUTSENKO
AND V. P. BORONKOV
P. N. Lebedev Physical Institute,
Academy of Sciences, USSR

(Submitted to JETP editor August 12, 1955)
J. Exper. Theoret. Phys. USSR **29**, 894-895
(December 1955)

IN recent years thick photographic emulsions have been used widely in a large number of physical problems. The study of the tracks left by particles in their passage through an emulsion enable us to derive information about the properties of the particles, the nature of nuclear reactions etc. However, the sign of a particle is seldom determined by this method and in many instances (when the entire track is not contained in the emulsion) the energy is not determined with sufficient accuracy.

A more complete solution of these problems can be achieved if the nuclear track plate is placed in a strong magnetic field during the period of irradiation. A calculation shows that an analysis of the momenta and signs of the particles can achieve sufficiently accurate results only in strong magnetic fields of the order of $1\text{-}1.5 \times 10^5$ gauss and above. It is known that such strong fields can be set up, at least at the present time, only in the form of pulses. However, in working with accelerators which also produce pulsed beams of particles, the use of pulsed magnetic fields seems to us especially advantageous because of the possibility of synchronizing the particle beam with the field*. We have used this kind of pulsed magnetic field to measure the spectrum of photons from the synchrotron of the Physical Institute of the Academy of Sciences of the USSR.

The apparatus consists of a current source[1] a control circuit and a solenoid within which the photographic films are placed. As a source of energy we use a bank of IM-3/100 pulse capacitors with a capacity of 3300 μf. The current-switching element is an IG-100/5000 ignitron. The pulse which fires the ignitron is timed so that the field peak coincides with the arrival of the particle beam from the accelerator. In order to avoid exposure of the nuclear emulsion in the absence of the magnetic field the accelerator operates under a so-called single-pulse regime**. The coil, which was made according to our own design, enabled us to set up a magnetic field of $1\text{-}1.5 \times 10^5$ gauss with a 5 mm space between sections of the coil and an inside diameter of 2.5cm. Axial asymmetry in the working part of the coil is 2-3% and radial asymmetry is 5-7%. A test coil was used to measure the field. The field was determined with an accuracy of 5%.

In order to determine the sign of the charge and the energy of the particles, measurements were made of the magnetic curvature and multiple scattering. For analysis of the tracks we used a MBI-8 microscope with a special ocular scale which makes for a great saving of time. Up to the present time we have studied 800 pairs found in an emulsion which was exposed in a magnetic field of 120,000 gauss. The total length of the tracks of these pairs is 221.6 cm. The mean energy per particle as determined by the magnetic method for 1600 components is 43.3 ± 2.7 mev; by the multiple scattering method the mean energy is 46.5 ± 1.7 mev. The scattering constant per 100 μ for electrons in a type «P» NIKFI (Cine-Photographic Scientific Research Institute) emulsion is 23.4 ± 0.7.

Preliminary data on the spectral distribution of the pairs is given in the figure. The results obtained by the multiple scattering method are shown by the dashed line; the solid line gives the results obtained by measuring the magnetic curvature.

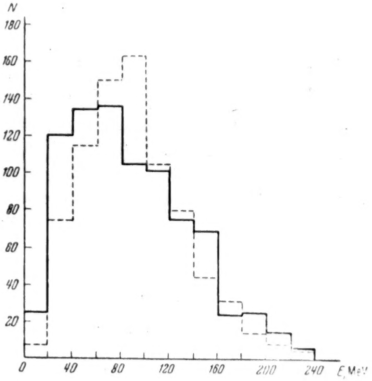

It is of interest that in a total of 78 cm (with 39 cm of the distance for positrons) only 2 instances were observed in which the particles disappeared suddenly without leaving a visible trace. In both cases the "disappearing" particles were positrons. Not a single similar instance was detected for negatively charged particles. We also observed a few cases of single scattering of electrons and positrons at angles above 100° and pair creation in the field of an electron.

In conclusion we wish to express our thanks to Prof. V. I. Veksler for his constant interest and assistance.

---

* This was first suggested by G. M. Strakhovskii in 1951.

** By the single-pulse regime we mean a regime under which the accelerator emits a single pulse at the appropriate "command" from an automatic device.

[1] P. L. Kapitza Proc. Roy. Soc. (London) A **105**, 691 (1924)

Translated by I. Emin
301

Inelastic Scattering of Mesons in the Semi-Phenomenological Theory of the Interaction of π-Mesons with Nucleons

IU. M. POPOV AND A. A. RUKHADZE
The P. N. Lebedev Physical Institute,
Academy of Sciences, USSR

(Submitted to JETP editor July 29, 1955)
J. Exper. Theoret. Phys. USSR **29**, 893 (December, 1955)

THE problem of inelastic scattering of π-mesons with nucleons (inelastic scattering emanating from the energy of incident mesons higher than 400 mev) has been solved on the basis of the semi-phenomenological theory of the interaction of π-mesons with nucleons[1]. Calculations were carried out according to the first nonvanishing approximation of Heitler's theory of damping[2]. After scattering, the following states were considered: nucleon + meson and "isobar" + meson, but the state of a nucleon + two mesons was not investigated. The creation of the second meson was regarded as the disintegration of the isobaric state of the nucleon. The present study does not contain new constants in comparison with the work.[1]

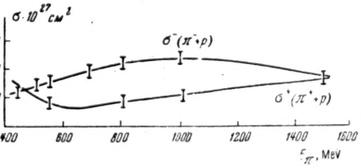

Total cross sections were obtained for the scattering of π^+- and π^-- mesons on protons with calculation of the contribution of $S_{1/2}$, $P_{1/2}$ and $P_{3/3}$ waves. The evaluation of the D wave showed that its contribution to the total cross section was less than 10%.

Comparison was made with experiment for energies of incident mesons greater than 400 mev (up to 400 mev results of the present study agree with the results of reference 1). Experimental data are shown on the graph[3]. The results obtained theoretically are given in the Table below. As is evident from comparison, the theoretical values of σ^+ $(\pi^+ + p)$ agree favorably with the experimental data, but the values of $\sigma^-(\pi^- + p)$ were noticeably smaller than those obtained experimentally.

Theoretical Values of Cross Sections

E_π, mev	$\sigma^+(\pi^+ + p)_3 \cdot 10^{27}$ cm^3	$\sigma^-(\pi^- + p)_3 \cdot 10^{27}$ cm^3
600	18.5	22.2
800	22.2	24
1000	23	25.5
1200	22.7	25

It is possible that the experimental values for σ^- $(\pi^- + p)$ are diminished as the result of their being made more precise[4]. But even in this instance agreement with the experiment is to be expected only in the calculation of the state nucleon + two mesons. This state should significantly increase the cross section $\sigma^-(\pi^- + p)$ with an insignificant increase in $\sigma^+(\pi^+ + p)$.

In conclusion the authors express their thanks to I. E. Tamm, Iu. A. Gol'fand and V. Ia. Fainberg for their continuous interest in the work as well as to L. V. Pariski, N. E. Nikulkina and L. I. Grachev, who performed a great computational task.

---

[1] I. E. Tamm, Iu. A. Gol'fand and V. Ia. Fainberg, J. Exper. Theoret. Phys. USSR **26**, 649 (1954)

[2] W. Heitler, Proc. Cambr. Phil. Soc. **37**, 291 (1941)

[3] Annual Review of Nuclear Science, **4**, 229 (1954)

[4] L. M. Shutt, A. M. Thorndicke and W. L. Whittemore, Phys. Rev. **97**, 797 (1955).

Translated by D. Tarris
299

The Relation Between our Criterion of Stability for a Homogenious Phase and that of S. V. Tiablikov

I. Z. FISHER

(Submitted to JETP editor June, 24, 1955)
J. Exper. Theoret. Phys. USSR 29, 884 (December, 1955)

BOGOLIUBOV and S. V. Tiablikov have noted that the criterion for the stability of a homogeneous distribution of particles, given in reference 1, coincides with the similar criterion, given earlier and and in different form by Tiablikov[2] in the case of limit points of the second kind. Equation (9) of reference 2 and the first of Eq. (34) of reference 3 can be put in the same form

$$-\frac{4\pi}{vkT}\int_0^\infty \frac{\sin\beta r}{\beta}\left\{\int_\infty^r \Phi'(t)\,g(t)\,dt\right\} r\,dr = 1, \qquad (1)$$

where $\Phi(r)$ is the intermolecular potential, $g(r)$ is the radial distribution function. This equation must be satisfied by the equation for the determination of β. The second of Eq. (34) in reference 2, which serves for this purpose, similarly to Eq. (1), is written in the expanded form

$$\int_0^\infty (\sin\beta r - \beta r\cos\beta r)\left\{\int_\infty^r \Phi'(t)\,g(t)\,dt\right\} r\,dr = 0. \qquad (2)$$

This condition is absent in reference 2, but a graphical method is applied there to the determination of β, which, as can be shown, is approximately equivalent to the requirement of Eq. (2). The approximation of the graphical method of Tiablikov consists of this, that the temperature on the left side of Eq. (9) in reference 2 is considered as an unknown and variable, while the term on the right is considered given and constant. A general and precise condition for determining β in reference 2 is not given.

The different approach to the problem in references 1 and 2, and, in part, the differences in notation account for the fact that the equivalence of the two stability criteria remained unknown to us. An attempt to determine the sign of the derivative (dv/dt) along the fusion curve by the theory of Tiablikov led us, as a consequence of an admitted error, to the physically inadmissible result of which mention was made in reference 3. Actually, as is clear from the above, the sign of the derivative must be the same in the two cases. It was shown in reference 4 that $(dv/dT)_{\lim} < 0$ for systems of the argon type, in accord with the experimental facts. Therefore the author acknowledges the error of his statement on the unfitness of the stability criterion for a liquid of S. V. Tiablikov, which statement was based on a misunderstanding of what was contained in reference 3.

The author thanks N. N. Bogoliubov and S. V. Tiablikov for their discussion of the question and for pointing out the error.

---

[1] I. Fisher, J. Exper. Theoret. Phys. USSR **28**, 171 (1955); Soviet Phys. JETP **1**, 171 (1955)

[2] S. Tiablikov, J. Exper. Theoret. Phys. USSR **17**, 386 (1947)

[3] I. Fisher, J. Exper. Theoret. Phys. USSR **28**, 437 (1955); Soviet Phys. JETP **1**, 273 (1955)

[4] I. Fisher, J. Exper. Theoret. Phys. USSR **28**, 447 (1955); Soviet Phys. **1**, 289 (1955)

Translated by R. T. Beyer
294

Capture of Thermal Neutrons by Isotopes of Lead

A. V. SHUT'KO AND D. F. ZARETSKII

(Submitted to JETP editor August 31, 1955)
J. Exper. Theoret. Phys. USSR 29, 866-868
(December, 1955)

1. CHARACTERISTIC of the capture of thermal neutrons by a natural mixture of lead isotopes is a gamma-ray spectrum consisting of only two lines[1]. The gamma quanta appear as quanta of the electric dipole type, the energies ($E_{\gamma_1} = 7.380 \pm 0.008$ mev and $E_{\gamma_2} = 6.734 \pm 0.008$ mev) being equal to the binding energies of a neutron in Pb^{208} and Pb^{207}, respectively. This simplicity of the spectrum represents the exception among the spectra of heavy elements and is associated with the "magic" attribute of Pb^{208}. An analysis of levels Pb^{208} and Pb^{207} shows that the simplicity of the spectrum can be explained if one assumes that an intermediate nucleus is not created during the capture, but that the process consists of an immediate transition of a neutron from a continuous spectrum into bound states. This same mechanism also specifies the correct magnitude of the cross section for capture of thermal neutrons by lead.

2. Having investigated gamma rays accompanied by beta decay of Tl^{208}, Elliott[2] et al obtained the energy level scheme of Pb^{208} (Fig. 1), from which it is seen that for capture of thermal neutrons by Pb^{207} transitions to excited levels of Pb^{208} are possible for only a high multipolarity. It is necessary to note also that these levels apparently correspond to an excited proton since: 1, spins and parity, shown in Fig. 1, can be obtained from the shell model, assuming that a proton from the filled shell (82 protons) is shifted to the succeeding unfilled shell; 2, lower levels ($E = 2.6$ mev and $E = 3.2$ mev) are not excited in the reaction Pb^{207} (dp) Pb^{208*} (energy of deuteron is 14 mev[3]); 3, these levels arise from beta decay of Tl^{208}, i.e., it can be assumed that radiation results from the transition of a proton from its excited state, arising from the conversion of a neutron into a proton, to its low-lying state.

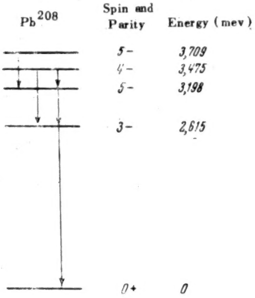

Fig. 1

The first two levels excited in the reaction[3] Pb^{207} (dp) Pb^{208*} have energies respectively equal to 3.37 mev and 3.60 mev. It is assumed that these levels have spins of 4 and 5, and parity opposite to the parity of the ground state of Pb^{208} (spins and parities of levels in (dp) experiments have been identified in accordance with the shell model). The next levels lie near the energy 5-6 mev. Thus it is seen that electric dipole capture must dominate for the ground state of Pb^{208}.

Let us consider Pb^{207}. The scheme of low-lying energy levels of odd nuclei can be divided into three classes[4]: "consecutive" system of levels, "hole" system and mixed system. The excitation of "consecutive" and "hole" levels in nuclei corresponds to the excitation of optical and x-ray terms in an atom. Now one can count it as an established fact[4] that the lower excited levels of Pb^{207} appear "hole like" (Fig. 2). As the figure shows, the spins and parities allow electric dipole transitions to the ground state $p_{1/2}$, and also to the excited state $p_{3/2}$ ($E_{\text{level}} = 0.870$ mev). If one assumes that the shell model holds for higher levels, then their spins and parities exclude dipole transitions.

Transitions between levels of a continuous spectrum, which evidently have the appearance of "consecutive", and the "hole" level $p_{3/2}$ appear forbidden compared with the transitions to level $p_{1/2}$, since the "cross-over" transitions appear particle-like. From the point of view of the intermediate nucleus, which we ordinarily understand as many-particle excitation, transitions to levels $p_{3/2}$ and $p_{1/2}$ are equally proper, and the absence of a transition to the $p_{3/2}$ level is difficult to explain.

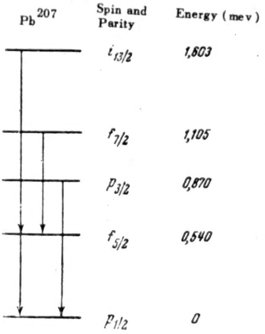

Fig. 2

3. Let us evaluate the magnitude of the cross section for capture of thermal neutrons by Pb^{207}. Taking into account the preceding, we assume that during capture only a single neutron, which is moving in a field described by a certain effective potential, $U(r)$, changes state. The total cross section of the electric dipole capture is equal to

$$\sigma_c = \frac{16\pi\,\mu\omega^3}{9h^2k_nc^4}\,Q_{10}^2, \tag{1}$$

$$Q_{10} = -\frac{Ze}{A}\sqrt{\frac{3}{4\pi}}\int \varphi_b^*(\mathbf{r})\,z\,\varphi_a(\mathbf{r})\,d\mathbf{r},$$

where φ_a and φ_b are the wave functions of the neutron in the initial and final states, k_n is the wave number of the incident neutron. Assuming that the potential changes sharply enough on the surface of the nucleus, we obtain (see, for example, reference 5)

$$Q_{10} \approx -(ZeU_0R^2 / A\mu\cdot\omega^2)\,L_{k_n0}(R)\,R_{E1}(R), \tag{2}$$

where U_0 is the magnitude of the effective potential inside the nucleus; $L_{k_n0}(r)$ and $R_{E1}(r)$ are the radial wave functions corresponding to the incident (l=0) and the bound neutron (l=0). In the limit where $k_n \to 0$ the value of the wave function $L_{k_n0}(R)$ is expressed in terms of the scattering amplitude and radius of the nucleus:

$$\lim_{k_n\to 0} L_{k_n0}(R) = (R-a)/R, \tag{3}$$

where a is the experimentally determined scattering amplitude of thermal neutrons in Pb^{207}. In addition if $(2\mu E/h)^{1/2}R \gg 1$ and $U_0^{1/2} \gg E^{1/2}$ (E is the order of magnitude of the binding energy of neutrons in Pb^{208}), one can find that

$$R_{E1}(R) \approx R^{-3/2}. \tag{4}$$

From Eqs. (1)-(4) it follows

$$\sigma_c = \frac{32\pi}{9}\left(\frac{Z}{A}\right)^2 \frac{e^2}{hc}\,\frac{(R-a)^2}{k_nR}\,\frac{U_0^2}{\mu c^2E}. \tag{5}$$

For $U_0 = 42$ mev, $R = 7.8 \times 10^{-13}$ cm, $a = 9.6 \times 10^{-13}$ cm,[6] the incident energy of thermal neutron $E_n = 0.025$ ev, and $E = 7$ mev, we obtain $\sigma_c \approx 0.42$ barn, which agrees with the experimentally determined value of 0.7 barn. Above we compared the theoretical evaluation of the cross section with data on the capture of thermal neutrons by Pb^{207}. Experiments[7] show that the cross section for capture of neutrons by Pb^{206} is within an order smaller than the cross section for capture by heavier isotopes. This diminution can be attributed to the fact that capture of neutrons by Pb^{206} is accompanied by a certain deformation of the self-consistent field, but in the case of Pb^{207} this deformation has practically no significance. One can say that capture by Pb^{206} appears less "single-particle-like" than in the case of Pb^{207}. Thus, the anomalous character of the capture radiation in isotopes of lead apparently is explained if it originates from a single-particle picture of capture. Obviously, such a consideration under no circumstances is applicable to heavy nuclei which are far from closed shells. These nuclei have great density of levels for the intermediate nucleus, and thus single-particle capture cannot compete with collective capture.

The authors thank Prof. A. S. Davydov for his discussion as well as B. F. Turchin for his valuable comments.

---

[1] B. B. Kinsey, G. A. Bartholomew, and W. H. Walker, Phys Rev. 82, 380 (1951).

[2] L. G. Elliott, R. L. Graham, J. Walker, and J. L. Wolfson, Phys. Rev. 93, 356 (1954).

[3] J. A. Harvey, Canad. J. Phys. **31**, 278 (1953).

[4] L. K. Peker and L. A. Sliv, Izv. Akad SSSR, Ser. Fiz. **17**, 411 (1953).

[5] E. D. Courant, Phys. Rev. **82**, 703 (1951).

[6] C. G. Shull and E. O. Wollan, Phys. Rev. 81, 527 (1951).

[7] H. Pomerance, Phys. Rev. **88**, 412 (1952).

Translated by B. G. Saunders
284

Crystalline Anisotropy of the Intermediate State

IU. V. SHARVIN AND V. L. SEDOV
Institute of Physical Problems,
Academy of Sciences, USSR

(Submitted to JETP editor July 18, 1955)
J. Exper. Theoret. Phys. USSR **29**, 897 (December, 1955)

WE have undertaken experiments on the investigation of the moments of forces which act through the agency of a magnetic field on a monocrystalline sphere of lead of high purity (99.998%), placed in the intermediate state. The specimen was mounted on a torsion suspension so that the [010] axis could be vertical and was placed (at a temperature of 3.65 °K) in a magnetic field whose direction could be changed in the horizontal plane. In addition, we superimposed a small (1-2 oersteds) magnetic field, which changed its sign with a period of 30 sec. Under these conditions we could observe the moments, which evidently have a reversible equilibrium character, and which arise as a consequence of the dependence of the surface tension at the boundary of the superconducting and normal phases on the orientation of this boundary with respect to the lattice. The great scatter of the results of various experiments, which is connected with the imperfections of the lattice of the specimens, does not permit a completely reliable quantitative check. However, qualitatively speaking, the two samples that we investigated gave results in agreement, namely, that the free energy of the specimen, as a function of the angle between the field and the tetragonal axis has maxima in the [100] and [001] directions. The intermediate minimum is located approximately at an angle of 25-35° with respect to the tetragonal axis. The height of the maxima for our samples (diameter 12.6 mm, 50% superconducting phase) was of the order of 10^{-3} erg. These results are evidently in qualitative agreement with the anisotropies of the penetration depth found by Pippard[1].

We express our thanks to A. I. Shal'nikov for his interest in this work.

---

[1] A. B. Pippard, Proc. Roy. Soc. (London) **203**, 195 (1950).

Translated by R. T. Beyer
303

Heat of Vaporization of Oxygen in the Temperature Range 80-106°K

R. A. ALIKHANOV
Institute of Physical Problems,
Academy of Sciences, USSR

(Submitted to JETP editor July 21, 1955)
J. Exper. Theoret. Phys. USSR **29**, 902-903
(December, 1955)

UP to the present time the heats of vaporization of condensable gases as a function of temperature have been little studied, although they are of both practical and theoretical interest. The basic theoretical methods of calculating heats of vaporization require the knowledge of a great number of other quantities. Experimental determinations have been few and insufficiently reliable.

We have undertaken to investigate the heat of vaporization of oxygen from 80° to 106°K by a precision method which we have developed, carried out as follows. A calorimeter contains an evaporator filled with the liquid, and a measured amount of power is applied. The vapor which forms is collected by condensation in a light tank and weighed at room temperature on an analytical balance. During the weighing period the evaporation process goes on in another similar flask.

The apparatus which has been constructed for this purpose includes:

(1) a vacuum adiabatic calorimeter, similar to the one described previously[1], with a number of changes and improvements;

(2) a system of two capillaries leading out of the calorimeter; one is used during filling and evaporation, and the other is connected to a mercury manometer;

(3) a gas system consisting of two thin-walled stainless steel tanks, closed by vents of original construction, a Bourdon manometer, and operating valves used during the period of evaporation.

Thirty-five measurements were made of the heat of evaporation at seven different temperatures. The value of the heat of vaporization at the normal boiling point served as a check on the method. The following table compares the heats of vaporization at the normal boiling point as measured by various workers in recent years:

	L (cal/mole)	T (°K)
Giauque and Johnston[2]	1628.8 ± 1.6	90.13
Clusius and Konnertz[3]	1630.0 ± 1.5	90.19
Present measurement	1628.7 ± 1.3	90.19

Our measurement agrees satisfactorily with the previous results.

The heats of vaporization at different temperatures are presented below, and are shown in the figure compared to the experimental data of Alt[4] and to values calculated from the empirical formula of Mathias[5].

T° K	80.0	81.5	85.4	90.2	95.1	100.0	106.0
L (cal /mole)	1706	1696	1665	1628	1587	1544	1490

The dashed line on the graph represents the curve calculated from our choice of empirical expression:

$$L^2 = 67208{,}68\,(T_{cr} - T) - 555{,}221\,(T_{cr} - T)^2 + 2{,}32505\,(T_{cr} - T)^3.$$

I should like to express my deep gratitude to P. G. Strelkov for his constant attention and interest in this work.

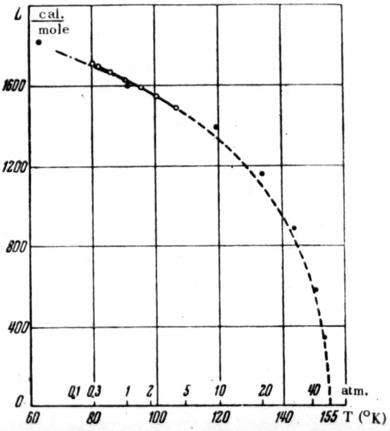

Broken line – Set[4]; solid circles – Mathius et al[5]; open circles – author's data

---

[1] V. N. Kostriukov, R. A. Alikhanov, B. N. Samoilov and P. G. Strelkov, Zh. Fiz. Khim. **28**, 650 (1954)

[2] W. F. Giauque and H. L. Johnston J. Am. Chem. Soc. 51, 2300 (1929).

[3] R. Clusius and F. Konnertz, Naturforsch. **4a**, 117 (1949)

[4] H. Alt, Ann. d. Physik 19, 739 (1906)

[5] Mathius et al., Leiden Comm. No. 162a (1922)

Translated by D. C. West
307

Measurement of the Absolute Quantum Yield of Photoluminescence of Alkali-Halide Crystals

Z. L. MORGENSHTERN
P. N. Lebedev Physical Institute,
Academy of Sciences, USSR

(Submitted to JETP editor July 19, 1955)
J. Exper. Theoret. Phys. USSR **29**, 903-904
(December, 1955)

IN earlier works the dependence of the relative quantum yield of photoluminescence of crystals of KI-Tl and NaI-Tl on the concentration of the activator[1] and the wavelengths of the exciting light[2] was investigated. In the present work the absolute quantum yield of luminescence of these crystals during excitation in the absorption region of the activator was investigated.

For determining the absolute quantum yield a method was used in which the number of luminescent quanta and the number of absorbed quanta of exciting light was measured with the aid of a substance which is luminescent under the action of the one as well as the other radiation, and which has a constant quantum yield in the entire measurable region. This method has been applied earlier to the measurement of the absolute luminescence yield of powdered phosphors which radiate in the ultra-violet[3], and also of some finely-crystalline organic phosphors[4].

Our measurements were carried out in a photometric sphere, which made it possible to take into account the entire flux of luminescence. As a measurable luminescent substance a powdered, light yellow phosphor was taken. The preliminary tests showed that the quantum luminescence yield of this phosphor does not depend on the wavelength in the region 240-500 mμ, and the absorption coefficient of the surface of the powdered layer of phosphor is constant (about 0.95) in this region. The excitation and radiation spectrum of the crystals KCl-Tl, KI-Tl, and NaI-Tl is in this region.

The measurements were carried out with light excitation from a hydrogen lamp through a spectrometer SF-4, with a cap enclosing an FEY-19 photomultiplier and an amplifier*. The crystal was placed in an aluminum sphere (ϕ4cm), which had a slot (4 × 10 mm) for the entrance of the exciting light, and an aperture (ϕ 10 mm) for the exit of the luminescent light. The sphere was lined in the interior with a thick layer of phosphor. The exciting light fell on the crystal and part of it was reflected while the remainder was absorbed, producing luminescence of the crystal (special attention was given so that the absorption of exciting light in the crystal was complete). The reflected light as well as the luminescent light of the crystal caused a glow of the phosphor, which was registered by the photomultiplier.

The reflected (Fresnel) exciting light was measured with the help of another nonabsorbing crystal, the back face of which was blackened. A crystal of NaCl was used for this purpose. The small difference in the index of refraction is unimportant, in view of the small size of the correction. The incident exciting light (in order to preserve the geometry) was similarly measured with the aid of a nonabsorbing crystal, the back face of which in this case was covered with magnesium oxide. It is obvious that if in the first measurement we obtain the reading a, in the second b, and in the third c, then the quantum yield will equal $\eta = (a - b)/(c - d)$. The results of the measurements of yield are presented in the following Table.

Crystal	$\lambda_{\text{excit.}}$ (mμ)	η	Note
KCl-Tl	246	0.80	
KJ-Tl	245	0.80 0.70 0.93	Different crystals
KJ-Tl	285	0.77 0.74 0.76	One and the same crystal, different method of calculation of the reflected light
NaJ-Tl	260	0.40	
NaJ-Tl	293	0.61	

The concentration of Tl in the crystals KI-Tl and NaI-Tl was sufficient so that during the excitation in the shortwave region of absorption the Tl yield no longer depended on its concentration[1]. In KCl-Tl, according to our measurements, the concentration of Tl was 1.5×10^{-4}gm Tl/gmKCl; the data for KCl-Tl correspond well with those available in the literature[5]. It should be noted that in KI-Tl the variations in the value of the yield for various crystals (with high content of Tl) is found to be greater during excitation with $\lambda = 245\ m\mu$ than with $\lambda = 285\ m\mu$. This is easily explained by the different degree of overlapping of the short wave region of Tl absorption with the boundary of absorption of the lattice itself, which, as has been shown[2], is inactive.

The above method was also used to measure the quantum yield of several organic monocrystals. The coefficient of reflection in this case was measured directly. With excitation of $\lambda = 250\ m\mu$ the yield amounts to: for tolane 0.57; for dibenzyl 0.44; for stilbene 0.43; for naphthalene 0.18. These values correspond satisfactorily with the data of other authors.

I thank M. N. Alentsev and M. D. Galanin for their valuable advice and help during the completion of this work.

---

* The cap was constructed by E. E. Bukke.

[1] L. M. Beliaev, M. D. Galanin, Z. L. Morgenshtern and Z. A. Chizhikova, Dokl. Akad. Nauk SSSR **99**, 691 (1954); Dokl. Akad. Nauk SSSR **105**, 57 (1955).

[2] Z. L. Morgenshtern, Dokl. Akad. Nauk SSSR **105**, 250 (1955).

[3] M. N. Alentsev and L. A. Vinokurov, Izv. Akad. Nauk SSSR, Ser. Fiz. **15**, 725 (1951).

[4] M. D. Galanin and Z. A. Chizhikova, J. Exper. Theoret. Phys. USSR **26**, 624 (1954).

[5] W. Bünger, Z. Physik **66**, 311 (1930).

Translated by L. A. D'Asaro
308

The Surface Tension of Liquid He³ in the Region of Very Low Temperatures (1.0-0.35°K)

K. N. ZINOV'EVA
Institute of Physical Problems,
Academy of Sciences, USSR

(Submitted to JETP editor September 15, 1955)

J. Exper. Theoret. Phys. USSR **29**, 899-900
(December, 1955)

EARLIER[1] we discussed our measurements of the surface tension of liquid He^3 from the critical temperature to 0.93°K by the method of capillary rise[4]. In the present work we have continued the measurements to lower temperatures using our earlier capillaries with diameters of 0.360, 0.224, and 0.188 mm. By pumping on He^3 vapor, we were able to carry the measurements to 0.35°K.

The temperature of liquid He^3 was determined by the vapor pressure of He^3, measured with a Mcleod gauge. In the temperature interval 0.5-1.0°K we used the temperature scale of Sydoriak and Roberts (see reference 2). Below 0.5°K, the temperature was calculated from the vapor pressure, using an empirical formula given in reference 2. The pressure of the saturated vapor of He^3 at a temperature of 0.35°K was 0.008 mm Hg. To measure the position of the level in the capillary we used a cathetometer, KM-5, which enabled us to read the height with an accuracy of 0.001 mm. However, as in the previous work, the actual accuracy of the reading was no better than several hundredths of a millimeter, since the observation of the meniscus was made through eight dewar vessel walls. The shape of the meniscus did not vary, and the guide line was adjusted for some average position of the division line. The error, introduced by the deformations of the heterogeneous glass, and noted by us earlier[1], was no greater than ±2%.

The measurement proceeded in the following way. After the temperature had reached the lowest point, around 0.3°K, the pumping was stopped and the liquid slowly warmed up. In the warming process, regular measurements were taken of the vapor pressure of He^3 and the height of rise of the liquid in the capillary. The warm-up time from 0.3° to 1.0°K took approximately 2.5 hours.

The calculation of the coefficient of surface tension was made according to the equation $\alpha = \rho g r h/2$, where the value of ρ, the density of liquid He^3, was taken from the paper of E. C. Kerr[3]. The results obtained in the temperature interval 0.35-1.0°K, averaged for the three capillaries, are shown in Fig. 1 together with earlier data[1]. Also shown are the results obtained by others[4,5]. As we can see from the figure, the results from all three papers are in satisfactory agreement. (The old data have been recalculated using the new densities[3].)

The error in determining the value of the surface tension in the region of very low temperature is approximately 5%. The maximum scatter of the individual points is shown by the arrows on the figure.

As we can see from the graph, the surface tension of He^3 below 0.6°K approaches its limiting value equal to 0.152 dyne/cm. This value is 2.3 times smaller than the limiting value α_0 for He^4, which is assumed to be equal to 0.35 dyne/cm on the basis of extrapolated experimental data[6,7].

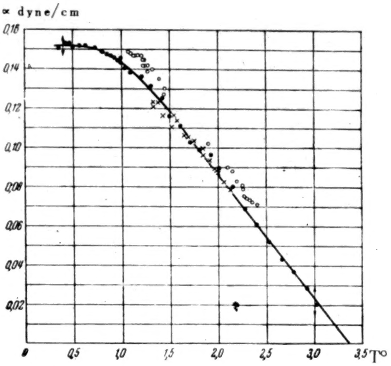

FIG. 1. ●-data from this work and reference 1; ×-Esel'son and Berezniak[4]; O-Lovejoy[5].

It is interesting to note that the character of the dependence of the temperature on the surface tension in He^4 and He^3 is exactly the same and differs only in magnitude. This is easy to see from Fig. 2, which shows α/α_0 as a function of T/T_{cr} for He^3 and He^4. Both curves coincide, within the limit of the accuracy of the measurements. Thus, we see that the different statistics of the isotopes leads to no noticeable difference in the temperature dependence of surface tension down to $T/T_{cr} = 0.19$.

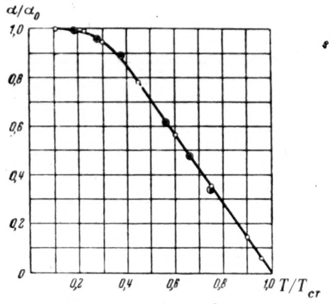

FIG. 2. ⊖-He^4, O-He^3

In closing I wish to express my deep gratitude to Prof. V. P. Peshkov for his sustained interest in our work, and to N. I. Iakovlev who helped with the measurements.

---

[1] K. N. Zinov'eva, J. Exper. Theoret. Phys. USSR **28**, 125 (1955); Soviet Phys. JETP **1**, 173 (1955)

[2] C. J. Gorter, Progress in Low Temperature Physics, (North-Holland Publishing Co., Amsterdam, 1955), p.82.

[3] E. C. Kerr, Phys. Rev. **96**, 551 (1954)

[4] B. N. Esel'son and N. G. Berezniak, Dokl. Akad. Nauk SSSR **99**, 365 (1954).

[5] D. R. Lovejoy, Can. J. Phys. **39**, 49 (1955).

[6] A. T. van Urk, W. H. Keesom and H. Kammerlingh Onnes, Leid. Comm., No. 179a, Proc. Roy. Akad. Amsterdam **28**, 58 (1925).

[7] J. F. Allen and A. D. Misener, Proc. Cambridge Phil. Soc. **34**, 299 (1938).

Translated by S. G. Sydoriak
305

Surface Ionization of Calcium, Strontium and Magnesium on Oxidized Tungsten

IU. K. SZHENOV

(Submitted to JETP editor June 2, 1955)
J. Exper. Theoret. Phys. USSR **29**, 901-902
(December, 1955)

THE surface ionization effects in alkali metal atoms are known to be well described by the Saha-Langmuir equations [1]. In the case of the alkaline earth elements, no satisfactory agreement with theory has yet been obtained. The existing data on surface ionization of barium[2-4], calcium and magnesium[5,6] on tungsten were obtained under various experimental conditions and differ noticeably among themselves. It is possible that in some of these experiments the tungsten had become oxidized, thus altering the work function of the surface and complicating the observations. In this letter we shall describe some results of attempts to study the surface ionization of calcium, strontium and magnesium atoms on tungsten, undertaken with the aim of exploring the possibility of ionizing them effectively. A mass spectrometer method was used to measure the flow of ions, thus enabling the joint surface ionization of different types of atoms to be followed, and comparative measurements to be made[6].

It was found that the change of surface ionization with temperature for calcium on tungsten satisfies the Saha-Langmuir equation. Similar results for magnesium were obtained in the work reported in reference 6.

Attempts to increase the effectiveness of surface ionization of calcium by a preliminary oxidation of the tungsten did not give positive results. However, when a continuous stream of oxygen was directed at the incandescent tungsten, the ion current at first increased by two orders of magnitude, after which the equilibrium current, and the time required to establish it, were observed to depend on the pressure of oxygen near the filament, over a small range of pressure (of the order of 10^{-6} to 10^{-5} mm Hg). A further increase in pressure did not affect the magnitudes of the ion currents. At tungsten filament temperatures of about 2000°K there was a maximum in the ion current, and with increasing oxygen pressure the location of this maximum shifted slightly in the direction of higher temperatures. If the glowing filament were suddenly heated to temperatures above 2600°K and then reduced to its former temperature, a sudden initial jump in ion current was observed, followed by a drop to values noticeably lower than the initial current and then by a gradual recovery to the initial value. The recovery time decreased at higher pressures.

The intensity of the calcium beam was varied over such wide limits that the time required to form a monomolecular layer of calcium oxide on the filament would have required from a few seconds to several hours. None the less, an interruption in the oxygen supply invariably led to a sharp decrease in the ion current. Consequently, under these conditions the increased effectiveness of surface ionization of the calcium cannot be due to the formation of a layer of calcium oxide on the tungsten[5].

Analogous results were obtained with strontium, magnesium and sodium. In the case of sodium, the increased surface ionization at the much lower filament temperatures persisted even after the oxygen supply was cut off, as is usually observed on oxidized tungsten.[6] (It is known that lithium is also effectively ionized on incandescent tungsten which is kept in a stream of oxygen[7]).

Thus in our experiments we have observed the surface ionization of calcium, strontium and magnesium on oxidized tungsten, under conditions of continuous regeneration of the decomposing layer of tungsten oxide. The greatest effect was obtained in a narrow interval of high temperatures and at suitably high oxygen pressures, where apparently adsorption of calcium, strontium or magnesium atoms on the surface does not play a substantial role but the rate of oxidation of the tungsten is considerable, so that the values of temperature and mean work function of the surface are optimal. It is to be expected that an increased degree of surface ionization, due to the increased work function of the tungsten when it becomes oxidized, would occur under definite conditions regardless of the type of atoms. It is proposed to make use if this effect to detect atomic beams of the alkaline earth metals in measuring their nuclear moments.

---

[1] L. N. Dobretsov, *Electronic and Ionic Emission*, (1952), p. 245.

[2] A. N. Guthrie, Phys. Rev. **49**, 868 (1936).

[3] R. H. Hay, Phys. Rev. **60**, 2 (1941).

[4] G. A. Morozov, Zh. Tekhn. Fiz. **17**, 1143 (1947).

[5] L. N. Dobretsov, S. V. Starodubtsev and Iu. I. Timokhina, Dokl. Akad. Nauk SSSR **55**, 303 (1947).

[6] S. V. Starodubtsev and Iu. I. Timokhina, *Collection in Honor of the 70th Year of Academician A. F. Ioffe* (1950) p. 117.

[7] J. H. Manley and S. Millman, Phys. Rev. **51**, 19 (1937).

Translated by D. C. West
309

Phosphorescence of the Crystal Phosphor ZnS-Cu during Excitation by an Electron Beam

T. P. BELIKOVA
P. N. Lebedev Physical Institute,
Academy of Sciences, USSR

(Submitted to JETP editor July 19, 1955)
J. Exper. Theoret. Phys. USSR **29**, 905-906
(December, 1955)

NOTWITHSTANDING the large number of investigations of cathodoluminescence, there are almost no works in the literature in which a comparison is carried out, on the very same specimens, of the kinetics of the after-glow of phosphors under excitation by light and electrons. For the beginning stages of afterglow (about 10^{-3} sec) such an investigation has been carried out[1]. In this work it was shown that the decay takes place nonspecifically with regard to the sort of excitation and that the difference in the observed decay curves can be explained by means of the difference in density of excitation during various types of excitation (light λ = 365 or 313 mμ, or an electron beam).

In the present work the continuous decay of luminescence of a ZnS-Cu phosphor (10^{-4} g/cm^3) was measured during excitation by an electron beam (energy of 2000 v, current density of 3μamp/cm^2) and, for comparison, under excitation by light with λ = 365 mμ. Figure 1 gives decay curves in double logarithmic coordinates, obtained with various intensities of exciting light *a* and with various densities of current *b*. The numbers on the curves indicate, respectively, the relative intensity of exciting light and the relative stationary brightness of luminescence under excitation by electrons.

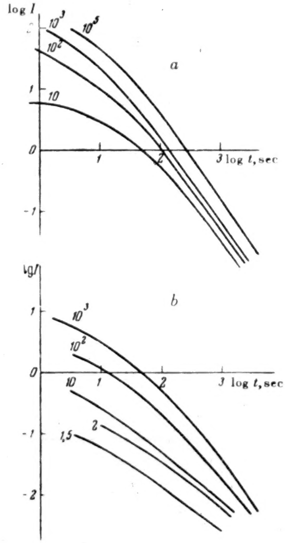

FIG. 1

According to these data, the decay of cathodoluminescence to the last stages of after-glow follows, as in photoluminescence, a hyperbolic law, in which the slope of the decay curves during electron excitation is somewhat smaller than is the case with light, despite the fact that in the first case with the very same brightness of phosphor the density of excitation is much larger than in the second case.

The appearance of the decay curve must essentially depend on the initial distribution of the exciting electrons in the phosphor according to different levels of localization. In Fig. 2 are curves of the temperature induced glow of the investigated phosphor during light (curve 1) and during electron (curve 2) excitation*. The similarity of these curves shows that the system of local levels and their filling is essentially unchanged by electron excitation as compared with excitation by light. The reason for the difference in the decay curves can consequently not be found directly from the obtained curves of temperature induced glow. Clarification of the difference requires a more detailed investigation.

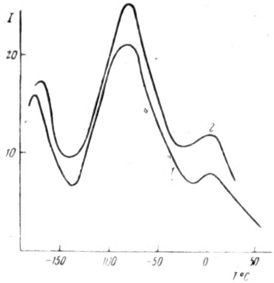

FIG. 2

The author expresses hid gratitude to V. L. Levshin, who suggested this work.

---

* In taking the curves of temperature glow, the intensity of excitation was matched by means of the maximum of the intensities used in obtaining the decay curves.

[1] V. A. Arkhangelskaia, A. M. Bonch-Bruevich, N. A. Tolstoi and P. P. Feofilov, J. Exper. Theoret. Phys. USSR **21**, 290, 297 (1951).

Translated by L. A. D'Asaro
309

Author Index to Volume 2

References with L are Letters to the Editor

Abrosimov, A. T., A. A. Bedniakov, V. I. Zatsepin, Iu. A. Nechin, V. I. Solov'eva, G. B. Kristiansen and P. S. Chikin. Investigation of the Structure of Extensive Air Showers at Sea Level – 357L

Adirovich, E. I. and V. G. Kolotilova. Propagation of a Short Pulse in a Semiconductor Bounded by Two Electron-Hole Transitions – 670

Agrest, M. M. Calculation of the Ultimate Thickness of the Emulsion Layer in the Investigation of Nuclear Processes by the Photographic Method – 166L

Alekseevskii, N. E. and Iu. P. Gaidukov, The Effect of Pressure on the Superconductivity of Cadmium. –762L

Alikhanov, R. A. Heat Evaporation of Oxygen in the Temperature Range 80-106°K –771L

Andronikashivili, G. L. and G. G. Mírskaia. The Behavior of Helium II in the neighborhood of a Heat Diffusing Surface – 406L

Antonov-Romanovskii, V. V. and L. A. Vinokurov. On the Lowering of the Luminescence Yield of Phosphors in Intense Excitation – 711L

Aptekar', I. L., and B. L. Timan. Adiabatic Processes at High Temperatures – 327L

Askar'ian, G. A. The Radiation of a Rapidly Moving Electric Image of a Uniformly Moving Charge – 334L

Azbel', M. Ia. Determination of the Dielectric Constant of Superconductors – 354L

——— **and E. A. Kaner.** Anamolous Skin Effect in an Arbitrary Integral of Collision –749L

Azbel', M. Ia. and E. A. Kaner. Anamalous Skin Effect in an Arbitrary Integral of Collision –573L

Balandin, M. P., B. D. Balashov, V. A. Zhukov, B. M. Pontecorvo and G. I. Silivanov. The Possibility of the Formation of Λ^0 Particles by Protons with Energies up to 700 mev – 98

Balashov, B. D. (see Balandin, M. P.) – 98

Baluev, B. M., B. I. Gavrilov, G. N. Zatsepina and L. E. Lazereva. The Average Number of Neutrons Per Fission Event in the Photodisintegration of Uranium and Thorium – 106

Balygin, I. E. On the Development by Means of Leaders of the Process of Breakdown of Liquids – 749L

Barchukov, A. I., T. M. Minaeva and A. M. Prokhorov. Microwave Spectrum of the C_2H_5Cl Molecule –760L

Bedniakov, A. A. (see Abrosimov, A. T) – 357L

Belen'kii, S. Z. and G. A. Milekhin. Multiple Production of Particles in the Collisions of High-Energy Nucleons with Nuclei – 14

Belikova, T. P. Phosphorence of the Crystal Phosphor ZuS-Cu During Excitation by an Electron Beam –776L

Belovitskii, G. E., T. A. Romanova, L. V. Sukhov and I. M. Frank. Fission of Uranium by Slow π-Mesons, Fast Neutrons and X-Rays of Energies up to 250 mev –493

Berestetskii, V. B. Asymptotic Behavior of the Electromagnetic Vacuum-Polarization in the Presence of Meson Interactions –540

——— **and I. Ia. Pomeranchuk.** Formation of a μ- Meson Pair in Positron Annihilation –580

——— Formation of a μ-Meson Pair in Positron Annihilation –580L

Blokhintsev, D. I. On the Theory of Nucleons – 23

Bobovich, Ia. S. and V. M. Pivovarov. Photoelectric Recording of Spectra of Combination (Raman) Scattering of Powdery Materials – 574L

Bolotin, I. B. Levinson and L. I. Levin. The Double Configurational Approximation in the Case of Carbon-like Atoms – 391

Borovik-Romanov, A. S. and N. N. Kreines. Magnetic Properties of Trivalent Ions of Europium and Samarium – 657

Bozhulin, P. A., S. G. Rautian, A. I. Sakolovskaia and N. M. Sushchinskii. Methods of Investigating the Width of Raman Lines and Their Application – 663

Bronshtein, I. M. and T. A. Storodina. Secondary Electron Emission in Thin Layers of Be. II – 410

——— Secondary Electron Emission in Thin Layers of Silver – 414

Chernavskii, D. S. (see Gerasimova, N. M.) – 344L

——— **(see Podgoretskii, M. I.)** – 211

Chikin, P. S. (see Abrosimov, A. T.) – 357L

Davidov, A. S. The Connection Between the Vibrations of the Surface of a Nucleus and Single Nucleon Excitation – 62

Dentsov, N. G. The Interaction of Ordinary and Extraordinary Waves in the Ionosphere and the Effect of Multiplication of Reflected Signals – 342L

Dimitrieva, M. M. (see Solntsev, G. S.) – 533

Drokin, A. I. and V. L. Il'iushenko. The Effect of the Method of Demagnetization of the Specimen on the Temperature Dependence of the Magnetization of Nickel in Weak Fields – 191L

Dukel'skii, V. M. and N. V. Fedorenko. Loss of Two Electrons by Negative Ions in Collisions with Atoms and Molecules – 307

Dzhelepov, V. P., K. O. Oganesian and V. B. Fliagin. Formation of Neutral π-Mesons in (*n* – *p*) Collisions at Effective Neutron Energies of 590 mev –757L

——— **V. I. Satarov and B. M. Golovin.** Total Cross Sections of Nuclei of Certain Elements for Neutrons with Energies of 590 mev – 349L

Eidus, I, M. (See Stepanov, A. V.) – 377

Fain, V. M. Radiation of Molecules in the Presence of a Strong High-Frequency Field –747L

Fainberg, V. Ia, (see Silin, V. P.) – 3

Fedorenko, N. V. (see Dukel'skii, V. M.) – 307

Feinberg, E. L. The Interaction of Fast Deuterons with Nuclei – 58

—— (see **Lazareva, L. E.**) – 351L

Feofilov, P. P. (see **Grechushnikov, B. N.**) – 330L

Filippov, S. S. The Fermi-Yang Hypothesis – 572L

Fisher, I. Z. The Relation Between our Criterion of Stability for a Homogeneous Phase and that of S. V. Tiablikov – 768L

Fliagin, V. B. (see **Dzhelepov, V. P.**) – 757L

Fogel', Ia. M. and L. I. Krupnik. The Formation of Negative Oxygen Ions in the Collisions of Positive Oxygen Ions with Gas Molecules – 252

Fradkin, E. S. Concerning Some General Relations of Quantum Electrodynamics – 361L

—— The Quantum Theory of Fields I – 148

—— The Problem of the Asymptote of the Green Function in the Theory of Mesons with Pseudoscalar Coupling – 340L

Fradkin, M. I. On the Problem of Anti-protons in the Primary Stream of Cosmic Rays – 87

Frank, I. M. (see **Belovitskii, G. E.**) – 493

Frank-Kamenetskii, D. A. Numerical Values of the Constant of the Triplet Beta Interaction – 162

Gaidukov, Iu. P. (see **Alekseevskii, N. E.**) – 762L

Galanin, A. D., B. L. Ioffe and I. Ia. Pomeranchuk. The Asymptotic Green's Function of Nucleon and Meson in Pseudoscalar Theory with Weak Interaction – 37

Gavrilov, B. I. (see **Baluev, B. M.**) – 106

Geilikman, B. T. The Theory of Strong Coupling for Meson Fields I – 509

—— The Theory of Strong Coupling for Meson Fields II – 601

—— The Theory of Strong Coupling for Meson Fields III – 451

Gerasimova, N. M., and D. S. Chernavskii. On Particle Energy Distribution at Multiple Formation – 344L

Gershtein, S. S. and Ia. B. Zel'dovich. Meson Corrections in the Theory of Beta Decay – 576L

Ginzburg, V. L. On the Macroscopic Theory of Superconductivity – 589

—— The Surface Energy Associated with a Tangential Velocity Discontinuity in Helium II – 170L

—— **and V. P. Silin.** The Effect of Interelectronic Collisions on the Electrical Conductivity and Skin Effect in Metals – 46

Glembotskii, I. I., V. V. Kibartas and A. P. Iutsis. Fock Self-Consistent Field for the Boron Atom in the Two-Configuration Approximation – 476

Gol'danskii, V. I., V. S. Pen'kina and E. Z. Tarunev. Fission of Heavy Nuclei by High Energy Neutrons* – 677

—— **and M. I. Podgoretskii.** On the Correlation Method for the Determination of the Absolute Yield of Nuclear Reactions – 441

Golovin, B. M. (see **Dzhelepov, V. P.**) – 349L

Gorngi, N. G. Investigation of the Structure of the Surface of Films of Copper Oxide on Different Faces of a Monocrystal of Copper, and the Determination of the Contact Potential Difference between these Surfaces – 687

Grechushnikov, B. N. and P. P. Feofilov. Fluctuating Structure in the Absorption Spectrum of Ruby – 330L

Gribov, V. N. (see **Gurevich, L. E.**) – 565

Grigoruk, L. V. (see **Kokhanenko, P. N.**) – 530

Gurevich, L. E., and V. N. Gribov. Dielectric Losses in Ionic Dielectrics in Strong Electric Fields – 565

Gusev, A. A. The Quantum Theory of Magnetostriction – 126

—— The Quantum Theory of the Magnetostriction of Cubic Monocrystals of Ferromagnetics at Low Temperatures – 764L

Gvozdover, S. D. and N. M. Ievskaia. Determination of Transverse Relaxation Times in the Magnetic Resonnance of Atomic Nuclei in Weak High-Frequency Magnetic Fields – 90

—— Determination of Longitudinal Relaxation Times for Magnetic Resonance of Atomic Nuclei in an Intense High-Frequency Magnetic Field – 486

Iakobson, A. M. The Internal Compton Effect –

Ievskaia, N. M. (see **Gvozdover, S. D.**) – 90

—— (see **Gbozdover, S. D.**) – 486

Il'iushenko, V. L. (see **Drokin, A. I.**) – 191

Ioffe, B. L. (see **Galanin, A. D.**) – 37

Isaev, P. S. and M. A. Markov. The Theory of Λ^0 Particles – 84

Iutsis, A. P. (see **Glembotskii, I. I.**) – 476

—— (see **Kibartas, V. V.**) – 476

Iuzhakov, V. M. The Measurement of the Specific Charge of Conduction Electrons – 332L

Ivanova, N. S. (see **Perfilov, N. A.**) – 433

Kagan, Ia. M. and V. I. Perel'. Concerning the Cross Section of Overcharging of Slow Ions in their Own Gas – 761L

—— On the Theory of Langmuir Probes – 326L

Kaganov, M. I. (see **Lifshitz, I. M.**) – 172L

Kaner, E. A. (see **Azbel', M. Ia.**) – 749L

Kaniukov, M. V. and Ia. P. Terletskii. Electroacoustic Waves in Gas Discharge Plasma with Consideration of Volume Recombination – 742L

Kaplan, S. A. The Theory of the Acceleration of Charged Particles by Isotropic Gas Magnetic Turbulent Fields – 203

Kapustinskii, A. F. The Rotation of the Plane of Polarization in Electrolyte Solutions by a Magnetic Field – 744L

Karmen, K. N. Electrical After-Effects in Rochelle Salt – 578L

Karpova, V. I. (see **Zamchalova, E. A.**) – 165L

Kartuzhanskii, A. L. The Photographic Action of Ionizing Particles I – 550

Kavetskii, V. T. (see **Kibartas, V. V.**) – 476

Khalatnikov, I. M. (see **Landau, L. D.**) – 69

—— The Second Viscosity of Monatomic Gases – 169L

Kharitonov, V. M. Orientation of Planes in Double V^0 Decay Events – 741L

Khokhlov, M. Z. The Question of the Possibility of Measuring the Temperature of the Column of a Jet Discharge Using the 3064 Å Hydroxyl band – 559

Khristiansen, G. B. (see **Abrosimov, A. T.**) – 357L

Khutseshvili, G. R. Polarization of the Nuclei of Ferromagnetic Atoms – 744L

Kibartas, V. V. (see **Glembotskii, I. I.**) – 476

—— **V. T. Kavetskii and A. P. Iutsis.** Fock Self-Consistant Field in the Three-Configuratuon Approximation for the Beryllium Atom —476

Kizel', V. A. Study of the Structure of the Surface of a Liquid by the Method of Reflection of Light — 520

Klinger, M. I. The Theory of the Hall Effect in Ionic Semiconductors —383

Kokhanenko, P. N., and L. V. Grigoruk. Absorption Spectrum of Excess Silver in the Low Temperature and High Temperature Modifications of Silver Iodide —530

Kolotilova, V. G. (see Adirovich, E. I.) — 670

Korostyleva, L. A. (see Striganov, A. R.) — 277

Kosevich, A. M. and I. M. Lifshitz. The de-Haas-van Alphen Effect in Thin Metal Layers —646

—— **(see Lifshitz, I. M.)** —172L

Kreines, N. M. (see Borovik-Romanov, A. S.) —657

Krupnik, L. I. (see Fogel', Ia. M.) — 252

Kutsenko, A. V. (see Lukhachev, V. M) —766L

Kutsishvili, G. R. The Thermodynamic Theory of Magnetic Relaxation — 187

Landau, L. D. and I. M. Khalatnikov. The Gradient Representation of the Green's Function for Charged Particles — 69

Lazareva, L. E., E. L. Feinberg and F. L. Shapiro. Neutron Spectrometry Based on the Measurement of of the Decelerating Time of Neutrons — 351L

——— **B. S. Ratner and I. V. Shtranikh.** Delayed Neutrons Which Accompany Photofission of Uranium

—— **(see Baluev, B. M.)**— 106

Levin, L. I. (see Bolotin, A. B.) —391

Levin, M. L. An Elementary Derivation of the formula for the Electromagnetic Energy in a Dispersive Medium — 168L

Levinson, I. B. (see Bolotin, A. B.) —391

Levitskaia, M. A. The Characteristics of "Specific" Zones —119

Liapidevskii, V. K. Investigation of the Field of Partial Pressures in a Diffusing Condensing Chamber — 346L

Lifshitz, E. M. The Theory of Molecular Attractive Forces between Solids — 73

Lifshitz, I. M. and M. I. Kaganov. The Effective Density of Rotating Liquid Helium II — 172L

—— **and A. M. Kosevich.** Theory of Magnetic Susceptability in Metals at Low Temperatures —636

—— **(see Kosevich, A. M.)** —646

Litvinenko, I. A. (see Tolstoi, N. A.) —

Logunov, A. A. Green's Function in Scalar Electrodynamics in the Region of Small Momenta — 337L

——— **and Ia. P. Terletskii.** Diffusion Coefficient of Particles in a Magnetized Interstellar Medium — 353L

Lozhkin, O. V. (see Shamov, V. P.) — 111

—— **N. A. Perfilov and V. P. Shamov.** The Angular Distribution Fragments from Fission of Uranium at High Excitation Energies — 116

Lukhachev, V. M., A. V. Kutsenko and V. P. Voronkov. The Study of Relativistic Particles by the Use of Nuclear Emulsions in a Pulsed Magnetic Field —766L

Magalinskii, V. B. and Ia. P. Terletskii. The Statistics of Charge Conserving System and their Application to the Theory of Multiple Production — 143

Markov, M. A. (see Isaev, P. S.) —84

Mash, D. I. Rotation of the Plane of Polarization in a Longitudinal Magnetic Field at a Wavelength of 3cm. — 364L

Matveev, A. N. The Role of Spin in the Study of the Radiation Electron — 356L

Melankholin, N. M. and V. R. Regel'. Experiments on the Investigation of the Breakdown of NaCl Crystals — 696

Miamlin, V. A. The Consideration of the Nuclear Quadrupole Moment in Electron Scattering — 163

Milekhin, G. A. (see Belen'kii, S. Z.) — 14

Minaeva, T. M. (see Barchukov, A. I.) —760L

Mirskaia, G. G. (see Andronikashivili, G. L.) — 406L

Mitskevich, N. V. The Scalar Field of a Stationary Nucleon in a Nonlinear Theory — 197

Morgenshtern, Z. L. Measurement of the Absolute Quantum Yield of Photoluminescence of Alkali-Halide Crystals —773L

Nechin, Iu. A. (see Abrosimov, A. T.) —357L

Neporent, B. S. (see Zaitsev, G. A.) —733

Nikishov, A. I. The Role of Isobaric States of Nucleons in Meson Creation — 161

Nosov, V. G. Towards a Statistical Theory of Fission Width —746L

Novikov, A. N., B. M. Pontecorvo and G. I. Selivanov. Possibility of Formation of Penetrating Radiation in (μ^0-Mesons) in the Collision of High Energy Protons with Nuclei* —754L

Oganesian, K. O. (see Dzhelepov, V. P.) — 757L

Ogievetskii, V. I. The Theory of the Propagation of Gamma Rays through Matter — 312

——— Angular Distribution of Gamma Rays at Great Depths of Penetration in Matter — 319

Ordzhonikidze, K. and V. Shiuttse. Investigation of the Isotopic Constitution of Lithium — 396

Ostroumov, G. A. Observation of Electroconductive Convection in Electrolytes —428

Papov, Iu. M. and A. A. Rukhadze. Inelastic Scattering of Mesons in the Semi-Phenomenological Theory of the Interaction of π-Mesons with Nucleons —767L

Peker, L. K. Radiative Capture of Thermal Neutrons without Formation of a Compound Nucleus —753L

Pen'kina, V. S. (see Gol'danskii, V. I.) 677

Perel', V. I. (see Kagan, Ia. M.) —761 L

——— **(see Kagan, Iu. M.)** — 326L

Perfilov, N. A. and N. S. Ivanova. Fission of Heavy Nuclei by Slow π-Mesons* — 433

——— **(see Lozhkin, O. V.)** — 116

Pershits, Ia. N. The Mechanism of the Formation of Anode Layers in Molded Dielectrics — 272

Pikar, S. I. Existence of Quantum Stationary States of Point Nucleons which Interact with the Meson Field — 462

Pil'shchikov, A. I. Method of Determination of Parameters of Ferromagnetic Resonance from Experimental Data — 703

Pivovarov, V. M. (see Babovich, Ia. S.) — 574L

Podgoretskii, M. I., L. L. Rozental' and D. S. Chernavskii . Fluctuations During Collision of High Energy

Particles — 211
—— Note on Subsequent Transitions in Meson Atoms — 363L
—— (see **Gol'danskii, V. I.**) — 441
Pomeranchuk, I. Ia. Solution of the Equations of Pseudoscalar Meson Theory with Pseudoscalar Coupling — 739L
—— (see **Berestetskii, V. B.**) — 580
—— (see **Ioffe, B. L.**) — 37
Pomerantsev, N. M. Relaxation Processes in the Interaction of Nuclear Magnetic Moments with an Oscillator Loop — 581
Pontecorvo, B. M. The Processes of Production of Heavy Mesons and V_1^0 Particles — 135
—— (see **Balandin, M. P.**) — 98
—— (see **Novikov, A. N.**) — 754L
Prokhorov, A. M. (see **Barchukov, A. I.**) — 760L
Rapoport, L. P. The Problem of the Generalization of the Statistical Theory of the Atom — 347L
Ratner, B. S. (see **Lazareva, L. E.**) — 301
Rautian, S. G. (see **Bozhulin, P. A.**) — 663
Regel', V. R. (see **Melankholin, N. M.**) — 696
Romanova, T. A. (see **Belovitskii, G. E.**) — 493
Rozental', L. L. (see **Podgoretskii, M. I.**) — 211
Rukhadze, A. A. Interaction of Nucleons through a Pseudoscalar Meson Field — 570L
—— (see **Papov, Iu. M.**) — 767L
Rytov, S. M. Electromagnetic Properties of a Finely Stratified Medium — 466
—— Fluctuations in Oscillating Systems of the Thomson Type I — 217
—— Fluctuations in Oscillating Systems of the Thomson Type II — 225
—— The Connection between the Distribution of a Quasi-Monochromatic Stationary Process and the Distribution of its Envelope — 571L
Ryzhanov, S. G. On the Problem of Rotational Levels and the Spectra of Heavy Nuclei II — 334L
Sakolovskaia, A. I. (see **Bozhulin, P. A.**) — 663
Satarov, V. I. (see **Dzhelepov, V. P.**) — 349L
Sedov, V. I. (see **Sharvin, Iu. V.**) — 771
Selivanov, G. I. (see **Novikov, A. N.**) — 754L
Shamov, V. P. and O. V. Lozhkin. Asymmetry of Fragment Ranges in the Fission of Heavy Nuclei by Ultrafast Particles — 111
—— (see **Lozhkin, O. V.**) — 116
Shapiro, F. L. (see **Lazareva, L. E.**) — 351L
Sharvin, Iu. V. and V. I. Sedov. Crystalline Anisotropy of the Intermediate State — 771L
Shatalov, A. A. Photochemical Conversion of Color Centers in Heated Crystals of Potassium Chloride — 725
Shchelkin, K. I. Phenomena in the Vicinity of Detonation Formation in a Gas — 296
Shchukin, I. P. Some Problems in Recombination Luminescence Associated with Various Forms of Excitation in KCl-Tl Phosphors — 714
Shiuttse, V. An Investigation of the Isotopic Constitution of Boron — 402
—— (see **Ordzhonikidze, K.**) — 396
Shtranikh, I. V. (see **Lazareva, L. E.**) — 301
Shut'ko, A. V. and D. F. Zaretskii. Capture of Thermal Neutrons by Isotopes of Lead — 769
Silin, V. P., I. E. Tamm and V. Ia. Fainberg. The Method of Terminated Field Equations and its Application to the Scattering of Mesons by Nucleons — 3
—— (see **Ginzburg, V. L.**) — 46
Silivanov, G. I. (see **Balandin, M. P.**) — 98
Solntsev, G. S. and M. M. Dimitrieva. Two Electrode High Frequency Discharge at Pressures from 100 mm Hg to Atmospheric — 533
Solov'ev, V. G. Bremsstrahlung, from the Collisions of II-Mesons with Nucleons — 159L
——
Solov'eva, V. I. (see **Abrosimov, A. T.**) — 357L
Spartakov, A. A. and N. A. Tolstoi. Stable Dipole Moment of Aerosol Particles — 329L
Stepanov, A. V. and I. M. Eidus. Temperature Dependence of the Elastic Constants of Monocrystals of Sodium Chloride and Silver Chloride — 377
Storodina, T. A. (see **Bronshtein, I. M.**) — 410
—— (see **Bronshtein, I. M.**) — 414
Striganov, A. R. and L. A. Korostyleva. Investigation of the Isotopic Effect in the Uranium Spectrum — 277
Sukhov, L. V. (see **Belovitskii, G. E.**) — 493
Sushchinskii, M. M. (see **Bozhulin, P. A.**) — 663
Szhenov, Iu. K. Surface Ionization of Calcium, Strontium and Magnesium on Oxidized Tungsten — 775
Tamm, I. E. (see **Silin, V. P.**) — 3
Tarunov, E. Z. (see **Gol'danskii, V. I.**) — 677
Terletskii, Ia. P. Further Discussion of Fluctuations in Gravitating Systems — 262
—— (see **Kaniukov, M. V.**) — 742L
—— (see **Maglinskii, V. B.**) — 143
—— (see **Logunov, A. A.**) — 353L
Ter-Martirosian, K. A. The (d, p,) Reaction on Heavy Nuclei — 620
Tkachuk, A. M. (see **Tolstoi, N. A.**) — 331L
Tkachuk, N. N. (see **Tolstoi, N. A.**) — 331L
Tolstoi, N. A. and I. A. Litvinenko. Direct Measurement of the Total Light of Rapidly Decaying Processes of Luminescence — 420
—— **Tkachuk, A. M. and N. N. Tkachuk.** Temperature Dependence of the Relaxation Time of Luminescence of Platino Cyanides of Barium and of Potassium, and of Flourite activated with Europium — 331L
—— (see **Spartakov, A. A.**) — 329L
Tret'iakova, M. I. (see **Zamchalova, E. A.**) — 165L
Turov, E. A. (see **Vonsovskii, S. V.**) — 26
Veksler, A. Z. Photoelectron Emission in a Ferromagnetic — 266
Vlasov, K. B. (see **Vonsovskii, S. V.**) — 26
Vinokurov, L. A. (see **Antonov-Romanovskii, V. V.**) — 711L
Vonsovskii, S. V., K. B. Vlasov and E. A. Turov. The Quantum Theory of Ferromagnetism — 26
Voronkov, V. P. (see **Lukhachev, V. M.**) — 766
Zaitsev, G. A. Real Spinors in Curvilinear Coordinates

and in Pseudo-Riemannian Space – 290
——— Tensers which are Characterized by Two Real Spinors – 240
——— The Problem of the Interpretation of Dirac's Equation for the Electron – 140
——— **and B. S. Neporent.** Anisotropy of the Absorption of Gypsum Crystals in the Infra-red Region –733
Zamchalova, E. A., V. I. Karpova and M. I. Tret'iakova. Nuclear Capture of a Negative Heavy Meson – 165L
Zaretskii, D. F. (see Shut'ko, A. V.) –769
Zatsepin, V. I. (see Abrosimov, A. T.) – 357L
Zatsepina, G. N. (see Baluev, B. N.) – 106
Zel'dovich, Ia. B. (see Gershtein, S. S.) –\576L
Zharkov, G. F. Nucleon-Nucleon Scattering According to the Theory of Damping – 55
Zhukov, V. A. (see Balandin, M. P.) – 98
Zhukova, N. V. Investigation of the Origin of Levels of Electron Localization in Zinc Sulfide Phosphors – – 608
Zil'berman, G. E. Thermal and Galvanometric Effects in Strong Fields at Low Temperatures – 650
Zmov'eva, K. N. The Surface Tension of Liquid He^3 in the Region of very Low Temperatures (1.0-0.35°K) – 774L
Zuborev, D. N. Distribution Function of a Non-Ideal Bose Gas at the Temperature of Absolute Zero – 745
Zyrianov, P. S. Relaxation Fluctuations in Condensed Systems – 236
——— On a Theory of the Electrical Conductivity of Metals – 247

SOVIET PHYSICS JETP VOLUME 3, NUMBER 1 AUGUST, 1956

Analytic Subject Index to Volume 2

References with L are Letters to the Editor. Items are listed under the following categories:

- Atomic Mass and Abundance
- Atomic Structure and Spectra
- Biographical Material
- Chemical Effects and Properties
- Cosmic Radiation
- Crystalline State
- Dielectrics and Dielectric Properties
- Diffusion
- Elasticity and Plasticity
- Electrical Conductivity and Resistance
- Electrical Discharges
- Electrical Properties
- Electromagnetic Theory and Electrodynamics
- Electrons and Positrons
- Elementary Particle Interactions
- Errata
- Field Theory
- Films, Properties
- Fluid Dynamics
- Gamma Rays
- Gases
- Helium, Liquid
- Imperfections in Solids
- Ionization
- Ions
- Ions and Electrons, Mobility
- Liquids
- Luminescence
- Magnetic Properties
- Magnetic Resonance
- Mathematical Methods
- Mesons and Hyperons
- Methods and Instruments
- Microwaves
- Molecular Aggregates
- Molecular Structure and Spectra
- Nuclear Fission
- Nuclear Moments and Spin
- Nuclear Reactions, General
- Nuclear Reactions Induced by Deuterons and Tritons
- Nuclear Reactions Induced by Mesons
- Nuclear Reactions Induced by Neutrons
- Nuclear Reactions Induced by Protons
- Nuclear Spectra
- Nuclear Structure Theory
- Optical Properties
- Quantum Electrodynamics
- Quantum Mechanics
- Radiation
- Radioactivity
- Range and Energy Loss of Particles
- Relativity and Gravitation
- Scattering, General
- Scattering of Deuterons
- Scattering of Electrons and Positrons
- Scattering of Mesons
- Scattering of Neutrons
- Scattering of Protons
- Semiconductors
- Spectra, General
- Statistical Mechanics and Thermodynamics
- Superconductivity
- Thermal Properties

Absorption of Radiation (see **Radiation**)
Afterglow (see **Electrical Discharges**)
Alloys (see **Crystalline State**)
Annihilation (see **Electrons and Positrons**)
Antiferroelectric Phenomena (see **Dielectrics and Dielectric Properties**)
Antiferromagnetism (see **Magnetic Properties**)
Arcs (see **Electrical Discharges**)
Atomic Mass and Abundance
- An Investigation of the Isotopic Constitution of Boron, V. Shiuttse – 402
- Investigation of the Isotopic Constitution of Lithium, K. Ordzhonikidze and V. Shiuttse – 396

Atomic Structure and Spectra
- Fock Self-Consistent Field for the Boron Atom in the Two-Configuration Approximation, I. I. Glembotskii, V. V. Kilbartas and A. P. Iutsis – 476
- Fock Self-Consistent Field in the Three-Configuration Approximation for the Beryllium Atom, V. V. Kibartas, V. T. Kavetskii and A. P. Iutsis – 481
- Surface Ionization of Calcium, Strontium, and Magnesium on Oxidized Tungsten, Iu. K. Szhenov – 775L
- Investigation of the Isotopic Effect in the Uranium Spectrum, A. R. Striganov and L. A. Korostyleva – 277
- The Double Configurational Approximation in the Case of Carbon-like Atoms, A. B. Bolotin, I. B. Levinson and L. I. Levin – 391
- The Problem of the Generalization of the Statistical Theory of the Atom, L. P. Rapoport – 347L

Auger Effect (see **Atomic Structure and Spectra**)

Barkhausen Effect (see **Magnetic Properties**)
Biographical Material
- Academician Nikolai Nikolaevich Andreev – 184
- Academician Igor' Evgen'evich Tamm – 1

Boson Theory (see **Field Theory**)
Bremsstrahlung (see **Radiation**)
Broadening of Spectral Lines (see **Atomic Structure and Spectra; Spectra, General**)
Capture Cross Sections (see **Electrons and Positrons; Nuclear Reactions; Radiation**)
Cerenkov Effect (see **Radiation**)
Chemical Effects and Properties
- Investigation of the Origin of Levels of Electron Localization in Zinc Sulfide Phosphors – 608

Chemiluminescences (see Luminescence)

Cold Emission (see Electrical Properties)

Campton Effect (see Radiation)

Conductivity, Electrical (see Electrical Conductivity and Resistance)

Cosmic Radiation

- Diffusion Coefficient of Particles in a Magnetized Interstellar Medium, A. A. Logunov and Ia. P. Terletskii – 353
- Investigation of the Structure of Extensive Air Showers at Sea Level, A. T. Abrosimov, A. A. Bedniakov, V. I. Zatsepin, Iu. A. Nechin, V. I. Solov'eva, G. B. Kristiansen and P. S. Chikin – 357L
- On the Problem of Anti-protons in the Primary Stream of Cosmic Rays, M. I. Fradkin – 187
- Orientation of Planes in Double V^0 Decay Events, V. M. Kharitonov – 741L

Cosmology (see Relativity and Gravitation)

Critical Potentials (see Atomic Structure and Spectra)

Cross Section (see Electrons and Positrons; Nuclear Reactions; Radiation; Scattering)

Crystal Counters (see Methods and Instruments)

Crystalline State (see also Electrical Properties; Magnetic Properties; Semiconductors, etc)

- Electrical After-Effects in Rochelle Salt, K. N. Karmen – 578
- Dielectric Losses in Ionic Dielectrics in Strong Electric Fields, L. E. Gurevich and V. N. Gribov – 565
- Experiments on the Investigation of the Breakdown of NaCl Crystals, N. M. Melenkholin and V. R. Regel' – 696
- Investigation of the Structure of the Surface of Films of Copper Oxide on Different Faces of a Monocrystal of Copper and the Determination of the Contact Potential Difference between these Surfaces, N. G. Gorngi – 687
- Magnetic Properties of Trivalent Ions of Europium and Samarium, A. S. Borovik-Romanov and N. M. Kreines – 657
- Measurement of the Absolute Quantum Yield of Photoluminescence of Alkali-Halide Crystals, Z. L. Morgenshtern – 773L
- Phosphorescence of the Crystal Phosphor ZuS-Cu During Excitation by an Electron Beam, T. P. Belikova–776L
- Photochemical Conversion of Color Centers in Heated Crystals of Potassium Chloride, A. A. Shatalov – 725
- Photoelectric Recording of Spectra of Combination (Raman) Scattering of Powdery Materials, Ia. S. Bobovich, and V. M. Pivovarov – 574L
- Temperature Dependence of the Elastic Constants of Monocrystals of Sodium Chloride and Silver Chloride, A. V. Stepanov and I. M. Eidus – 377
- The Theory of the Hall Effect in Ionic Semi-Conductors, M. I. Klinger – 383
- Theory of Magnetic Susceptibility in Metals at Low Temperatures, I. M. Lifshitz and A. M. Kosevich -636
- Thermal and Galvanometric Effects in Strong Fields at Low Temperatures G. E. Zil'berman – 650

Diamagnetism (see Magnetic Properties)

Dielectrics and Dielectric Properties

- Dielectric Losses in Ionic Dielectrics in Strong Electric Fields, L. E. Gurevich and V. N. Gribov – 565
- Electromagnetic Properties of a Finely Stratified Medium, S. M. Rytov – 466
- On the Development by Means of Leaders of the Process of Breakdown of Liquids, I. E. Balygin – 573L
- The Mechanism of the Formation of Anode Layers in Molded Dielectrics, Ia. N. Pershits – 272

Diffusion

- Propagation of a Short Pulse in a Semiconductor Bounded by Two Electron-Hole Transitions, E. I. Adirovich and V. G. Kolotilova – 670

Discharge of Electricity in Gases (see Electrical Discharges)

Disintegration and Excitation of Nucleus (see Nuclear Reactions)

Elasticity and Plasticity

- Experiments on the Investigation of the Breakdown of NaCl Crystals, N. M. Melankholin and V. R. Regel' – 696
- Temperature Dependence of the Elastic Constants of Monocrystals of Sodium Chloride and Silver Chloride, A. V. Stepanov and I. M. Eidus – 377

Electrical Breakdown (see Dielectrics and Dielectric Properties; Electrical Discharges)

Electrical Conductivity and Resistance (see also **Electrical Properties; Semiconductors; Superconductors**)

- Anamalous Skin Effect in an Arbitrary Integral of Collision, M. Ia. Azbel' – 749L
- Crystalline Anisotropy of the Intermediate State, Iu. V. Sharvin and V. I. Sedov – 771L
- Determination of the Dielectric Constant of Superconductors, M. Ia. Azbel' – 354
- Observation of Electroconductive Convection in Electrolytes, G. A. Ostroumov – 428
- On a Theory of the Electrical Conductivity of Metals P. S. Zyrianov – 247
- The Effect of Interelectronic Collisions on the Electrical Conductivity and Skin Effect in Metals, V. L. Ginzburg and V. P. Silin – 46
- Thermal and Galvanometric Effects in Strong Fields at Low Temperatures, G. E. Zil'berman – 650
- Two Electrode High Frequency Discharge at Pressures from 100 mm Hg to Atmospheric, G. S. Solntsev and M. M. Dimitrieva – 533

Electrical Discharges

- Electroacoustic Waves in Gas Discharge Plasma with Consideration of Volume Recombination, M. V. Kaniukov and Ia. P. Terletskii – 742L
- On the Development by Means of Leaders of the Process of Breakdown of Liquids, I. E. Balygin – 573L
- On the Theory of Langmuir Probes, Iu. M. Kagan and V. I. Perel' – 326L
- The Question of the Possibility of Measuring the Temperature of the Column of a Jet Discharge Using the 3064A Hydroxyl Band, M. Z. Khokhlov – 559
- Two Electrode High Frequency Discharge at Pressures

from 100 mm Hg to Atmospheric, G. S. Solntsev and M. M. Dimitrieva – 533

Electrical Properties (see also Dielectrics and Dielectric Properties; Electrical Conductivity and Resistance; Semiconductors; Superconductors)
- Anamalous Skin Effect in an Arbitrary Integral of Collision, M. Ia. Azbel' – 749L
- Dielectric Losses in Ionic Dielectrics in Strong Electric Fields, L. E. Gurevich and V. N. Gribov – 565
- Electrical After-Effects in Rochelle Salt, K. N. Karmen – 578L
- Electromagnetic Properties of a Finely Stratified Medium, S. M. Rytov – 466
- Fluctuations in Oscillating Systems of the Thomson Type I, S. M. Rytov – 217
- Fluctuations in Oscillating Systems of the Thomson Type II, S. M. Rytov – 225
- Investigation of the Structure of the Surface of Films of Copper Oxide on Different Faces of a Monocrystal of Copper and the determination of the Contact Potential Difference between these Surfaces, N. G. Gorngi – 687
- Measurement of the Absolute Quantum Yield of Photoluminescence of Alkali-Halide Crystals, Z. L. Morgenshtern – 773L
- Phosphorescence of the Crystal Phosphor ZuS-Cu During Excitation by an Electron Beam, T. P. Belikova – 776L
- Rotation of the Plane of Polarization in a Longitudinal Magnetic Field at a Wavelength of 3 cm, D. I. Mash – 364L
- Stable Dipole Moment of Aerosol Particles, A. A. Spartakov and N. A. Tolstoi – 329L
- Thermal and Galvanometric Effects in Strong Fields at Low Temperatures, G. E. Zil'berman – 650

Electrodynamics (see Electromagnetic Theory and Electrodynamics)

Electromagnetic Theory and Electrodynamics (see also **Microwaves)**
- An Elementary Derivation of the Formula for the Electromagnetic Energy in a Dispersive Medium, M. L. Levin, – 168L
- Asymptotic Behavior of the Electromagnetic Vacuum-Polarization in the Presence of Meson Interactions, V. B. Berestetskii – 540
- Dielectric Losses in Ionic Dielectrics in Strong Electric Fields, L. E. Gurevich and V. N. Gribov – 565
- Electromagnetic Properties of a Finely Stratified Medium, S. M. Rytov – 466
- Green's Function in Scalar Electrodynamics in the Region of Small Momenta, A. A. Logunov – 337L
- Radiation of Molecules in the Presence of a Strong High Frequency Field, V. M. Fain – 747L
- The Gradient Representation of the Green's Function for Charged Particles, L. D. Landau and I. M. Khalatnikov – 69
- The Interaction of Ordinary and Extraordinary Waves in the Ionosphere and the Effect of Multiplication of Reflected Signals, N. G. Dentsov – 342L
- The Radiation of a Rapidly Moving Electric Image of a Uniformly Moving Charge, G. A. Askar'ian – 334L
- The Theory of the Acceleration of Charged Particles by Isotropic Gas Magnetic Turbulent Fields, S. A. Kaplan – 203

Electron Diffraction (see Scattering of Electrons and Positrons)

Electron Optics (see Electromagnetic Theory and Electrodynamics)

Electronic Tubes (see Methods and Instruments)

Electrons and Positrons (see also **Electromagnetic Theory and Electrodynamics; Elementary Particle Interactions; Scattering of Electrons and Positrons)**
- Method of Determination of Parameters of Ferromagnetic Resonance from Experimental Data, A. I. Pil'shchikov 703
- Numerical Values of the Constant of the Triplet Beta Interaction, D. A. Frank-Kamenetskii – 162
- Photoelectron Emission in a Ferromagnetic, A. Z. Veksler – 266
- Secondary Electron Emission in Thin Layers of Be. II, I. M. Bronshtein and T. A. Storodina – 410
- Secondary Electron Emission in Thin Layers of Silver, I. M. Bronshtein and T. A. Storodina – 414
- The Measurement of the Specific Charge of Conduction Electrons, V. M. Iuzhakov – 332L
- The Problem of the Interpretation of Dirac's Equation for the Electron, G. A. Zaitsev – 140
- The Role of Spin in the Study of the Radiating Electron, A. N. Matveev – 356

Electrons, Scattering of (see Scattering of Electrons and Positrons)

Electrons, Secondary (see Electrical Properties)

Electro-Optical Effects (see Optical Properties)

Electrostriction (see Dielectrics and Dielectric Properties)

Elementary Particle Interactions
- Asymptotic Behavior of the Electromagnetic Vacuum-Polarization in the Presence of Meson Interactions, V. B. Berestetskii – 540
- Formation of a μ-Meson Pair in Positron Annihilation, V. B. Berestetskii and I. Ia. Pomeranchuk – 580L
- Formation of Neutral π-Mesons in $(n-p)$ Collisions at Effective Neutron Energies of 590 mev, V. P. Dzhelepov, K. O. Oganesian and V. B. Fliagin – 757L
- Interaction of Nucleons through a Pseudoscalar Meson Field, A. A. Rukhadze – 570L
- Orientation of Planes in Double V^0 Decay Events, V. M. Kharitonov – 741L
- Possibility of Formation of Penetrating Radiation in (μ^0-Mesons) in the Collision of High Energy Protons with Nuclei*, A. N. Novikov, B. M. Pontecorvo, and G. I. Selivanov – 754L
- Solution of the Equations of Pseudoscalar Meson Theory with Pseudoscalar Coupling, I. Ia. Pomeranchuk – 739
- The Asymptotic Green's Function of Nucleon and Meson in Pseudoscalar Theory with Weak Interaction, A. D. Galanin, B. L. Ioffe, and I. Ia. Pomeranchuk – 37
- The Fermi-Yang Hypothesis, S. S. Filippov – 572L
- The Theory of Strong Coupling for Meson Fields I, B. T. Geilikman – 509
- Theory of Strong Coupling for Meson Fields III, B. T. Geilikman – 451

Elements (see Atomic Mass and Abundance)

Energy Loss of Particles (see Range and Energy Loss)

Energy States of Atoms (see Atomic Structure and Spectra)

Energy States of Nucleus (see Nuclear Reactions; Nuclear Spectra; Nuclear Structure Theroy)

Errata – 174, 793

p. 563, column 1, 5th line from bottom

reads	should read
"fissions"	"disintegrations"

Index to J. Tech. Phys.
p. 374
Our apologies to Academician Abram Fedorovich Iotte for interpreting his anniversary biography as an obituary. Like the report of Mark Twain's demise, it was a great exaggeration.

Evaporation (see Liquids)
Excitation of Atoms (see Atomic Structure and Spectra)
Excitation of Nucleus (see Nuclear Reactions; Nuclear Spectra; Nuclear Structure Theory)

Faraday Effect (see Optical Properties)
Ferroelectric Phenomena (see Dielectrics and Dielectric Properties)
Field Emission (see Electric Properties)
Field Theory (see also Quantum Electrodynamics)
- Asymptotic Behavior of the Electromagnetic Vacuum-Polarization in the Presence of Meson Interactions, V. B. Berestetskii – 540
- Formation of a π-Meson Pair in Positron Annihilation, V. B. Berestetskii and I. Ia. Pomeranchuk – 580L
- Interaction of Nucleons through a Pseudoscalar Meson Field, A. A. Rukhadze – 570L
- Meson Corrections in the Theory of Beta Decay, S. S. Gershtein and Ia. B. Zel'dovich – 576L
- Tensors Which are Characterized by Two Real Spinors, G. A. Zaitsev – 240
- The Asymptotic Green's Function of Nucleon and Meson in Pseudoscalar Theory with Weak Interaction, A. D. Galanin, B. L. Ioffe, and I. Ia. Pomeranchuk – 37
- The Gradient Representation of the Green's Function for Charged Particles, L. D. Landau and I. M. Khalatnikov – 69
- The Method of Terminated Field Equations and Its Application to the Scattering of Mesons by Nucleons, V. P. Silin, I. E. Tamm and V. Ia. Fainberg – 3
- The Quantum Theory of Fields, I. E. S. Fradkin – 148
- The Scalar Field of a Stationary Nucleon in a Nonlinear Theory, N. V. Mitskevich – 197
- The Theory of Molecular Attractive Forces between Solids, E. M. Lifshitz – 73
- The Theory of Strong Coupling for Meson Fields I, B. T. Geilikman – 509
- The Theory of Strong Coupling for Meson Fields II, B. T. Geilikman – 601
- Theory of Strong Coupling for Meson Fields III, B. T. Geilikman – 451

Films, Properties
- Investigation of the Structure of the Surface of Films of Copper Oxide, on Different Faces of a Monocrystal of Copper, and the Determination of the Contact Potential Difference between these Surfaces, N. G. Gorngi – 687
- Study of the Structure of the Surface of a Liquid by the Method of Reflection of Light, V. A. Kizel' – 520
- Surface Ionization of Calcium, Strontium, and Magnesium on Oxidized Tungsten, Iu. K. Szhenov – 775
- The Photographic Action of Ionizing Particles I, A. L. Kartuzhanskii – 550
- The Study of Relativistic Particles by the Use of Nuclear Emulsions in a Pulsed Magnetic Field, V. M. Lukhachev, A. V. Kutsenko and V. P. Voronkov – 766L

Fine Structure (see Atomic Structure and Spectra)
Fission of Nucleus (see Nuclear Fission)
Fluid Dynamics
- Phenomena in the Vicinity of Detonation Formation in a Gas, K. I. Shchelkin – 296

Fluorescence (see Luminescence)

Galvanomagnetic Effect (see Magnetic Properties)
Gamma Rays
- Angular Distribution of Gamma Rays at Great Depths of Penetration in Matter, V. I. Ogievetskii – 319
- Capture of Thermal Neutrons by Isotopes of Lead, A. V. Shut'ko and D. F. Zaretskii – 764L
- The Internal Compton Effect, A. M. Iakobson –
- The Theory of the Propagation of Gamma Rays through Matter, V. I. Ogievetskii – 312

Gases
- Concerning the Cross Section of Overcharging of Slow Ions in their Own Gas, Ia. M. Kagan and V. I. Perel' – 761L
- Distribution Function of a Non-Ideal Bose Gas at the Temperature of Absolute Zero, D. N. Zuborev – 745L
- Heat Evaporation of Oxygen in the Temperature Range 80-106°K, R. A. Alikhanov – 771L
- Phenomena in the Vicinity of Detonation Formation in a Gas, K. I. Schelkin – 296
- The Question of the Possibility of Measuring the Temperature of the Column of a Jet Discharge Using the 3064A Hydroxyl Band, M. Z. Khokhlov – 559
- The Second Viscosity of Monotomic Gases, I. M. Khalatnikov – 169L

Gravitation (see Relativity and Gravitation)
Gyromagnetization (see Magnetic Properties)

Hall Effect (see Electrical Conductivity and Resistance; Semiconductors)
Helium, Liquid
- The Behavior of Helium II in the Neighborhood of a Heat Diffusing Surface, G. L. Andronikashivili and G. G. Mirskaia – 406
- The Effective Density of Rotating Liquid Helium II, I. M. Lifshitz, and M. I. Kaganov – 172L
- The Surface Energy Associated with a Tangential Velocity Discontinuity in Helium II, V. L. Ginzburg – 170L
- The Surface Tension of Liquid He^3 in the Region of Very Low Temperatures, (1.0-0.35°K), K. N. Zmov'eva – 774L

High-Voltage Tubes and Machines (see Methods and Instruments)
Hyperfine Structure (see Atomic Structure and Spectra; Nuclear Moments and Spin)
Hyperons (see Mesons and Hyperons)
Imperfections in Solids
- Investigation of the Origin of Levels of Electron Localization in Zinc Sulfide Phosphors, N. V. Zhukova – 608
- Investigation of the Structure of the Surface of Films of Copper Oxide on Different Faces of a Monocrystal of Copper, and the Determination of the Contact Potential Difference between these Surfaces N. G. Gorngi – 687
- Photochemical Conversion of Color Centers in Heated

Crystals of Potassium Chloride, A. A. Shatalov –
Thermal and Galvanometric Effects in Strong Fields at Low Temperatures, G. E. Zil'berman – 650
Inelastic Scattering (see Nuclear Reactions; Scattering)
Instruments (see Methods and Instruments)
Internal Conversion (see Nuclear Spectra)
Ionization (see also Electrical Discharges; Range and Energy Loss of Particles)
Electroacoustic Waves in Gas Discharge Plasma with Consideration of Volume Recombination, M. V. Kaniukov and Ia. P. Terletskii – 742L
Surface Ionization of Calcium, Strontium and Magnesium on Oxidized Tungsten, Iu. K. Szhenov – 775L
The Photographic Action of Ionizing Particles I, A. L. Kartuzhanskii – 550
Ionization Potentials of Atoms (see Atomic Structure and Spectra)
Ions (see also Electrical Discharges)
Concerning the Cross Section of Overcharging of Slow Ions in their Own Gas, Ia. M. Kagan and V. I. Perel' – 761L
Electroacoustic Waves in Gas Discharge Plasma with Consideration of Volume Recombination, M. V. Kaniukov and Ia. P. Terletskii – 742L
Investigation of the Isotopic Constitution of Lithium, K. Ordzhonikidze and V. Shiuttse – 396
Loss of Two Electrons by Negative Ions in Collisions with Atoms and Molecules, V. M. Dukel'skii and N. V. Fedorenko – 307
Magnetic Properties of Trivalent Ions of Europium and Samarium, A. S. Borovik-Romanov and N. M. Kreines– 657
The Formation of Negative Oxygen Ions in the Collisions of Positive Oxygen Ions with Gas Molecules, Ia. M. Fogel' and L. I. Krupnik – 252
The Photographic Action of Ionizing Particles I. A. L. Kartuzhanskii – 550
The Rotation of the Plane of Polarization in Electrolyte Solutions by a Magnetic Field, A. F. Kapustinskii – 744L
Ions and Electrons, Mobility
Concerning the Cross Section of Overcharging of Slow Ions in their own Gas, Ia. M. Kagan and V. I. Perel' – 761L
Electroacoustic Waves in Gas Discharge Plasma with Consideration of Volume Recombination, M. V. Kaniukov and Ia. P. Terletskii – 742L
Isobars (see Atomic Mass and Abundance)
Isomers, Nuclear (see Nuclear Spectra)
Isotopes (see Atomic Mass and Abundance; Radioactivity)
Liquid Helium (see Helium, Liquid)
Liquids
Observation of Electroconductive Convection in Electrolytes, G. A. Ostroumov – 428
On the Development by Means of Leaders of the Process of Breakdown of Liquids, I. E. Balygin - 513L
Study of the Structure of the Surface of a Liquid by the Method of Reflection of Light, V. A. Kizel' 520
The Rotation of the Plane of Polarization in Electrolyte Solutions by a Magnetic Field, A. F. Kapustinskii – 744L
Luminescence
Direct Measurement of the Total Light of Rapidly Decaying Processes of Luminescence, N. A. Tolstoi and I. A. Litvinenko – 420
Investigation of the Origin of Levels of Electron Localization in Zinc Sulfide Phosphors, N. V. Zhukova – 608
Measurement of the Absolute Quantum Yield of Photoluminescence of Alkali-Halide Crystals, Z. L. Morgenshtern – 773L
The Lowering of the Luminescence Yield of Phosphors in Intense Excitation, V. V. Antonov-Romanovskii, and L. A. Vinokurov – 711
Phosphorescence of the Crystal Phosphor ZuS-Cu During Excitation by an Electron Beam, T. P. Belikova – 776L
Some Problems in Recombination Luminescence Associated with Various Forms of Excitation in KCl-Tl Phosphors, I. P. Shchukin – 714
Temperature Dependence of the Relaxation Time of Luminescence of Platino Cyanides of Barium and of Potassium, and of Fluorite activated with Europium, N. A. Tolstoi, A. M. Tkachuk, and N. N. Tkachuk – 331L

Magnetic Fields (see Electromagnetic Theory and Electrodynamics)
Magnetic Properties
Electromagnetic Properties of a Finely Stratified Medium, S. M. Rytov – 466
Magnetic Properties of Trivalent Ions of Europium and Samarium, A. S. Borovik-Romanov and N. M. Kreines – 657
Method of Determination of Parameters of Ferromagnetic Resonance from Experimental Data, A. I. Pil'shchikov – 703
The Effect of Pressure on the Superconductivity of Cadmium, N. E. Akekseevskii and Iu. P. Gaidukov – 762L
The Effect of the Method of Demagnetization of the Specimen on the Temperature Dependence of the Magnetization of Nickel in Weak Fields, A. I. Drokin and V. L. Il'iushenko – 191L
The Quantum Theory of Ferromagnetism, S. V. Vonsovskii, K. B. Vlasov and E. A. Turov – 26
The Quantum Theory of Magnetostriction, A. A. Gusev – 126
The Rotation of the Plane of Polarization in Electrolyte Solutions by a Magnetic Field, A. F. Kapustinskii – 744L
The Theory of the Acceleration of Charged Particles by Isotropic Gas Magnetic Turbulent Fields, S. A. Kaplan – 203
The Thermodynamic Theory of Magnetic Relaxation, G. R. Kutsishvili – 187
Theory of Magnetic Susceptibility in Metals at Low Temperatures, I. M. Lifshitz and A. M. Kosevich – 636
Thermal and Galvanometric Effects in Strong Fields at Low Temperatures, G. E. Zil'berman – 650
Magnetic Resonance
Determination of Longitudinal Relaxation Times for Magnetic Resonance of Atomic Nuclei in an Intense High Frequency Magnetic Field, S. D. Gvozdover and N. M. Ievskaia – 486
Determination of Transverse Relaxation Times in the Magnetic Resonance of Atomic Nuclei in Weak High-Frequency Magnetic Fields, S. D. Gvozdover and N. M. Ievskaia – 90
Method of Determination of Parameters of Ferromag-

netic Resonance from Experimental Data, A. I. Pil'shchikov – 703
Relaxation Processes in the Interaction of Nuclear Magnetic Moments with an Oscillator Loop, N. M. Pomerantsev – 581L
Magneto-Optical Effects (see Optical Properties)
Magnetoresistance (see Electrical Conductivity and Resistance; Semiconductors)
Magnetostriction (see Magnetic Properties)
Mass Defects (see Atomic Mass and Abundance)
Mass Spectroscopy (see Atomic Mass and Abundance; Methods and Instruments)
Mathematical Methods
On the Correlation Method for the Determination of the Absolute Efficiency of Nuclear Reactions, V. I. Gol'danskii, and M. I. Podgoretskii – 441
Real Spinors in Curvilinear Coordinates and in Pseudo-Riemannian Space, G. A. Zaitsev – 290
Tensors Which are Characterized by Two Real Spinors , G. A. Zaitsev – 240
Measurements (see Methods and Instruments)
Mechanics, Quantum (see Quantum Mechanics)
Mechanics, Quantum - Atomic Structure and Spectra (see Atomic Structure and Spectra)
Mechanics, Quantum - Nuclear (see Nuclear Structure Theory)
Mechanics, Quantum - of Solid Bodies (see Crystalline State)
Mechanics, Statistical (see Statistical Mechanics and Thermodynamics)
Meson Field Theory (see Field Theory)
Mesons and Hyperons (see also Cosmic Radiation; Elementary Particle Interactions; Nuclear Reactions Induced by Mesons; Scattering of Mesons)
Existence of Quantum Stationary States of Point Nucleons which Interact with the Meson Field, S. I. Pikar – 462
Fission of Heavy Nuclei by Slow π-Mesons*, N. A. Perfilov and N. S. Ivanova – 433
Formation of a μ-Meson Pair in Positron Annihilation, V. B. Berestetskii and I. Ia. Pomeranchuk – 580L
Formation of Neutral π-Mesons in $(n-p)$ Collisions at Effective Neutron Energies of 590 mev, V. P. Dzhelepov, K. O. Oganesian, and V. B. Fliagin – 757L
Interaction of Nucleons through a Pseudoscalar Meson Field, A. A. Rukhadze – 570L
Note on Subsequent Transitions in Meson-Atoms, M. I. Podgoretskii – 363L
Nuclear Capture of a Negative Heavy Meson, E. A. Zamchalova, V. I. Karpova and M. I. Tret'iakova – 165L
Orientation of Planes in Double V^0 Decay Events, V. M. Kharitonov – 741L
Possibility of Formation of Penetrating Radiation in (μ^0-Mesons) in the Collision of High Energy Protons with Nuclei*, A. N. Novikov, B. M. Pontecorvo, and G. I. Selivanov – 754L
Solution of the Equations of Pseudoscalar Meson Theory with Pseudoscalar Coupling, I. Ia. Pomeranchuk – 739L
The Asymptotic Green's Function of Nucleon and Meson in Pseudoscalar Theory with Weak Interaction, A. D. Galanin, B. L. Ioffe and I. Ia. Pomeranchuk – 37
The Fermi-Yang Hypothesis, S. S. Filippov – 572L
The Possibility of the Formation of Λ^0 Particles by Protons with Energies up to 700 mev, M. P. Balandin, B. D. Balashiv, V. A. Zhukov, B. M. Pontecorvo and G. I. Silivanov – 98
The Problem of the Asymptote of the Green Function in the Theory of Mesons with Pseudoscalar Coupling, E. S. Fradkin – 340L
The Processes of Production of Heavy Mesons and V_1^0 Particles, B. M. Pontecorvo – 135
The Role of Isobaric States of Nucleons in Meson Creation, A. I. Mikishov – 161
The Theory of Strong Coupling for Meson Fields I, B. T. Geilikman – 509
The Theory of Strong Coupling for Meson Fields II, B. T. Geilikman – 601
The Theory of Λ^0 Particles, P. S. Isaev and M. A. Markov – 84
Theory of Strong Coupling for Meson Fields III, B. T. Geilikman – 451
Metals (see Crystalline State)
Metastable Atoms (see Atomic Structure and Spectra)
Methods and Instruments
Calculation of the Ultimate Thickness of the Emulsion Layer in the Investigation of Nuclear Processes by the Photographic Method, M. M. Agrest – 166L
Investigation of the Field of Partial Pressures in a Diffusing Condensing Chamber, V. K. Liapidevskii – 346L
Magnetic Properties of Trivalent Ions of Europium and Samarium, A. S. Borovik-Romanov and N. M. Kreines – 657
Method of Determination of Parameters of Ferromagnetic Resonance from Experimental Data, A. I. Pil'shchikov – 703
Neutron Spectrometry Based on the Measurement of the Decelerating Time of Neutrons, L. E. Lazareva, E. L. Feinberg and F. L. Shapiro – 351L
On the Correlation Method for the Determination of the Absolute Efficiency of Nuclear Reactions, V. I. Gol'danskii, and M. I. Podgoretskii – 441
On the Theory of Langmuir Probes, Iu. M. Kagan and V. I. Perel' – 326L
Photoelectric Recording of Spectra of Combination (Raman) Scattering of Powdery Materials, Ia. S. Bobovich and V. M. Pivovarov – 574L
The Question of the Possibility of Measuring the Temperature of the column of a Jet Discharge Using the 3064 Å Hydroxyl band, M. Z. Khokhlov – 559
Microwaves
Dielectric Losses in Ionic Dielectrics in Strong Electric Fields, L. E. Gurevich, V. N. Gribov – 565
Electromagnetic Properties of a Finely Stratified Medium, S. M. Rytov – 466
Method of Determination of Parameters of Ferromagnetic Resonance from Experimental Data, A. I. Pil'shchikov – 703
Microwave Spectrum of the C_2H_5Cl Molecule, A. I. Barchukov, T. M. Minaeva and A. M. Prokhorov – 760L
Molecular Aggregates
Photoelectric Recording of Spectra of Combination Scattering of Powdery Material, Ia. S. Bobovich and V. M. Pivovarov – 574L

  The Theory of Molecular Attractive Forces between Solids, E. M. Lifshitz — 73
Molecular Structure and Spectra
  Methods of Investigating the Width of Raman Lines and Their Application, P. A. Bozhulin, S. G. Rautian, A. I. Sakolovskaia and N. M. Sushchinskii — 663
  Microwave Spectrum of the C_2H_5Cl Molecule, A. I. Barchukov, T. M. Minaeva and A. M. Prokhorov — 760L
  The Question of the Possibility of Measuring the Temperature of the Column of a Jet Discharge Using the 3064 Å Hydroxyl band, M. Z. Khokhlov — 559
Moments, Nuclear (see Nuclear Moments and Spin)
Neutrons (see Elementary Particle Interactions)
Nuclear Fission
  Asymmetry of Fragment Ranges in the Fission of Heavy Nuclei by Ultrafast Particles, V. P. Shamov and O. V. Lozhkin — 111
  Delayed Neutrons Which Accompany Photofission of Uranium and Thorium, L. E. Lazareva, B. S. Ratner and I. V. Shtranikh — 301
  Fission of Heavy Nuclei by High Energy Neutrons*, V. I. Gol'danskii,V. S. Pen'kina and E. Z. Tarunev — 677
  Fission of Heavy Nuclei by Slow π- Mesons, N. A. Perfilov and N. S. Ivanova — 433
  Fission of Uranium by Slow π-Mesons, Fast Neutrons and X-Rays of energies up to 250 mev, G. E. Belovitskii T. A. Romanova, L. V. Sukhov and I. M. Frank — 493
  Inelastic Scattering of Mesons in the Semi-Phenomenological Theory of the Interaction of π-Mesons with Nucleons, Iu. M. Papov and A. A. Rukhadze — 767L
  International Values for the Thermal Cross Section of Fissionable Materials —
  The Role of Isobaric States of Nucleons in Meson Creation, A. I. Mikishov — 161
  Towards a Statistical Theory of Fission Width, V. G. Nosov — 746L
  The Angular Distribution Fragments from Fission of Uranium at High Excitation Energies, O. V. Lozhkin, N. A. Perfilov and V. P. Shamov — 116
  The Average Number of Neutrons Per Fission Event in the Photodisintegration of Uranium and Thorium, B. M. Baluev, B. I. Gavrilov, G. N. Zatsepina and L. E. Lazareva — 106
Nuclear Forces (see Elementary Particle Interactions; Field Theory; Nuclear Structure Theory)
Nuclear Induction (see Magnetic Resonance
Nuclear Moments and Spin
  Determination of Longitudinal Relaxation Times for Magnetic Resonance of Atomic Nuclei in an Intense High Frequency Magnetic Field, S. D. Gvozdover and N. M. Ievskaia — 486
  On the Problem of Rotational Levels and the Spectra of Heavy Nuclei II, S. G. Ryzhanov — 334L
  Polarization of the Nuclei of Ferromagnetic Atoms, G. R. Khutseshvili — 744L
  Relaxation Processes in the Interaction of Nuclear Magnetic Moments with an Oscillator Loop, N. M. Pomerantsev — 581L
  Surface Ionization of Calcium, Strontium and Magnesium on Oxidized Tungsten, Iu. K. Szhenov — 775L
  The Consideration of the Nuclear Quadrupole Moment in Electron Scattering, V. A. Miamlin — 163
Nuclear Reactions, General
  Calculation of the Ultimate Thickness of the Emulsion Layer in the Investigation of Nuclear Processes by the Photographic Method, M. M. Agrest — 166L
  Fission of Heavy Nuclei by High Energy Neutrons*, V. I. Gol'danskii, V. S. Pen'kina and E. Z. Tarunev — 677
  Fluctuations during Collision of High Energy Particles, M. I. Podgoretskii, L. L. Rozental' and D. S. Chernavskii — 211
  Multiple Production of Particles in the Collisions of High-Energy Nucleons with Nuclei, S. Z. Belen'kii and G. A. Milekhin — 14
  Numerical Values of the Constant of the Triplet Beta Interaction, D. A. Frank-Kamenetskii — 162
  On Particle Energy Distribution at Multiple Formation, N. M. Gerasimova and D. S. Chernavskii — 344L
  On the Correlation Method for the Determination of the Absolute Efficiency of Nuclear Reactions, V. I. Gol'danskii and M. I. Podgoretskii — 441
  The (*d* - *p*) Reaction on Heavy Nuclei, K. A. Ter-Martirosian — 620
  The Statistics of Charge Conserving System and their Application to the Theory of Multiple Production, V. B. Magalinskii and Ia. P. Terletskii — 143
  The Study of Relativistic Particles by the Use of Nuclear Emulsions in a Pulsed Magnetic Field, V. M. Lukhachev,A.V.Kutsenkoand V. P. Voronkov — 766L
Nuclear Reactions Induced by Deuterons and Tritons
  The (*d*, *p*) Reaction on Heavy Nuclei, K. A. Ter-Martirosian — 620
  The Interaction of Fast Deuterons with Nuclei, E. L. Feinberg — 58
  The Theory of Λ° Particles, P. S. Isaev and M. A. Markov — 84
Nuclear Reactions Induced by Mesons.
  Fission of Heavy Nuclei by Slow π-Mesons, N. A. Perfilov and N. S. Ivanova — 433
Nuclear Reactions Induced by Neutrons
  Capture of Thermal Neutrons by Isotopes of Lead, A. V. Shut'ko and D. F. Zaretskii — 769L
  Fission of Heavy Nuclei by High Energy Neutrons*, V. I. Gol'danskii, V. S. Pen'kina and E. Z. Tarunev — 677
  Fission of Uranium by Slow π-Mesons, Fast Neutrons and X-Rays of Energies up to 250 mev, G. E. Belovitskii T. A. Romanova, L. V. Sukhov, and I. M. Frank — 493
  Formation of Neutral π- Mesons in (*n* — *p*) Collisions at Effective Neutron Energies of 590 mev, V. P. Dzhelepov, K. O. Oganesian and V. B. Fliagin — 757L
  Inelastic Scattering of Mesons in the Semi-Phenomenological Theory of the Interactionof π-Mesons with Nucleons, Iu. M. Papov and A. A. Rukhadze — 767L
  International Values for the Thermal Cross Section of Fissionable Materials —

Radiative Capture of Thermal Neutrons without Formation of a Compound Nucleus, L. K. Peker — 753L

Nuclear Reactions Induced by Protons
The Possibility of the Formation of Λ° Particles by Protons with Energies up to 700 mev, M. P. Balandin, B. D. Balashiv, V. A. Zhukov, B. M. Pontecorvo and G. I. Silivanov — 98

Nuclear Scattering (see Scattering)

Nuclear Spectra (see also Nuclear Reactions; Radioactivity)
Capture of Thermal Neutrons by Isotopes of Lead, A. V. Shut'ko and D. F. Zaretskii — 769L
On the Problem of Rotational Levels and the Spectra of Heavy Nuclei II, S. G. Ryzhanov — 334L
Radiative Capture of Thermal Neutrons without Formation of a Compound Nucleus, L. K. Peker — 753L

Nuclear Structure Theory
Capture of Thermal Neutrons by Isotopes of Lead, A. V. Shut'ko and D. F. Zaretskii — 769L
On the Problem of Rotational Levels and the Spectra of Heavy Nuclei II, S. G. Ryzhanov — 334L
On the Theory of Nucleons, D. I. Blokhintsev — 23
The Characteristics of "Specific" Zones, M. A. Levitskaia — 119
The Connection Between the Vibrations of the Surface of a Nucleus and Single Nucleon Excitation, A. S. Davidov — 62

Optical Instruments (see Methods and Instruments)

Optical Properties (see also Luminescence)
Absorption Spectrum of Excess Silver in the Low Temperature and High Temperature Modifications of Silver Iodide, P. N. Kokhanenko and L. V. Grigoruk — 530
Anisotropy of the Absorption of Gypsum Crystals in the Infra-red Region, G. A. Zaitsev and B. S. Neporent — 733
Dielectric Losses in Ionic Dielectrics in Strong Electric Fields, L. E. Gurevich, V. E. Gribov — 565
Fluctuating Structure in the Absorption Spectrum of Ruby, B. N. Grechushnikov and P. P. Feofilov — 330L
Photochemical Conversion of Color Centers in Heated Crystals of Potassium Chloride, A. A. Shatalov — 725
Photoelectron Emission in a Ferromagnetic, A. Z. Veksler — 266
Polarization of the Nuclei of Ferromagnetic Atoms, G. R. Khutseshvili — 744L
Study of the Structure of the Surface of a Liquid by the Method of Reflection of Light, V. A. Kizel' — 520
The Photographic Action of Ionizing Particles I, A. L. Kartuzhanskii — 550

Pair Production (see Electrons and Positrons)

Phosphors and Phosphorescence (see Luminescence; Semiconductors)

Photoconductivity (see Electrical Conductivity and Resistance)

Photodisintegration (see Nuclear Photoeffects)

Photoelectric Effect (see Electrical Properties)

Photography and Photographic Emulsions (see Methods and Instruments; Optical Properties)

Photometry (see Methods and Instruments; Optical Properties)

Photons (see Radiation)

Photovoltaic Effect (see Electrical Properties; Semiconductors)

Piezoelectric Effect (see Dielectrics and Dielectric Properties)

Polarization, Electrical (see Dielectrics and Dielectric Properties)

Positrons (see Electrons and Positrons)

Probability (see Mathematical Methods)

Protons (see Elementary Particle Interactions)

Quantum Electrodynamics (see also Field Theory)
Asymptotic Behavior of the Electromagnetic Vacuum-Polarization in the Presence of Meson Interactions, V. B. Berestetskii — 540
Concerning Some General Relations of Quantum Electrodynamics, E. S. Fradkin — 361L
Existence of Quantum Stationary States of Point Nucleons which Interact with the Meson Field, S. I. Pikar — 462
Formation of a μ-Meson Pair in Positron Annihilation V. I. Berestetskii and I. Ia. Pomeranchuk — 580L
Green's Function in Scalar Electrodynamics in the Region of Small Momenta, A. A. Logunov — 337L
Meson Corrections in the Theory of Beta Decay, S. S. Gershtein and Ia. B. Zel'dovich — 576L
Radiation of Molecules in the Presence of a Strong High Frequency Field, V. M. Fain — 747L
Solution of the Equations of Pseudoscalar Meson Theory with Pseudoscalar Coupling, I. Ia. Pomeranchuk — 739L
The Asymptotic Green's Function of Nucleon and Meson in Pseudoscalar Theory with Weak Interaction, A. D. Galanin, B. L. Ioffe and I. Ia. Pomeranchuk — 37
The Problem of the Asymptote of the Green Function in the Theory of Mesons with Pseudoscalar Coupling, E. S. Fradkin — 340L
The Quantum Theory of Fields, I, E. S. Fradkin — 148
The Role of Spin in the Study of the Radiating Electron, A. N. Matveev— 356L
The Theory of Molecular Attractive Forces between Solids, E. M. Lifshitz — 73
The Theory of Strong Coupling for Meson Fields I, B. T. Geilikman — 509
The Theory of Strong Coupling for Meson Fields II, B. T. Geilikman — 601
Theory of Strong Coupling for Meson Fields III, B. T. Geilikman — 451

Quantum Mechanics
Fock Self-Consistant Field for the Boron Atom in the Two-Configuration Approximation L. I. Glembotskii, V. V. Kibartas and A. P. Iutsis — 476
Fock Self-Consistant Field in the Three-Configuration Approximation for the Beryllium Atom, V. V. Kibartas, V. T. Kavetskii and A. P. Iutsis — 481
The Problem of the Interpretation of Dirac's Equation for the Electron, G. A. Zaitsev — 140
The Quantum Theory of Ferromagnetism, S. V. Vonsovskii, K. B. Vlasov and E. A. Turov — 26
The Quantum Theory of Fields I, E. S. Fradkin — 148
The Quantum Theory of Magnetostriction, A. A. Gusev — 126
The Quantum Theory of the Magnetostriction of Cubic Monocrystals of Ferromagnetics at Low Temperatures, A. A. Gusev — 764L

Quenching of Radiation (see Radiation)

Radar (see **Methods and Instruments; Radiation**)
Radiation (see also **Range and Energy Loss**)
  Bremsstrahlung from the Collisions of π-Mesons with Nucleons, V, G. Solov'ev – 159L
  Capture of Thermal Neutrons by Isotopes of Lead, A. V. Shut'ko and D. F. Zaretskii – 769L
  Measurement of the Absolute Quantum Yield of Photoluminescence of Alkali-Halide Crystals, Z. L. Morgenshtern – 773L
  Phosphorescence of the Crystal Phosphor ZuS-Cu During Excitation by an Electric Beam, T. P. Belikova – 776L
  Radiation of Molecules in the Presence of a Strong High Frequency Field, V. M. Fain – 747L
  The Photographic Action of Ionizing Particles I, A. L. Kartuzhanskii – 550
  The Radiation of a Rapidly Moving Electric Image of a Uniformly Moving Charge, G. A. Askar'ian – 334L
  The Role of Spin in the Study of the Radiating Electron, A. N.Matveev – 356L

Radioactivity (see also **Nuclear Spectra**)
  Capture of Thermal Neutrons by Isotopes of Lead, A. V. Shut'ko and D. F. Zaretskii – 769L
  Meson Corrections in the Theory of Beta Decay, S. S. Gershtein and Ia. B. Zel'dovich – 576L
  On the Correlation Method for the Determination of the Absolute Efficiency of Nuclear Reactions, V. I. Gol'danskii and M. I. Podgoretskii – 441
  On the Problem of Rotational Levels and the Spectra of Heavy Nuclei II, S. G. Ryzhanov – 334L

Radio Waves (see **Radiation**)
Range and Energy Loss of Particles
  Asymmetry of Fragment Ranges in the Fission of Heavy Nuclei by Ultrafast Particles, V. P. Shamov and O.V. Lozhkin – 111
  Fluctuations during Collisions of High Energy Particles, M. I. Podgoretskii, L. I. Rozental' and D. S. Chernavskii – 211
  The Photographic Action of Ionizing Particles I, A. L. Kartuzhanskii – 550
Relativity and Gravitation
  Further Discussion on Fluctuations in Gravitating Systems, Ia. P. Terletskii – 262
Rectifiers (see **Electrical Conductivity and Resistance; Semiconductors**)
Resistance, Electrical (see **Electrical Conductivity and Resistance**)
Resonance Radiation (see **Radiation**)
Scattering, General (see also **Elementary Particle Interactions; Nuclear Reactions; Range and Energy Loss of Particles**)
  Nucleon-Nucleon Scattering According to the Theory of Damping, G. F. Zharkov – 55
Scattering of Deuterons
  The Interaction of Fast Deuterons with Nuclei, E. L. Feinberg – 58
  The Theory of Λ^0 Particles, P. S. Isaev and M. A. Markov – 84
Scattering of Electrons and Positrons (see also **Electrons and Positrons**)
  Anamalous Skin Effect in an Arbitrary Integral of Collision, M. Ia. Azbel' – 749L
  The Consideration of the Nuclear Quadrupole Moment in Electron Scattering, V. A. Miamlin – 163
Scattering of Mesons (see also **Mesons; Nuclear Reactions Induced by Mesons**)
  Inelastic Scattering of Mesons in the Semi-Phemomenological Theory of the Interaction of π-Mesons with Nucleons, Iu. M. Papov and A. A. Rukhadze – 767L
  Phosphorescence of the Crystal Phosphor ZuS-Cu During Excitation by an Electron Beam, T. P. Belikova – 776L
  Solution of the Equations of Pseudoscalar Meson Theory with Pseudoscalar Coupling, I. Ia. Pomeranchuk – 739L
  The Method of Terminated Field Equations and Its Application to the Scattering of Mesons by Nucleons, V. P. Silin, I. E. Tamm and V. Ia. Fainberg – 3
  The Relation between our Criterion of Stability for a Homogeneous Phase and that of S. V. Tiablikov, I. Z. Fisher – 768L
Scattering of Neutrons (see also **Nuclear Reactions Induced by Neutrons**)
  Bremsstrahlung from the Collisions of π- Mesons with Nucleons, V. G. Solov'ev – 159L
  Inelastic Scattering of Mesons in the Semi-Phenomenological Theory of the Interaction of π- Mesons with Nucleons, Iu. M. Papov and A. A. Rukhadze – 767L
  Nucleon-Nucleon Scattering According to the Theory of Damping, G. F. Zharkov – 55
  Total Cross Sections of Nuclei of Certain Elements for Neutrons with Energies of 590 mev, V. P. Dzhelepov, V. I. Satarov and B. M. Golovin – 349L
Scattering of Protons (see also **Nuclear Reactions Induced by Protons**)
  Nucleon-Nucleon Scattering According to the Theory of Damping, G. F. Zharkov – 55
Semiconductors
  Investigation of the Structure of the Surface of Films of Copper Oxide on Different Faces of a Monocrystal of Copper and the Determination of the Contact Potential Difference between these Surfaces, N. G. Gorngi – 687
  Measurement of the Absolute Quantum Yield of Photoluminescence of Alkali-Halide Crystals, Z. L. Morgenshtern – 773L
  Photochemical Conversion of Color Centers in Heated Crystals of Potassium Chloride, A. A. Shatalov – 725
  Propagation of a Short Pulse in a Semiconductor Bounded by Two Electron-Hole Transitions, E. I. Adirovich and V. G. Kolotilova – 670
  The Theory of the Hall Effect in Ionic Semi-Conductors, M. I. Klinger – 383
Solid State (see **Crystalline State**)
Spallation (see **Nuclear Reactions**)
Spark Discharge (see **Electrical Discharges**)
Spectra, Atomic (see **Atomic Structure and Spectra**)
Spectra, General
  Anisotropy of the Absorption of Gypsum Crystals in the Infra-red Region, G. A. Zaitsevand B. S. Neporent – 733
  Methods of Investigating the Width of Raman Lines and Their Application, P. A. Bozhulin, S. G. Rau-

tian, A. I. Sakolovskaia and N. M. Sushchinskii –663
Photoelectric Recording of Spectra of Combination Scattering of Powdery Material, Ia. S. Bobovich and V. M. Pivovarov – 574L

Spectra, Nuclear (see Nuclear Spectra)

Spinor Fields (see Field Theory)

Statistical Mechanics and Thermodynamics
- Distribution Function of a Non-Ideal Bose Gas at the Temperature of Absolute Zero, D. N. Zuborev – 745L
- Fluctuations in Oscillating Systems of the Thomson Type I, S. M. Rytov – 217
- Fluctuations in Oscillating Systems of the Thomson Type II, S. M. Rytov – 225
- Relaxation Fluctuations in Condensed Systems, P. S. Zyrianov – 236
- The Connection between the Distribution of a Quasi-Monochromatic Stationary Process and the Distribution of its Envelope, S. M. Rytov – 571L
- The Problem of the Generalization of the Statistical Theory of the Atom, L. P. Rapoport – 347L
- Towards a Statistical Theory of Fission Width, V. G. Nosov – 746L

Statistical Methods (see Mathematical Methods)

Superconductivity
- Crystalline Anisotropy of the Intermediate State, Iu. V. Sharvin and V. I. Sedov – 771L
- Determination of the Dielectric Constant of Superconductors, M. Ia. Azbel' – 354L
- On the Macroscopic Theory of Superconductivity, V. L. Ginzburg – 589
- The de-Haas-van Alphen Effect in Thin Layers, A. M. Kosevich and I. M. Lifshitz – 646
- The Effect of Pressure on the Superconductivity of Cadmium, N. E. Alekseevskii and Iu. P. Gaidukov – 762L

Thermal Properties
- Adiabatic Processes at High Temperatures, I. L. Aptekar' and B. L. Timan – 327L
- Heat Evaporation of Oxygen in the Temperature Range 80-106°K, R. A. Alikhanov – 771L
- Magnetic Properties of Trivalent Ions of Europium and Samarium, A. S. Borovik-Romanov and N. M. Kreines – 657
- Phenomena in the Vicinity of Detonation Formation in a Gas, K. I. Shchelkin – 296
- The Behavior of Helium II in the neighborhood of a Heat Diffusing Surface, G. L. Andronikashivili and G. G. Mirskaia – 406
- The Thermodynamic Theory of Magnetic Relaxation, G. R. Kutsishvili – 187
- Thermal and Galvanometric Effects in Strong Fields at Low Temperatures, G. E. Zil'berman – 650

Thermionic Emission (see Electrical Properties)

Thermodynamics (see Statistical Mechanics and Thermodynamics)

Thermoelectric Effect (see Electrical Properties; Semiconductors)

Thermoluminescence (see Luminescence)

Total Cross Sections (see Electrons and Positrons; Nuclear Reactions)

Transmutation (see Nuclear Reactions)

Uncertainty Principle (see Quantum Mechanics)

Vacuum Tubes (see Methods and Instruments)

Viscosity (see Liquids)

Wave Mechanics (see Quantum Mechanics)

Work Function (see Electrical Properties)

ERRATA

	reads	should read
Rodionov et al, Soviet Phys. JETP 1, 64 (July, 1955)		
p. 64, column 2, line 19	methyl or ethyl	methylal or ethylal
Bogoliubov and Zubarev, Soviet Phys. 1, 83 (July, 1955)		
p. 88, column 1, line 6	omits	is taken over
p. 88, col. 1, 4th line from bottom	appears in	are
Grametitskii et al, Soviet Phys. JETP 1, 562 (November, 1955)		
p. 562, title	"fissions"	"disintegrations"
p. 562, paragraphs 1 and 2 (3times)	"fissions"	"disintegrations"
p. 563, column 1, 5th line from bottom	"fissions"	"disintegrations"

Index to J. Tech. Phys.
p. 374

Our apologies to Academician Abram Fedorovich Ioffe for interpreting his anniversary biography as an obituary. Like the report of Mark Twain's demise, it was a great exaggeration.

ANNOUNCEMENT

Beginning with the next issue (August, 1956), Soviet Physics JETP will appear monthly. Volume 3 (August, 1956-January, 1957) will contain translations of all articles appearing in Volume 30 of the Journal of Experimental and Theoretical Physics of the USSR (January-June, 1956). Volume 4 (February-July, 1957) will be a translation of Volume 31 (July-December, 1956) of the Soviet Journal.

Subscribers to Soviet Physics JETP for the calender year 1956 will receive Volume 3 as the completion of their subscription. For new subscribers (beginning with Volume 3) the subscription price will be $60.00 per year (two volumes, twelve issues) in the United States and Canada, $64.00 per year elsewhere. The single issue price will remain at $6.00.

Beginning in either July or August, 1956, the American Institute of Physics will commence translations of the Journal of Technical Physics of the USSR, the Acoustics Journal of the USSR and the physical sciences portions of Doklady. Price schedules for these journals are given below. Subscriptions should be addressed to the American Institute of Physics, 57 East 55 Street, New York 22, N. Y.

Soviet Physics—Technical Physics

A translation of the "Journal of Technical Physics" of the Academy of Sciences of the U.S.S.R. Eighteen issues per year, approximately 4,000 Russian pages. Annually, $90.00 domestic, $95.00 foreign.

Soviet Physics—Acoustics

A translation of the "Journal of Acoustics" of the Academy of Sciences of the U.S.S.R. Four issues per year, approximately 500 Russian pages. Annually, $20.00 domestic, $22.00 foreign. The 1955 issues of "Journal of Acoustics" U.S.S.R. will also be published. Will consist of two volumes, approximately 500 pages, and the subscription price will be $20.00 for the set.

Soviet Physics—Dokaldy

A translation of the "Physics Section" of the Proceedings of the Academy of Sciences of the U.S.S.R. Six issues per year, approximately 900 Russian pages. Annually $25.00 domestic, $27.50 foreign.

CONTENTS – *continued*

Letters to the Editor:

Solution of the Equation of Pseudo-scalar Meson Theory with Pseudo-scalar Coupling . . . I. Ia. Pomeranchuk 739 29, 869
Orientation of Planes in Double V^{0}Decay Events . . . V. M. Kharitonov 741 29, 868
Electroacoustic Waves in a Gas Discharge Plasma with Consideration of Volume Recombination . . . M. V. Koniukov and Ia. P. Terletskii 742 29, 874
Polarization of the Nuclei of Ferromagnetic Atoms . . . G. R. Khutsishvili 744 29, 894
The Rotation of the Plane of Polarization in Electrolytic Solutions by a Magnetic Field . . . A. F. Kapustinskii 744 29, 883
Distribution Function of a Non-ideal Bose Gas at the Temperature of Absolute Zero 745 29, 881
Towards a Statistical Theory of Fission Width . . . V. G. Nosov 746 29, 880
Radiation of Molecules in the Presence of a Strong High-Frequency Field . . . V. M. Fain 747 29, 878
Anamalous Skin Effect with Arbitrary Collision Integral . . . M. Ia. Azbel' and E. A. Kaner . . . 749 29, 876
The Internal Compton Effect . . . A. M. Iakobson 751 29, 703
Radiative Capture of Thermal Neutrons without Formation of a Compound Nucleus . . . L. K. Peker 753 29, 865
Possibility of Formation of Penetrating Radiation (μ-Mesons) in the Collision of High Energy Protons with Nuclei . . . A. N. Novikov, B. M. Pontecorvo and G. I. Selivanov 754 29, 889
Formation of Neutral π-Mesons in (n – p) Collisions at Effective Neutron Energies of 590 mev . . . V. P. Dzhelepov, K. O. Oganesian and V. B. Fliagin 757 29, 886
Microwave Spectrum of the C_2H_5Cl Molecule . . . A. I. Barchukov, T. M. Minaeva and A. M. Prokhorov 760 29, 892
Concerning the Cross Section of Overcharging of Slow Ions in their own Gas . . . Ia. M. Kagan and V. I. Perel' 761 29, 884
The Effect of Pressure on the Superconductivity of Cadmium . . . N. E. Alekseevskii and Iu. P. Gaidukov 762 29, 898
The Quantum Theory of the Magnetostriction of Cubic Monocrystals of Ferromagnetics at Low Temperatures . . . A. A. Gusev 764 29, 895
The Study of Relativistic Particles by the Use of Nuclear Emulsions in a Pulsed Magnetic Field . . . V. M. Likhachev, A. V. Kutsenko and V. P. Boronkov 766 29, 894
Inelastic Scattering of Mesons in the Semi-Phenomenological Theory of the Interaction of π-Mesons with Nucleons . . . Iu. M. Popov and A. A. Rukhadze 767 29, 893
The Relation Between our Criterion of Stability for a Homogeneous and that Phase of S. V. Tiablikov . . . I. Z. Fisher 768 29, 884

Capture of Thermal Neutrons by Isotopes of Lead . . . 769 29, 866
Crystalline Anisotropy of the Intermediate State . . . Iu. V. Sharvin and V. L. Sedov 771 29, 897
Heat of Vaporization of Oxygen in the Temperature Range 80-106°K . . . R. A. Alikhanor 771 29, 902
Measurement of the Absolute Quantum Yield of Photoluminescence of Alkali-Halide Crystals . . . Z. L. Morgenshtern 773 29, 903
The Surface Tension of Liquid He^3 in the Region of Very Low Temperatures (1.0-0.35°K . . . K. N. Zinov'eva 774 29, 899
Surface Ionization of Calcium, Strontium, and Magnesium on Oxidized Tungsten . . . Iu. K. Szhenov 775 29, 901
Phosphorescence of the Crystal Phosphor ZnS-Cu during Excitation by an Electron Beam . . . T. P. Belikova 776 29, 905
Author Index to Volume 1 . . . 778
Analytic Index to Volume 1 . . . 783
Errata . . . 793
Announcement . . . 793

SOVIET PHYSICS JETP VOLUME 2, NUMBER 4 JULY, 1956

CONTENTS

On the Macroscopic Theory of Superconductivity	V. L. Ginzburg	589	29, 748
The Strong Coupling Theory of Meson Fields. II	B. T. Geilikman	601	29, 430
Investigation of the Origin of Levels of Electron Localization in Zinc Sulfide Phosphors	N. V. Zhukova	608	29, 680
The (d–p) Reaction on Heavy Nuclei	K. A. Ter-Martirosian	620	29, 713
Theory of Magnetic Susceptibility in Metals at Low Temperatures	I. M. Lifshitz and A. M. Kosevich	636	29, 730
The de Haas-van Alphen Effect in Thin Metal Layers	A. M. Kosevich and I. M. Lifshitz	646	29, 743
Thermal and Galvanometric Effects in Strong Fields at Low Temperatures	G. E. Zil'berman	650	29, 762
Magnetic Properties of Trivalent Ions of Europium and Samarium	A. S. Borovik-Romanov and N. M. Kreines	657	29, 790
Methods of Investigating the Width of Raman Lines and Their Application	P. A. Bazhulin, S. G. Rautiian, A. I. Sokolovskaia and M. Sushchinskii	663	29, 822
Propagation of a Short Pulse in a Semiconductor Bounded by Two Hole-Electron Transistors	E. I. Adirovich and V. G. Kolotilova	670	29, 770
Fission of Heavy Nuclei by High Energy Neutrons*	V. I. Gol'danskii, V. S. Pen'kina and E. Z. Tarumov	677	29, 778
Investigation of the Structure of the Surface of Films of Copper Oxide on Different Faces of a Monocrystal of Copper, and the Determination of the Contact Potential Difference between These Surfaces	N. B. Gorngy	687	29, 808
Experiments on the Investigation of the Breakdown of NaCl Crystals	N. M. Melankholin and V. R. Regel'	696	29, 817
Method of Determination of Parameters of Ferromagnetic Resonance from Experimental Data	A. I. Pil'shchikov	703	29, 798
On the Lowering of the Luminescence Yield of Phosphors in Intense Excitation	V. V. Antonov-Romanovskii and L. A. Vinokurov	711	29, 830
Some Problems in Recombination Luminescence Associated With Various Forms of Excitation in KCl-Tl Phosphors	I. P. Shchukin	714	29, 834
Photochemical Conversion of Color Centers in Heated Crystals of Potassium Chloride	A. A. Shatalov	725	29, 847
Anisotropy of the Absorption of Gypsum Crystals in the Infrared Region	G. S. Zaitsev and B. C. Neporent	733	29, 857

(Contents continued on inside back cover)